Land Cover CCI

PRODUCT VALIDATION AND INTERCOMPARISON REPORT V2

YEAR 2&3 - 1.1

DOCUMENT REF:	CCI-LC-PVIRV2
DELIVERABLE REF:	D4.1
VERSION:	1.1
CREATION DATE:	2017-07-07
LAST MODIFIED:	2017-08-21

This page is intentionally blank.

Document Signature Table

	NAME	FUNCTION	COMPANY	SIGNATURE	DATE
PREPARED	Kirches G.		BC		
PREPARED	Militzer J.		BC		
PREPARED	Boettcher M.		BC		
PREPARED	Brockmann C.		BC		
PREPARED	Bontemps S.		UCL		
VERIFIED	Defourny P.	Science leader	UCL		
APPROVED					

Document Change Record

VERSION	DATE	DESCRIPTION	APPROVED
1.0	2015-04-30	First version of the PVIRv2 (based on PVIRv1)	
1.1	2017-08-21	Updated regarding ESA RIDs	

From version 1.0 to version 1.1

RID	SECTION	COMMENTS
FR-01	Symbols and Acronyms	The link related to BEAM has been corrected.
FR-02	Symbols and Acronyms	The link related to GlobCover Project has been corrected.
FR-03	Symbols and Acronyms	The link related to S-2 Mission has been corrected.
FR-04	Symbols and Acronyms	The link related to S-2 Mission has been corrected.
FR-05	Page 39 / Section 2.5 "Products planned in the LC-CCI Phase2"	The reference to the 2015 epoch was removed because it was not produced.

Document Diffusion List

ORGANISATION	NAME	QUANTITY
ESA	O. Arino, F. Ramoino	

SYMBOLS AND ACRONYMS

AATSR	: Advance Along Track Scanning Radiometer
ATSR	: Along Track Scanning Radiometer
ACRI-ST	: ACRI subsidiaries
A/D converter	: Analog-to-Digital-Converter
AMF	: Air Mass Factor
AMORGOS	: Accurate MERIS Ortho Rectified Geo-location Operational Software
ANN	: Artificial Neural Network
ANOVA	: Analysis of variance
AOD	: Aerosol Optical Depth
AOT	: Aerosol Optical Thickness
ASAR	: Advanced Synthetic Aperture Radar
ATBD	: Algorithm Theoretical Basis Document
AVHRR	: Advanced Very High Resolution Radiometer
BC	: Brockmann Consult GmbH
BDC	: Bi-directional compositing algorithm
BEAM	: Basic ENVISAT Tool for AATSR & MERIS ('http://www.brockmann-consult.de/cms/web/beam/)
BELMANIP	: Benchmark Land Multi-site Analysis and Intercomparison of Products
BISE	: Best Index Slope Extraction
BOA	: Bottom-Of-Atmosphere
BRDF	: Bidirectional Reflectance Distribution Function
BRF	: Bidirectional Reflectance Factor
CBH	: Cloud Base Height
CCD	: Charge-Coupled Device
CCI	: Climate Change Initiative
LC-CCI	: CCI Land Cover
CESBIO	: Center for the Study of the Biosphere from Space
CFI	: Customer Furnished Item
CEOS	: Committee on Earth Observation Satellites
CMC	: Climate Modelling Community
CoastColour	: ESA DUE project (http://www.coastcolour.org/)

CTH	: Cloud Top Height
CWV	: Water Vapour Column Content
CYC	: Hagolle Algorithm
DARD	: Data Access Requirements Document
DBT2	: Database for Task 2
DEM	: Digital Elevation Model
DJF	: Design Justification File
DOM	: Dark Object Method
DOY	: Day of year
DPM	: Detailed Processing Model
ECV	: Essential Climate Variable
EEA	: European Environment Agency
ELEV	: Elevation
ENVISAT	: Environnement Satellite (http://ENVISAT.esa.int)
EO	: Earth Observation
ERA Interim	: Global atmospheric reanalysis from 1979
ERS	: European Remote Sensing Satellite
ESA	: European Space Agency
ECV	: Essential Climate Variable
EUMETSAT	: European Meteorological Satellites Agency
f_{APAR}	: Fraction of Absorbed Photosynthetically Active Radiation
FR	: Full Resolution
FRS	: Full Resolution Swath
FSG	: Full Swath Geo-corrected
GCOS	: Global Climate Observing System
GlobAlbedo	: ESA DUE project
GlobCover	: ESA DUE project (http://due.esrin.esa.int/globcover/)
GMES	: Global Monitoring for Environment and Security
GOME	: Global Ozone Monitoring Experiment
HDF	: Hierarchical Data Format
HOT	: Haze Optimized Transform
HSV	: Hue Saturation Value colour space
IdePix	: Pixel Identification
IKONOS	: Commercial Earth Observation Satellite

IODD	: Input and Output Data Description
KO	: Kick-Off
L0, L1, L2, L3	: Level 0, Level 1, Level 2, Level 3
LAI	: Leaf Area Index
LARS	: Land Aerosol Remote Sensing
LC	: Land Cover
LC-condition	: Land Cover condition
LC-maps	: Land Cover maps
LUT	: Look-Up Table
MAX	: Maximum
MC	: Mean Compositing
MDSI	: MERIS Differential Snow Index
MERIS	: Medium Resolution Imaging Spectrometer
MIN	: Minimum
MIR	: Mid-wavelength InfraRed
LUT	: Look-Up Table
MODIS	: Moderate Resolution Imaging Spectroradiometer
MOMO	: Matrix-Operator-Model
MSI	: Multi-Spectral Imager
NDII	: Normalized Difference Ice Index
NDVI	: Normalized Difference Vegetation Index
NDSI	: Normalized Difference Snow Index
NIR	: Near InfraRed
NN	: Neuronal Net
NOAA	: National Oceanic and Atmospheric Administration
NRT	: Near Real Time
OLCI	: Ocean and Land Colour Instrument
OZO	: Ozone Column Content
PCA	: Principal Component Analysis
PG	: Projects Guidelines
PROBA	: Project for On-Board Autonomy; ESA's Project for On-Board Autonomy satellite
PROBA-V	: Proba Vegetation
PROSPECT	: Model of Leaf Optical Properties Spectra
PSD	: Product Specification Document

PUG	: Product User Guide
PVASR	: Product Validation and Algorithm Selection Report
PVP	: Product Validation Plan
PVIR	: Product Validation and Intercomparison Report
RAA	: Relative Azimuth Angle
RD	: Reference Dataset
RGB	: Red Green Blue colour space
RMS	: Root Mean Square
RR	: Reduced Resolution
RRG	: AMORGOS- Processed MERIS RR
RTC	: Radiative Transfer Code
RTE	: Radiative Transfer Equation
S-2	: GMES Sentinel-2 (https://sentinel.esa.int/web/sentinel/missions/sentinel-2)
S-3	: GMES Sentinel-3 (https://sentinel.esa.int/web/sentinel/missions/sentinel-3)
SAIL	: Scattering by Arbitrary Inclined Leaves (SAIL) 1D radiative transfer model
SAR	: Synthetic Aperture Radar
SCIAMACHY	: Scanning Imaging Spectrometer for Atmospheric CHartographY
SDR	: Surface Directional Reflectance
SLSTR	: Sea and Land Surface Temperature Radiometer
SMAC	: Simplified Method for Atmospheric Correction
SoW	: Statement of Work
SPOT	: Satellite Pour l'Observation de la Terre
SPOT-VGT	: SPOT-VEGETATION
SPOT VGT P	: SPOT VGT P Product (physical product)
SPOT VGT S1	: SPOT VGT S1 Product (daily surface product)
SR	: Surface Reflectance
SRTM	: Shuttle Radar Topography Mission
SRD	: System Requirements Document
SSD	: System Specifications Document
SVR	: System Verification Report
SWBD	: SRTM Water Body Data
SWIR	: Short-Wave InfraRed
SZA	: Sun Zenith Angle
TIR	: Thermal InfraRed

TN	: Technical Note
TOA	: Top Of Atmosphere
TP	: Technical Proposal
UCL	: Université catholique de Louvain
URD	: Users Requirement Document
USGS	: United States Geological Survey
UV	: Ultra Violet
VIS	: Visible
VIIRS	: Visible Infrared Imaging Radiometer Suite
VITO	: Vison on Technology (Flemish Institute for Technological Research NV)
VEU	: Video Electronic Unit
VGT	: SPOT Vegetation
VNIR	: Visible Near InfraRed
VZA	: View Zenith Angle
WB	: Water Bodies
WGS84	: World Geodetic System 84

REFERENCE DOCUMENTS

Applicable documents

ID	TITLE	ISSUE	DATE
[Ph1_SoWv1.4, 2009]	ESA Climate Change Initiative Phase I - Scientific User Consultation and Detailed Specification Statement of Work	1.4	09/11/2009
[Ph2_SoWv1.2, 2013]	Statement of Work for ESA Climate Change Initiative Phase II - CCI-PRGM-EOPS-SW-12-0012	1.2	07/06/2013
[Ph1_PGv1.0, 2013]	ESA Climate Change Initiative – Projects guidelines (EOP-DTEX-EOPS-SW-10-0002)	1.0	05/11/2010
[Ph1_TPv1.0, 2011]	ESA Climate Change Initiative Phase I - Land Cover ECV Technical proposal	1.0	05.03.2011
[Ph2_TPv1.0, 2014]	ESA Climate Change Initiative Phase II - Land Cover ECV Technical baseline for the project (update of the technical proposal with clarification and negotiation items)	1.0	13/03/2014
[Ph1_URDv2.2, 2011]	LC-CCI URD Phase I. Land Cover Climate Change Initiative - User Requirements Document	2.2	23/02/2011
[Ph2_URDv1.0, 2014]	LC-CCI URD Phase II. Land Cover Climate Change Initiative - User Requirements Document	1.0	28/07/2014
[Ph1_PSDv1.11, 2012]	LC-CCI URD Phase I. Land Cover Climate Change Initiative - Product Specification Document	1.11	03/07/2014
[Ph1_PVPv1.3, 2011]	LC-CCI PVR Phase I. Land Cover Climate Change Initiative - Product Validation Plan	1.3	04/07/2011
[Ph1_ATBDv2.3, 2013]	LC-CCI ATBD Phase I. Land Cover Climate Change Initiative - Algorithm Technical Basis Document	2.3	28/11/2013
[Ph1_PVASRv2.1, 2012]	LC-CCI PVASR Phase I. Land Cover Climate Change Initiative - Product Validation and Algorithm Selection Report	2.1	14/12/2012
[Ph1_IPVRv1.2, 2012]	LC-CCI IPVIR Phase I. Land Cover Climate Change Initiative - Internal Preliminary Validation Report	1.2	17/12/2012
[Ph1_PVIRv1.2, 2011]	LC-CCI PVIR Phase I. Land Cover Climate Change Initiative - Product Validation and Intercomparison Report v1	1.2	03/07/2014
[Ph2_ATBDv1_1.2, 2015]	LC-CCI ATBD Phase II. Land Cover Climate Change Initiative - Algorithm Technical Basis Document v1	1.2	11/09/2015

ID	TITLE	ISSUE	DATE
[Ph2_CECRv2_1.1, 2015]	LC-CCI CECR Phase II. Land Cover Climate Change Initiative - Comprehensive Error Characterisation Report v2	1.1	16/12/2015

Reference documents

ID	TITLE	ISSUE	DATE
[Arino et al., 2012]	Arino, O., Kalogirou, V., Ramos Perez, J. & Pinnock, S., 2012. Culture-MERIS: an ESA weekly service for agriculture. Remote Sensing Letters, 3:6, 461-469.	/	2012
[Eidenshink & Faundeen, 1994]	Eidenshink, J. C. & Faundeen, J. L., 1994The 1 km AVHRR global land data set: first stages in implementation, International Journal of Remote Sensing Vol. 15, Iss. 17, 3443-3462	/	1994
[GlobCover - PVR, 2008]	GlobCover - Products and Validation Report	1	01/12/2008
[GlobCover - TSD, 2008]	GlobCover 2005 project: Technical Specification Document, End-User meeting 3	4.0	27/11/2008
[USGS-CEOS, 2008]	USGS - CEOS Reference Sites Web Page http://calval.cr.usgs.gov/sites_catalog_ceos_sites.php#CEOS	/	28/08/2009
[CEOS-RVP, 2009]	QA4EO-WGCV-IVO-CSP-001-Questionnaire for information regarding the CEOS WGCV IVOS subgroup Cal/Val test sites for land imager radiometric gain - Questionnaire on Railroad Valley Playa http://calvalportal.ceos.org/railroad-valley-playa	1.1	18/02/2009
[CEOS-NV, 2009]	QA4EO-WGCV-IVO-CSP-001-Questionnaire for information regarding the CEOS WGCV IVOS subgroup Cal/Val test sites for land imager radiometric gain - Questionnaire on Negev http://calvalportal.ceos.org/negev	2.0	20/04/2009
[CEOS-LC, 2009]	QA4EO-WGCV-IVO-CSP-001-Questionnaire for information regarding the CEOS WGCV IVOS subgroup Cal/Val test sites for land imager radiometric gain - Questionnaire on La Crau http://calvalportal.ceos.org/la-crau	1.1	18/02/2009
[CEOS-IP, 2009]	QA4EO-WGCV-IVO-CSP-001-Questionnaire for information regarding the CEOS WGCV IVOS subgroup Cal/Val test sites for land imager radiometric gain - Questionnaire on Ivanpah Playa http://calvalportal.ceos.org/ivanpah-playa	1.1	18/02/2009
[CEOS-FF, 2009]	QA4EO-WGCV-IVO-CSP-001-Questionnaire for information regarding the CEOS WGCV IVOS subgroup Cal/Val test sites for land imager radiometric gain - Questionnaire on Frenchman Flat http://calvalportal.ceos.org/frenchman-flat	1.1	18/02/2009

ID	TITLE	ISSUE	DATE
[CEOS-DG, 2009]	QA4EO-WGCV-IVO-CSP-002-Questionnaire for information regarding the CEOS WGCV IVOS subgroup Cal/Val test sites for land imager radiometric gain - Questionnaire on Dunhuang http://calvalportal.ceos.org/dunhuang	2.0	20/04/2009
[CIMT, 2012]	CIMT, 2012 Analysis of Variance (ANOVA), A-Level Course Material, Further Statistics, Centre for Innovation in Mathematics Teaching, Plymouth, UK http://www.cimt.plymouth.ac.uk/projects/mepres/alevel/fstats_ch7.pdf		
[Kalogirou et al., 2013]	Kalogirou, V., Ramos Perez, J. & Arino, O., 2013. A first analysis on the Culture-MERIS products. Remote Sensing Letters, 4:3, 211-218.	/	/
[Kneubuehler et al., 2006]	Mathias Kneubuehler, Michael Schaepman and Kurt Thome, 2006. LONG - TERM VICARIOUS CALIBRATION EFFORTS OF MERIS AT RAILROAD VALLEY PLAYA (NV) - AN UPDATE, 2nd Working Meeting on MERIS and AATSR Calibration and Geophysical Validation, MAVT, 20.-24.3. 2006, ESRIN	/	2006
[Lane et al., 2015]	Online Statistics Education: A Multimedia Course of Study (http://onlinestatbook.com/) Project Leader: David M. Lane, Rice University	2.0	2015
[Rohatgi, 2015]	Rohatgi, A., 2015. WebPlotDigitalizer: HTML5 based online tool to extract numerical data from plot images Version 3.9	3.9	2015
[Santoro et al., 2014]	Santoro, M., Wegmueller, U., "Multi-temporal Synthetic ApertureRadar metrics applied to map open water bodies," IEEE Journal of Selected Topics in Applied Earth Observations and Remote Sensing, vol. 7, 8, pp. 3225-3238, 2014.	/	2014
[Pesaresi et al., 2016]	Pesaresi M., Ehrlich D., Ferri S., Florczyk A.J., Freire S., Halkia S., Julea A.M., Kemper T., Soille P. and V. Syrris. Operating procedure for the production of the Global Human Settlement Layer from Landsat data of the epochs 1975, 1990, 2000, and 2014. Publications Office of the European Union, EUR 27741 EN, 2016. doi: 10.2788/253582	/	2016
[DLR, 2016]	Global Urban Footprint, GUF; DLR 2016	/	2016
[Sulla-Menashe et al., 2011]	Sulla-Menashe, D.; Friedl, M. a.; Krankina, O. N.; Baccini, A.; Woodcock, C. E.; Sibley, A.; Sun, G.; Kharuk, V.; Elsakov, V. Hierarchical mapping of Northern Eurasian land cover using MODIS data. Remote Sensing of Environment 2011, 115, 392–403	/	2011
[Bartholome and Belward, 2005]	Bartholome, E. and Belward, A., 2005, “GLC2000: a new approach to ´ global land cover mapping from Earth Observation data”, International Journal of Remote Sensing, 26, 1959–1977	/	2005
[Pekel et al., 2016]	Pekel J-F., Cottam A., Gorelick N., Belward AS. High-resolution mapping of global surface water and its long-term changes. Nature. 540, 418–422 (15 December 2016). doi:10.1038/nature20584	/	2016

ID	TITLE	ISSUE	DATE
[Bontemps et al., 2010]	Bontemps, S., Defourny, P., Van Bogaert, E., Kalogirou, V. and Arino, O., GlobCover 2009 - Products Description and Validation Report (2010). Available at: http://due.esrin.esa.int/page_globcover.php	/	2010
[Strahler et al., 2006]	Strahler, A.H., Boschetti, L., Foody, G.M., Friedl, M.A., Hansen, M.C., Herold, M.; Mayaux, P., Morisette, J.T., Stehman, S.V., Woodcock, C. E. Global Land Cover Validation: Recommendations for Evaluation and Accuracy Assessment of Global Land Cover Maps. European Communities 2006, 51	/	2006

TABLE OF CONTENTS

LIST OF FIGURES

LIST OF TABLES

1 INTRODUCTION

1.1 Scope

The European Space Agency (ESA) Climate Change Initiative (CCI) projects will deliver the next generation of satellite derived geophysical parameters, with quantified uncertainties that will allow each parameter to be assessed against requirements from the Global Climate Observing System (GCOS) for Essential Climate Variables (ECV) and the Climate Modelling Community (CMC), represented within the CCI program by the Climate Modelling User Group (CMUG). A critical step in the acceptance of the CCI products by the GCOS and CMC communities is providing confidence in the quality of each CCI product and its uncertainties through validation against independent data such as ground based reference measurements or alternate estimates from other projects and sensors.

The Product Validation and Intercomparison Report version 2 gives a complete report of the activities executed to assess the quality of the products that were generated during the 2nd year of the Phase 2: the global surface reflectance (SR) composite time series and the CCI annual global Land Cover maps.

The document includes

- a description of all in situ observations used for product validation
- a description of all alternative products from other initiatives used for product inter-comparison
- a description of the quality control procedures applied for the selection of the most appropriate validation data and a characterisation of the errors and biases associated to them
- a detailed analysis of the uncertainty associated to the independent validation data
- a description of the match-up analyses performed on the derived ECV products against the selected spatially and temporally coincident in situ observations
- a detailed analysis of the uncertainty of the ECV products with reference to the independent validation data
- recommendations for fixing errors and/or improving the overall product quality

This report is based on the validation plan which gives a description of the methods and designs that has been applied so far in the validation of the LC-CCI products.

1.2 Structure of the document

After this introduction, the document is organized in 3 main sections:

- Section 2 gives an overview of the processing in LC-CCI Phase II and lists all the products that will be generated during the LC-CCI Phase 2;

- Section 3 describes the validation and inter-comparison as well as presents the results for the LC-CCI SR time series ;
- Section 4 describes the validation and inter-comparison as well as presents the results for the LC-CCI map products;
- Section 5 refers to the annex.

2 PROCESSING IN THE YEARS 1 AND 2 OF PHASE II

2.1 General overview

During the Phase I, the LC-CCI project delivered (i) global LC databases made of LC state products for three epochs, (ii) the ENVISAT MERIS Full and Reduced Resolutions (FR and RR respectively) time series which served as input for generating the global LC maps and (iii) a global Water Body (WB) product derived from the ENVISAT Advanced Synthetic Aperture Radar (ASAR) archives. To do so, the processing was organized in three distinct modules (Figure 2-1).

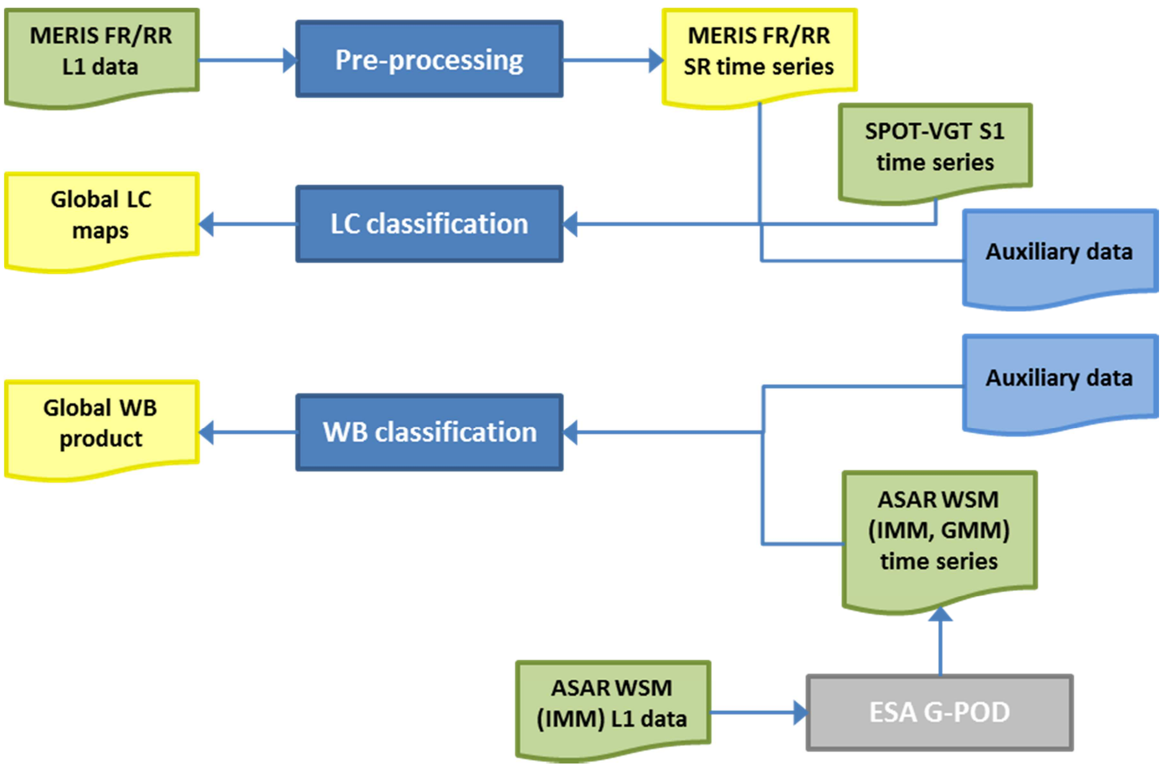

Figure 2-1 : Flowchart of the LC-CCI processing chains.

2.2 Overview of the pre-processing module

The completed automated pre-processing chain performs the following operations (Figure 2-2): radiometric and geometric correction, pixel identification, atmospheric correction with aerosol retrieval as well as compositing and mosaicking (possibly including sensor merging). This pre-processing chain was already implemented in Phase I and during the first and second years of the Phase II, improved and new algorithms are developed and validated for each of these steps. They are exhaustively detailed in a separate document [Ph2_ATBDv1_1.2, 2015].

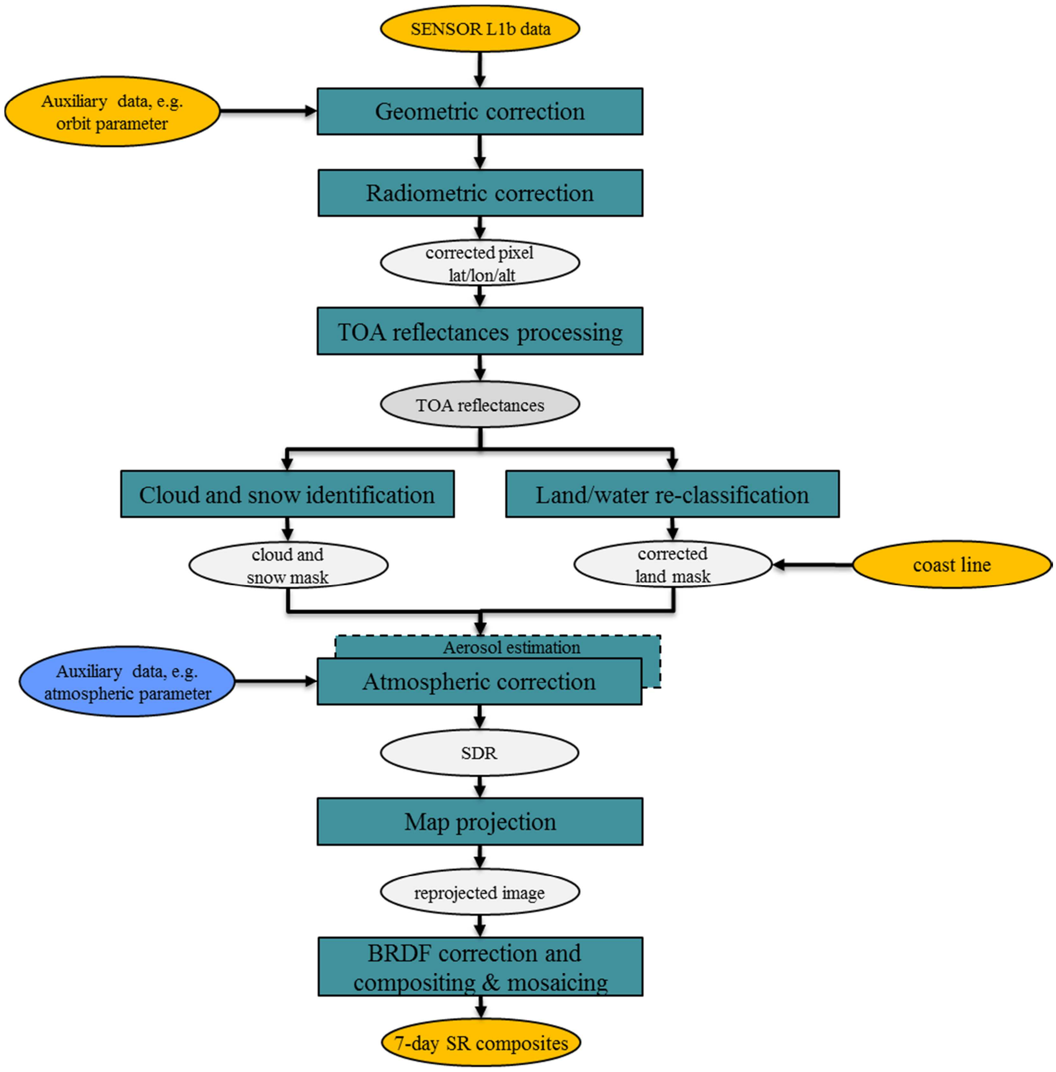

Figure 2-2 Schematic representation of the LC-CCI pre-processing chain including input (pre-processing chain based on the GlobAlbedo chain)

In case of PROBA-V, the input products in the pre-processing chain are the PROBA-V Level 3 Top of Atmosphere daily synthesis product at 333m spatial resolution. Therefore, the pre-processing includes pixel identification, atmospheric correction with aerosol retrieval as well as compositing and mosaicking only.

Table 2-1 details the satellite dataset that are planned to be used in order to generate the global SR composite time series in the first and second year of the Phase II. The time series are made of temporal synthesis obtained over a specific compositing period. The compositing period most suitable for the classification chain – and so the temporal resolution of the SR products delivered by the project – has been decided in Phase 1 to be 7 days. The exact schema for the 7-day periods is to start at January 1 and go on 7-day by 7-day periods until the end of the year. In this way, it should be noted that the last period of December comprises 8 days. As for leap years, the 7-day period including February 29 comprises 8 days.

Table 2-1: Satellite data that are planned to be used to generate the LC-CCI SR time series in the 1st and 2nd years of the Phase II

Global SR composite time series	Reference period	Satellite data source	Technical specifications of the satellite data source
AVHRR global SR composite time series[1]	1992-1998	AVHRR 2	• 1km • 5 spectral bands in visible and infrared • Global coverage
PROBA-V global SR composite time series	2014-2015 (and beyond)	PROBA-V S1 TOA	• 300 m resolution • spectral bands in visible and infrared • Global coverage
MERIS global SR composite time series	2003-2012	ENVISAT MERIS FR & RR	• 300-m or 1000- m resolution full swath • 15 spectral bands in visible and near infrared (NIR) • Global coverage

[1] It was planned to apply the complete pre-processing chain to AVHRR data and to deliver 7-day SR composites in Phase II year1. As a result of the delay in data delivery, it was decided to adapt the delivery plan as follows: deliver 7-day SR composites in Phase II year1. As a result of the delay in data delivery, it was decided to adapt the delivery plan as follows:

- Year1: delivery of 7-day TOA cloud free composites
- Year2: delivery of 7-day SR composites

For the production of the 7-day free cloud composites of AVHRR, the pre-processing chain includes only the radiometry, radiance to reflectance calculation, IdePix and compositing module. Only related modules are described in this document version.

2.3 Overview of the land cover classification module

The classification chain is organized into 2 main processes: (i) the generation of a baseline global LC map using the entire archive of the ENVISAT MERIS data and (ii) the generation of global LC maps representative of different 5-year epochs from this baseline product. An overall overview is provided in Figure 2-3.

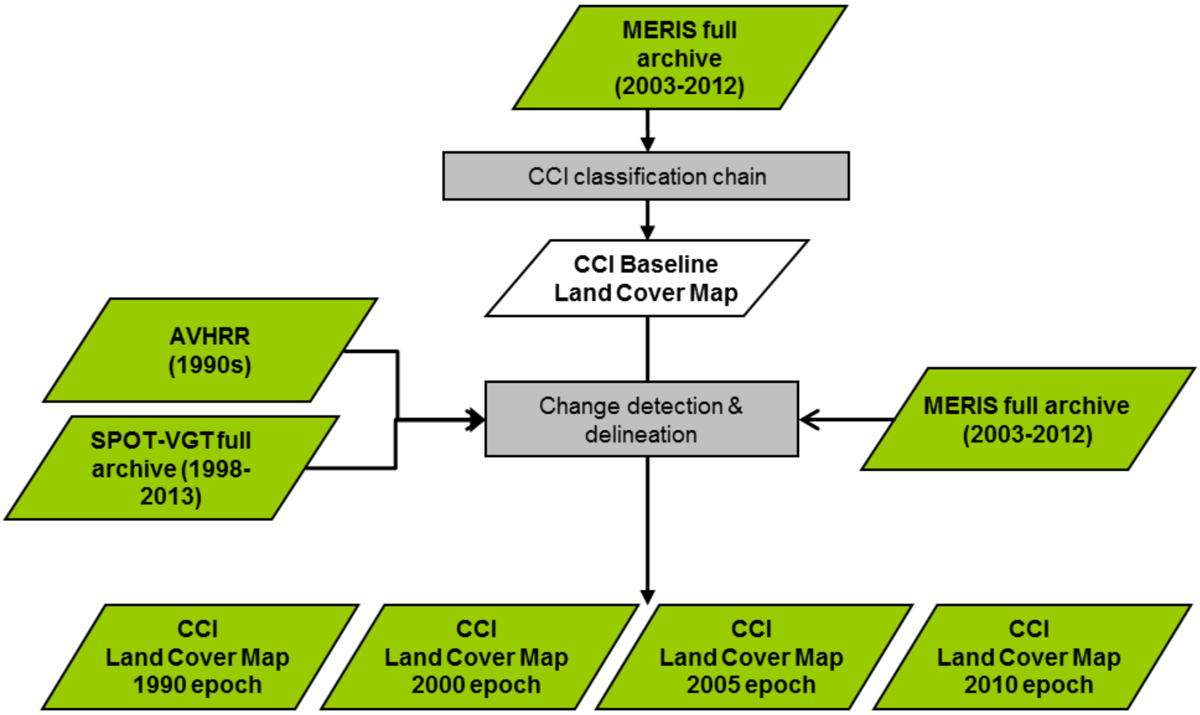

Figure 2-3: Schematic representation of the LC-CCI classification chain made of 2 main processes to generate global LC maps representative of 5-year epochs using the entire archives of ENVISAT MERIS and SPOT-VGT data and the AVHRR data over the 1990s

Figure 2-4 presents the different steps developed to generate the baseline global LC map: preliminary steps, classification algorithms with the use of 2 parallel techniques which are a machine learning algorithm and an unsupervised methodology, classification merging and post-classification editions.

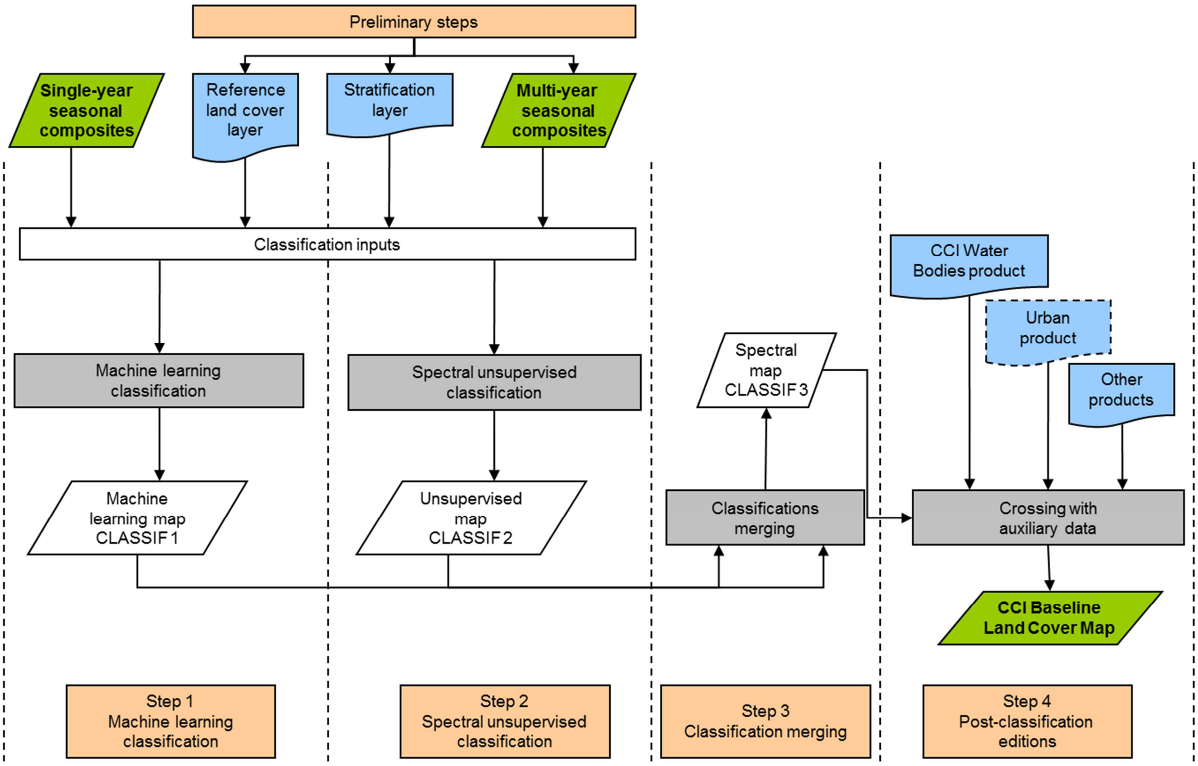

Figure 2-4: Schematic representation of the classification process developed to generate a baseline global LC map over the period 2003-2012 using the entire archives of ENVISAT MERIS data

The method implemented to derive global LC maps specific to 5-year epochs from the baseline global LC map is illustrated in Figure 2-5.

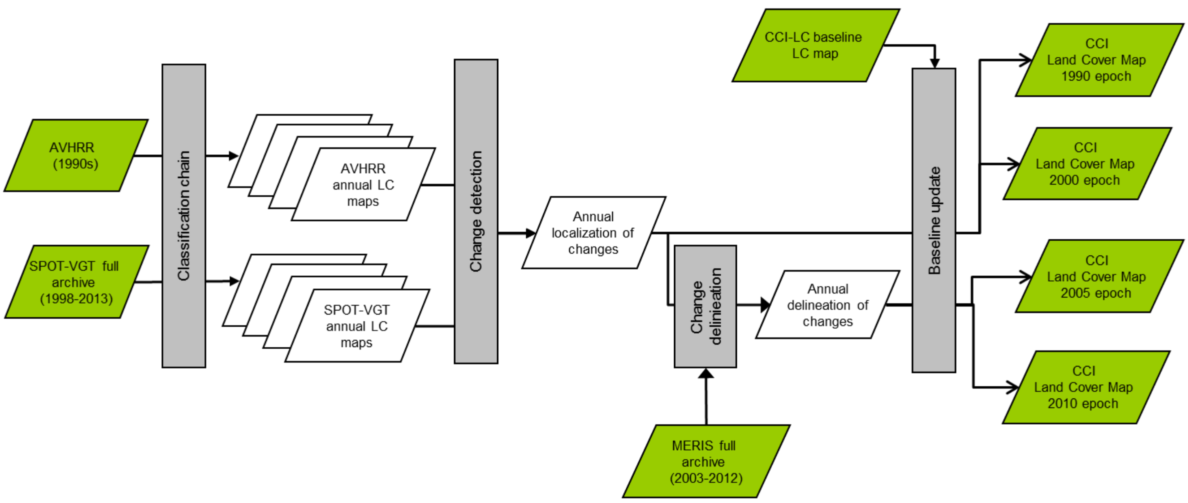

Figure 2-5: Schematic representation of the methodology developed to derive global LC maps specific to 5-year epochs from the baseline global LC map

Table 2-2 lists the satellite dataset that are planned to be used in order to generate the four LC maps.

Table 2-2: Satellite data sources that are planned to be used for the global LC maps generated during the 1st and 2nd years of Phase II

GLOBAL LC DATABASE	REFERENCE PERIOD	SATELLITE DATA SOURCE
Baseline 10-year global LC map	2003-2012	MERIS FR/RR global SR composites between 2003 and 2012
Global LC database for the 1990 epoch	1992-1998	Baseline 10-year global LC map AVHRR global SR composites between 1992 and 1998
Global LC database for the 2000 epoch	1998-2002	Baseline 10-year global LC map SPOT-VGT global SR composites between 1998 and 2002
Global LC map for the 2005 epoch	2003-2007	Baseline 10-year global LC map SPOT-VGT global SR composites between 2003 and 2007 to identify and date the changes MERIS FR global SR composites between 2003 and 2007 to map the identified changes at 300m spatial resolution
Global LC map for the 2010 epoch	2008-2012	Baseline 10-year global LC map SPOT-VGT global SR composites between 2008 and 2012 to identify and date the changes MERIS FR global SR composites between 2008 and 2012 to map the identified changes at 300m spatial resolution

2.4 Overview of the water body classification module

The generation of the WB product of the LC-CCI project followed a separated approach from the major LC classification activities described above (section 0) because of the start of the activities at a later stage during Phase I and of the use of a different source of EO data compared to the global LC maps.

To detect water bodies, a novel approach based on multi-temporal metrics from time series of Synthetic Aperture Radar (SAR) observations of the backscattering coefficient was developed and applied. The classification approach was applied to ENVISAT ASAR data of the backscattering coefficient. The major requirement was a number of observations sufficient to obtain a reliable classification. To fulfil the requirement, all ENVISAT ASAR data acquired in Wide Swath Mode (WSM - 150 m resolution) between summer 2005 and December 2010 were used .Gap fillers consisting of images in Image Mode Medium (IMM) resolution mode and Global Monitoring mode (GM1) were used locally, also at 150 m spatial resolution. The classification consisted of a binary map containing either water or land. In addition, areas of no or poor coverage by SAR data were labelled as unclassified. Because the SAR dataset covered primarily land, gaps occurred in correspondence of isolated islands and oceans. Occasionally, gaps would occur over land as well. Figure 2-6 shows the so-called Water Body Indicator (WBI) obtained straight from the SAR data.

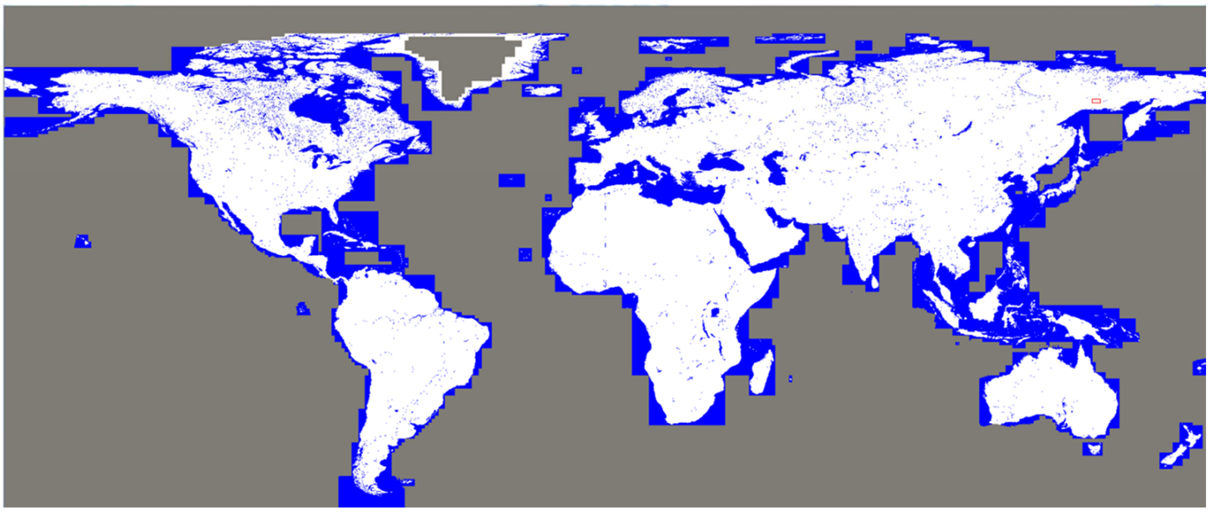

Figure 2-6: Illustration of LC-CCI WB Indicator obtained straight from the ENVISAT ASAR backscatter data. Pixel size: 150 m.

To obtain a truly global coverage of the Earth, the unclassified pixels were removed during a consolidation phase of the product obtained straight from the SAR data (i.e. the WBI) and filled with land or water information from other sources. The consolidation also served to check for major systematic errors and compensate for these wherever possible. At the end of the consolidation (end of Phase I), the LC-CCI WB product was obtained. It is shown in Figure 2-7.

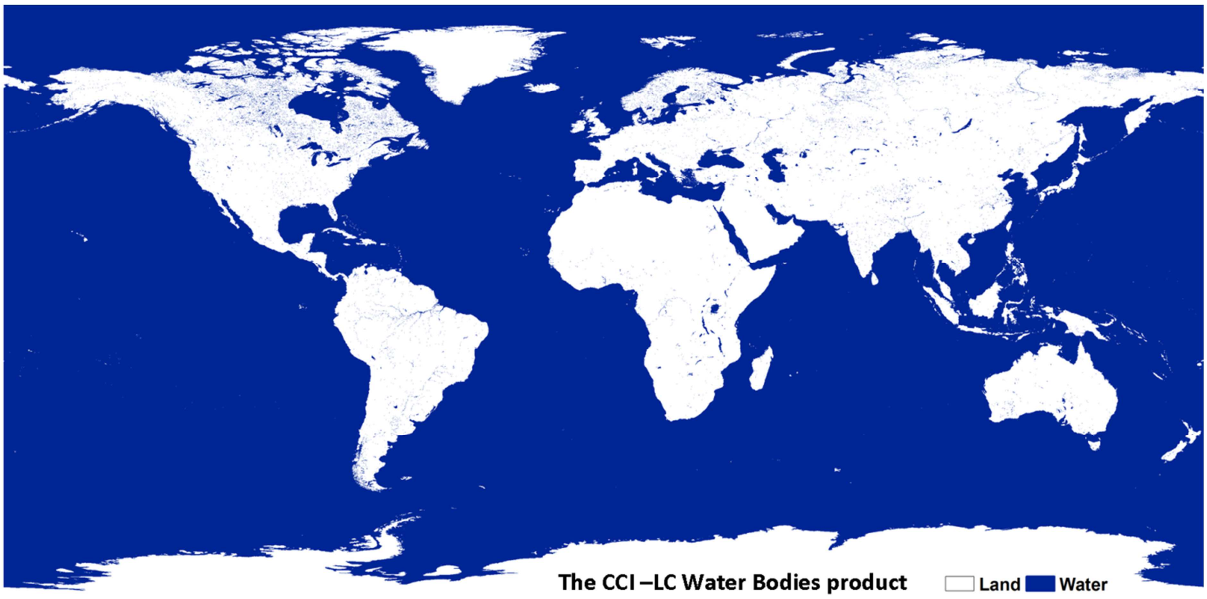

Figure 2-7 : Illustration of LC-CCI WB product derived at the end of Phase I from ENVISAT ASAR backscatter data and consolidated with additional EO data products of water bodies. Pixel size: 300 m.

The classification chain is here summarized into bullet points:

- Gathering of ENVISAT ASAR data and pre-processing from radar geometry to stacks of calibrated, geocoded, co-registered, normalized and speckle-filtered images of the SAR backscatter. A 1×1 degree tiling system is adopted to make the classification more flexible;
- Generation of multi-temporal metrics from the SAR backscatter:
    - Temporal variability (TV),
    - Minimum backscatter (MB),
    - Average backscatter (AVE);
- Thresholding in the feature space of TV and MB using a global rule [Santoro et al., 2014] generation of a map of potential water bodies (binary map);
- Refinement of potential water bodies to generate the WBI using regional rules and all three backscatter metrics to account for:
    - Commissions in cropland, land, snow and ice surfaces, glaciers,
    - Omissions over long-lasting sea ice;
- Consolidation of WBI to remove remaining macroscopic errors and obtain truly global coverage with EO imagery and Shuttle Radar Topography (SRTM) Water Body Database (SWBD);
- Aggregation of consolidated WBI from 150 m to 300 m: generation of LC-CCI WB product;

- Further refinement of the WB products with further auxiliary water body products and seasonal WB maps derived from the ASAR data.

The last point refers to the advances in Phase II. Given the high thematic accuracy of the WB product and the evidence that the algorithm already performs at its best, a new round of classification aims at focusing primarily on the removal or existing errors in the WB product derived at the end of Phase I.

2.5 Products planned in the LC-CCI Phase2

The outputs of the LC-CCI Phase 2 project concern global SR time series, global LC maps, global LS seasonality products and a global water bodies' product, all of them being delivered along with metadata. The outputs also include software systems, products documentation and validation reports. The PSD focuses on the datasets.

At the end of the 3-year long Phase 2, the key global datasets for the end-users will be:

1) Global SR time series and associated metadata over different epochs and from different sensors:
    a. Time series of AVHRR 7-day composites[2] from 1992 through 1999;
    b. Time series of ENVISAT MERIS Full Resolution 7-day composites from 2003 through 2012;
    c. Time series of ENVISAT MERIS Reduced Resolution 7-day composites from 2003 through 2012;
    d. Time series of PROBA-V 7-day composites from 2014 through 2015 (and beyond);
    e. Time series of Sentinel-3 OLCI and SLSTR 7-day composites from 2015 (and beyond).
2) Global LC maps for the 1990s, 2000, 2005 and 2010 epochs based on the above AVHRR, SPOT-VGT, MERIS FR and RR, PROBA-V, MODIS composites and associated metadata;
3) An updated global LC map for 2015 including the above Sentinel-3 OLCI and SLSTR composites and associated metadata[3];
4) A global LS seasonality product and associated metadata for the NDVI;
5) Global map of permanent open water bodies for the 2010 epoch based on ENVISAT ASAR time series.

In addition, prototypes products are foreseen, which will demonstrate the pre-processing and classification algorithms developed for the Sentinel-1 and -2 missions and to expand historical time series. They include:

[2] A 7-day compositing period is foreseen to be consistent with the other sensors, but this has to be confirmed according to the data coverage

[3] According to the availability of Sentinel-3 data in terms of quantity and timing with respect to the overall project planning

1) Sentinel-2 and Landsat 8 time series of regional SR composites from 2014 (and beyond) and associated metadata;
2) Regional LC maps based on the above Sentinel-2 and Landsat 8 composites and associated metadata;
3) Change maps dedicated to critical LC classes and/or regions according to users' priorities based on the above Sentinel-2 and Landsat 8 composites and associated metadata;
4) Prototype water body and urban products based on Sentinel-1 SAR data, tuned geographically to the regional LC maps obtained with Sentinel-2 data;
5) A consistent coarse spatial resolution LC map for continental or sub-continental regions for the 1980s based on the AVHRR Global Inventory Monitoring and Modelling System (GIMMS) dataset;
6) An EvapoTranspiration (ET) Feasibility study will be performed during the first year of this second phase. Encouraging results may lead to the production of an ET seasonality product;
7) As backup the time series of SPOT-VGT 7-day composites from 1998 through 2012 in case of delayed delivery of the reprocessed SPOT VGT S1 products.

Those products will be generated throughout the project, following the planning illustrated in Figure 2-8.

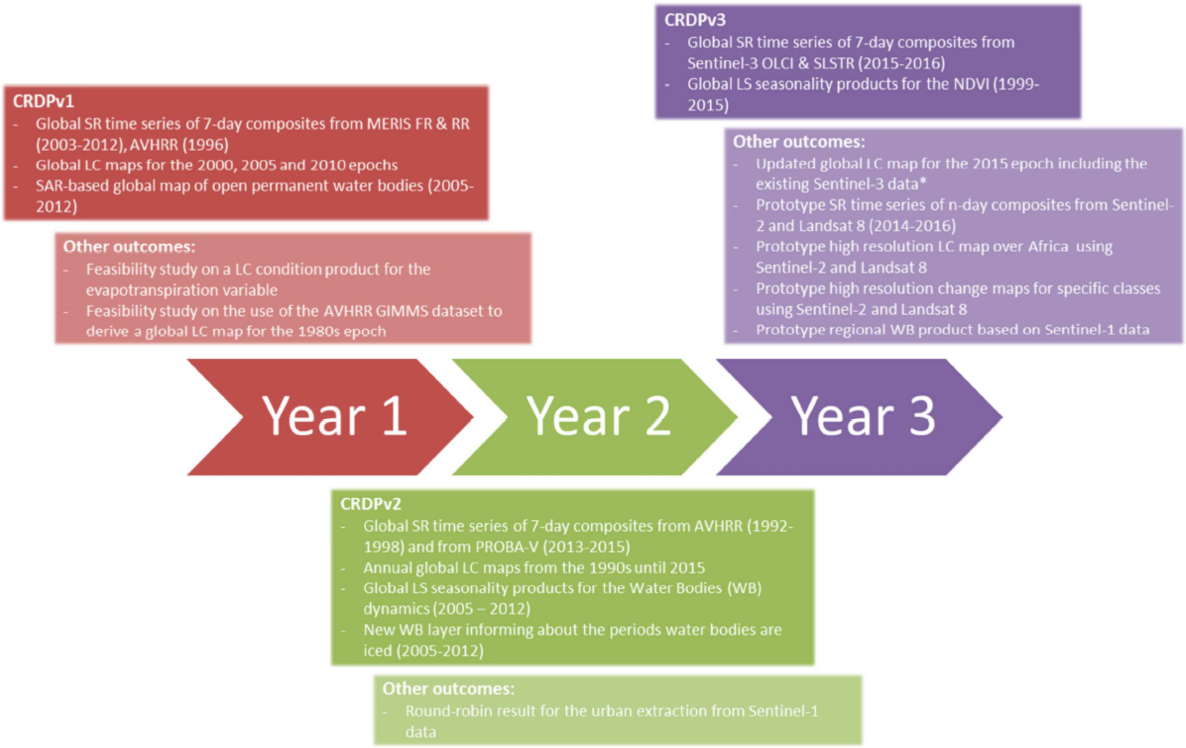

Figure 2-8: Planning of datasets to be produced in the LC-CCI Phase 2

* The reason why this update is not included in the CRDPv3 is that it will be delivered at the end of the year 3, thus not available for climate assessment

This version of the document focuses on the products that will be generated during the first and the second year of the project, i.e. not the Sentinel-3 time series and not the high resolution prototype products.

3 SR 7-DAY COMPOSITE TIME SERIES

3.1 Validation plan for the global SR composite time series [Ph1_PVPv1.3, 2011]

The quality of each global multispectral SR composite is described, on a per-pixel basis, by a set of flags and values:

- the temporal standard deviation, for each spectral band;
- the number of valid observations, for each pixel;
- the number of clear sky values available for the BRDF correction and compositing steps, for each pixel;
- the number of observations of cloudy coverage, for each pixel;
- the number of observations of snow and ice coverage, for each pixel;
- the risk of incorrect BRDF-correction, for each pixel.

Besides assessing the quality of individual composites, the quality of the global SR time series is also documented, with the aim of quantifying its discrimination potential. The following indicators are used:

- the intra- and inter-annual reflectance dynamics (range and standard deviation) computed from the overall spectral reflectance distribution, for each spectral band and stratum (if a stratification is used in the classification process);
- the temporal variance at the pixel level for the various spectral reflectance values;
- the local variance for the various spectral reflectance values within a LC class and across LC classes.

Furthermore, the obtained SR values are compared with in-situ measurements, with other correspondent reflectance products, e.g. with the products of the ESA Culture MERIS project. In addition, the geometric accuracy is quality controlled and reported in the LC-CCI Product Validation and Algorithm Selection Report [Ph1_PVASRv2.1, 2012] and in the LC-CCI Comprehensive Error Characterisation report [Ph2_CECRv2_1.1, 2015] in detail.

3.2 The temporal variance at the pixel level for the various spectral reflectance values

The purpose of this paragraph is to present the results of the validation of the global 7 day MERIS FR and RR, PROBA-V as well as AVHRR composites based on the analysis of the temporal variance at pixel-level for the various spectral reflectance values.

For this part of the validation, 26 reference points, including the CEOS LandNet sites (without Dome C and Tuz Golu) [USGS-CEOS, 2008], have been selected and the corresponding time series have been analysed afterwards by statistical measurements like calculating the mean and variance. The selected reference points are globally distributed and cover a wide range of different natural surfaces (see Figure 3-1and Table 3-1 and Table 5-1).

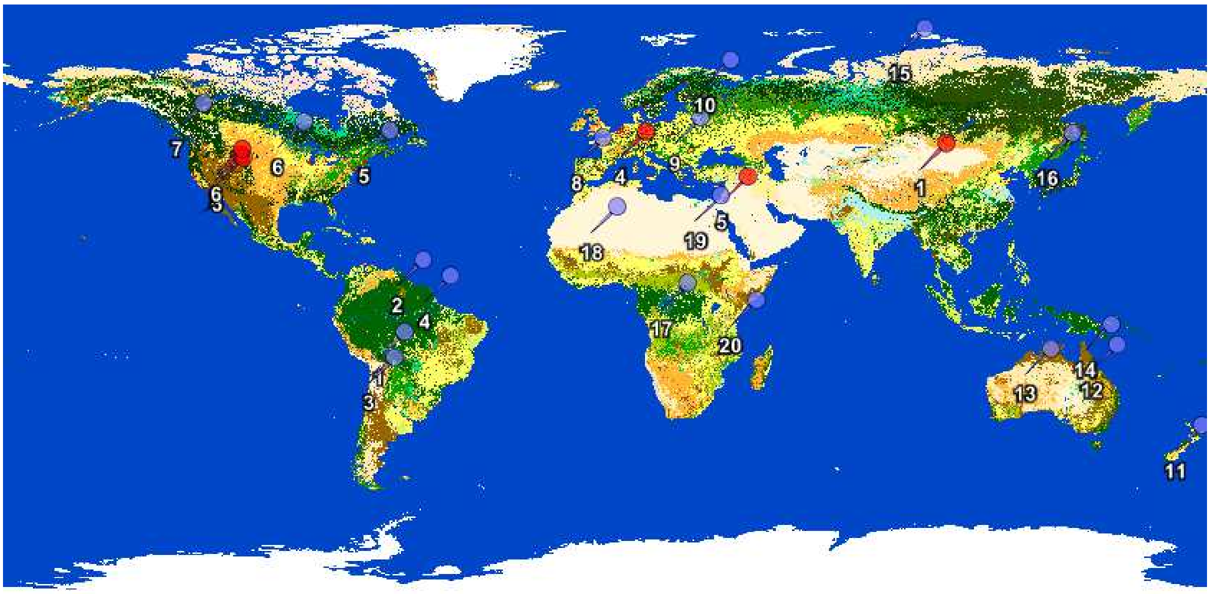

Figure 3-1: CEOS LandNet sites (red pin) and selected reference points (blue pin) (see also Table 3-2)

Table 3-1: CEOS LandNet sites

NAME	LONGITUDE	LATITUDE	COMMENTS
Railroad Valley Playa	-115.69	38.50	Affiliation: NASA/GSFC [CEOS-RVP, 2009]
Negev	35.01	30.11	Affiliation: Ben Gurion Univerisity [CEOS-NV, 2009]
La Crau	4.86	43.56	Affiliation: CNES [CEOS-LC, 2009]
Ivanpah Playa	-115.40	35.57	Affiliation: NASA/GSFC [CEOS-IP, 2009]
Frenchman Flat	-115.93	36.81	Affiliation: NASA/JPL [CEOS-FF, 2009]
Dunhuang	94.34	40.13	Affiliation: NSMC/CMA [CEOS-DG, 2009]

For the analysis and illustration only, the reflectance values of those pixels which are classified as clear land have been considered.

3.2.1 MERIS FR and RR

The following table (Table 3-2) shows the relation between the number of the valid observations taken by the sensor and the number of observations taking into account the specific surface condition.

Table 3-2: Number of valid observations of the sensor and w.r.t. observation conditions for MERIS FR and RR for 2003 - 2012 for the CEOS LandNet sites and reference points

	PIN NUMBER	LCCS CLASS	FR ACQUISITION	FR CLEAR LAND OBSERVATION	RR ACQUISITION	RR CLEAR LAND OBSERVATION
Dunhuang	1	130	443	356	476	377
Frenchman Flat	2	200	400	20	477	38
Ivanpah Playa	3	120	366	275	477	390
La Crau	4	130	471	404	479	406
Negev	5	200	465	407	478	442
Railroad Valley Playa	6	200	395	141	477	160
Yungas Coroico	1	50	67	16	473	177
Gran Sabana	2	50	230	28	473	68
Atacama Desert	3	200	269	255	475	463
Amazon	4	50	273	31	473	65
White Mountain National Forest	5	61	309	117	478	195
Sheyenne National Grassland	6	130	419	187	474	246
Great Bear Rainforest	7	70	395	68	398	58
National Park Peneda Geres	8	90	461	314	478	314
National Park Horto Bagy	9	130	470	253	471	247
Kalevalsky Bor National Park	10	70	292	78	302	83
Mackenzie Country - New Zealand	11	130	353	223	391	274
Great Basalt Wall National Park	12	62	422	276	477	341
Great Sandy Dessert	13	150	297	241	478	436
Coen Tropical	14	50	392	150	474	158
Tundra - Tajmyr	15	150	227	42	243	53
Boreal Forest - Wladiwostok	16	90	256	87	475	208
Tumba Lediima - Kongo	17	50	337	64	477	119
Timbuktu - Sahara	18	200	435	411	479	460
New Valley - Sahara	19	200	456	451	478	477
Mikumi National Park	20	10	415	112	474	107

The following figures (Figure 3-2 through Figure 3-25) show SR time series of MERIS FR and RR data (2003-2012) over the CEOS-LANDNET SITES as well as the mean spectra. The tables (Table 3-3 through Table 3-6) show the corresponding mean and variance values.

The analysis of different 10-year temporal profiles highlights the level remaining noise in the SR 7-day composite. This analysis leads to three main conclusions which can be summarized as follows:

- the number of pixels which contribute to the analysis of the time series is very variable whereas this can be caused by the data availability (number of acquisition) or by the cloud coverage (number of "clear land" pixels); the number of RR acquisition count is always higher than the FR one and logically, the number of RR clear observation is also higher than the number of clear observation from FR;
- the impact of undetected clouds is visible (see discussion below related to Figure 3-26) in the time series and influences the statistical parameter estimate;
- the standard deviation values reach an order of magnitude from 2.1% through 63 % (mean 21%).

The Figure 3-26 shows two time series of the 7 day SR composites from the LC-CCI project for the CEOS LANDNET sites Negev. They only differ which valid pixel expression is applied. Taking only into account those values with status count greater 2 for calculation of the 7 day composites, some fluctuations are eliminated due to BRDF for example as shown in Figure 3-26-b. The variation of the values may be caused by undetected clouds which strongly influence the retrieved 7-day SR composites values due to their spectral characteristics which may be completely differ from the underlying surface.

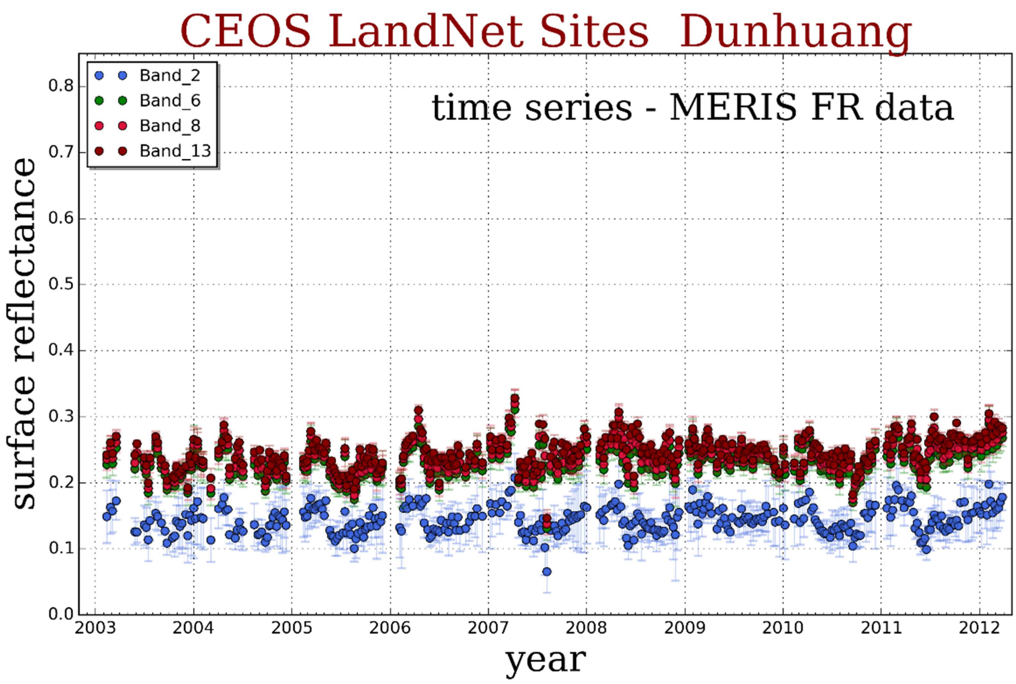

Figure 3-2: SR time series from MERIS FR data - 2003-2012 - CEOS-LANDNET SITES - Dunhuang

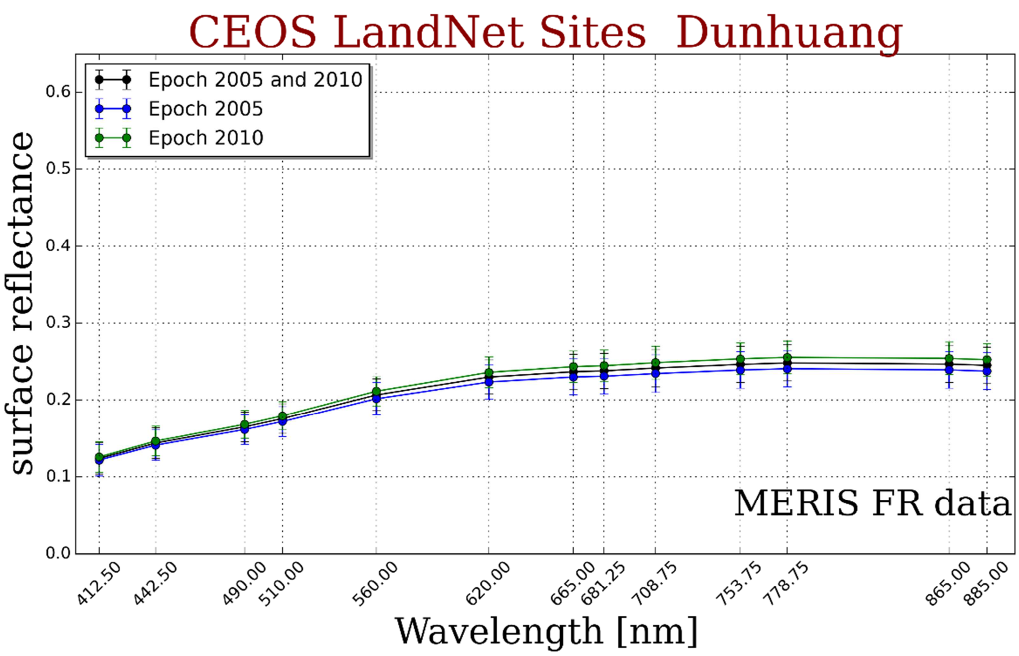

Figure 3-3: Spectra - CEOS-LANDNET SITES - Dunhuang - MERIS FR data

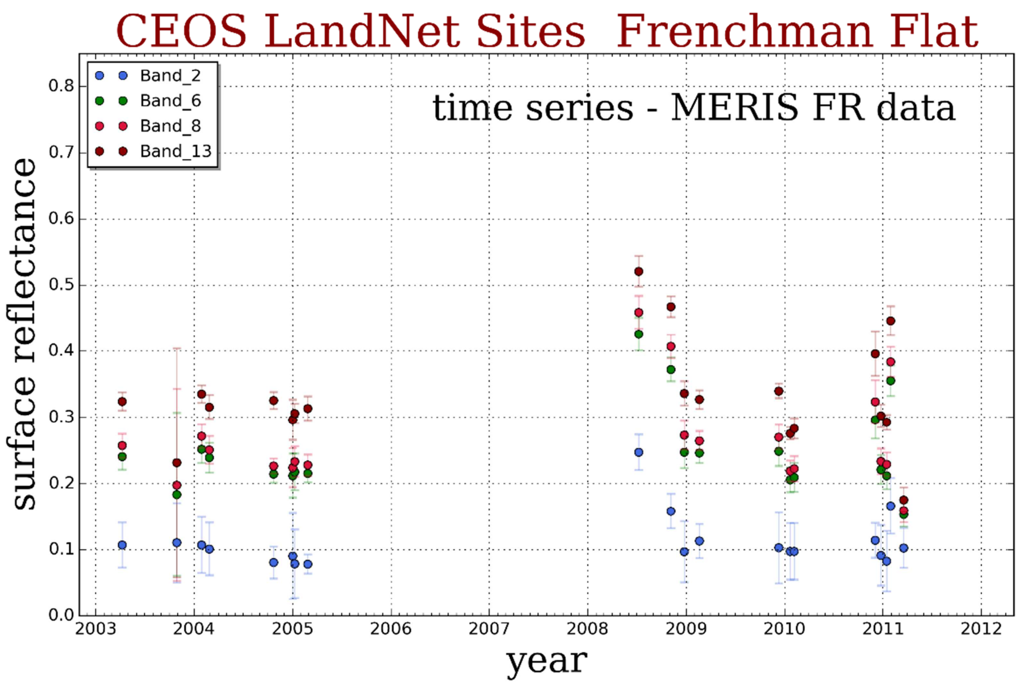

Figure 3-4: SR time series from MERIS FR data - 2003-2012 - CEOS-LANDNET SITES - Frenchman Flat

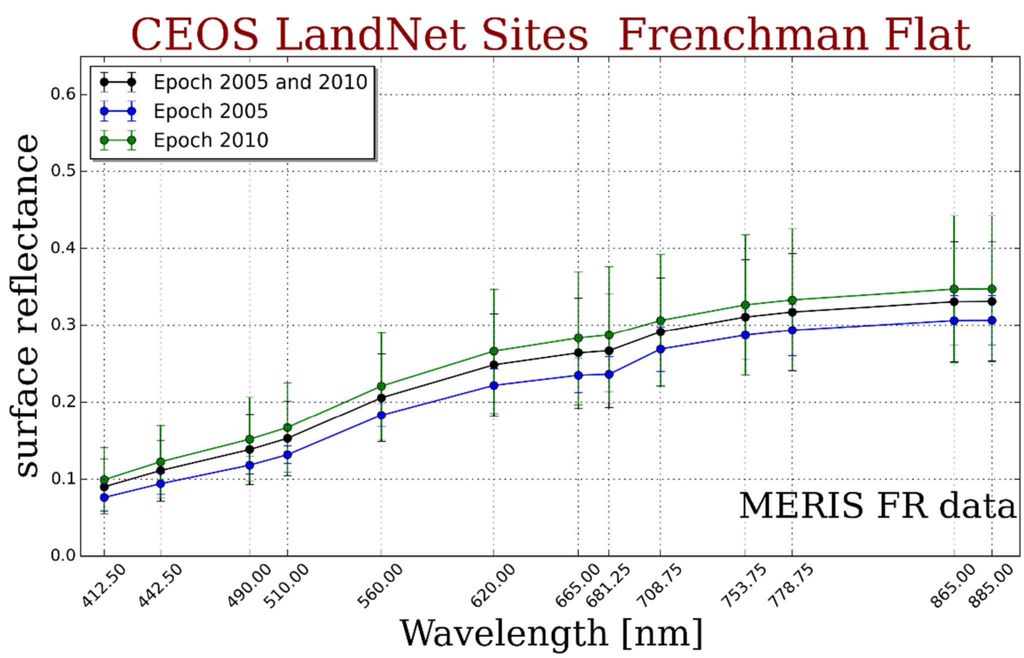

Figure 3-5: Spectra - CEOS-LANDNET SITES - Frenchman Flat - MERIS FR data

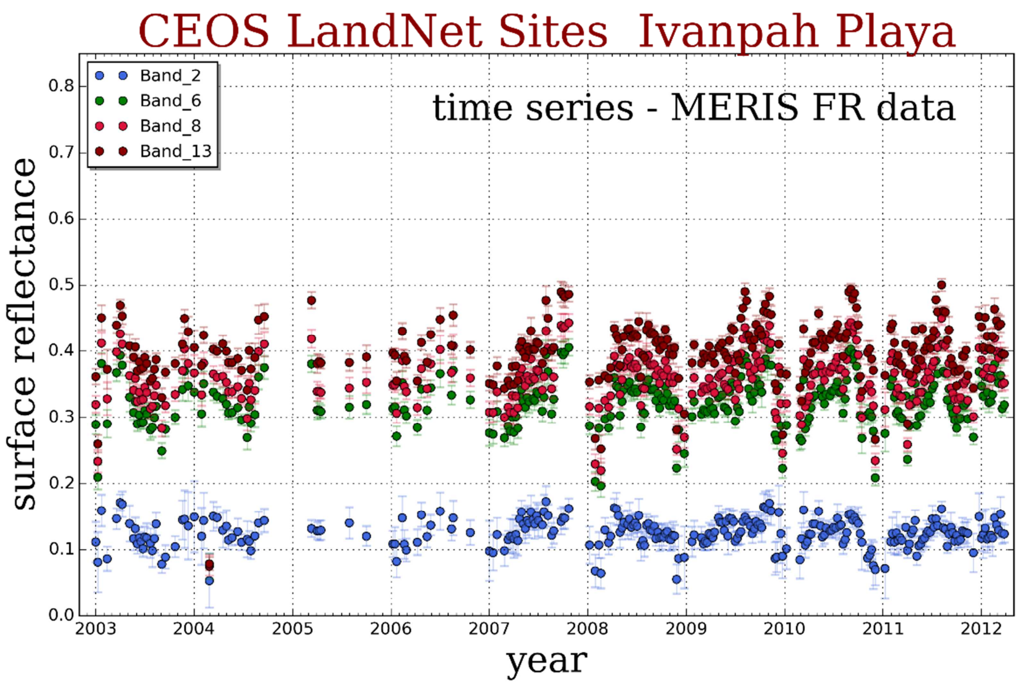

Figure 3-6: SR time series from MERIS FR data - 2003-2012 - CEOS-LANDNET SITES - Ivanpah Playa

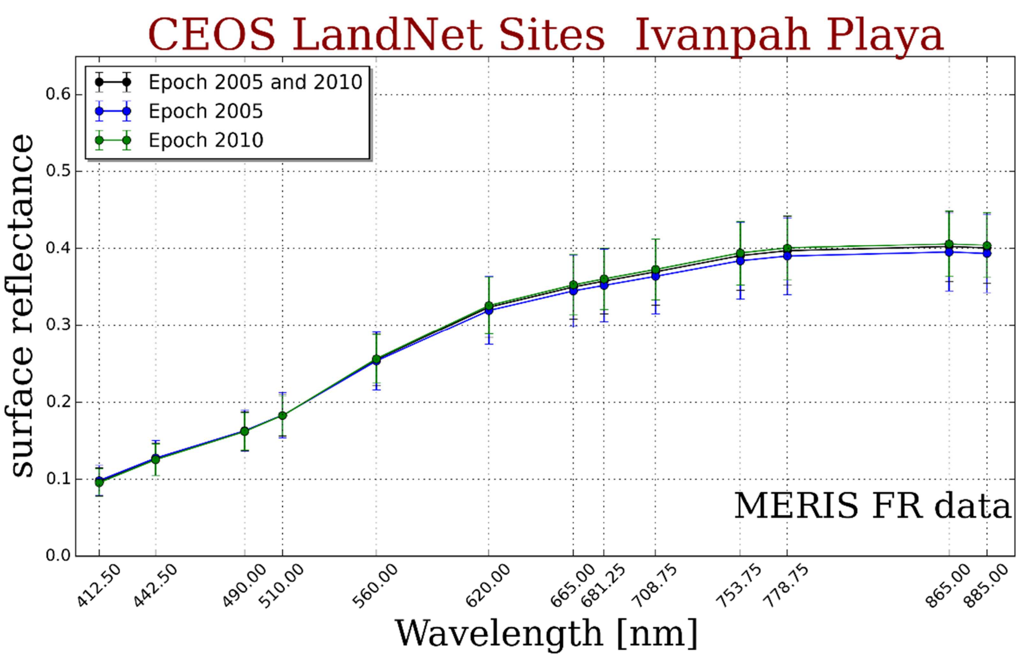

Figure 3-7: Spectra - CEOS-LANDNET SITES - Ivanpah Playa - MERIS FR data

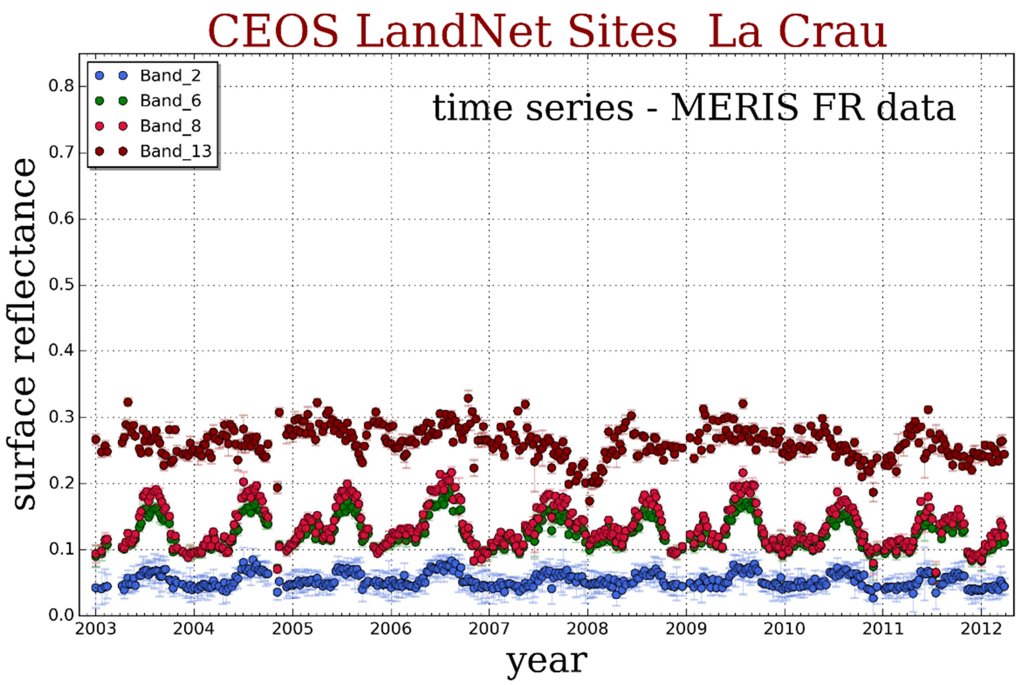

Figure 3-8: SR time series from MERIS FR data - 2003-2012 - CEOS-LANDNET SITES - La Crau

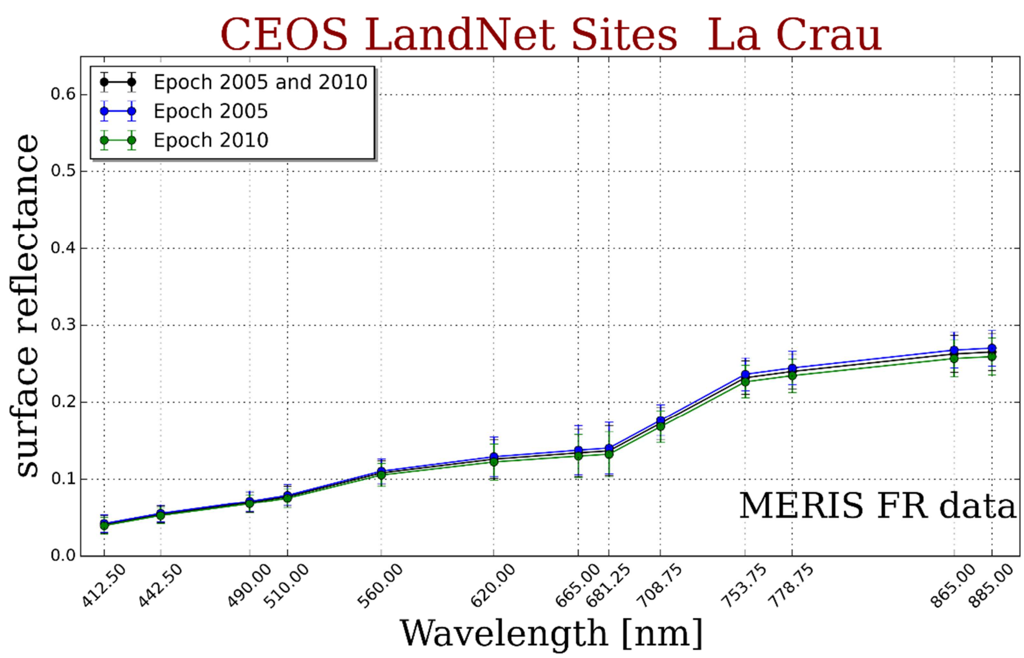

Figure 3-9: Spectra - CEOS-LANDNET SITES - La Crau - MERIS FR data

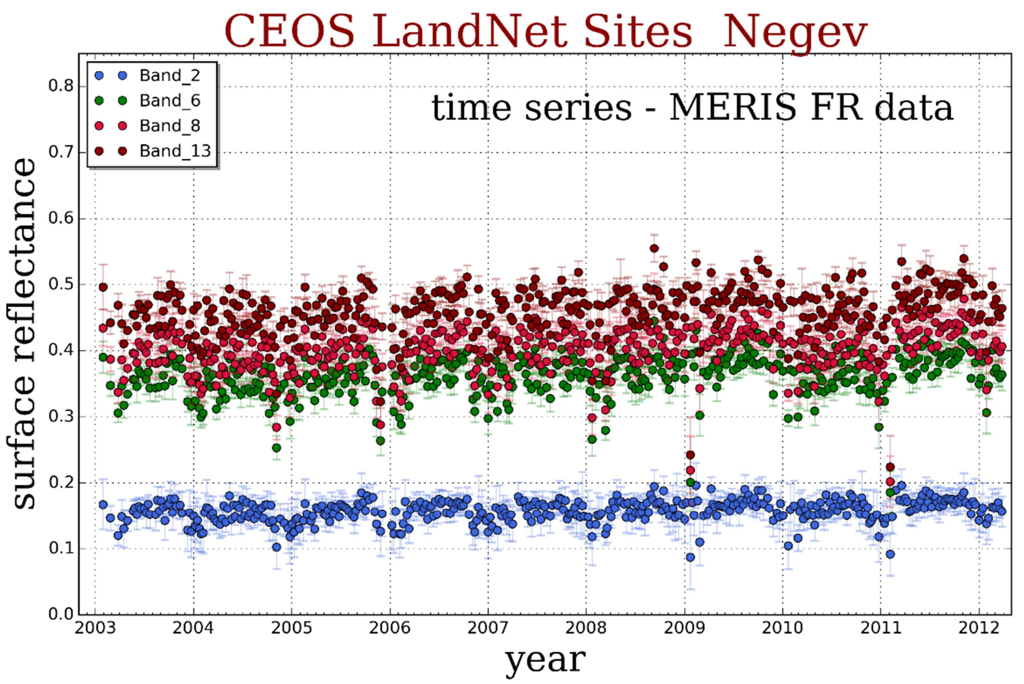

Figure 3-10: SR time series from MERIS FR data - 2003-2012 - CEOS-LANDNET SITES - Negev

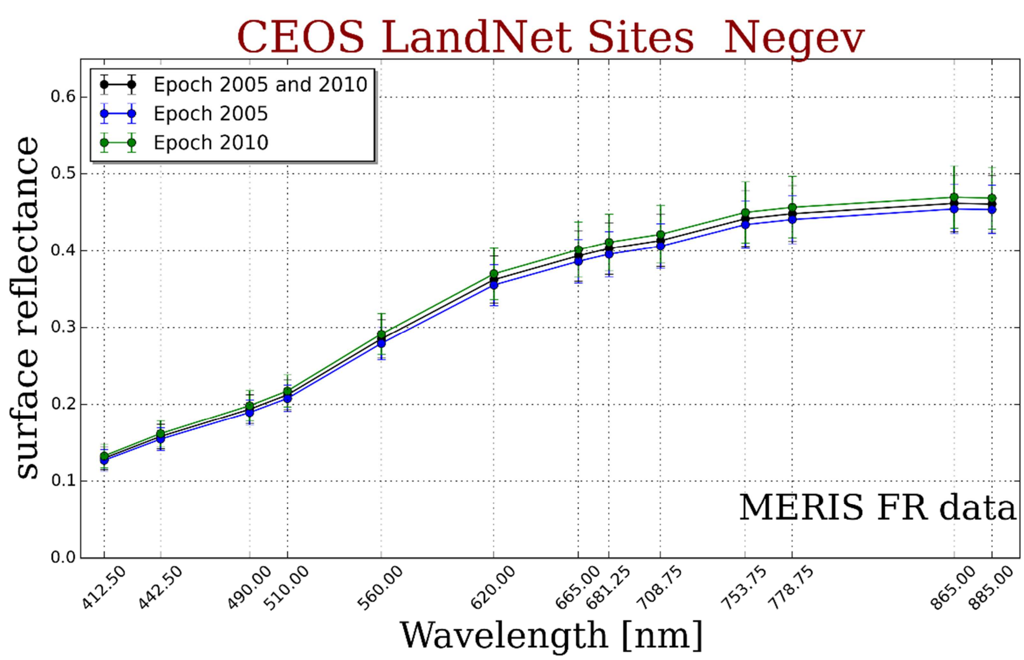

Figure 3-11: Spectra - CEOS-LANDNET SITES - Negev - MERIS FR data

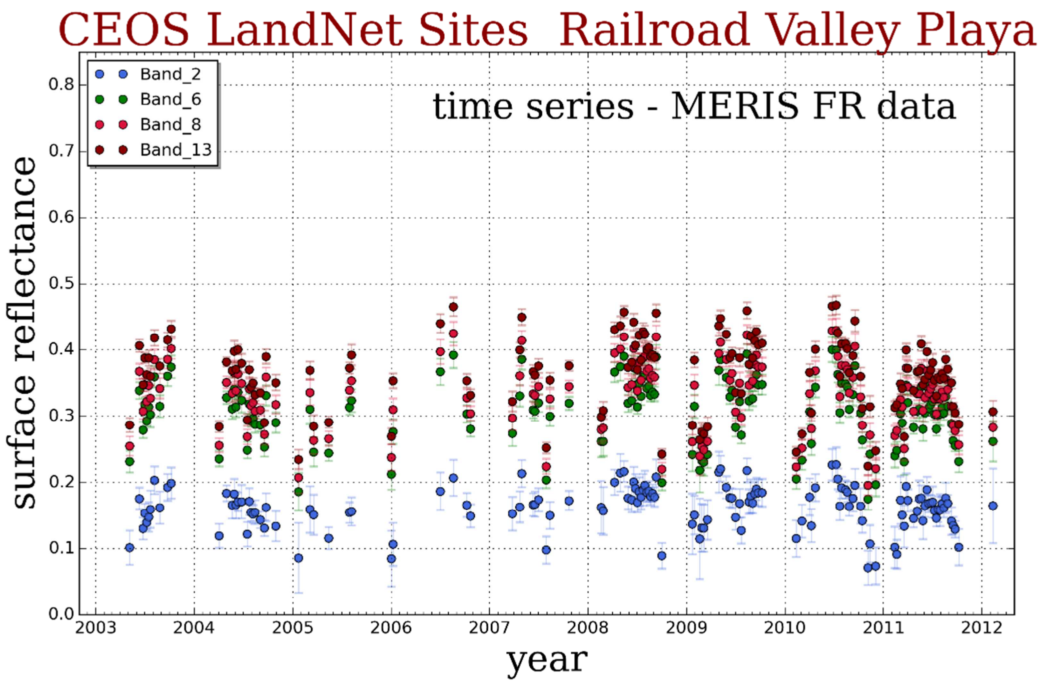

Figure 3-12: SR time series from MERIS FR data - 2003-2012 - CEOS-LANDNET SITES - Railroad Valley Playa

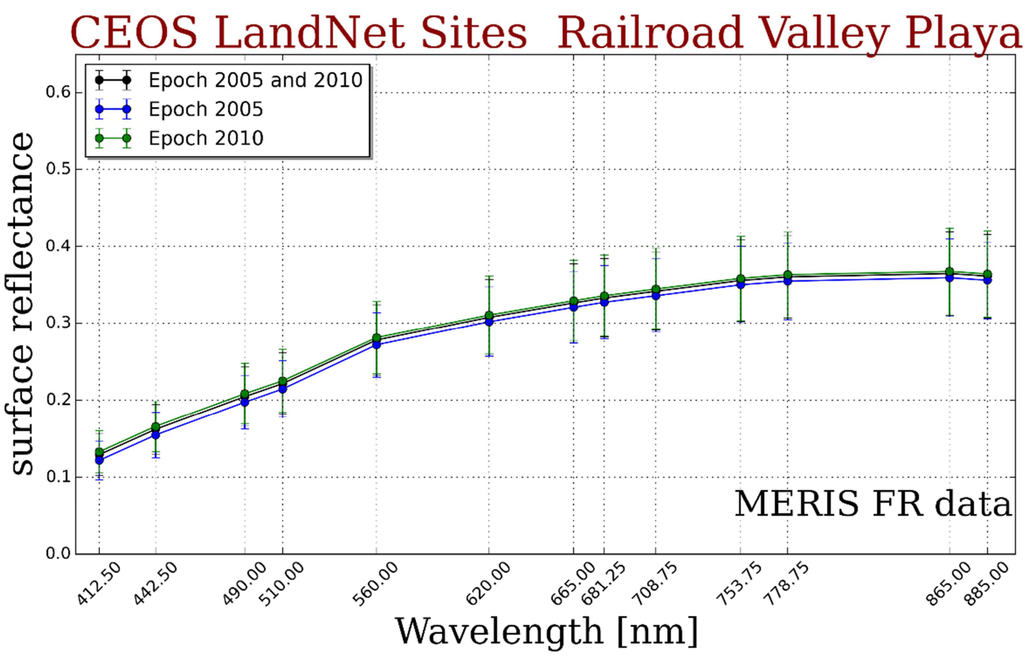

Figure 3-13: Spectra - CEOS-LANDNET SITES - Railroad Valley Playa - MERIS FR data

Table 3-3: Temporal mean and variance (σ^2) at the pixel level for the various spectral reflectance values - CEOS LandNet sites - MERIS FR time series and band1 to band7

	OBS. COUNTS CLEAR LAND		MERIS FR SR BAND 1	MERIS FR SR BAND 2	MERIS FR SR BAND 3	MERIS FR SR BAND 4	MERIS FR SR BAND 5	MERIS FR SR BAND 6	MERIS FR SR BAND 7
Dunhuang	356	mean	0.1239	0.1440	0.1651	0.1758	0.2067	0.2298	0.2367
		sigma	0.0202	0.0196	0.0191	0.0193	0.0204	0.0220	0.0225
		variance	0.0004	0.0004	0.0004	0.0004	0.0004	0.0005	0.0005
Frenchman Flat	20	mean	0.0905	0.1114	0.1386	0.1530	0.2058	0.2485	0.2640
		sigma	0.0353	0.0393	0.0453	0.0481	0.0568	0.0665	0.0715
		variance	0.0012	0.0015	0.0021	0.0023	0.0032	0.0044	0.0051
Ivanpah Playa	275	mean	0.0968	0.1261	0.1622	0.1827	0.2553	0.3235	0.3499
		sigma	0.0183	0.0211	0.0251	0.0272	0.0338	0.0397	0.0419
		variance	0.0003	0.0004	0.0006	0.0007	0.0011	0.0016	0.0018
La Crau	404	mean	0.0411	0.0542	0.0700	0.0776	0.1083	0.1262	0.1342
		sigma	0.0111	0.0107	0.0127	0.0134	0.0154	0.0246	0.0303
		variance	0.0001	0.0001	0.0002	0.0002	0.0002	0.0006	0.0009
Negev	407	mean	0.1299	0.1582	0.1939	0.2125	0.2849	0.3624	0.3936
		sigma	0.0150	0.0162	0.0184	0.0197	0.0249	0.0310	0.0331
		variance	0.0002	0.0003	0.0003	0.0004	0.0006	0.0010	0.0011
Railroad Valley Playa	141	mean	0.1293	0.1622	0.2048	0.2215	0.2779	0.3077	0.3265
		sigma	0.0271	0.0320	0.0380	0.0398	0.0454	0.0490	0.0508
		variance	0.0007	0.0010	0.0014	0.0016	0.0021	0.0024	0.0026

Table 3-4: Temporal mean and variance (σ^2) at the pixel level for the various spectral reflectance values - CEOS LandNet sites - MERIS FR time series and band8 to band14

	OBS. COUNTS CLEAR LAND		MERIS FR SR BAND 8	MERIS FR SR BAND 9	MERIS FR SR BAND 10	MERIS FR SR BAND 12	MERIS FR SR BAND 13	MERIS FR SR BAND 14
Dunhuang	356	mean	0.2378	0.2415	0.2462	0.248	0.2466	0.2449
		sigma	0.0226	0.0239	0.0233	0.0233	0.0235	0.0236
		variance	0.0005	0.0006	0.0005	0.0005	0.0006	0.0006
Frenchman Flat	20	mean	0.2668	0.2913	0.3107	0.3172	0.3307	0.331
		sigma	0.0737	0.0699	0.0748	0.076	0.0782	0.0777
		variance	0.0054	0.0049	0.0056	0.0058	0.0061	0.0060
Ivanpah Playa	275	mean	0.3574	0.3695	0.3905	0.3969	0.4024	0.4005
		sigma	0.0425	0.0434	0.0448	0.0452	0.0458	0.0456
		variance	0.0018	0.0019	0.0020	0.0020	0.0021	0.0021
La Crau	404	mean	0.1369	0.1727	0.2318	0.2399	0.2625	0.265
		sigma	0.0321	0.0209	0.0216	0.0223	0.024	0.0241
		variance	0.0010	0.0004	0.0005	0.0005	0.0006	0.0006
Negev	407	mean	0.4031	0.4134	0.4417	0.4483	0.4617	0.4608
		sigma	0.0338	0.0339	0.0362	0.0364	0.0366	0.0363
		variance	0.0011	0.0011	0.0013	0.0013	0.0013	0.0013
Railroad Valley Playa	141	mean	0.333	0.3417	0.3556	0.3603	0.3647	0.3614
		sigma	0.0512	0.0509	0.0533	0.0538	0.0546	0.0544
		variance	0.0026	0.0026	0.0028	0.0029	0.0030	0.0030

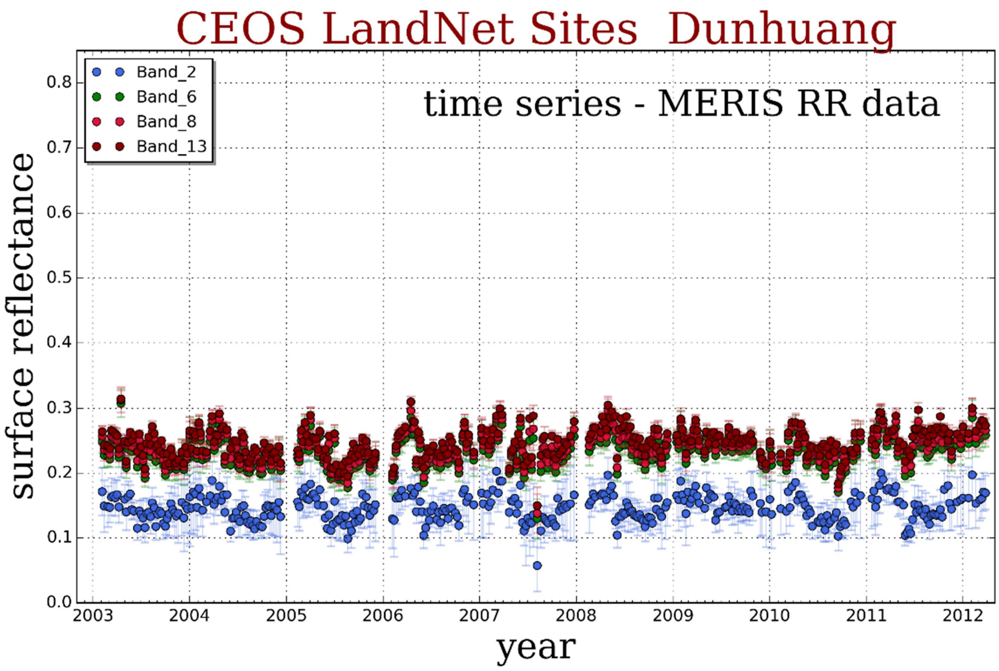

Figure 3-14: SR time series from MERIS RR data - 2003-2012 - CEOS-LANDNET SITES - Dunhuang

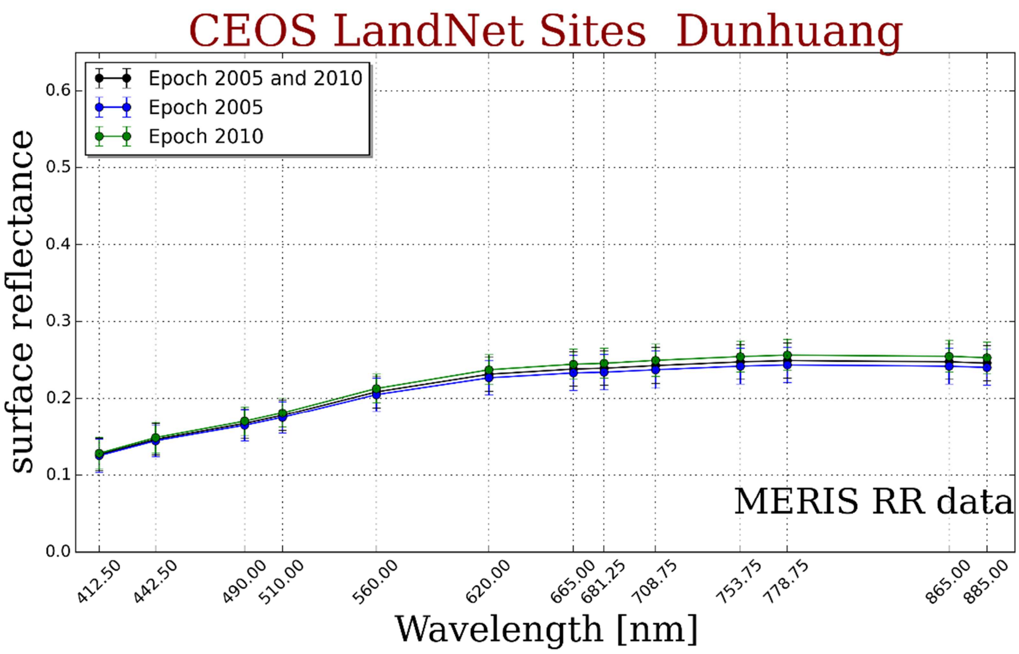

Figure 3-15: Spectra - CEOS-LANDNET SITES – Dunhuang - MERIS RR data

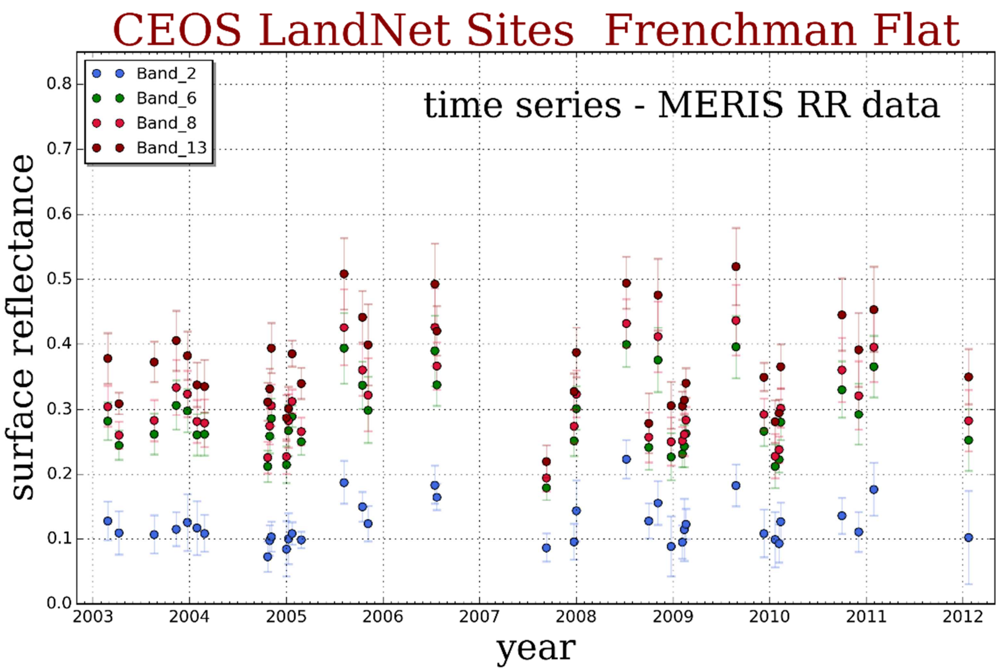

Figure 3-16: SR time series from MERIS RR data - 2003-2012 - CEOS-LANDNET SITES - Frenchman Flat

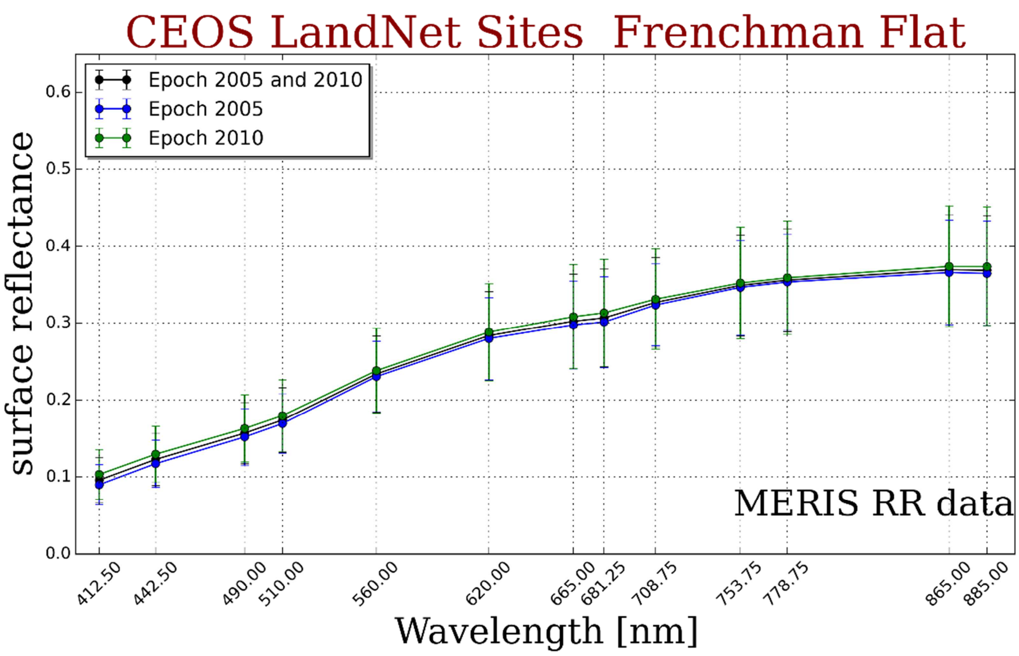

Figure 3-17: Spectra - CEOS-LANDNET SITES - Frenchman Flat - MERIS RR data

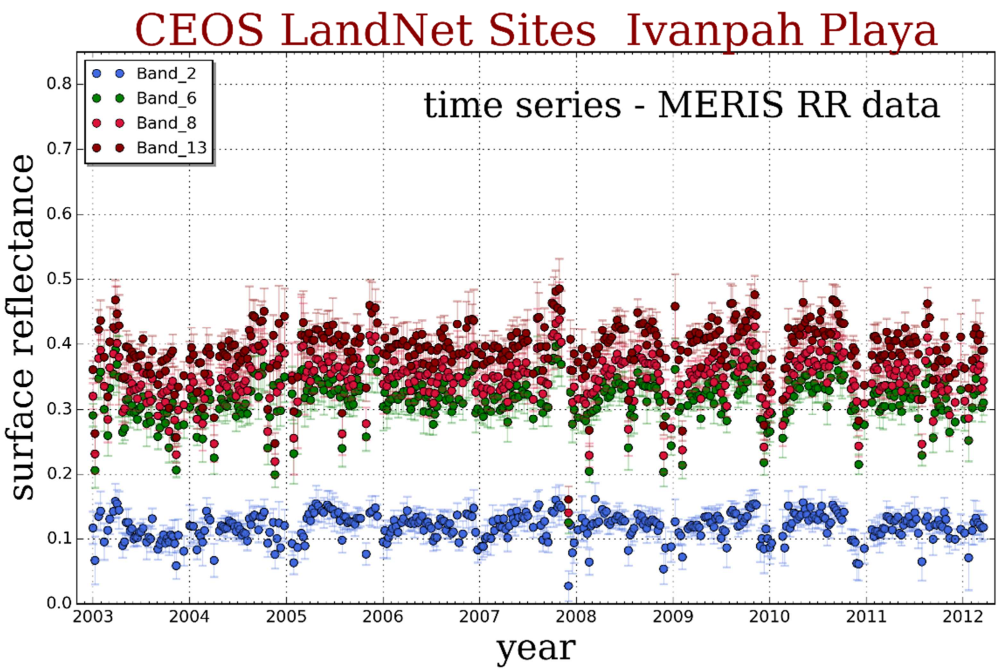

Figure 3-18: SR time series from MERIS RR data - 2003-2012 - CEOS-LANDNET SITES - Ivanpah Playa

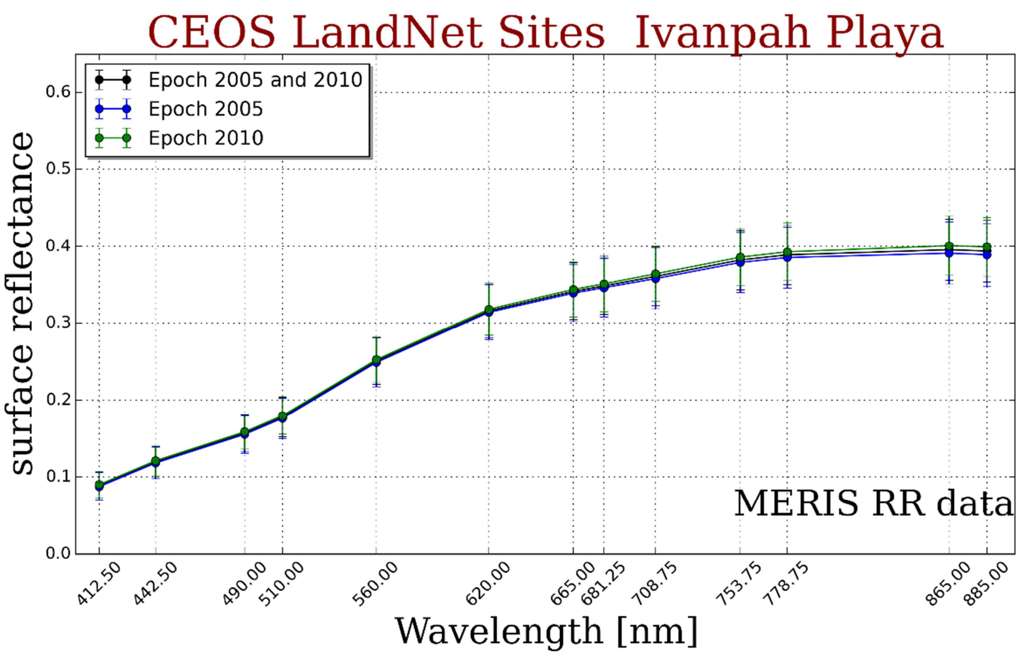

Figure 3-19: Spectra - CEOS-LANDNET SITES - Ivanpah Playa - MERIS RR data

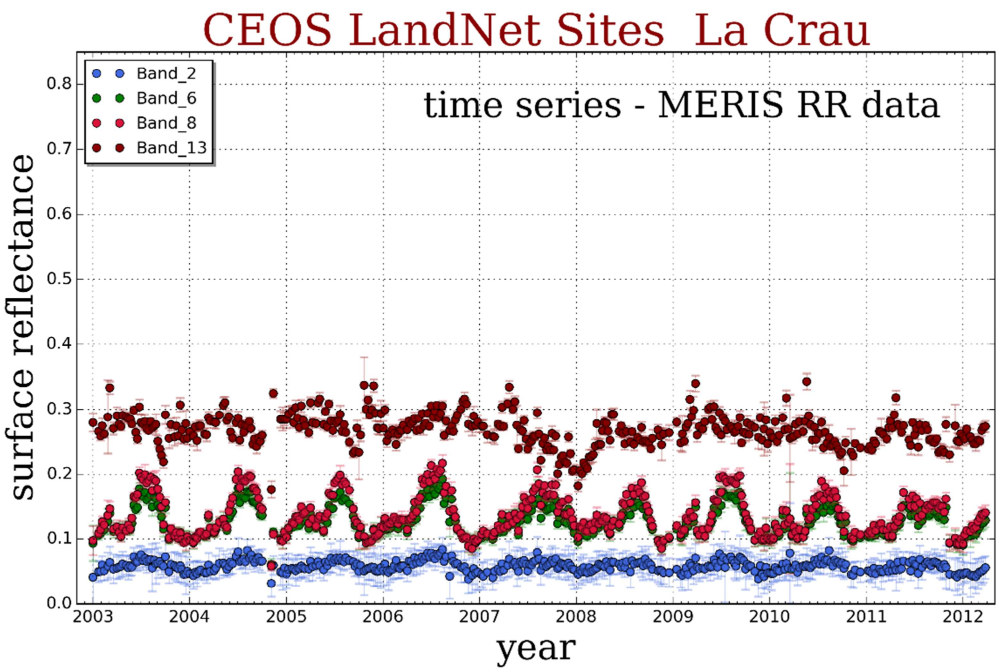

Figure 3-20: SR time series from MERIS RR data - 2003-2012 - CEOS-LANDNET SITES - La Crau

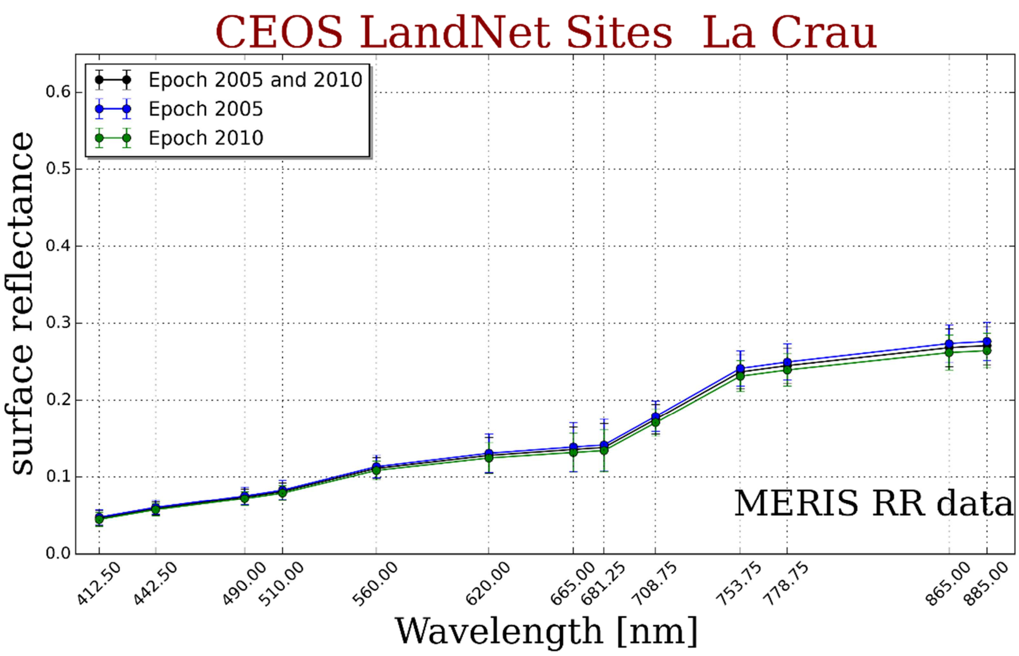

Figure 3-21: Spectra - CEOS-LANDNET SITES - La Crau - MERIS RR data

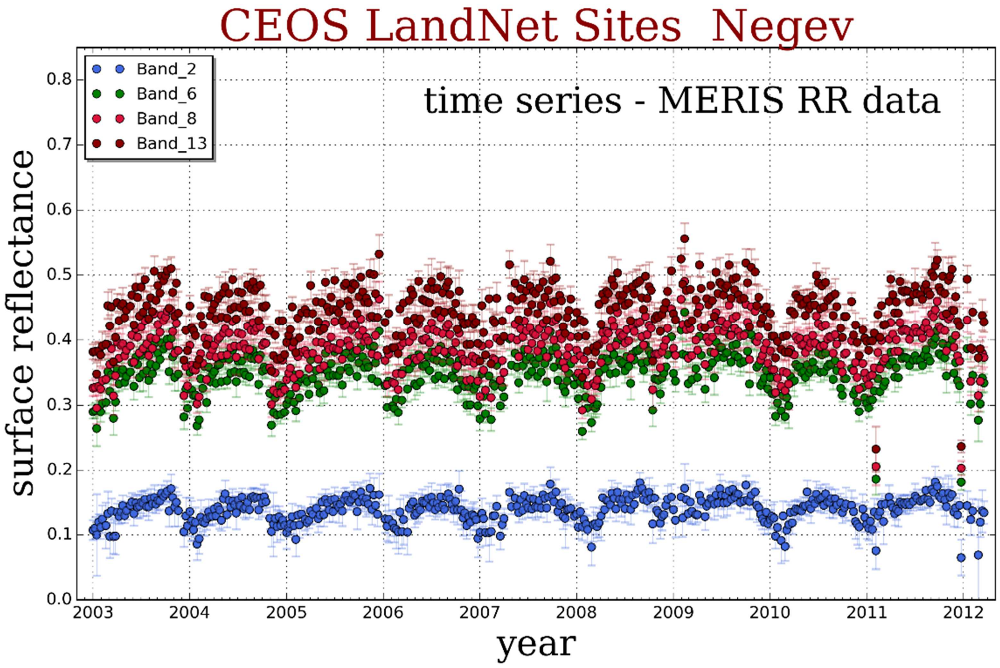

Figure 3-22: SR time series from MERIS RR data - 2003-2012 - CEOS-LANDNET SITES - Negev

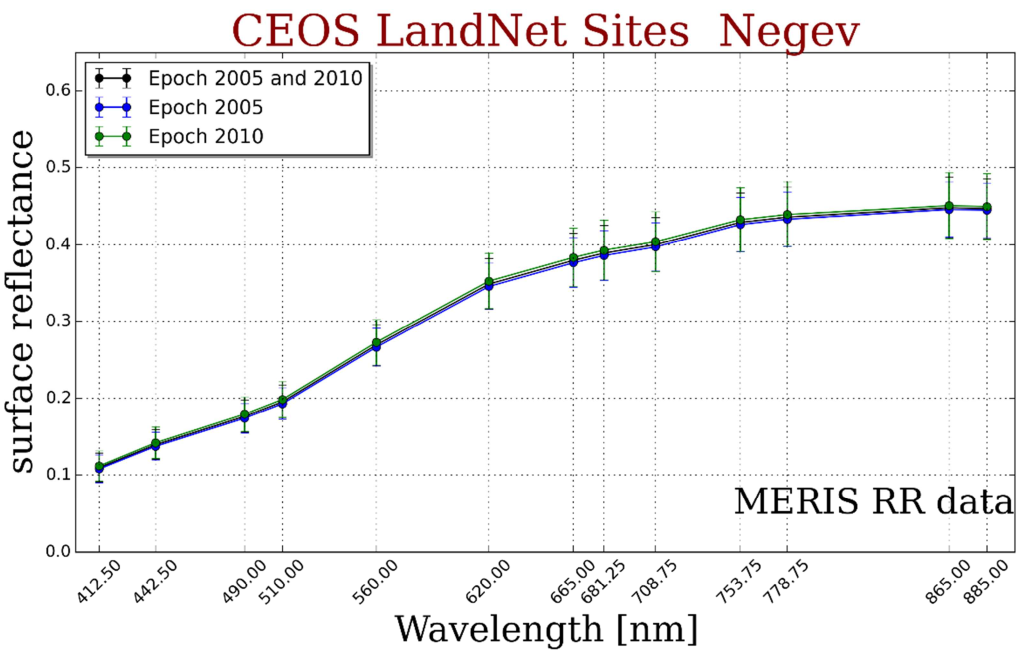

Figure 3-23: Spectra - CEOS-LANDNET SITES – Negev - MERIS RR data

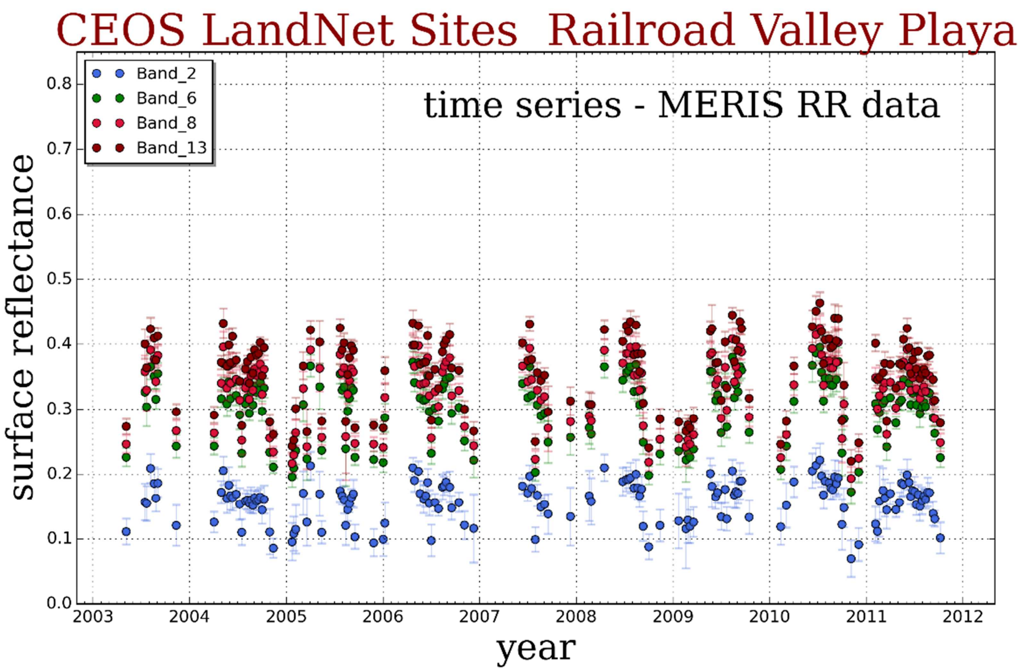

Figure 3-24: SR time series from MERIS RR data - 2003-2012 - CEOS-LANDNET SITES - Railroad Valley Playa

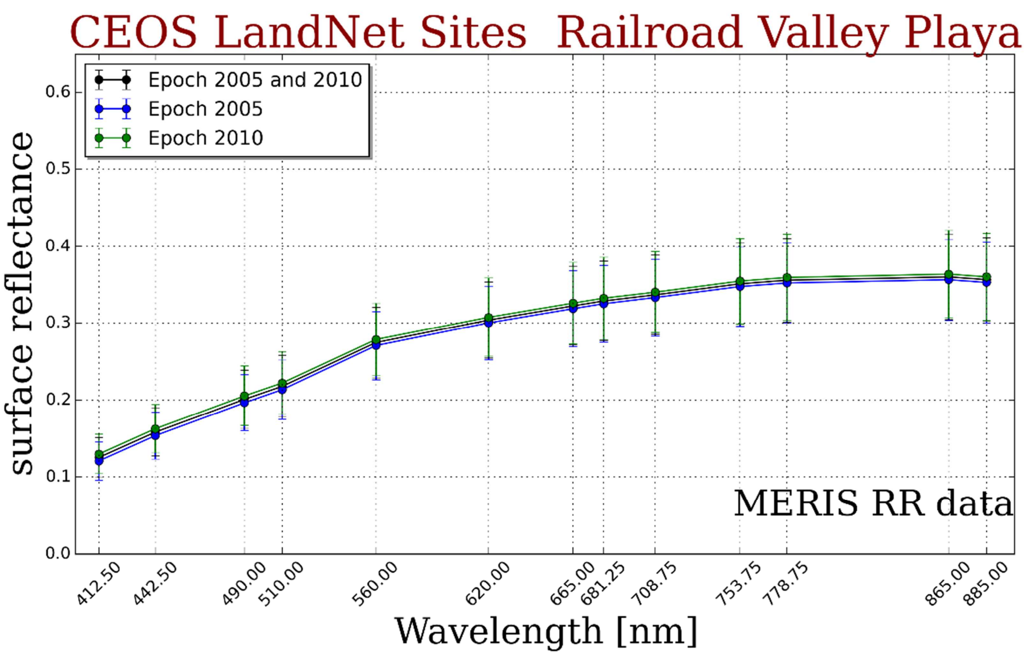

Figure 3-25: Spectra - CEOS-LANDNET SITES - Railroad Valley Playa - MERIS RR data

Table 3-5: Temporal mean and variance (σ^2) at the pixel level for the various spectral reflectance values - CEOS LandNet sites - MERIS RR time series and band1 to band7

	OBS. COUNTS CLEAR LAND		MERIS RR SR Band 1	MERIS RR SR Band 2	MERIS RR SR Band 3	MERIS RR SR Band 4	MERIS RR SR Band 5	MERIS RR SR Band 6	MERIS RR SR Band 7
Dunhuang	377	mean	0.1267	0.1466	0.1673	0.1779	0.2085	0.2314	0.2381
		sigma	0.0212	0.0204	0.0197	0.0198	0.0206	0.0217	0.0222
		variance	0.0004	0.0004	0.0004	0.0004	0.0004	0.0005	0.0005
Frenchman Flat	38	mean	0.096	0.1228	0.1571	0.1742	0.234	0.2837	0.3025
		sigma	0.0296	0.0336	0.0399	0.0422	0.0495	0.0573	0.0615
		variance	0.0009	0.0011	0.0016	0.0018	0.0025	0.0033	0.0038
Ivanpah Playa	390	mean	0.0887	0.1196	0.1571	0.178	0.2505	0.316	0.3414
		sigma	0.0174	0.0201	0.0236	0.0254	0.0302	0.0348	0.0367
		variance	0.0003	0.0004	0.0006	0.0006	0.0009	0.0012	0.0013
La Crau	406	mean	0.0462	0.0588	0.0738	0.0812	0.1112	0.1281	0.1358
		sigma	0.0092	0.0086	0.0106	0.0115	0.0137	0.0232	0.0292
		variance	0.0001	0.0001	0.0001	0.0001	0.0002	0.0005	0.0009
Negev	442	mean	0.1098	0.1396	0.1767	0.1955	0.2692	0.3487	0.3796
		sigma	0.0188	0.0193	0.021	0.022	0.0269	0.033	0.0351
		variance	0.0004	0.0004	0.0004	0.0005	0.0007	0.0011	0.0012
Railroad Valley Playa	160	mean	0.1255	0.1583	0.2011	0.2179	0.2747	0.304	0.3225
		sigma	0.0257	0.0312	0.0377	0.0397	0.0458	0.0495	0.0512
		variance	0.0007	0.0010	0.0014	0.0016	0.0021	0.0025	0.0026

Table 3-6: Temporal mean and variance (σ^2) at the pixel level for the various spectral reflectance values - CEOS LandNet sites - MERIS RR time series and band8 to band14

	OBS. COUNTS CLEAR LAND		MERIS RR SR BAND 8	MERIS RR SR BAND 9	MERIS RR SR BAND 10	MERIS RR SR BAND 12	MERIS RR SR BAND 13	MERIS RR SR BAND 14
Dunhuang	377	mean	0.2391	0.2426	0.2473	0.249	0.2474	0.2457
		sigma	0.0222	0.0233	0.0226	0.0226	0.0227	0.0227
		variance	0.0005	0.0005	0.0005	0.0005	0.0005	0.0005
Frenchman Flat	38	mean	0.3067	0.3271	0.3491	0.3559	0.3695	0.3688
		sigma	0.0635	0.0581	0.066	0.0672	0.0718	0.0715
		variance	0.0040	0.0034	0.0044	0.0045	0.0052	0.0051
Ivanpah Playa	390	mean	0.3485	0.3609	0.3821	0.3888	0.3955	0.3937
		sigma	0.0373	0.0379	0.0386	0.0389	0.0398	0.0399
		variance	0.0014	0.0014	0.0015	0.0015	0.0016	0.0016
La Crau	406	mean	0.1383	0.1752	0.2366	0.2447	0.2679	0.2705
		sigma	0.0311	0.0193	0.022	0.0227	0.0244	0.0246
		variance	0.0010	0.0004	0.0005	0.0005	0.0006	0.0006
Negev	442	mean	0.389	0.4002	0.429	0.4358	0.448	0.447
		sigma	0.0358	0.0352	0.0383	0.0386	0.0391	0.0386
		variance	0.0013	0.0012	0.0015	0.0015	0.0015	0.0015
Railroad Valley Playa	160	mean	0.3289	0.3369	0.3512	0.3559	0.3602	0.3566
		sigma	0.0517	0.0514	0.0538	0.0543	0.0552	0.0548
		variance	0.0027	0.0026	0.0029	0.0029	0.0030	0.0030

a) valid pixel expression: pixel status - clear land

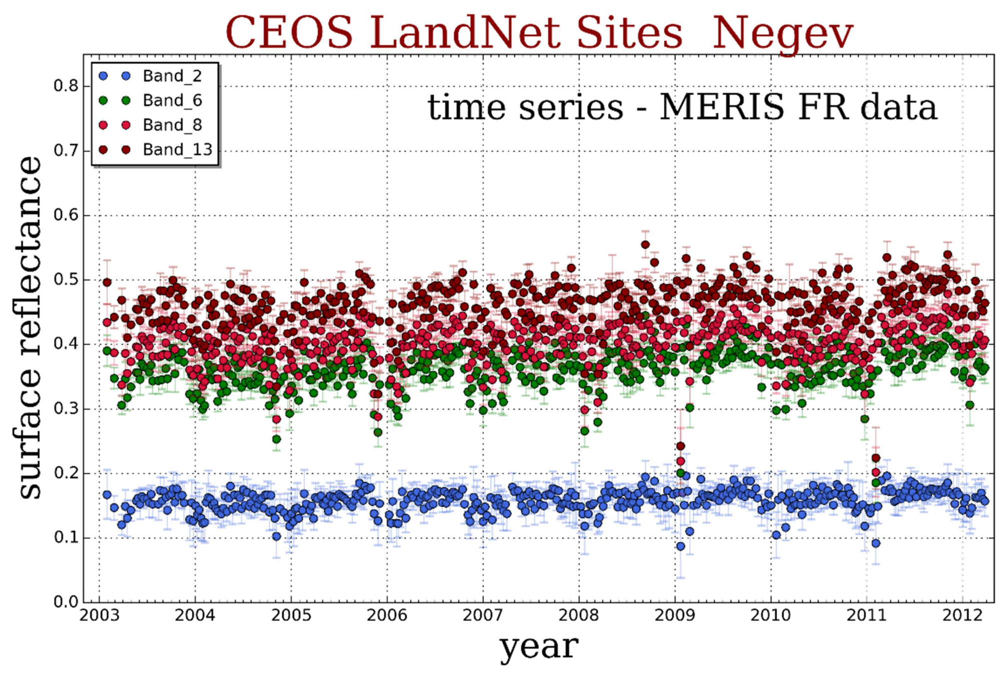

b) valid pixel expression: pixel status - clear land and clear_land_count >2

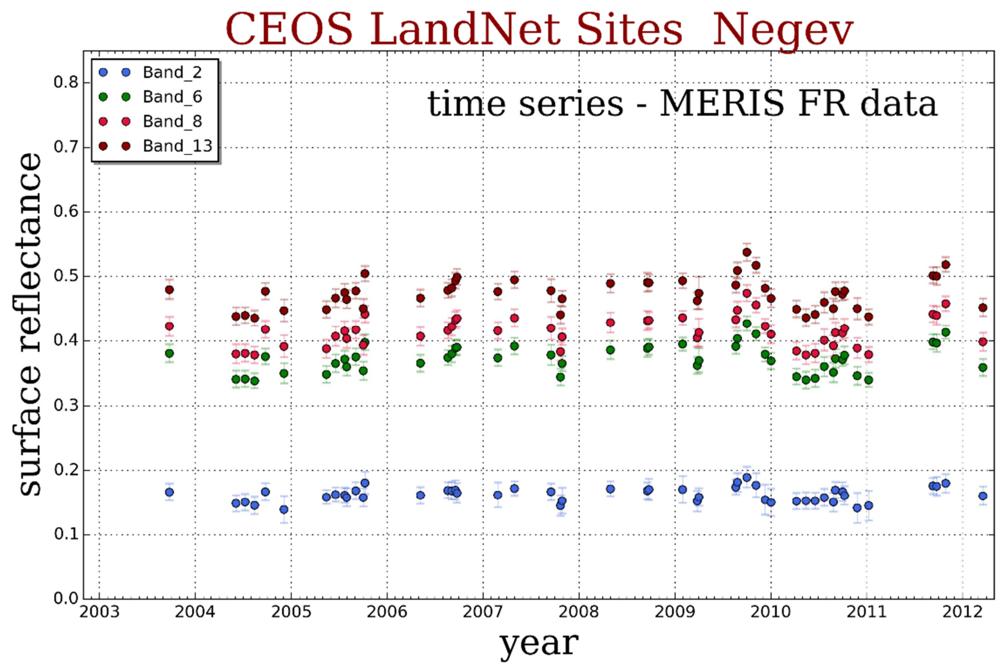

Figure 3-26: SR time series from MERIS FR data - 2003-2012 - CEOS-LANDNET SITES - Negev a) valid pixel expression: pixel status - clear land b) valid pixel expression: pixel status - clear land and clear_land_count >2

3.2.2 PROBA-V

The following table (Table 3-7) shows the relation between the number of the valid observations taken by the sensor and the number of observations taking into account the specific surface condition.

Table 3-7: Number of valid observations of the sensor and w.r.t. observation conditions for PROBA-V for 2014 - 2016 over the CEOS LandNet sites and reference points

	PIN NUMBER	LCCS CLASS	OBS. COUNTS	CLEAR LAND OBS. COUNTS
Dunhuang	1	130	91	6
Frenchman Flat	2	200	91	1
Ivanpah Playa	3	120	91	77
La Crau	4	130	90	87
Negev	5	200	91	76
Railroad Valley Playa	6	200	91	1
Yungas Coroico	1	50	93	66
Gran Sabana	2	50	92	22
Atacama Desert	3	200	93	48
Amazon	4	50	91	26
White Mountain National Forest	5	61	91	55
Sheyenne National Grassland	6	130	93	72
Great Bear Rainforest	7	70	91	11
National Park Peneda Geres	8	90	88	51
National Park Horto Bagy	9	130	93	67
Kalevalsky Bor National Park	10	70	72	7
Mackenzie Country - New Zealand	11	130	92	77
Great Basalt Wall National Park	12	62	93	81
Great Sandy Dessert	13	150	93	90
Coen Tropical	14	50	89	61
Tundra - Tajmyr	15	150	44	9
Boreal Forest - Wladiwostok	16	90	87	48
Tumba Lediima - Kongo	17	50	93	20
Timbuktu - Sahara	18	200	93	91
New Valley - Sahara	19	200	93	93
Mikumi National Park	20	10	90	41

The following figures (Figure 3-27 through Figure 3-38) show SR time series of PROBA-V data (2015-2016) over the CEOS-LANDNET SITES as well as the mean spectra. The Table 3-8 shows the corresponding mean and variance values.

The analysis of different 2-year temporal profiles leads to three main conclusions which can be summarized as follows again:

- the number of pixels which contribute to the analysis of the time series is very variable whereas this can be caused by the data availability or by the cloud coverage or by commission errors in the pixel identification;
- the impact of undetected clouds and cloud shadows is visible (see discussion below related to Figure 3-39) in the time series and influences the statistical parameter estimate;
- the standard deviation values reach an order of magnitude from 2.0 % through 86 % (mean 18%).

Figure 3-39 shows two time series of the 7 day SR composites from the LC-CCI project for the CEOS LANDNET sites Ivanpah Playa. As explained before, the only difference between these two time series is the way the valid pixels are identified again. The first figure represents the time series if all cloud-free observations are used; the second one takes pixels only into account were cloud-free observations are higher than 2. This second situation allows eliminating some fluctuations due to BRDF, but significantly lowers the number of available pixels. The variation of the values may be caused by undetected clouds or cloud shadows which strongly influence the retrieved 7-day SR composites values.

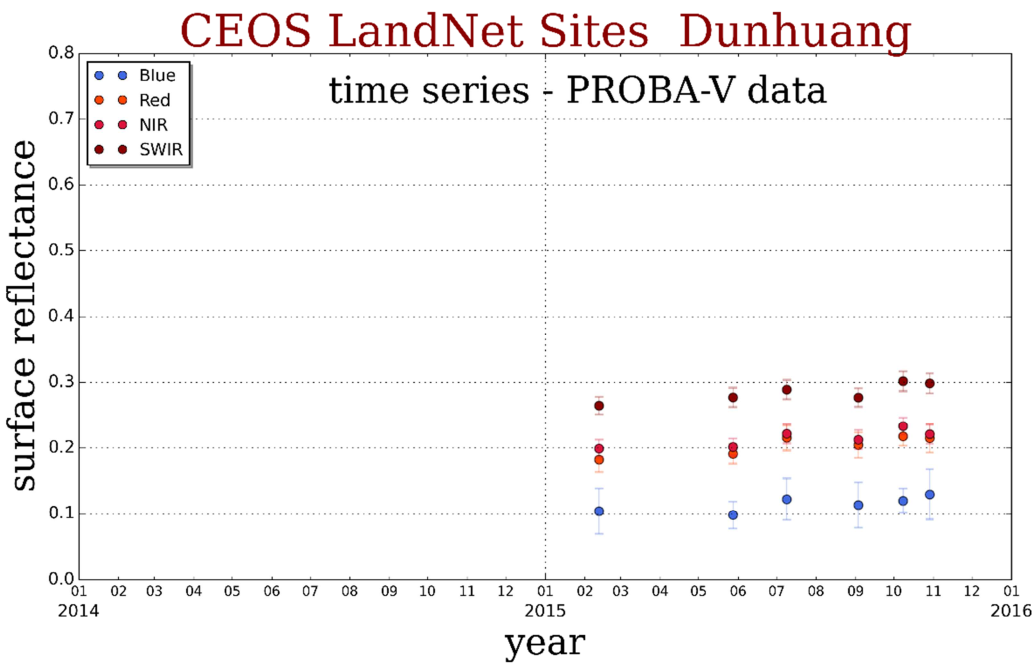

Figure 3-27: SR time series from PROBA-V data - 2014-2015 - CEOS-LANDNET SITES – Dunhuang

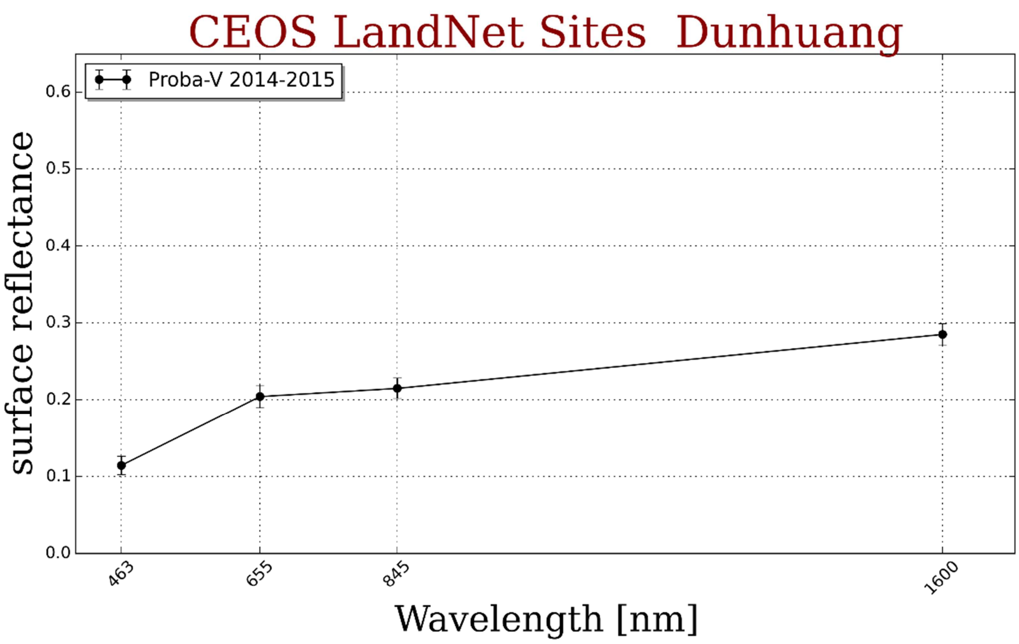

Figure 3-28: Spectra - CEOS-LANDNET SITES – Dunhuang – PROBA-V data

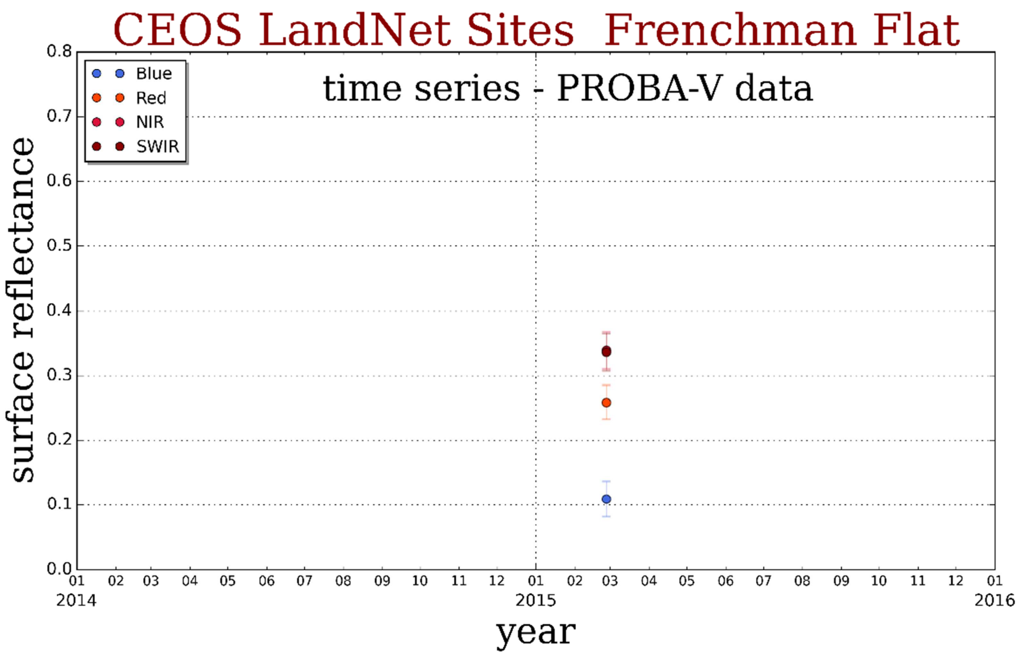

Figure 3-29: SR time series from PROBA-V data - 2014-2015 - CEOS-LANDNET SITES - Frenchman Flat

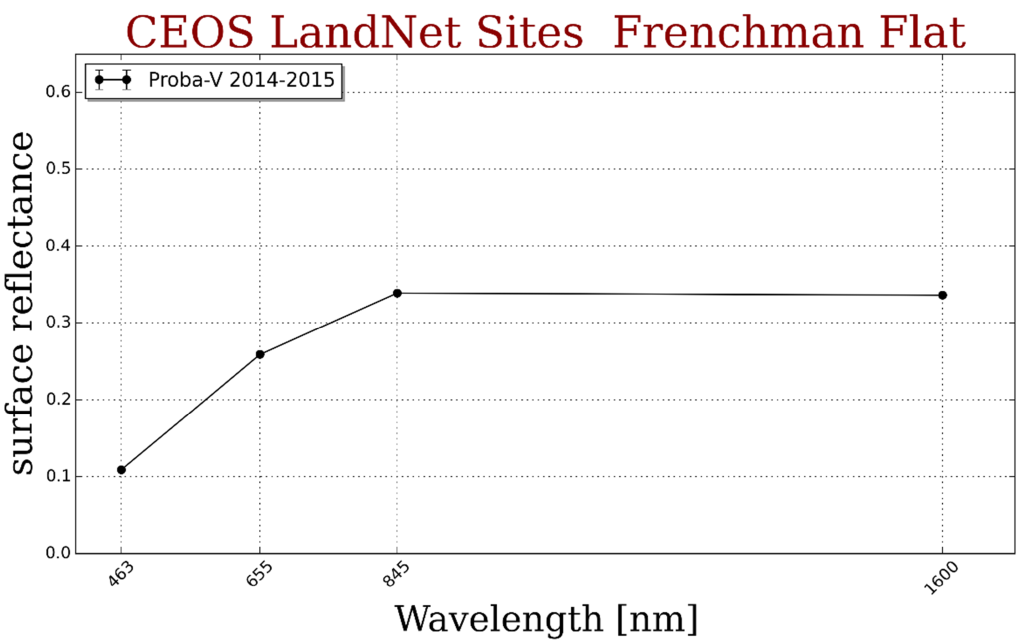

Figure 3-30: Spectra - CEOS-LANDNET SITES - Frenchman Flat – PROBA-V data

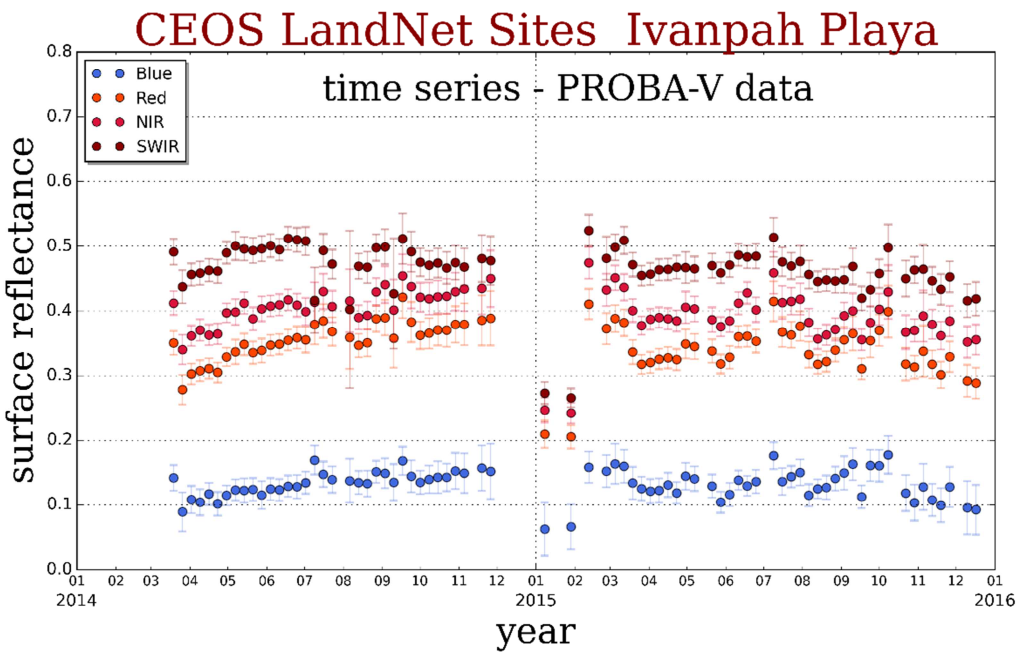

Figure 3-31: SR time series from PROBA-V data - 2014-2015 - CEOS-LANDNET SITES - Ivanpah Playa

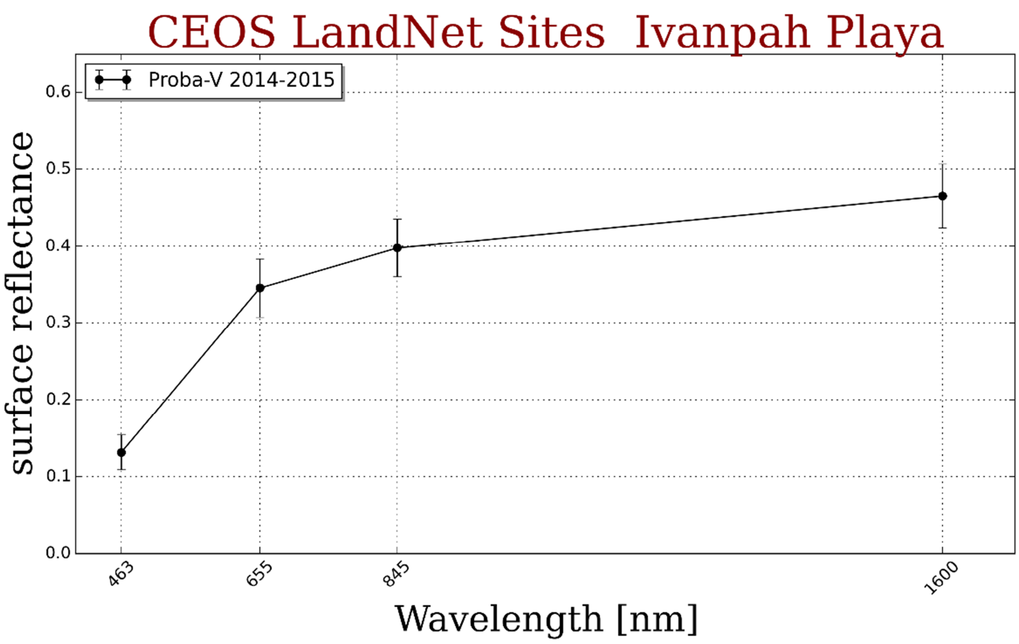

Figure 3-32: Spectra - CEOS-LANDNET SITES - Ivanpah Playa – PROBA-V data

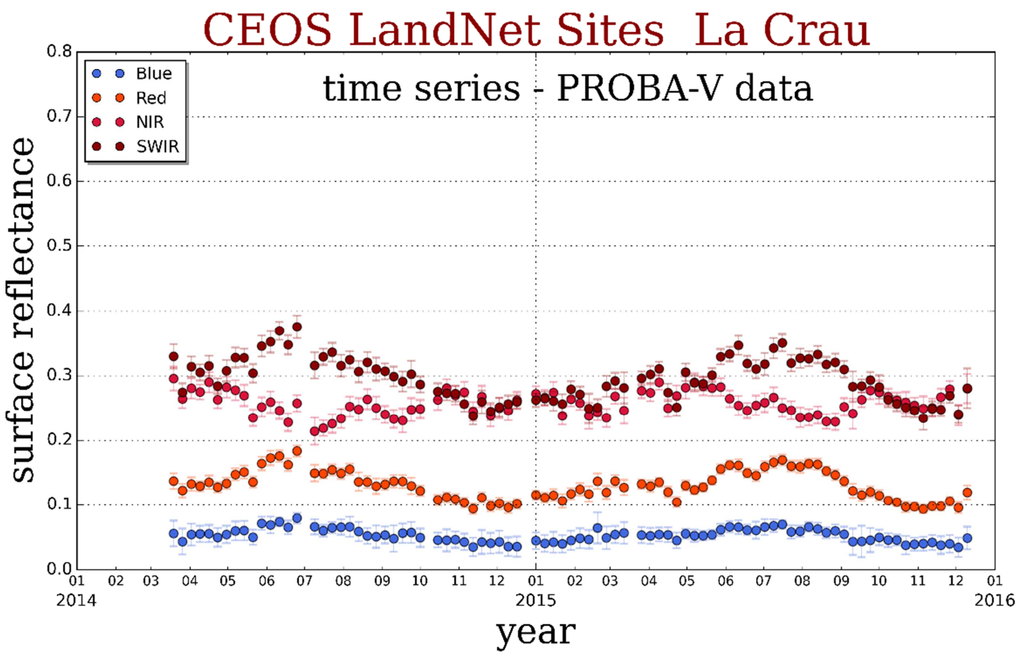

Figure 3-33: SR time series from PROBA-V data - 2014-2015 - CEOS-LANDNET SITES - La Crau

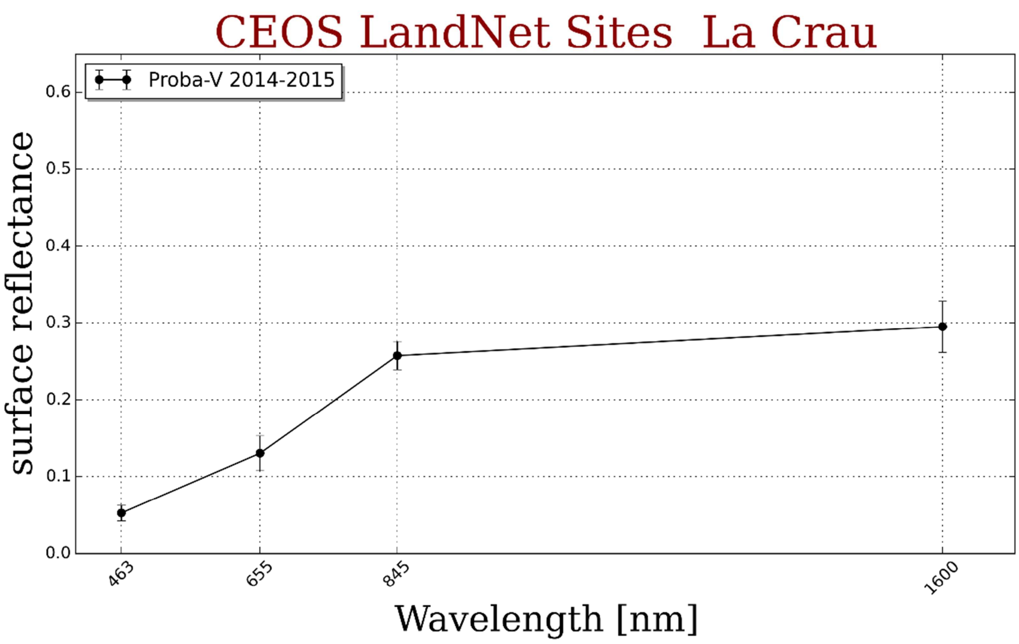

Figure 3-34: Spectra - CEOS-LANDNET SITES - La Crau – PROBA-V data

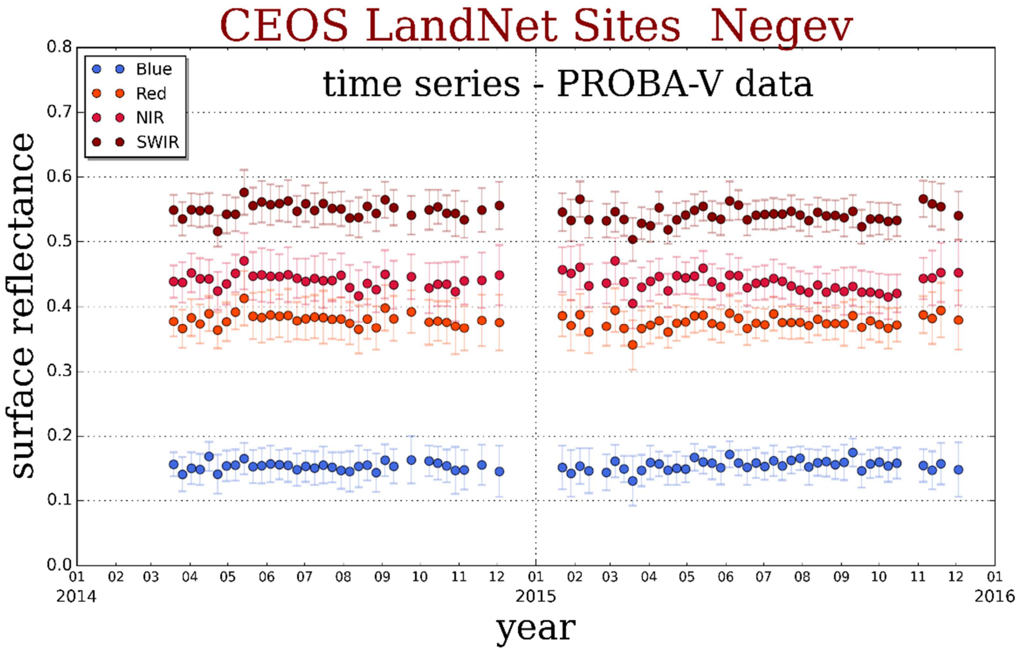

Figure 3-35: SR time series from PROBA-V data - 2014-2015 - 2003-2012 - CEOS-LANDNET SITES - Negev

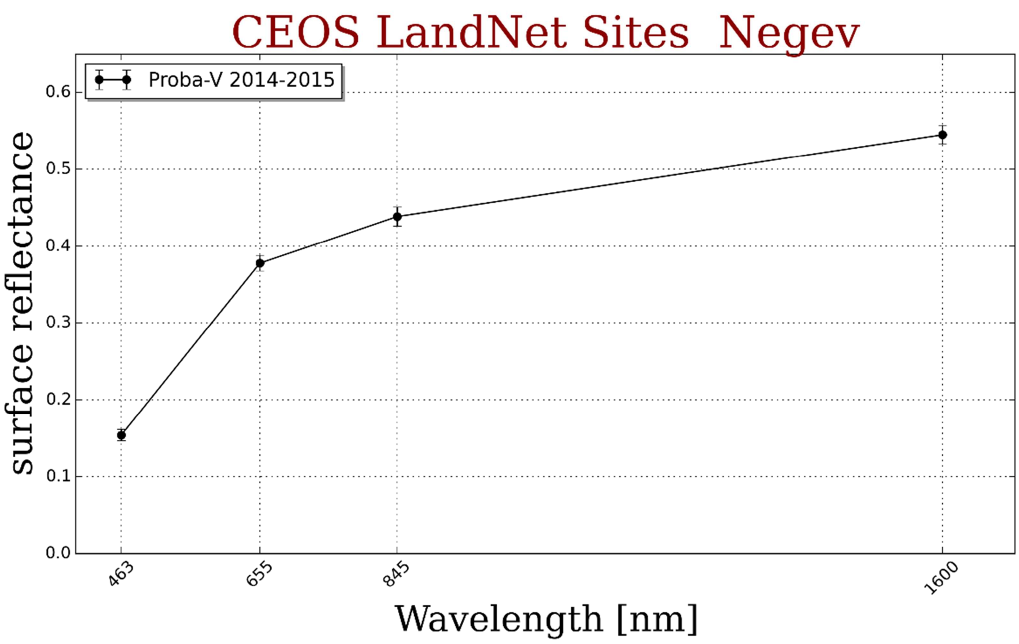

Figure 3-36: Spectra - CEOS-LANDNET SITES – Negev – PROBA-V data

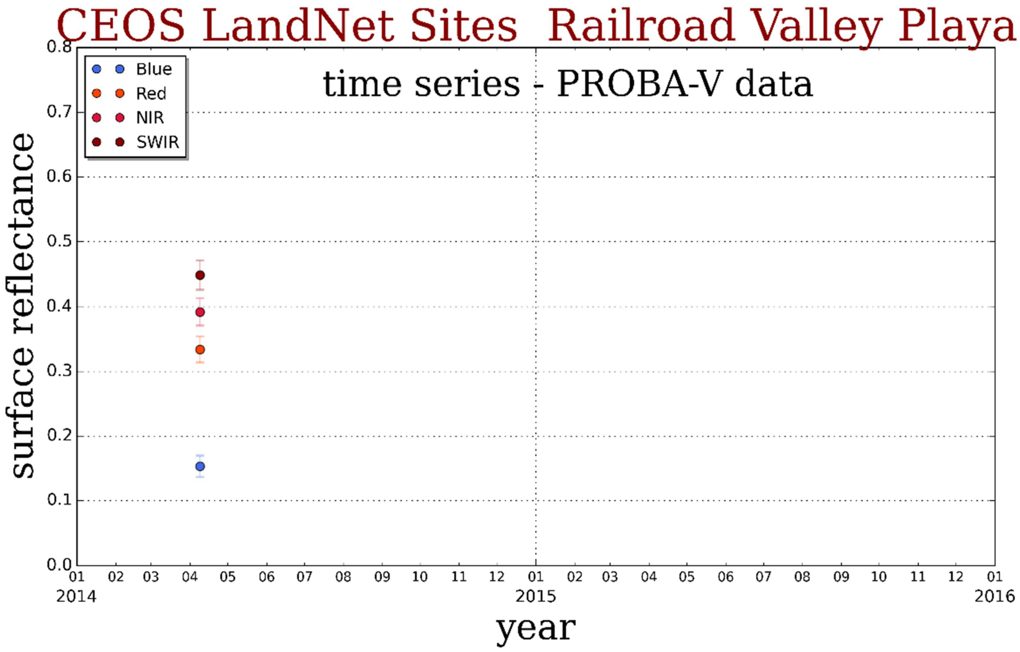

Figure 3-37: SR time series from PROBA-V data - 2014-2015 - CEOS-LANDNET SITES - Railroad Valley Playa

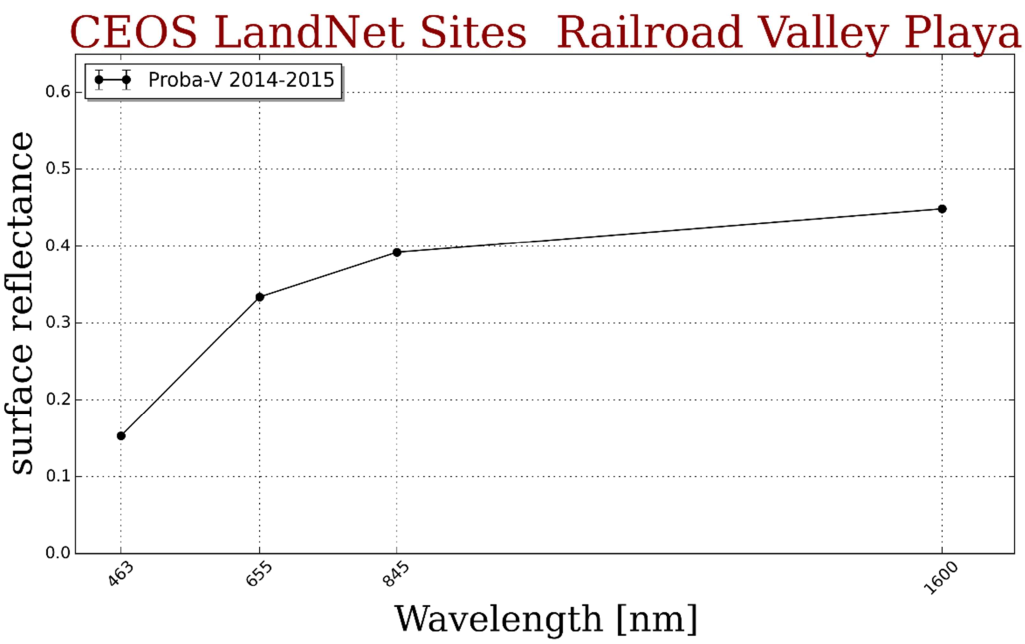

Figure 3-38: Spectra - CEOS-LANDNET SITES - Railroad Valley Playa – PROBA-V data

Table 3-8: Temporal mean and variance (σ^2) at the pixel level for the various spectral reflectance values - CEOS LandNet sites - PROBA-V time series and band1 to band4

	OBS. COUNTS CLEAR LAND		PROBA-V SR Band 1	PROBA-V SR Band 2	PROBA-V SR Band 3	PROBA-V SR Band 4
Dunhuang	6	mean	0.1145	0.2042	0.2148	0.2845
		sigma	0.0119	0.0146	0.0131	0.0143
		variance	0.0001	0.0002	0.0002	0.0002
Frenchman Flat	1	mean	0.1089	0.2589	0.3388	0.3361
		sigma	-	-	-	-
		variance	-	-	-	-
Ivanpah Playa	77	mean	0.1315	0.3454	0.3975	0.4651
		sigma	0.0227	0.0378	0.0375	0.0411
		variance	0.0005	0.0014	0.0014	0.0017
La Crau	87	mean	0.0525	0.1304	0.2573	0.2949
		sigma	0.0101	0.0226	0.0183	0.0333
		variance	0.0001	0.0005	0.0003	0.0011
Negev	76	mean	0.1541	0.3778	0.4386	0.5448
		sigma	0.0074	0.0103	0.0123	0.0124
		variance	0.0001	0.0001	0.0002	0.0002
Railroad Valley Playa	1	mean	0.1533	0.3339	0.3920	0.4486
		sigma	-	-	-	-
		variance	-	-	-	-

a) valid pixel expression: pixel status - clear land

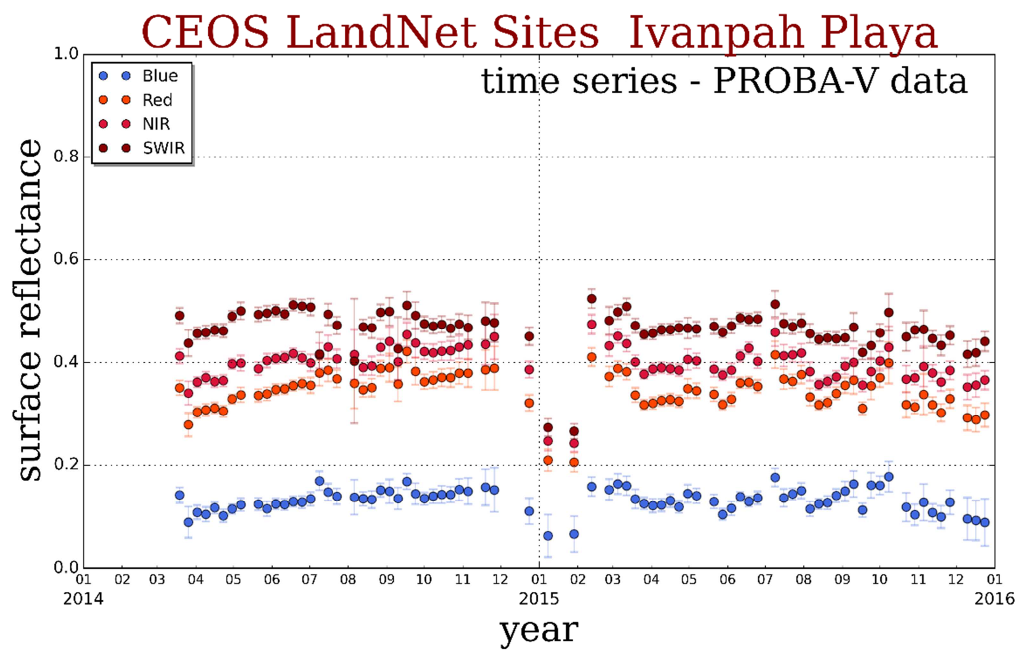

b) valid pixel expression: pixel status - clear land and clear_land_count >2

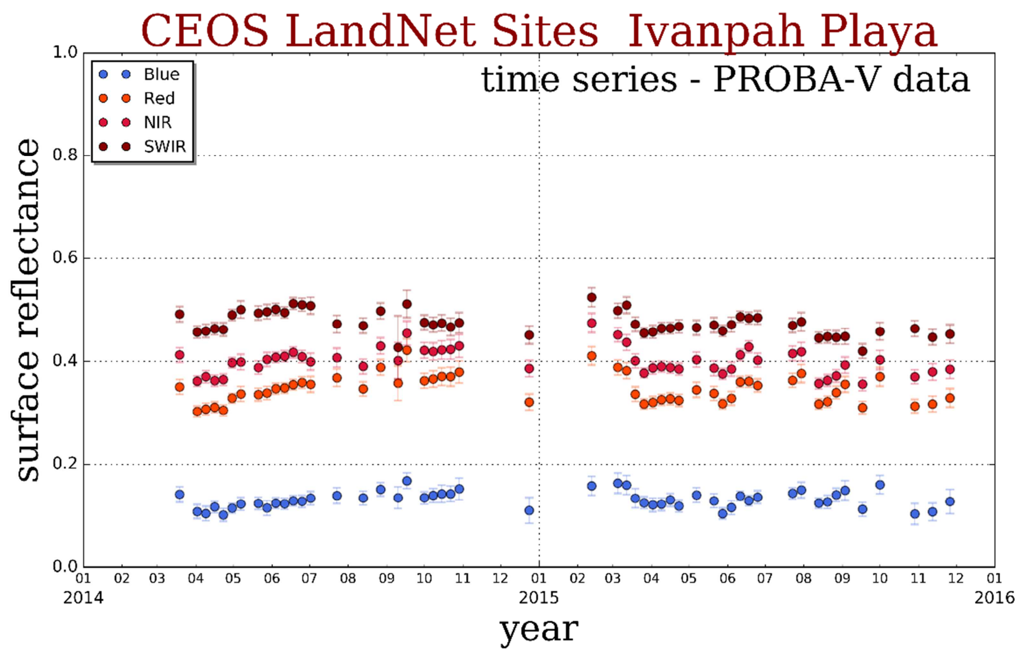

Figure 3-39: SR time series from PROBA-V data - 2014-2015 - CEOS-LANDNET SITES – Ivanpah Playa a) valid pixel expression: pixel status - clear land b) valid pixel expression: pixel status - clear land and clear_land_count >2

3.2.3 AVHHR

The following table (Table 3-9) shows the relation between the number of the valid observations taken by the sensor and the number of observations taking into account the specific surface condition.

Table 3-9: Number of valid observations of the sensor and w.r.t. observation conditions for AVHRR for 1992 - 1999 over the CEOS LandNet sites and reference points

	PIN NUMBER	LCCS CLASS	OBS. COUNTS	CLEAR LAND OBS. COUNTS
Dunhuang	1	130	273	182
Frenchman Flat	2	200	279	112
Ivanpah Playa	3	120	282	149
La Crau	4	130	279	178
Negev	5	200	298	260
Railroad Valley Playa	6	200	286	137
Yungas Coroico	1	50	292	87
Gran Sabana	2	50	223	20
Atacama Desert	3	200	272	246
Amazon	4	50	237	65
White Mountain National Forest	5	61	271	88
Sheyenne National Grassland	6	130	259	104
Great Bear Rainforest	7	70	243	36
National Park Peneda Geres	8	90	276	119
National Park Horto Bagy	9	130	255	103
Kalevalsky Bor National Park	10	70	202	82
Mackenzie Country - New Zealand	11	130	189	98
Great Basalt Wall National Park	12	62	287	147
Great Sandy Dessert	13	150	276	219
Coen Tropical	14	50	280	143
Tundra - Tajmyr	15	150	114	8
Boreal Forest - Wladiwostok	16	90	278	102
Tumba Lediima - Kongo	17	50	256	69
Timbuktu - Sahara	18	200	239	206
New Valley - Sahara	19	200	284	264
Mikumi National Park	20	10	288	81

The following figures (Figure 3-40 through Figure 3-45) show SR time series of AVHRR data (1992-1999) over the CEOS-LANDNET SITES. The Table 3-10 shows the corresponding mean and variance values.

The analysis of different 8-year temporal profiles highlights the level remaining noise in the SR 7-day composite again. This analysis leads to four main conclusions which can be summarized as follows:

- the number of pixels which contribute to the analysis of the time series is variable whereas this can be caused by the data availability or by the cloud coverage or by commission error of the pixel identification or by an incorrect identification of L1b product as erroneous due to the quality control;
- outlier can be caused by usage of climatology regarding the aerosol optical depth and of the coarse resolution data of other atmospheric condition values for the atmospheric correction
- the impact of the cloud screening, which is rather clear-sky conservative than cloud conservative is visible (see discussion below related to Figure 3-46) in the time series and influences the statistical parameter estimate;
- the standard deviation values reach an order of magnitude from 6.3% through 67 % (mean 26%).

Figure 3-46 shows two time series of the 7 day SR composites from the LC-CCI project for the CEOS LANDNET sites La Crau. As mentioned before, the only difference between these two time series is the way the valid pixels are identified. The first figure represents the time series if all cloud-free observations are used; the second one takes pixels only into account were cloud-free observations are higher than 2. This second situation significantly lowers the number of available pixels, which strongly influence the retrieved 7-day SR composites values. Furthermore, the resultant time series is often too sparse for the further analysis, e.g. the expected vegetation cycle is not observable for the CEOS LANDNET sites La Crau.

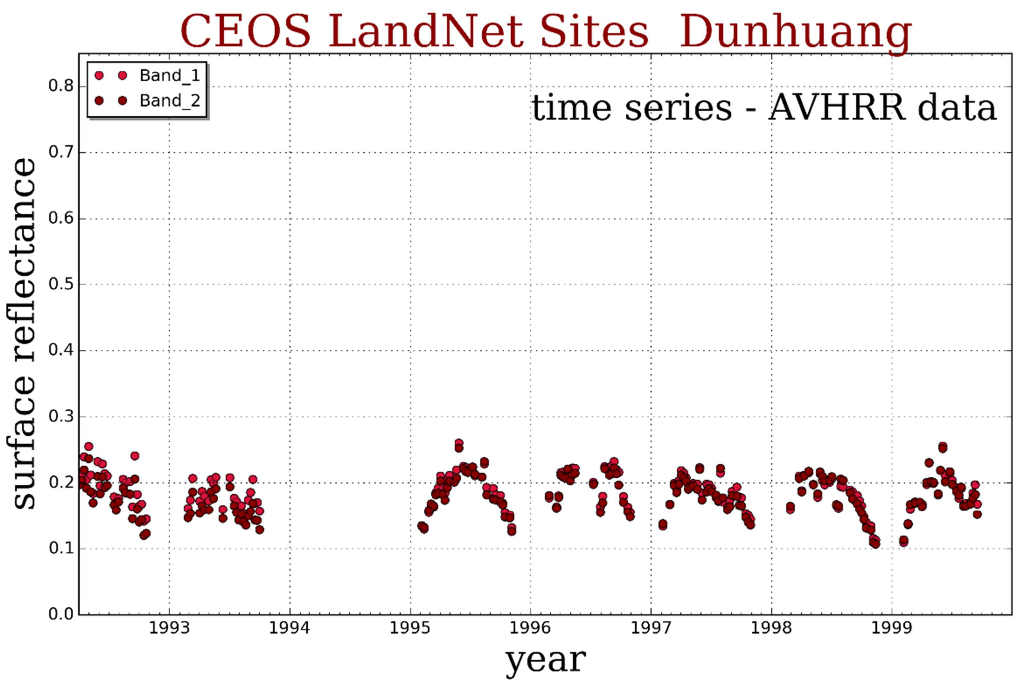

Figure 3-40: SR time series from AVHRR data - 1992-1999 - CEOS-LANDNET SITES – Dunhuang

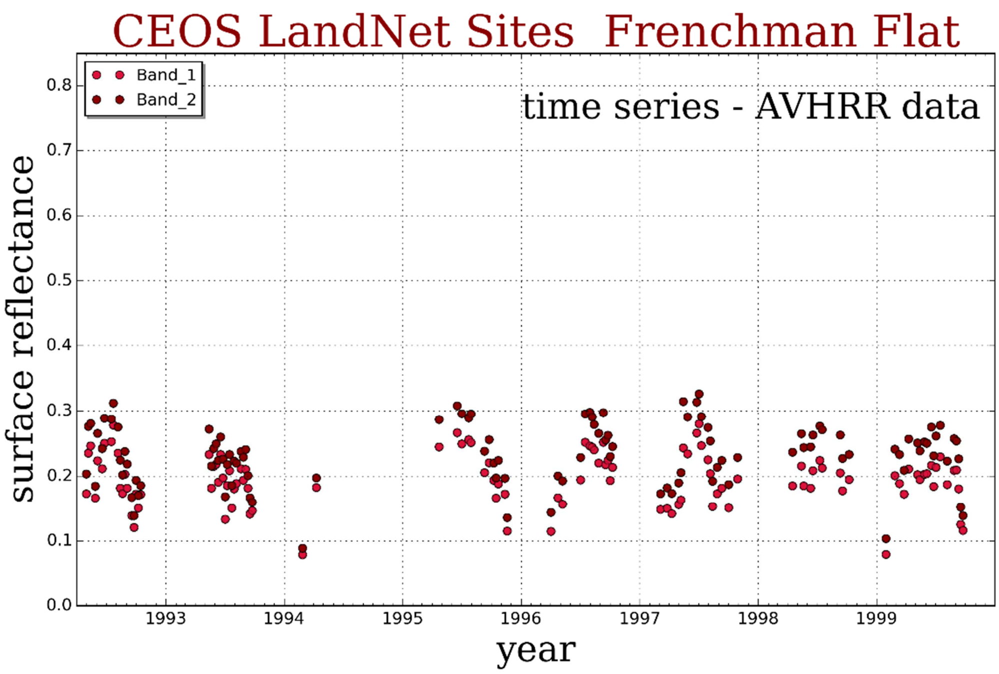

Figure 3-41: SR time series from AVHRR data - 1992-1999 - CEOS-LANDNET SITES - Frenchman Flat

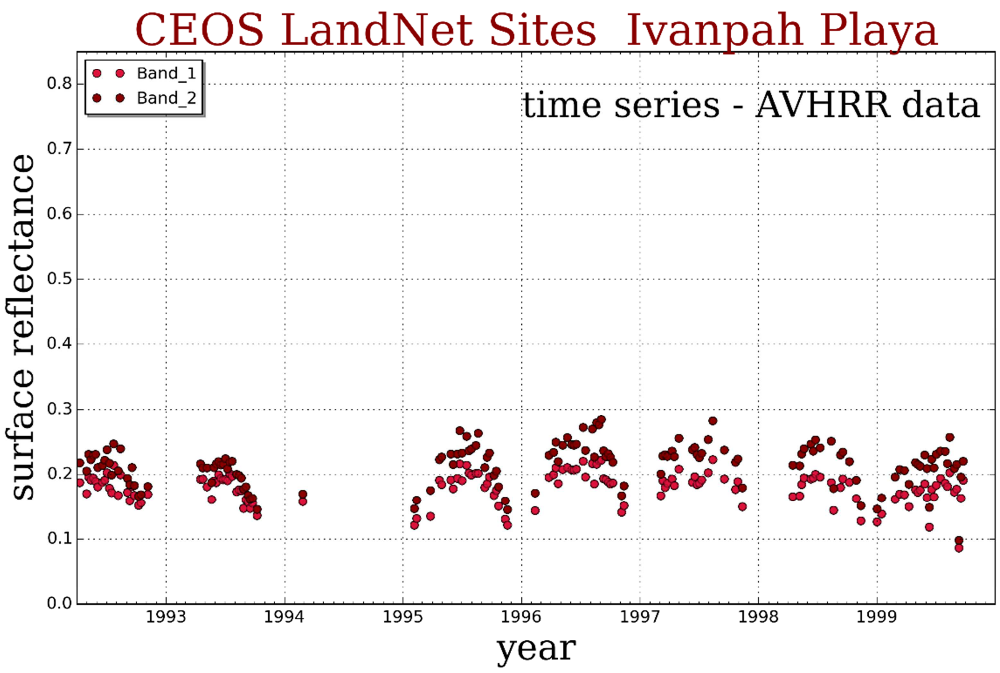

Figure 3-42: SR time series from AVHRR data - 1992-1999 - CEOS-LANDNET SITES - Ivanpah Playa

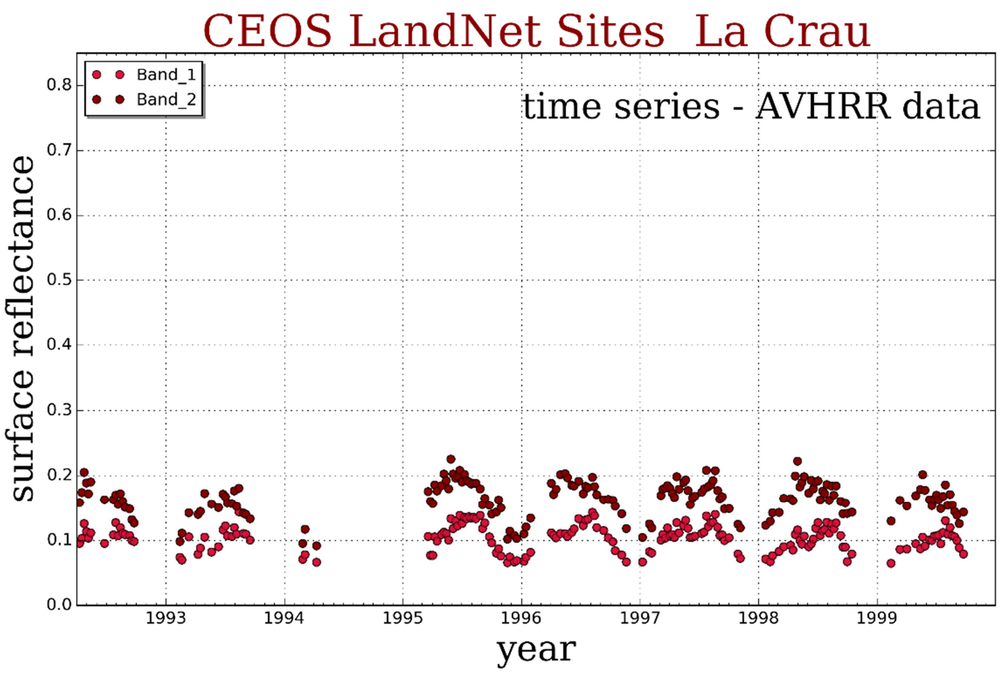

Figure 3-43: SR time series from AVHRR data - 1992-1999 - CEOS-LANDNET SITES - La Crau

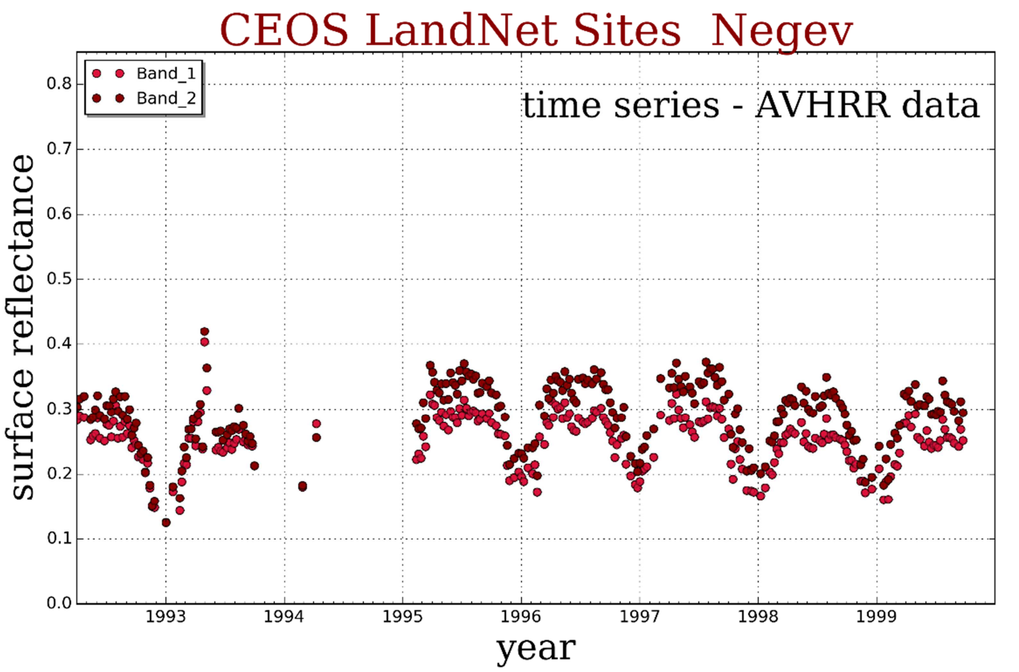

Figure 3-44: SR time series from AVHRR data - 1992-1999 - 2003-2012 - CEOS-LANDNET SITES - Negev

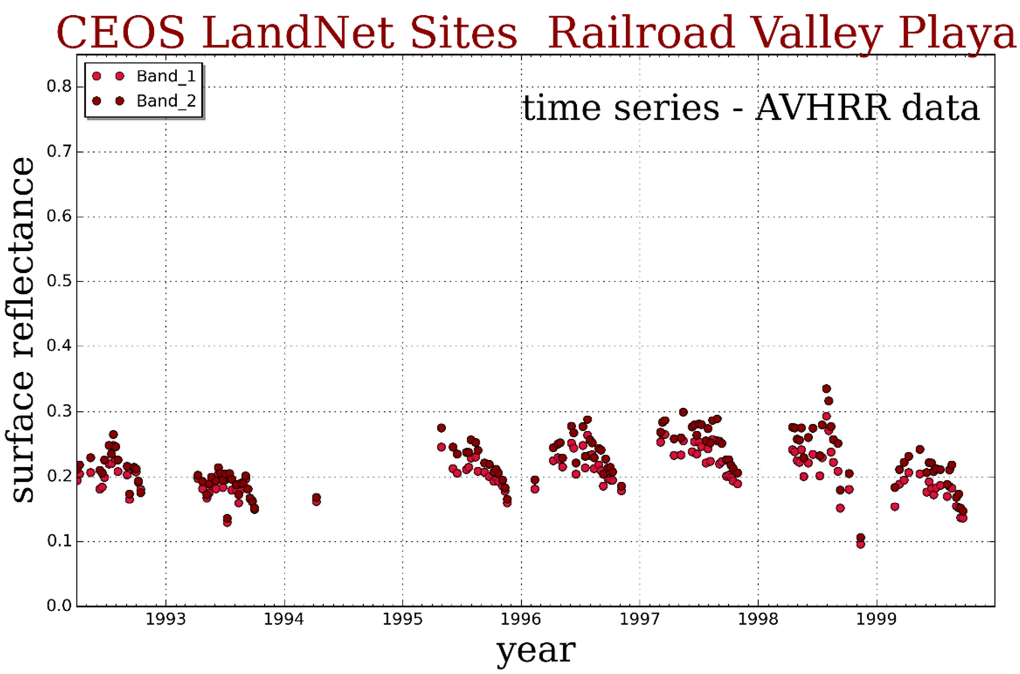

Figure 3-45: SR time series from AVHRR data - 1992-1999 - CEOS-LANDNET SITES - Railroad Valley Playa

Table 3-10: Temporal mean and variance (σ^2) at the pixel level for the various spectral reflectance values - CEOS LandNet sites - AVHRR time series and band1 and band2

	OBS. COUNTS CLEAR LAND		AVHRR SR Band 1	AVHRR SR Band 2
Dunhuang	182	mean	0.1881	0.1803
		sigma	0.0278	0.0286
		variance	0.0008	0.0008
Frenchman Flat	112	mean	0.1958	0.2334
		sigma	0.0402	0.0470
		variance	0.0016	0.0022
Ivanpah Playa	149	mean	0.1800	0.2155
		sigma	0.0237	0.0317
		variance	0.0006	0.0010
La Crau	178	mean	0.1048	0.1649
		sigma	0.0194	0.0265
		variance	0.0004	0.0007
Negev	260	mean	0.2525	0.2930
		sigma	0.0404	0.0496
		variance	0.0016	0.0025
Railroad Valley Playa	137	mean	0.2045	0.2257
		sigma	0.0320	0.0391
		variance	0.0010	0.0015

a) valid pixel expression: pixel status - clear land

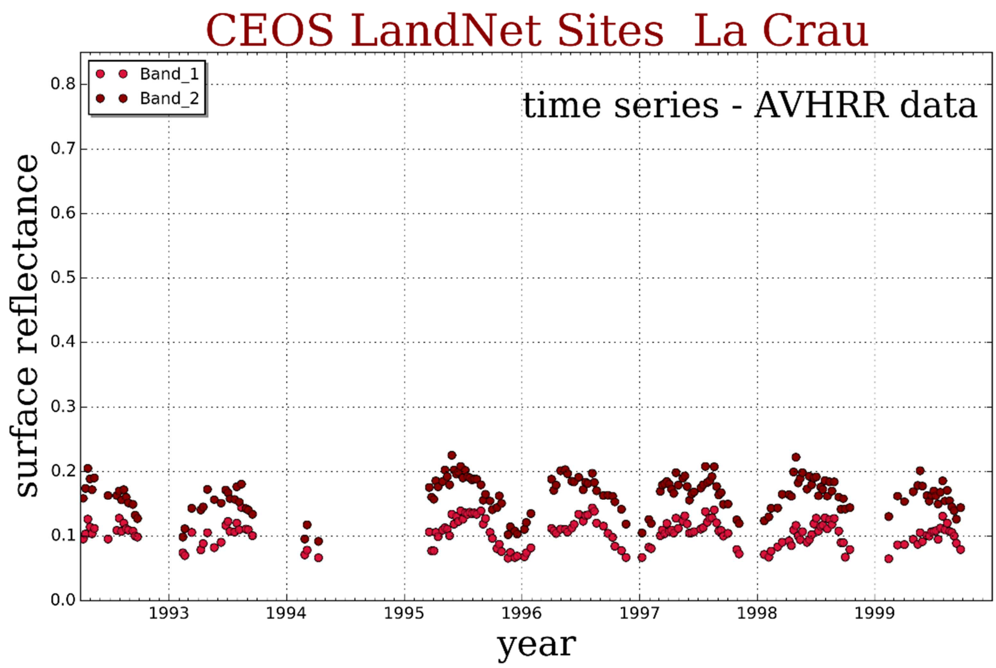

b) valid pixel expression: pixel status - clear land and clear_land_count >2

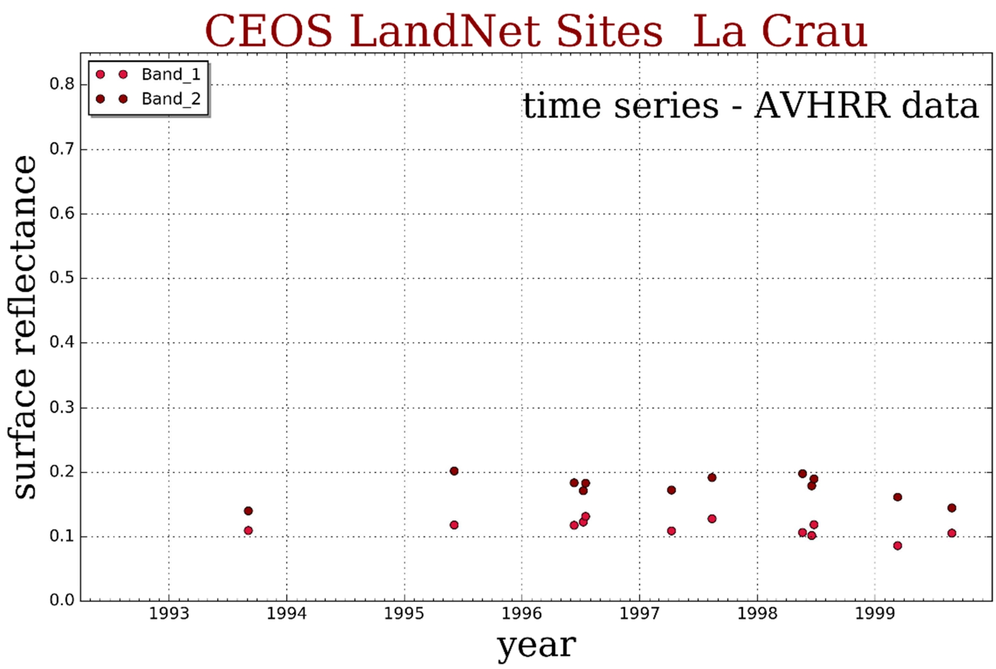

Figure 3-46: SR time series from AVHRR data - 1992-1999 - CEOS-LANDNET SITES – La Crau a) valid pixel expression: pixel status - clear land b) valid pixel expression: pixel status - clear land and clear_land_count >2

3.3 The local variance for the various spectral reflectance values within a LC class and across LC classes

The purpose of this paragraph is to present the method and the results of the validation of the global 7-day MERIS FR and RR, PROBA-V and AVHRR composites based on the analysis of the local variance for the various spectral reflectance values within a LC class and across LC classes.

3.3.1 Analysis of variance [CIMT, 2012] and [Lane et al., 2015]

Analysis of variance (ANOVA) is a statistical method used to analyse the differences between class means and their variation "among and between classes. ANOVA provides a statistical test of whether or not the means of several classes are equal and is therefore useful in comparing means for statistical significance.

First, some notations are introduced.

Number of conditions	k
Number of observations for i^{th} condition	n_i , $i = 1, ..., k$
Total number of observation	$n = \Sigma_i n_i$
Observation j for i^{th} condition	x_{ij}, $j = 1, ..., n_i$
Mean of all observations in i^{th} condition	$X_i = 1/n_i \Sigma_j x_{ij}$
Mean of all observations	$X = 1/n \Sigma_{ij} x_{ij}$
Degree of freedom	$df = dfn + dfd = n - 1$
degrees of freedom numerator	$dfn = k - 1$
degrees of freedom for the denominator	$dfd = n - k$

The computational formulae now follow.

Total sum of squares	$SSQ_{total} = \Sigma_{ij} (x_{ij}-X)^2 = SSQ_{condition} + SSQ_{error}$
Sum of squares condition	$SSQ_{condition} = \Sigma_i [n_i \cdot (X_i-X)^2]$
Sum of squares error	$SSQ_{error} = \Sigma_i \Sigma_j (x_{ij}-X_i)^2$
Total mean square	$MST = 1/df\ SSQ_{total} = 1/(n-1) \cdot SSQ_{total}$
Mean Square Between (MSB) estimates	$MSB = 1/dfn\ SSQ_{condition} = 1/(k-1) \cdot SSQ_{condition}$
Mean Square Error (MSE) estimate	$MSE = 1/dfd\ SSQ_{error} = 1/(n-k) \cdot SSQ_{error}$
F ratio	$F= MSB/MSE$

The ANOVA summary table (Figure 3-47) shown below is a good way to summarize the partitioning of the variance. The first column shows the sources of variation, the second column shows the sums of squares, the third shows the degrees of freedom, the fourth shows the mean squares, the fifth shows the F ratio, and the last shows the critical value of F ratio at a user defined significance level. The critical value of F ratio is a function of dfd, dfn and significance level (α). If $F \geq F_{Critical}$ (dfn, dfd, α) then the differences between class means and their variation among and between classes have a statistical significance or, in other words reject the null hypothesis that the means of several classes are equal.

Source of variation	**Sum of squares**	**Degrees of Freedom**	**Mean square**	**F ratio**	$\mathbf{F_{(dfn,dfd)}}$ significance level 0.05
Condition	$SSQ_{condition}$	dfn = k - 1	MSB	F= MSB/MSE	$F_{Critical}$
Error	SSQ_{error}	dfd = n - k	MSE		
Total	SSQ_{total}				

Figure 3-47: Example of ANOVA summary table

For the analysis of the local variance for the various spectral reflectance values within a LC class and across LC classes a couple of preparative steps are necessary. The preparative phase includes: (i) identification of the to be analysed LC-CCI classes and (ii) selection of reference points for each LC-CCI class, as well as (iii) the extraction of the 7-day surface reflectance values of the complete MERIS FR and RR, PROBA-V and AVHRR data for all selected reference points.

The following classes have been selected for the analysis:

- LC-CCI-Class 10 and 20 - Cropland -
- LC-CCI-Class 50 - Tree cover, broadleaved, evergreen, closed to open
- LC-CCI-Class 60 - Tree cover, broadleaved, deciduous, closed to open
- LC-CCI-Class 70 - Tree cover, needleleaved, evergreen, closed to open
- LC-CCI-Class 80 - Tree cover, needleleaved, deciduous, closed to open
- LC-CCI-Class 90 - Tree cover, mixed leaf type (broad - and needleleaved)
- LC-CCI-Class 130 - Grassland
- LC-CCI-Class 150 - Sparse vegetation
- LC-CCI-Class 160 and 170 - Tree cover, flooded
- LC-CCI-Class 180 - Shrub or herbaceous cover, flooded
- LC-CCI-Class 190 - Urban areas
- LC-CCI-Class 200 - Bare areas

The selection of the reference points is a two-steps procedure and the LC-CCI yearly map products (1992-2015) form the basis for the identification of the reference points. At first, every 50 pixels and their 5x5 neighbourhood pixels have been collected and filtered, so that all resultant central pixels have the same LC-CCI class in a 5x5 window. Afterwards, the resultant central pixels have been grouped by the LC-CCI classes and filtered again to avoid changes in the LC-CCI class from the correspondent years. Finally, 50 reference pixels (points, central pixel) per to be analysed LC-CCI classes have been randomly selected from the automatic collection. If there are not enough automatic collected points available, the remaining reference points have been manually selected. The selected reference points are shown in the following figure (Figure 3-48).

Figure 3-48: Selected reference points for MERIS FR, MERIS RR, PROBA-V and AVHRR data

3.3.2 Results of the analysis of the local variance for the various spectral reflectance values within a LC class and across LC classes for the MERIS FR and RR data

The following tables (Table 3-11 through Table 3-14) show the variance of the spectral reflectance values at the class level for the SR time series of MERIS FR and RR data for the yearly maps (2003-2012) The subsequent tables (Table 3-15 through Table 3-30) show the corresponding ANOVA summary table.

The results of ANOVA for the all analysed combinations of LC-CCI classes show that the differences between class means and their variation among and between classes are statistical significance. The ANOVA of individual MERIS bands can also result in rejection of the null hypothesis, e.g. MERIS FR band 5 and 9 for the ANOVA for cropland and grassland (see Table 3-18).

The number of pixels which contribute to the analysis is very variable whereas this can be caused by the data availability or by the cloud coverage (see also section 3.2).

Table 3-11: Variance of the spectral reflectance values at the class level - MERIS FR time series and band 1 to 7

	OBS. COUNTS	MERIS FR SR BAND 1	MERIS FR SR BAND 2	MERIS FR SR BAND 3	MERIS FR SR BAND 4	MERIS FR SR BAND 5	MERIS FR SR BAND 6	MERIS FR SR BAND 7
Cropland	5170	0.00023	0.00035	0.00060	0.00072	0.00116	0.00260	0.00365
Forest - LC-CCI Class 50	2274	0.00007	0.00006	0.00006	0.00007	0.00011	0.00022	0.00035
Forest - LC-CCI Class 60	2863	0.00008	0.00006	0.00007	0.00008	0.00014	0.00031	0.00052
Forest - LC-CCI Class 70	1374	0.00006	0.00004	0.00003	0.00003	0.00008	0.00011	0.00021
Forest - LC-CCI Class 80	250	0.00015	0.00011	0.00009	0.00009	0.00014	0.00009	0.00008
Forest - LC-CCI Class 90	4488	0.00051	0.00066	0.00096	0.00109	0.00146	0.00237	0.00302
Grassland	552	0.00017	0.00017	0.00023	0.00026	0.00035	0.00066	0.00089
Sparse vegetation	6433	0.00066	0.00095	0.00146	0.00180	0.00334	0.00611	0.00780
Inundated forest	2246	0.00006	0.00004	0.00003	0.00003	0.00007	0.00008	0.00009
Wetland	3317	0.00110	0.00171	0.00270	0.00313	0.00472	0.00716	0.00899
Urban areas	3173	0.00122	0.00161	0.00215	0.00240	0.00327	0.00434	0.00486
Bare areas	13283	0.00058	0.00083	0.00135	0.00172	0.00404	0.00876	0.01106

Table 3-12: Variance of the spectral reflectance values at the class level - MERIS FR time series and band 8 to 14

	OBS. COUNTS	MERIS FR SR BAND 8	MERIS FR SR BAND 9	MERIS FR SR BAND 10	MERIS FR SR BAND 12	MERIS FR SR BAND 13	MERIS FR SR BAND 14
Cropland	5170	0.00400	0.00270	0.00469	0.00526	0.00566	0.00554
Forest - LC-CCI Class 50	2274	0.00040	0.00041	0.00309	0.00340	0.00363	0.00355
Forest - LC-CCI Class 60	2863	0.00059	0.00038	0.00504	0.00566	0.00583	0.00566
Forest - LC-CCI Class 70	1374	0.00023	0.00024	0.00238	0.00250	0.00258	0.00253
Forest - LC-CCI Class 80	250	0.00009	0.00029	0.00331	0.00395	0.00484	0.00475
Forest - LC-CCI Class 90	4488	0.00323	0.00243	0.00328	0.00357	0.00431	0.00437
Grassland	552	0.00096	0.00074	0.00352	0.00396	0.00424	0.00410
Sparse vegetation	6433	0.00844	0.00784	0.00901	0.00942	0.01039	0.01035
Inundated forest	2246	0.00010	0.00023	0.00137	0.00152	0.00173	0.00172
Wetland	3317	0.00969	0.00621	0.00569	0.00579	0.00573	0.00566
Urban areas	3173	0.00500	0.00397	0.00340	0.00343	0.00345	0.00334
Bare areas	13283	0.01187	0.01254	0.01514	0.01563	0.01623	0.01613

Table 3-13: Variance of the spectral reflectance values at the class level - MERIS RR time series and band 1 to 7

	OBS. COUNTS	MERIS FR SR BAND 1	MERIS FR SR BAND 2	MERIS FR SR BAND 3	MERIS FR SR BAND 4	MERIS FR SR BAND 5	MERIS FR SR BAND 6	MERIS FR SR BAND 7
Cropland	6782	0.00019	0.00030	0.00055	0.00067	0.00106	0.00243	0.00343
Forest - LC-CCI Class 50	3799	0.00007	0.00006	0.00007	0.00008	0.00012	0.00026	0.00043
Forest - LC-CCI Class 60	4249	0.00006	0.00005	0.00007	0.00009	0.00014	0.00029	0.00049
Forest - LC-CCI Class 70	2598	0.00006	0.00004	0.00003	0.00004	0.00008	0.00012	0.00022
Forest - LC-CCI Class 80	1020	0.00014	0.00011	0.00008	0.00008	0.00012	0.00009	0.00009
Forest - LC-CCI Class 90	6781	0.00041	0.00056	0.00085	0.00099	0.00135	0.00207	0.00265
Grassland	1235	0.00021	0.00023	0.00031	0.00034	0.00042	0.00080	0.00107
Sparse vegetation	10956	0.00056	0.00086	0.00137	0.00170	0.00314	0.00547	0.00688
Inundated forest	2540	0.00006	0.00004	0.00003	0.00003	0.00006	0.00007	0.00009
Wetland	4630	0.00099	0.00150	0.00239	0.00276	0.00418	0.00648	0.00813
Urban areas	4444	0.00106	0.00139	0.00185	0.00207	0.00284	0.00379	0.00424
Bare areas	14742	0.00061	0.00087	0.00139	0.00176	0.00409	0.00877	0.01103

Table 3-14: Variance of the spectral reflectance values at the class level - MERIS RR time series and band 8 to 14

	OBS. COUNTS	MERIS FR SR BAND 8	MERIS FR SR BAND 9	MERIS FR SR BAND 10	MERIS FR SR BAND 12	MERIS FR SR BAND 13	MERIS FR SR BAND 14
Cropland	6782	0.00375	0.00243	0.00398	0.00448	0.00481	0.00470
Forest - LC-CCI Class 50	3799	0.00049	0.00041	0.00255	0.00282	0.00305	0.00299
Forest - LC-CCI Class 60	4249	0.00056	0.00032	0.00420	0.00468	0.00485	0.00470
Forest - LC-CCI Class 70	2598	0.00024	0.00025	0.00195	0.00205	0.00211	0.00207
Forest - LC-CCI Class 80	1020	0.00009	0.00025	0.00248	0.00295	0.00355	0.00346
Forest - LC-CCI Class 90	6781	0.00284	0.00220	0.00266	0.00291	0.00375	0.00386
Grassland	1235	0.00114	0.00082	0.00313	0.00360	0.00398	0.00382
Sparse vegetation	10956	0.00742	0.00678	0.00762	0.00797	0.00881	0.00878
Inundated forest	2540	0.00010	0.00018	0.00129	0.00142	0.00158	0.00156
Wetland	4630	0.00873	0.00589	0.00504	0.00510	0.00497	0.00488
Urban areas	4444	0.00437	0.00355	0.00335	0.00341	0.00348	0.00339
Bare areas	14742	0.01183	0.01249	0.01505	0.01554	0.01616	0.01608

3.3.2.1 *ANOVA - Different forest classes (50, 60, 70, 80 and 90) - MERIS FR data*

Table 3-15: ANOVA summary table - different forest classes - MERIS FR data

	Source of variation	Sum of squares	Degrees of Freedom	Mean square	F ratio	$F_{(dfn,dfd)}$ significance level 0.05
Band 1	Condition	0.033	4	0.00820	119.607	2.372
	Error	0.617	9002	0.00007		
	Total	0.650				
Band 2	Condition	0.041	4	0.01028	210.247	2.372
	Error	0.440	9002	0.00005		
	Total	0.481				
Band 3	Condition	0.072	4	0.01797	344.702	2.372
	Error	0.469	9002	0.00005		
	Total	0.541				
Band 4	Condition	0.092	4	0.02301	388.964	2.372
	Error	0.533	9002	0.00006		
	Total	0.625				
Band 5	Condition	0.204	4	0.05091	472.095	2.372
	Error	0.971	9002	0.00011		
	Total	1.174				
Band 6	Condition	0.335	4	0.08376	437.627	2.372
	Error	1.723	9002	0.00019		
	Total	2.058				
Band 7	Condition	0.464	4	0.11597	372.165	2.372
	Error	2.805	9002	0.00031		
	Total	3.269				
Band 8	Condition	0.523	4	0.13066	372.620	2.372
	Error	3.157	9002	0.00035		

	Source of variation	Sum of squares	Degrees of Freedom	Mean square	F ratio	$F_{(dfn,dfd)}$ significance level 0.05
	Total	3.679				
Band 9	Condition	0.825	4	0.20618	637.810	2.372
	Error	2.910	9002	0.00032		
	Total	3.735				
Band 10	Condition	3.029	4	0.75727	238.335	2.372
	Error	28.602	9002	0.00318		
	Total	31.632				
Band 12	Condition	3.720	4	0.93004	263.726	2.372
	Error	31.746	9002	0.00353		
	Total	35.466				
Band 13	Condition	5.096	4	1.27411	341.846	2.372
	Error	33.552	9002	0.00373		
	Total	38.648				
Band 14	Condition	5.194	4	1.29848	356.482	2.372
	Error	32.790	9002	0.00364		
	Total	37.984				

3.3.2.2 *ANOVA - Forest (50, 60, 70, 80 and 90) and inundated forest (160 and 170) - MERIS FR data*

Table 3-16: ANOVA summary table - forest classes and inundated forest classes - MERIS FR data

	Source of variation	Sum of squares	Degrees of Freedom	Mean square	F ratio	$F_{(dfn,dfd)}$ significance level 0.05
Band 1	Condition	0.007	1	0.00658	84.337	3.843
	Error	0.746	9557	0.00008		
	Total	0.752				
Band 2	Condition	0.008	1	0.00762	126.185	3.843

	Source of variation	Sum of squares	Degrees of Freedom	Mean square	F ratio	$F_{(dfn,dfd)}$ significance level 0.05
	Error	0.577	9557	0.00006		
	Total	0.585				
Band 3	Condition	0.011	1	0.01059	151.089	3.843
	Error	0.670	9557	0.00007		
	Total	0.681				
Band 4	Condition	0.012	1	0.01170	146.175	3.843
	Error	0.765	9557	0.00008		
	Total	0.777				
Band 5	Condition	0.020	1	0.01995	139.409	3.843
	Error	1.367	9557	0.00014		
	Total	1.387				
Band 6	Condition	0.018	1	0.01764	69.673	3.843
	Error	2.420	9557	0.00025		
	Total	2.438				
Band 7	Condition	0.012	1	0.01223	31.077	3.843
	Error	3.762	9557	0.00039		
	Total	3.774				
Band 8	Condition	0.012	1	0.01150	26.125	3.843
	Error	4.207	9557	0.00044		
	Total	4.218				
Band 9	Condition	0.038	1	0.03763	86.772	3.843
	Error	4.144	9557	0.00043		
	Total	4.182				
Band 10	Condition	0.194	1	0.19383	55.182	3.843
	Error	33.570	9557	0.00351		

	Source of variation	Sum of squares	Degrees of Freedom	Mean square	F ratio	$F_{(dfn,dfd)}$ significance level 0.05
	Total	33.764				
Band 12	Condition	0.242	1	0.24226	61.500	3.843
	Error	37.646	9557	0.00394		
	Total	37.889				
Band 13	Condition	0.380	1	0.37986	88.575	3.843
	Error	40.986	9557	0.00429		
	Total	41.366				
Band 14	Condition	0.386	1	0.38619	91.720	3.843
	Error	40.240	9557	0.00421		
	Total	40.627				

3.3.2.3 *ANOVA - Inundated forest (160 and 170) and wetland (180) - MERIS FR data*

Table 3-17: ANOVA summary table - inundated forest classes and wetland class - MERIS FR data

	Source of variation	Sum of squares	Degrees of Freedom	Mean square	F ratio	$F_{(dfn,dfd)}$ significance level 0.05
Band 1	Condition	0.137	1	0.13654	140.958	3.843
	Error	3.746	3867	0.00097		
	Total	3.882				
Band 2	Condition	0.280	1	0.28021	188.264	3.843
	Error	5.756	3867	0.00149		
	Total	6.036				
Band 3	Condition	0.533	1	0.53349	227.177	3.843
	Error	9.081	3867	0.00235		
	Total	9.615				
Band 4	Condition	0.645	1	0.64505	237.435	3.843

	Source of variation	Sum of squares	Degrees of Freedom	Mean square	F ratio	$F_{(dfn,dfd)}$ significance level 0.05
	Error	10.506	3867	0.00272		
	Total	11.151				
Band 5	Condition	0.985	1	0.98495	240.282	3.843
	Error	15.851	3867	0.00410		
	Total	16.836				
Band 6	Condition	1.944	1	1.94370	311.910	3.843
	Error	24.098	3867	0.00623		
	Total	26.041				
Band 7	Condition	2.478	1	2.47807	316.118	3.843
	Error	30.314	3867	0.00784		
	Total	32.792				
Band 8	Condition	2.637	1	2.63715	312.359	3.843
	Error	32.648	3867	0.00844		
	Total	35.285				
Band 9	Condition	2.232	1	2.23201	410.938	3.843
	Error	21.004	3867	0.00543		
	Total	23.236				
Band 10	Condition	0.263	1	0.26337	48.934	3.843
	Error	20.813	3867	0.00538		
	Total	21.076				
Band 12	Condition	0.239	1	0.23929	43.268	3.843
	Error	21.387	3867	0.00553		
	Total	21.626				
Band 13	Condition	0.214	1	0.21417	38.820	3.843
	Error	21.335	3867	0.00552		

	Source of variation	Sum of squares	Degrees of Freedom	Mean square	F ratio	$F_{(dfn,dfd)}$ significance level 0.05
	Total	21.549				
Band 14	Condition	0.222	1	0.22228	40.881	3.843
	Error	21.026	3867	0.00544		
	Total	21.248				

3.3.2.4 *ANOVA - Cropland (10, 11, 12) and grassland (130) - MERIS FR data*

Table 3-18: ANOVA summary table - cropland classes and grassland class - MERIS FR data

	Source of variation	Sum of squares	Degrees of Freedom	Mean square	F ratio	$F_{(dfn,dfd)}$ significance level 0.05
Band 1	Condition	0.050	1	0.04977	137.157	3.843
	Error	3.504	9656	0.00036		
	Total	3.554				
Band 2	Condition	0.039	1	0.03861	78.699	3.843
	Error	4.737	9656	0.00049		
	Total	4.776				
Band 3	Condition	0.039	1	0.03924	51.271	3.843
	Error	7.390	9656	0.00077		
	Total	7.429				
Band 4	Condition	0.029	1	0.02892	32.396	3.843
	Error	8.619	9656	0.00089		
	Total	8.648				
Band 5	Condition	0.001	1	0.00061	0.468	3.843
	Error	12.527	9656	0.00130		
	Total	12.528				
Band 6	Condition	0.090	1	0.09013	36.181	3.843

	Source of variation	Sum of squares	Degrees of Freedom	Mean square	F ratio	$F_{(dfn,dfd)}$ significance level 0.05
	Error	24.055	9656	0.00249		
	Total	24.145				
Band 7	Condition	0.147	1	0.14726	43.847	3.843
	Error	32.429	9656	0.00336		
	Total	32.577				
Band 8	Condition	0.147	1	0.14684	40.308	3.843
	Error	35.176	9656	0.00364		
	Total	35.323				
Band 9	Condition	0.000	1	0.00000	0.001	3.843
	Error	24.831	9656	0.00257		
	Total	24.831				
Band 10	Condition	3.158	1	3.15836	783.423	3.843
	Error	38.928	9656	0.00403		
	Total	42.086				
Band 12	Condition	3.765	1	3.76519	841.323	3.843
	Error	43.214	9656	0.00448		
	Total	46.979				
Band 13	Condition	4.507	1	4.50741	895.908	3.843
	Error	48.580	9656	0.00503		
	Total	53.088				
Band 14	Condition	4.281	1	4.28121	856.924	3.843
	Error	48.242	9656	0.00500		
	Total	52.523				

3.3.2.5 *ANOVA - Cropland (10, 11, 12) and sparse vegetation (150, 151, 152, 153) - MERIS FR data*

Table 3-19: ANOVA summary table - cropland classes and sparse vegetation classes - MERIS FR data

	Source of variation	Sum of squares	Degrees of Freedom	Mean square	F ratio	$F_{(dfn,dfd)}$ significance level 0.05
Band 1	Condition	0.887	1	0.88661	1897.699	3.843
	Error	5.420	11601	0.00047		
	Total	6.307				
Band 2	Condition	1.577	1	1.57697	2320.656	3.843
	Error	7.883	11601	0.00068		
	Total	9.460				
Band 3	Condition	2.921	1	2.92107	2712.094	3.843
	Error	12.495	11601	0.00108		
	Total	15.416				
Band 4	Condition	3.576	1	3.57621	2704.371	3.843
	Error	15.341	11601	0.00132		
	Total	18.917				
Band 5	Condition	7.446	1	7.44564	3148.002	3.843
	Error	27.439	11601	0.00237		
	Total	34.884				
Band 6	Condition	24.799	1	24.79885	5452.100	3.843
	Error	52.767	11601	0.00455		
	Total	77.566				
Band 7	Condition	33.028	1	33.02772	5550.319	3.843
	Error	69.033	11601	0.00595		
	Total	102.061				
Band 8	Condition	35.386	1	35.38642	5476.951	3.843
	Error	74.954	11601	0.00646		

	Source of variation	Sum of squares	Degrees of Freedom	Mean square	F ratio	$F_{(dfn,dfd)}$ significance level 0.05
	Total	110.340				
Band 9	Condition	25.740	1	25.74045	4638.990	3.843
	Error	64.371	11601	0.00555		
	Total	90.111				
Band 10	Condition	7.747	1	7.74679	1093.548	3.843
	Error	82.183	11601	0.00708		
	Total	89.929				
Band 12	Condition	6.500	1	6.50035	859.231	3.843
	Error	87.765	11601	0.00757		
	Total	94.266				
Band 13	Condition	4.179	1	4.17902	504.763	3.843
	Error	96.047	11601	0.00828		
	Total	100.226				
Band 14	Condition	3.894	1	3.89435	474.561	3.843
	Error	95.200	11601	0.00821		
	Total	99.095				

3.3.2.6 *ANOVA - Cropland (10, 11, 12) and bare areas (200, 201, 202) - MERIS FR data*

Table 3-20: ANOVA summary table - cropland classes and bare areas classes - MERIS FR data

	Source of variation	Sum of squares	Degrees of Freedom	Mean square	F ratio	$F_{(dfn,dfd)}$ significance level 0.05
Band 1	Condition	12.180	1	12.17971	25107.561	3.843
	Error	8.951	18451	0.00049		
	Total	21.130				
Band 2	Condition	17.520	1	17.52050	25171.557	3.843

	Source of variation	Sum of squares	Degrees of Freedom	Mean square	F ratio	$F_{(dfn,dfd)}$ significance level 0.05
	Error	12.843	18451	0.00070		
	Total	30.363				
Band 3	Condition	25.704	1	25.70425	22559.671	3.843
	Error	21.023	18451	0.00114		
	Total	46.727				
Band 4	Condition	31.098	1	31.09811	21588.249	3.843
	Error	26.579	18451	0.00144		
	Total	57.677				
Band 5	Condition	59.794	1	59.79415	18487.201	3.843
	Error	59.677	18451	0.00323		
	Total	119.471				
Band 6	Condition	131.078	1	131.07784	18633.670	3.843
	Error	129.793	18451	0.00703		
	Total	260.871				
Band 7	Condition	158.516	1	158.51602	17637.936	3.843
	Error	165.823	18451	0.00899		
	Total	324.339				
Band 8	Condition	166.180	1	166.17970	17187.973	3.843
	Error	178.391	18451	0.00967		
	Total	344.571				
Band 9	Condition	130.657	1	130.65680	13355.162	3.843
	Error	180.511	18451	0.00978		
	Total	311.167				
Band 10	Condition	65.680	1	65.68027	5379.890	3.843
	Error	225.259	18451	0.01221		

	Source of variation	Sum of squares	Degrees of Freedom	Mean square	F ratio	$F_{(dfn,dfd)}$ significance level 0.05
	Total	290.939				
Band 12	Condition	60.556	1	60.55624	4759.372	3.843
	Error	234.763	18451	0.01272		
	Total	295.319				
Band 13	Condition	44.563	1	44.56288	3359.778	3.843
	Error	244.727	18451	0.01326		
	Total	289.290				
Band 14	Condition	41.952	1	41.95237	3187.573	3.843
	Error	242.838	18451	0.01316		
	Total	284.790				

3.3.2.7 *ANOVA - Cropland (10, 11, 12) and urban (190) - MERIS FR data*

Table 3-21: ANOVA summary table - cropland classes and urban area class - MERIS FR data

	Source of variation	Sum of squares	Degrees of Freedom	Mean square	F ratio	$F_{(dfn,dfd)}$ significance level 0.05
Band 1	Condition	0.190	1	0.19045	313.737	3.843
	Error	5.063	8341	0.00061		
	Total	5.254				
Band 2	Condition	0.274	1	0.27353	331.216	3.843
	Error	6.888	8341	0.00083		
	Total	7.162				
Band 3	Condition	0.324	1	0.32395	272.733	3.843
	Error	9.907	8341	0.00119		
	Total	10.231				
Band 4	Condition	0.287	1	0.28665	210.578	3.843

	Source of variation	Sum of squares	Degrees of Freedom	Mean square	F ratio	$F_{(dfn,dfd)}$ significance level 0.05
	Error	11.354	8341	0.00136		
	Total	11.641				
Band 5	Condition	0.089	1	0.08941	45.629	3.843
	Error	16.344	8341	0.00196		
	Total	16.434				
Band 6	Condition	0.017	1	0.01702	5.217	3.843
	Error	27.211	8341	0.00326		
	Total	27.228				
Band 7	Condition	0.002	1	0.00204	0.496	3.843
	Error	34.282	8341	0.00411		
	Total	34.284				
Band 8	Condition	0.018	1	0.01756	4.008	3.843
	Error	36.530	8341	0.00438		
	Total	36.548				
Band 9	Condition	0.572	1	0.57188	179.831	3.843
	Error	26.525	8341	0.00318		
	Total	27.097				
Band 10	Condition	4.291	1	4.29145	1022.542	3.843
	Error	35.006	8341	0.00420		
	Total	39.297				
Band 12	Condition	5.383	1	5.38294	1179.483	3.843
	Error	38.067	8341	0.00456		
	Total	43.450				
Band 13	Condition	8.998	1	8.99806	1868.043	3.843
	Error	40.177	8341	0.00482		

	Source of variation	Sum of squares	Degrees of Freedom	Mean square	F ratio	$F_{(dfn,dfd)}$ significance level 0.05
	Total	49.175				
Band 14	Condition	9.595	1	9.59476	2039.922	3.843
	Error	39.232	8341	0.00470		
	Total	48.827				

3.3.2.8 *ANOVA - Urban (190) and bare areas (200, 201, 202) - MERIS FR data*

Table 3-22: ANOVA summary table - urban area class and bare areas classes - MERIS FR data

	Source of variation	Sum of squares	Degrees of Freedom	Mean square	F ratio	$F_{(dfn,dfd)}$ significance level 0.05
Band 1	Condition	5.746	1	5.74623	8137.163	3.843
	Error	11.619	16454	0.00071		
	Total	17.366				
Band 2	Condition	8.269	1	8.26870	8418.357	3.843
	Error	16.161	16454	0.00098		
	Total	24.430				
Band 3	Condition	12.648	1	12.64765	8413.703	3.843
	Error	24.734	16454	0.00150		
	Total	37.382				
Band 4	Condition	16.122	1	16.12173	8711.949	3.843
	Error	30.449	16454	0.00185		
	Total	46.570				
Band 5	Condition	36.889	1	36.88908	9476.653	3.843
	Error	64.049	16454	0.00389		
	Total	100.938				
Band 6	Condition	87.403	1	87.40305	11052.267	3.843

	Source of variation	Sum of squares	Degrees of Freedom	Mean square	F ratio	$F_{(dfn,dfd)}$ significance level 0.05
	Error	130.121	16454	0.00791		
	Total	217.524				
Band 7	Condition	110.172	1	110.17206	11165.499	3.843
	Error	162.355	16454	0.00987		
	Total	272.527				
Band 8	Condition	117.624	1	117.62409	11151.779	3.843
	Error	173.550	16454	0.01055		
	Total	291.174				
Band 9	Condition	107.033	1	107.03315	9830.237	3.843
	Error	179.154	16454	0.01089		
	Total	286.187				
Band 10	Condition	82.583	1	82.58350	6415.647	3.843
	Error	211.799	16454	0.01287		
	Total	294.383				
Band 12	Condition	82.876	1	82.87587	6242.024	3.843
	Error	218.461	16454	0.01328		
	Total	301.337				
Band 13	Condition	80.308	1	80.30812	5835.292	3.843
	Error	226.448	16454	0.01376		
	Total	306.756				
Band 14	Condition	79.362	1	79.36170	5808.375	3.843
	Error	224.816	16454	0.01366		
	Total	304.178				

3.3.2.9 *ANOVA - Different forest classes (50, 60, 70, 80 and 90) - MERIS RR data*

Table 3-23: ANOVA summary table - different forest classes - MERIS RR data

	Source of variation	Sum of squares	Degrees of Freedom	Mean square	F ratio	$F_{(dfn,dfd)}$ significance level 0.05
Band 1	Condition	0.040	4	0.00992	147.425	2.372
	Error	0.955	14201	0.00007		
	Total	0.995				
Band 2	Condition	0.055	4	0.01381	268.129	2.372
	Error	0.732	14201	0.00005		
	Total	0.787				
Band 3	Condition	0.107	4	0.02685	462.585	2.372
	Error	0.824	14201	0.00006		
	Total	0.932				
Band 4	Condition	0.137	4	0.03426	533.854	2.372
	Error	0.911	14201	0.00006		
	Total	1.048				
Band 5	Condition	0.260	4	0.06505	617.663	2.372
	Error	1.495	14201	0.00011		
	Total	1.756				
Band 6	Condition	0.525	4	0.13135	666.340	2.372
	Error	2.799	14201	0.00020		
	Total	3.325				
Band 7	Condition	0.798	4	0.19954	614.890	2.372
	Error	4.608	14201	0.00032		
	Total	5.406				
Band 8	Condition	0.905	4	0.22631	617.367	2.372
	Error	5.206	14201	0.00037		

	Source of variation	Sum of squares	Degrees of Freedom	Mean square	F ratio	$F_{(dfn,dfd)}$ significance level 0.05
	Total	6.111				
Band 9	Condition	0.953	4	0.23827	788.826	2.372
	Error	4.289	14201	0.00030		
	Total	5.243				
Band 10	Condition	2.964	4	0.74098	273.918	2.372
	Error	38.416	14201	0.00271		
	Total	41.379				
Band 12	Condition	3.962	4	0.99046	330.791	2.372
	Error	42.521	14201	0.00299		
	Total	46.483				
Band 13	Condition	5.657	4	1.41437	443.645	2.372
	Error	45.274	14201	0.00319		
	Total	50.931				
Band 14	Condition	5.612	4	1.40301	451.068	2.372
	Error	44.171	14201	0.00311		
	Total	49.783				

3.3.2.10 *ANOVA - Forest (50, 60, 70, 80 and 90) and inundated forest (160 and 170) - MERIS RR data*

Table 3-24: ANOVA summary table - forest classes and inundated forest classes - MERIS RR data

	Source of variation	Sum of squares	Degrees of Freedom	Mean square	F ratio	$F_{(dfn,dfd)}$ significance level 0.05
Band 1	Condition	0.020	1	0.01972	242.911	3.843
	Error	1.253	15439	0.00008		
	Total	1.273				
Band 2	Condition	0.019	1	0.01932	277.803	3.843

	Source of variation	Sum of squares	Degrees of Freedom	Mean square	F ratio	$F_{(dfn,dfd)}$ significance level 0.05
	Error	1.074	15439	0.00007		
	Total	1.093				
Band 3	Condition	0.023	1	0.02290	268.126	3.843
	Error	1.318	15439	0.00009		
	Total	1.341				
Band 4	Condition	0.025	1	0.02498	263.725	3.843
	Error	1.463	15439	0.00009		
	Total	1.488				
Band 5	Condition	0.051	1	0.05116	347.683	3.843
	Error	2.272	15439	0.00015		
	Total	2.323				
Band 6	Condition	0.024	1	0.02389	85.529	3.843
	Error	4.313	15439	0.00028		
	Total	4.336				
Band 7	Condition	0.009	1	0.00914	20.975	3.843
	Error	6.725	15439	0.00044		
	Total	6.734				
Band 8	Condition	0.007	1	0.00721	14.813	3.843
	Error	7.515	15439	0.00049		
	Total	7.522				
Band 9	Condition	0.048	1	0.04771	117.748	3.843
	Error	6.256	15439	0.00041		
	Total	6.303				
Band 10	Condition	0.914	1	0.91378	311.850	3.843
	Error	45.239	15439	0.00293		

	Source of variation	Sum of squares	Degrees of Freedom	Mean square	F ratio	$F_{(dfn,dfd)}$ significance level 0.05
	Total	46.153				
Band 12	Condition	1.129	1	1.12949	342.404	3.843
	Error	50.929	15439	0.00330		
	Total	52.058				
Band 13	Condition	1.516	1	1.51559	419.021	3.843
	Error	55.842	15439	0.00362		
	Total	57.358				
Band 14	Condition	1.466	1	1.46566	415.248	3.843
	Error	54.494	15439	0.00353		
	Total	55.959				

3.3.2.11 *ANOVA - Inundated forest (160 and 170) and wetland (180) - MERIS RR data*

Table 3-25: ANOVA summary table - inundated forest classes and wetland class - MERIS RR data

	Source of variation	Sum of squares	Degrees of Freedom	Mean square	F ratio	$F_{(dfn,dfd)}$ significance level 0.05
Band 1	Condition	0.167	1	0.16693	202.900	3.843
	Error	4.823	5863	0.00082		
	Total	4.990				
Band 2	Condition	0.382	1	0.38229	309.955	3.843
	Error	7.231	5863	0.00123		
	Total	7.614				
Band 3	Condition	0.773	1	0.77284	396.567	3.843
	Error	11.426	5863	0.00195		
	Total	12.199				
Band 4	Condition	0.948	1	0.94773	420.841	3.843

	Source of variation	Sum of squares	Degrees of Freedom	Mean square	F ratio	$F_{(dfn,dfd)}$ significance level 0.05
	Error	13.203	5863	0.00225		
	Total	14.151				
Band 5	Condition	1.422	1	1.42228	419.627	3.843
	Error	19.872	5863	0.00339		
	Total	21.294				
Band 6	Condition	2.881	1	2.88136	545.137	3.843
	Error	30.989	5863	0.00529		
	Total	33.871				
Band 7	Condition	3.743	1	3.74292	563.712	3.843
	Error	38.929	5863	0.00664		
	Total	42.672				
Band 8	Condition	4.004	1	4.00353	561.404	3.843
	Error	41.811	5863	0.00713		
	Total	45.814				
Band 9	Condition	3.195	1	3.19502	662.559	3.843
	Error	28.273	5863	0.00482		
	Total	31.468				
Band 10	Condition	0.090	1	0.08993	19.381	3.843
	Error	27.204	5863	0.00464		
	Total	27.294				
Band 12	Condition	0.048	1	0.04839	10.120	3.843
	Error	28.035	5863	0.00478		
	Total	28.084				
Band 13	Condition	0.022	1	0.02248	4.723	3.843
	Error	27.906	5863	0.00476		

	Source of variation	Sum of squares	Degrees of Freedom	Mean square	F ratio	$F_{(dfn,dfd)}$ significance level 0.05
	Total	27.929				
Band 14	Condition	0.029	1	0.02913	6.259	3.843
	Error	27.291	5863	0.00465		
	Total	27.320				

3.3.2.12 *ANOVA - Cropland (10, 11, 12) and grassland (130) - MERIS RR data*

Table 3-26: ANOVA summary table - cropland classes and grassland class - MERIS RR data

	Source of variation	Sum of squares	Degrees of Freedom	Mean square	F ratio	$F_{(dfn,dfd)}$ significance level 0.05
Band 1	Condition	0.012	1	0.01198	40.111	3.843
	Error	4.051	13561	0.00030		
	Total	4.063				
Band 2	Condition	0.004	1	0.00364	8.495	3.843
	Error	5.813	13561	0.00043		
	Total	5.816				
Band 3	Condition	0.002	1	0.00186	2.659	3.843
	Error	9.507	13561	0.00070		
	Total	9.509				
Band 4	Condition	0.000	1	0.00006	0.075	3.843
	Error	11.223	13561	0.00083		
	Total	11.223				
Band 5	Condition	0.034	1	0.03429	28.427	3.843
	Error	16.358	13561	0.00121		
	Total	16.393				
Band 6	Condition	0.121	1	0.12137	53.950	3.843

	Source of variation	Sum of squares	Degrees of Freedom	Mean square	F ratio	$F_{(dfn,dfd)}$ significance level 0.05
	Error	30.508	13561	0.00225		
	Total	30.629				
Band 7	Condition	0.254	1	0.25442	83.745	3.843
	Error	41.199	13561	0.00304		
	Total	41.453				
Band 8	Condition	0.269	1	0.26881	81.609	3.843
	Error	44.669	13561	0.00329		
	Total	44.938				
Band 9	Condition	0.002	1	0.00247	1.069	3.843
	Error	31.365	13561	0.00231		
	Total	31.367				
Band 10	Condition	5.343	1	5.34271	1608.849	3.843
	Error	45.034	13561	0.00332		
	Total	50.376				
Band 12	Condition	6.508	1	6.50812	1762.418	3.843
	Error	50.077	13561	0.00369		
	Total	56.585				
Band 13	Condition	8.601	1	8.60079	2009.088	3.843
	Error	58.054	13561	0.00428		
	Total	66.655				
Band 14	Condition	8.412	1	8.41207	1965.489	3.843
	Error	58.040	13561	0.00428		
	Total	66.452				

3.3.2.13 *ANOVA - Cropland (10, 11, 12) and sparse vegetation (150, 151, 152, 153) - MERIS RR data*

Table 3-27: ANOVA summary table - cropland classes and sparse vegetation classes - MERIS RR data

	Source of variation	**Sum of squares**	**Degrees of Freedom**	**Mean square**	**F ratio**	$F_{(dfn,dfd)}$ significance level 0.05
Band 1	Condition	0.581	1	0.58084	1389.840	3.843
	Error	7.412	17736	0.00042		
	Total	7.993				
Band 2	Condition	1.046	1	1.04645	1622.796	3.843
	Error	11.437	17736	0.00064		
	Total	12.483				
Band 3	Condition	2.056	1	2.05585	1951.422	3.843
	Error	18.685	17736	0.00105		
	Total	20.741				
Band 4	Condition	2.505	1	2.50529	1919.585	3.843
	Error	23.148	17736	0.00131		
	Total	25.653				
Band 5	Condition	5.916	1	5.91560	2526.324	3.843
	Error	41.530	17736	0.00234		
	Total	47.446				
Band 6	Condition	26.808	1	26.80793	6225.209	3.843
	Error	76.377	17736	0.00431		
	Total	103.185				
Band 7	Condition	37.108	1	37.10832	6671.670	3.843
	Error	98.649	17736	0.00556		
	Total	135.757				
Band 8	Condition	40.040	1	40.03956	6655.250	3.843
	Error	106.704	17736	0.00602		

	Source of variation	Sum of squares	Degrees of Freedom	Mean square	F ratio	$F_{(dfn,dfd)}$ significance level 0.05
	Total	146.744				
Band 9	Condition	28.696	1	28.69580	5604.901	3.843
	Error	90.804	17736	0.00512		
	Total	119.500				
Band 10	Condition	7.126	1	7.12560	1144.300	3.843
	Error	110.443	17736	0.00623		
	Total	117.568				
Band 12	Condition	5.508	1	5.50833	830.121	3.843
	Error	117.688	17736	0.00664		
	Total	123.197				
Band 13	Condition	2.569	1	2.56886	352.962	3.843
	Error	129.083	17736	0.00728		
	Total	131.652				
Band 14	Condition	2.296	1	2.29580	318.040	3.843
	Error	128.029	17736	0.00722		
	Total	130.325				

3.3.2.14 *ANOVA - Cropland (10, 11, 12) and bare areas (200, 201, 202) - MERIS RR data*

Table 3-28: ANOVA summary table - cropland classes and bare areas classes - MERIS RR data

	Source of variation	Sum of squares	Degrees of Freedom	Mean square	F ratio	$F_{(dfn,dfd)}$ significance level 0.05
Band 1	Condition	14.228	1	14.22804	30004.917	3.843
	Error	10.206	21522	0.00047		
	Total	24.434				
Band 2	Condition	20.561	1	20.56112	29744.374	3.843

	Source of variation	Sum of squares	Degrees of Freedom	Mean square	F ratio	$F_{(dfn,dfd)}$ significance level 0.05
	Error	14.877	21522	0.00069		
	Total	35.438				
Band 3	Condition	30.283	1	30.28284	26890.559	3.843
	Error	24.237	21522	0.00113		
	Total	54.520				
Band 4	Condition	36.666	1	36.66605	25851.776	3.843
	Error	30.525	21522	0.00142		
	Total	67.191				
Band 5	Condition	71.039	1	71.03864	22662.510	3.843
	Error	67.464	21522	0.00313		
	Total	138.502				
Band 6	Condition	157.299	1	157.29860	23230.182	3.843
	Error	145.732	21522	0.00677		
	Total	303.031				
Band 7	Condition	190.729	1	190.72948	22098.265	3.843
	Error	185.756	21522	0.00863		
	Total	376.485				
Band 8	Condition	200.111	1	200.11139	21561.857	3.843
	Error	199.741	21522	0.00928		
	Total	399.853				
Band 9	Condition	156.138	1	156.13811	16748.227	3.843
	Error	200.642	21522	0.00932		
	Total	356.781				
Band 10	Condition	78.550	1	78.54997	6793.989	3.843
	Error	248.831	21522	0.01156		

	Source of variation	Sum of squares	Degrees of Freedom	Mean square	F ratio	$F_{(dfn,dfd)}$ significance level 0.05
	Total	327.381				
Band 12	Condition	72.361	1	72.36079	6003.148	3.843
	Error	259.422	21522	0.01205		
	Total	331.783				
Band 13	Condition	52.793	1	52.79306	4196.053	3.843
	Error	270.781	21522	0.01258		
	Total	323.574				
Band 14	Condition	49.523	1	49.52273	3963.776	3.843
	Error	268.892	21522	0.01249		
	Total	318.415				

3.3.2.15 *ANOVA - Cropland (10, 11, 12) and urban (190) - MERIS RR data*

Table 3-29: ANOVA summary table - cropland classes and urban area class - MERIS RR data

	Source of variation	Sum of squares	Degrees of Freedom	Mean square	F ratio	$F_{(dfn,dfd)}$ significance level 0.05
Band 1	Condition	0.808	1	0.80792	1513.464	3.843
	Error	5.992	11224	0.00053		
	Total	6.800				
Band 2	Condition	0.861	1	0.86077	1174.514	3.843
	Error	8.226	11224	0.00073		
	Total	9.087				
Band 3	Condition	0.796	1	0.79602	747.273	3.843
	Error	11.956	11224	0.00107		
	Total	12.752				
Band 4	Condition	0.667	1	0.66685	545.129	3.843

	Source of variation	Sum of squares	Degrees of Freedom	Mean square	F ratio	$F_{(dfn,dfd)}$ significance level 0.05
	Error	13.730	11224	0.00122		
	Total	14.397				
Band 5	Condition	0.190	1	0.18971	107.454	3.843
	Error	19.816	11224	0.00177		
	Total	20.005				
Band 6	Condition	0.034	1	0.03370	11.342	3.843
	Error	33.353	11224	0.00297		
	Total	33.387				
Band 7	Condition	0.002	1	0.00186	0.495	3.843
	Error	42.093	11224	0.00375		
	Total	42.095				
Band 8	Condition	0.023	1	0.02312	5.788	3.843
	Error	44.832	11224	0.00399		
	Total	44.855				
Band 9	Condition	0.922	1	0.92175	320.631	3.843
	Error	32.267	11224	0.00287		
	Total	33.188				
Band 10	Condition	7.130	1	7.12976	1910.530	3.843
	Error	41.886	11224	0.00373		
	Total	49.016				
Band 12	Condition	8.885	1	8.88466	2190.687	3.843
	Error	45.521	11224	0.00406		
	Total	54.405				
Band 13	Condition	14.446	1	14.44612	3371.585	3.843
	Error	48.091	11224	0.00428		

	Source of variation	Sum of squares	Degrees of Freedom	Mean square	F ratio	$F_{(dfn,dfd)}$ significance level 0.05
	Total	62.537				
Band 14	Condition	15.318	1	15.31842	3661.809	3.843
	Error	46.953	11224	0.00418		
	Total	62.272				

3.3.2.16 *ANOVA - Urban (190) and bare areas (200, 201, 202) - MERIS RR data*

Table 3-30: ANOVA summary table - urban area class and bare areas classes - MERIS RR data

	Source of variation	Sum of squares	Degrees of Freedom	Mean square	F ratio	$F_{(dfn,dfd)}$ significance level 0.05
Band 1	Condition	4.930	1	4.93012	6918.917	3.843
	Error	13.670	19184	0.00071		
	Total	18.600				
Band 2	Condition	8.074	1	8.07387	8142.236	3.843
	Error	19.023	19184	0.00099		
	Total	27.097				
Band 3	Condition	13.779	1	13.77892	9198.278	3.843
	Error	28.737	19184	0.00150		
	Total	42.516				
Band 4	Condition	18.239	1	18.23932	9936.347	3.843
	Error	35.214	19184	0.00184		
	Total	53.454				
Band 5	Condition	45.363	1	45.36349	11938.235	3.843
	Error	72.896	19184	0.00380		
	Total	118.260				
Band 6	Condition	111.222	1	111.22248	14605.262	3.843

	Source of variation	Sum of squares	Degrees of Freedom	Mean square	F ratio	$F_{(dfn,dfd)}$ significance level 0.05
	Error	146.091	19184	0.00762		
	Total	257.313				
Band 7	Condition	141.361	1	141.36096	14951.472	3.843
	Error	181.378	19184	0.00945		
	Total	322.739				
Band 8	Condition	151.294	1	151.29362	14983.649	3.843
	Error	193.706	19184	0.01010		
	Total	344.999				
Band 9	Condition	139.152	1	139.15164	13351.231	3.843
	Error	199.943	19184	0.01042		
	Total	339.095				
Band 10	Condition	112.577	1	112.57665	9123.029	3.843
	Error	236.727	19184	0.01234		
	Total	349.304				
Band 12	Condition	113.528	1	113.52770	8918.772	3.843
	Error	244.195	19184	0.01273		
	Total	357.722				
Band 13	Condition	110.588	1	110.58849	8364.016	3.843
	Error	253.650	19184	0.01322		
	Total	364.238				
Band 14	Condition	109.152	1	109.15205	8307.625	3.843
	Error	252.054	19184	0.01314		
	Total	361.206				

3.3.3 Results of the analysis of the local variance for the various spectral reflectance values within a LC class and across LC classes for the PROBA-V data

The following table (Table 3-31) show the variance of the spectral reflectance values at the class level for the SR time series of PRPOBA-V data for the yearly maps (2014- 2015) The subsequent tables (Table 3-32 through Table 3-39) show the corresponding ANOVA summary table.

The results of ANOVA for the all analysed combinations of LC-CCI classes show that the differences between class means and their variation among and between classes are statistical significance. The ANOVA of individual PROBA-V bands can also result in rejection of the null hypothesis, e.g. PROBA-V band 1 for the ANOVA for forest and inundated forest (see Table 3-32).

The number of pixels which contribute to the analysis is very variable whereas this can be caused by the data availability or by the cloud coverage (see also section 3.2).

Table 3-31: Variance of the spectral reflectance values at the class level – PROBA-V time series and band 1 to 4

	OBS. COUNTS	PROBA-V SR BAND 1	PROBA-V SR BAND 2	PROBA-V SR BAND 3	PROBA-V SR BAND 4
Cropland	2453	0.00034	0.00287	0.00579	0.00634
Forest - LC-CCI Class 50	1284	0.00009	0.00032	0.00332	0.00172
Forest - LC-CCI Class 60	1983	0.00008	0.00044	0.00472	0.00144
Forest - LC-CCI Class 70	928	0.00007	0.00028	0.00247	0.00085
Forest - LC-CCI Class 80	686	0.00018	0.00012	0.00167	0.00048
Forest - LC-CCI Class 90	2565	0.00068	0.00226	0.00329	0.00492
Grassland	600	0.00022	0.00099	0.00301	0.00258
Sparse vegetation	2946	0.00122	0.00645	0.00804	0.01311
Inundated forest	487	0.00006	0.00014	0.00173	0.00066
Wetland	1166	0.00079	0.00390	0.00519	0.00715
Urban areas	1487	0.00034	0.00063	0.00110	0.00079
Bare areas	2772	0.00087	0.01028	0.01452	0.02398

3.3.3.1 *ANOVA - Different forest classes (50, 60, 70, 80 and 90) – PROBA-V data*

Table 3-32: ANOVA summary table - different forest classes - PROBA-V data

	Source of variation	**Sum of squares**	**Degrees of Freedom**	**Mean square**	**F ratio**	$F_{(dfn,dfd)}$ significance level 0.05
Band 1	Condition	0.062	4	0.01551	166.109	2.372
	Error	0.501	5363	0.00009		
	Total	0.563				
Band 2	Condition	0.389	4	0.09733	307.649	2.372
	Error	1.697	5363	0.00032		
	Total	2.086				
Band 3	Condition	2.239	4	0.55982	167.921	2.372
	Error	17.879	5363	0.00333		
	Total	20.119				
Band 4	Condition	1.820	4	0.45505	375.566	2.372
	Error	6.498	5363	0.00121		
	Total	8.318				

3.3.3.2 *ANOVA - Forest (50, 60, 70, 80 and 90) and inundated forest (160 and 170) - PROBA-V data*

Table 3-33: ANOVA summary table - forest classes and inundated forest classes - PROBA-V data

	Source of variation	**Sum of squares**	**Degrees of Freedom**	**Mean square**	**F ratio**	$F_{(dfn,dfd)}$ significance level 0.05
Band 1	Condition	0.000	1	0.00004	0.379	3.843
	Error	0.692	5966	0.00012		
	Total	0.692				
Band 2	Condition	0.002	1	0.00228	5.077	3.843
	Error	2.678	5966	0.00045		
	Total	2.681				

	Source of variation	Sum of squares	Degrees of Freedom	Mean square	F ratio	$F_{(dfn,dfd)}$ significance level 0.05
Band 3	Condition	0.322	1	0.32161	87.518	3.843
	Error	21.924	5966	0.00367		
	Total	22.246				
Band 4	Condition	0.018	1	0.01774	10.727	3.843
	Error	9.865	5966	0.00165		
	Total	9.882				

3.3.3.3 *ANOVA - Inundated forest (160 and 170) and wetland (180) - PROBA-V data*

Table 3-34: ANOVA summary table - inundated forest classes and wetland class - PROBA-V data

	Source of variation	Sum of squares	Degrees of Freedom	Mean square	F ratio	$F_{(dfn,dfd)}$ significance level 0.05
Band 1	Condition	0.048	1	0.04761	80.426	3.843
	Error	1.044	1764	0.00059		
	Total	1.092				
Band 2	Condition	0.550	1	0.55017	188.948	3.843
	Error	5.136	1764	0.00291		
	Total	5.687				
Band 3	Condition	0.015	1	0.01499	3.369	3.843
	Error	7.852	1764	0.00445		
	Total	7.867				
Band 4	Condition	1.266	1	1.26565	226.121	3.843
	Error	9.873	1764	0.00560		
	Total	11.139				

3.3.3.4 *ANOVA - Cropland (10, 11, 12) and grassland (130) - PROBA-V data*

Table 3-35: ANOVA summary table - cropland classes and grassland class - PROBA-V data

	Source of variation	**Sum of squares**	**Degrees of Freedom**	**Mean square**	**F ratio**	$F_{(dfn,dfd)}$ significance level 0.05
Band 1	Condition	0.002	1	0.00193	3.753	3.843
	Error	2.582	5016	0.00051		
	Total	2.584				
Band 2	Condition	0.089	1	0.08939	34.950	3.843
	Error	12.829	5016	0.00256		
	Total	12.918				
Band 3	Condition	2.519	1	2.51938	558.967	3.843
	Error	22.608	5016	0.00451		
	Total	25.128				
Band 4	Condition	0.104	1	0.10393	18.511	3.843
	Error	28.162	5016	0.00561		
	Total	28.266				

3.3.3.5 *ANOVA - Cropland (10, 11, 12) and sparse vegetation (150, 151, 152, 153) – PROBA-V data*

Table 3-36: ANOVA summary table - cropland classes and sparse vegetation classes - PROBA-V data

	Source of variation	**Sum of squares**	**Degrees of Freedom**	**Mean square**	**F ratio**	$F_{(dfn,dfd)}$ significance level 0.05
Band 1	Condition	0.181	1	0.18141	221.799	3.843
	Error	4.414	5397	0.00082		
	Total	4.596				
Band 2	Condition	12.921	1	12.92147	2680.794	3.843
	Error	26.014	5397	0.00482		
	Total	38.935				

	Source of variation	Sum of squares	Degrees of Freedom	Mean square	F ratio	$F_{(dfn,dfd)}$ significance level 0.05
Band 3	Condition	0.935	1	0.93463	133.253	3.843
	Error	37.854	5397	0.00701		
	Total	38.789				
Band 4	Condition	16.779	1	16.77946	1672.323	3.843
	Error	54.151	5397	0.01003		
	Total	70.931				

3.3.3.6 *ANOVA - Cropland (10, 11, 12) and bare areas (200, 201, 202) - PROBA-V data*

Table 3-37: ANOVA summary table - cropland classes and bare areas classes - PROBA-V data

	Source of variation	Sum of squares	Degrees of Freedom	Mean square	F ratio	$F_{(dfn,dfd)}$ significance level 0.05
Band 1	Condition	5.954	1	5.95407	9569.123	3.843
	Error	3.250	5223	0.00062		
	Total	9.204				
Band 2	Condition	63.809	1	63.80937	9387.555	3.843
	Error	35.502	5223	0.00680		
	Total	99.311				
Band 3	Condition	21.446	1	21.44602	2058.641	3.843
	Error	54.411	5223	0.01042		
	Total	75.857				
Band 4	Condition	79.211	1	79.21062	5045.298	3.843
	Error	82.001	5223	0.01570		
	Total	161.211				

3.3.3.7 *ANOVA - Cropland (10, 11, 12) and urban (190) - PROBA-V data*

Table 3-38: ANOVA summary table - cropland classes and urban area class - PROBA-V data

	Source of variation	**Sum of squares**	**Degrees of Freedom**	**Mean square**	**F ratio**	**$F_{(dfn,dfd)}$** significance level 0.05
Band 1	Condition	0.043	1	0.04325	127.691	3.843
	Error	1.334	3938	0.00034		
	Total	1.377				
Band 2	Condition	0.140	1	0.13962	69.030	3.843
	Error	7.965	3938	0.00202		
	Total	8.105				
Band 3	Condition	7.288	1	7.28801	1813.829	3.843
	Error	15.823	3938	0.00402		
	Total	23.111				
Band 4	Condition	9.081	1	9.08150	2139.163	3.843
	Error	16.718	3938	0.00425		
	Total	25.800				

3.3.3.8 *ANOVA - Urban (190) and bare areas (200, 201, 202) - PROBA-V data*

Table 3-39: ANOVA summary table - urban area class and bare areas classes - PROBA-V data

	Source of variation	**Sum of squares**	**Degrees of Freedom**	**Mean square**	**F ratio**	**$F_{(dfn,dfd)}$** significance level 0.05
Band 1	Condition	3.578	1	3.57827	5206.638	3.843
	Error	2.926	4257	0.00069		
	Total	6.504				
Band 2	Condition	52.864	1	52.86408	7651.821	3.843
	Error	29.410	4257	0.00691		
	Total	82.274				

	Source of variation	Sum of squares	Degrees of Freedom	Mean square	F ratio	$F_{(dfn,dfd)}$ significance level 0.05
Band 3	Condition	45.615	1	45.61494	4638.669	3.843
	Error	41.862	4257	0.00983		
	Total	87.477				
Band 4	Condition	115.700	1	115.69954	7284.358	3.843
	Error	67.615	4257	0.01588		
	Total	183.315				

3.3.4 Results of the analysis of the local variance for the various spectral reflectance values within a LC class and across LC classes for the AVHRR data

The following table (Table 3-40) show the variance of the spectral reflectance values at the class level for the SR time series of AVHRR data for the yearly maps (1992 - 1999). The subsequent tables (Table 3-41 through Table 3-48) show the corresponding ANOVA summary table.

The results of ANOVA for the all analysed combinations of LC-CCI classes show that the differences between class means and their variation among and between classes are statistical significance. The ANOVA of individual AVHRR bands can also result in rejection of the null hypothesis, e.g. AVHRR band 1 for the ANOVA for forest and inundated forest (see Table 3-42).

The number of pixels which contribute to the analysis is very variable whereas this can be caused by the data availability or by the cloud coverage (see also section 3.2).

Table 3-40: Variance of the spectral reflectance values at the class level – AVHRR time series and band 1 to 2

	OBS. COUNTS	AVHRR SR BAND 1	AVHRR SR BAND 2
Cropland	2070	0.00341	0.00501
Forest - LC-CCI Class 50	1621	0.00072	0.00106
Forest - LC-CCI Class 60	1629	0.00082	0.00222
Forest - LC-CCI Class 70	806	0.00066	0.00075
Forest - LC-CCI Class 80	385	0.00062	0.00161
Forest - LC-CCI Class 90	1992	0.00222	0.00329
Grassland	686	0.00082	0.00188

	OBS. COUNTS	AVHRR SR BAND 1	AVHRR SR BAND 2
Sparse vegetation	3251	0.00900	0.01307
Inundated forest	1115	0.00087	0.00113
Wetland	1818	0.00413	0.00320
Urban areas	1911	0.00310	0.00323
Bare areas	4979	0.00945	0.01446

3.3.4.1 *ANOVA - Different forest classes (50, 60, 70, 80 and 90) – AVHRR data*

Table 3-41: ANOVA summary table - different forest classes - AVHRR data

	Source of variation	Sum of squares	Degrees of Freedom	Mean square	F ratio	$F_{(dfn,dfd)}$ significance level 0.05
Band 1	Condition	0.197	4	0.04923	64.464	2.372
	Error	4.239	5551	0.00076		
	Total	4.436				
Band 2	Condition	1.085	4	0.27133	192.543	2.372
	Error	7.823	5551	0.00141		
	Total	8.908				

3.3.4.2 *ANOVA - Forest (50, 60, 70, 80 and 90) and inundated forest (160 and 170) - AVHRR data*

Table 3-42: ANOVA summary table - forest classes and inundated forest classes - AVHRR data

	Source of variation	Sum of squares	Degrees of Freedom	Mean square	F ratio	$F_{(dfn,dfd)}$ significance level 0.05
Band 1	Condition	0.003	1	0.00295	3.682	3.843
	Error	5.000	6240	0.00080		
	Total	5.003				
Band 2	Condition	0.289	1	0.28943	177.090	3.843

	Source of variation	Sum of squares	Degrees of Freedom	Mean square	F ratio	$F_{(dfn,dfd)}$ significance level 0.05
	Error	10.198	6240	0.00163		
	Total	10.488				

3.3.4.3 *ANOVA - Inundated forest (160 and 170) and wetland (180) - AVHRR data*

Table 3-43: ANOVA summary table - inundated forest classes and wetland class - AVHRR data

	Source of variation	Sum of squares	Degrees of Freedom	Mean square	F ratio	$F_{(dfn,dfd)}$ significance level 0.05
Band 1	Condition	0.550	1	0.54990	170.391	3.843
	Error	8.075	2502	0.00323		
	Total	8.625				
Band 2	Condition	0.001	1	0.00094	0.332	3.843
	Error	7.096	2502	0.00284		
	Total	7.097				

3.3.4.4 *ANOVA - Cropland (10, 11, 12) and grassland (130) - AVHRR data*

Table 3-44: ANOVA summary table - cropland classes and grassland class - AVHRR data

	Source of variation	Sum of squares	Degrees of Freedom	Mean square	F ratio	$F_{(dfn,dfd)}$ significance level 0.05
Band 1	Condition	0.185	1	0.18543	65.685	3.843
	Error	11.461	4060	0.00282		
	Total	11.647				
Band 2	Condition	1.531	1	1.53084	367.466	3.843
	Error	16.914	4060	0.00417		
	Total	18.445				

3.3.4.5 *ANOVA - Cropland (10, 11, 12) and sparse vegetation (150, 151, 152, 153) – AVHRR data*

Table 3-45: ANOVA summary table - cropland classes and sparse vegetation classes - AVHRR data

	Source of variation	Sum of squares	Degrees of Freedom	Mean square	F ratio	$F_{(dfn,dfd)}$ significance level 0.05
Band 1	Condition	2.569	1	2.56935	376.442	3.843
	Error	36.304	5319	0.00683		
	Total	38.873				
Band 2	Condition	0.545	1	0.54531	54.894	3.843
	Error	52.839	5319	0.00993		
	Total	53.384				

3.3.4.6 *ANOVA - Cropland (10, 11, 12) and bare areas (200, 201, 202) - AVHRR data*

Table 3-46: ANOVA summary table - cropland classes and bare areas classes - AVHRR data

	Source of variation	Sum of squares	Degrees of Freedom	Mean square	F ratio	$F_{(dfn,dfd)}$ significance level 0.05
Band 1	Condition	33.220	1	33.21950	4329.478	3.843
	Error	54.071	7047	0.00767		
	Total	87.290				
Band 2	Condition	19.542	1	19.54196	1672.160	3.843
	Error	82.356	7047	0.01169		
	Total	101.898				

3.3.4.7 *ANOVA - Cropland (10, 11, 12) and urban (190) - AVHRR data*

Table 3-47: ANOVA summary table - cropland classes and urban area class - AVHRR data

	Source of variation	Sum of squares	Degrees of Freedom	Mean square	F ratio	$F_{(dfn,dfd)}$ significance level 0.05
Band 1	Condition	0.002	1	0.00171	0.524	3.843

	Source of variation	Sum of squares	Degrees of Freedom	Mean square	F ratio	$F_{(dfn,dfd)}$ significance level 0.05
	Error	12.976	3979	0.00326		
	Total	12.978				
Band 2	Condition	1.516	1	1.51589	364.956	3.843
	Error	16.527	3979	0.00415		
	Total	18.043				

3.3.4.8 *ANOVA - Urban (190) and bare areas (200, 201, 202) - AVHRR data*

Table 3-48: ANOVA summary table - urban area class and bare areas classes - AVHRR data

	Source of variation	Sum of squares	Degrees of Freedom	Mean square	F ratio	$F_{(dfn,dfd)}$ significance level 0.05
Band 1	Condition	31.924	1	31.92399	4153.334	3.843
	Error	52.944	6888	0.00769		
	Total	84.868				
Band 2	Condition	33.035	1	33.03550	2911.079	3.843
	Error	78.166	6888	0.01135		
	Total	111.202				

3.4 The intra- and inter-annual reflectance dynamics

The purpose of this paragraph is to present the method and the results of the validation of the global 7-day MERIS FR and RR, PROBA-V and AVHRR composites based on the analysis of the intra- and inter-annual reflectance dynamics.

3.4.1 Analysis of the intra- and inter-annual reflectance dynamics

The analysis of the intra- and inter-annual reflectance dynamics includes the computation of the mean and the standard deviation for each spectral band in the MERIS FR and RR, PROBA-V and AVHRR at the class level. The stratification is not used in the analysis.

The following classes have been selected for the analysis:

- LC-CCI-Class 10 and 20 - Cropland
- LC-CCI-Class 50 - Tree cover, broadleaved, evergreen, closed to open
- LC-CCI-Class 60 - Tree cover, broadleaved, deciduous, closed to open
- LC-CCI-Class 70 - Tree cover, needleleaved, evergreen, closed to open
- LC-CCI-Class 80 - Tree cover, needleleaved, deciduous, closed to open
- LC-CCI-Class 90 - Tree cover, mixed leaf type (broad - and needleleaved)
- LC-CCI-Class 130 - Grassland
- LC-CCI-Class 150 - Sparse vegetation
- LC-CCI-Class 160 and 170 - Tree cover, flooded
- LC-CCI-Class 180 - Shrub or herbaceous cover, flooded
- LC-CCI-Class 190 - Urban areas
- LC-CCI-Class 200 - Bare areas

For the analysis of the intra- and inter-annual reflectance dynamics the same preparative steps are necessary as for the local variance for the various spectral reflectance values within a LC class and across LC classes (see section 3.3). The selected reference points are shown in Figure 3-49.

LC-CCI-Class 10 and 20 - Cropland -

LC-CCI-Class 150 - Sparse vegetation -

LC-CCI-Class 180 - Shrub or herbaceous cover, flooded -

LC-CCI-Class 190 - Urban areas -

LC-CCI-Class 200 - Bare areas -

LC-CCI-Class 130 - Grassland -

LC-CCI-Class 50 - Tree cover, broadleaved, evergreen
LC-CCI-Class 60 - Tree cover, broadleaved, deciduous
LC-CCI-Class 70 - Tree cover, needleleaved, evergreen
LC-CCI-Class 80 - Tree cover, needleleaved, deciduous
LC-CCI-Class 90 - Tree cover, mixed leaf
LC-CCI-Class 160 and 170 - Tree cover, flooded

Figure 3-49: Selected reference points for MERIS FR and RR, PROBA-V and AVHRR data

3.4.2 Results of the analysis of the intra- and inter-annual reflectance dynamic for MERIS FR and RR

The following figures (Figure 3-50 through Figure 3-97) show the mean spectrum for each year and the mean (x_{mean}) and the range of the spectral reflectance values at the class level for the SR time series of MERIS FR and RR data for the years 2003-2012.

The range is given by twice the standard deviation (2σ). This means, that 95.45% of values lies in interval [x_{mean} $\pm 2\sigma$] under the assumption of a Gaussian distribution. Furthermore, the calculation of the mean and the standard deviation has been limited in particular to those cases in which at least 10 clear land observations per class and date are available.

The results of the analysis of the intra- and inter-annual reflectance dynamic can be summarized as follows:

- the spectra inside the class over the years are very similar but the standard deviation shows a great dispersion from the average, e.g. the very high standard deviation over the LC-CCCI class 'bare areas' reflects the natural variability of soils,
- the analysis of different 10-year temporal profiles of the mean and the range highlights similar intra-annual "structures" from year to year inside the class
- the different 10-year temporal profiles of the mean and the range do not show significant inter-annual changes,
- the number of pixels which contribute to the analysis is very variable whereas this can be caused by the data availability or by the cloud coverage (see also section 3.2).

3.4.2.1 *Cropland - LC-CCI-Class 10 and 20*

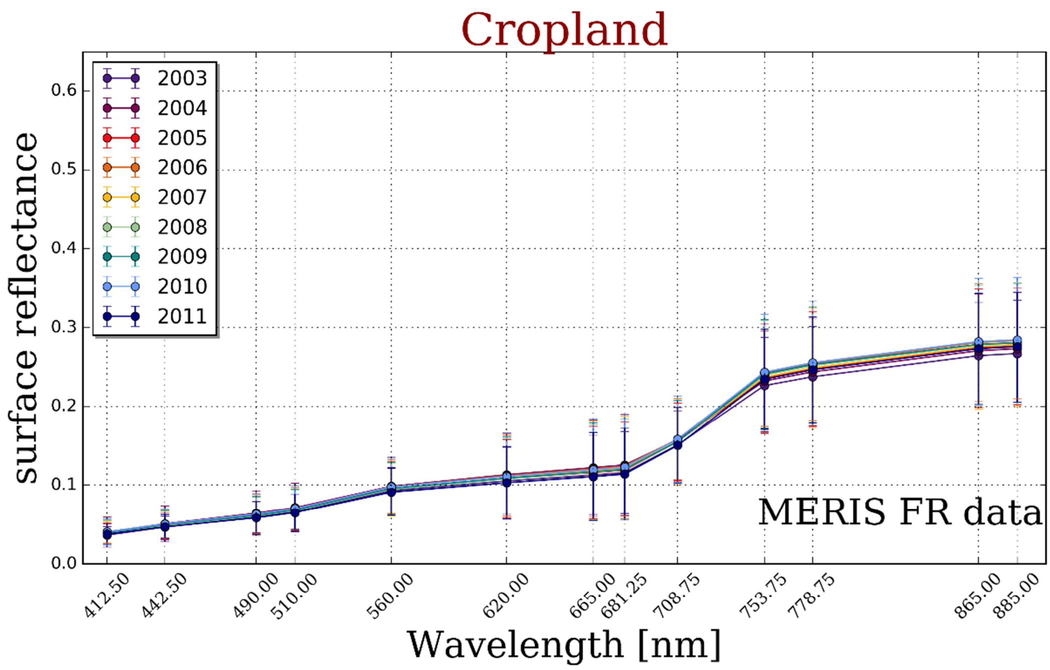

Figure 3-50: Spectra - LC-CCI-Class 10 and 20 - Cropland - MERIS FR data

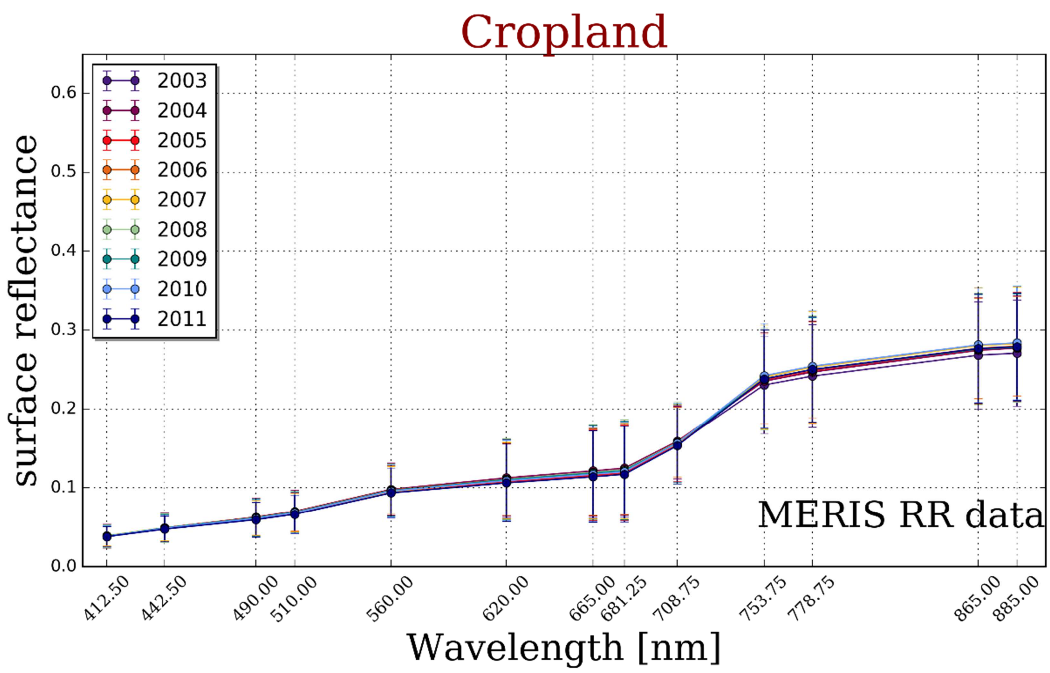

Figure 3-51: Spectra - LC-CCI-Class 10 and 20 - Cropland - MERIS RR data

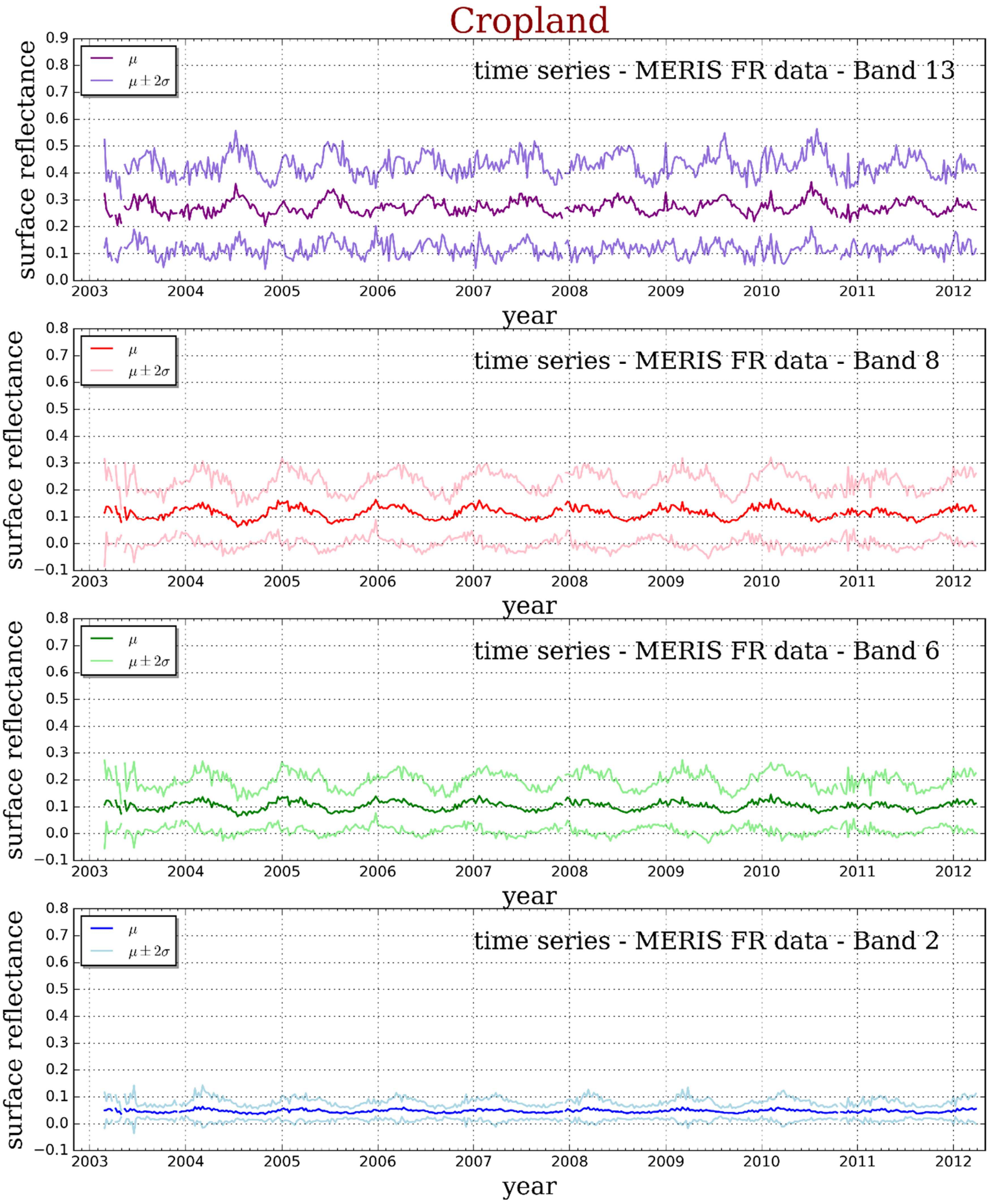

Figure 3-52: SR time series from MERIS FR data - 2003-2012 - LC-CCI-Class 10 and 20 - Cropland

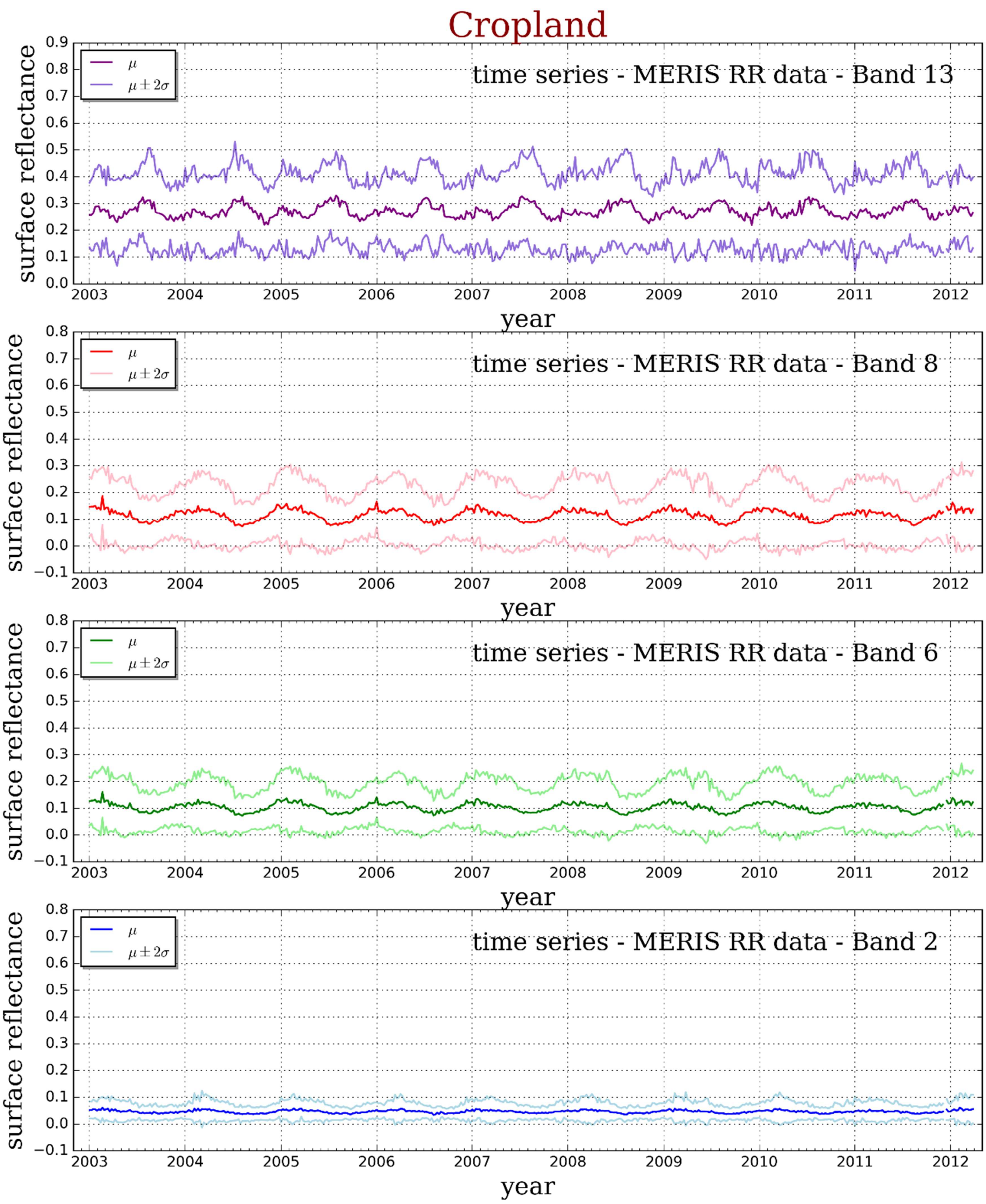

Figure 3-53: SR time series from MERIS RR data - 2003-2012 - LC-CCI-Class 10 and 20 - Cropland

3.4.2.2 *Forest - LC-CCI-Class 50 - Tree cover, broadleaved, evergreen, closed to open*

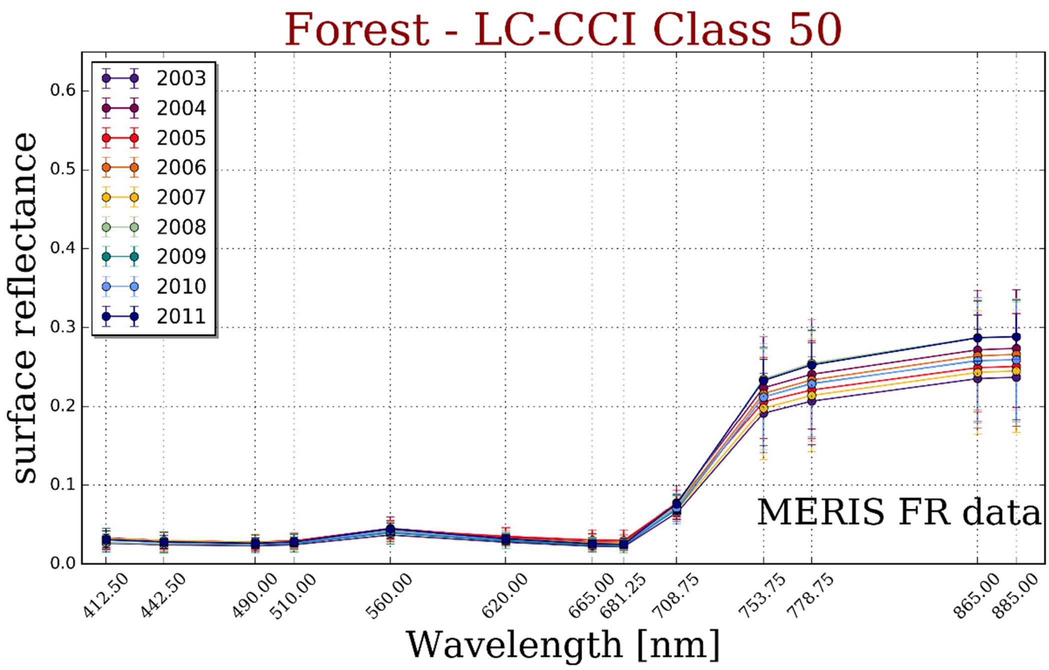

Figure 3-54: Spectra - LC-CCI-Class 50 - Tree cover, broadleaved, evergreen, closed to open - MERIS FR data

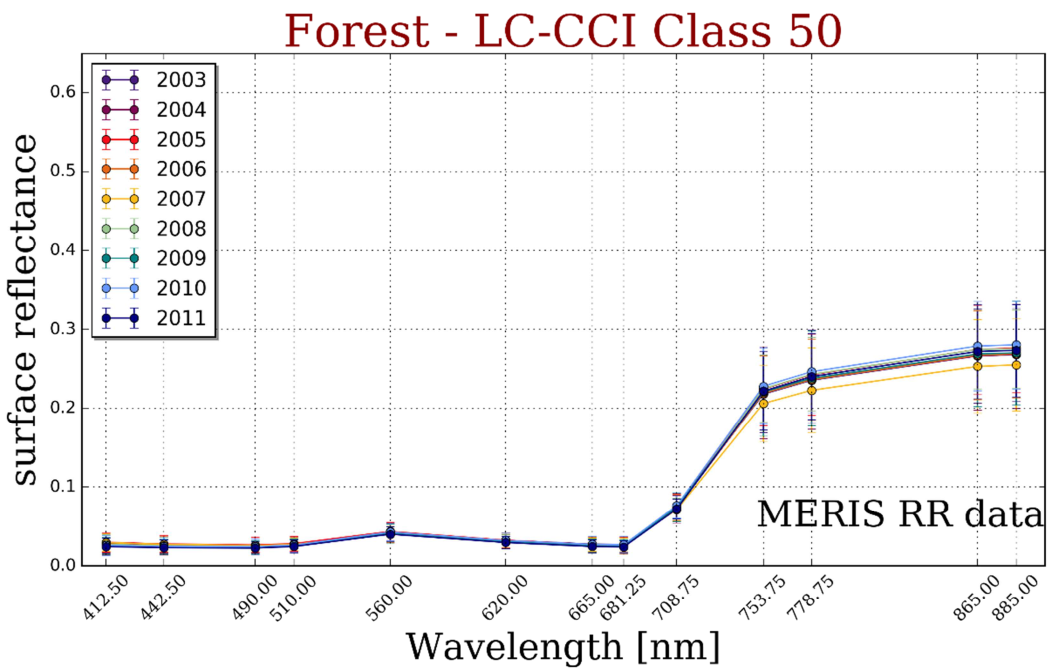

Figure 3-55: Spectra - LC-CCI-Class 50 - Tree cover, broadleaved, evergreen, closed to open - MERIS RR data

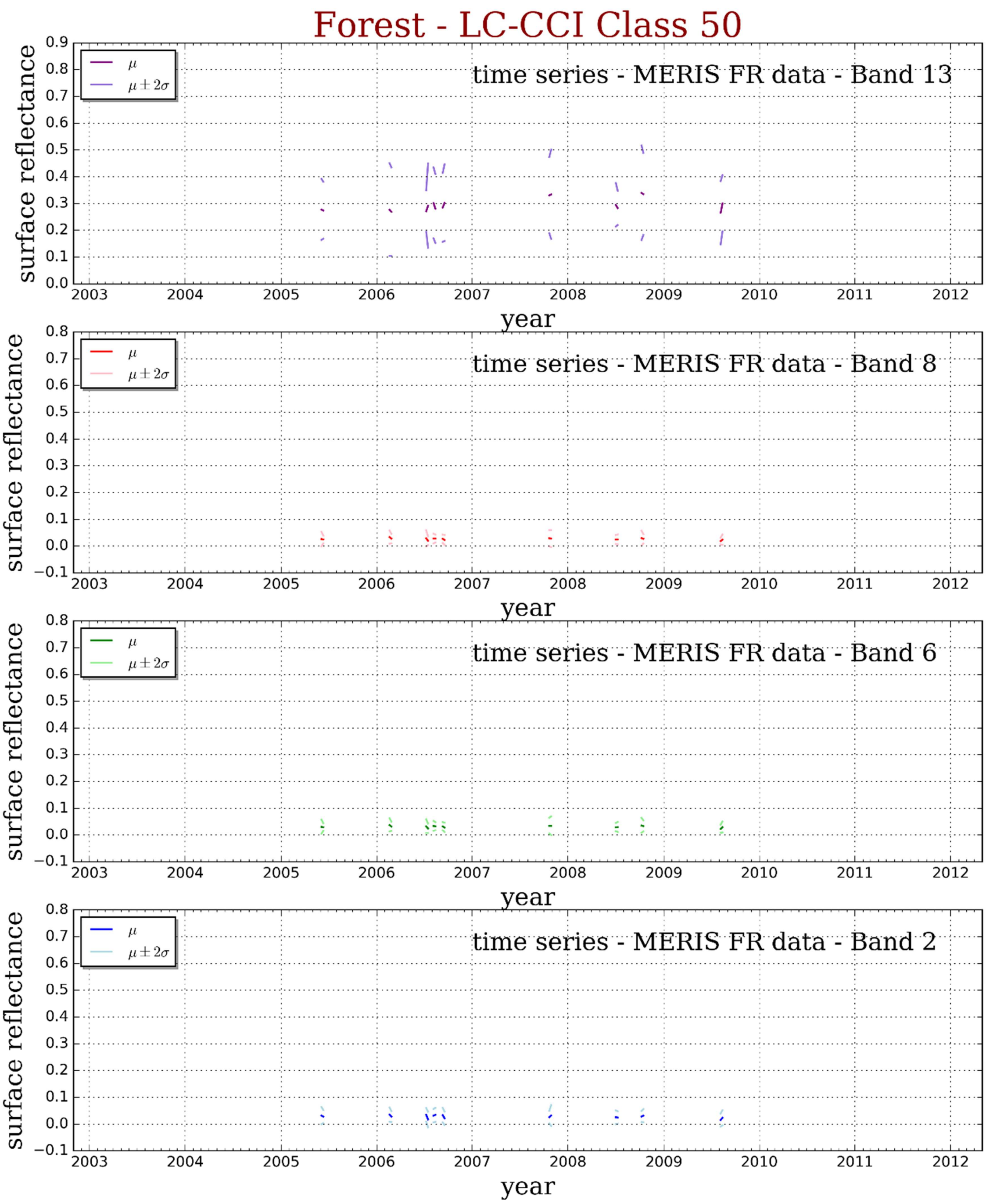

Figure 3-56: SR time series from MERIS FR data - 2003-2012 - LC-CCI-Class 50 - Tree cover, broadleaved, evergreen, closed to open

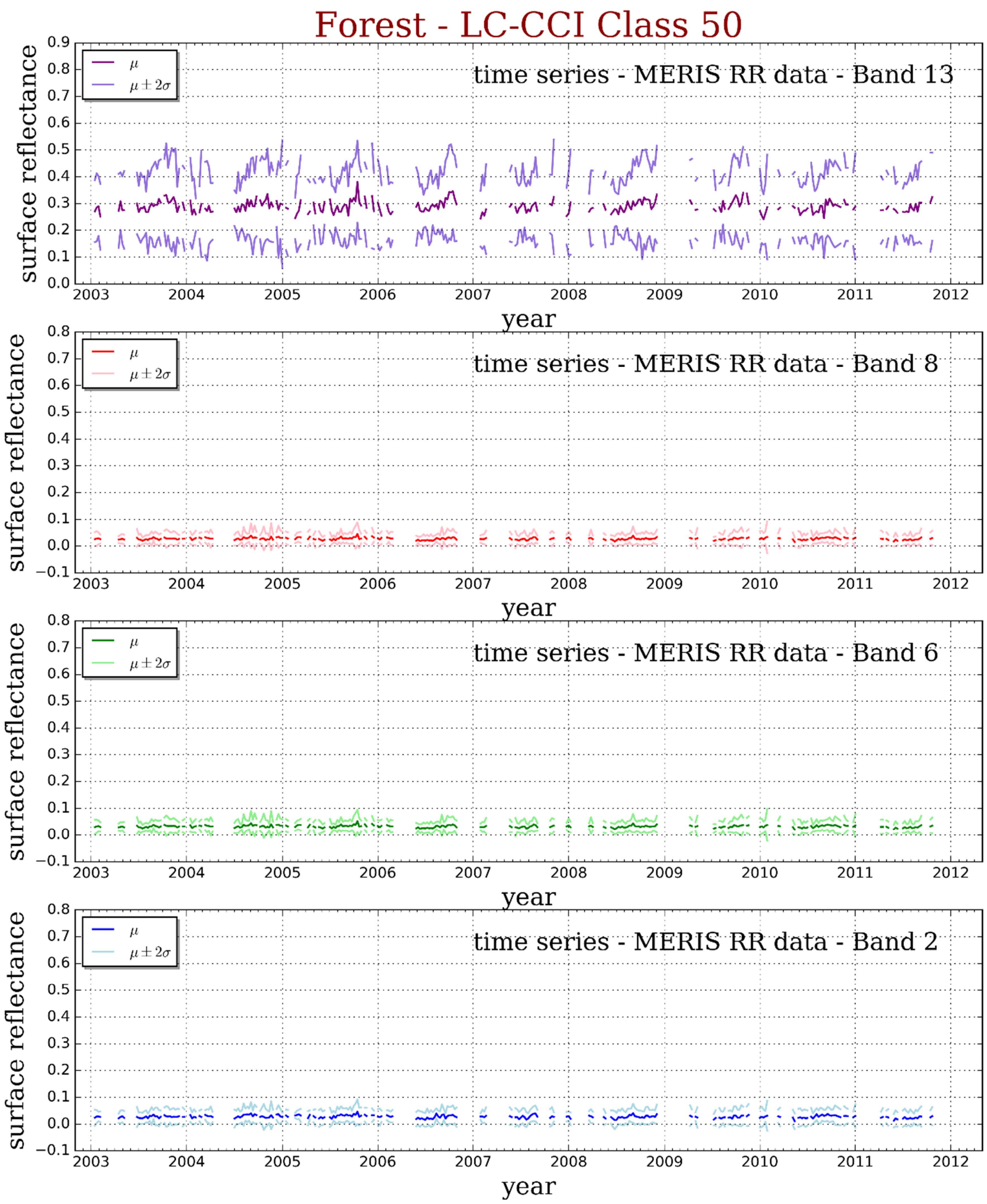

Figure 3-57: SR time series from MERIS RR data - 2003-2012 - LC-CCI-Class 50 - Tree cover, broadleaved, evergreen, closed to open

3.4.2.3 *Forest - LC-CCI-Class 60 - Tree cover, broadleaved, deciduous, closed to open*

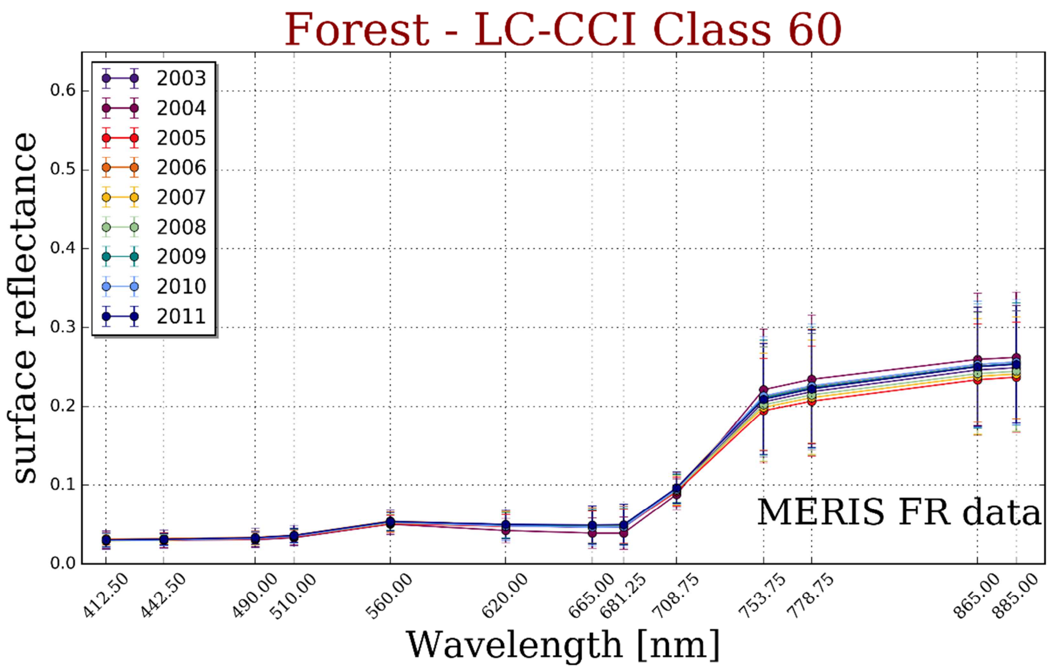

Figure 3-58: Spectra - LC-CCI-Class 60 - Tree cover, broadleaved, deciduous, closed to open - MERIS FR data

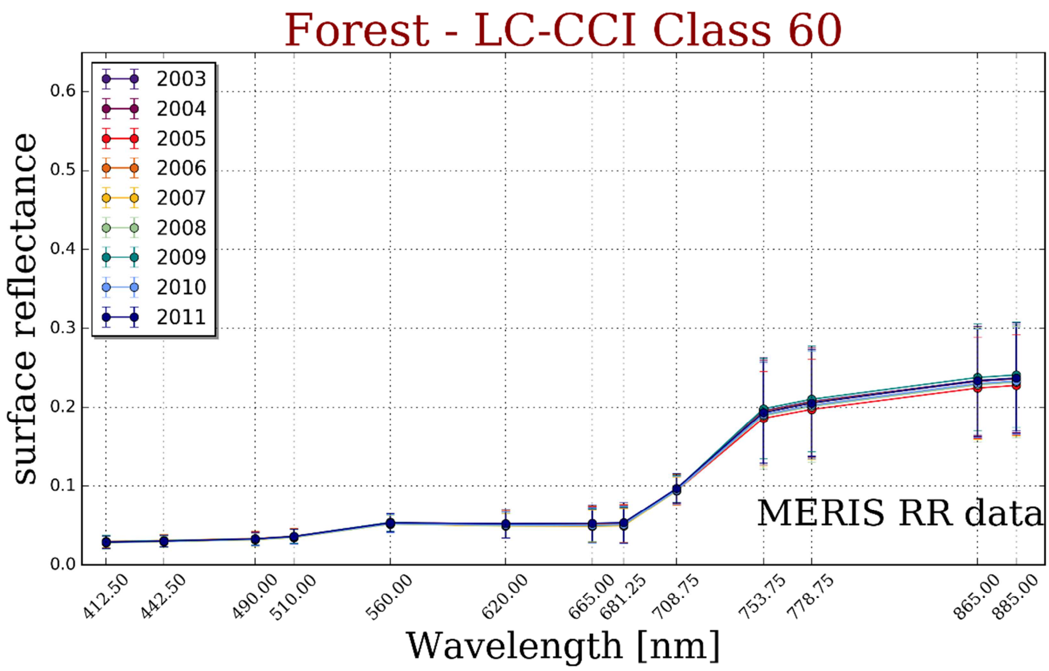

Figure 3-59: Spectra - LC-CCI-Class 60 - Tree cover, broadleaved, deciduous, closed to open - MERIS RR data

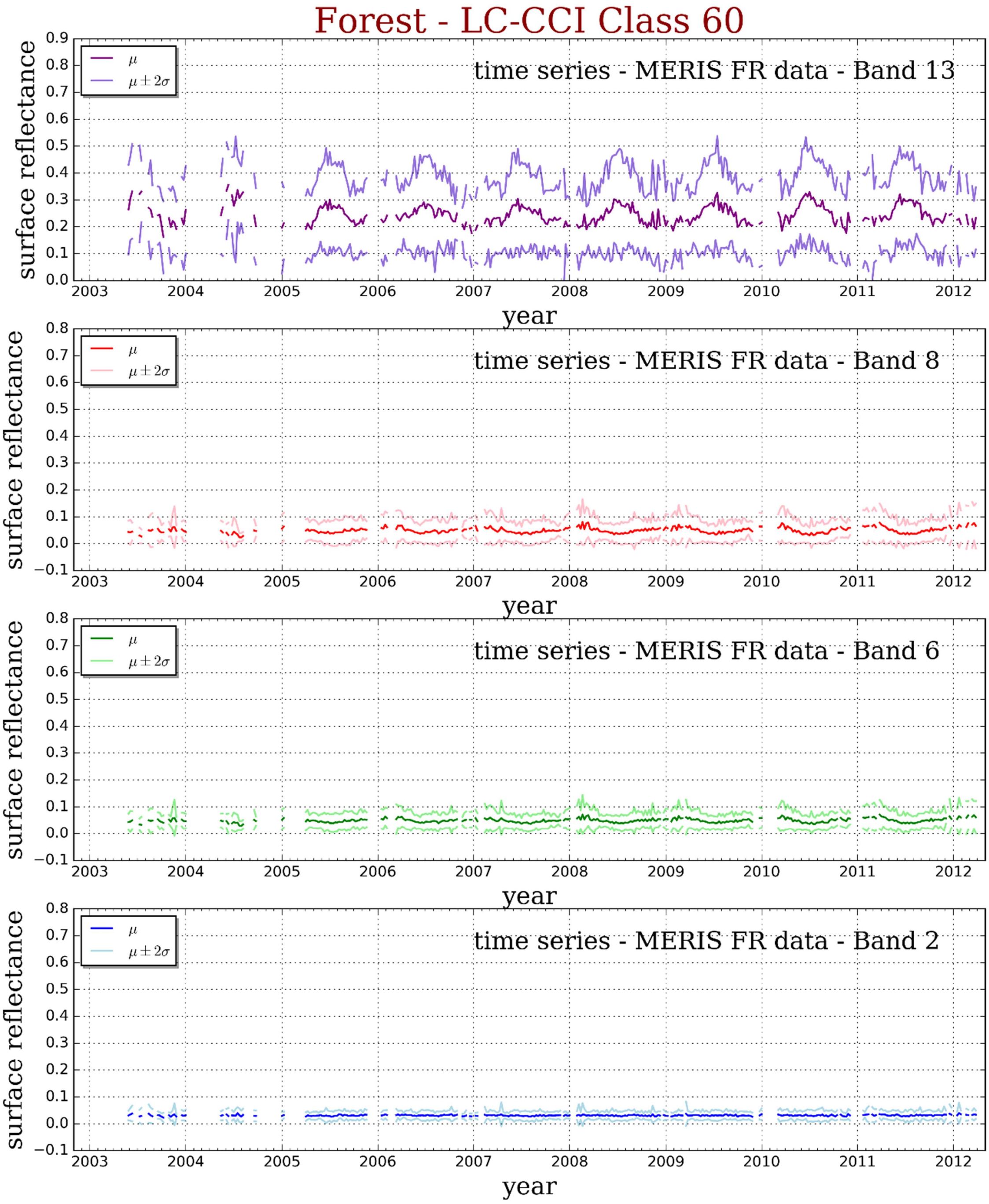

Figure 3-60: SR time series from MERIS FR data - 2003-2012 - LC-CCI-Class 60 - Tree cover, broadleaved, deciduous, closed to open

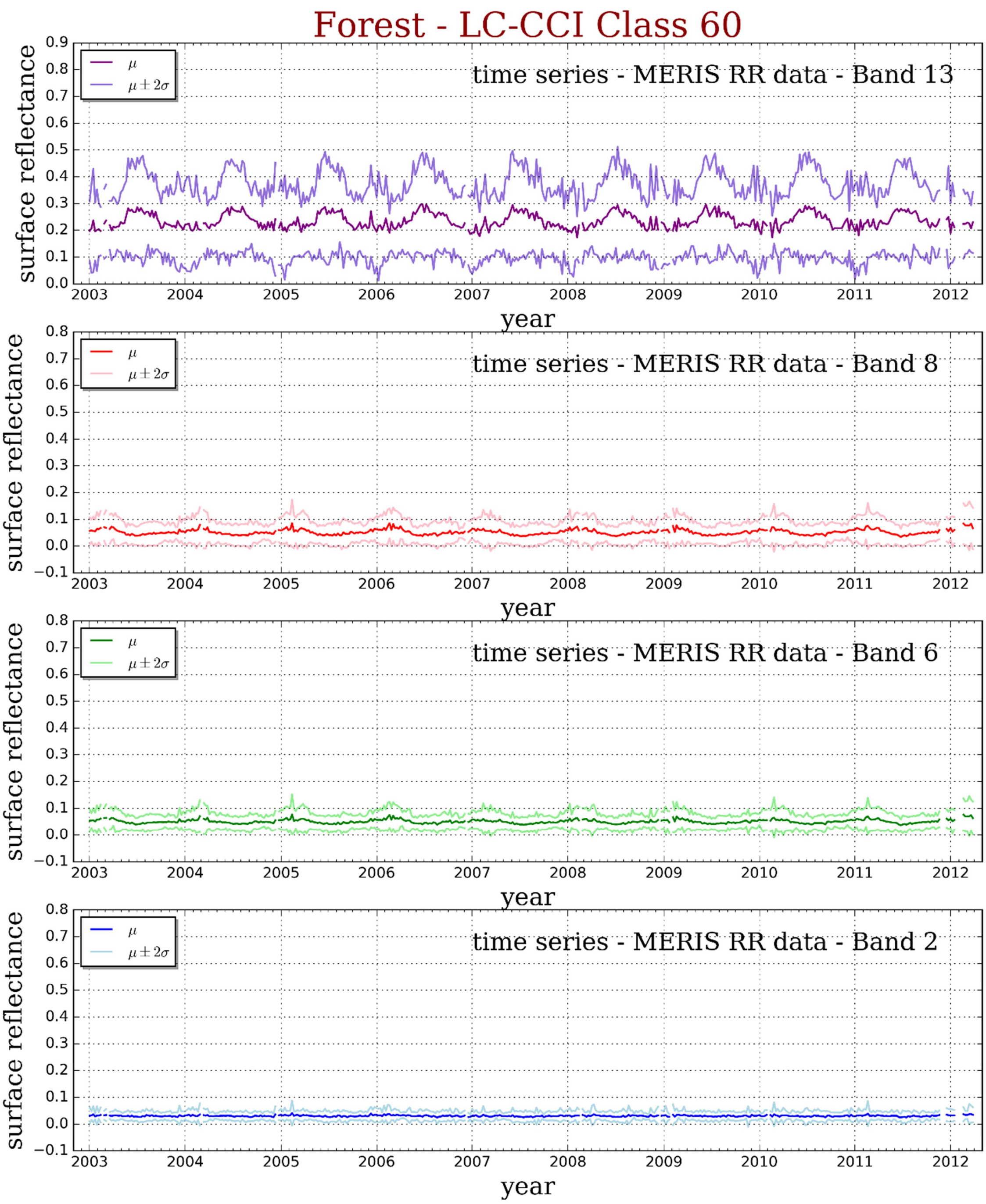

Figure 3-61: SR time series from MERIS RR data - 2003-2012 - LC-CCI-Class 60 - Tree cover, broadleaved, deciduous, closed to open

3.4.2.4 *Forest - LC-CCI-Class 70 - Tree cover, needleleaved, evergreen, closed to open*

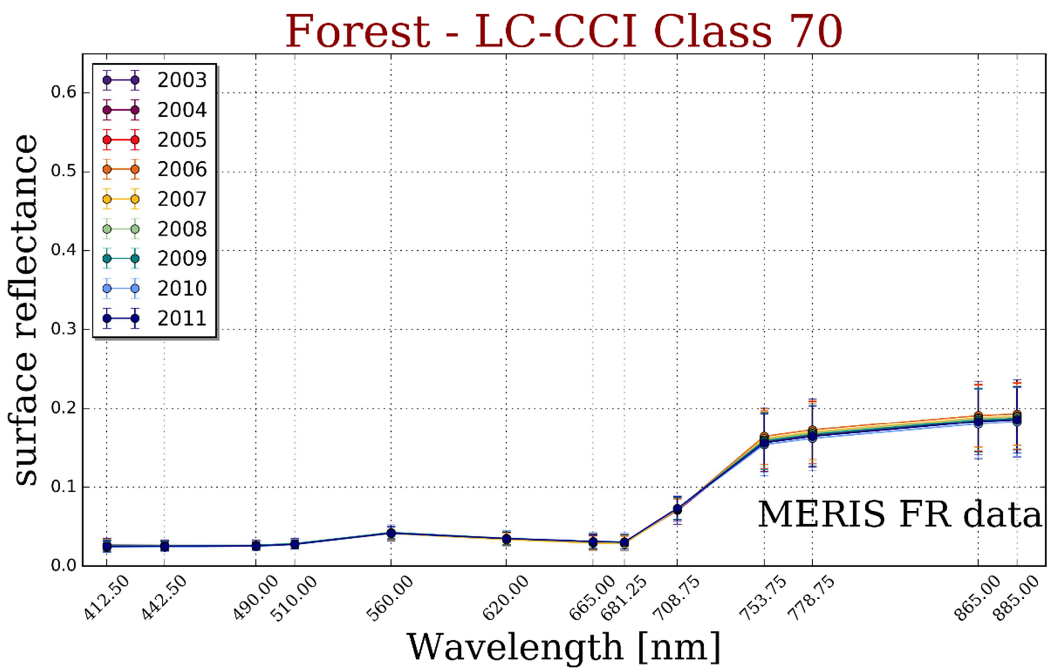

Figure 3-62: Spectra - LC-CCI-Class 70 - Tree cover, needleleaved, evergreen, closed to open - MERIS FR data

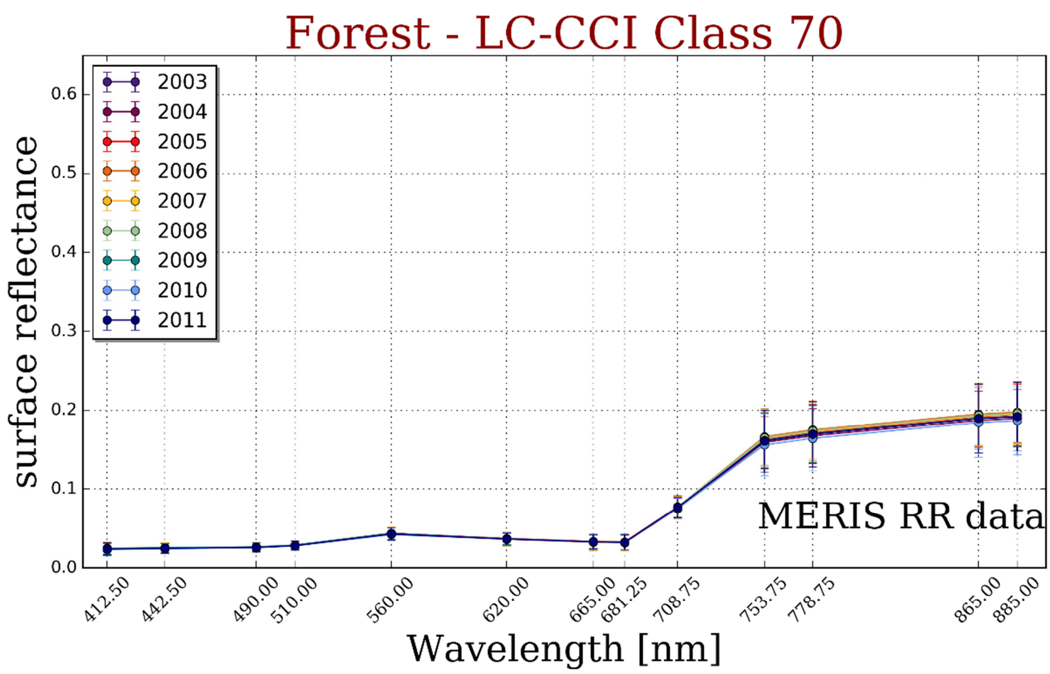

Figure 3-63: Spectra - LC-CCI-Class 70 - Tree cover, needleleaved, evergreen, closed to open - MERIS RR data

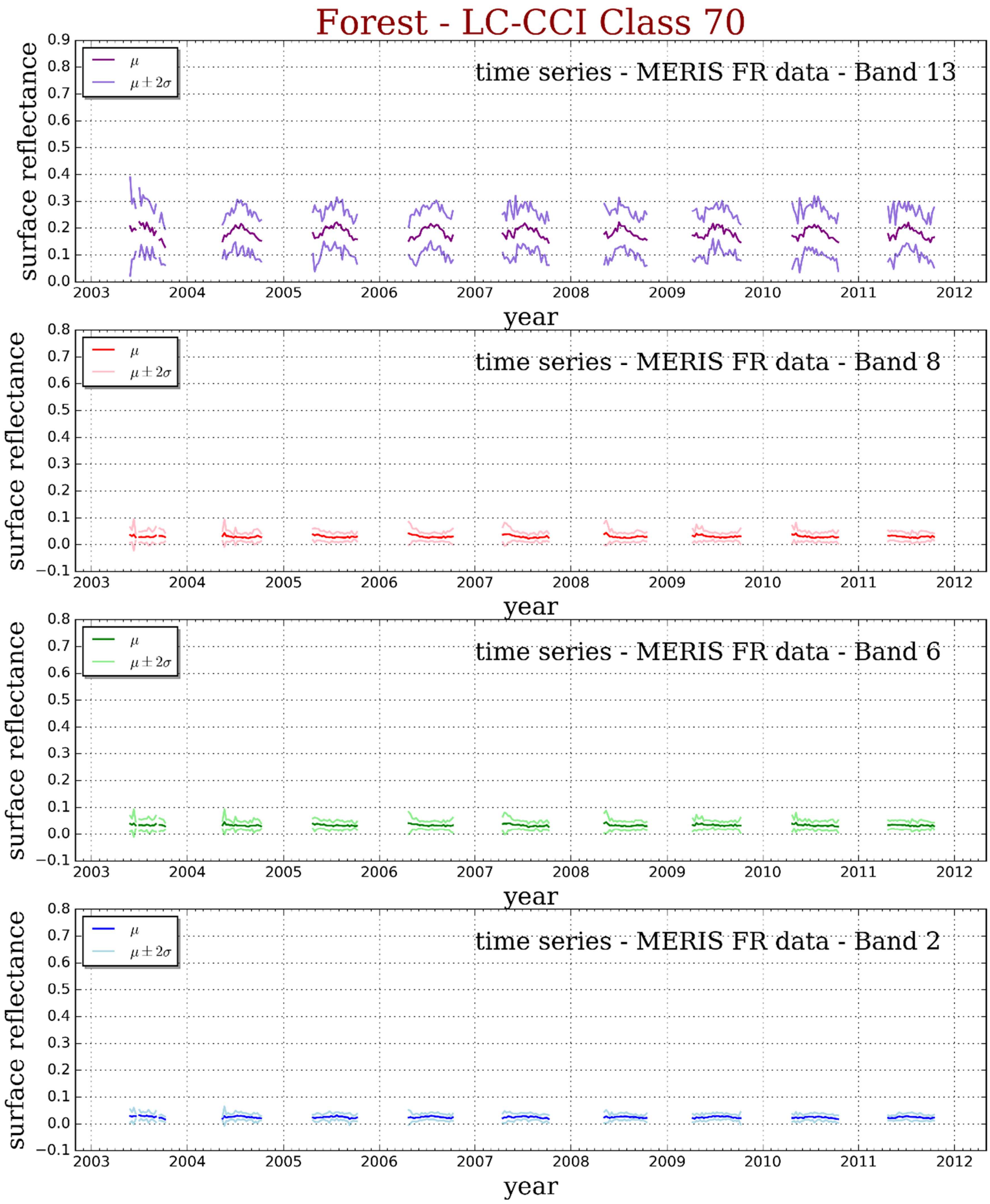

Figure 3-64: SR time series from MERIS FR data - 2003-2012 - LC-CCI-Class 70 - Tree cover, needleleaved, evergreen, closed to open

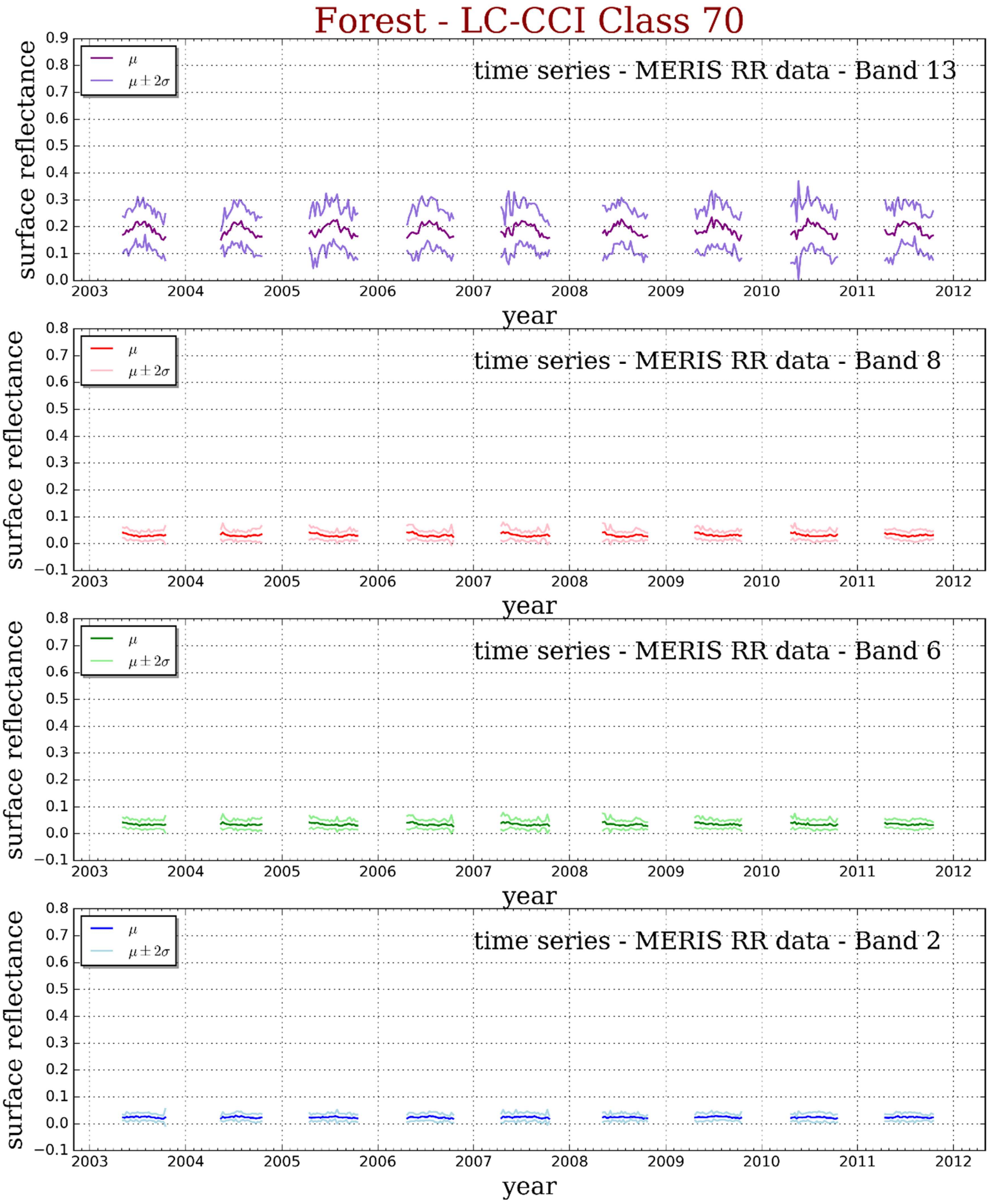

Figure 3-65: SR time series from MERIS RR data - 2003-2012 - LC-CCI-Class 70 - Tree cover, needleleaved, evergreen, closed to open

3.4.2.5 *Forest - LC-CCI-Class 80 - Tree cover, needleleaved, deciduous, closed to open*

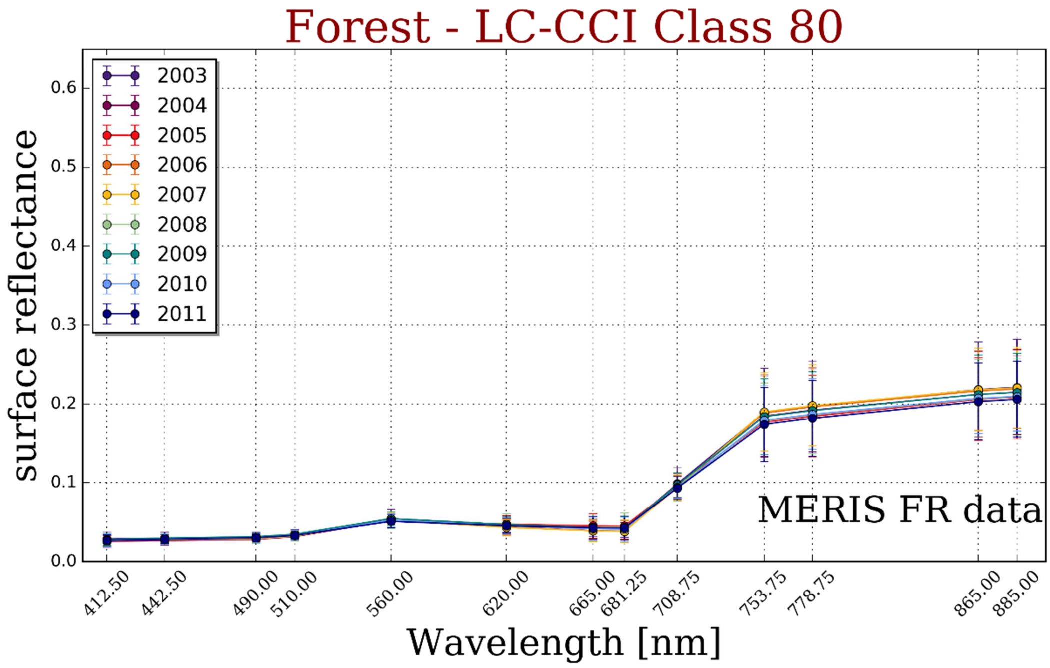

Figure 3-66: Spectra - LC-CCI-Class 80 - Tree cover, needleleaved, deciduous, closed to open - MERIS FR data

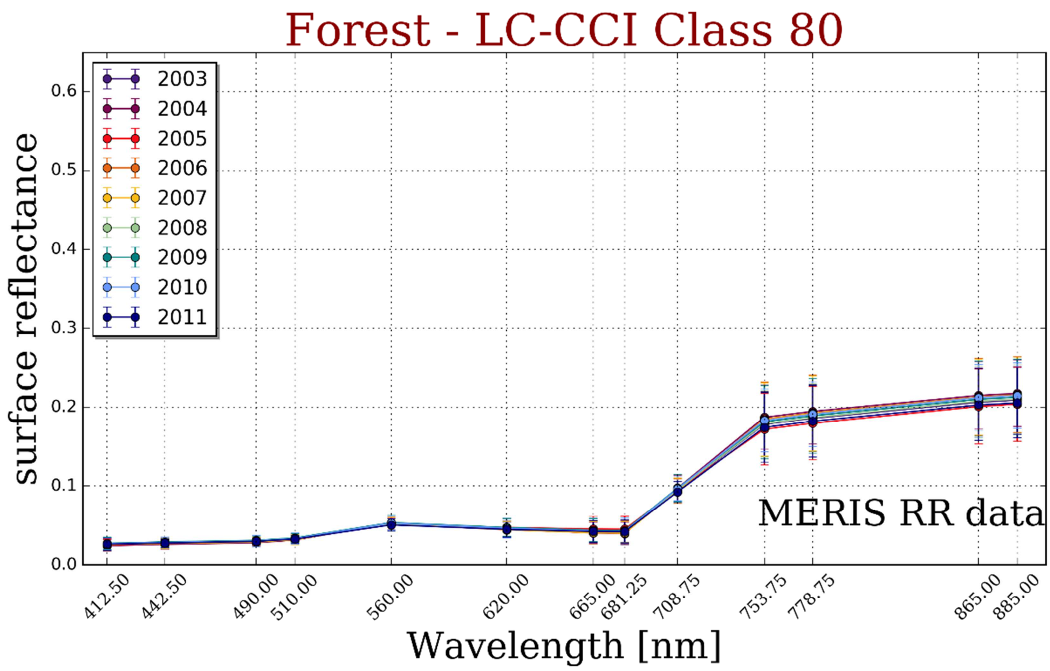

Figure 3-67: Spectra - LC-CCI-Class 80 - Tree cover, needleleaved, deciduous, closed to open - MERIS RR data

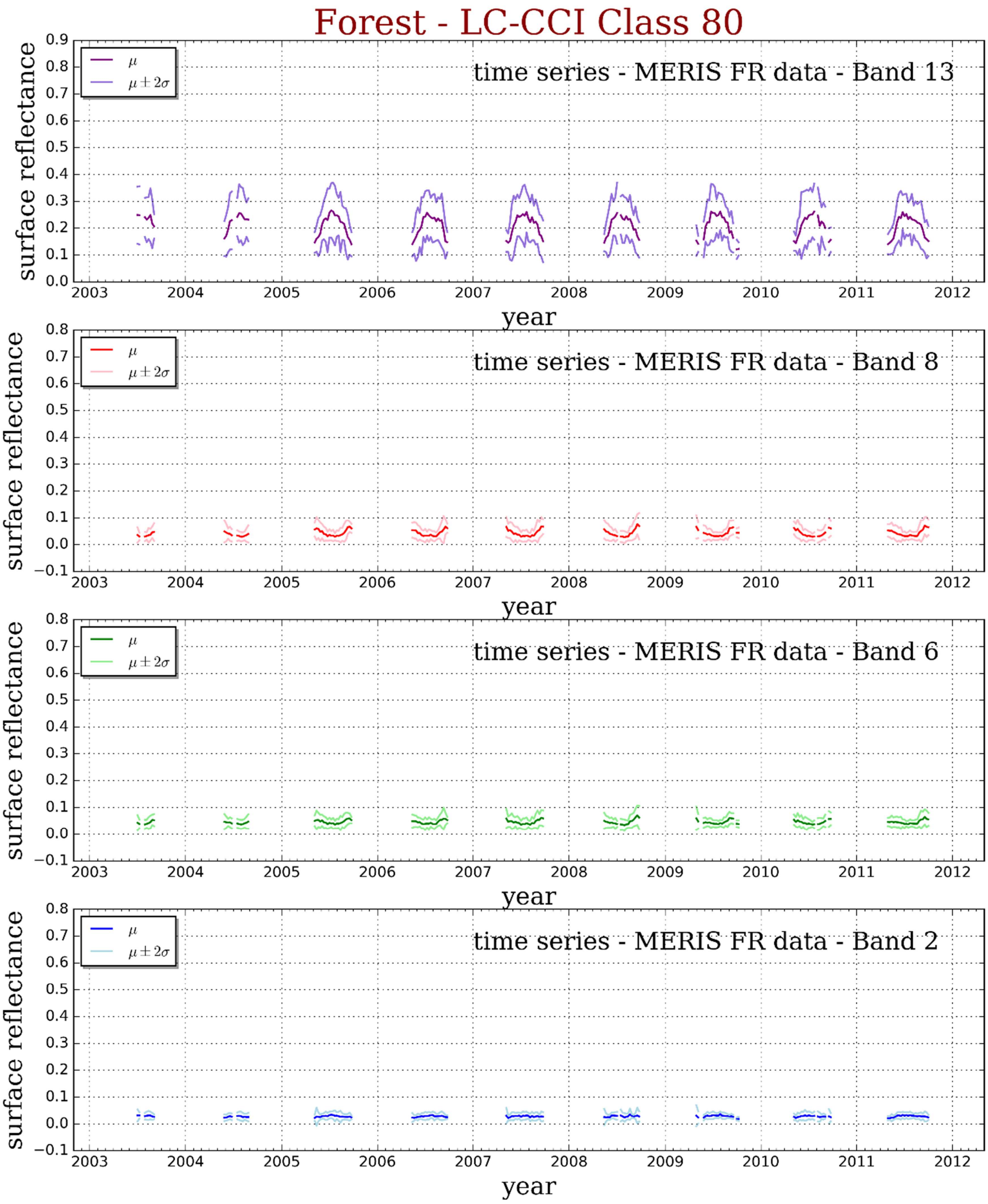

Figure 3-68: SR time series from MERIS FR data - 2003-2012 - LC-CCI-Class 80 - Tree cover, needleleaved, deciduous, closed to open

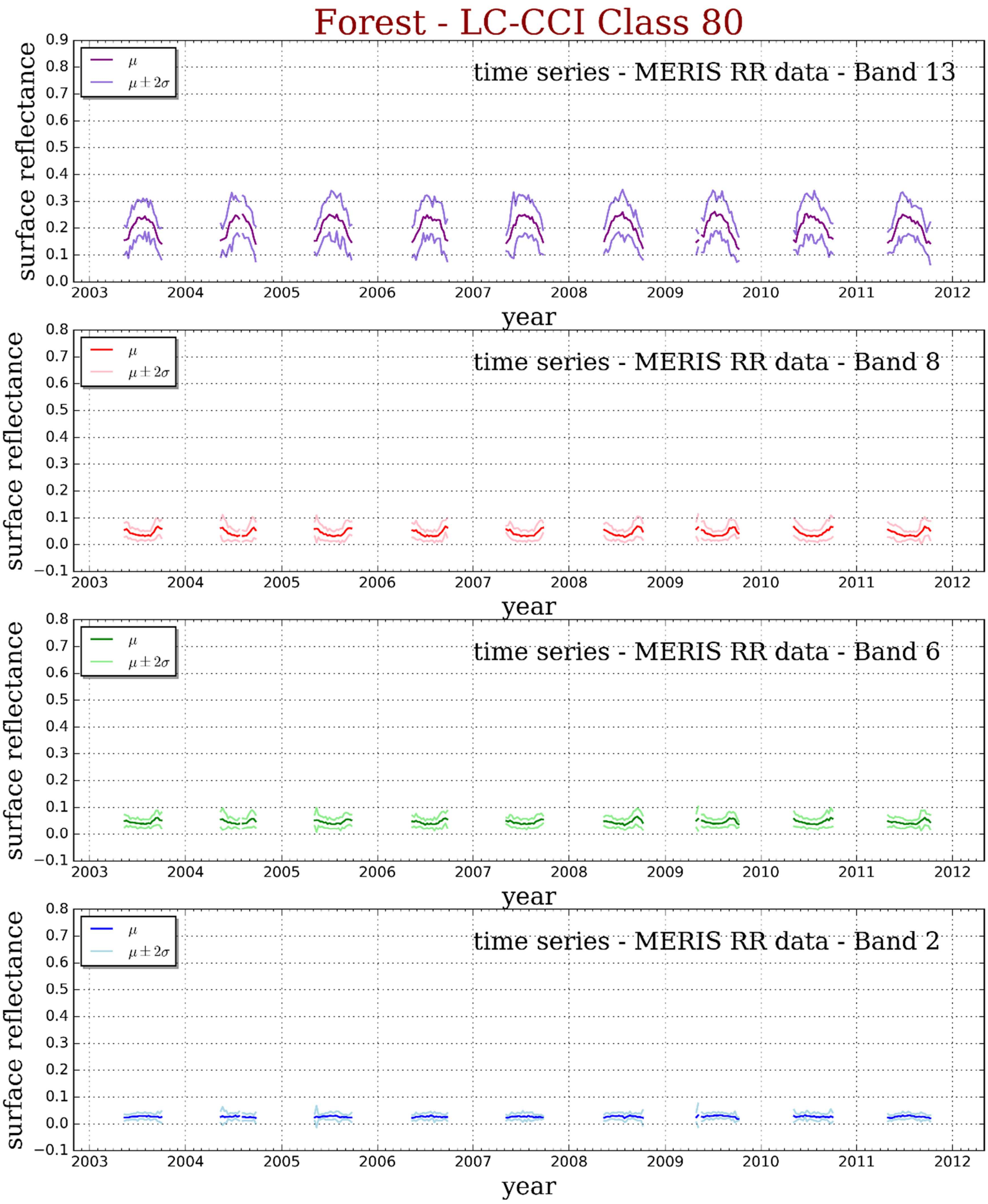

Figure 3-69: SR time series from MERIS RR data - 2003-2012 - LC-CCI-Class 80 - Tree cover, needleleaved, deciduous, closed to open

3.4.2.6 *Forest - LC-CCI-Class 90 - Tree cover, mixed leaf type (broadleaved and needleleaved)*

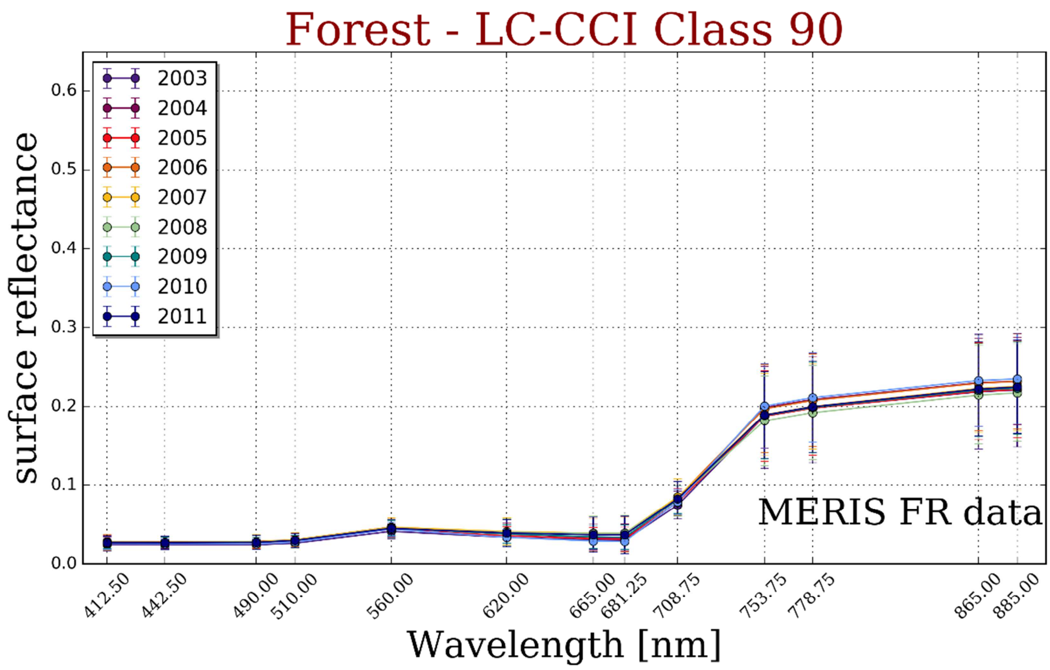

Figure 3-70: Spectra - LC-CCI-Class 90 - Tree cover, mixed leaf type (broad - and needleleaved) - MERIS FR data

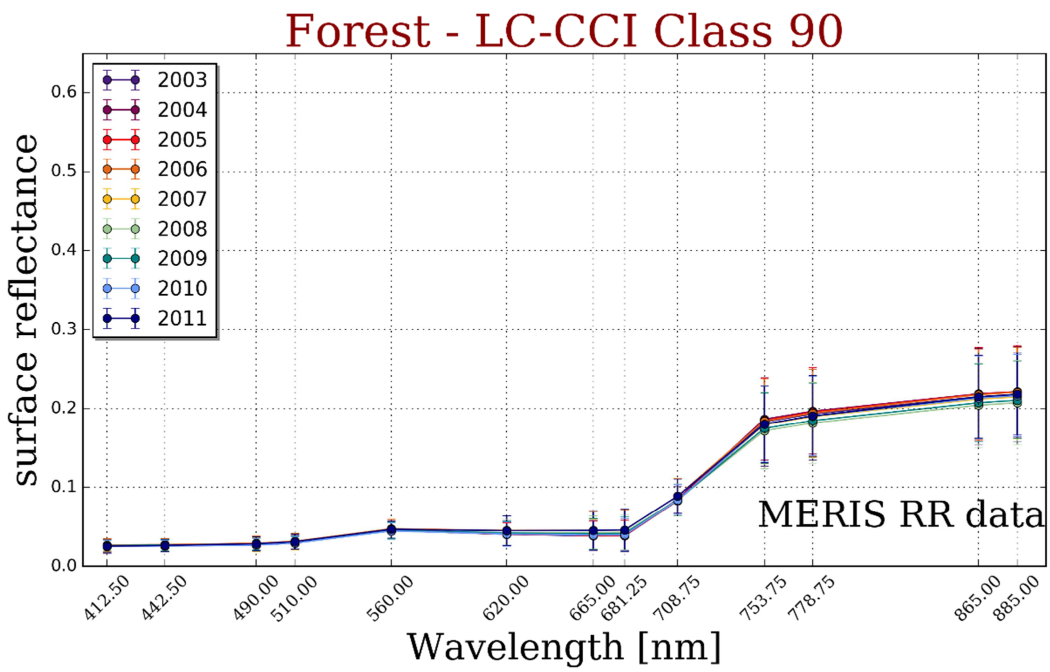

Figure 3-71: Spectra - LC-CCI-Class 90 - Tree cover, mixed leaf type (broad - and needleleaved) MERIS RR data

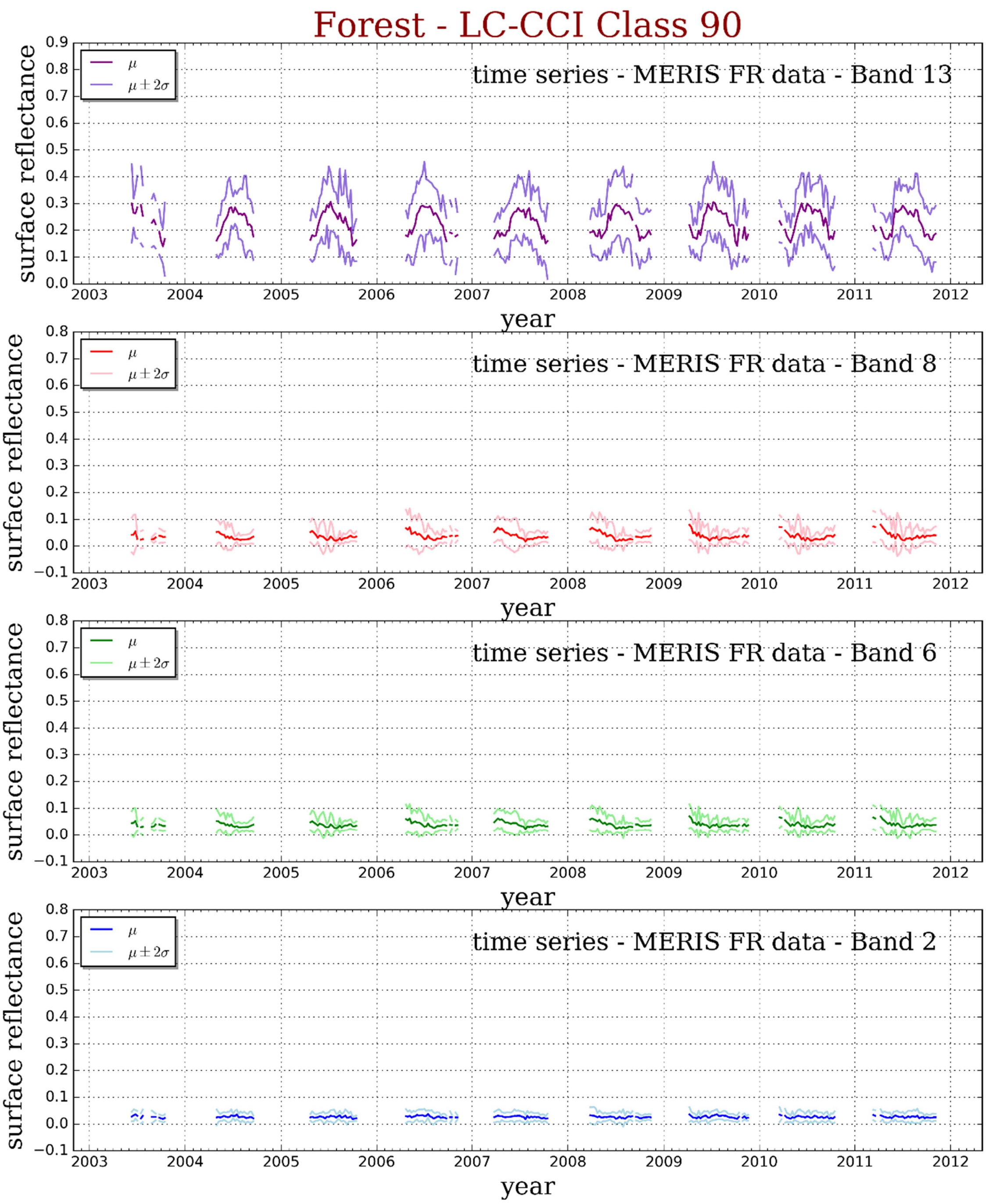

Figure 3-72: SR time series from MERIS FR data - 2003-2012 - LC-CCI-Class 90 - Tree cover, mixed leaf type (broad - and needleleaved)

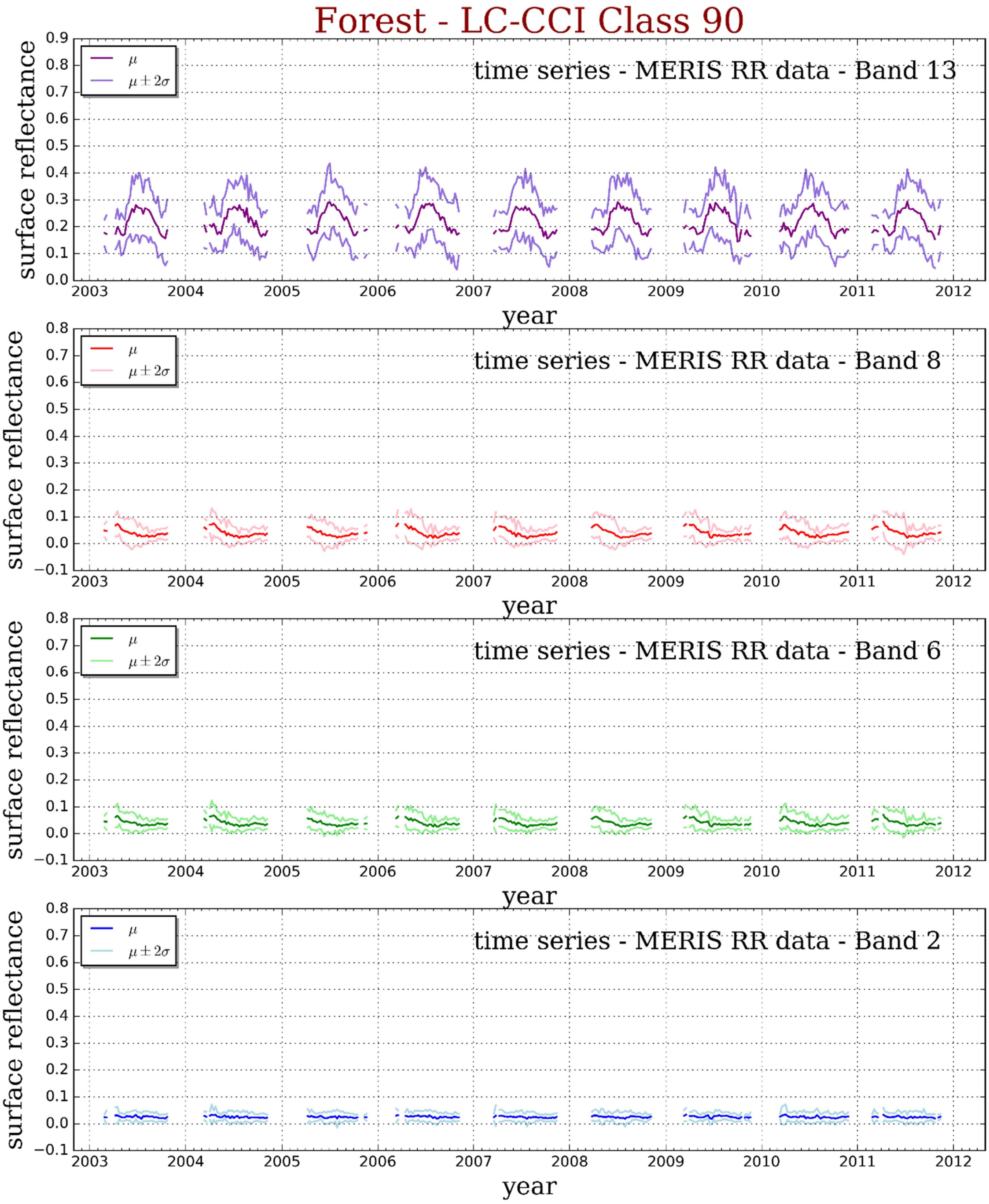

Figure 3-73: SR time series from MERIS FR data - 2003-2012 - LC-CCI-Class 90 - Tree cover, mixed leaf type (broad - and needleleaved)

3.4.2.7 *Grassland - LC-CCI-Class 130*

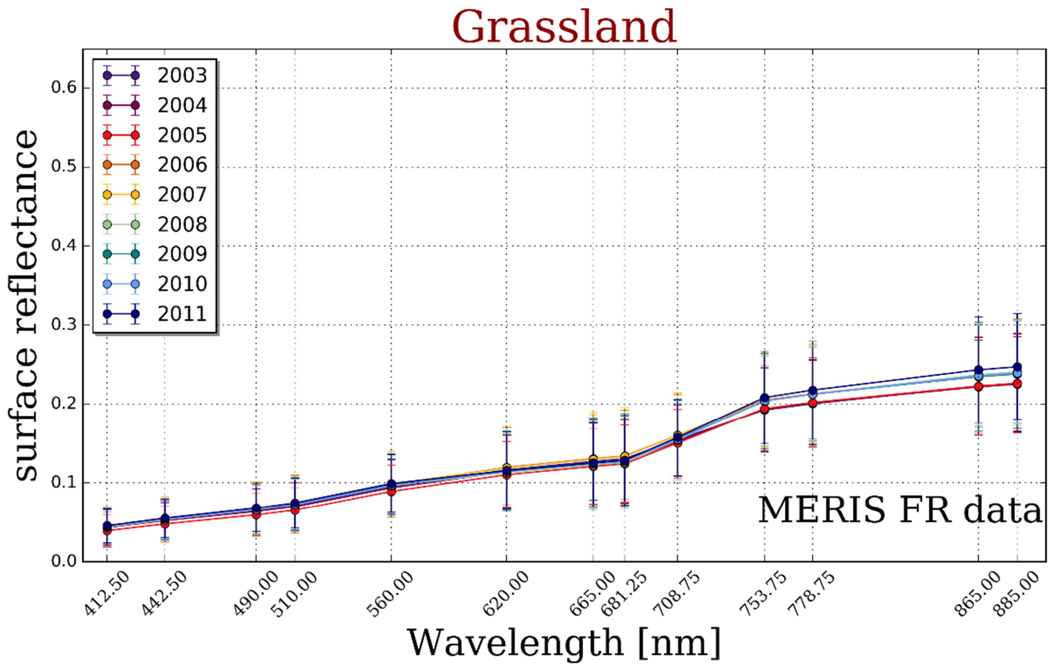

Figure 3-74: Spectra - LC-CCI-Class 130 - Grassland - MERIS FR data

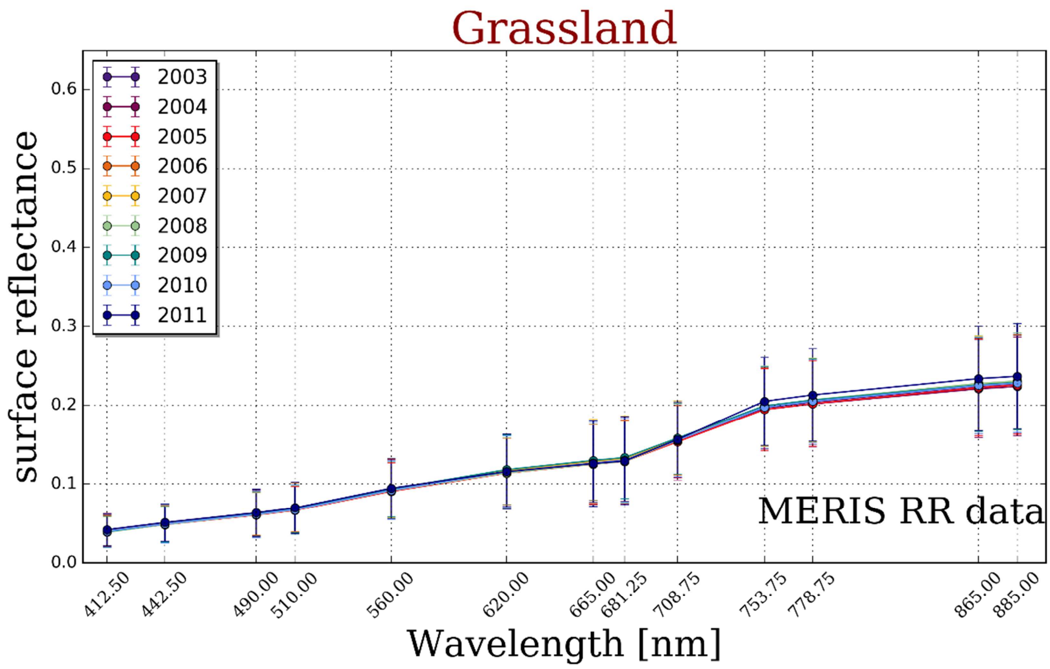

Figure 3-75: Spectra - LC-CCI-Class 130 - Grassland - MERIS RR data

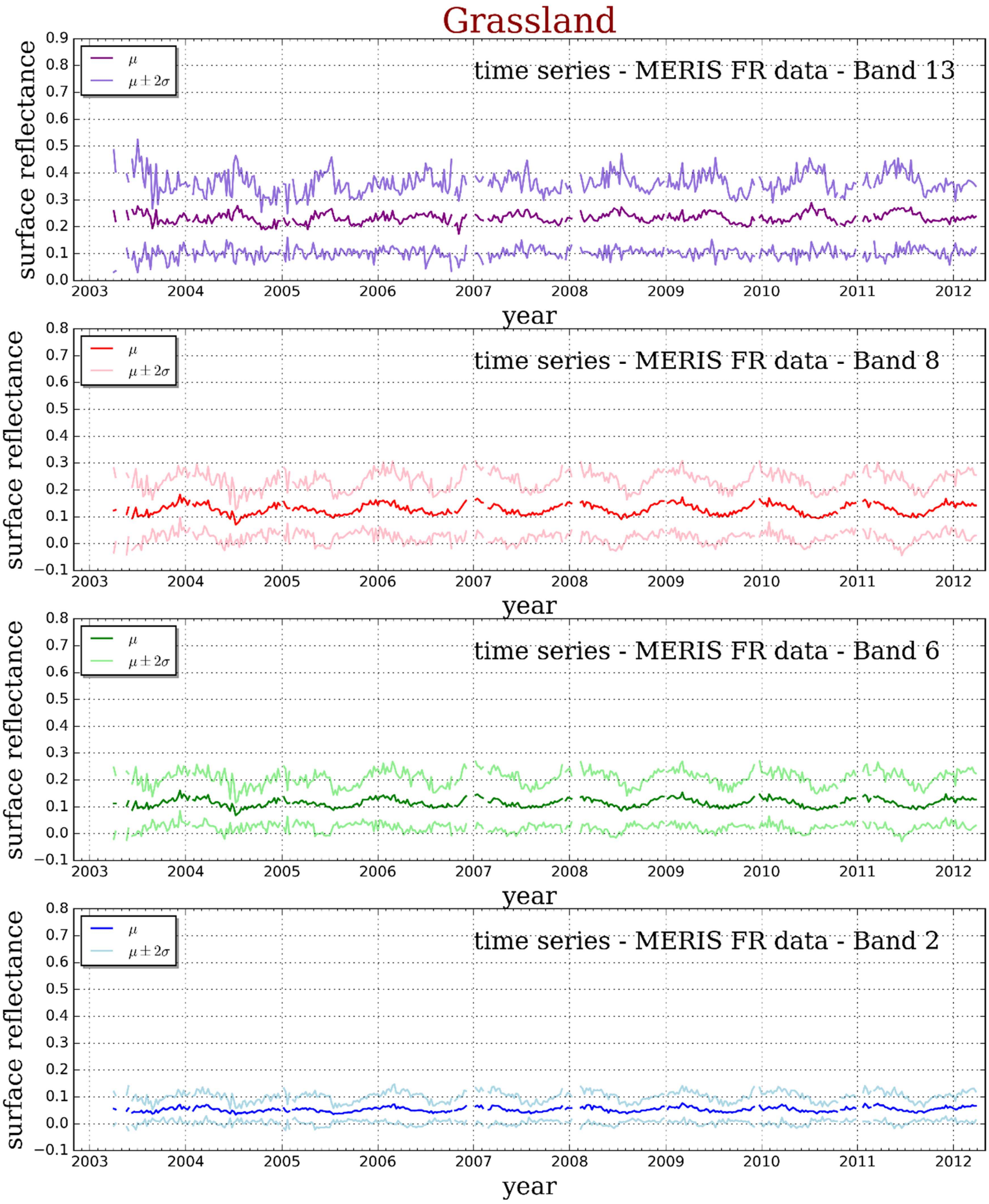

Figure 3-76: SR time series from MERIS FR data - 2003-2012 - LC-CCI-Class 130 - Grassland

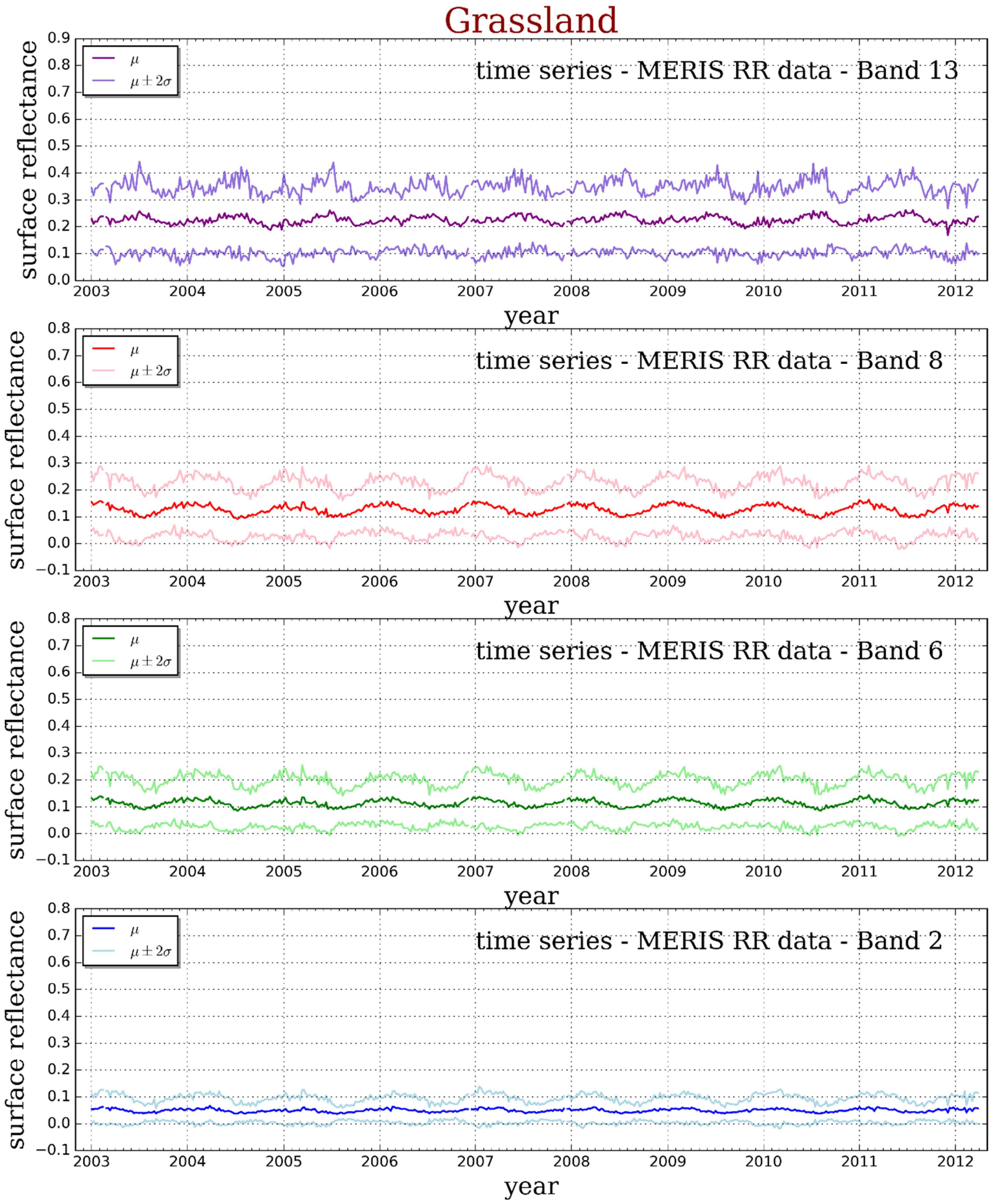

Figure 3-77: SR time series from MERIS FR data - 2003-2012 - LC-CCI-Class 130 - Grassland

3.4.2.8 *Sparse vegetation - LC-CCI-Class 150*

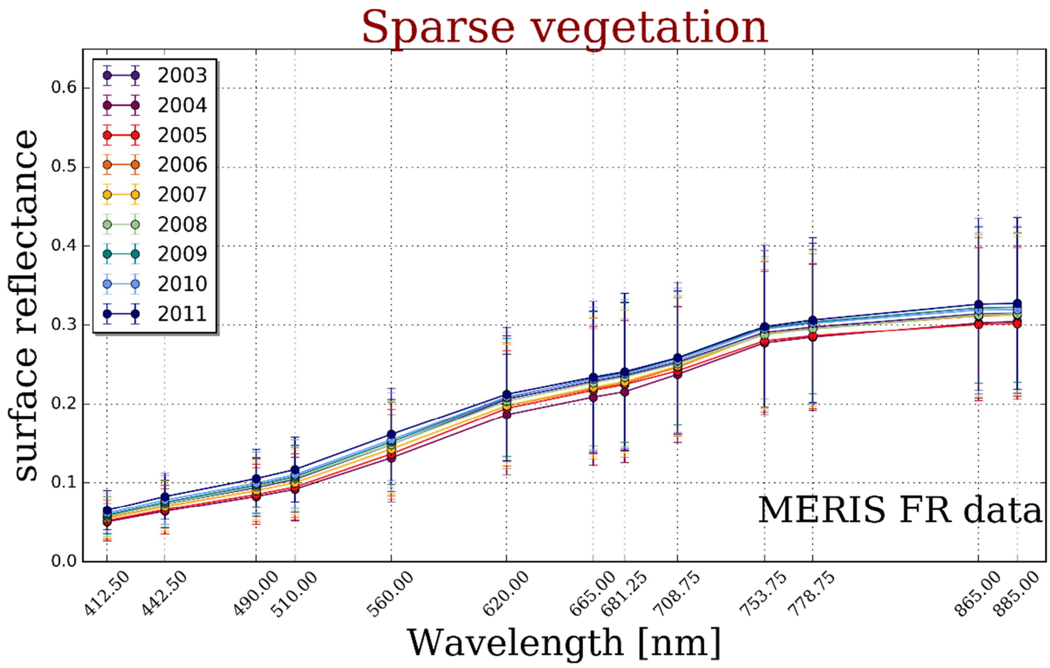

Figure 3-78: Spectra - LC-CCI-Class 150 - Sparse vegetation - MERIS FR data

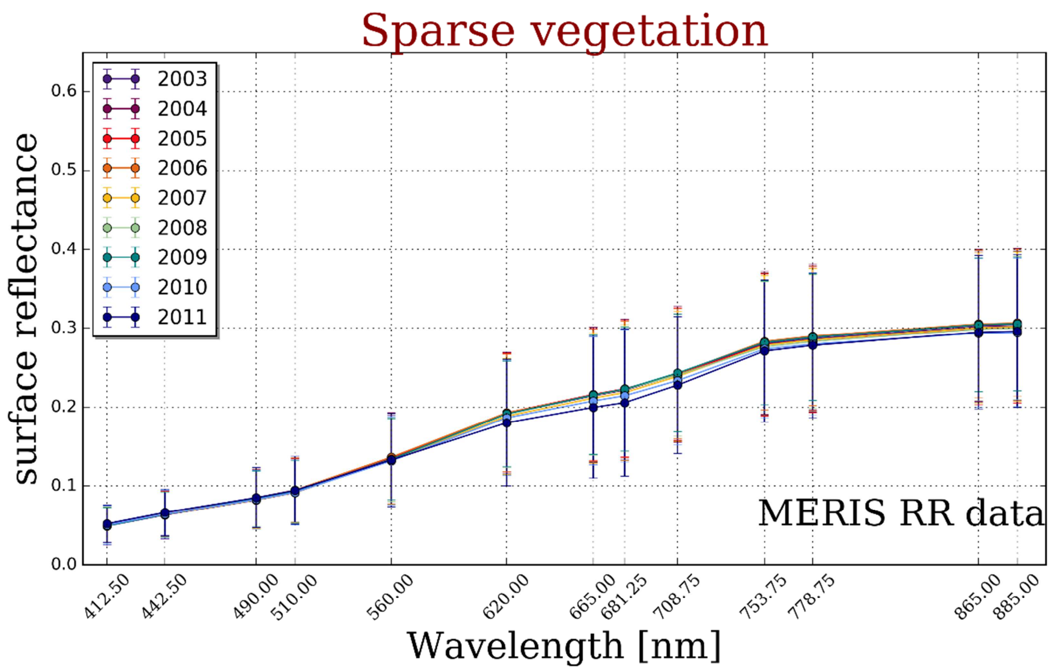

Figure 3-79: Spectra - LC-CCI-Class 150 - Sparse vegetation - MERIS RR data

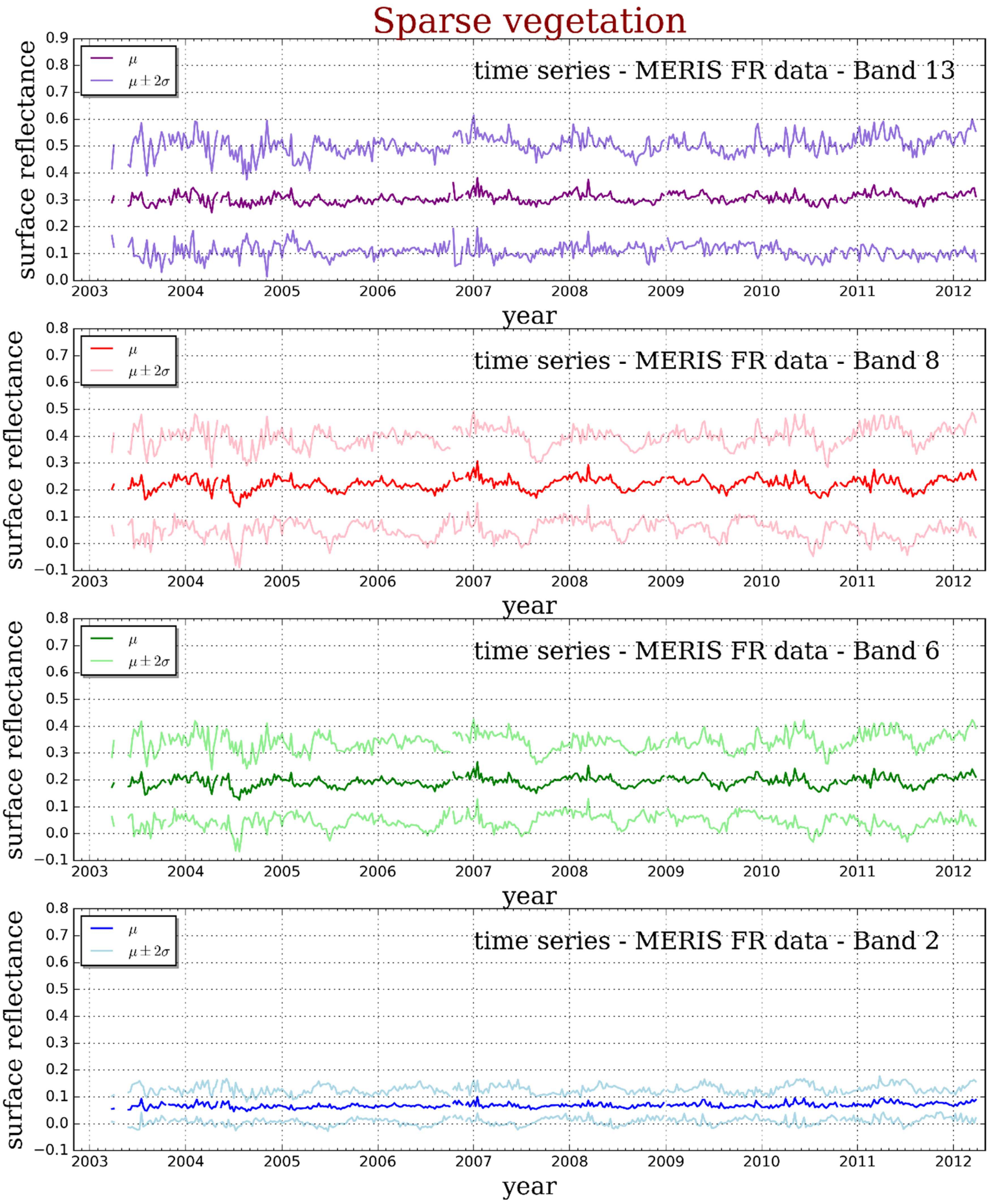

Figure 3-80: SR time series from MERIS FR data - 2003-2012 - LC-CCI-Class 150 - Sparse vegetation

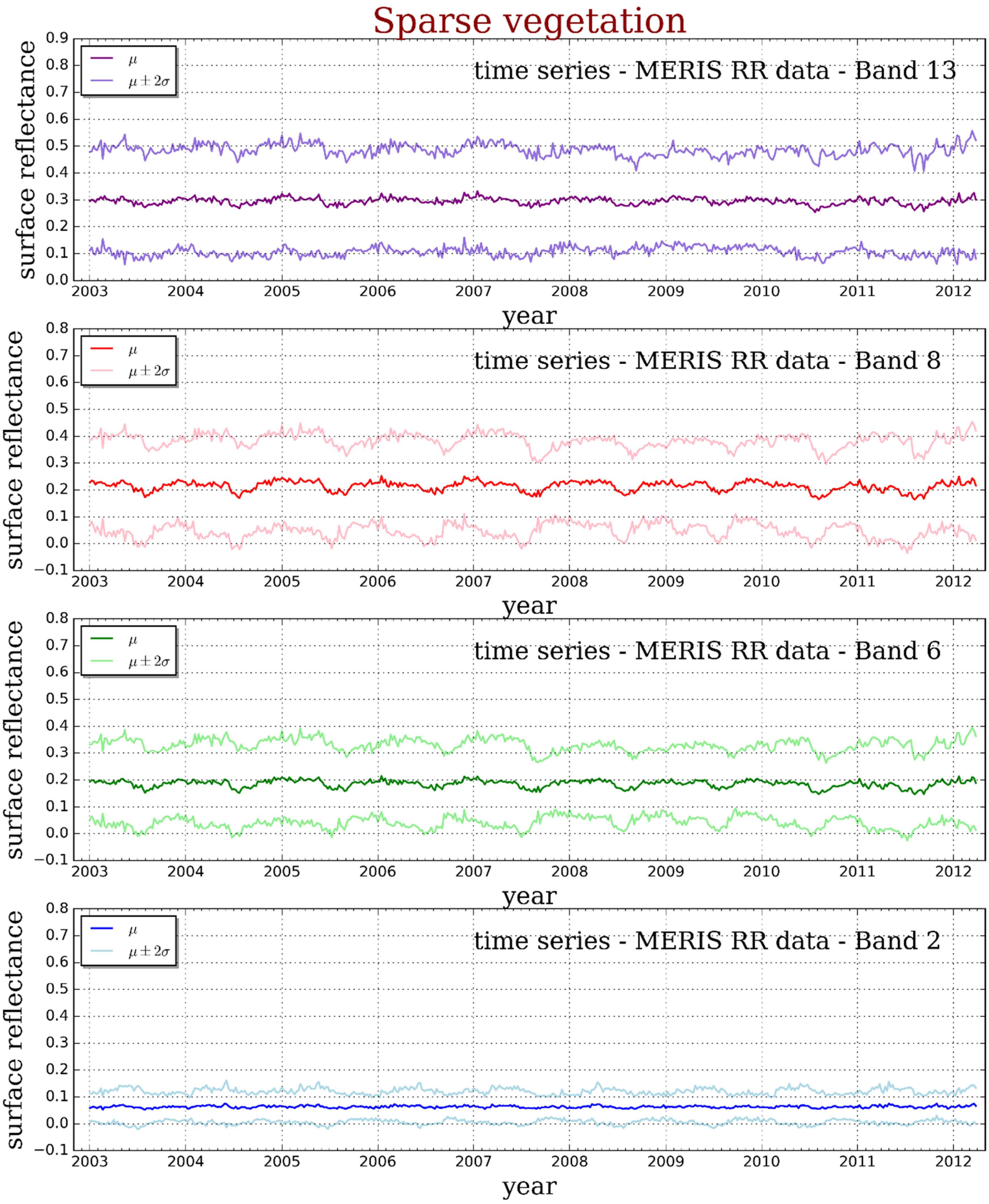

Figure 3-81: SR time series from MERIS RR data - 2003-2012 - LC-CCI-Class 150 - Sparse vegetation

3.4.2.9 *Inundated forest - LC-CCI-Class 160 and 170 - Tree cover, flooded*

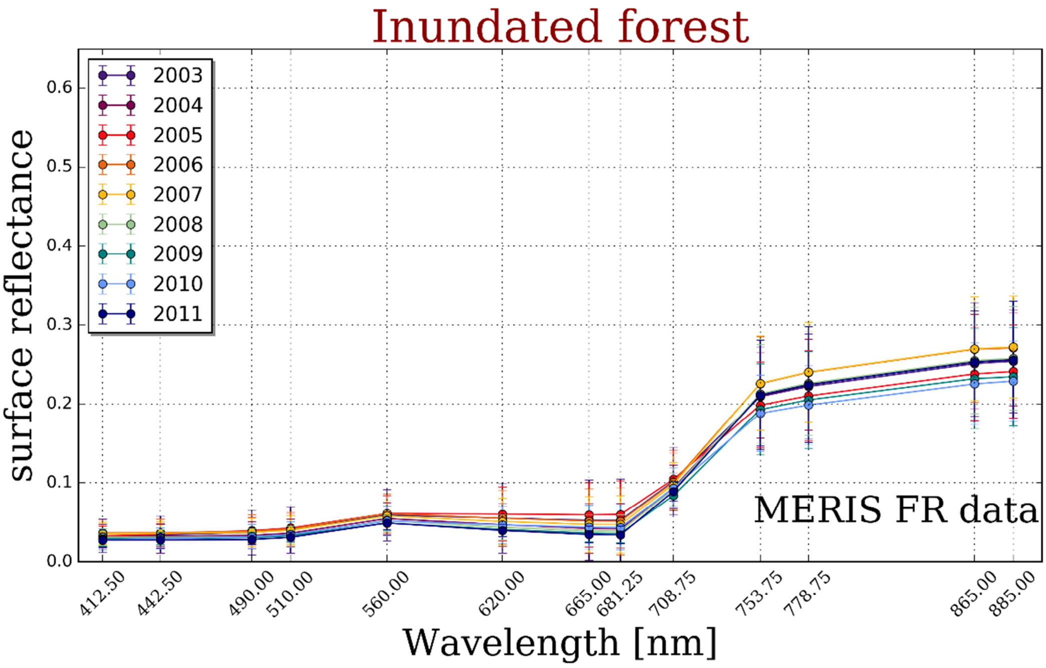

Figure 3-82: Spectra - LC-CCI-Class 160 and 170 - Tree cover, flooded - MERIS FR data

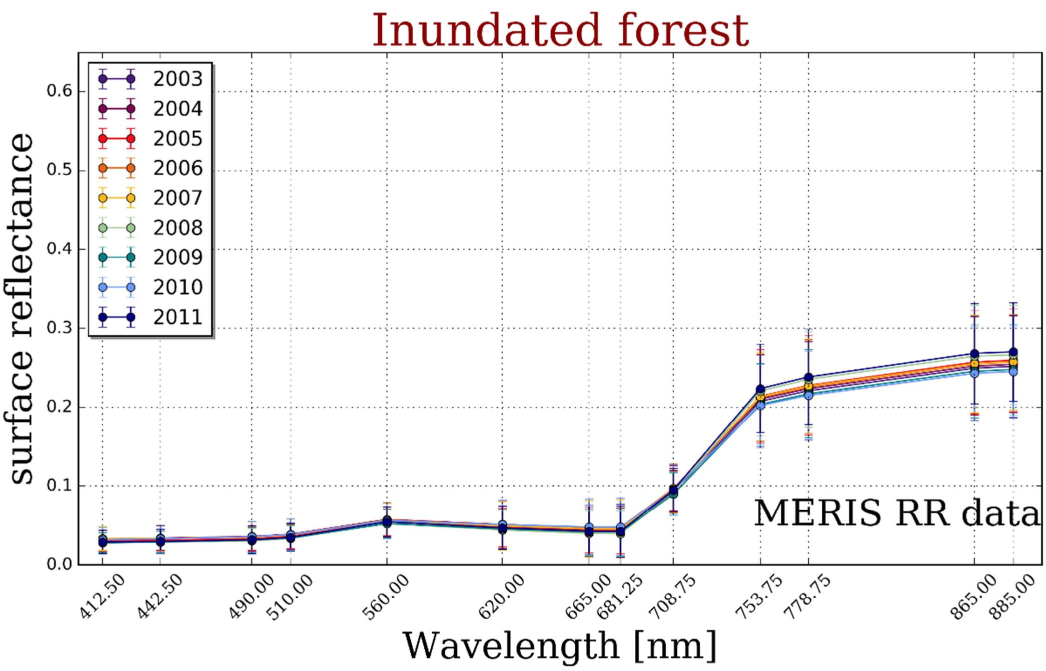

Figure 3-83: Spectra - LC-CCI-Class 160 and 170 - Tree cover, flooded - MERIS RR data

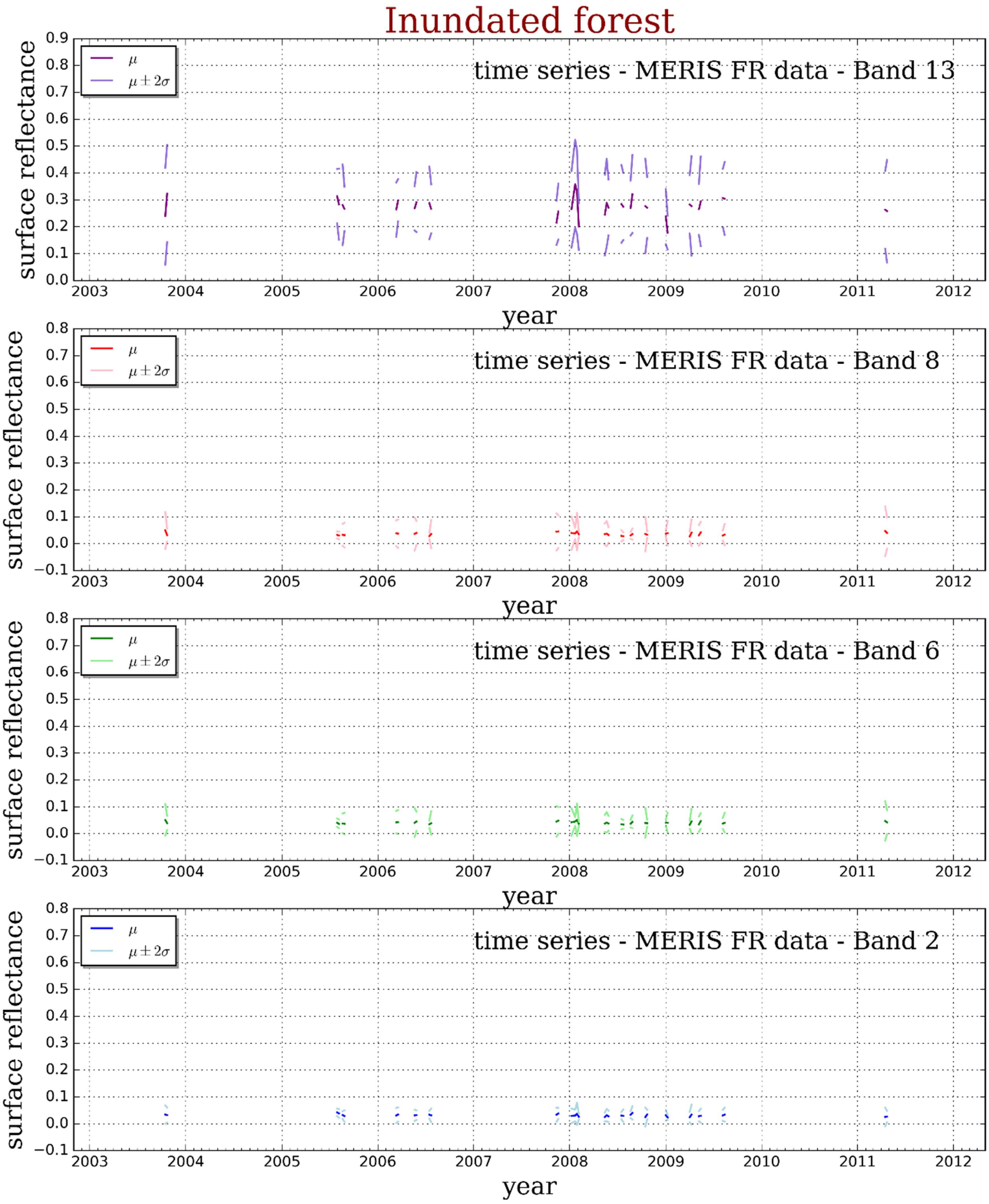

Figure 3-84: SR time series from MERIS FR data - 2003-2012 - LC-CCI-Class 160 and 170 - Tree cover, flooded

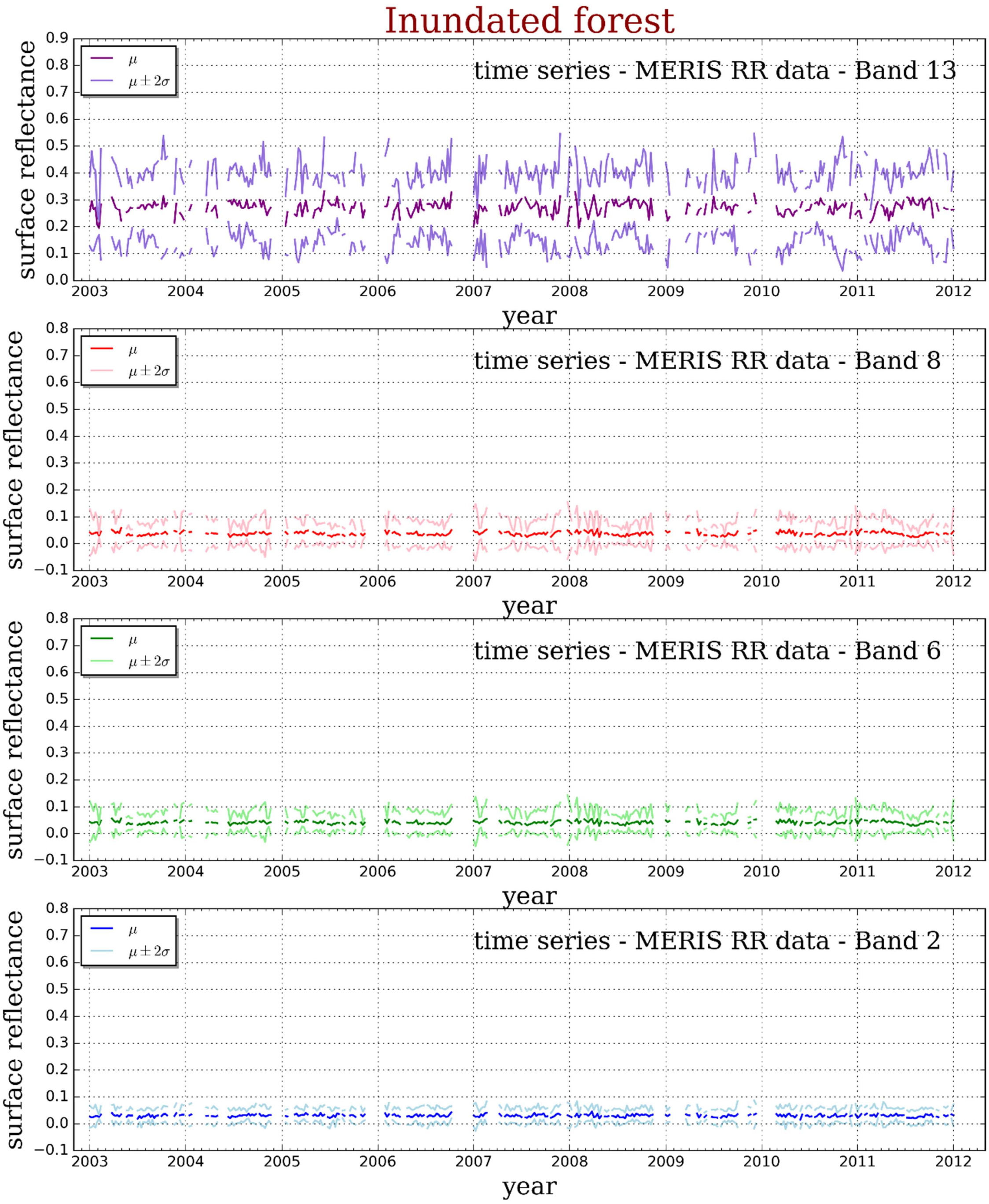

Figure 3-85: SR time series from MERIS RR data - 2003-2012 - LC-CCI-Class 160 and 170 - Tree cover, flooded

3.4.2.10 *Wetland - LC-CCI-Class 180 - Shrub or herbaceous cover, flooded*

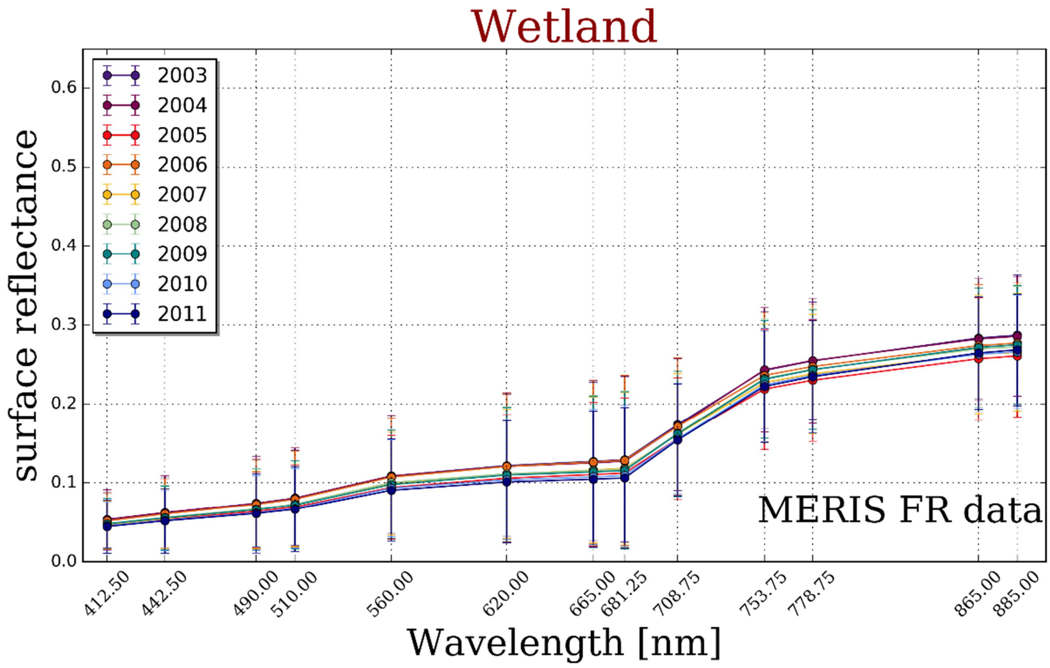

Figure 3-86: Spectra - LC-CCI-Class 180 - Shrub or herbaceous cover, flooded- MERIS FR data

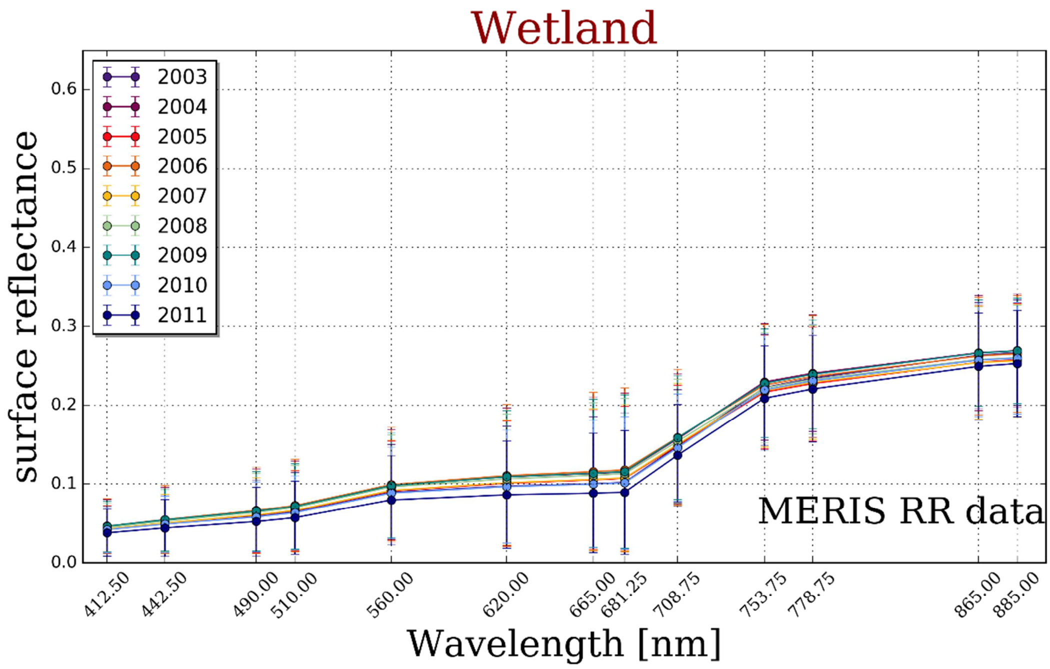

Figure 3-87: Spectra - LC-CCI-Class 180 - Shrub or herbaceous cover, flooded - MERIS RR data

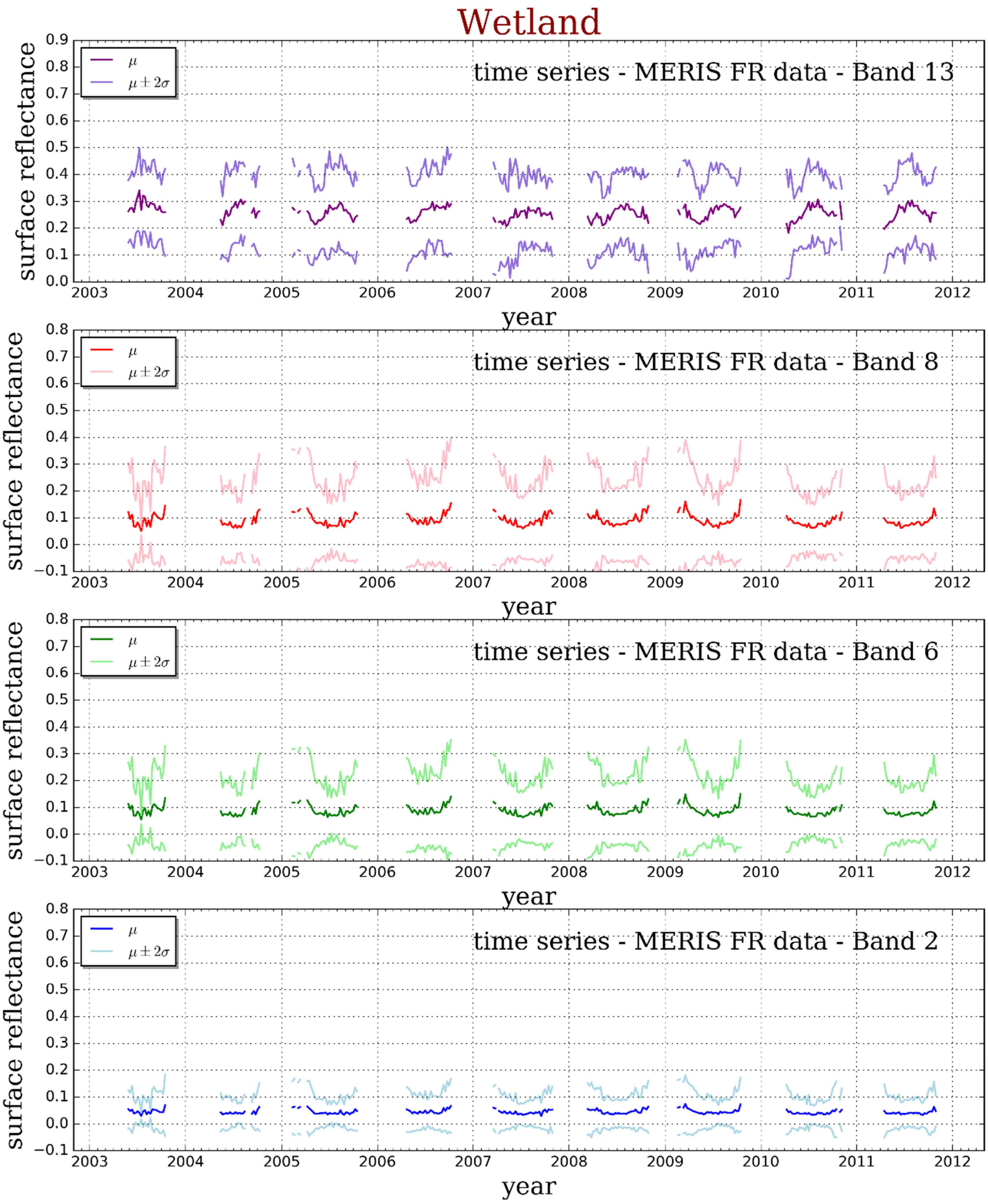

Figure 3-88: SR time series from MERIS FR data - 2003-2012 - LC-CCI-Class 180 - Shrub or herbaceous cover, flooded

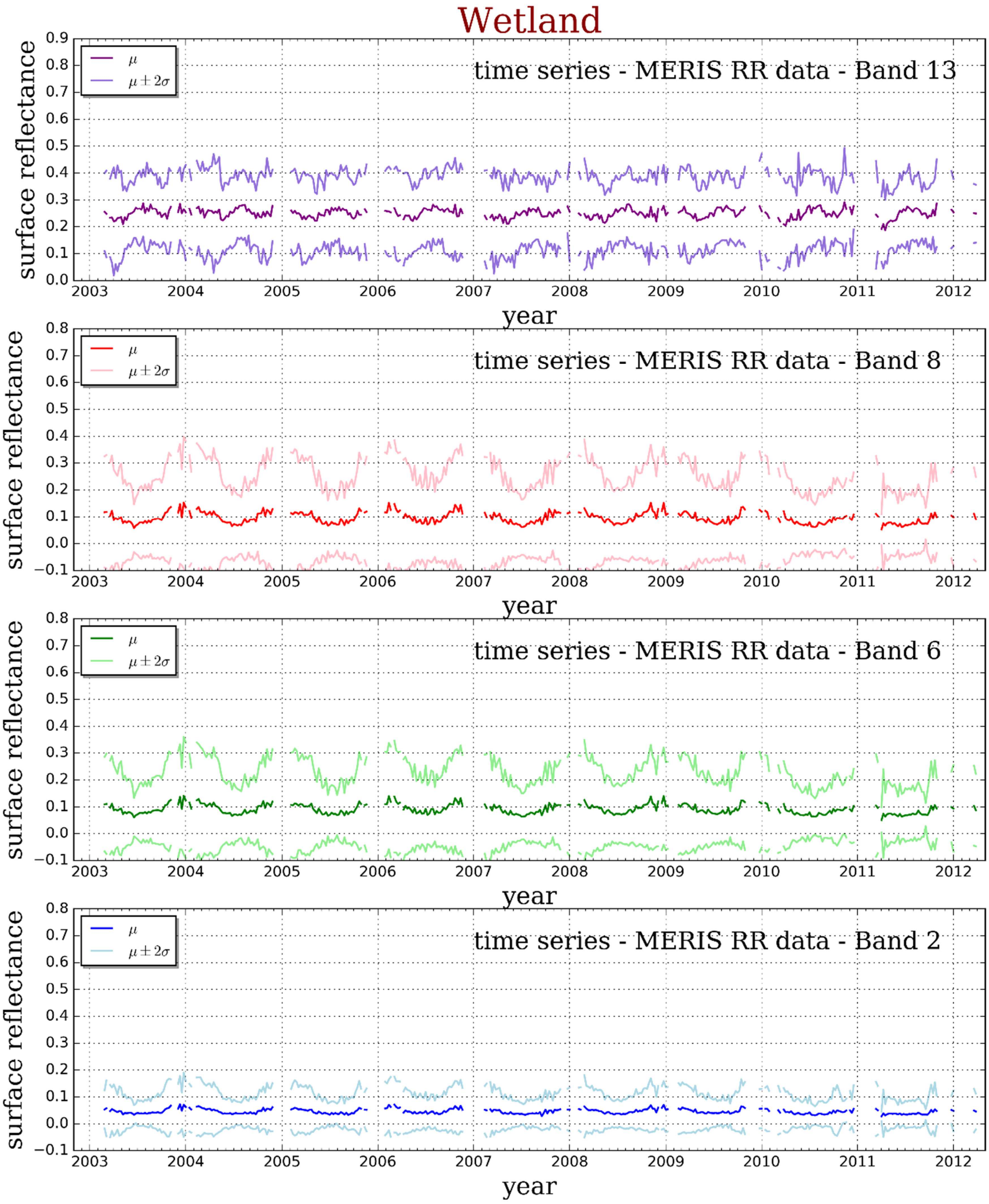

Figure 3-89: SR time series from MERIS RR data - 2003-2012 - LC-CCI-Class 180 - Shrub or herbaceous cover, flooded

3.4.2.11 *Urban areas - LC-CCI-Class 190 - Urban areas*

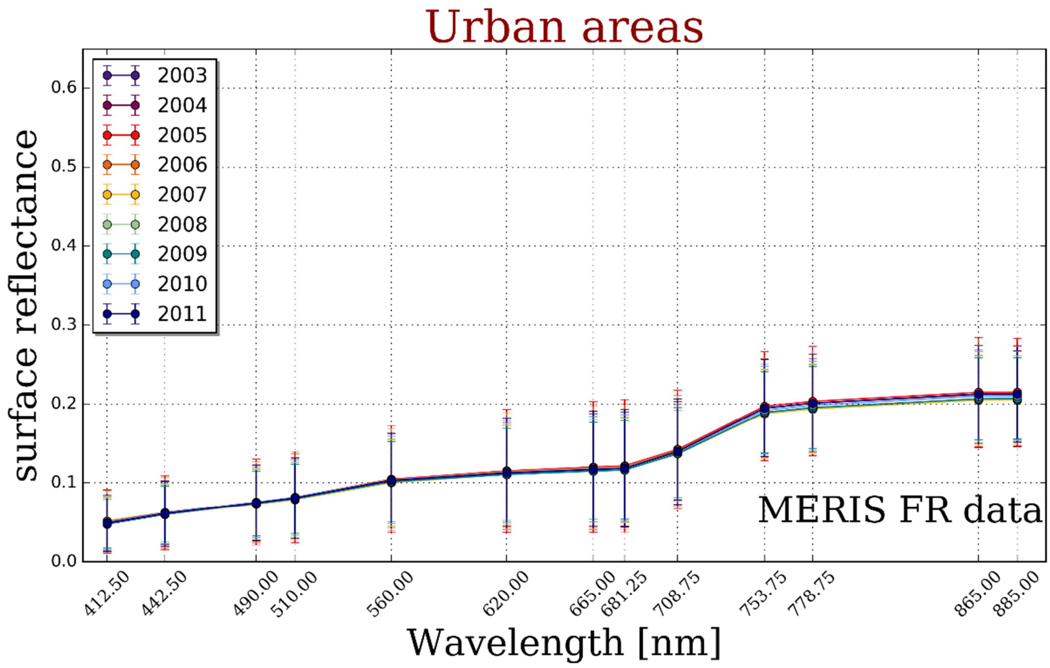

Figure 3-90: Spectra - LC-CCI-Class 190 - Urban areas - MERIS FR data

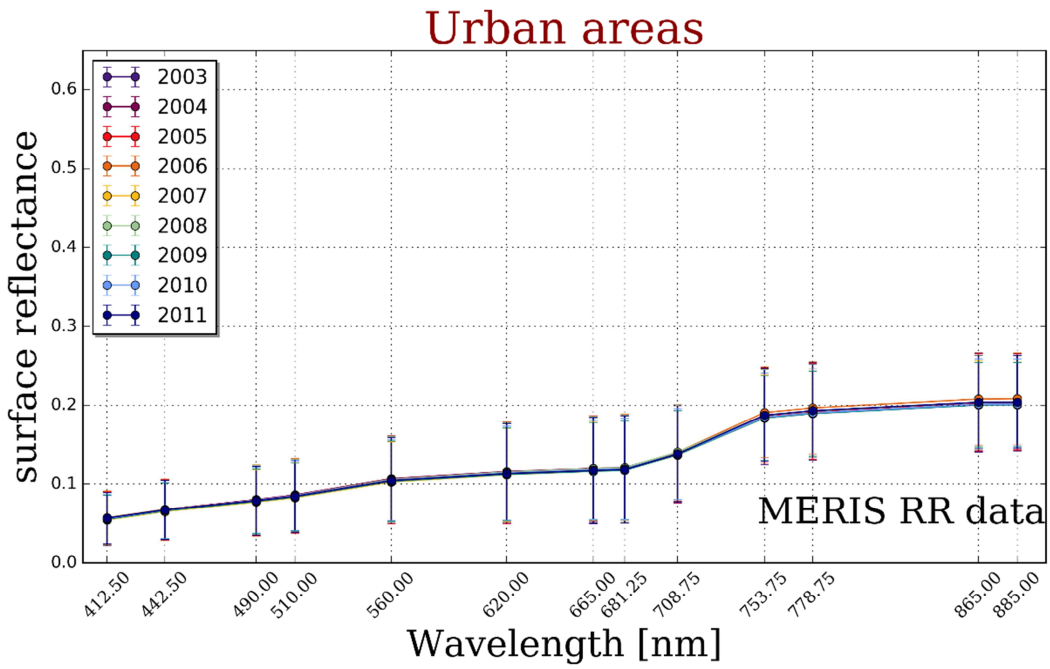

Figure 3-91: Spectra - LC-CCI-Class 190 - Urban areas - MERIS RR data

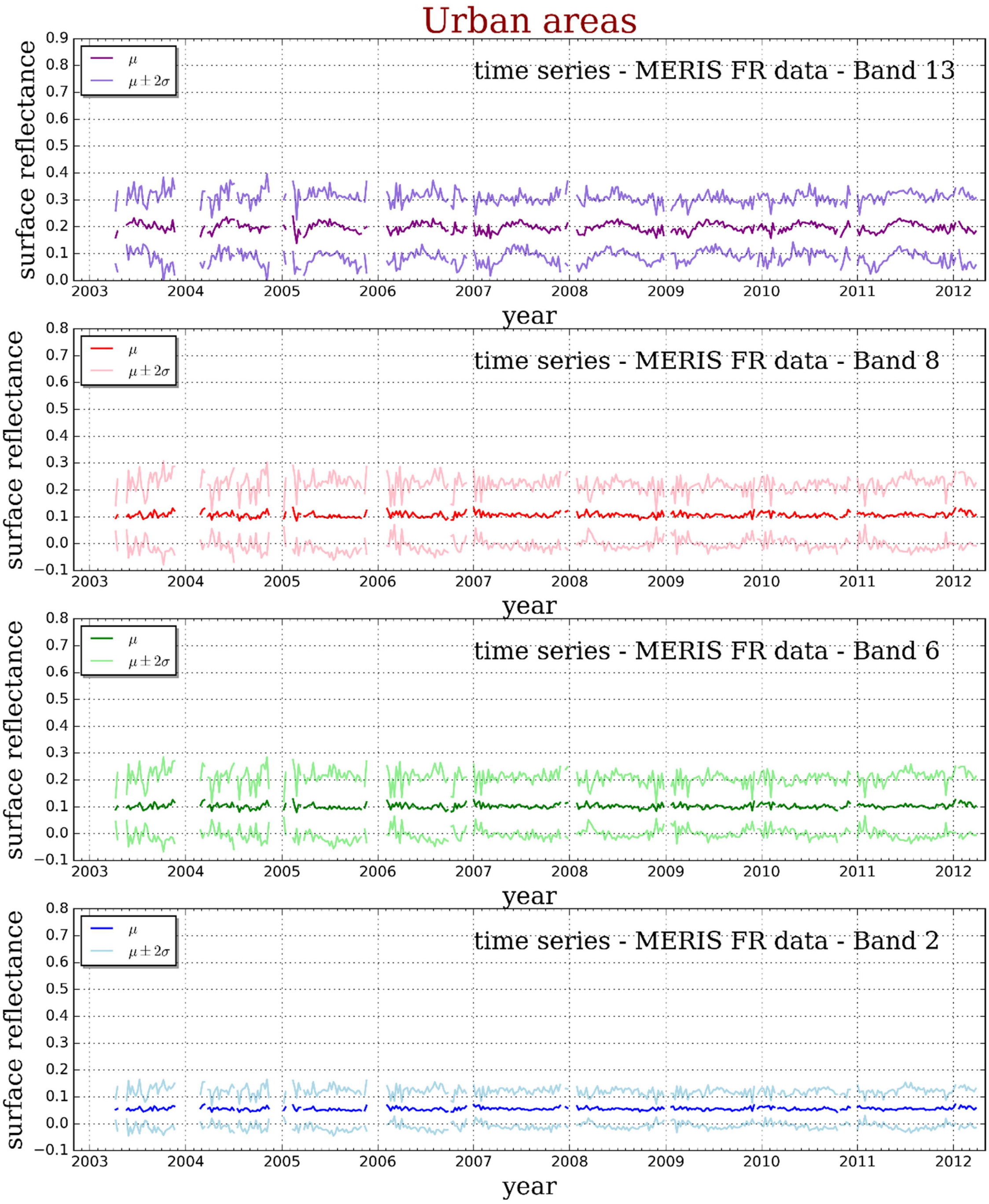

Figure 3-92: SR time series from MERIS FR data - 2003-2012 - LC-CCI-Class 190 - Urban areas

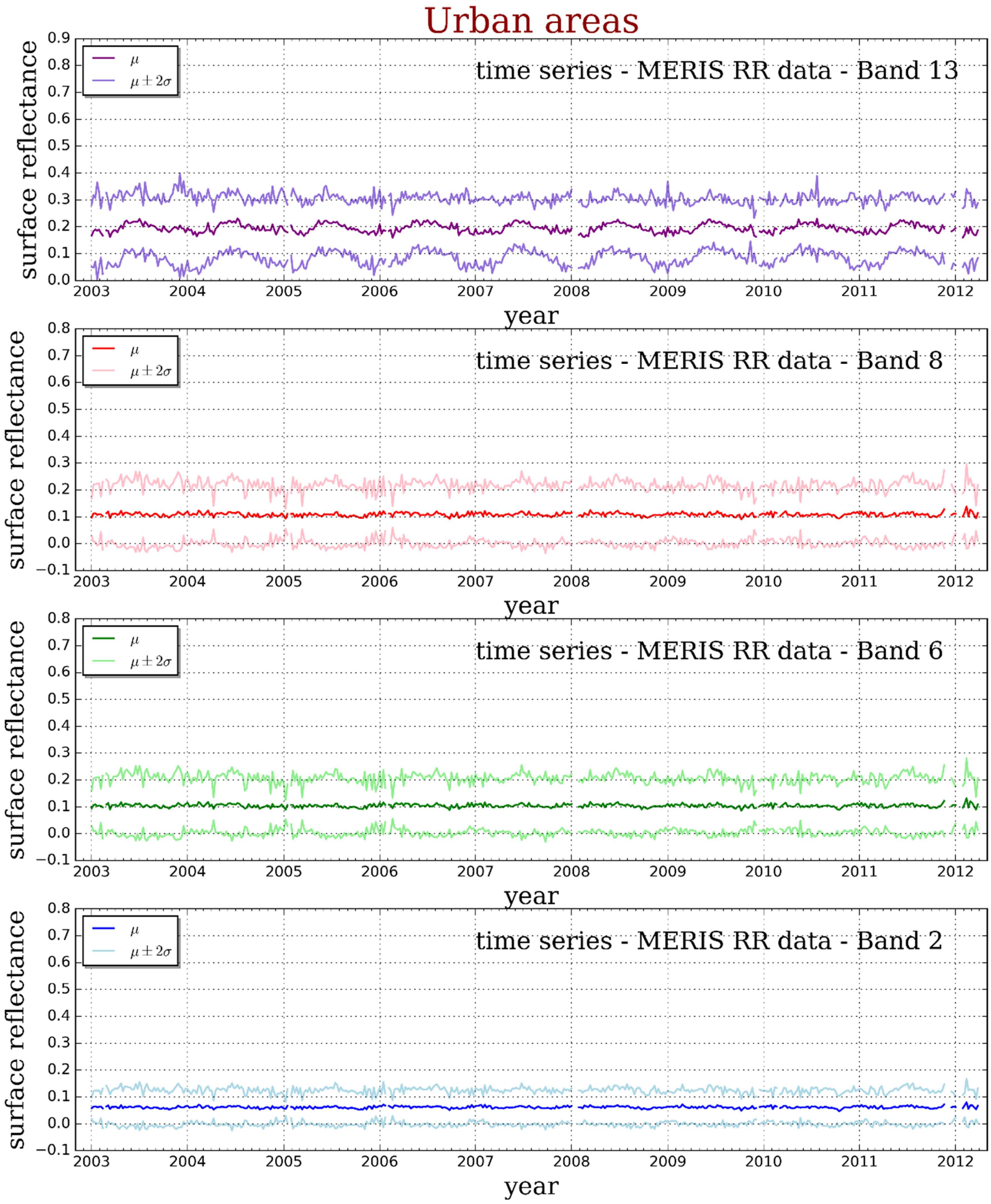

Figure 3-93: SR time series from MERIS RR data - 2003-2012 - LC-CCI-Class 190 - Urban areas

3.4.2.12 *Bare areas - LC-CCI-Class 200 - Bare areas*

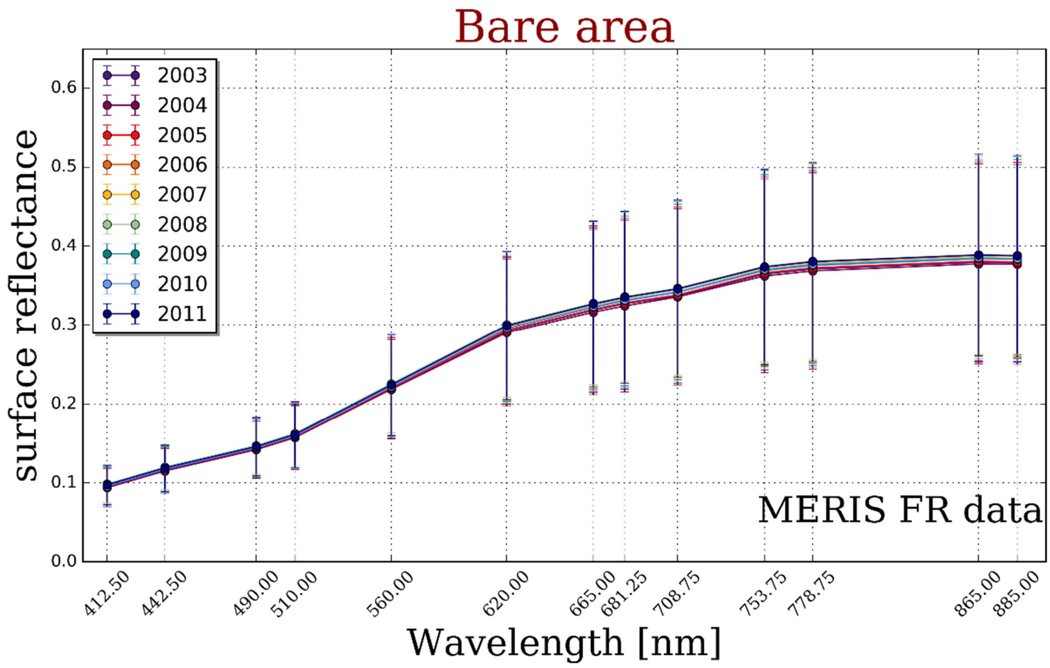

Figure 3-94: Spectra - LC-CCI-Class 200 - Bare areas - MERIS FR data

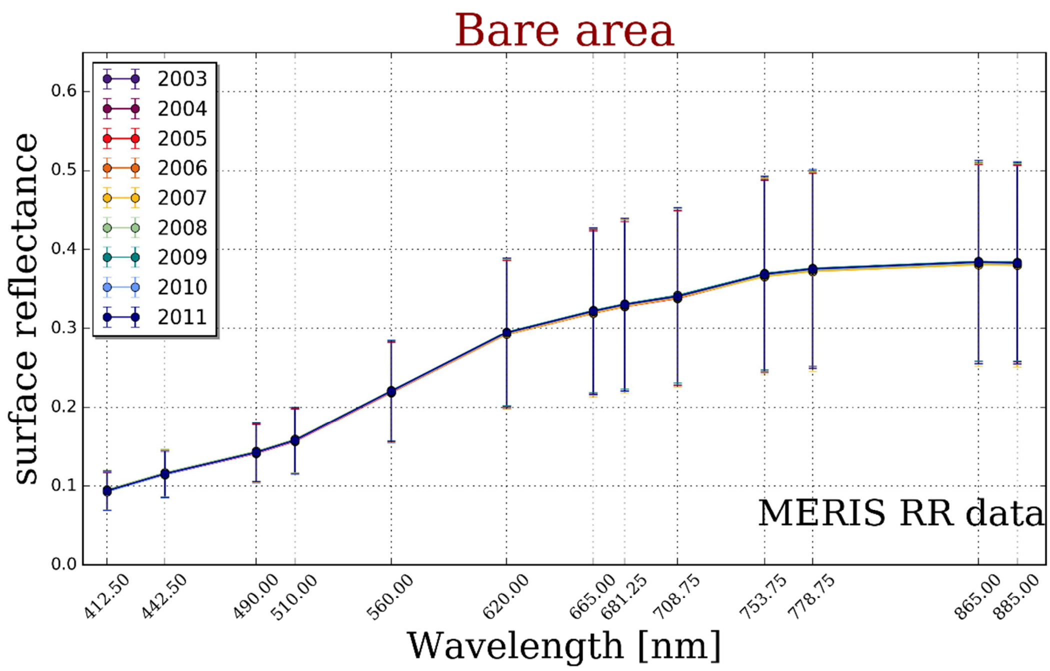

Figure 3-95: Spectra - LC-CCI-Class 200 - Bare areas - MERIS RR data

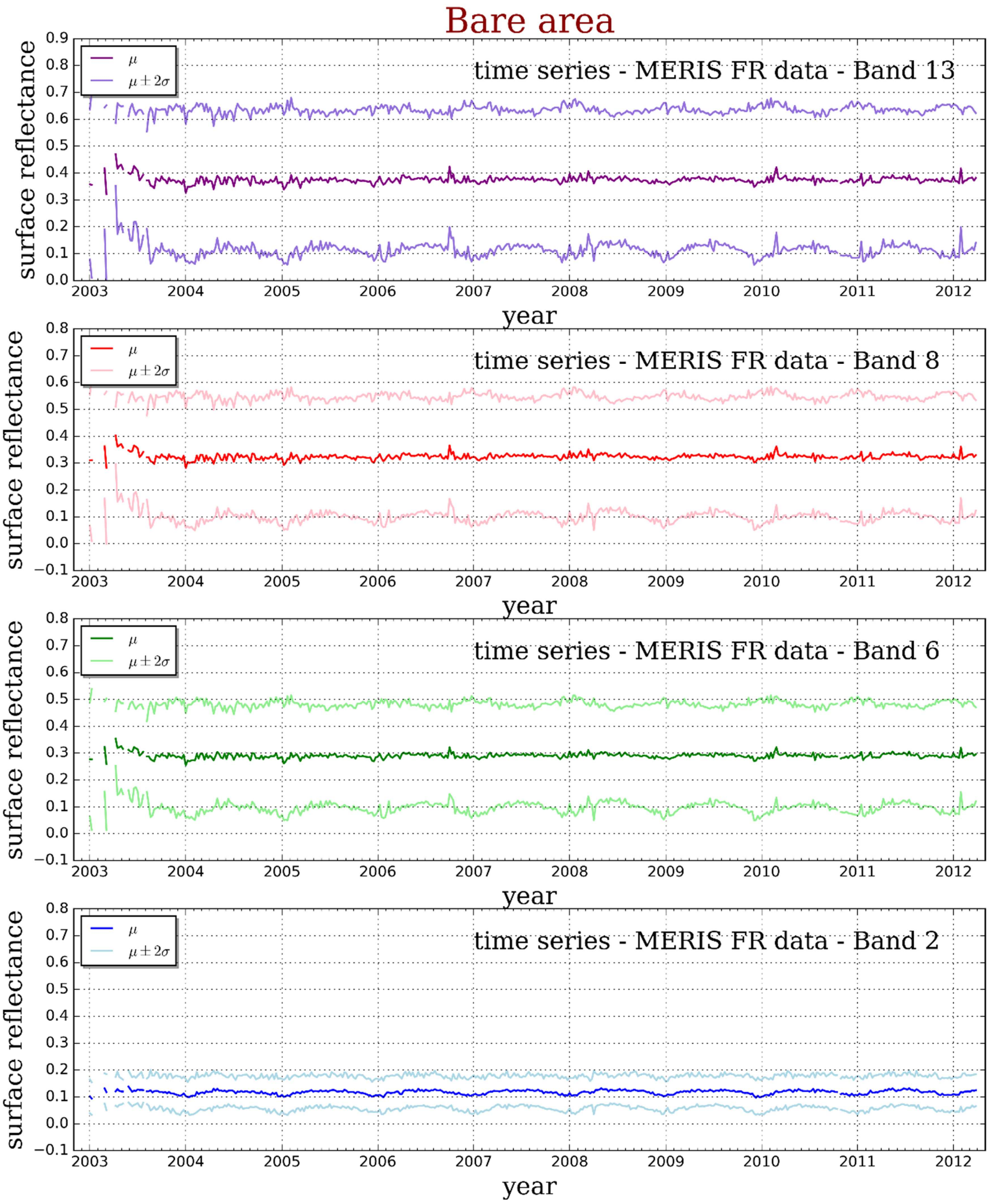

Figure 3-96: SR time series from MERIS FR data - 2003-2012 - LC-CCI-Class 200 - Bare areas - Cropland

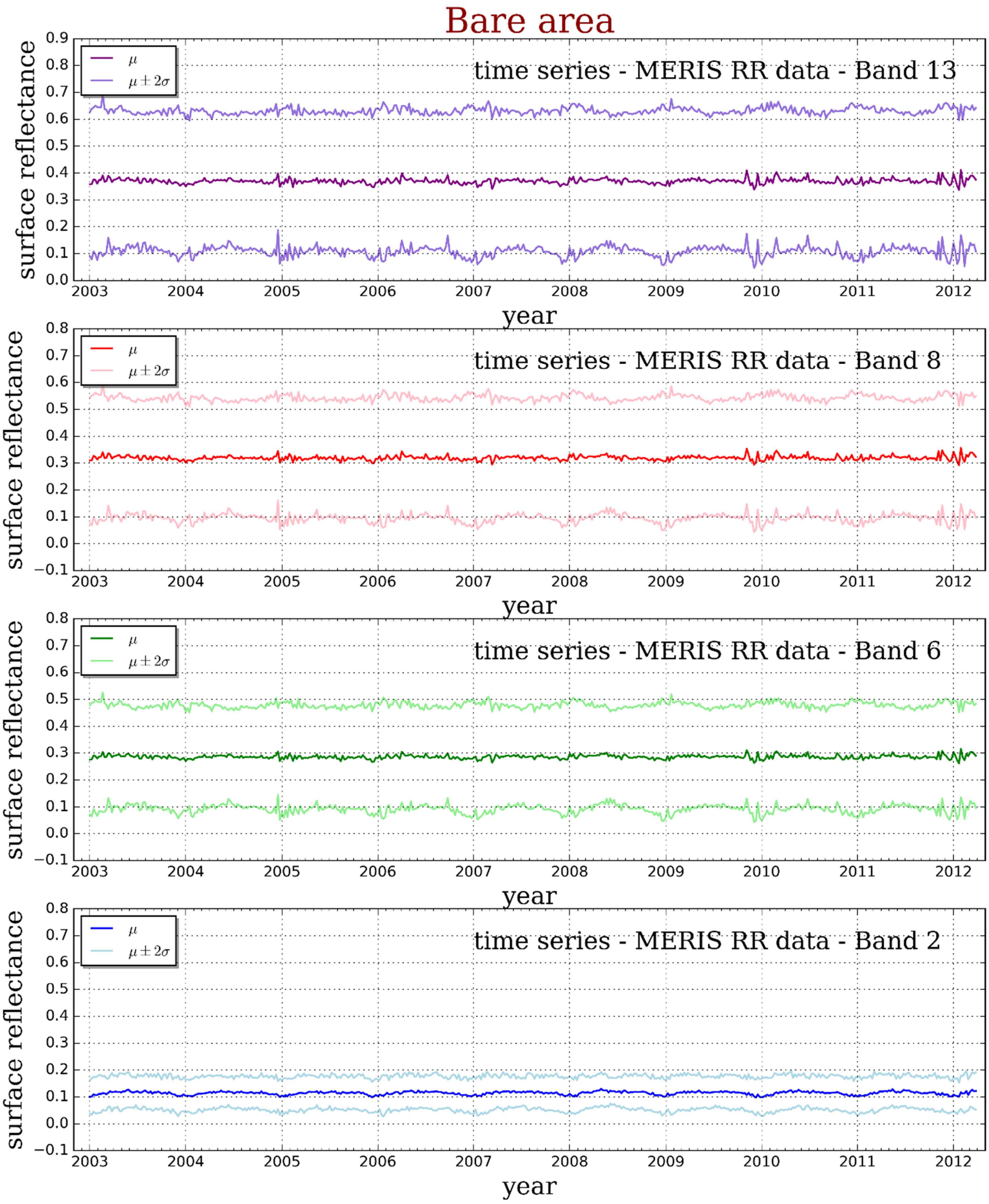

Figure 3-97: SR time series from MERIS RR data - 2003-2012 - LC-CCI-Class 200 - Bare areas

3.4.3 Results of the analysis of the intra- and inter-annual reflectance dynamic for PROBA-V

The following figures (Figure 3-98 through Figure 3-121) show the mean spectrum for each year and the mean (x_{mean}) and the range of the spectral reflectance values at the class level for the SR time series of PROBA-V data for the years 2014 and 2015.

The range refers to the twofold standard deviation (2σ) again. Furthermore, the calculation of the mean and the standard deviation has been limited in particular to those cases in which at least 10 clear land observations per class and date are available.

The results of the analysis of the intra- and inter-annual reflectance dynamic can be summarized as follows:

- the spectra inside the class over the years are very similar but the standard deviation shows a great dispersion from the average as well as for the MERIS FR and RR data,
- the analysis of different two-year temporal profiles of the mean and the range highlights similar intra-annual "structures" from year to year inside the class as well as for the MERIS FR and RR data,
- the different two-year temporal profiles of the mean and the range do not show significant inter-annual changes as well as for the MERIS FR and RR data,
- the number of pixels which contribute to the analysis is very variable (see also section 3.2) as well as for the MERIS FR and RR data.

3.4.3.1 *Cropland - LC-CCI-Class 10 and 20*

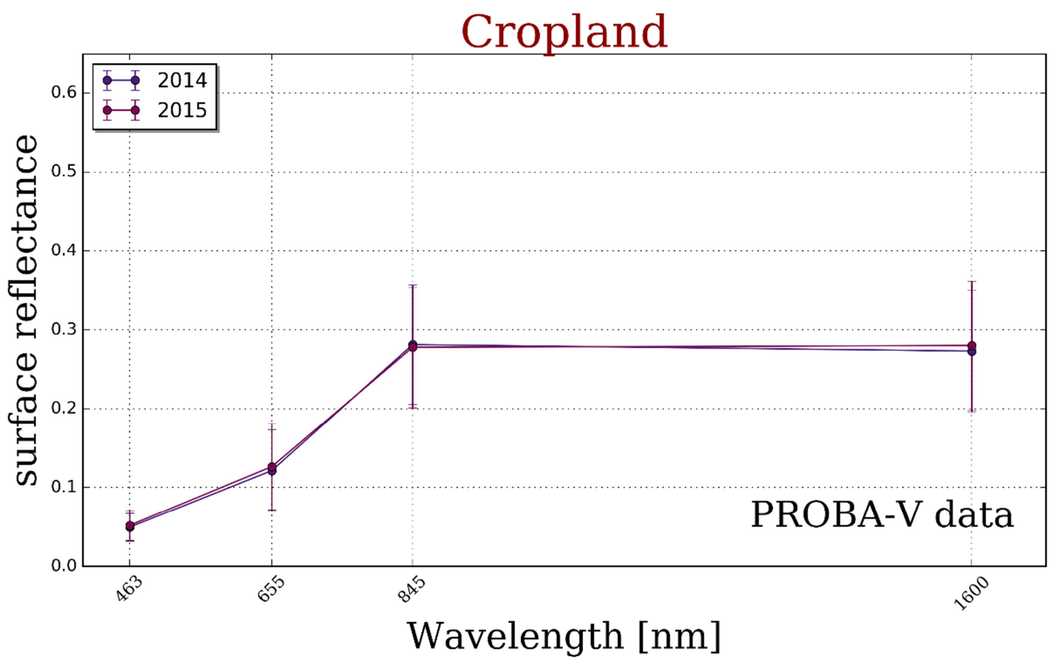

Figure 3-98: Spectra - LC-CCI-Class 10 and 20 - Cropland – PROBA-V data

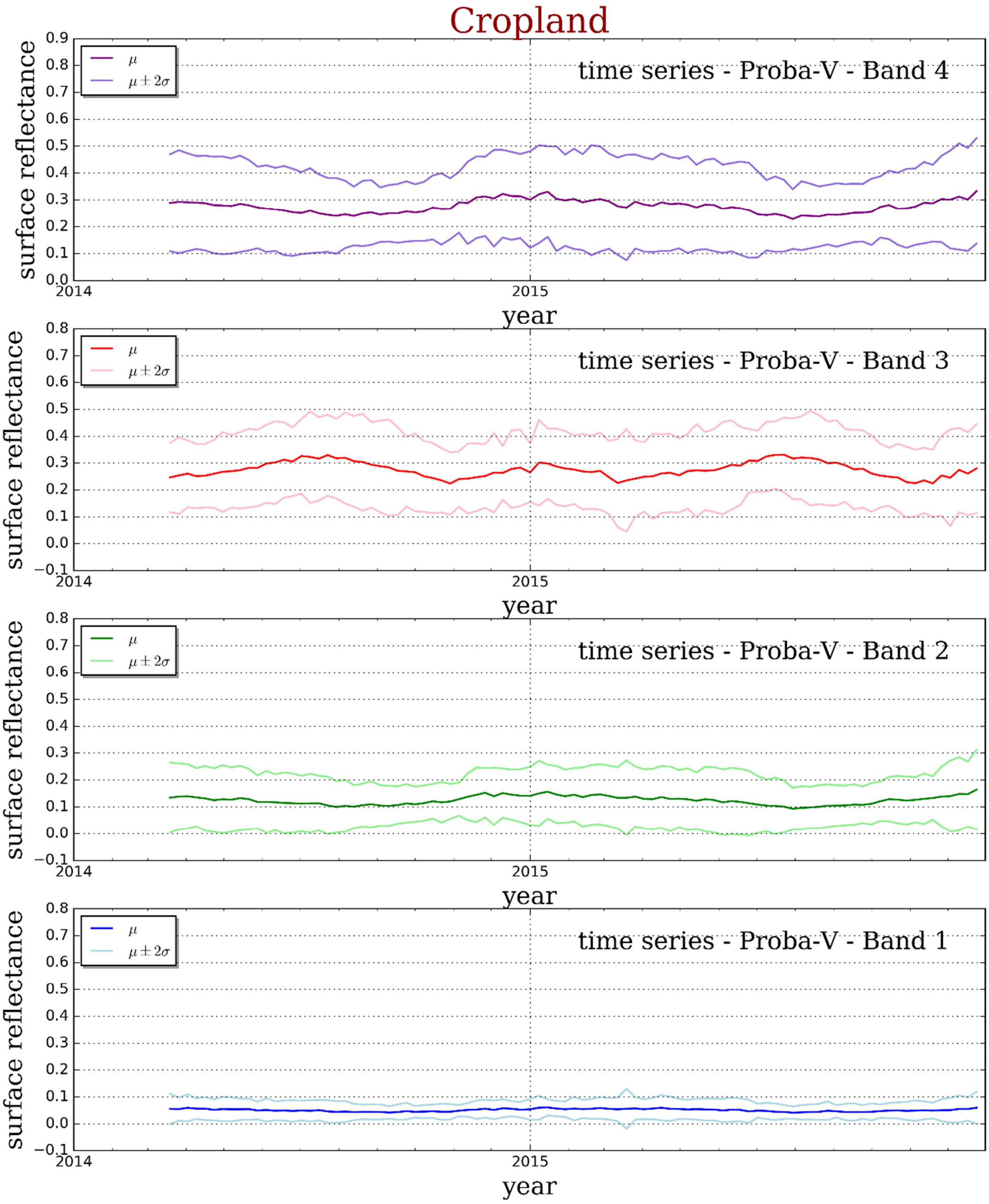

Figure 3-99: SR time series from PROBA-V data - 2014-2015 - LC-CCI-Class 10 and 20 - Cropland

3.4.3.2 *Forest - LC-CCI-Class 50 - Tree cover, broadleaved, evergreen, closed to open*

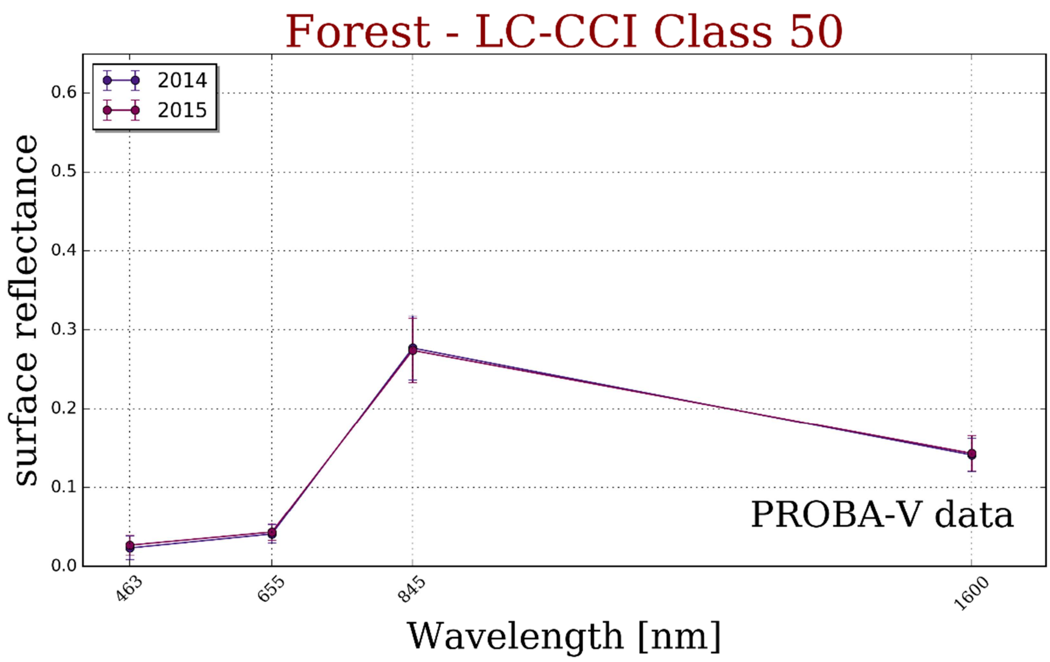

Figure 3-100: Spectra - LC-CCI-Class 50 - Tree cover, broadleaved, evergreen, closed to open – PROBA-V data

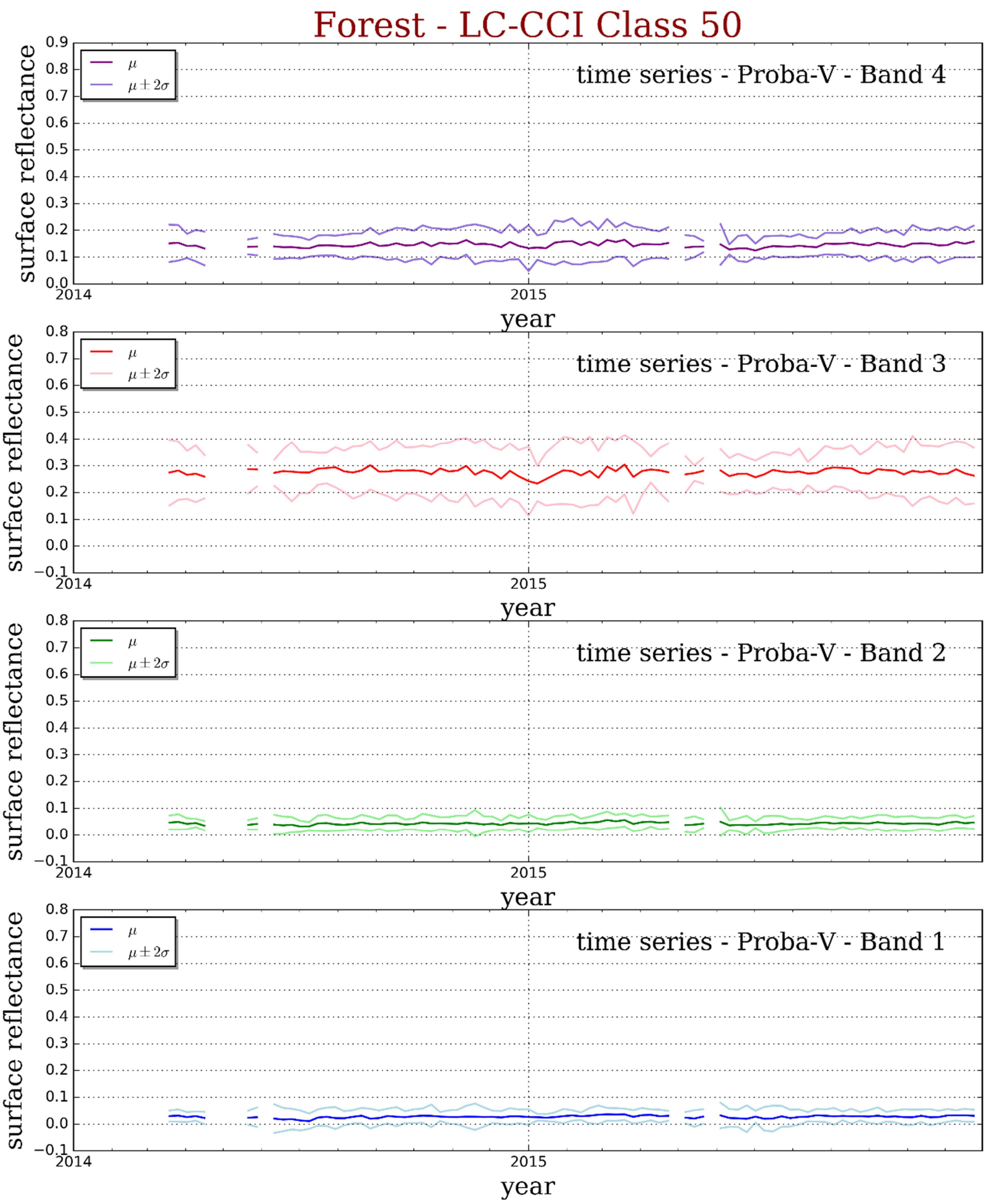

Figure 3-101: SR time series from PROBA-V data - 2014-2015 - LC-CCI-Class 50 - Tree cover, broadleaved, evergreen, closed to open

3.4.3.3 *Forest - LC-CCI-Class 60 - Tree cover, broadleaved, deciduous, closed to open*

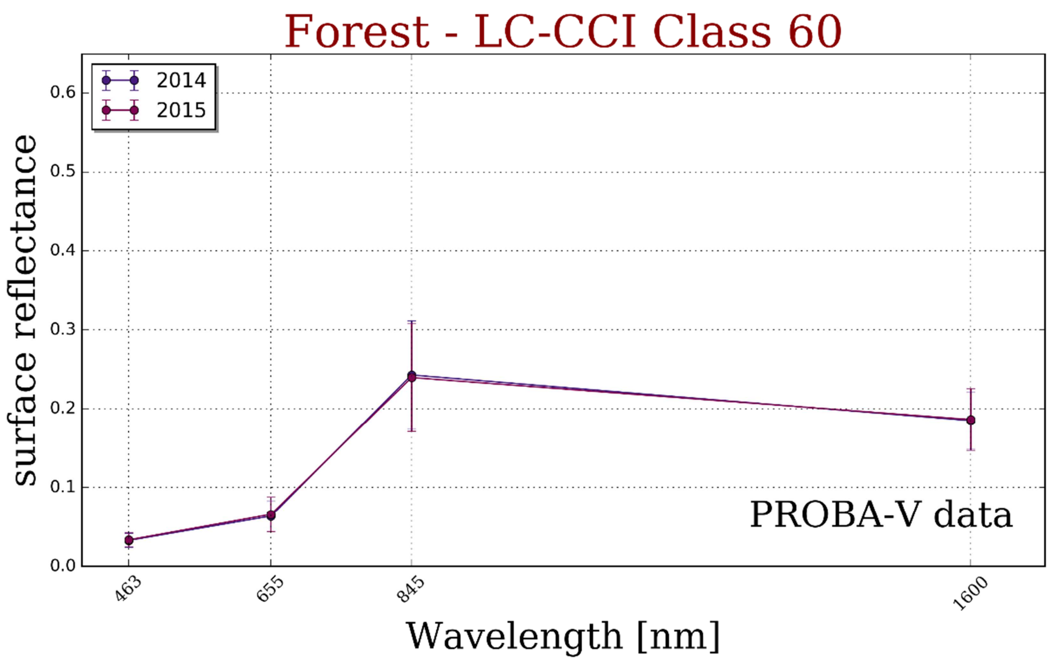

Figure 3-102: Spectra - LC-CCI-Class 60 - Tree cover, broadleaved, deciduous, closed to open – PROBA-V data

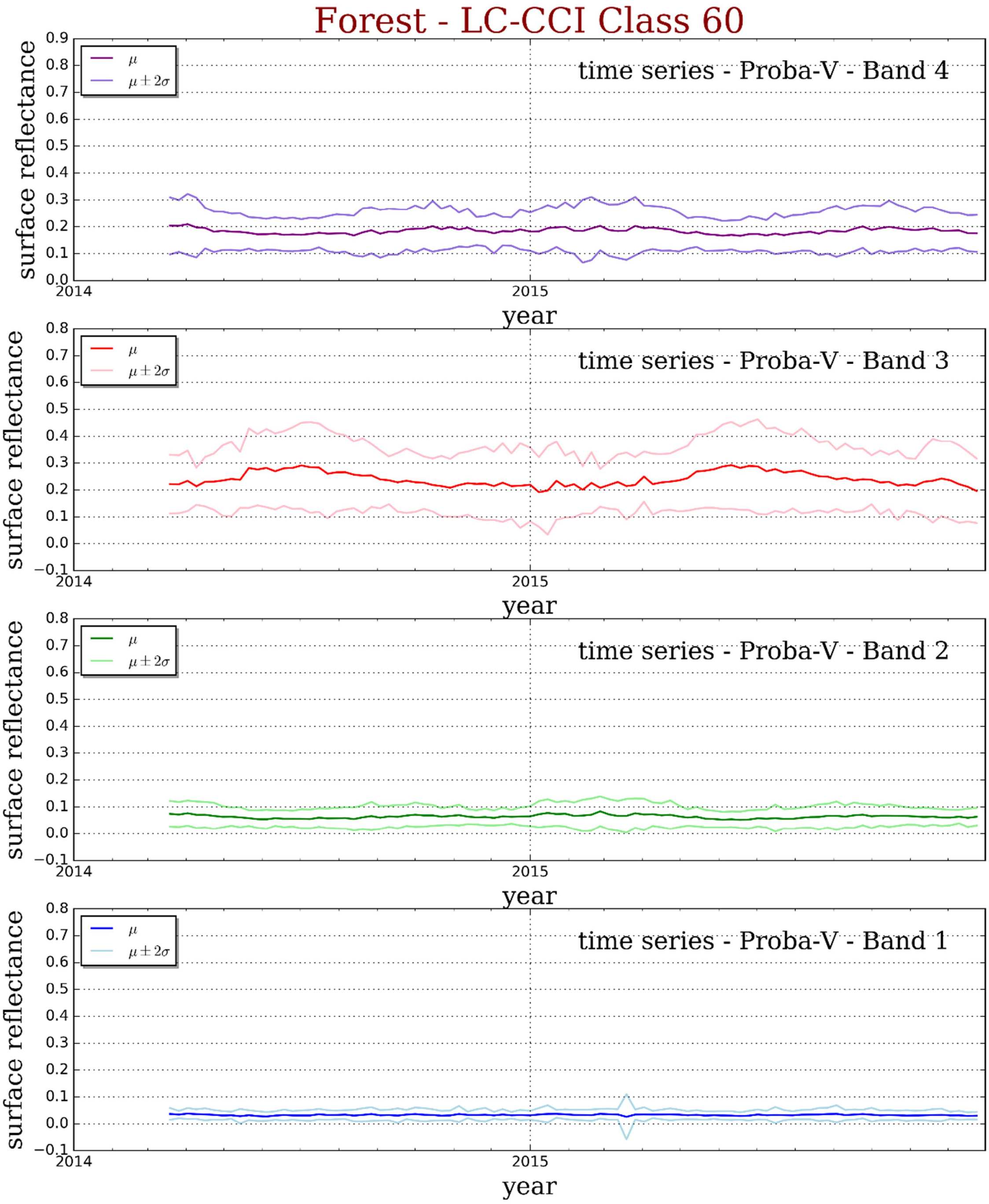

Figure 3-103: SR time series from PROBA-V data - 2014-2015 - LC-CCI-Class 60 - Tree cover, broadleaved, deciduous, closed to open

3.4.3.4 *Forest - LC-CCI-Class 70 - Tree cover, needleleaved, evergreen, closed to open*

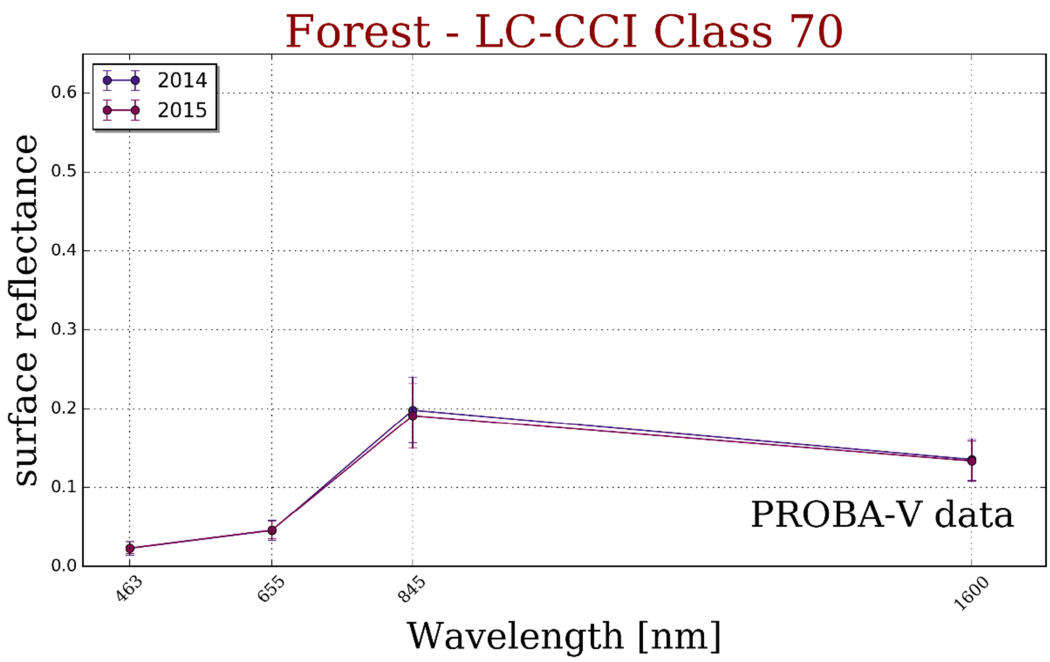

Figure 3-104: Spectra - LC-CCI-Class 70 - Tree cover, needleleaved, evergreen, closed to open – PROBA-V data

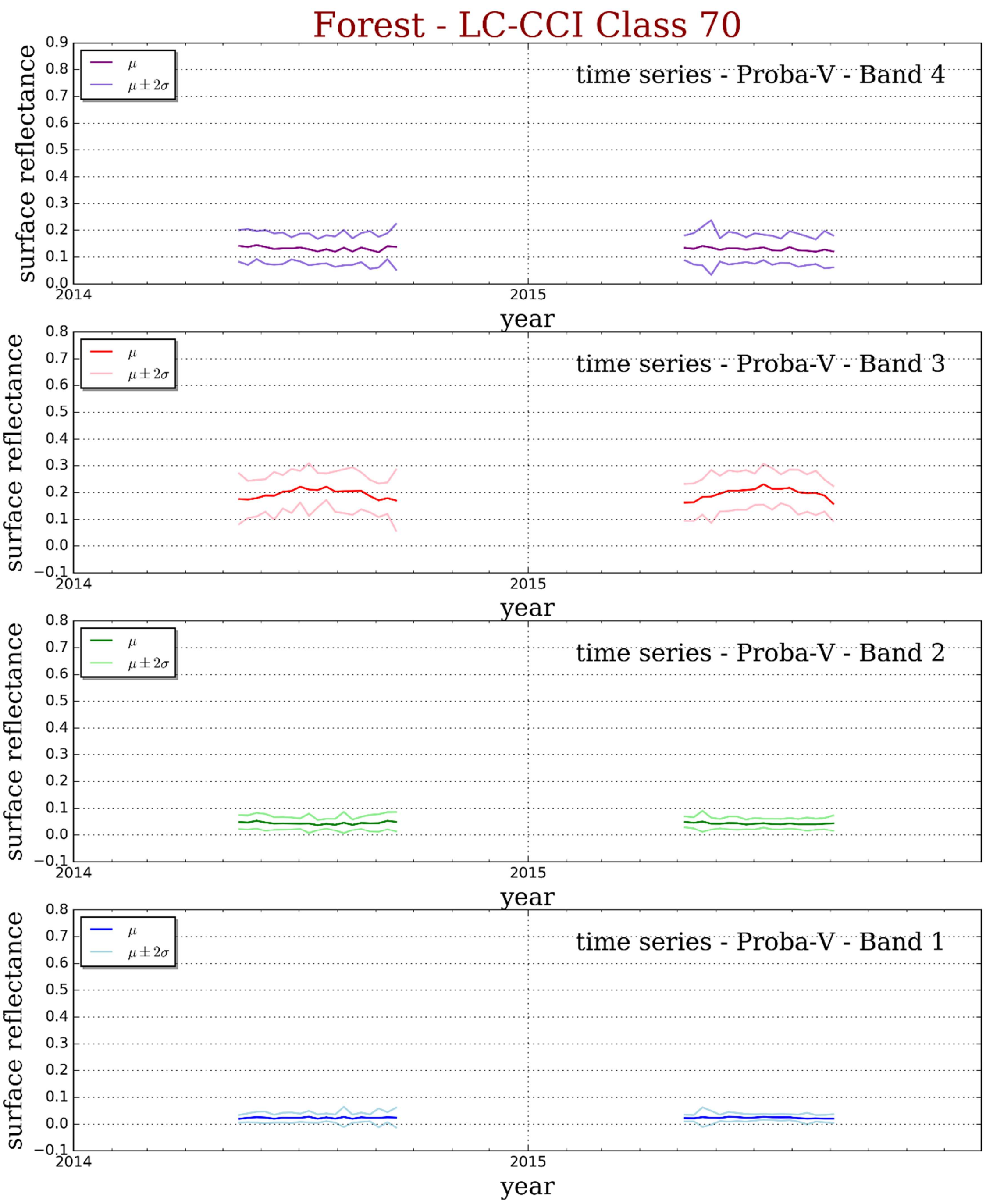

Figure 3-105: SR time series from PROBA-V data - 2014-2015 - LC-CCI-Class 70 - Tree cover, needleleaved, evergreen, closed to open

3.4.3.5 *Forest - LC-CCI-Class 80 - Tree cover, needleleaved, deciduous, closed to open*

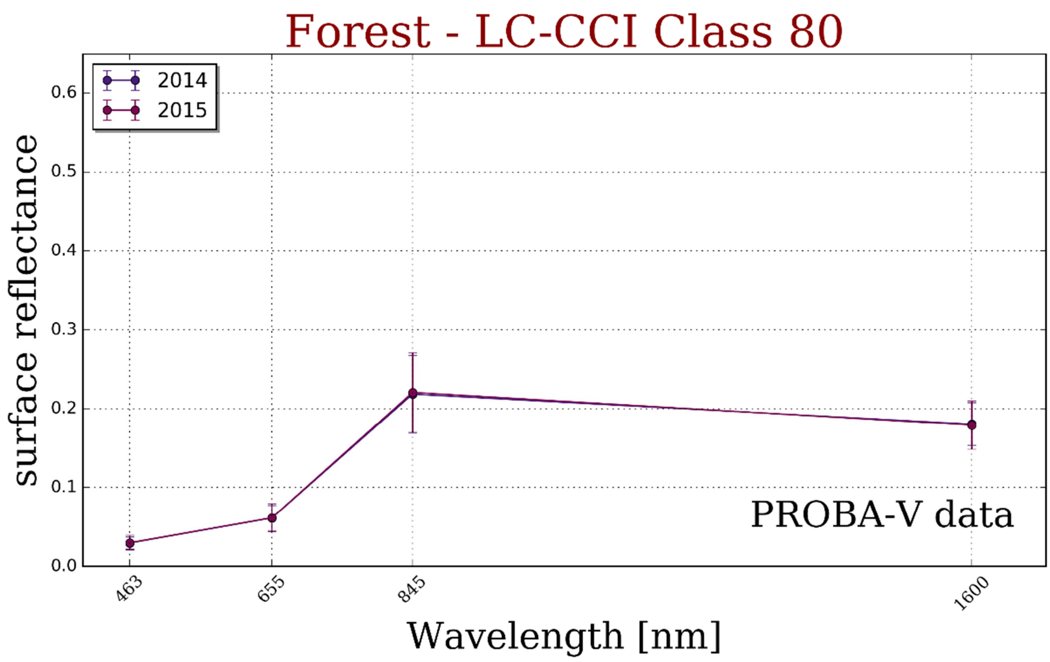

Figure 3-106: Spectra - LC-CCI-Class 80 - Tree cover, needleleaved, deciduous, closed to open – PROBA-V data

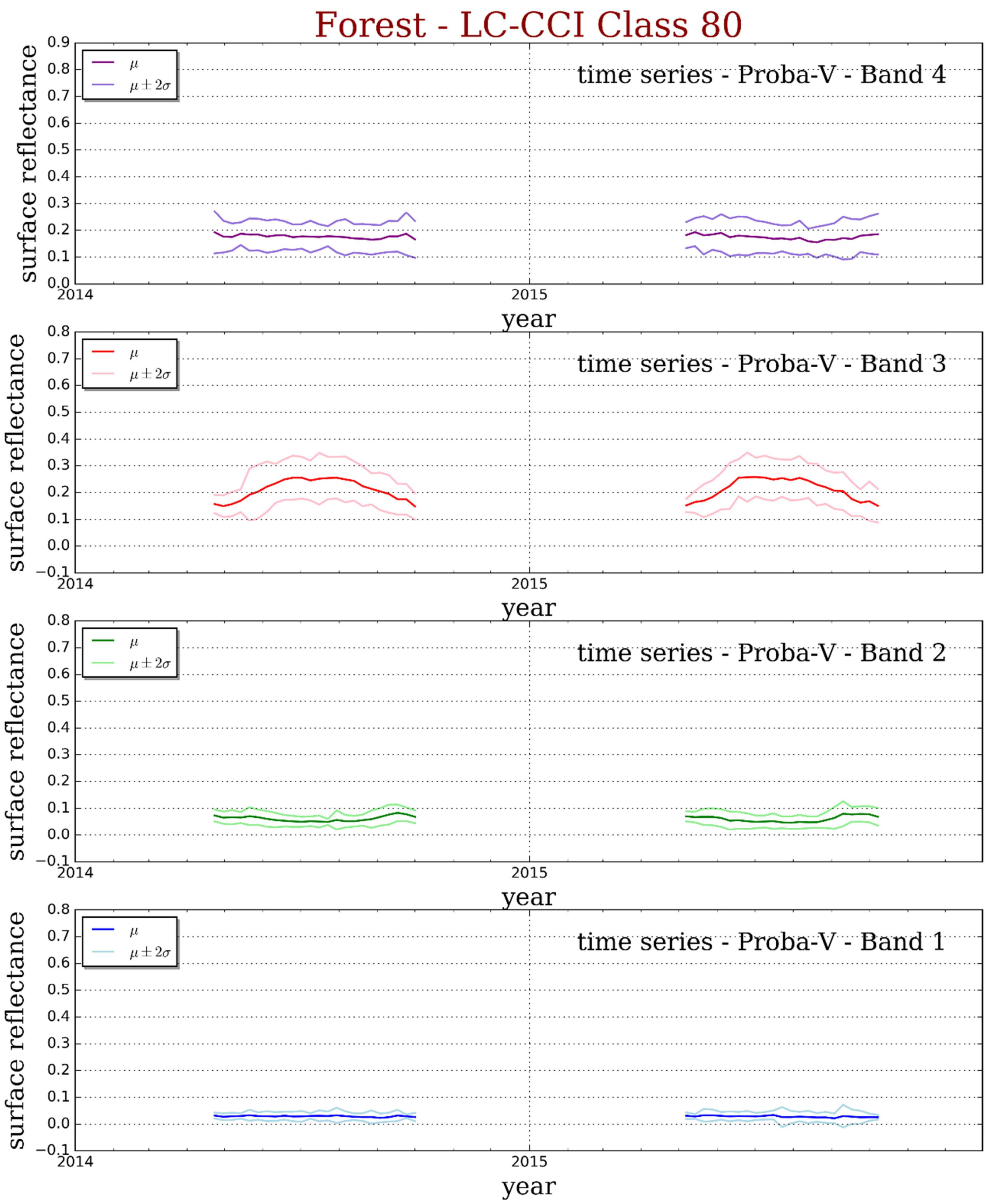

Figure 3-107: SR time series from PROBA-V data - 2014-2015 - LC-CCI-Class 80 - Tree cover, needleleaved, deciduous, closed to open

3.4.3.6 *Forest - LC-CCI-Class 90 - Tree cover, mixed leaf type (broadleaved and needleleaved)*

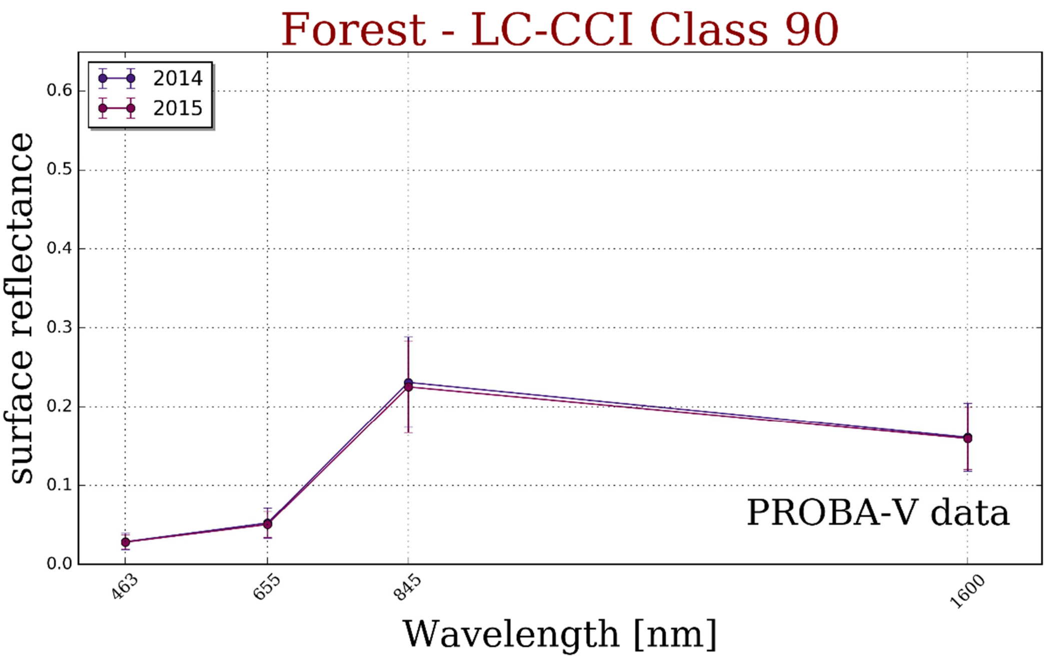

Figure 3-108: Spectra - LC-CCI-Class 90 - Tree cover, mixed leaf type (broad - and needleleaved) – PROBA-V data

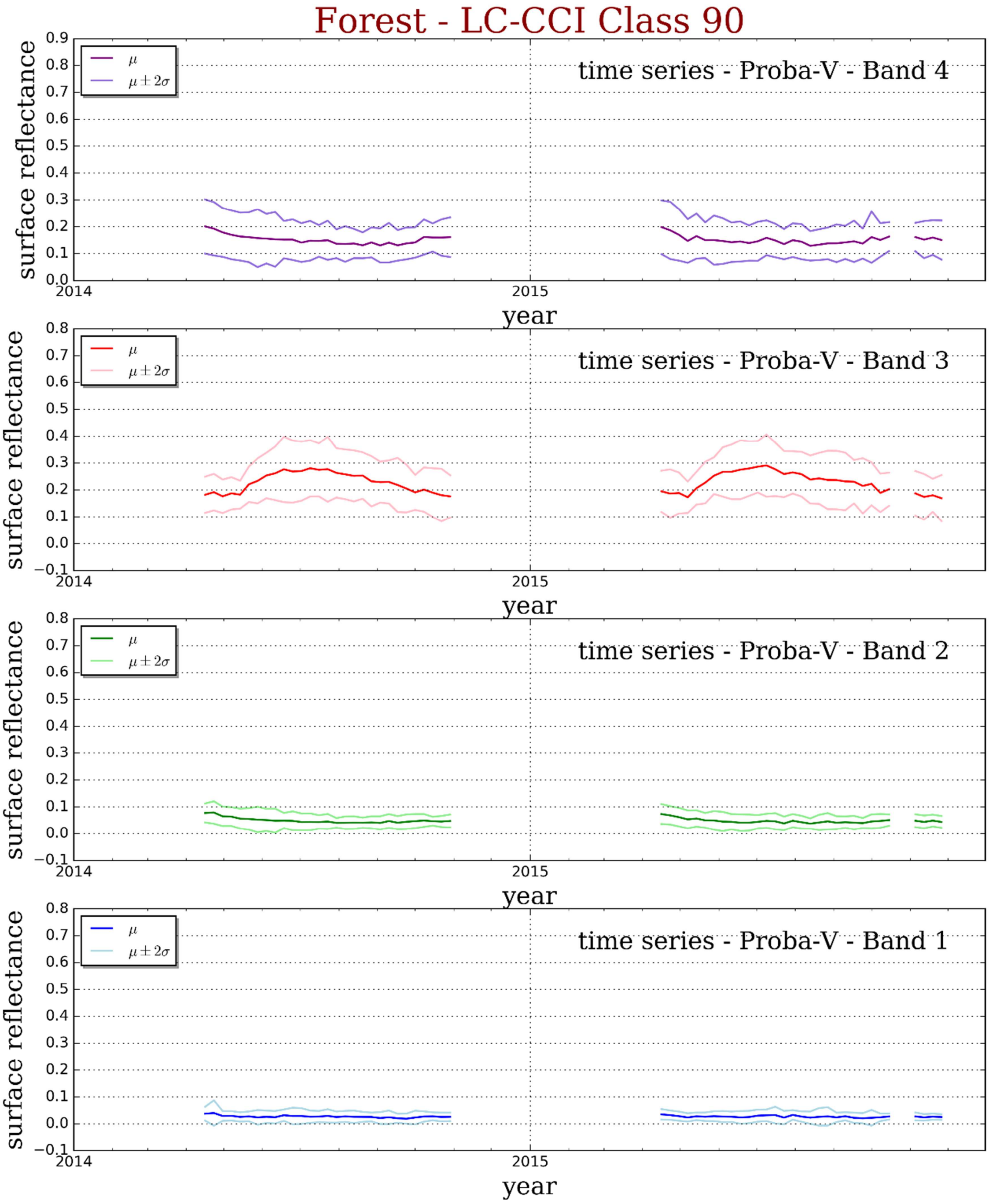

Figure 3-109: SR time series from PROBA-V data - 2014-2015 - LC-CCI-Class 90 - Tree cover, mixed leaf type (broad - and needleleaved)

3.4.3.7 *Grassland - LC-CCI-Class 130*

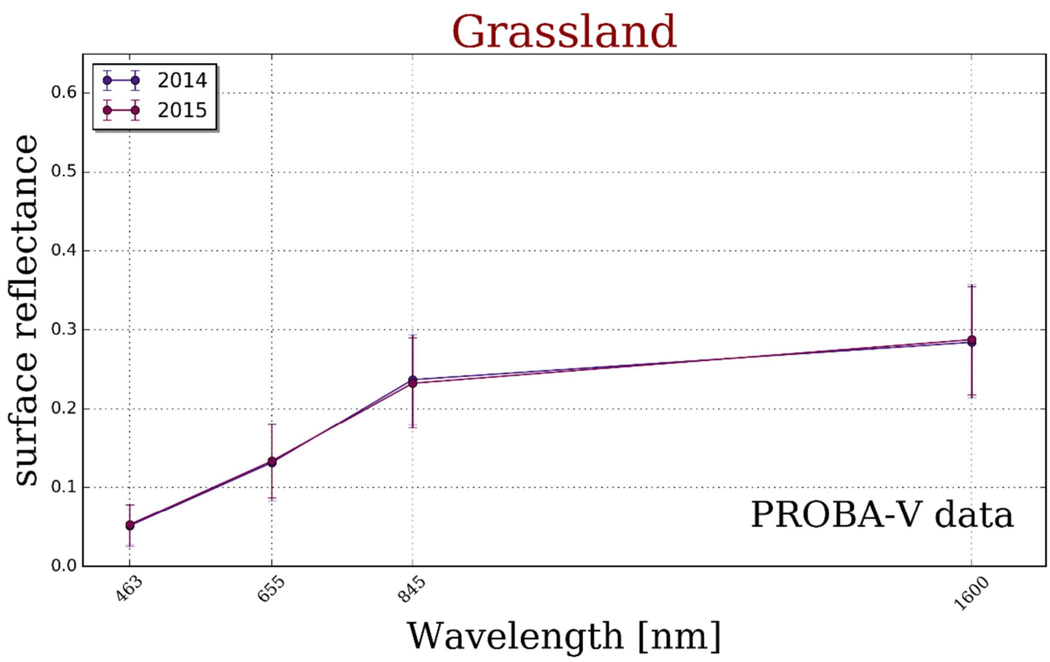

Figure 3-110: Spectra - LC-CCI-Class 130 - Grassland – PROBA-V data

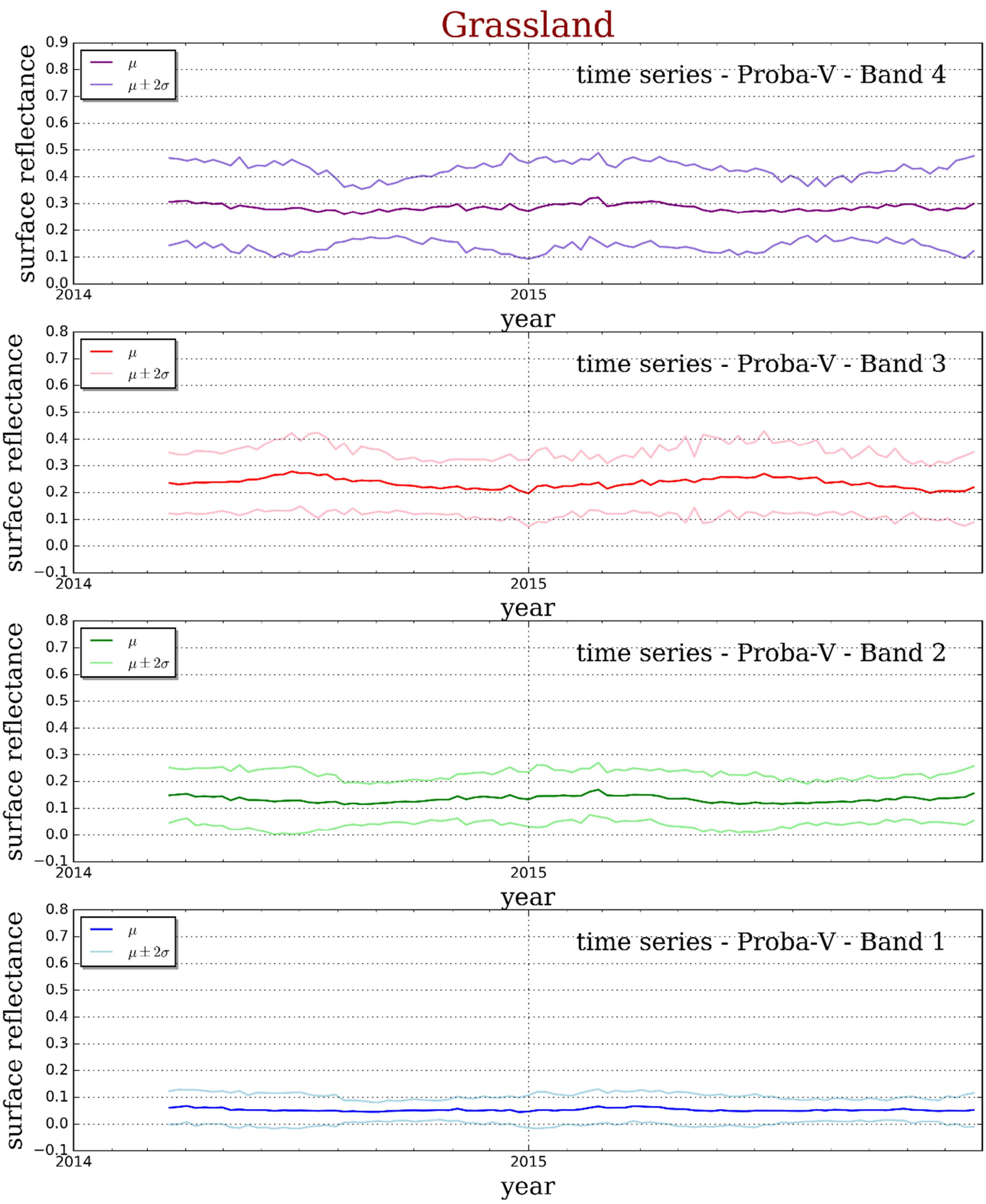

Figure 3-111: SR time series from PROBA-V data - 2014-2015 - LC-CCI-Class 130 - Grassland

3.4.3.8 *Sparse vegetation - LC-CCI-Class 150*

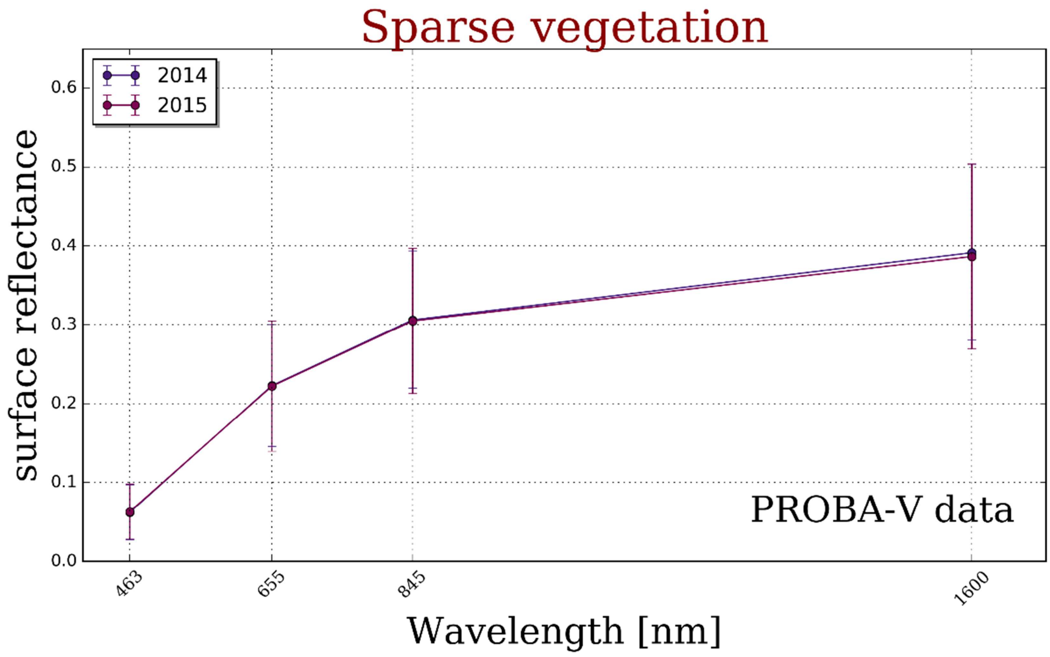

Figure 3-112: Spectra - LC-CCI-Class 150 - Sparse vegetation – PROBA-V data

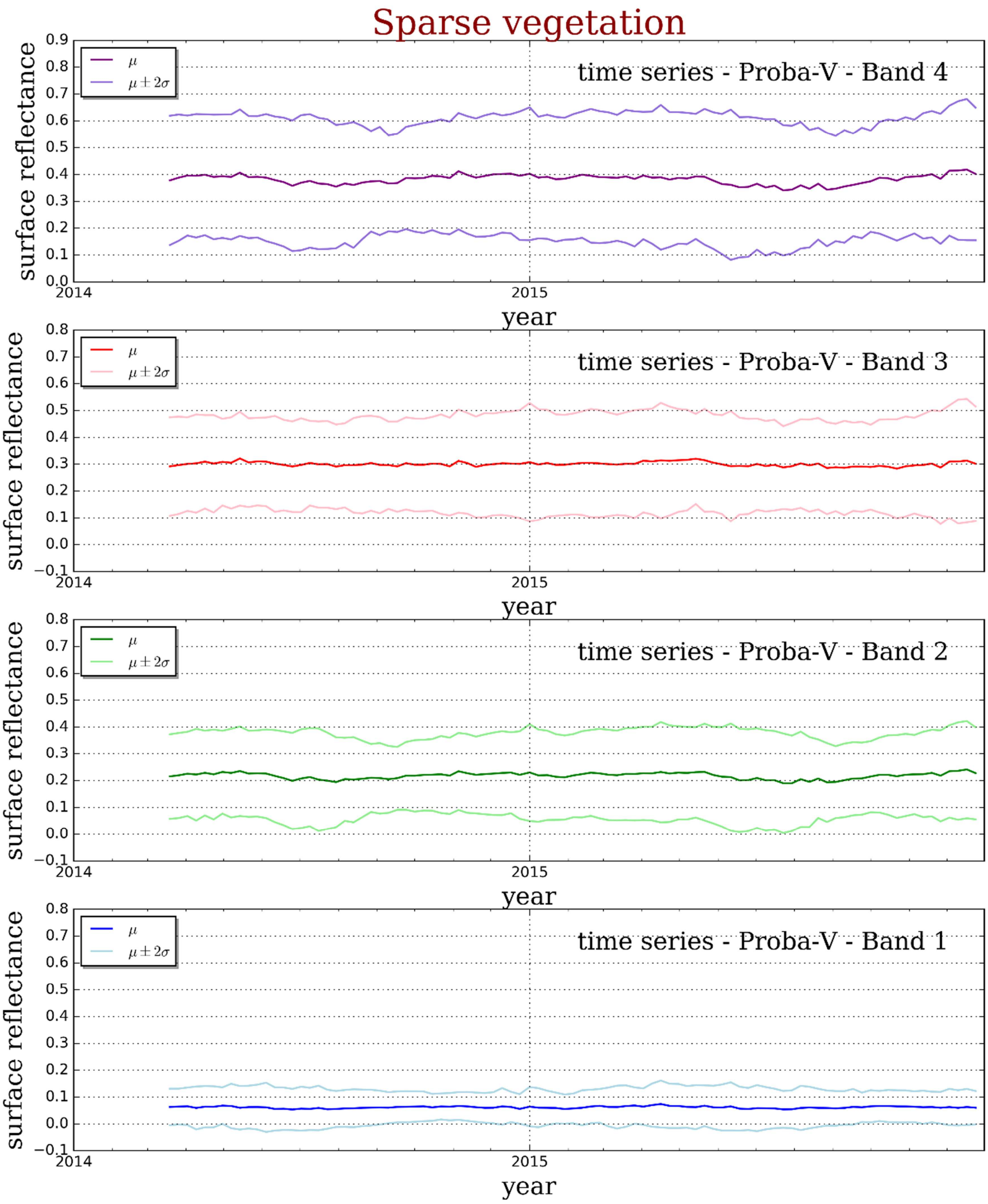

Figure 3-113: SR time series from PROBA-V data - 2014-2015 - LC-CCI-Class 150 - Sparse vegetation

3.4.3.9 *Inundated forest - LC-CCI-Class 160 and 170 - Tree cover, flooded*

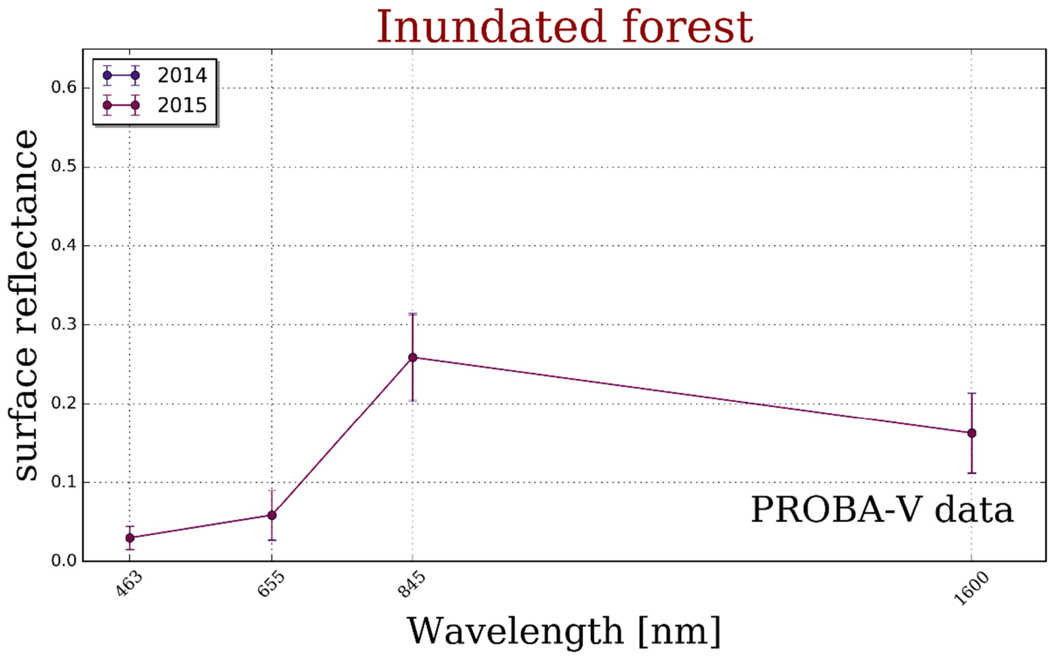

Figure 3-114: Spectra - LC-CCI-Class 160 and 170 - Tree cover, flooded – PROBA-V data

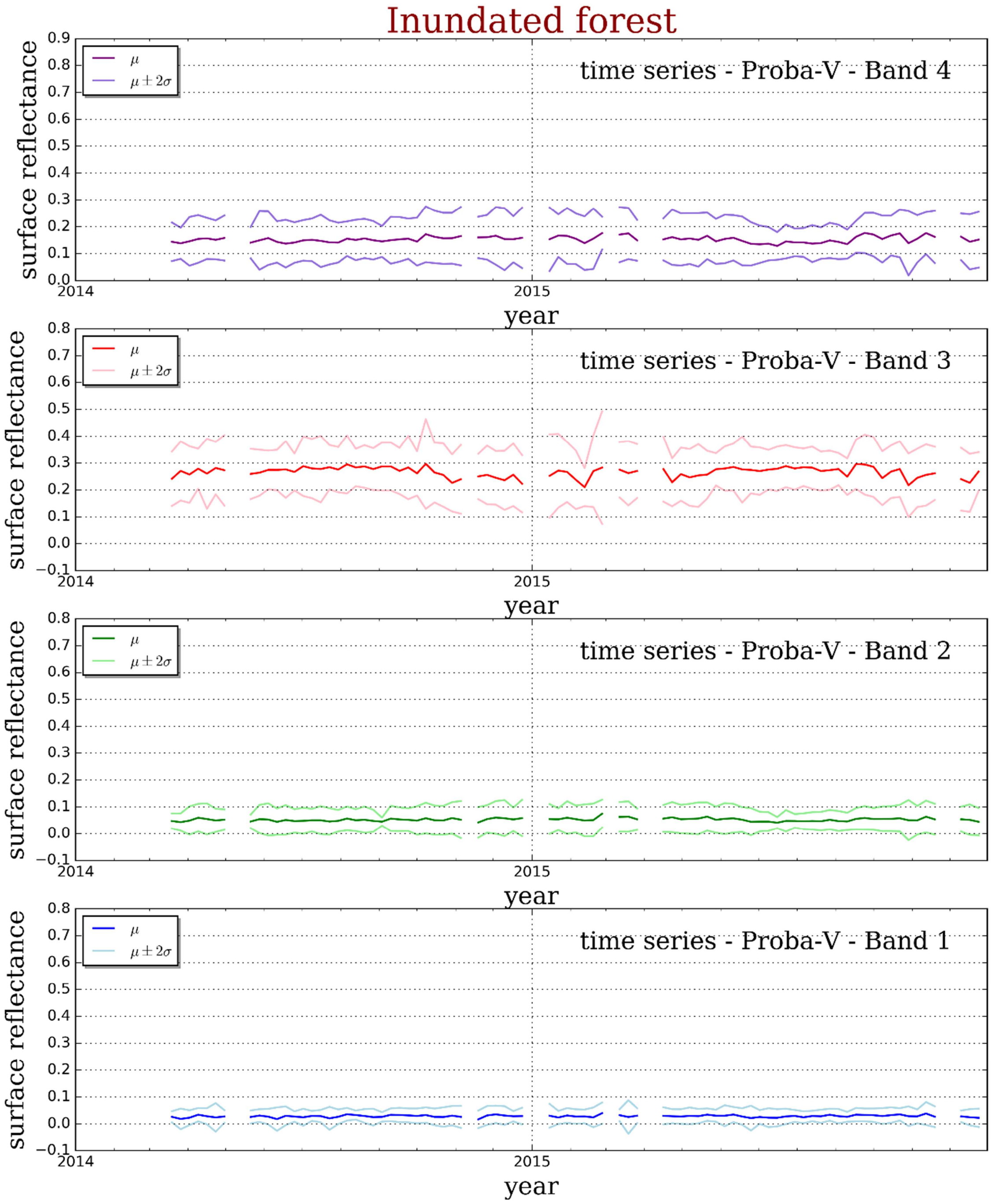

Figure 3-115: SR time series from PROBA-V data - 2014-2015 - LC-CCI-Class 160 and 170 - Tree cover, flooded

3.4.3.10 *Wetland - LC-CCI-Class 180 - Shrub or herbaceous cover, flooded*

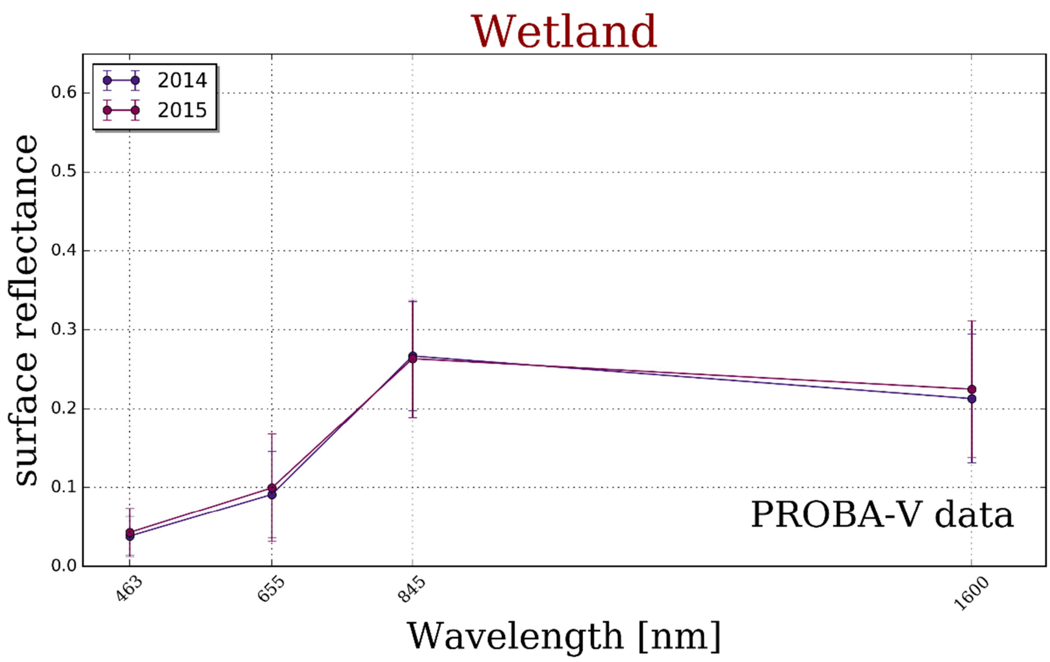

Figure 3-116: Spectra - LC-CCI-Class 180 - Shrub or herbaceous cover, flooded- PROBA-V data

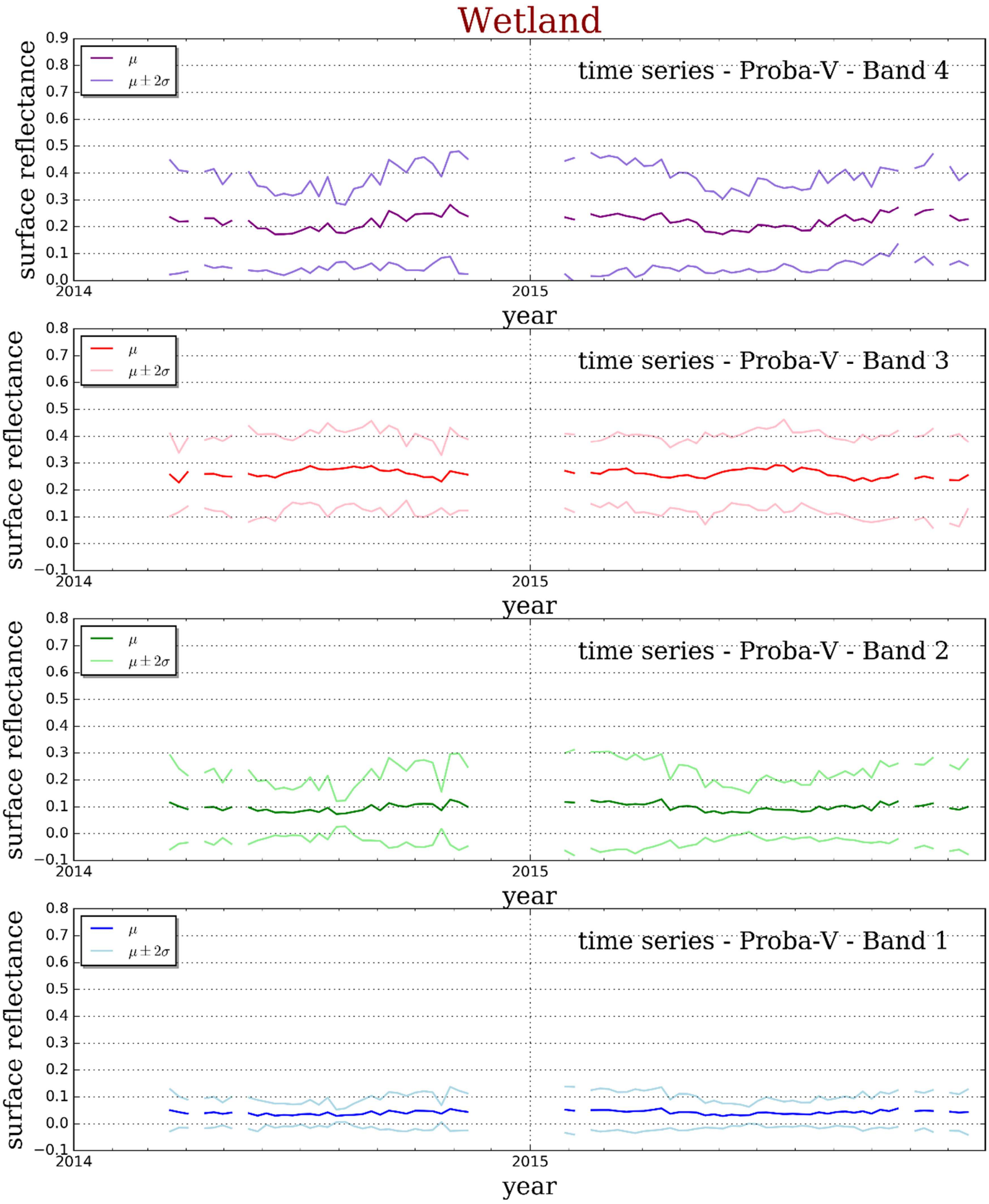

Figure 3-117: SR time series from PROBA-V data - 2014-2015 - LC-CCI-Class 180 - Shrub or herbaceous cover, flooded

3.4.3.11 *Urban areas - LC-CCI-Class 190 - Urban areas*

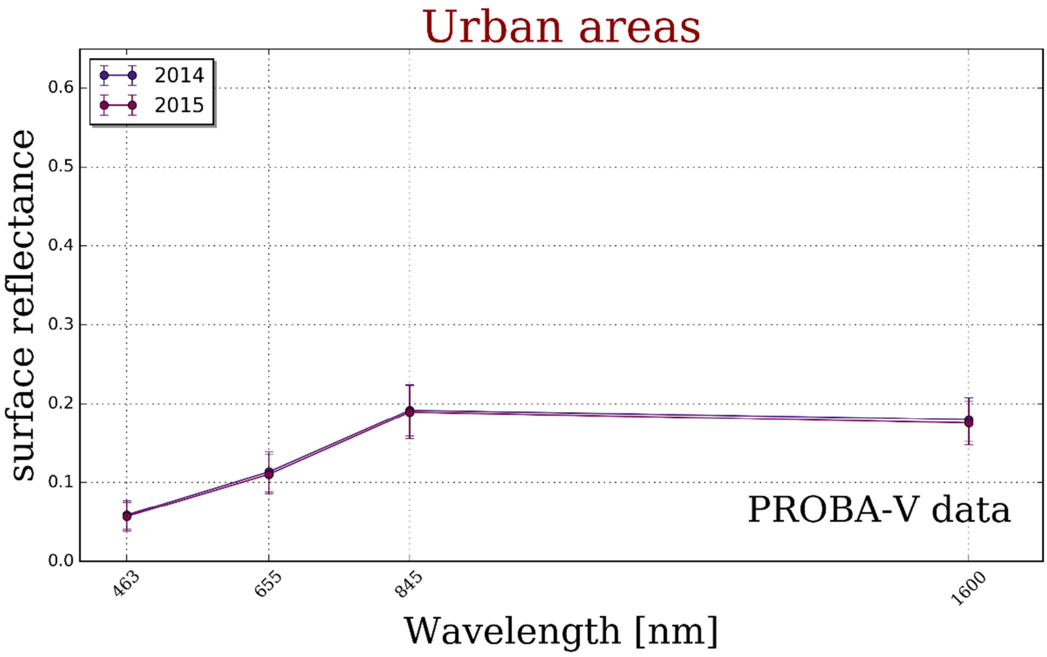

Figure 3-118: Spectra - LC-CCI-Class 190 - Urban areas – PROBA-V data

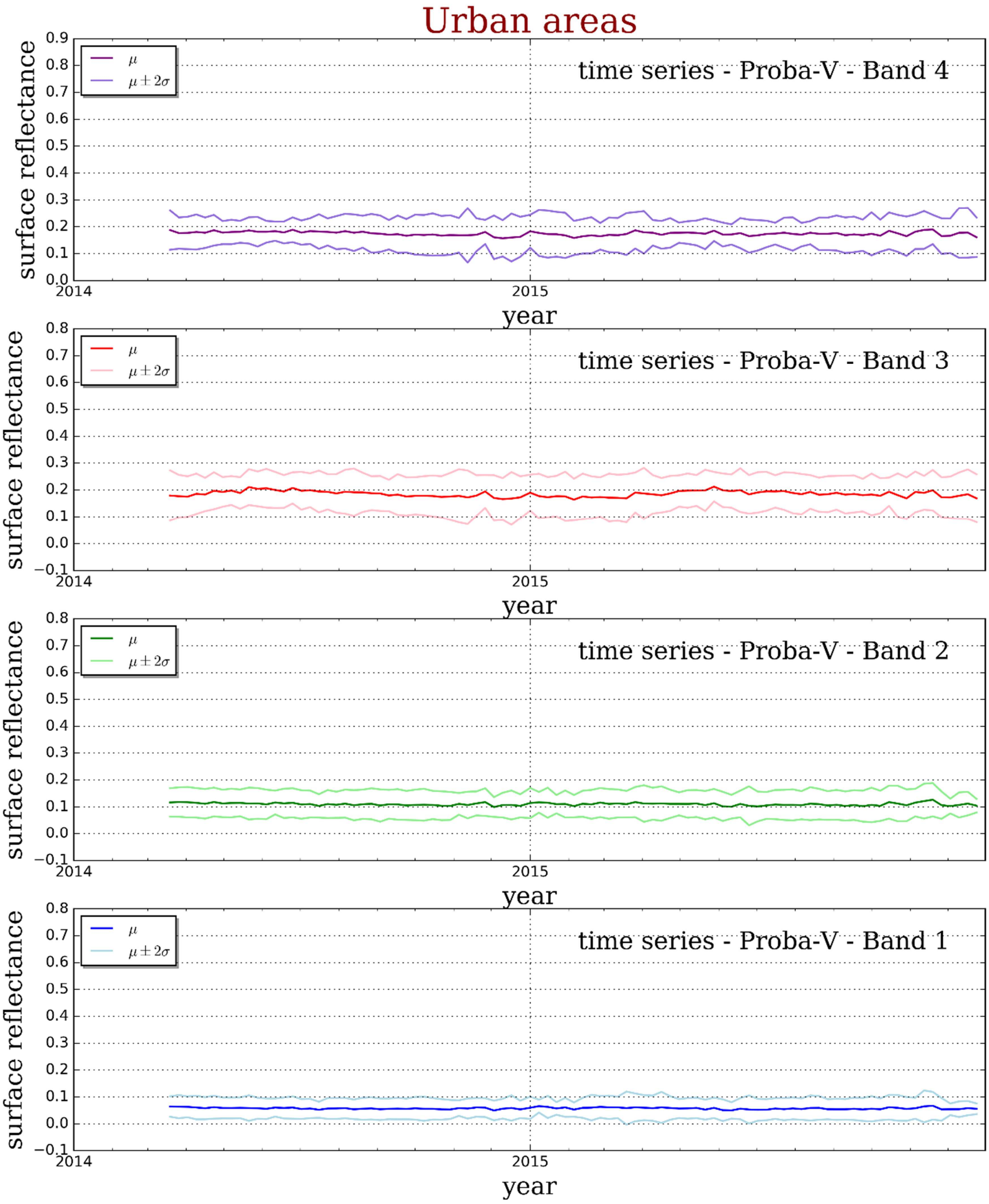

Figure 3-119: SR time series from PROBA-V data - 2014-2015 - LC-CCI-Class 190 - Urban areas

3.4.3.12 *Bare areas - LC-CCI-Class 200 - Bare areas*

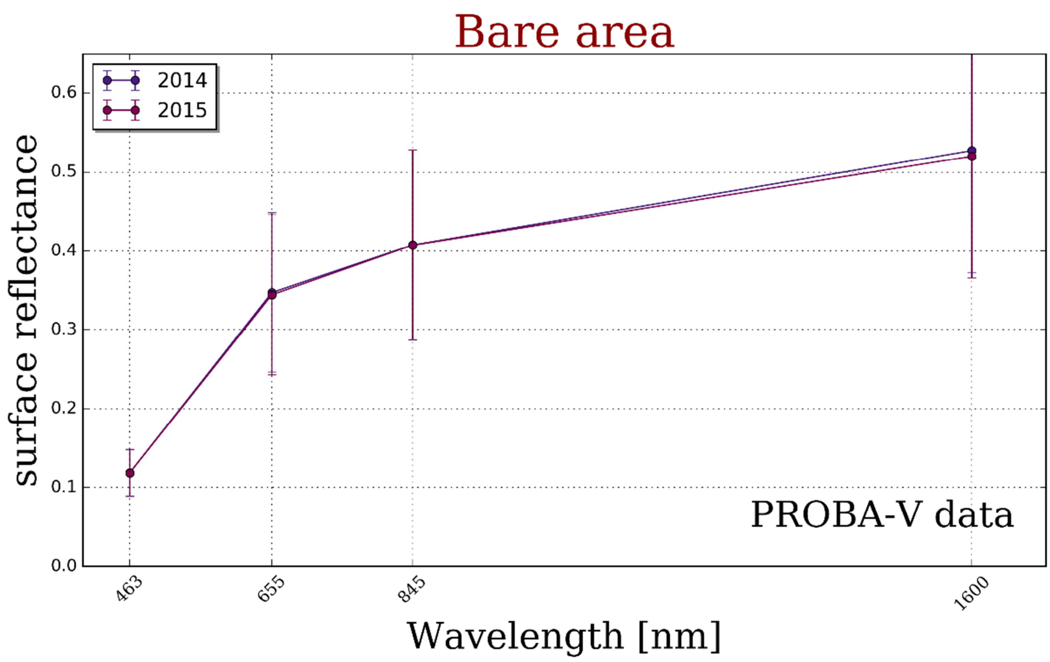

Figure 3-120: Spectra - LC-CCI-Class 200 - Bare areas – PROBA-V data

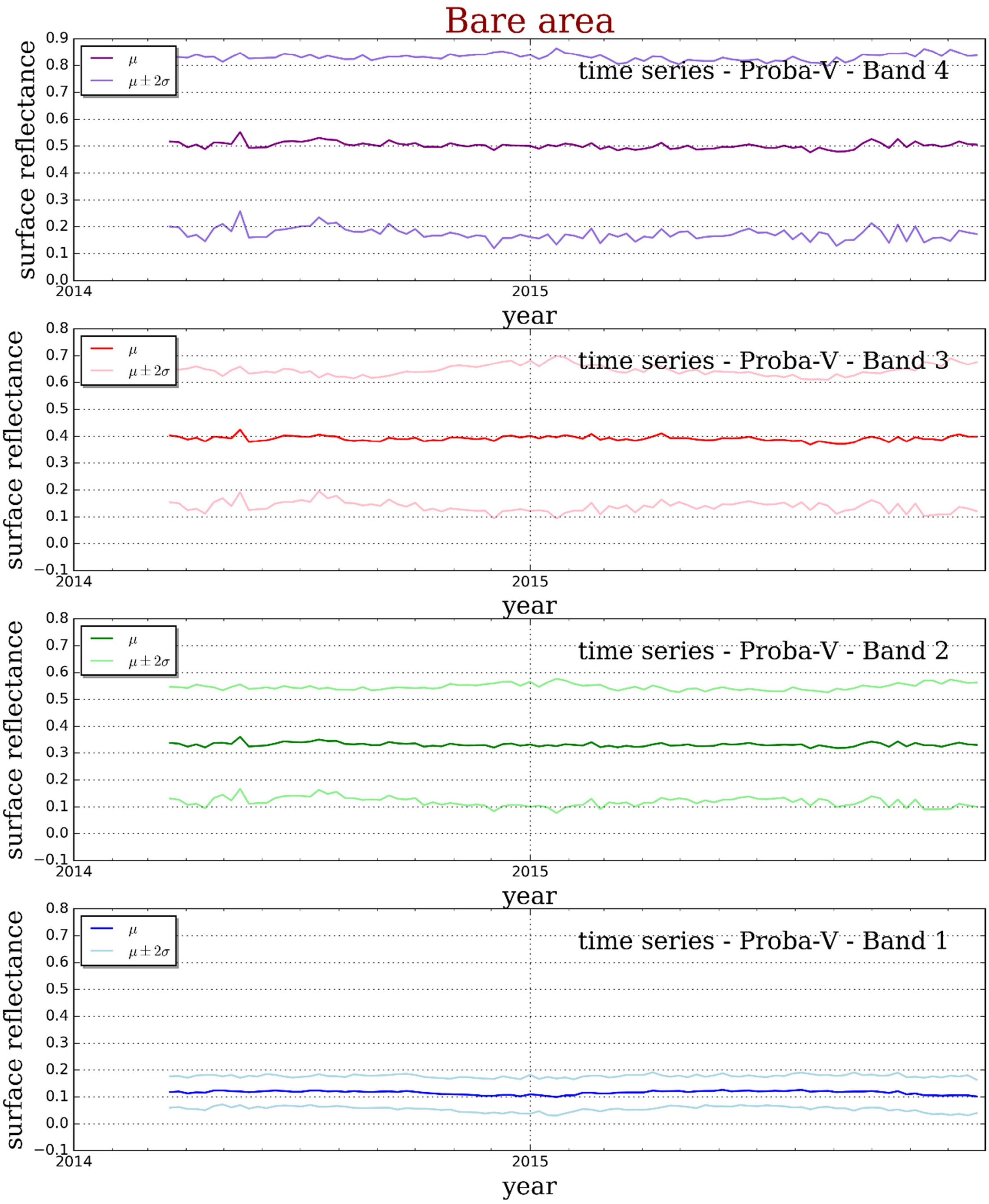

Figure 3-121: SR time series from PROBA-V data - 2014-2015 - LC-CCI-Class 200 - Bare areas – Cropland

3.4.4 Results of the analysis of the intra- and inter-annual reflectance dynamic for AVHRR

The following figures (Figure 3-122 through Figure 3-133) show the mean (x_{mean}) and the range of the spectral reflectance values at the class level for the SR time series of AVHRR data for the years 1992 through 1999.

The range is given by twice the standard deviation (2σ) again. Furthermore, the calculation of the mean and the standard deviation has been limited in particular to those cases in which at least 10 clear land observations per class and date are available.

The results of the analysis of the intra- and inter-annual reflectance dynamic can be summarized as follows:

- the spectra inside the class over the years are very similar but the standard deviation shows a great dispersion from the average as well as for the MERIS FR and RR and PROBA-V data,
- the analysis of different 7-year temporal profiles of the mean and the range highlights similar intra-annual "structures" from year to year inside the class as well as for the MERIS FR and RR and PROBA-V data
- the different 7-year temporal profiles of the mean and the range do not show significant inter-annual changes as well as for the MERIS FR and RR and PROBA-V data,
- the number of pixels which contribute to the analysis is very variable (see also section 3.2) as well as for the MERIS FR and RR and PROBA-V data.

3.4.4.1 *Cropland - LC-CCI-Class 10 and 20*

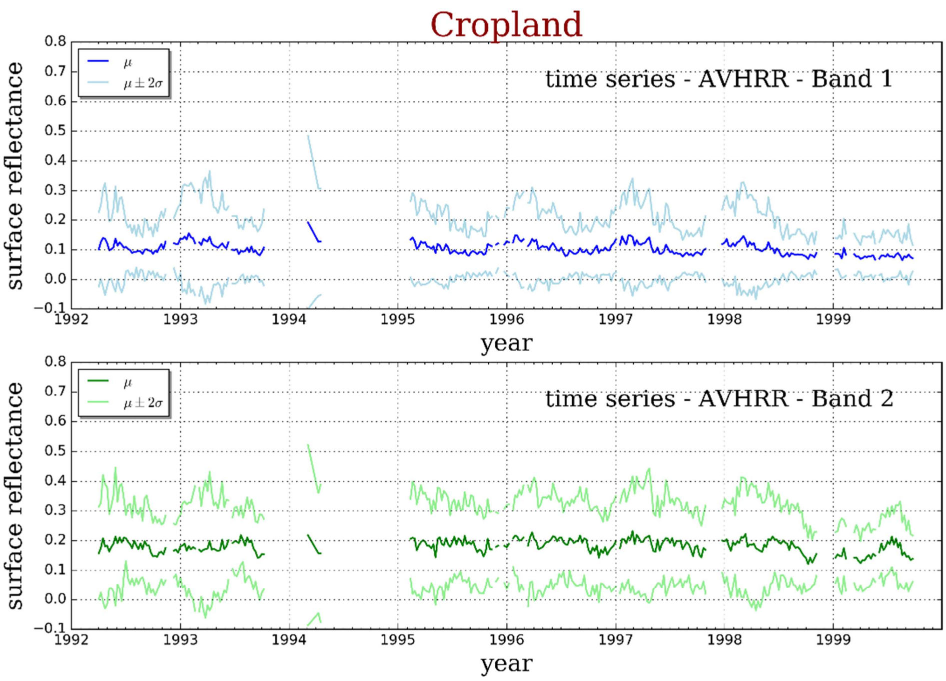

Figure 3-122: SR time series from AVHRR data - 1992-1999 - LC-CCI-Class 10 and 20 - Cropland

3.4.4.2 *Forest - LC-CCI-Class 50 - Tree cover, broadleaved, evergreen, closed to open*

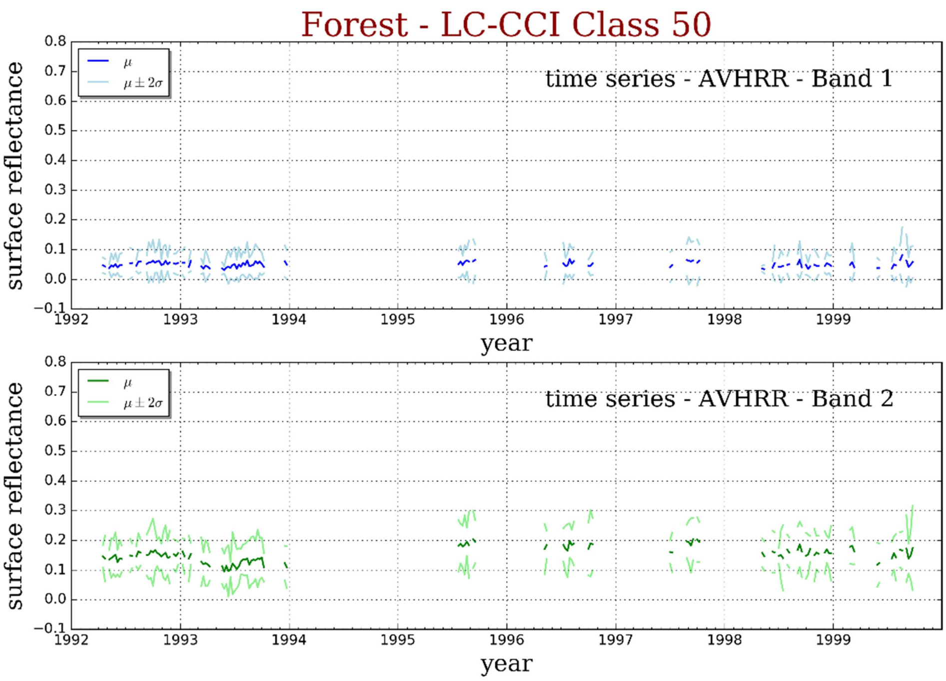

Figure 3-123: SR time series from AVHRR data - 1992-1999 - LC-CCI-Class 50 - Tree cover, broadleaved, evergreen, closed to open

3.4.4.3 *Forest - LC-CCI-Class 60 - Tree cover, broadleaved, deciduous, closed to open*

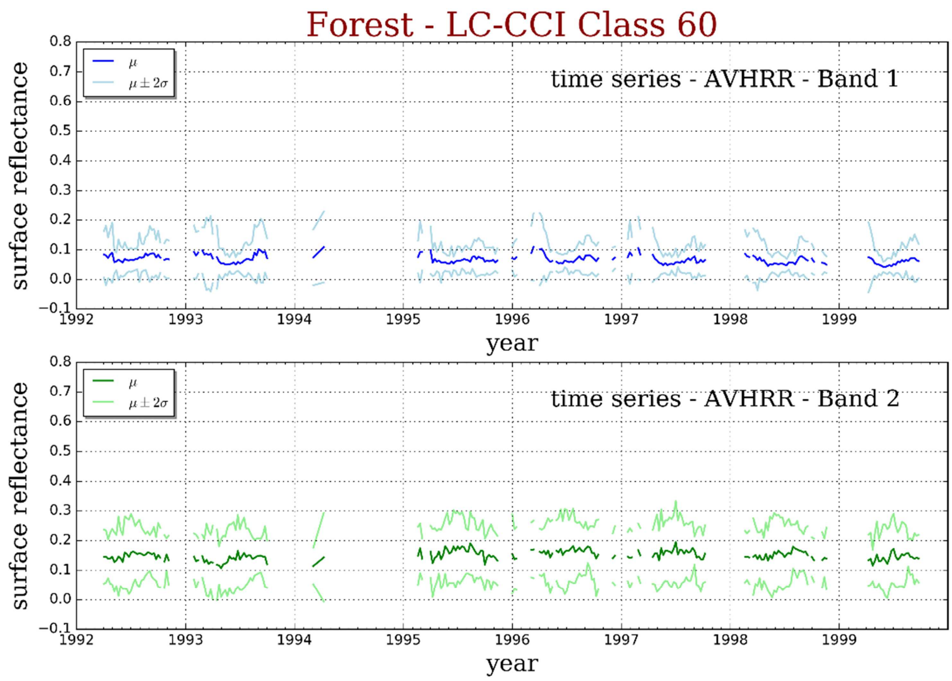

Figure 3-124: SR time series from AVHRR data - 1992-1999 - LC-CCI-Class 60 - Tree cover, broadleaved, deciduous, closed to open

3.4.4.4 *Forest - LC-CCI-Class 70 - Tree cover, needleleaved, evergreen, closed to open*

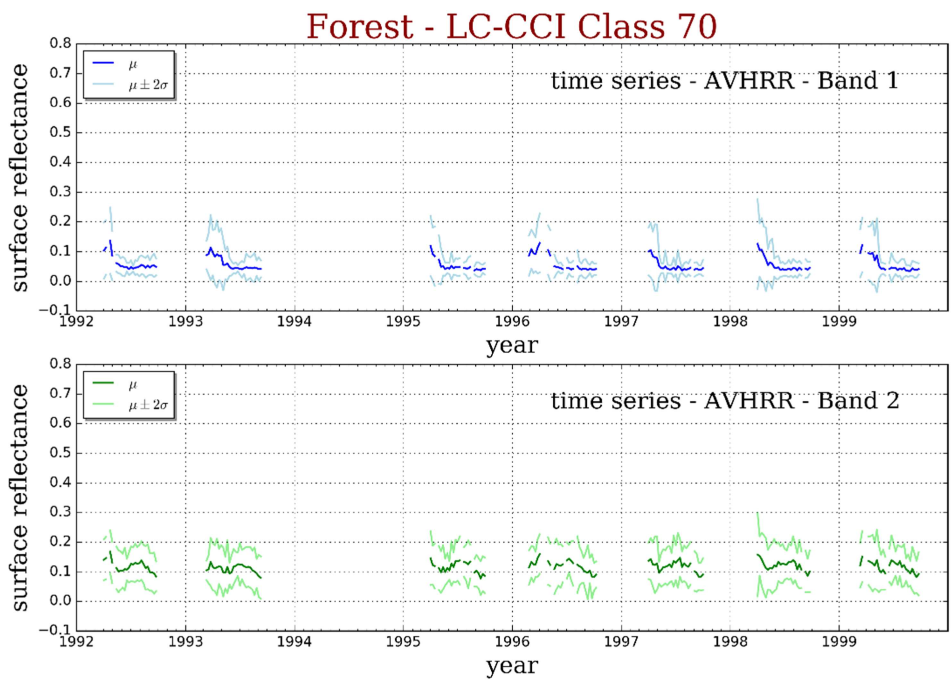

Figure 3-125: SR time series from AVHRR data - 1992-1999 - LC-CCI-Class 70 - Tree cover, needleleaved, evergreen, closed to open

3.4.4.5 *Forest - LC-CCI-Class 80 - Tree cover, needleleaved, deciduous, closed to open*

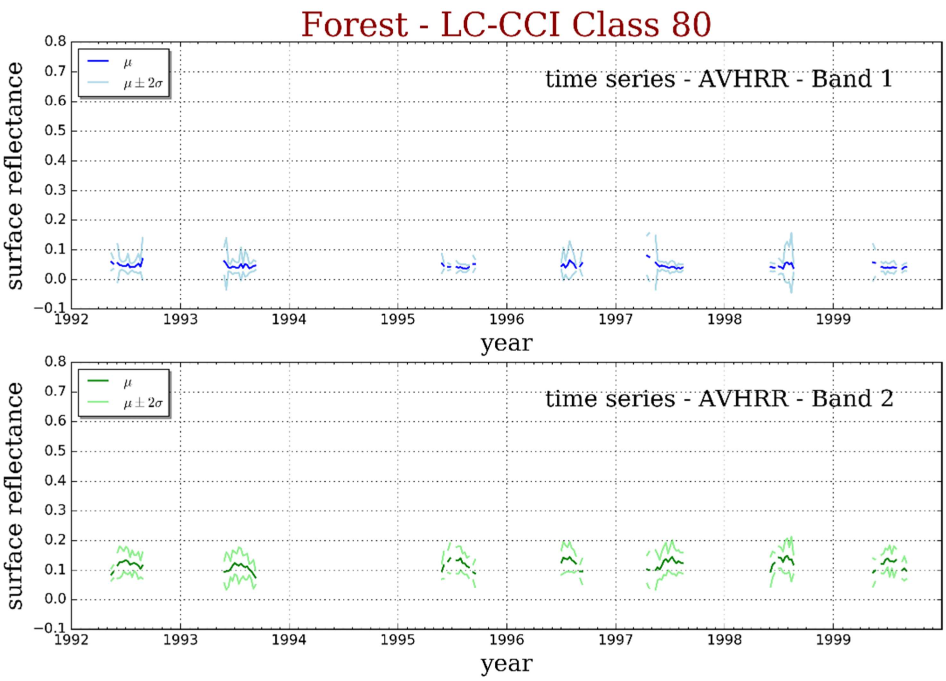

Figure 3-126: SR time series from AVHRR data - 1992-1999 - LC-CCI-Class 80 - Tree cover, needleleaved, deciduous, closed to open

3.4.4.6 *Forest - LC-CCI-Class 90 - Tree cover, mixed leaf type (broadl. and needleleaved)*

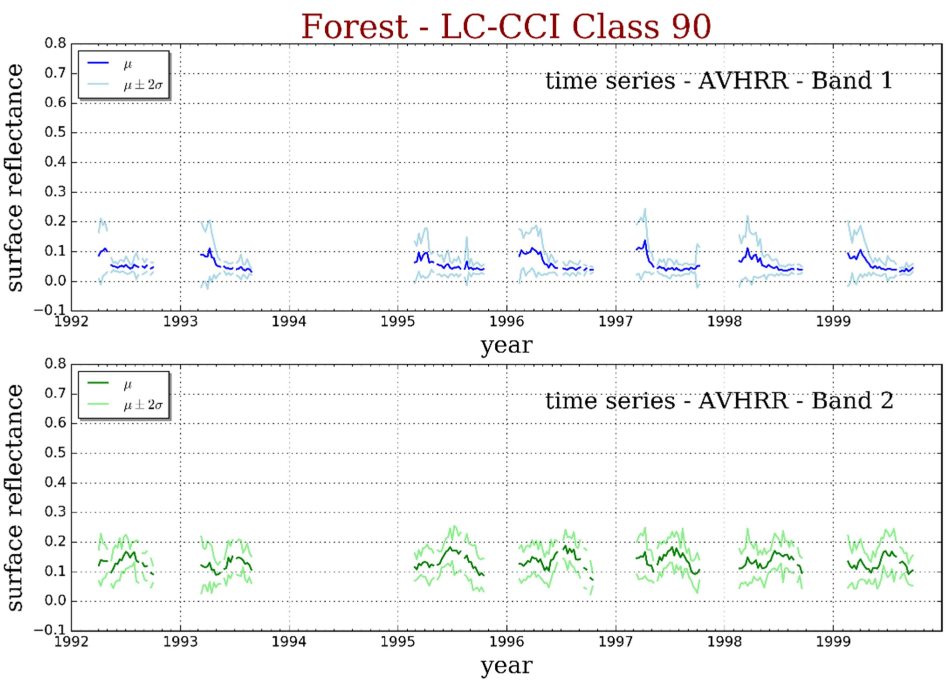

Figure 3-127: SR time series from AVHRR data - 1992-1999 - LC-CCI-Class 90 - Tree cover, mixed leaf type (broad - and needleleaved)

3.4.4.7 *Grassland - LC-CCI-Class 130*

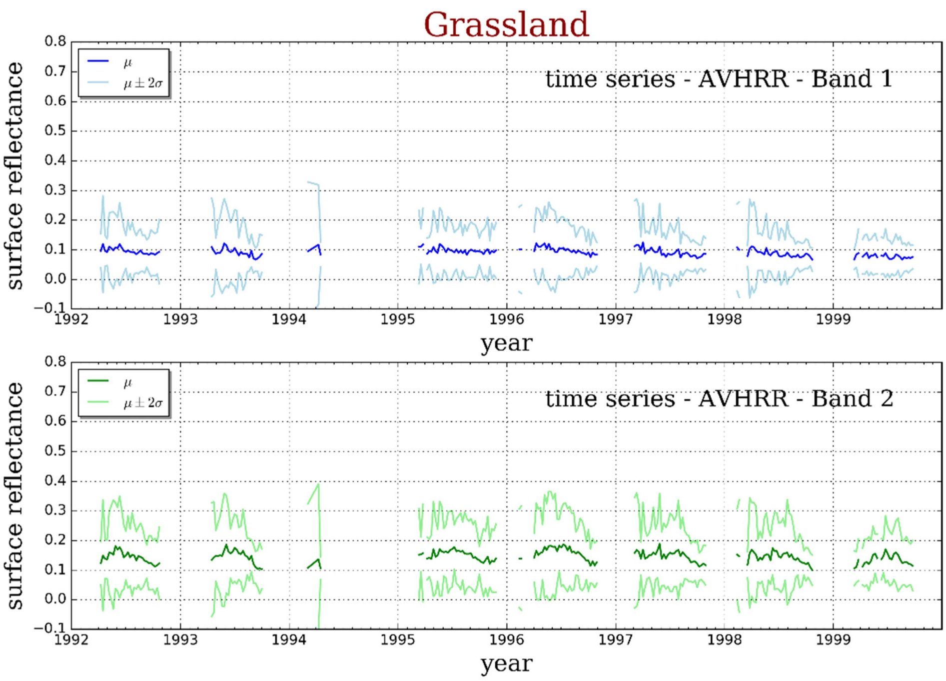

Figure 3-128: SR time series from AVHRR data - 1992-1999 - LC-CCI-Class 130 - Grassland

3.4.4.8 *Sparse vegetation - LC-CCI-Class 150*

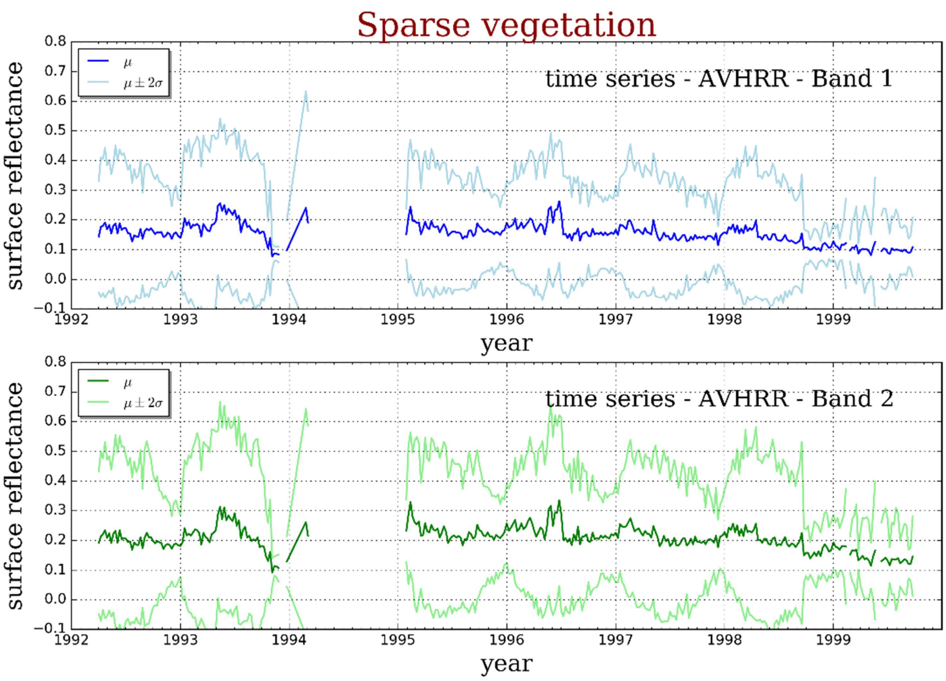

Figure 3-129: SR time series from AVHRR data - 1992-1999 - LC-CCI-Class 150 - Sparse vegetation

3.4.4.9 *Inundated forest - LC-CCI-Class 160 and 170 - Tree cover, flooded*

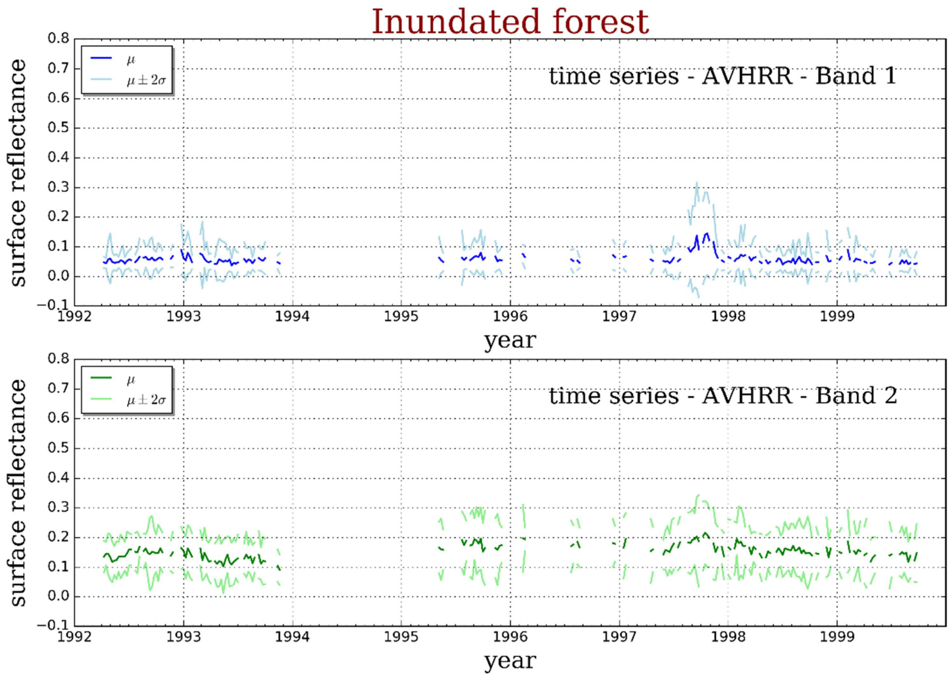

Figure 3-130: SR time series from AVHRR data - 1992-1999 - LC-CCI-Class 160 and 170 - Tree cover, flooded

3.4.4.10 *Wetland - LC-CCI-Class 180 - Shrub or herbaceous cover, flooded*

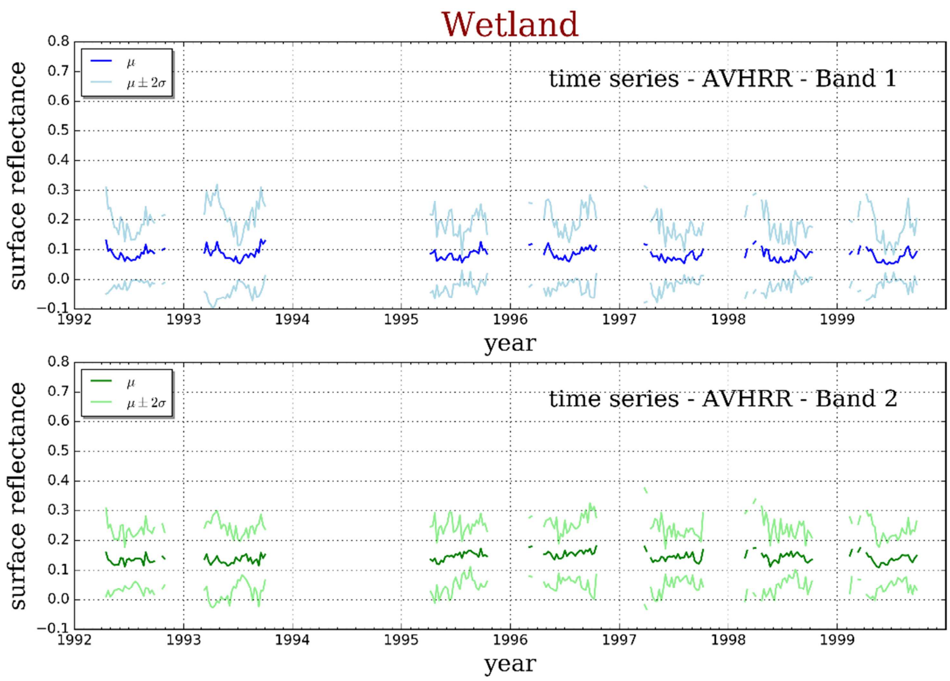

Figure 3-131: SR time series from AVHRR data - 1992-1999 - LC-CCI-Class 180 - Shrub or herbaceous cover, flooded

3.4.4.11 *Urban areas - LC-CCI-Class 190 - Urban areas*

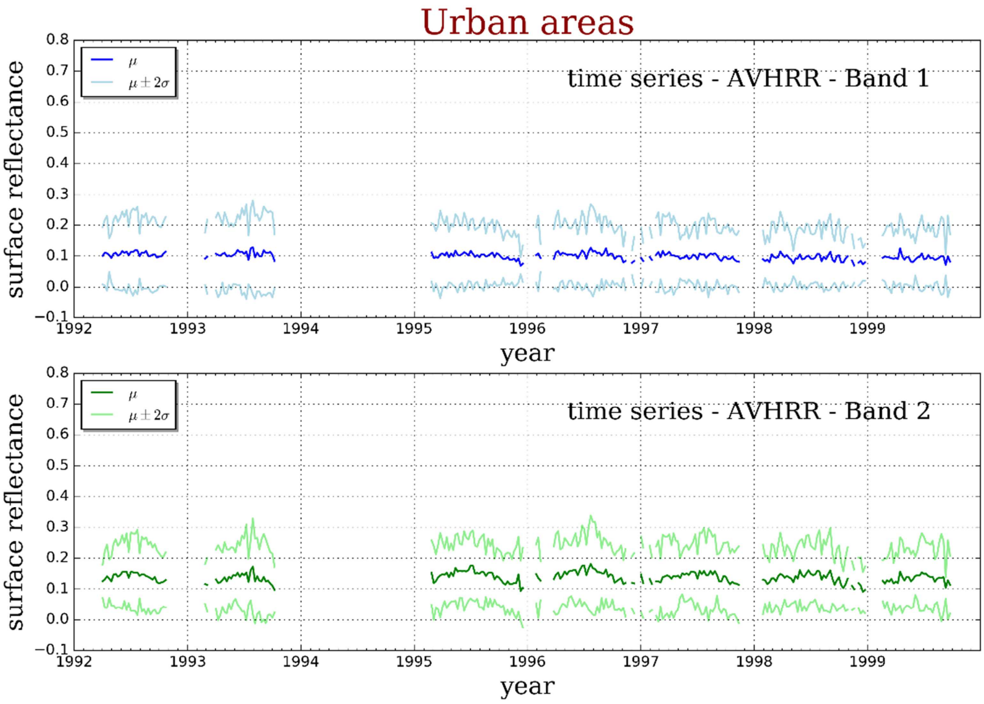

Figure 3-132: SR time series from AVHRR data - 1992-1999 - LC-CCI-Class 190 - Urban areas

3.4.4.12 *Bare areas - LC-CCI-Class 200 - Bare areas*

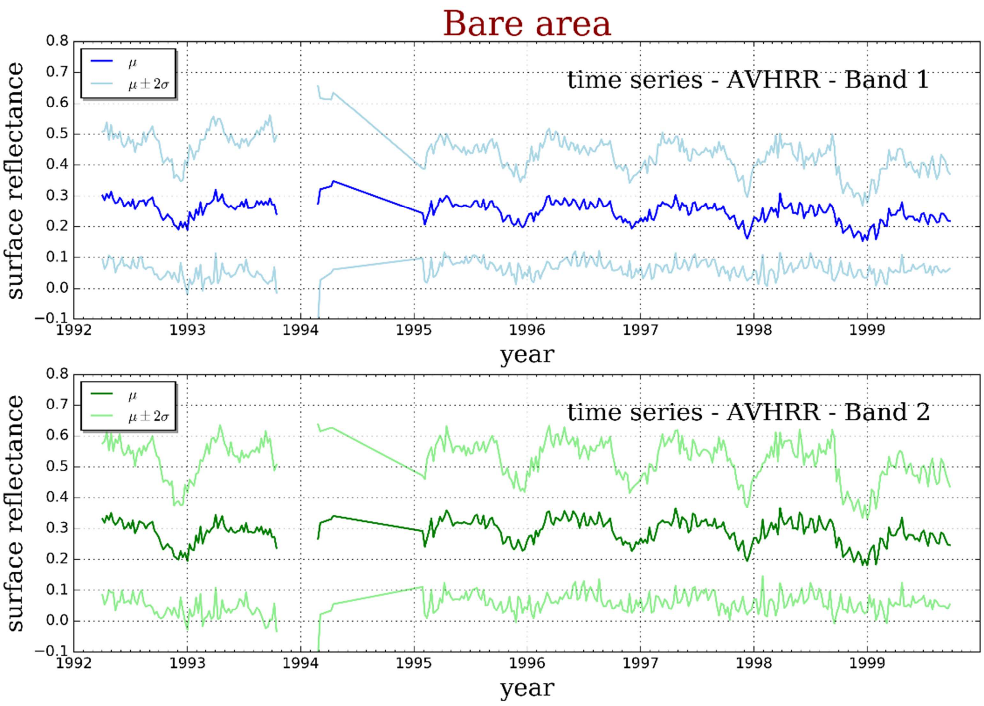

Figure 3-133: SR time series from AVHRR data - 1992-1999 - LC-CCI-Class 200 - Bare areas – Cropland

3.5 Validation against in-situ data

The validation of the 7-day SR composites should also comprise the comparison with in-situ data. For this purpose, the CEOS-LANDNET sites have been selected because they are accepted validation sites. At the present stage of the project the CEOS LANDNET site protocols with the in-situ data published herein are only accessible. But actually in-situ data has not been included to all protocols or there is a lack of information concerning the temporal variability of the measured spectra. Only for the CEOS LANDNET site La Crau, mean surface reflectances including the variation have been provided by the protocol. All other values should be used carefully by the evaluation because some of them reflect individual measurements only and uncertainties are not specified.

The Table 3-51 lists the in-situ data, that are taken from the figures or tables in the protocols of CEOS LANDNET sites ([CEOS-RVP, 2009], [CEOS-NV, 2009], [CEOS-LC, 2009], [CEOS-IP, 2009], [CEOS-FF, 2009], [CEOS-DG, 2009]) or figure, which is published in Kneubuehler et al., 2006 [Kneubuehler et al., 2006]. The images of the reference spectra have been digitalized using WebPlotDigitizer [Rohatgi, 2015].

The following figures (Figure 3-134 through Figure 3-137) show the mean spectra retrieved from time series of the CEOS LANDNET site Dunhuang, La Crau, Negev and Railroad Valley Playa. The characteristic of the spectra is similar, but the absolute values may differ.

As mentioned before, the in-situ data of CEOS LANDNET site La Crau can better use for the validation. The typical surface reflectance spectrum and values of this site are taken from [CEOS-LC, 2009]. Assuming that both in-situ measurements reflect the natural variability, then the mean of retrieved SR values from MERIS FR and RR as well as PROBA-V matched with the in-situ measurements reasonably well. In case of AVHRR the retrieved mean surface reflectance values are beyond the typical in-situ reflectance values. The reason for this may be that the atmospheric conditions cannot be retrieved from the sensor observations itself and therefore the era–interim data and aerosol climatology are used for the atmospheric correction of the AVHRR data.

a)

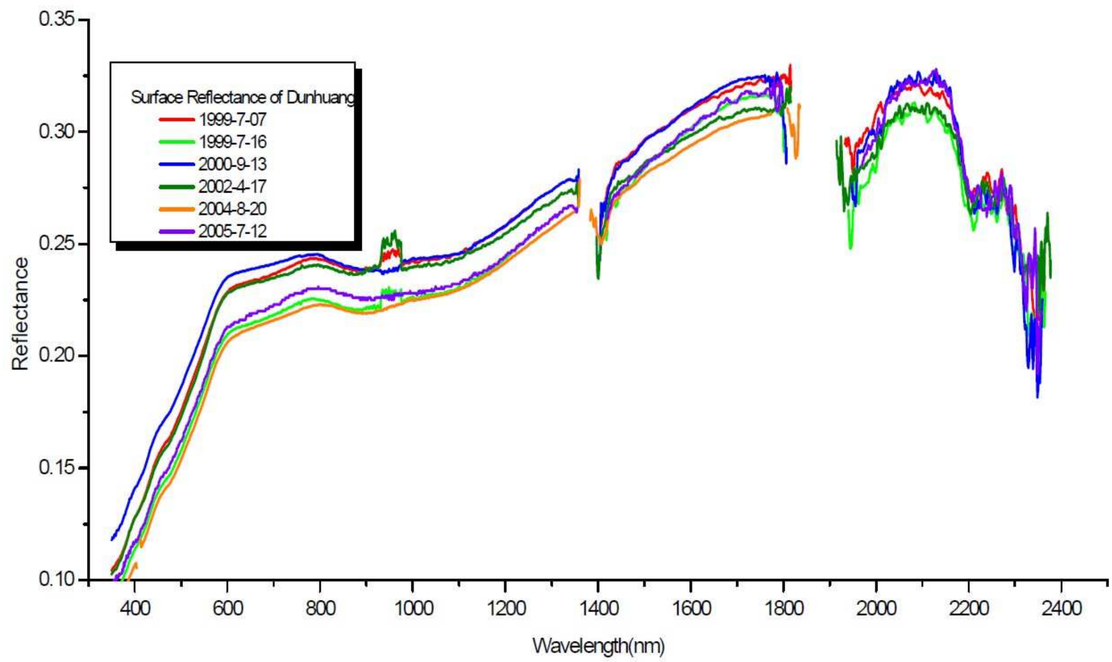
Surface Reflectance of Dunhuang
1999-7-07
1999-7-16
2000-9-13
2002-4-17
2004-8-20
2005-7-12
Reflectance
Wavelength(nm)

b)

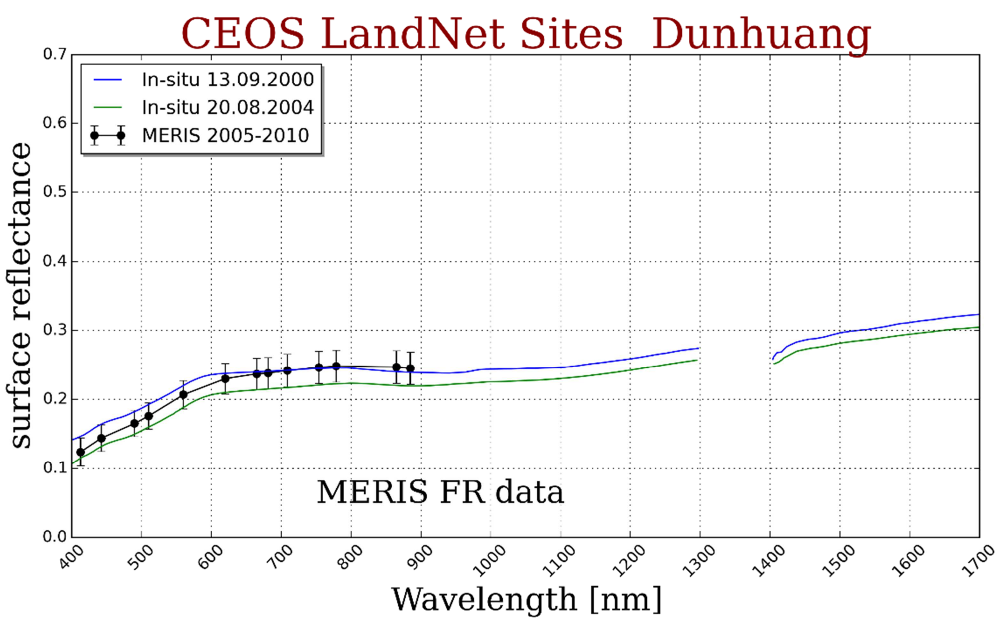
CEOS LandNet Sites Dunhuang
In-situ 13.09.2000
In-situ 20.08.2004
MERIS 2005-2010
surface reflectance
MERIS FR data
Wavelength [nm]

c)

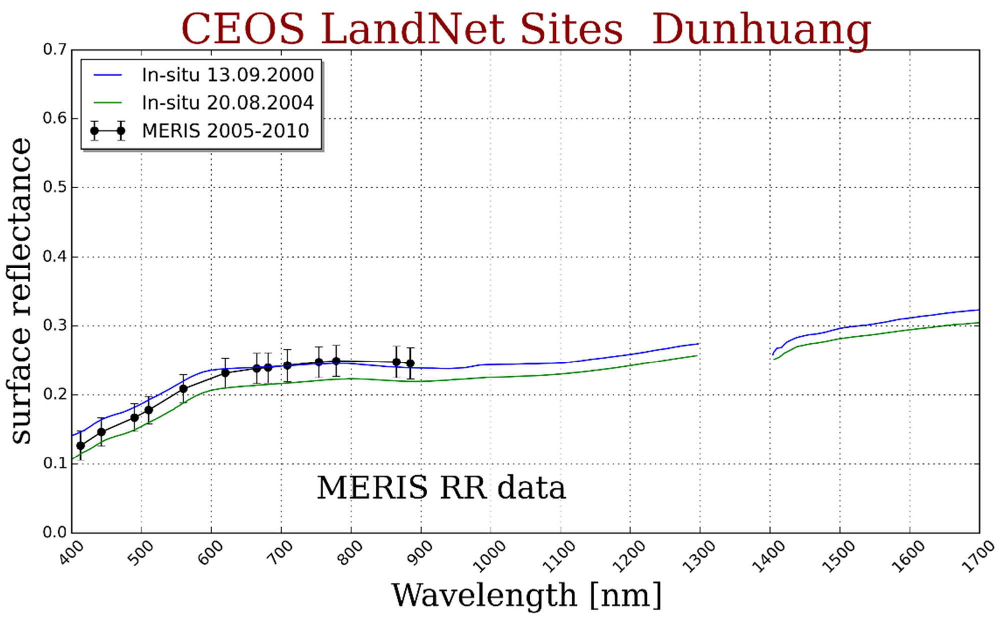
CEOS LandNet Sites Dunhuang
In-situ 13.09.2000
In-situ 20.08.2004
MERIS 2005-2010
surface reflectance
MERIS RR data
Wavelength [nm]

d)

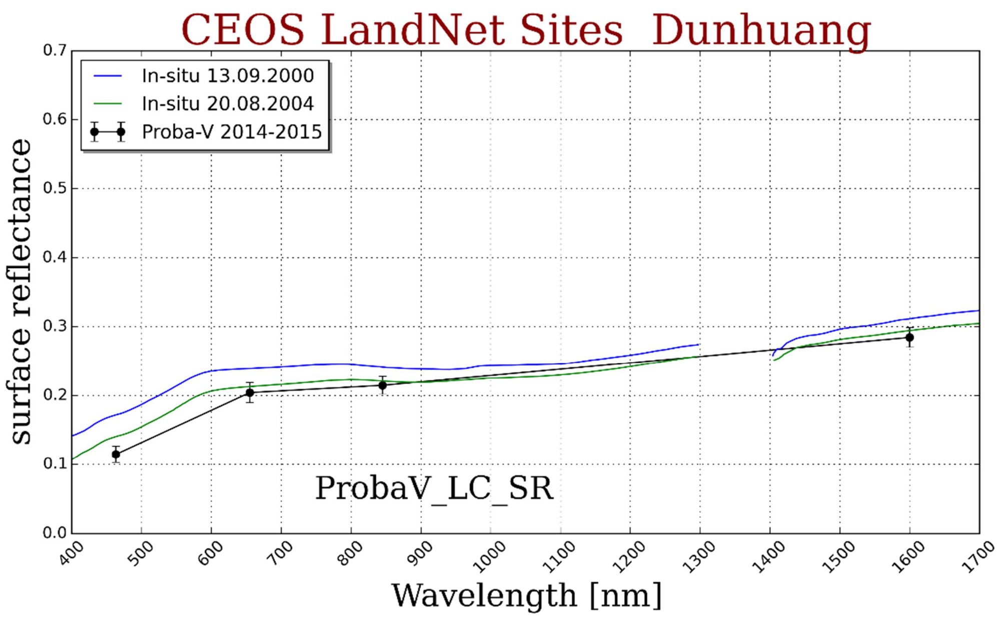
CEOS LandNet Sites Dunhuang
In-situ 13.09.2000
In-situ 20.08.2004
Proba-V 2014-2015
surface reflectance
ProbaV_LC_SR
Wavelength [nm]

e)

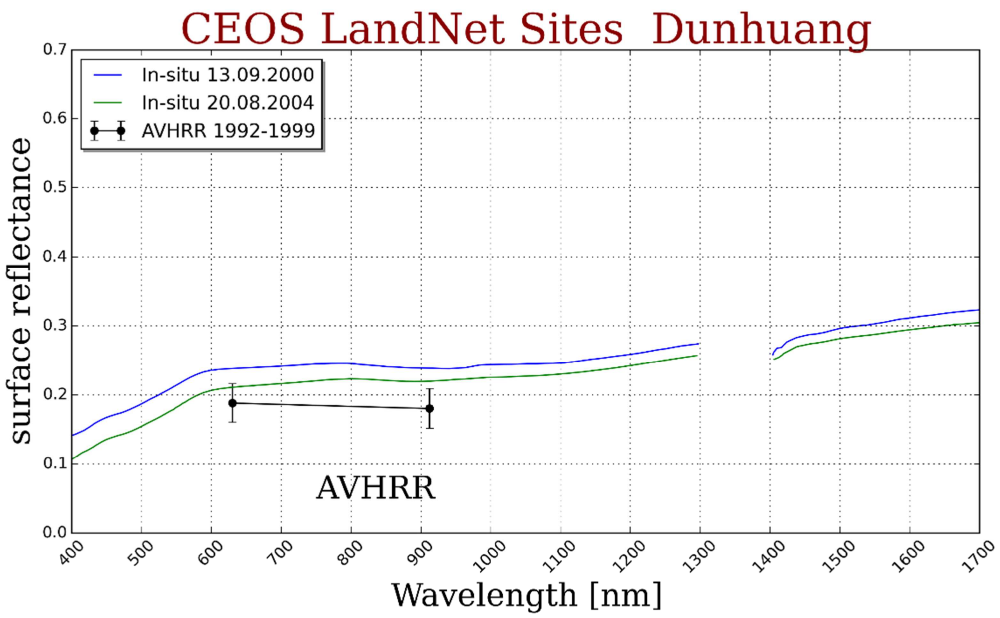

Figure 3-134: Comparison of Spectra - CEOS-LANDNET SITES - Dunhuang - a) in-situ data - fig. taken from [CEOS-DG, 2009] b) MERIS FR 2003-2012 c) MERIS RR 2003-2012 d) PROBA-V 2014-2016 e) AVHRR 1992-1999

a)

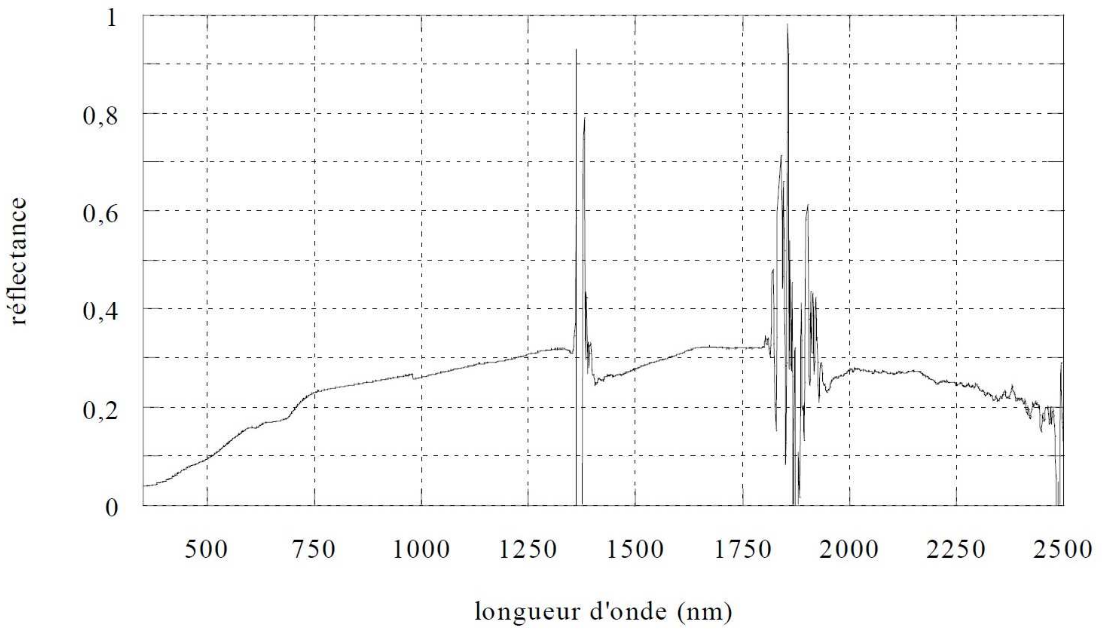

réflectance
0
0,2
0,4
0,6
0,8
1
500
750
1000
1250
1500
1750
2000
2250
2500
longueur d'onde (nm)

b)

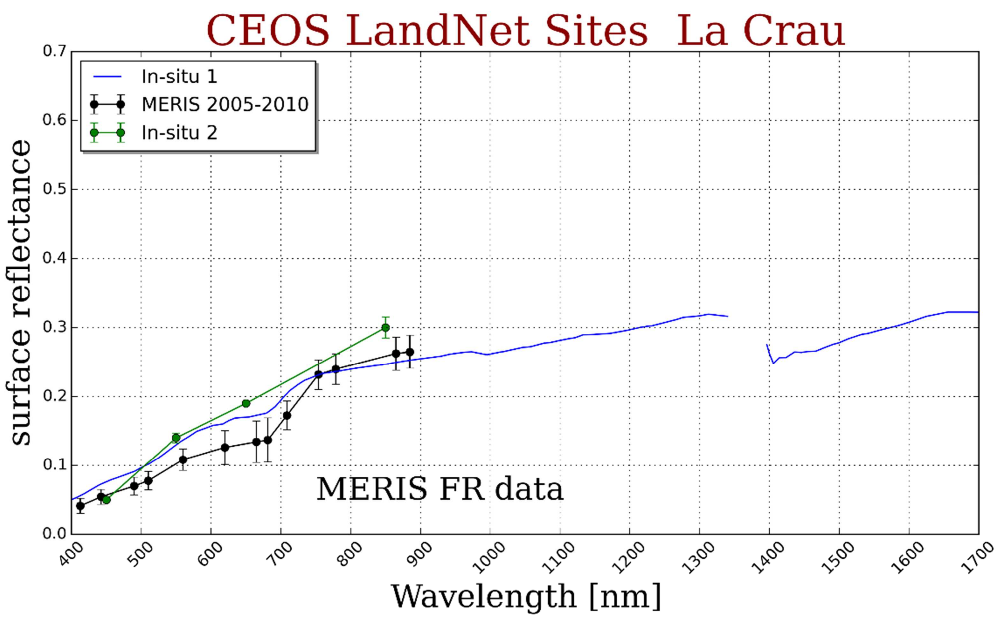

CEOS LandNet Sites La Crau
In-situ 1
MERIS 2005-2010
In-situ 2
surface reflectance
MERIS FR data
Wavelength [nm]

c)

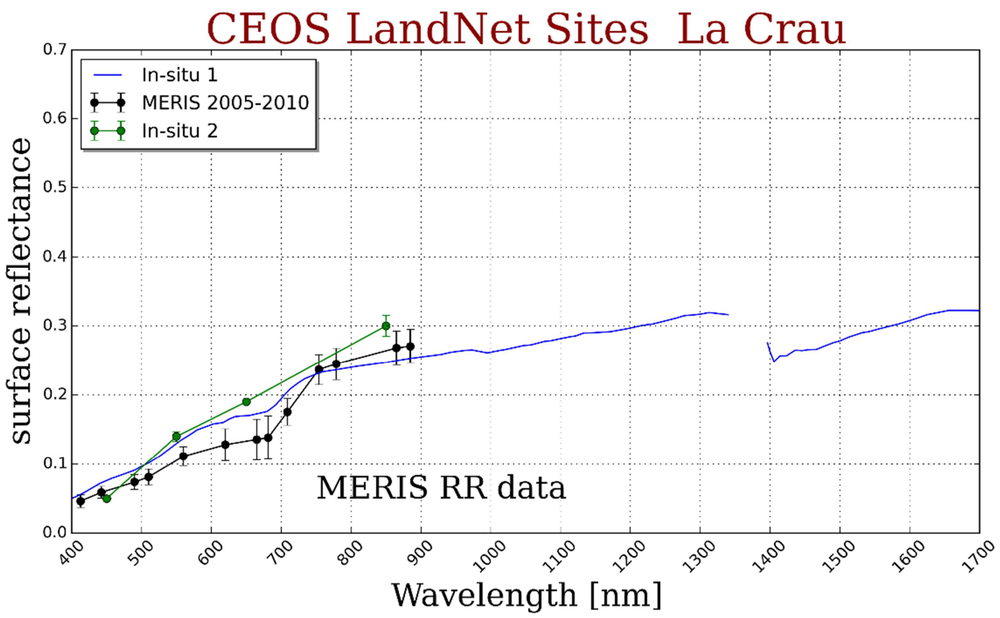
CEOS LandNet Sites La Crau
In-situ 1
MERIS 2005-2010
In-situ 2
MERIS RR data
surface reflectance
Wavelength [nm]
0.0
0.1
0.2
0.3
0.4
0.5
0.6
0.7
400
500
600
700
800
900
1000
1100
1200
1300
1400
1500
1600
1700

d)

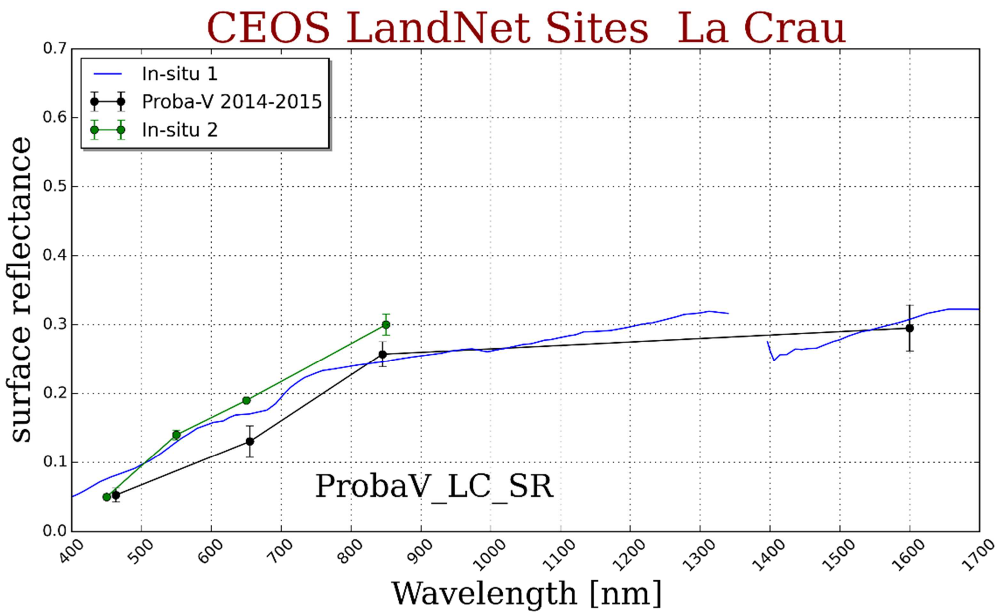
CEOS LandNet Sites La Crau
In-situ 1
Proba-V 2014-2015
In-situ 2
ProbaV_LC_SR
surface reflectance
Wavelength [nm]
0.0
0.1
0.2
0.3
0.4
0.5
0.6
0.7
400
500
600
700
800
900
1000
1100
1200
1300
1400
1500
1600
1700

e)

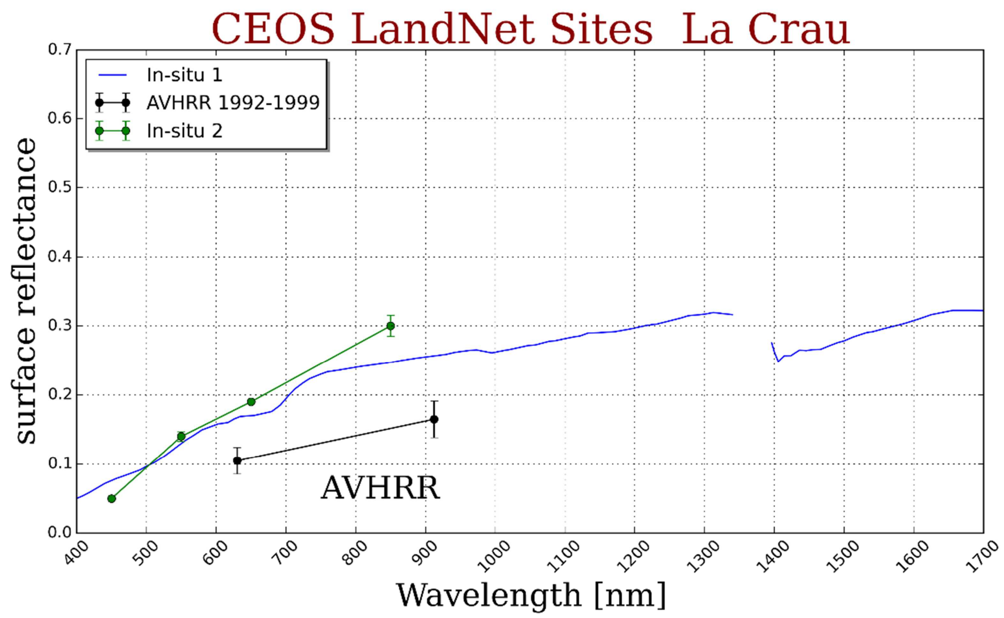

Figure 3-135: Comparison of Spectra - CEOS-LANDNET SITES - La Crau - a) in-situ data - fig. taken from [CEOS-LC, 2009] b) MERIS FR 2003-2012 c) MERIS RR 2003-2012 d) PROBA-V 2014-2016 e) AVHRR 1992-1999

a)

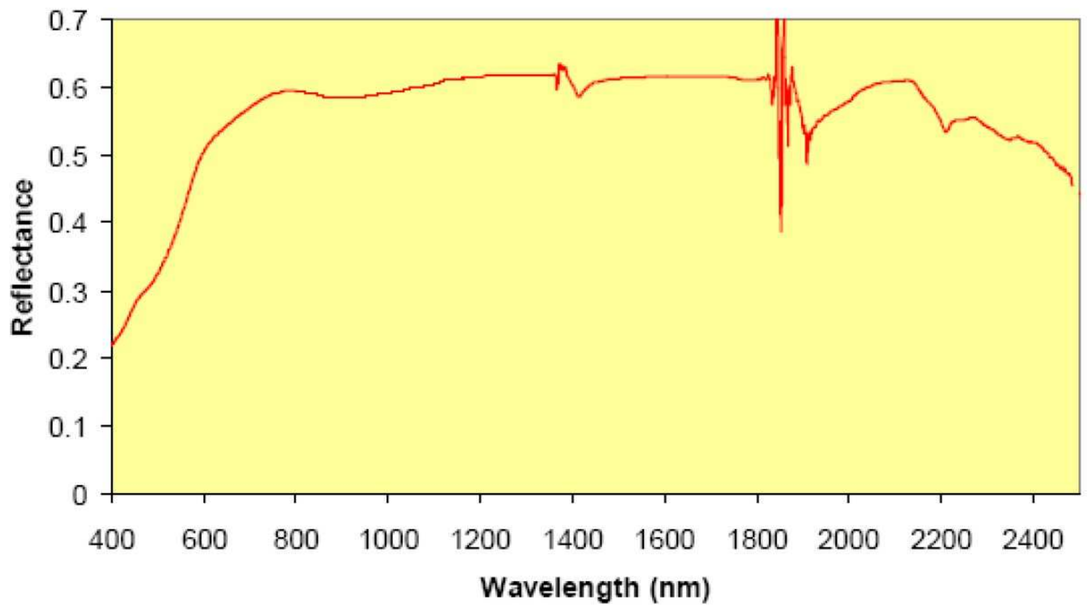

0.7
0.6
0.5
0.4
0.3
0.2
0.1
0
Reflectance
400
600
800
1000
1200
1400
1600
1800
2000
2200
2400
Wavelength (nm)

b)

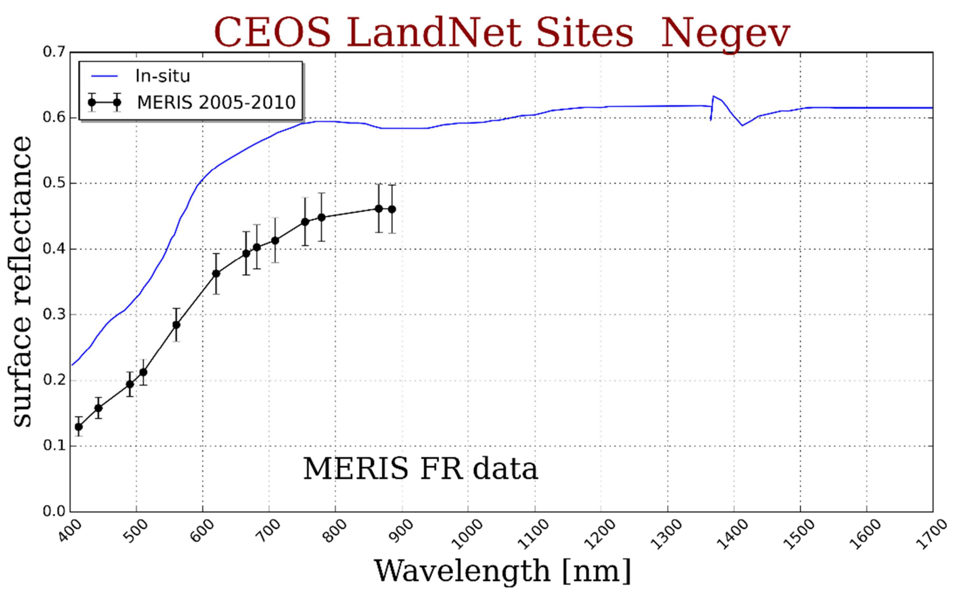

CEOS LandNet Sites Negev
In-situ
MERIS 2005-2010
surface reflectance
0.0
0.1
0.2
0.3
0.4
0.5
0.6
0.7
MERIS FR data
400
500
600
700
800
900
1000
1100
1200
1300
1400
1500
1600
1700
Wavelength [nm]

c)

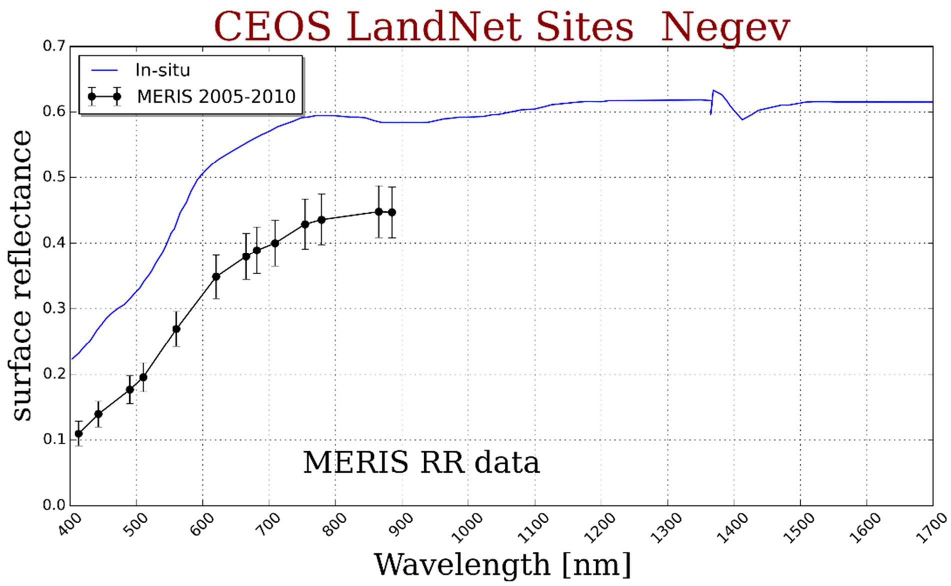

CEOS LandNet Sites Negev
In-situ
MERIS 2005-2010
surface reflectance
MERIS RR data
Wavelength [nm]
0.0
0.1
0.2
0.3
0.4
0.5
0.6
0.7
400
500
600
700
800
900
1000
1100
1200
1300
1400
1500
1600
1700

d)

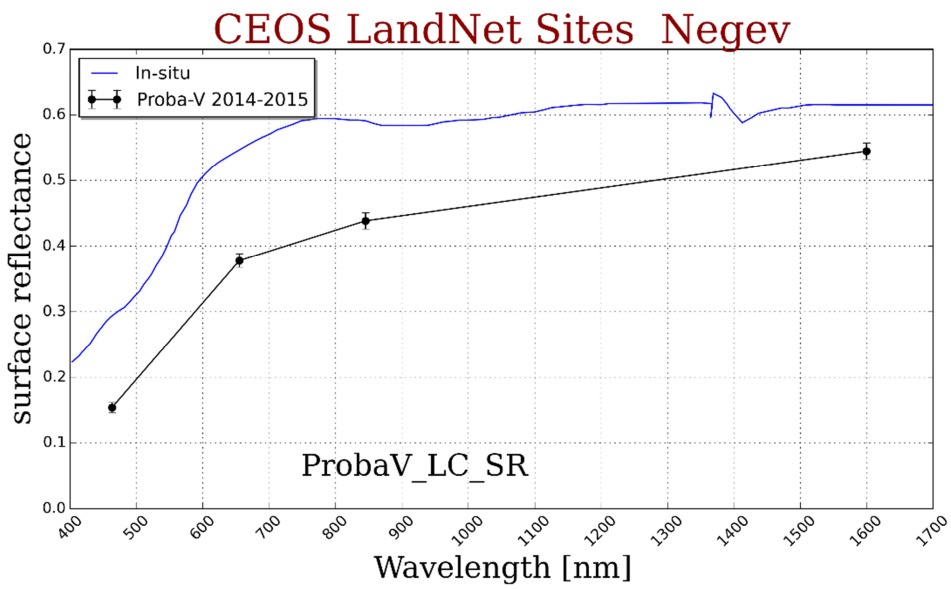

CEOS LandNet Sites Negev
In-situ
Proba-V 2014-2015
surface reflectance
ProbaV_LC_SR
Wavelength [nm]
0.0
0.1
0.2
0.3
0.4
0.5
0.6
0.7
400
500
600
700
800
900
1000
1100
1200
1300
1400
1500
1600
1700

e)

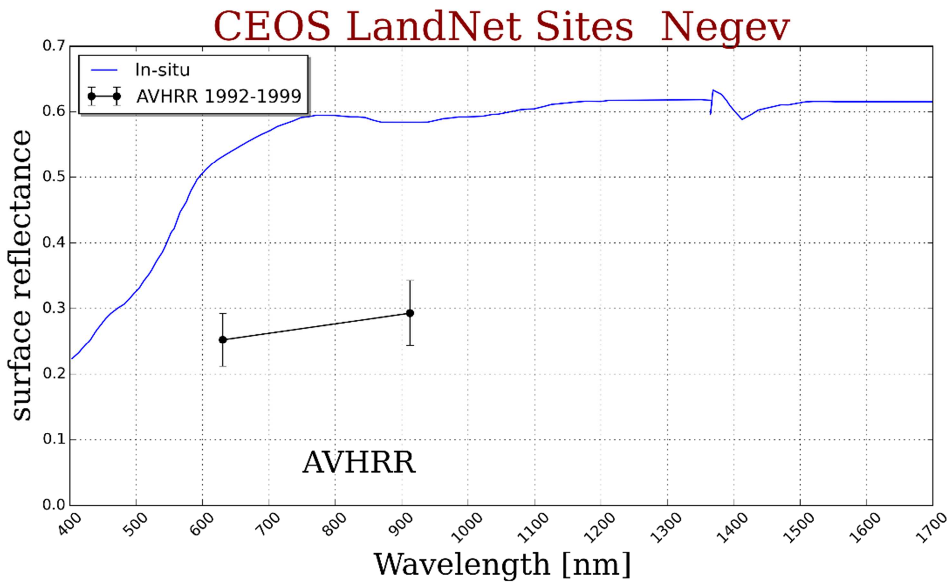

Figure 3-136: Comparison of Spectra - CEOS-LANDNET SITES - Negev - a) in-situ data - fig. taken from [CEOS-NG, 2009] b) MERIS FR 2003-2012 c) MERIS RR 2003-2012 d) PROBA-V 2014-2016 e) AVHRR 1992-1999

a)

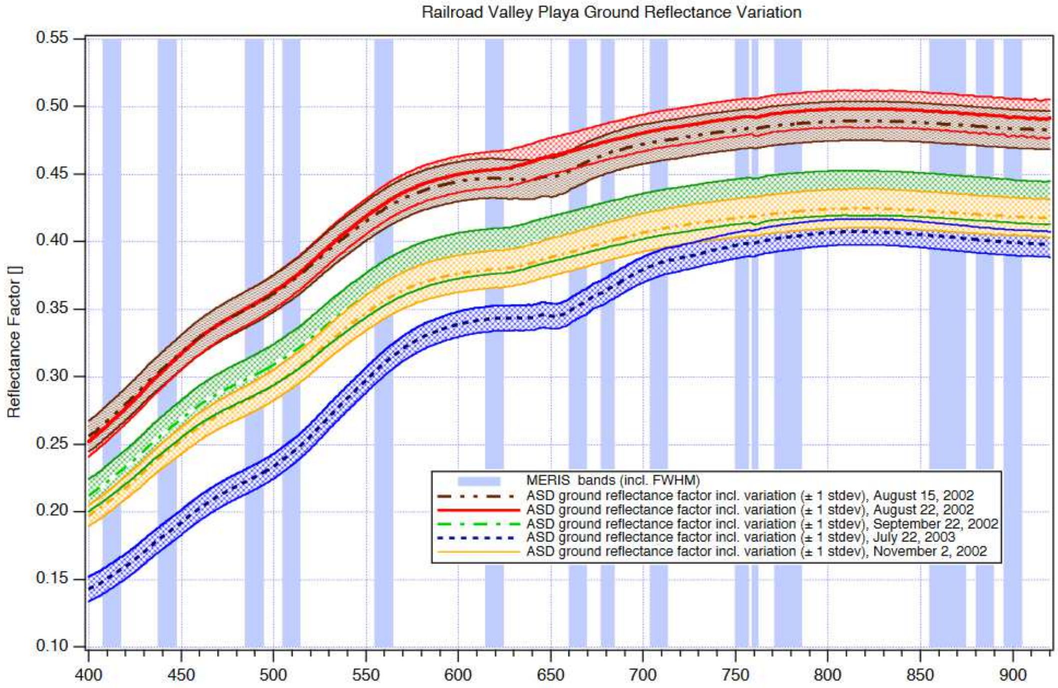
Railroad Valley Playa Ground Reflectance Variation
Reflectance Factor []
MERIS bands (incl. FWHM)
ASD ground reflectance factor incl. variation (± 1 stdev), August 15, 2002
ASD ground reflectance factor incl. variation (± 1 stdev), August 22, 2002
ASD ground reflectance factor incl. variation (± 1 stdev), September 22, 2002
ASD ground reflectance factor incl. variation (± 1 stdev), July 22, 2003
ASD ground reflectance factor incl. variation (± 1 stdev), November 2, 2002

b)

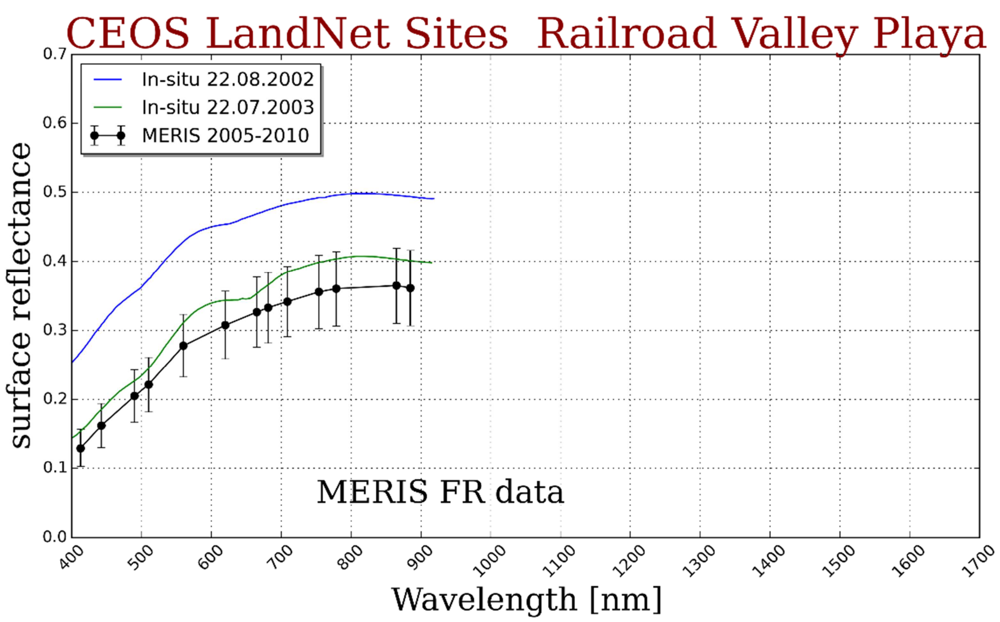
CEOS LandNet Sites Railroad Valley Playa
In-situ 22.08.2002
In-situ 22.07.2003
MERIS 2005-2010
surface reflectance
MERIS FR data
Wavelength [nm]

c)

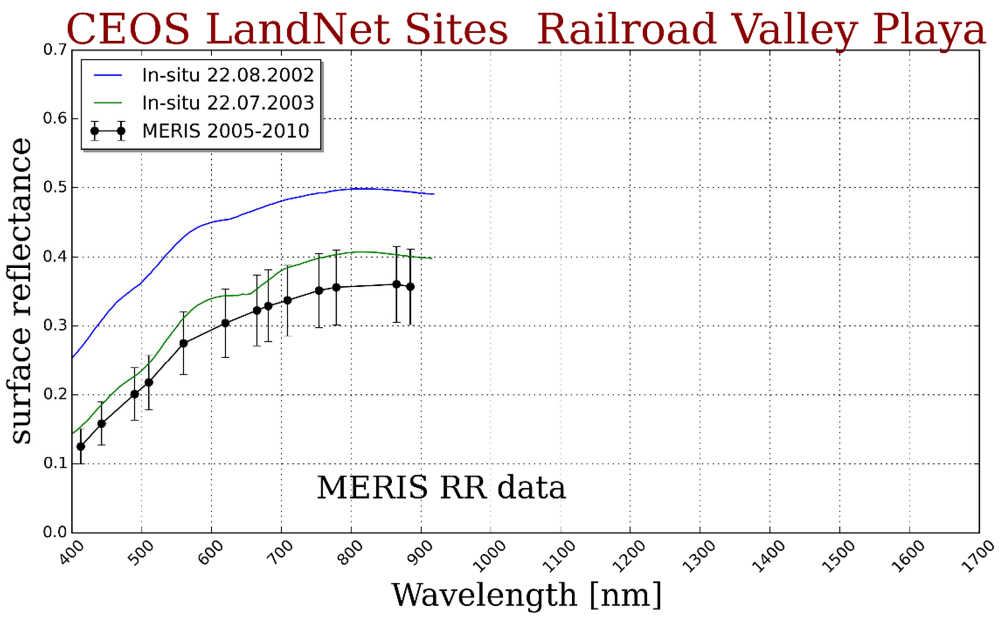
CEOS LandNet Sites Railroad Valley Playa
In-situ 22.08.2002
In-situ 22.07.2003
MERIS 2005-2010
surface reflectance
MERIS RR data
Wavelength [nm]
0.0
0.1
0.2
0.3
0.4
0.5
0.6
0.7
400
500
600
700
800
900
1000
1100
1200
1300
1400
1500
1600
1700

d)

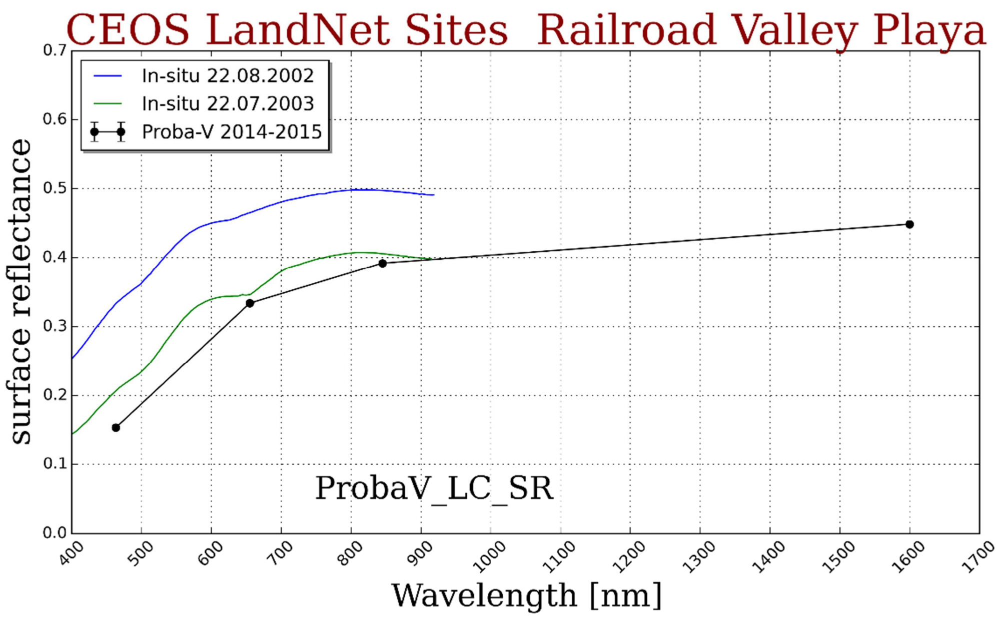
CEOS LandNet Sites Railroad Valley Playa
In-situ 22.08.2002
In-situ 22.07.2003
Proba-V 2014-2015
surface reflectance
ProbaV_LC_SR
Wavelength [nm]
0.0
0.1
0.2
0.3
0.4
0.5
0.6
0.7
400
500
600
700
800
900
1000
1100
1200
1300
1400
1500
1600
1700

e)

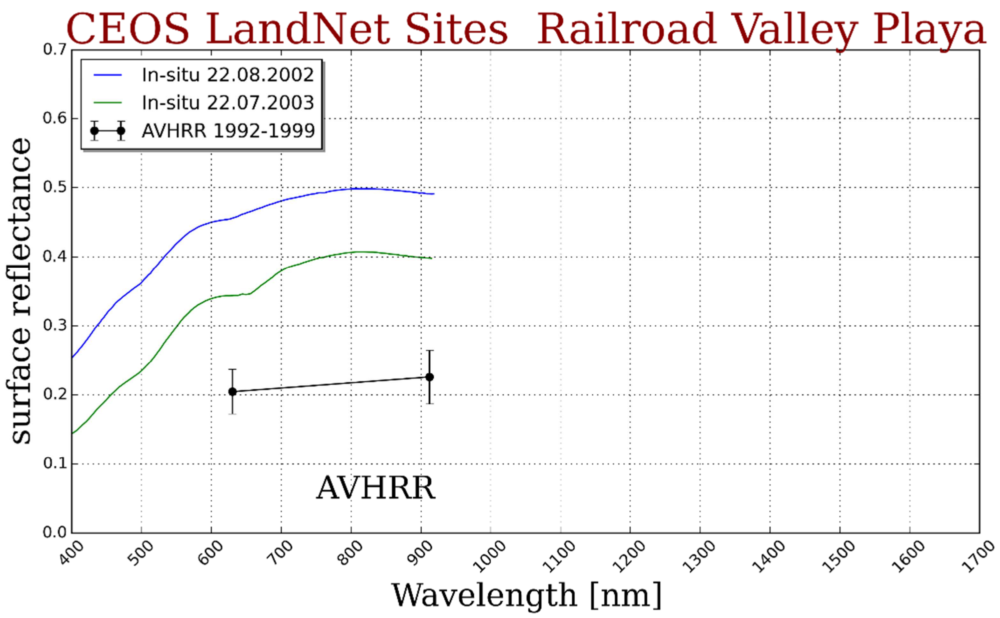

Figure 3-137: Comparison of Spectra - CEOS-LANDNET SITES - Railroad Valley Playa - a) in-situ data - fig. taken from [Kneubuehler et al., 2006] b) MERIS FR 2003-2012 c) MERIS RR 2003-2012 d) PROBA-V 2014-2016 e) AVHRR 1992-1999

3.6 Intercomparison with other products

The purpose of this paragraph is to present the method and the results of the intercomparison of the global 7-day MERIS FR and RR, AVHRR and PROBA-V composites with other products.

3.6.1 Radiometric intercomparison of the global 7-day MERIS FR SR composites processed in phase I and phase II

For the radiometric intercomparison of the global 7-day MERIS FR SR composites processed in phase I and phase II six different pairs of corresponding global 7-day MERIS FR SR composites processed in phase I and phase II have been chosen for the implementation of the radiometric intercomparison, which means at the same time that 6 different test areas have been selected (Sahara, Alps, Amazon, Australia, West Africa, and India). The global position of all test sites is illustrated in Figure 3-138.

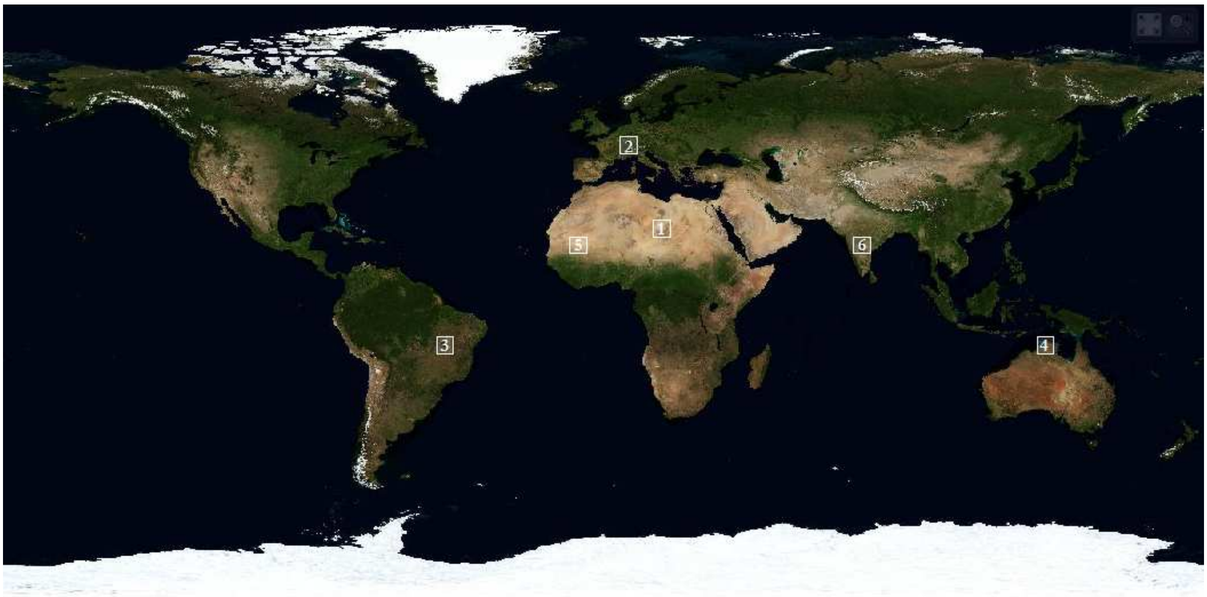

Figure 3-138: Location of all chosen test sites for the comparison of 7-day MERIS FR SR composites products (1 – Sahara h39v13, 2 – Alps h37v08, 3 – Brazil h26v20, 4 – Australia h62v20, 5 - West Africa h34v14, 6 – India h51v14)

For all examples investigated within this study the intercomparison results of the reflectance values of the 7-day MERIS FR SR composites are illustrated using scatter plots for all chosen test sites (e.g. Figure 3-145). Using a scatter plot is one option to graphically visualize observed values for two variables for a set of data.

In order to evaluate this effect, the line of best fit and the corresponding equation have been added to all scatter plots as well. The line of best fit can be obtained by the method of least squares. This mathematical standard method assumes that the best-fit curve of a predefined type is that one's which has the minimal sum of the deviations squared (least square error) from a given set of data. In the case that the predefined type of curve is a linear function, the best fitting curve is described by the following equation with the coefficients as well as the coefficient of determination R^2 are given by:

$$f(x) = \alpha_0 + \alpha_1 \cdot x$$

$$\alpha_1 = \frac{\sum_{i=1}^{n}(x_i - \bar{x})(y_i - \bar{y})}{\sum_{i=1}^{n}(x_i - \bar{x})^2} \; with\, \bar{x} = \frac{1}{n}\sum_{i=1}^{n} x_i \; and\; \bar{y} = \frac{1}{n}\sum_{i=1}^{n} y_i$$

$$\alpha_0 = \bar{y} - \alpha_1 \cdot \bar{x}$$

$$R^2 = \frac{\sum_{i=1}^{n}(\hat{y}_i - \bar{y})^2}{\sum_{i=1}^{n}(y_i - \bar{y})^2} \; with\; \hat{y}_i = \alpha_0 + \alpha_1 \cdot x_i$$

eq.: 3-1

The residual (also called coefficient of determination) R^2 represents a measure for the quality of the adaption for the predefined type of curve and has been considered in the evaluation of the results.

At first, the following figures (Figure 3-139 - Figure 3-144) show the RGB of the 7-day MERIS FR SR composite products processed in phase I and II over the selected test site.

Figure 3-139: RGB of 7-day MERIS FR SR composite products processed in phase I and II (test site Sahara)
ESACCI-LC-L3-SR-MERIS-300m-P7D-h39v13-20100423-v1.0.nc
ESACCI-LC-L3-SR-MERIS-300m-P7D-h39v13-20100423-v2.0.nc

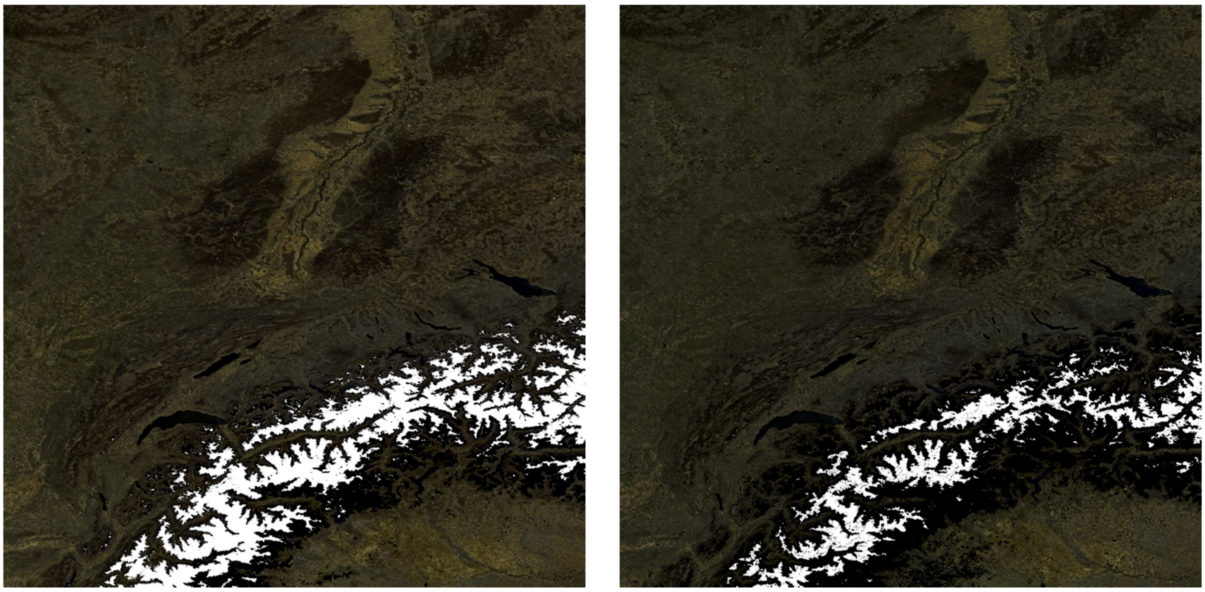

Figure 3-140: RGB of 7-day MERIS FR SR composite products processed in phase I and II (test site Alps)
ESACCI-LC-L3-SR-MERIS-300m-P7D-h37v08-20100423-v1.0.nc
ESACCI-LC-L3-SR-MERIS-300m-P7D-h37v08-20100423-v2.0.nc

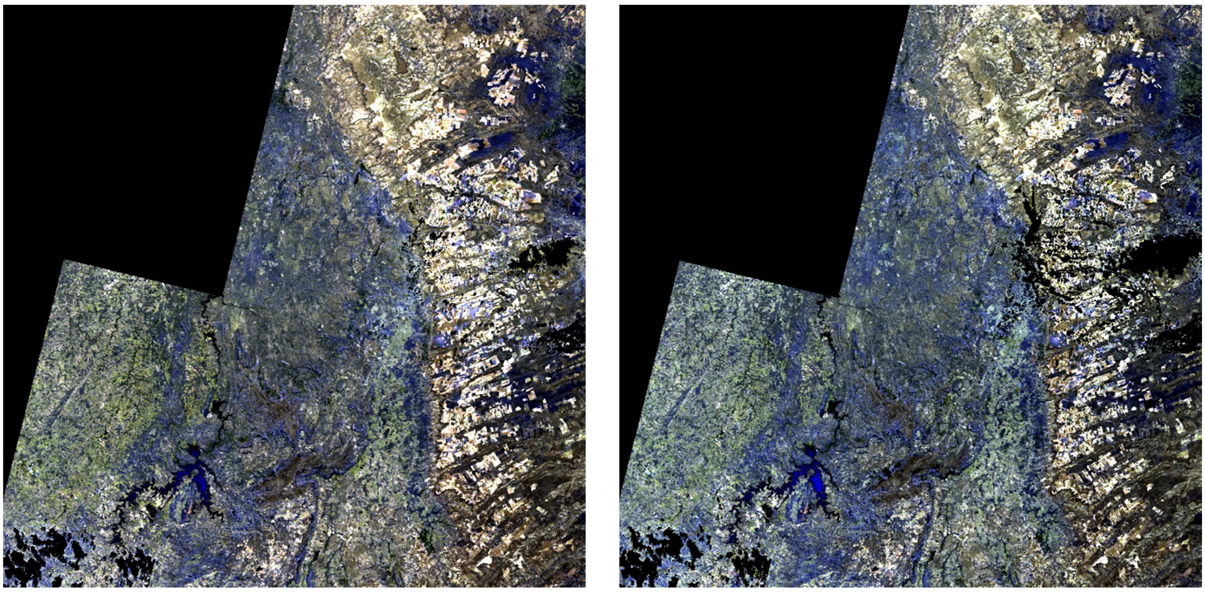

Figure 3-141: RGB of 7-day MERIS FR SR composite products processed in phase I and II (test site Brazil)
ESACCI-LC-L3-SR-MERIS-300m-P7D-h26v20-20100423-v1.0.nc
ESACCI-LC-L3-SR-MERIS-300m-P7D-h26v20-20100423-v2.0.nc

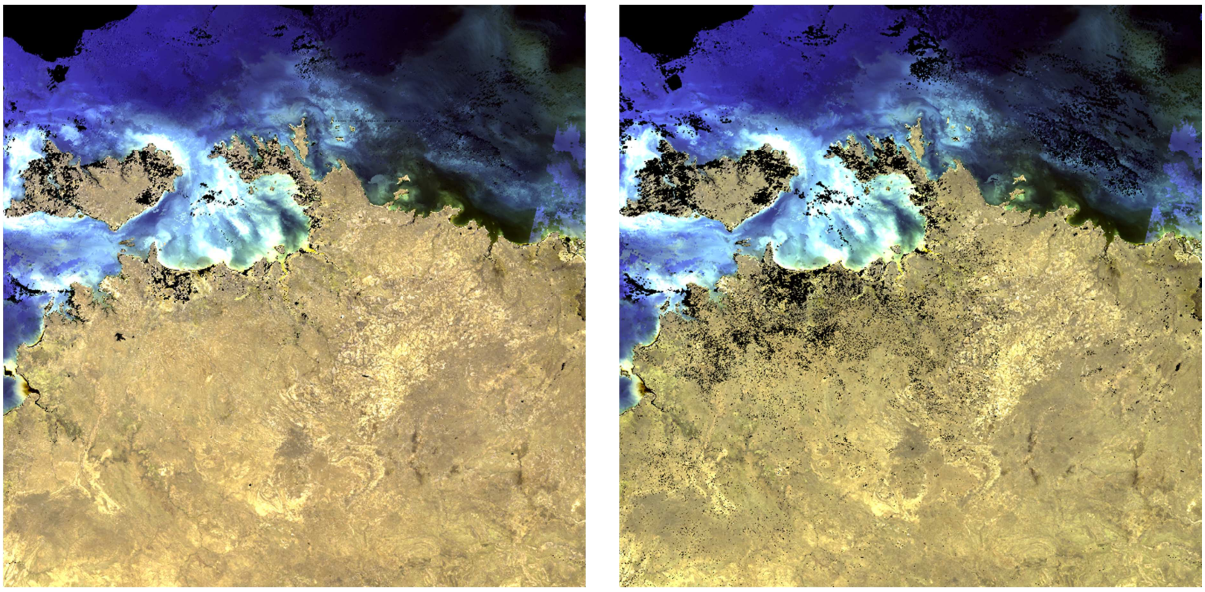

Figure 3-142: RGB of 7-day MERIS FR SR composite products processed in phase I and II (test site Australia)
ESACCI-LC-L3-SR-MERIS-300m-P7D-h62v20-20100423-v1.0.nc
ESACCI-LC-L3-SR-MERIS-300m-P7D-h62v20-20100423-v2.0.nc

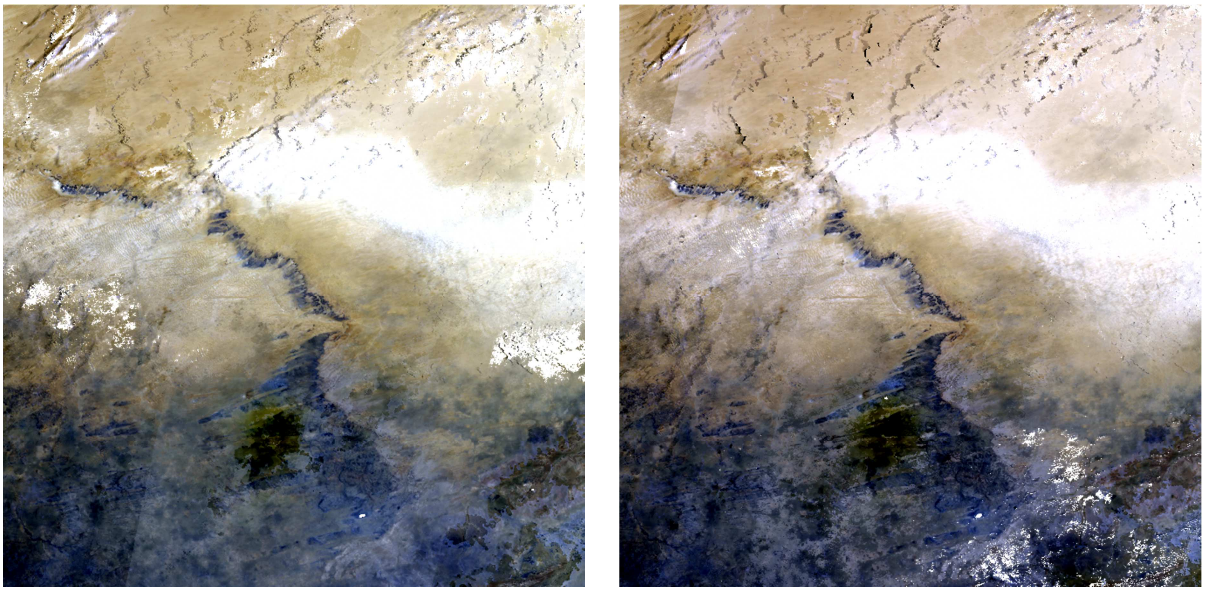

Figure 3-143: RGB of 7-day MERIS FR SR composite products processed in phase I and II (test site West Africa)
ESACCI-LC-L3-SR-MERIS-300m-P7D-h34v14-20100423-v1.0.nc
ESACCI-LC-L3-SR-MERIS-300m-P7D-h34v14-20100423-v2.0.nc

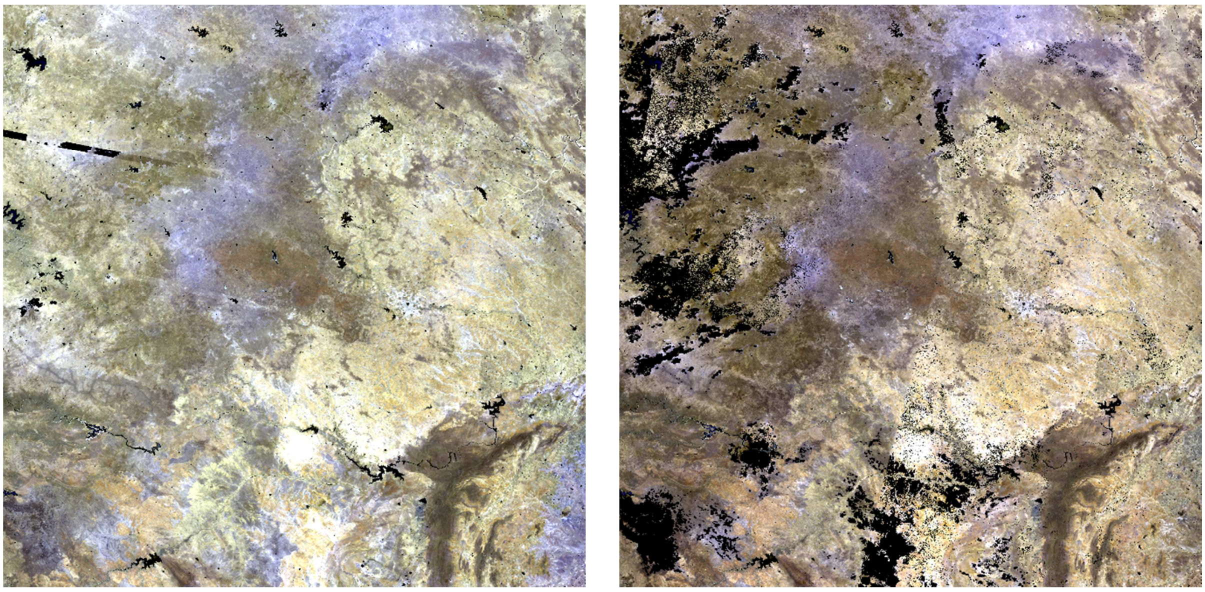

Figure 3-144: RGB of 7-day MERIS FR SR composite products processed in phase I and II (clear land pixel, test site India, bands B3, B5, B7 and B14)
ESACCI-LC-L3-SR-MERIS-300m-P7D-h51v14-20100423-v1.0.nc
ESACCI-LC-L3-SR-MERIS-300m-P7D-h51v14-20100423-v2.0.nc

In the following the results of the radiometric intercomparison of the 7-day MERIS FR SR composites products processed in phase I and phase II are presented.

7-day MERIS FR SR composite products processed in phase I and phase II data have been compared in their radiometric attributes at SR (surface reflectance) level and the scatterplots indicate in all cases a linear correlation. The variation of the values may be caused by omission and commission errors of the pixel identification.

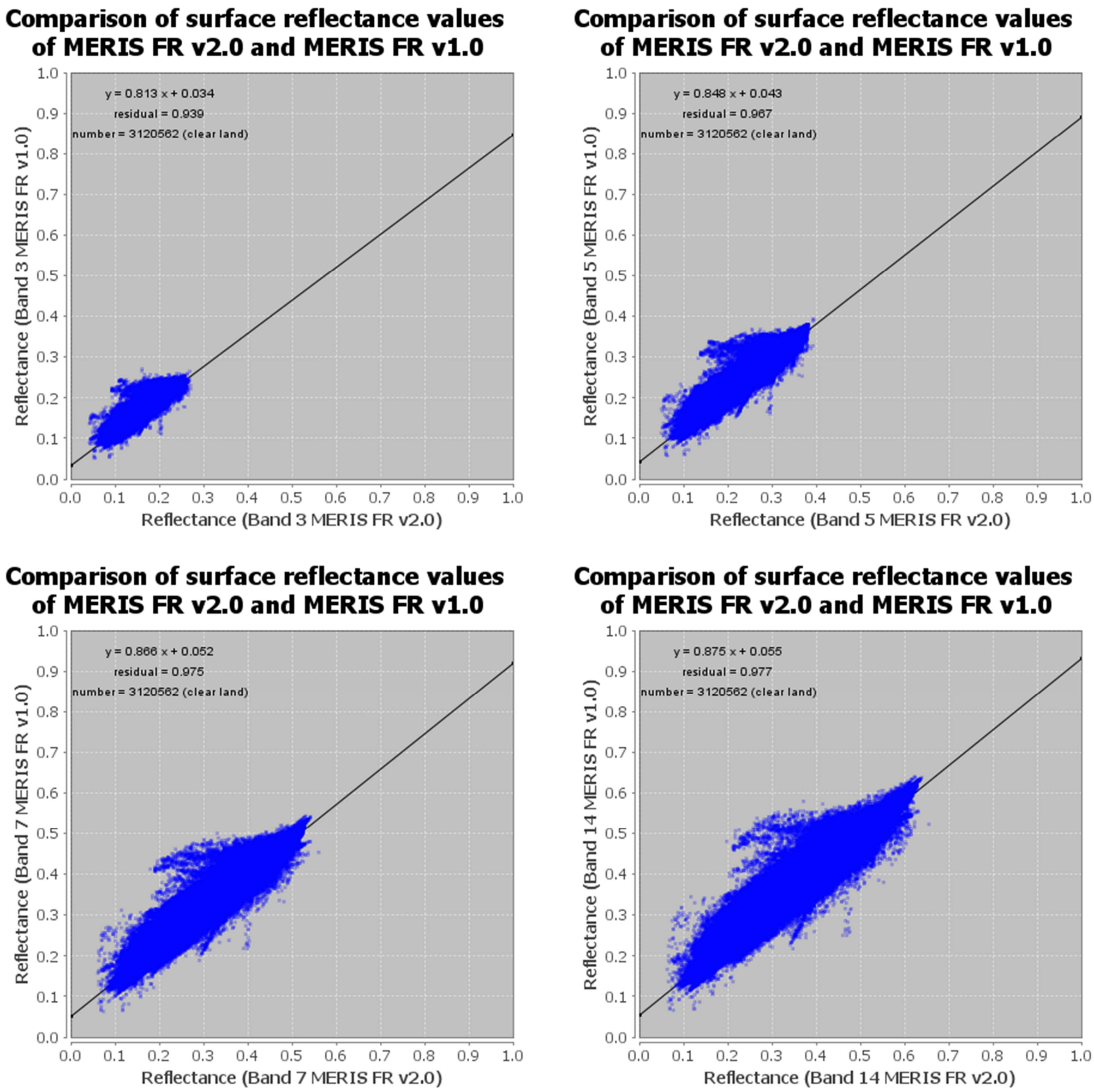

Figure 3-145: Comparison of reflectance values of 7-day MERIS FR SR composites products processed in phase I and II (clear land pixel, test site Sahara, bands B3, B5, B7 and B14)
ESACCI-LC-L3-SR-MERIS-300m-P7D-h39v13-20100423-v1.0.nc
ESACCI-LC-L3-SR-MERIS-300m-P7D-h39v13-20100423-v2.0.nc

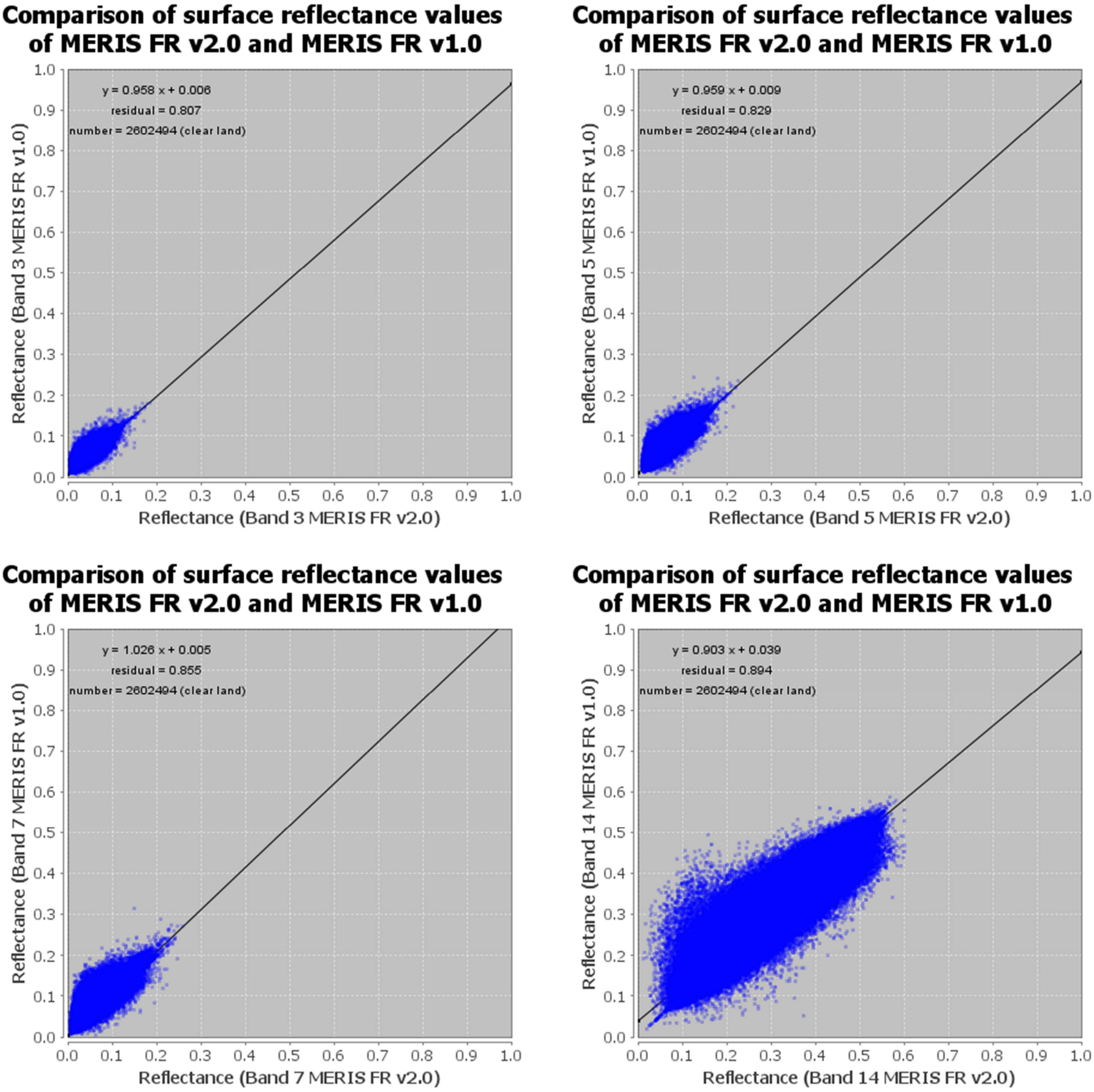

Figure 3-146: Comparison of reflectance values of 7-day MERIS FR SR composites products processed in phase I and II (clear land pixel, test site Alps, bands B3, B5, B7 and B14)
ESACCI-LC-L3-SR-MERIS-300m-P7D-h37v08-20100423-v1.0.nc
ESACCI-LC-L3-SR-MERIS-300m-P7D-h37v08-20100423-v2.0.nc

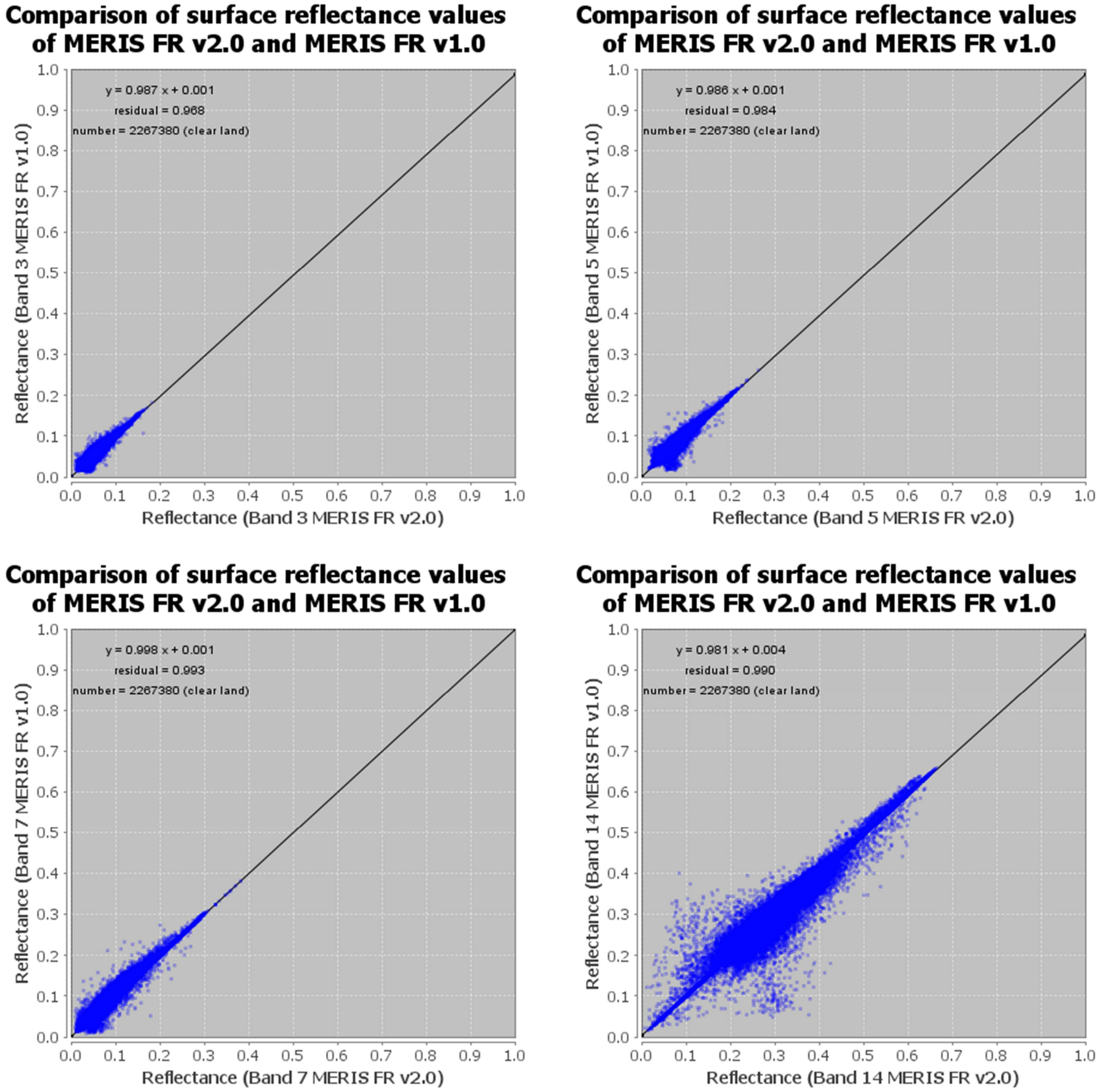

Figure 3-147: Comparison of reflectance values of 7-day MERIS FR SR composites products processed in phase I and II (clear land pixel, test site Brazil, bands B3, B5, B7 and B14)
ESACCI-LC-L3-SR-MERIS-300m-P7D-h26v20-20100423-v1.0.nc
ESACCI-LC-L3-SR-MERIS-300m-P7D-h26v20-20100423-v2.0.nc

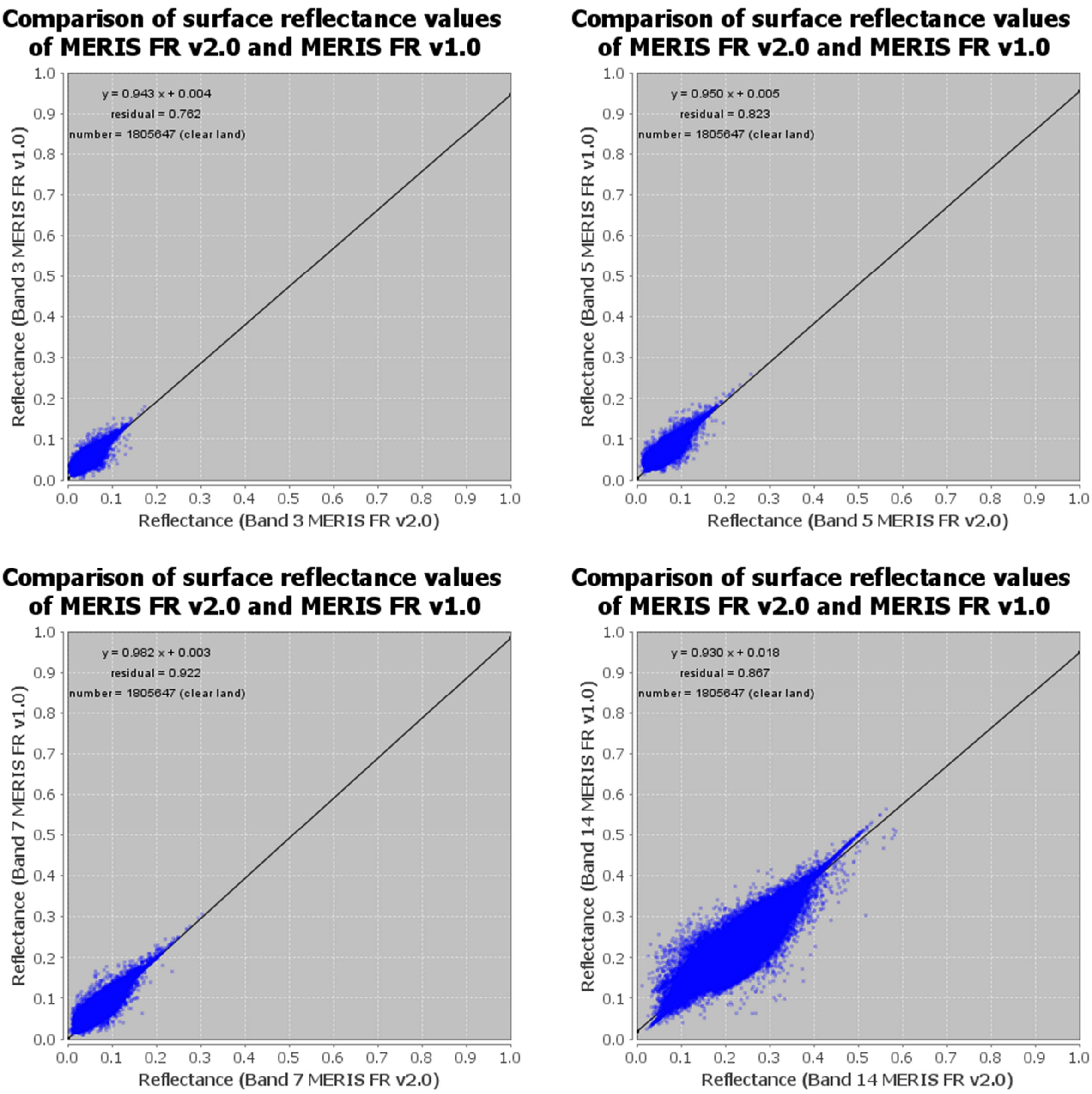

Figure 3-148: Comparison of reflectance values of 7-day MERIS FR SR composites products processed in phase I and II (clear land pixel, test site Australia, bands B3, B5, B7 and B14)
ESACCI-LC-L3-SR-MERIS-300m-P7D-h62v20-20100423-v1.0.nc
ESACCI-LC-L3-SR-MERIS-300m-P7D-h62v20-20100423-v2.0.nc

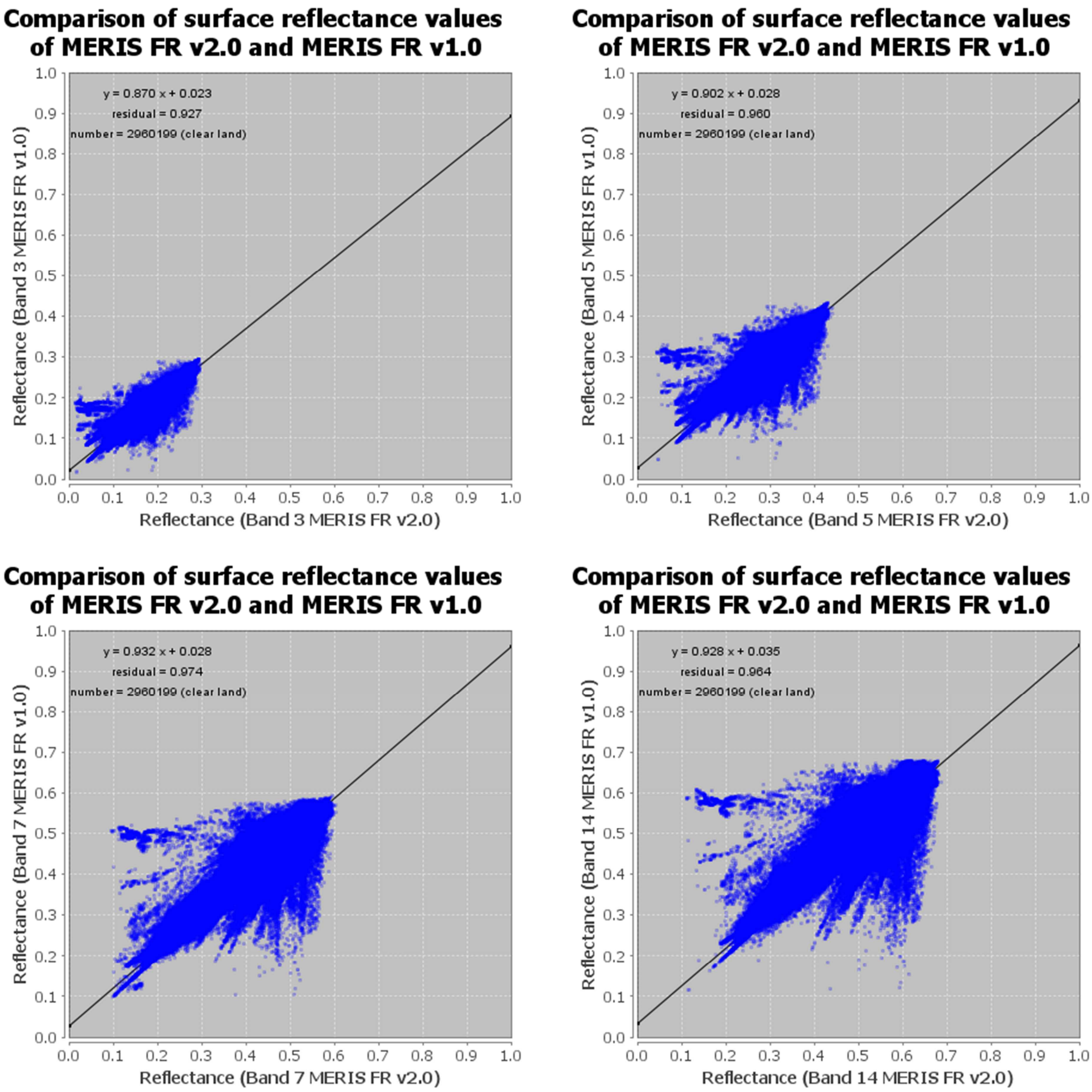

Figure 3-149: Comparison of reflectance values of 7-day MERIS FR SR composites products processed in phase I and II (clear land pixel, test site West Africa, bands B3, B5, B7 and B14)
ESACCI-LC-L3-SR-MERIS-300m-P7D-h34v14-20100423-v1.0.nc
ESACCI-LC-L3-SR-MERIS-300m-P7D-h34v14-20100423-v2.0.nc

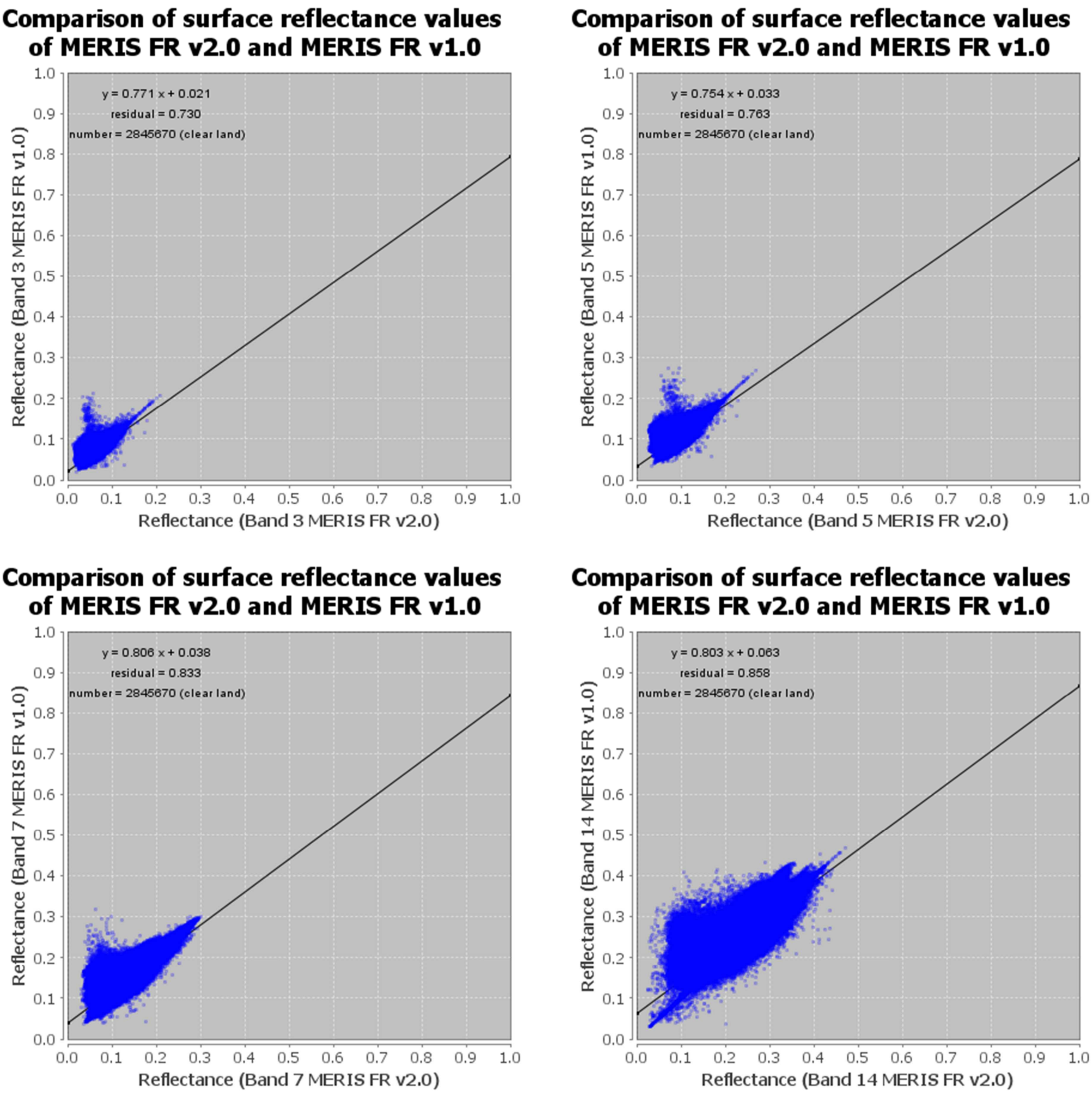

Figure 3-150: Comparison of reflectance values of 7-day MERIS FR SR composites products processed in phase I and II (clear land pixel, test site India, bands B3, B5, B7 and B14)
ESACCI-LC-L3-SR-MERIS-300m-P7D-h51v14-20100423-v1.0.nc
ESACCI-LC-L3-SR-MERIS-300m-P7D-h51v14-20100423-v2.0.nc

Table 3-49: Comparison of reflectance values of 7-day MERIS FR SR composites products processed in phase I and II; residual for the model $y = f(x) = \alpha_1 x + \alpha_0$

Results of the comparison of reflectance values								
	MERIS FR Band 3		MERIS FR Band 5		MERIS FR Band 7		MERIS FR Band 14	
Test site	**Line of best fit**	**Residual**	**Line of best fit**	**Residual**	**Line of best fit**	**Residual**	**Line of best fit**	**Residual**
Sahara (clear land)	y = 0.813x +0.0338	0.9388	y = 0.848x + 0.0434	0.9667	y = 0.866x + 0.0525	0.9753	y = 0.875x + 0.0549	0.9770
Alps (clear land)	y = 0.958x +0.0060	0.8073	y = 0.959x + 0.0088	0.8287	y = 1.026x + 0.0052	0.8549	y = 0.903x + 0.0390	0.8940
Brazil (clear land)	y = 0.987x +0.0008	0.9684	y = 0.986x + 0.0014	0.9841	y = 0.998x + 0.0007	0.9931	y = 0.981x + 0.0043	0.9897
Australia (clear land)	y = 0.943x +0.0036	0.7624	y = 0.951x + 0.0046	0.8228	y = 0.982x + 0.0026	0.9222	y = 0.930x + 0.0180	0.8669
West Africa (clear land)	y = 0.871x + 0.0230	0.9271	y = 0.902x + 0.0280	0.9595	y = 0.932+ 0.0280	0.9742	y = 0.928 + 0.0348	0.9645
India (clear land)	y = 0.771x + 0.0210	0.7300	y = 0.754x + 0.0326	0.7631	y = 0.806 + 0.0381	0.8329	y = 0.803 + 0.0629	0.8578

Table 3-50: Comparison of reflectance values of 7-day MERIS FR SR composites products processed in phase I and II - residual for the model y = f(x) = x

Results of the comparison of reflectance values				
	MERIS FR Band 3	MERIS FR Band 5	MERIS FR Band 7	MERIS FR Band 14
Test site	**Residual**	**Residual**	**Residual**	**Residual**
Sahara (clear land)	1.4349	1.3618	1.3085	1.2814
Alps (clear land)	1.0014	1.0044	0.8910	1.1136
Brazil (clear land)	0.9957	1.0127	0.9967	1.0301
Australia (clear land)	0.9073	0.9403	0.9662	1.0064
West Africa (clear land)	1.2241	1.1797	1.1219	1.1202
India (clear land)	1.5047	1.5850	1.4453	1.4487

3.6.2 Intercomparison of 7-day MERIS FR SR composite with CultureMeris products

Additionally, a direct comparison of the results of the evaluation with the CultureMeris dataset by using the in-situ data from the CEOS LANDNET sites (without Dome C and Tuz Golu) is provided. The complete description of the CultureMeris data set is given by Kalogirou et al, 2013 and Arino et al, 2012 ([Kalogirou et al., 2013], [Arino et al., 2012]). The complete description of the validation is part of the PVASR [Ph1_PVASRv2.1, 2012] and IPVR [Ph1_IPVRv1.2, 2012].

The Table 3-51 lists the in-situ data, that are taken from the figures or tables in the protocols of CEOS LANDNET sites ([CEOS-RVP, 2009], [CEOS-NV, 2009], [CEOS-LC, 2009], [CEOS-IP, 2009], [CEOS-FF, 2009], [CEOS-DG, 2009]) or figure, which is published in Kneubuehler et al. [Kneubuehler et al., 2006]. Only for the CEOS LANDNET site La Crau, mean surface reflectances including the variation have been provided by the protocol. All other values should be used carefully by the evaluation because some of them reflect individual measurements only and uncertainties are not specified.

The following figures (Figure 3-151- Figure 3-156) show the time series of the 7-day SR composites from the LC-CCI project and the CultureMeris project for the 6 CEOS LANDNET sites. The underlying coloured blocks are in accordance with the in-situ data.

The characteristic of both time series is similar, but the absolute values may differ. The variation of the values may be caused by undetected clouds which strongly influence the retrieved 7-day SR composites values due to their spectral characteristics which may be completely differ from the underlying surface.

Besides the general remark about the quality of the in-situ data from the CEOS LANDNET sites, the comparison of the 7-day SR composites from the LC-CCI project and the CultureMeris project with the in-situ measurements points out, that the 7 day SR composites values can be either greater or smaller than the in-situ values.

Table 3-51: In-situ data taken from [CEOS-RVP, 2009], [CEOS-NV, 2009], [CEOS-LC, 2009], [CEOS-IP, 2009], [CEOS-FF, 2009] and [CEOS-DG, 2009]

	Dunhang [CEOS-DG, 2009]	Frenchman Flat [CEOS-FF, 2009],	Ivanpah Playa [CEOS-IP, 2009]	La Crau [CEOS-LC, 2009]	Negev [CEOS-NV, 2009]	Railroad Valley Playa [CEOS-RVP, 2009]
Wavelength	**Mean surface reflectance**	**Mean surface reflectance**	**Mean surface reflectance**	**Mean surface reflectance**	**Mean surface reflectance**	**Mean surface reflectance**
490nm	0.15-0.18	-	-	0.05-0.09	0.305-0.315	0.24-0.25
560nm	0.18-0.22	-	-	0.13-0.14	0.42-0.43	0.31-0.32
665nm	0.21-0.24	-	-	0.17-0.19	0.545-0.555	0.34-0.35
885nm	0.22-0.24	-	-	0.25-0.30	0.58-0.59	0.37-0.38

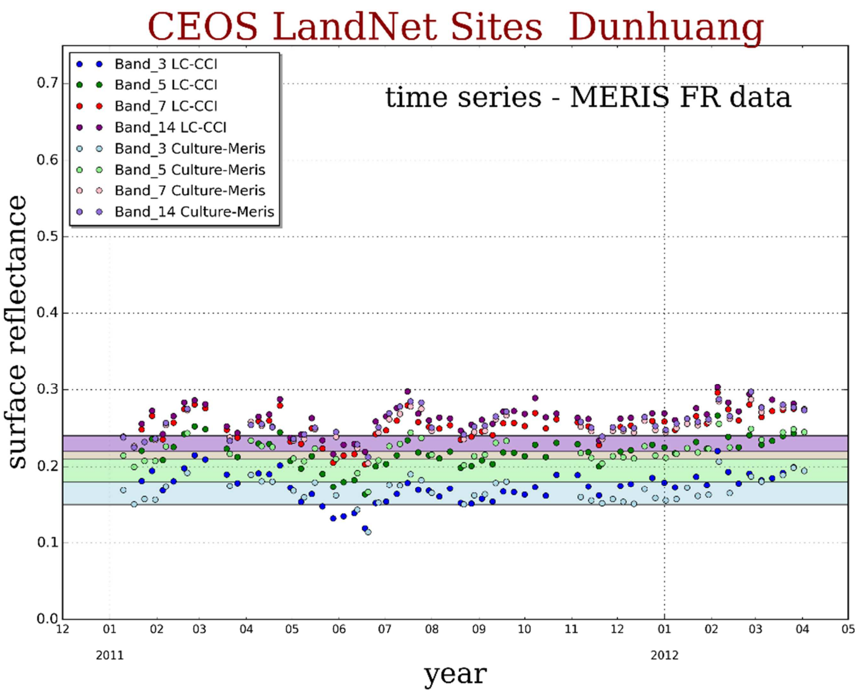

Figure 3-151: SR time series from MERIS FR data - 2011-2012 - CEOS-LANDNET SITES – Dunhuang – LC-CCI & CultureMeris + underlying colored blocks are in accordance with the in-situ data taken from [CEOS-DG, 2009]

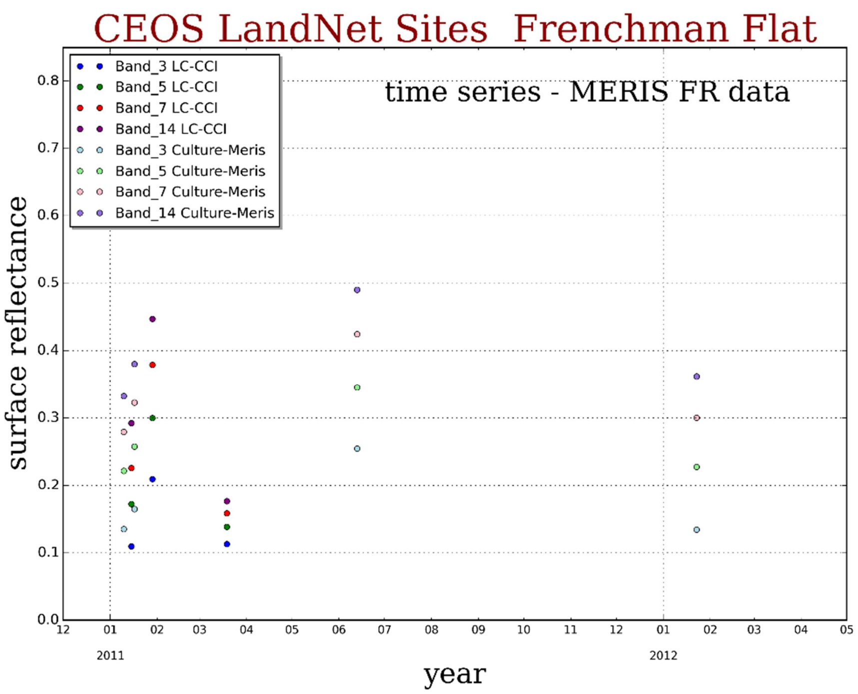

Figure 3-152: SR time series from MERIS FR data - 2011-2012 - CEOS-LANDNET SITES – Frenchman Flat – LC-CCI (no clear land data) & CultureMeris

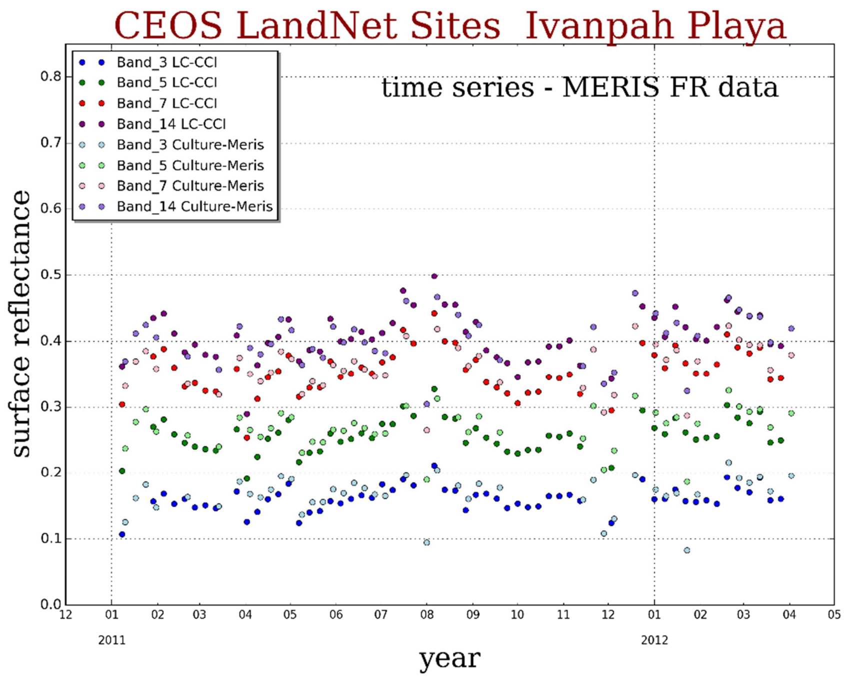

Figure 3-153: SR time series from MERIS FR data - 2011-2012 - CEOS-LANDNET SITES – Ivanpah Playa – LC-CCI & CultureMeris

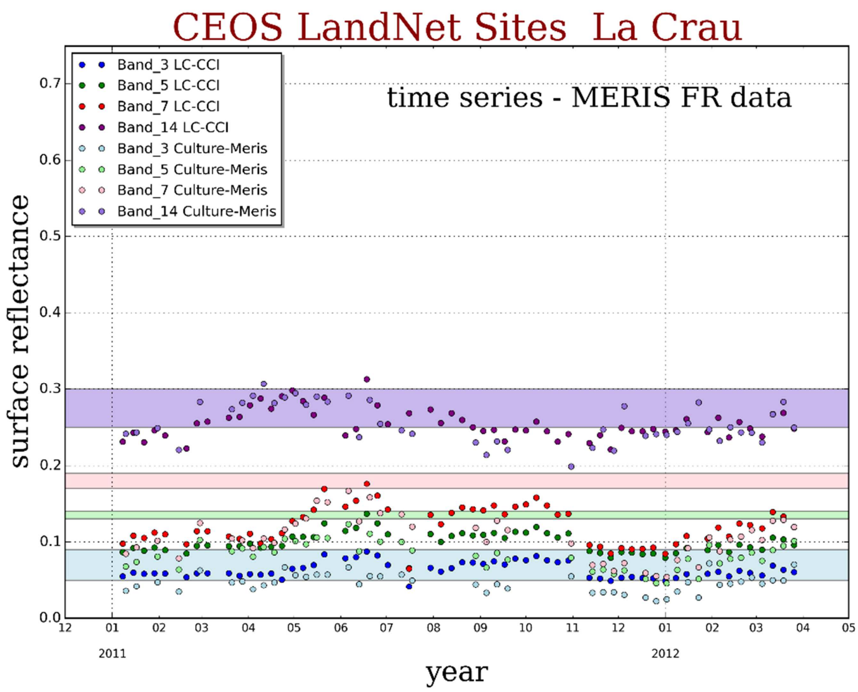

Figure 3-154: SR time series from MERIS FR data - 2011-2012 - CEOS-LANDNET SITES – La Crau – LC-CCI & CultureMeris + underlying colored blocks are in accordance with the in-situ data taken from [CEOS-LC, 2009]

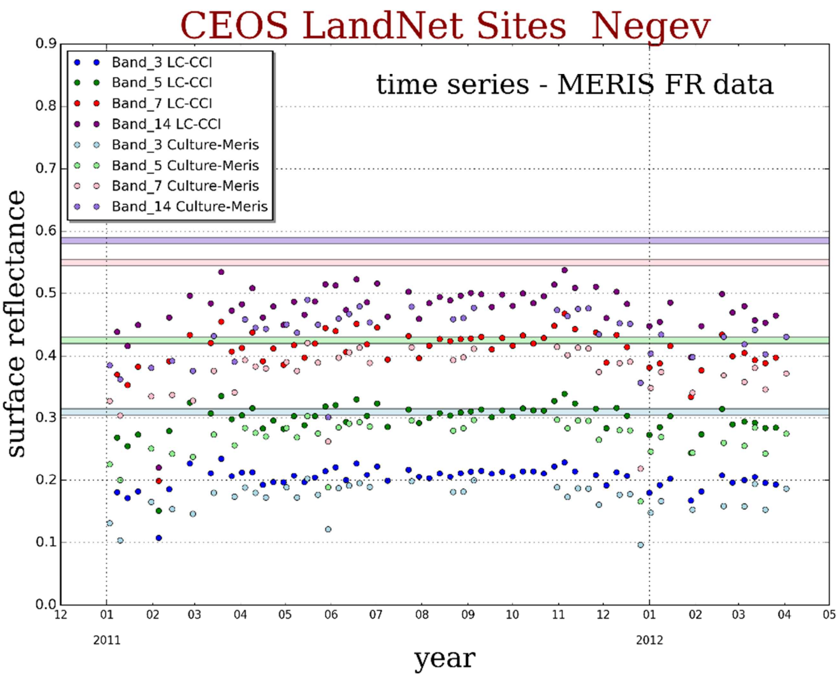

Figure 3-155: SR time series from MERIS FR data - 2011-2012 - CEOS-LANDNET SITES – Negev – LC-CCI & CultureMeris + underlying colored blocks are in accordance with the in-situ data taken from [CEOS-NV, 2009]

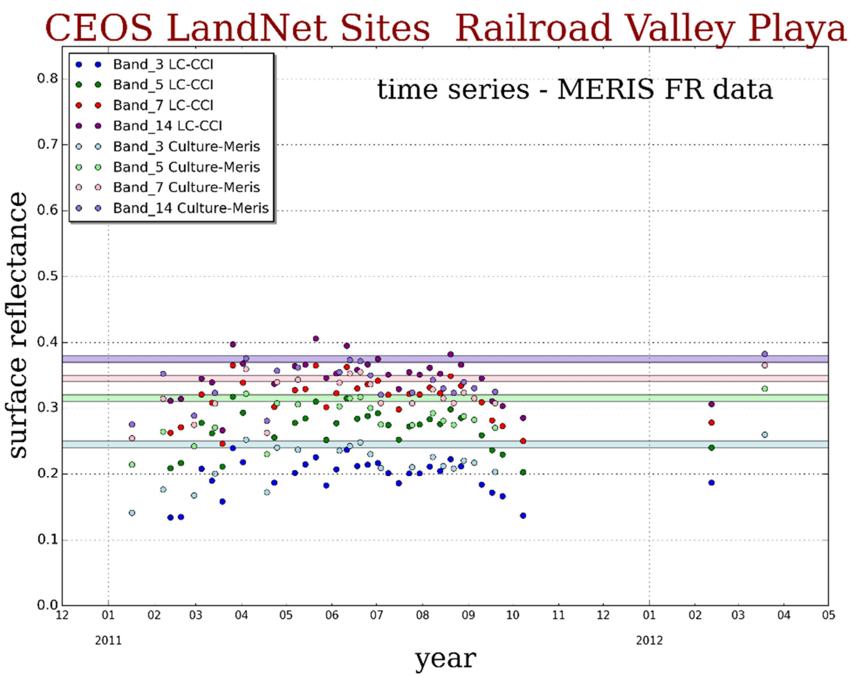

Figure 3-156: SR time series from MERIS FR data - 2011-2012 - CEOS-LANDNET SITES – Railroad Valley Playa – LC-CCI & CultureMeris + underlying colored blocks are in accordance with the in-situ data taken from [CEOS-RVP, 2009]

3.6.3 Intercomparison of the global 7-day PROBA-V composites and the PROBA-V S10 TOC products[4]

For the intercomparison of the global 7-day PROBA-V SR composites and the PROBA-V S10 TOC products the correspondent time series have been compared over the CEOS LANDNET sites (without Dome C and Tuz Golu) and six different pairs of corresponding composites have been chosen for visual comparison, which means at the same time that 6 different test areas have been selected (North America, South America, Europe, Near East, Asia and Australia). The global position of all test sites is illustrated in Figure 3-157.

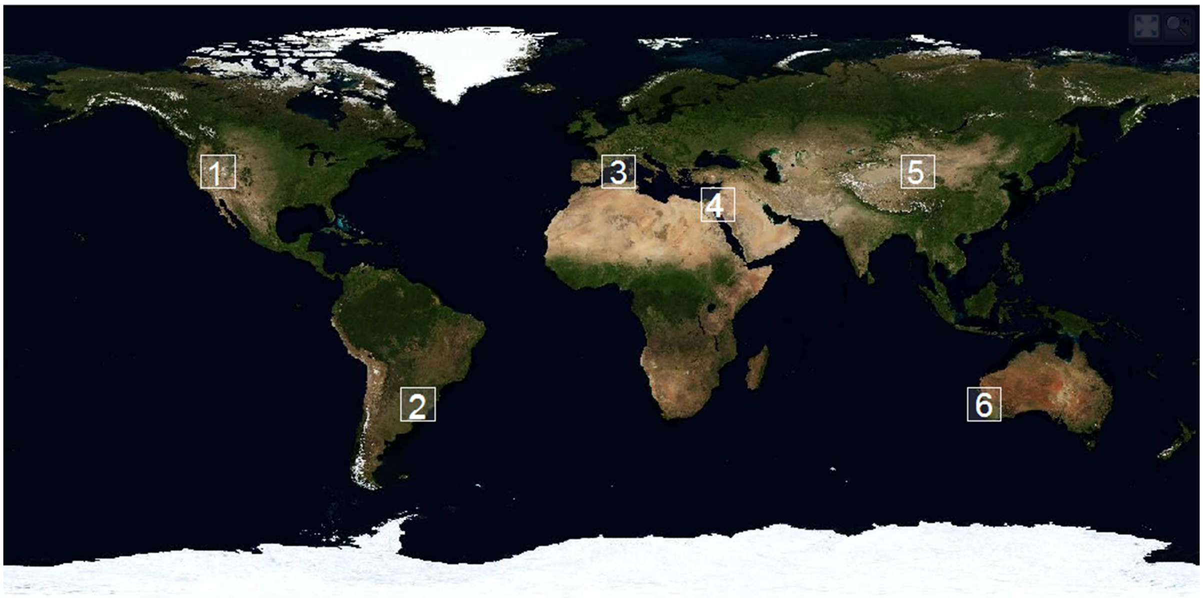

Figure 3-157: Location of all chosen test sites for the comparison of 7-day SR composites and the PROBA-V S10 TOC productss (1 – North America X06Y03, 2 – South America X12Y10, 3 – Europe X18Y03, 4 – Near East X12Y04, 5 – Asia X27Y03, 6 – Australia X29Y10)

At first, the following figures (Figure 3-158 - Figure 3-163) show the RGB of the 7-day SR composite and the S10 TOC products over the selected test site. The result of the visual comparison can summarize as follows:

- 7-day composites are less affected by residual clouds and haze than the S10 TOC products
- Number of SR values in 7-day composites is smaller than in the S10 TOC products,
  - Observations with unexpected and saturated values have been flagged as invalid in the 7-day composites, whereas a lot of these observations are consider in the calculation of the S10 TOC products

[4] Note: Further examination and verification regarding the uncertainty is needed.

- Bright surfaces are often flagged as cloud in the 7-day composites
- Some of the snow/ ice surface are also flagged as cloud in the 7-day composites

The following figures (Figure 3-164 - Figure 3-169) show the time series of the 7-day SR composite and the S10 TOC products for the 6 CEOS LANDNET sites. Besides the general remark about the quality of the 7-day SR composites, the intercomparison of the 7-day SR composite and the S10 TOC products points out, that the characteristic of both time series is similar, but the absolute values may differ. The variation of the values may be caused by undetected clouds which strongly influence the retrieved SR composites values due to their spectral characteristics which may be completely differ from the underlying surface.

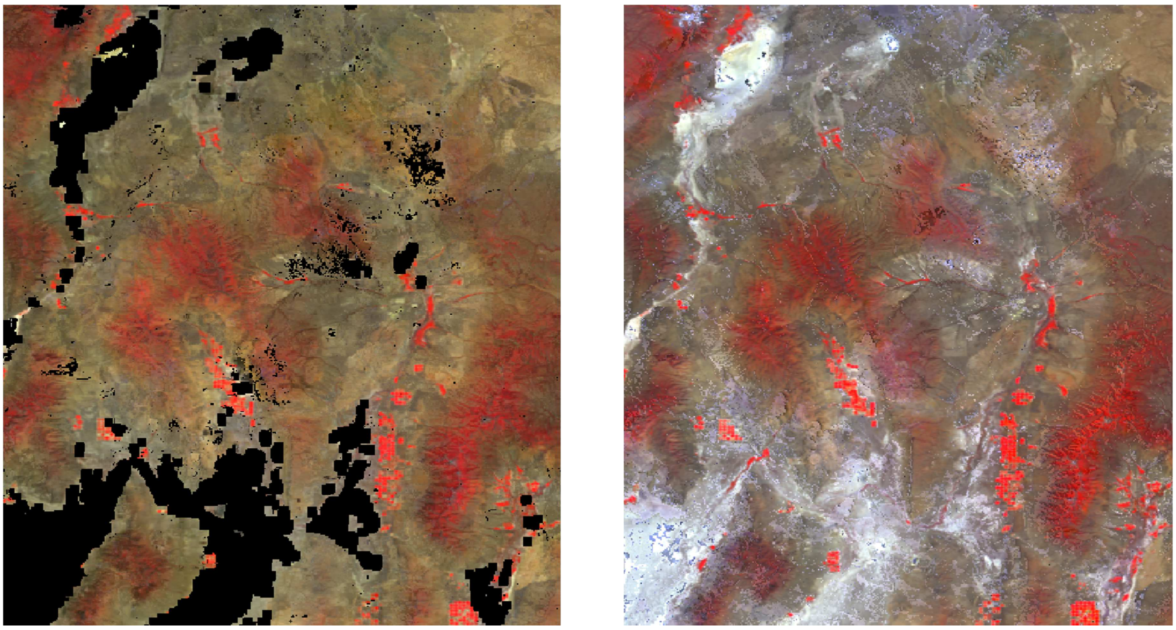

Figure 3-158: RGB of 7-day PROBA-V composite and of the PROBA-V S10 TOC products (test site North America, subset)
PROBAV_S10_TOC_X06Y03_20140611_333M_V002.hdf5
ESACCI-LC-L3-SR-VEGETATION-300m-P7D-h12v09-20140611-v2.0.nc
ESACCI-LC-L3-SR-VEGETATION-300m-P7D-h12v10-20140611-v2.0.nc
ESACCI-LC-L3-SR-VEGETATION-300m-P7D-h12v09-20140611-v2.0.nc
ESACCI-LC-L3-SR-VEGETATION-300m-P7D-h13v10-20140611-v2.0.nc

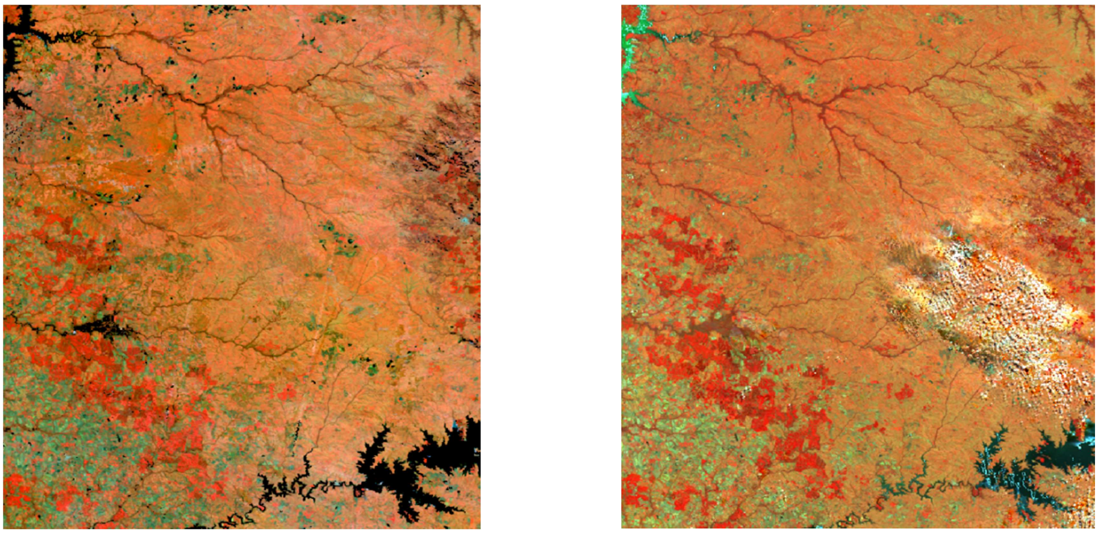

Figure 3-159: RGB of 7-day PROBA-V composite and of the PROBA-V S10 TOC products (test site South America, subset)
PROBAV_S10_TOC_X12Y10_20140611_333M_V002.hdf5
ESACCI-LC-L3-SR-VEGETATION-300m-P7D-h24v23-20140611-v2.0.nc
ESACCI-LC-L3-SR-VEGETATION-300m-P7D-h24v24-20140611-v2.0.nc
ESACCI-LC-L3-SR-VEGETATION-300m-P7D-h25v23-20140611-v2.0.nc
ESACCI-LC-L3-SR-VEGETATION-300m-P7D-h25v24-20140611-v2.0.nc

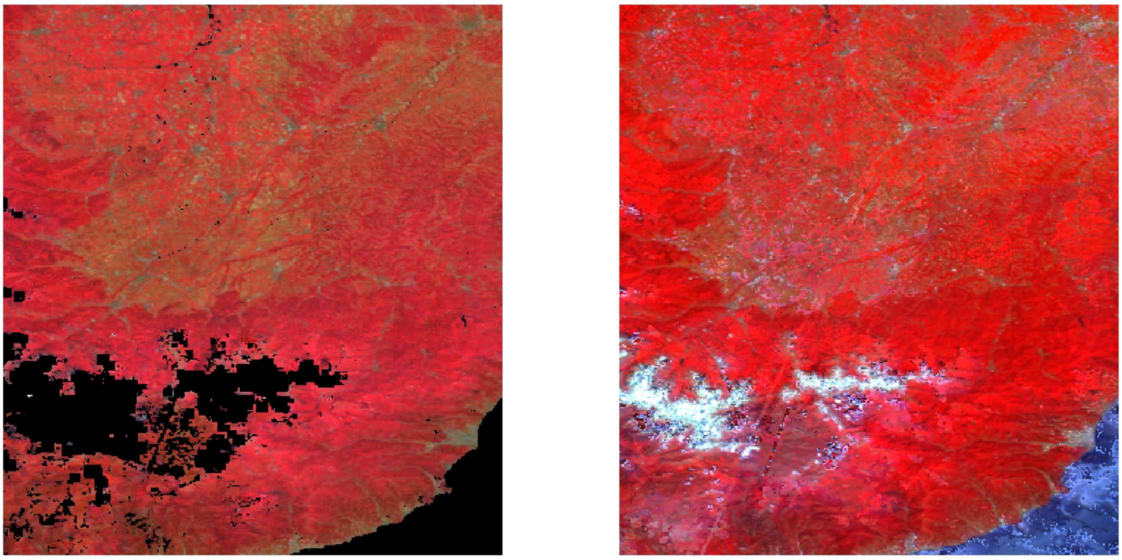

Figure 3-160: RGB of 7-day PROBA-V composite and of the PROBA-V S10 TOC products (test site Europe, subset)
PROBAV_S10_TOC_X18Y03_20140611_333M_V002.hdf5
ESACCI-LC-L3-SR-VEGETATION-300m-P7D-h36v09-20140611-v2.0.nc
ESACCI-LC-L3-SR-VEGETATION-300m-P7D-h36v10-20140611-v2.0.nc
ESACCI-LC-L3-SR-VEGETATION-300m-P7D-h37v09-20140611-v2.0.nc
ESACCI-LC-L3-SR-VEGETATION-300m-P7D-h37v10-20140611-v2.0.nc

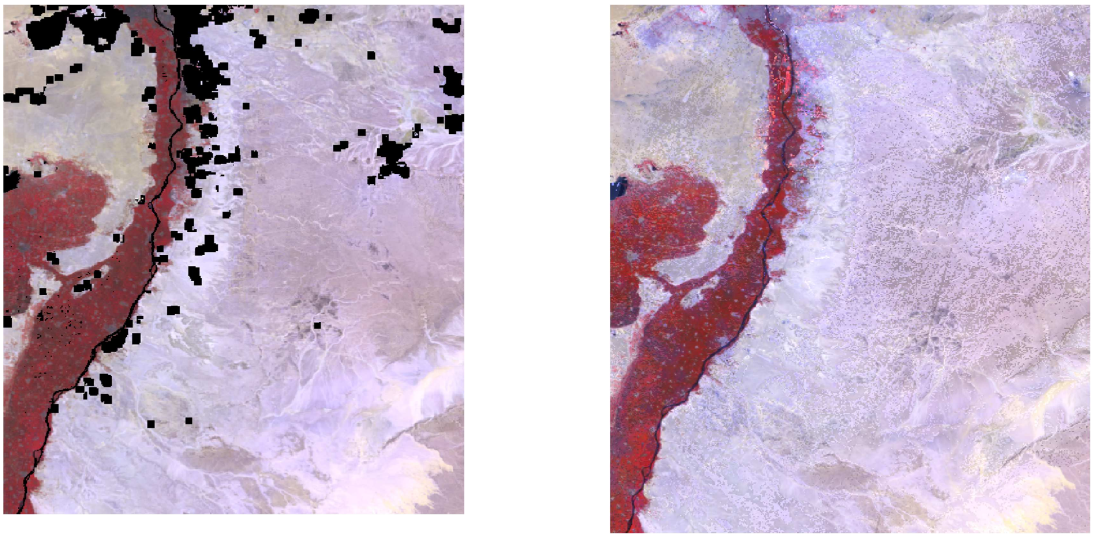

Figure 3-161: RGB of 7-day PROBA-V composite and of the PROBA-V S10 TOC products (test site Near East, subset)
PROBAV_S10_TOC_X21Y04_20140611_333M_V002.hdf5
ESACCI-LC-L3-SR-VEGETATION-300m-P7D-h42v11-20140611-v2.0.nc
ESACCI-LC-L3-SR-VEGETATION-300m-P7D-h42v12-20140611-v2.0.nc
ESACCI-LC-L3-SR-VEGETATION-300m-P7D-h43v11-20140611-v2.0.nc
ESACCI-LC-L3-SR-VEGETATION-300m-P7D-h43v12-20140611-v2.0.nc

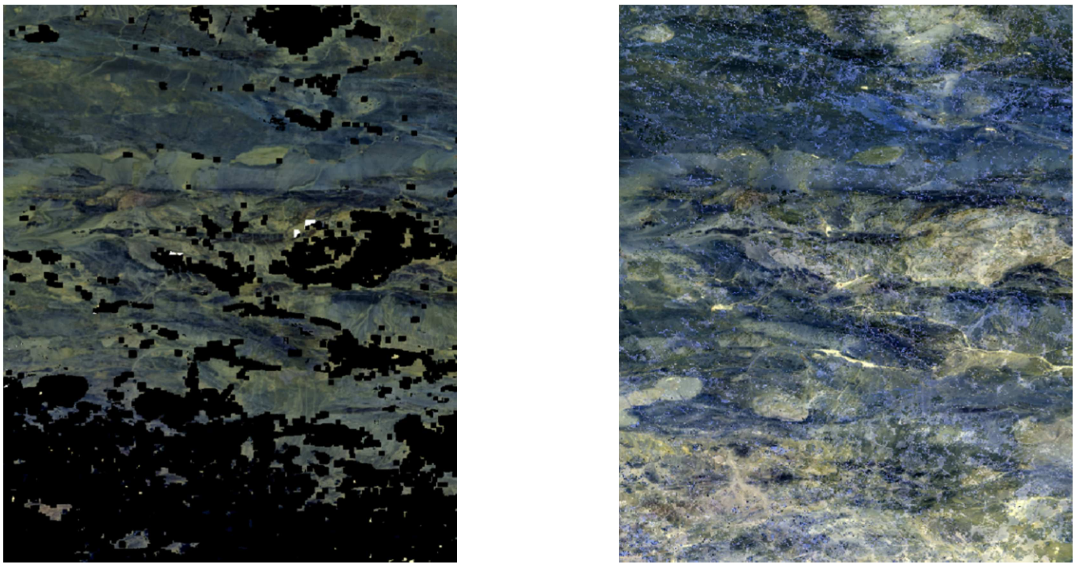

Figure 3-162: RGB of 7-day PROBA-V composite and of the PROBA-V S10 TOC products (test site Asia, subset)
PROBAV_S10_TOC_X27Y03_20140611_333M_V002.hdf5
ESACCI-LC-L3-SR-VEGETATION-300m-P7D-h54v09-20140611-v2.0.nc
ESACCI-LC-L3-SR-VEGETATION-300m-P7D-h54v10-20140611-v2.0.nc
ESACCI-LC-L3-SR-VEGETATION-300m-P7D-h55v09-20140611-v2.0.nc
ESACCI-LC-L3-SR-VEGETATION-300m-P7D-h55v10-20140611-v2.0.nc

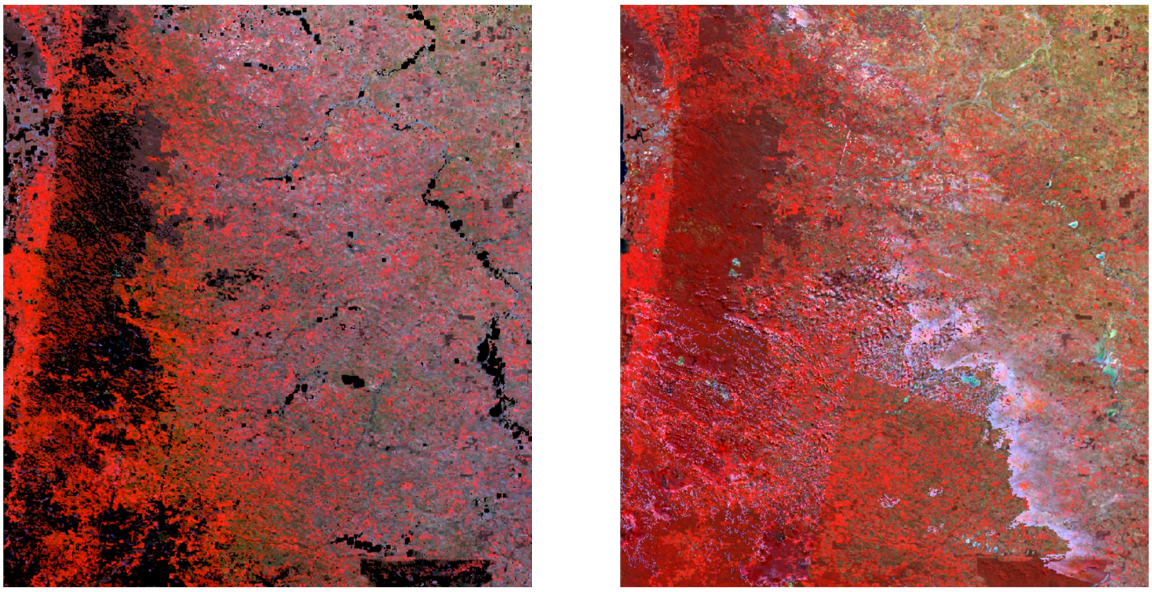

Figure 3-163: RGB of 7-day PROBA-V composite and of the PROBA-V S10 TOC products (test site Australia, subset)
PROBAV_S10_TOC_X29Y10_20140611_333M_V002.hdf5
ESACCI-LC-L3-SR-VEGETATION-300m-P7D-h58v23-20140611-v2.0.nc
ESACCI-LC-L3-SR-VEGETATION-300m-P7D-h58v24-20140611-v2.0.nc
ESACCI-LC-L3-SR-VEGETATION-300m-P7D-h59v23-20140611-v2.0.nc
ESACCI-LC-L3-SR-VEGETATION-300m-P7D-h59v24-20140611-v2.0.nc

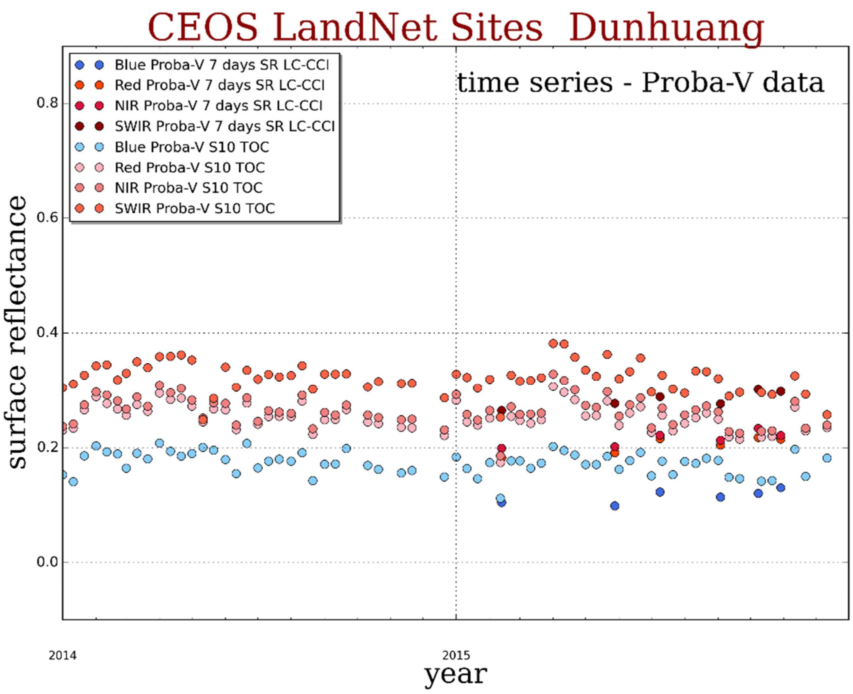

Figure 3-164: SR time series from PROBA-V data - 2014-2015 - CEOS-LANDNET SITES – Dunhuang – LC-CCI & S10 TOC dataset

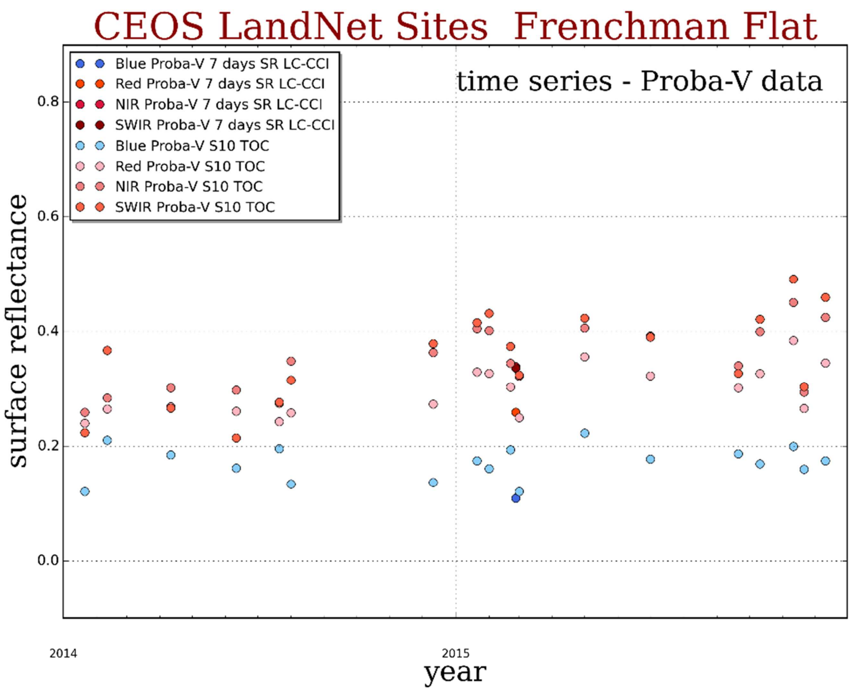

Figure 3-165: SR time series from PROBA-V data - 2014-2015 - CEOS-LANDNET SITES – Frenchman Flat – LC-CCI & S10 TOC dataset

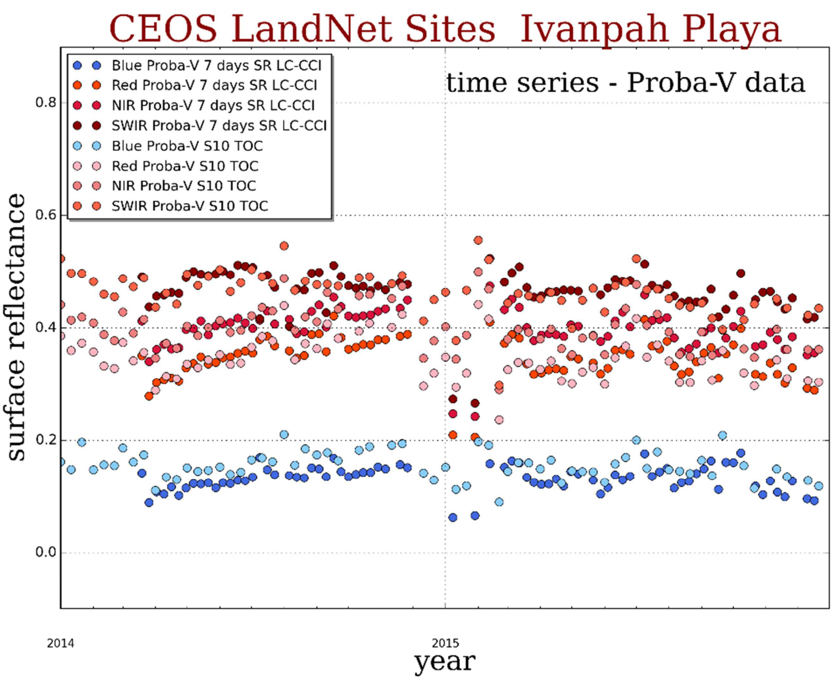

Figure 3-166: SR time series from PROBA-V data - 2014-2015 - CEOS-LANDNET SITES – Ivanpah Playa – LC-CCI & S10 TOC dataset

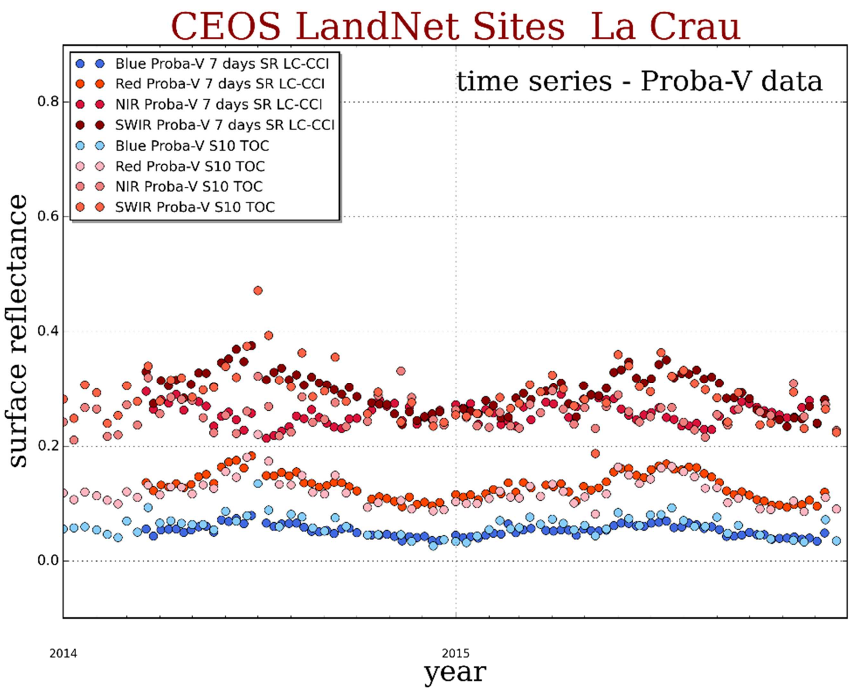

Figure 3-167: SR time series from PROBA-V data - 2014-2015 - CEOS-LANDNET SITES – La Crau – LC-CCI & S10 TOC dataset

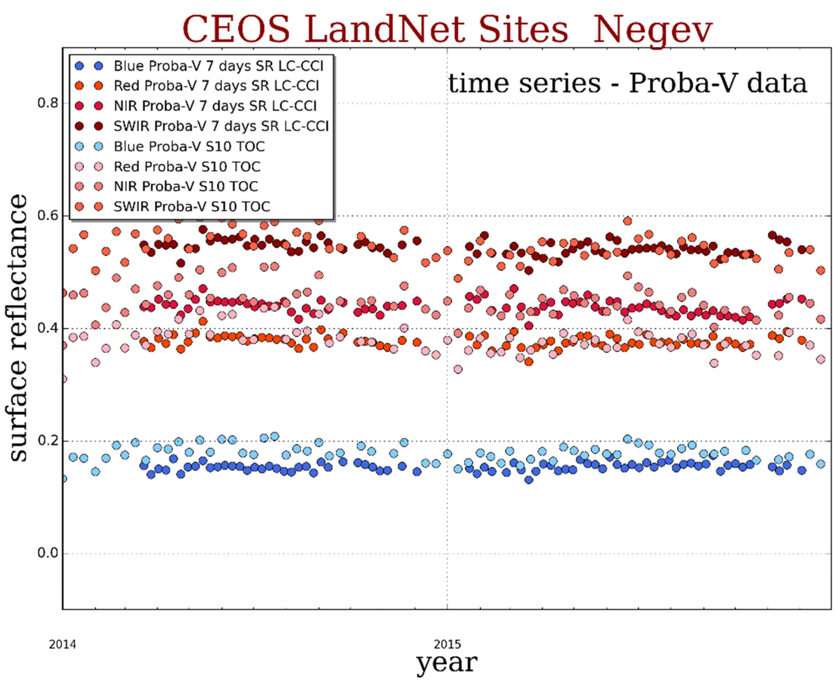

Figure 3-168: SR time series from PROBA-V data - 2014-2015 - CEOS-LANDNET SITES – Negev – LC-CCI & S10 TOC dataset -LANDNET SITES – Negev – LC-CCI & Global Land 1km dataset

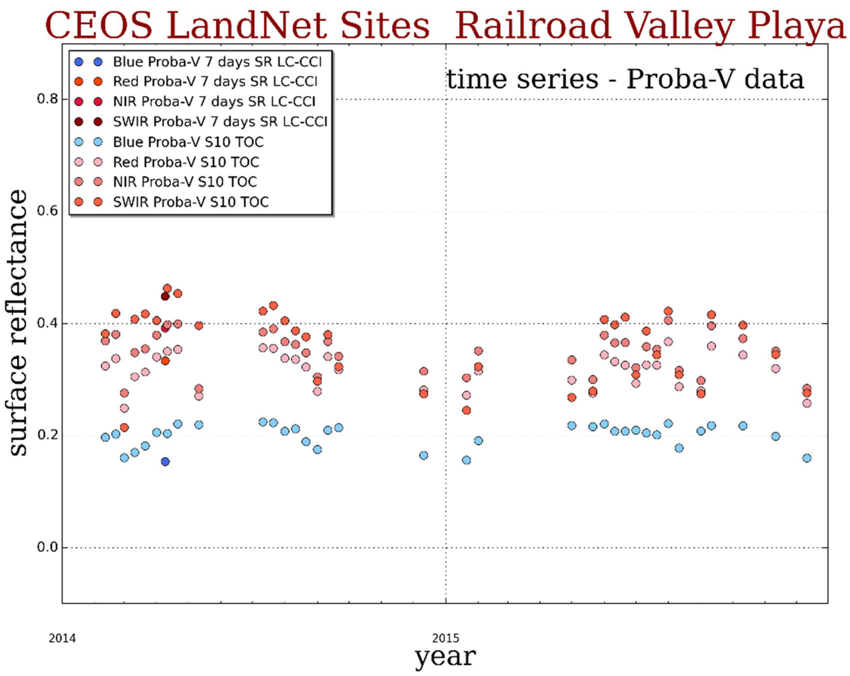

Figure 3-169: *SR time series from PROBA-V data - 2014-2015 - CEOS-LANDNET SITES – Railroad Valley Playa – LC-CCI & S10 TOC dataset*

3.6.4 Intercomparison of the global 7-day AVHRR composites and the Global Land 1-KM AVHRR products

In the framework of the Global Land 1-KM AVHRR Project [Eidenshink & Faundeen, 1994] surface reflectance composite has been also produced with the following characteristics:

- Temporal coverage: 10 day composites: from April 1992 through September 1993, from February 1995 through January 1996 and May 1996
- Spatial coverage: global
- Spatial resolution: 1km

The data products are available from the U.S. Geological Survey (USGS) and have been used for the intercomparison exercise. For the intercomparison of the global 7-day AVHRR SR composites and the Global Land 1km AVHRR products the correspondent time series have been compared over the CEOS LANDNET sites (without Dome C and Tuz Golu) and six different sites of the corresponding composite as well as one corresponding global composite have been chosen for visual comparison, which means at the same time that 6 different test areas have been selected (North America, South America, Europe, Near East, Asia and Australia). The global position of all test sites is illustrated in Figure 3-170.

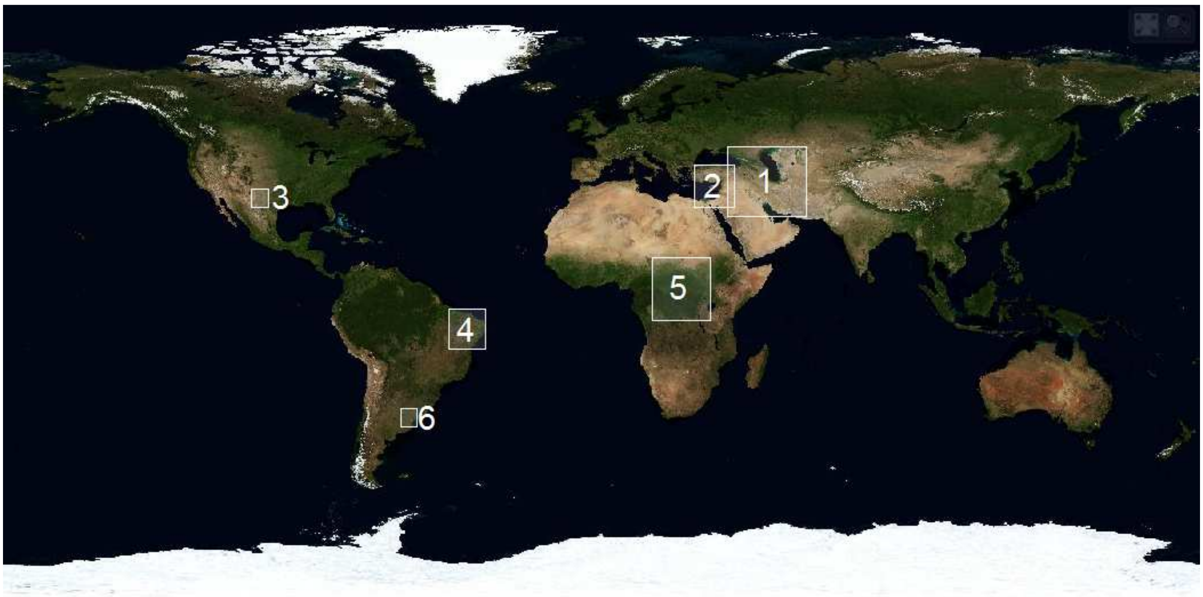

Figure 3-170: Location of all chosen test sites for the comparison of 7-day SR composites and the Global Land 1km AVHRR products (1 – Near East a, 2 – Near East b, 3 – America, 4 – Brazil, 5 – Africa, 6 – South America)

At first, the following figures (Figure 3-171 - Figure 3-178) show the RGB of the global 7-day AVHRR SR composites and the Global Land 1km AVHRR products over the selected test site and the global composite. The result of the visual comparison can summarize as follows:

- 7-day composites are less affected by residual clouds and haze than the Global Land 1km products
- Number of SR values in 7-day composites is smaller than in the Global Land 1km products,
  - Quality control of the input data (1344 corrupted products of 31597 products have been identified)
  - Border pixels have been removed (700 from each swath side)
  - Bright surfaces are often flagged as cloud in the 7-day composites
  - Some of the snow/ ice surface are also flagged as cloud in the 7-day composites
- Blurring effects and unsharpened coastlines can be visible through the weaker geolocation

The following figures (Figure 3-179 - Figure 3-184) show the time series of the 7-day SR composite and the Global Land 1km AVHRR products for the 6 CEOS LANDNET sites. Besides the general remark about the quality of the 7-day SR composites, the intercomparison of the 7-day SR composite and the Global Land 1km AVHRR products points out, that the characteristic of both time series is similar, but the absolute values may differ. The variation of the values may be caused by undetected clouds which strongly influence the retrieved SR composites values due to their spectral characteristics which may be completely differ from the underlying surface.

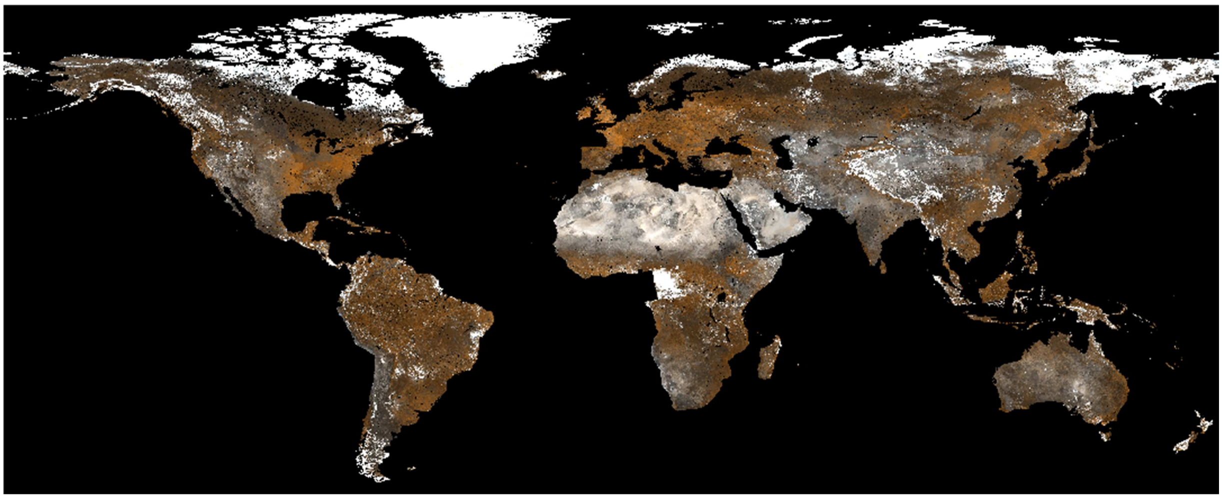

Figure 3-171: RGB of the Global Land 1km AVHRR products (ag1km14199605210530)

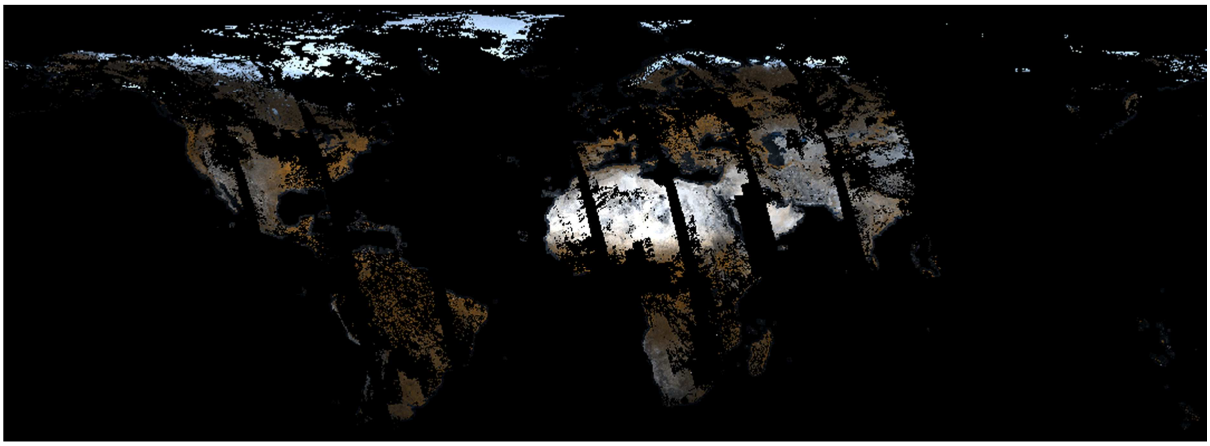

Figure 3-172: RGB of 7-day AVHRR composite
(ESACCI-LC-L3-SR-AVHRR-1000m-P7D- h00-71v00-35-19960521-v2.2.nc)

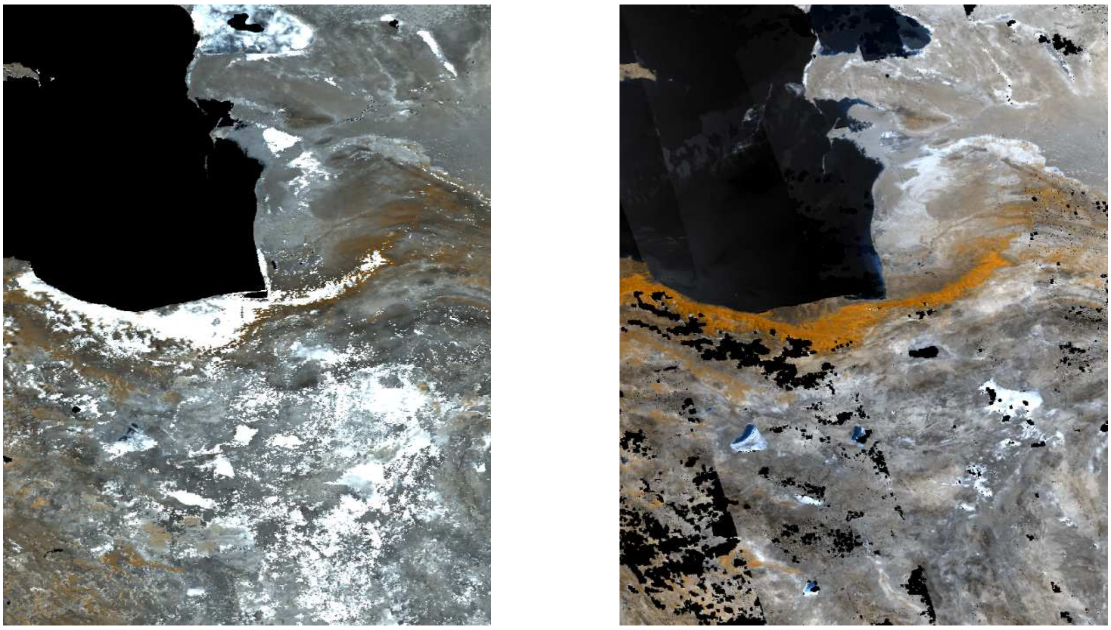

Figure 3-173: RGB of the Global Land 1km AVHRR products (left) and of the 7-day AVHRR composite(right) (test site Near East a, subset)
ag1km14199605210530
ESACCI-LC-L3-SR-AVHRR-1000m-P7D- h00-71v00-35-19960521-v2.2.nc

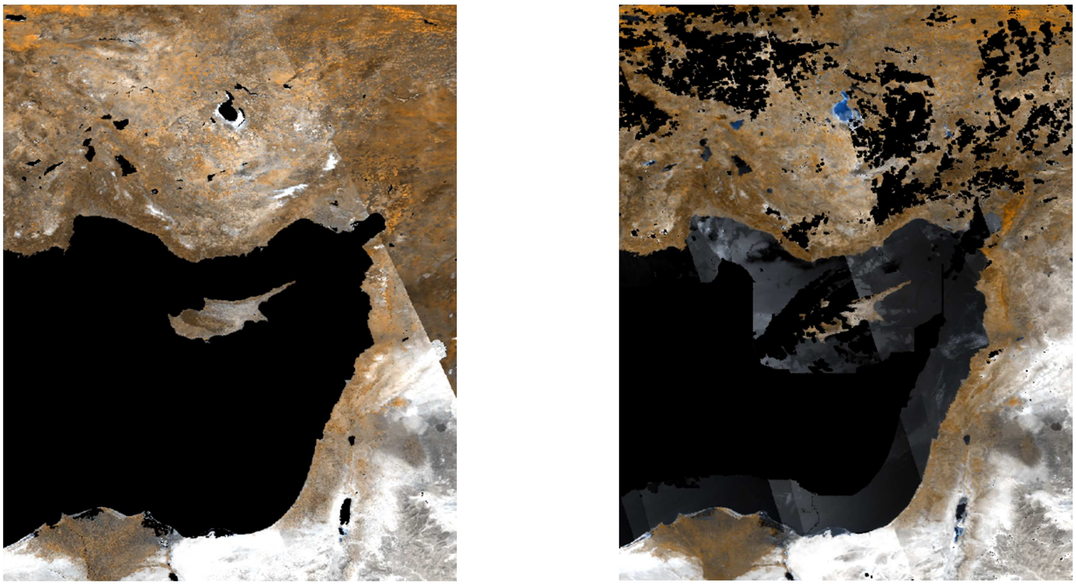

Figure 3-174: RGB of the Global Land 1km AVHRR products (left) and of the 7-day AVHRR composite(right) (test site Near East b, subset)
ag1km14199605210530
ESACCI-LC-L3-SR-AVHRR-1000m-P7D- h00-71v00-35-19960521-v2.2.nc

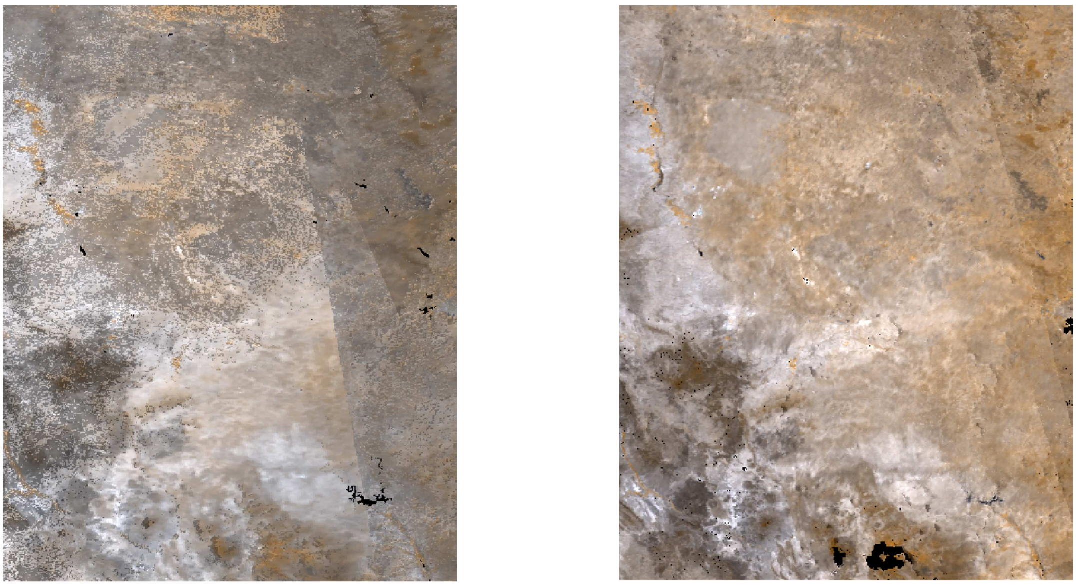

Figure 3-175: RGB of the Global Land 1km AVHRR products (left) and of the 7-day AVHRR composite(right) (test site America, subset)
ag1km14199605210530
ESACCI-LC-L3-SR-AVHRR-1000m-P7D- h00-71v00-35-19960521-v2.2.nc

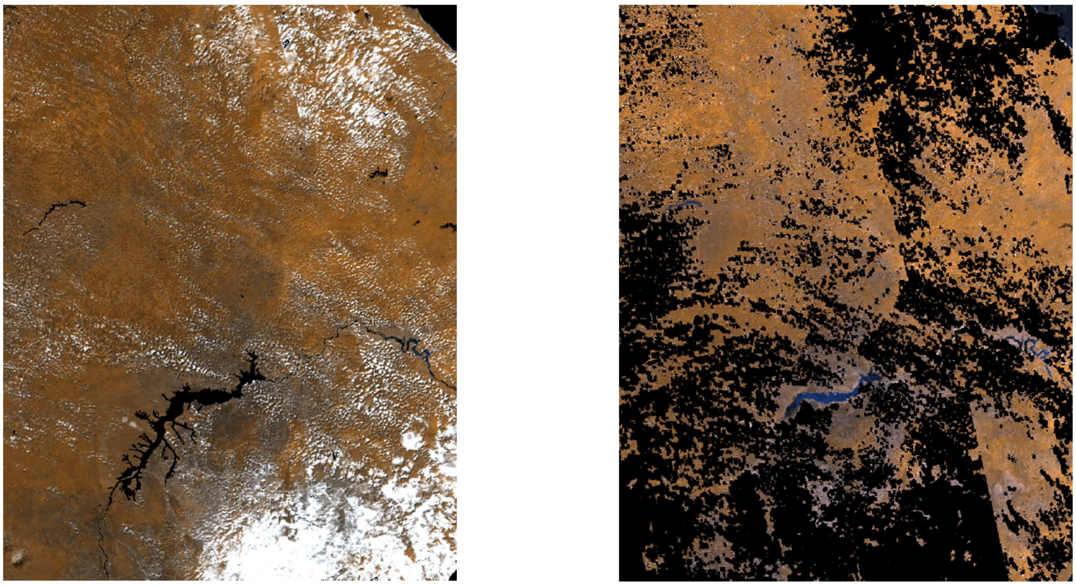

Figure 3-176: RGB of the Global Land 1km AVHRR products (left) and of the 7-day AVHRR composite(right) (test site Brazil, subset)
ag1km14199605210530
ESACCI-LC-L3-SR-AVHRR-1000m-P7D- h00-71v00-35-19960521-v2.2.nc

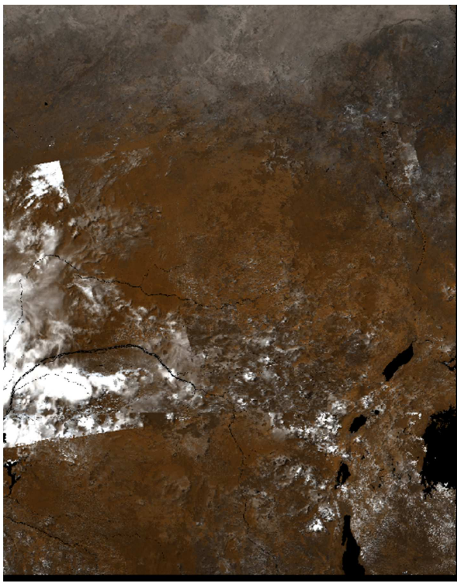

Figure 3-177: RGB of the Global Land 1km AVHRR products (left) and of the 7-day AVHRR composite(right) (test site Africa, subset)
ag1km14199605210530
ESACCI-LC-L3-SR-AVHRR-1000m-P7D- h00-71v00-35-19960521-v2.2.nc

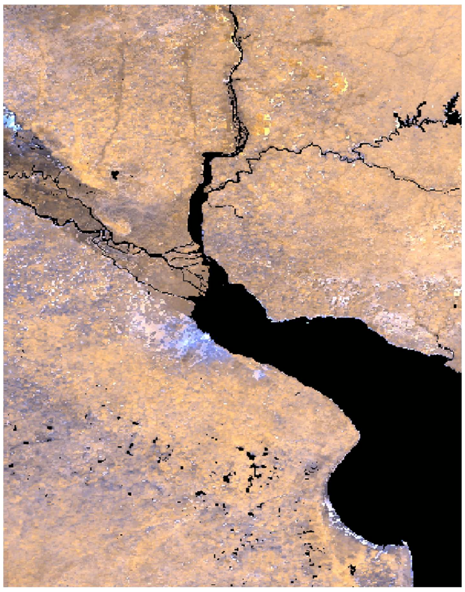

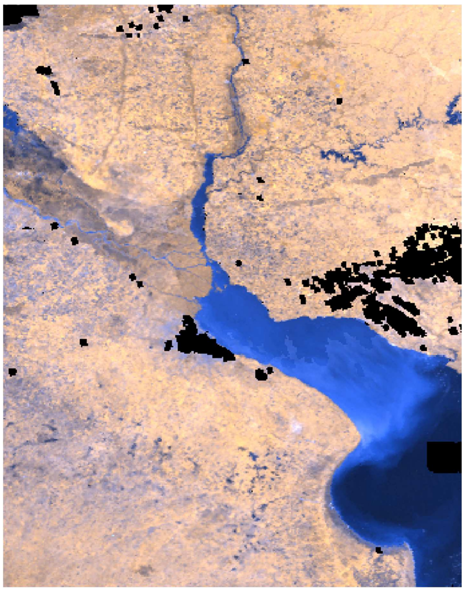

Figure 3-178: RGB of the Global Land 1km AVHRR products (left) and of the 7-day AVHRR composite(right) (test site South America, subset)
ag1km14199605210530
ESACCI-LC-L3-SR-AVHRR-1000m-P7D- h00-71v00-35-19960521-v2.2.nc

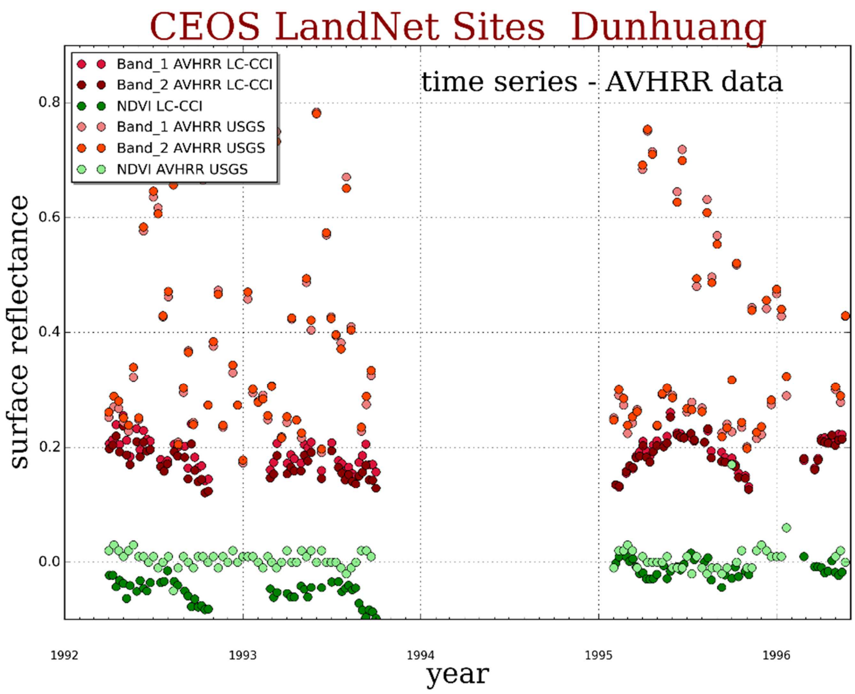

Figure 3-179: SR time series from AVHRR data - 1992-1997 - CEOS-LANDNET SITES – Dunhuang – LC-CCI & Global Land 1km dataset

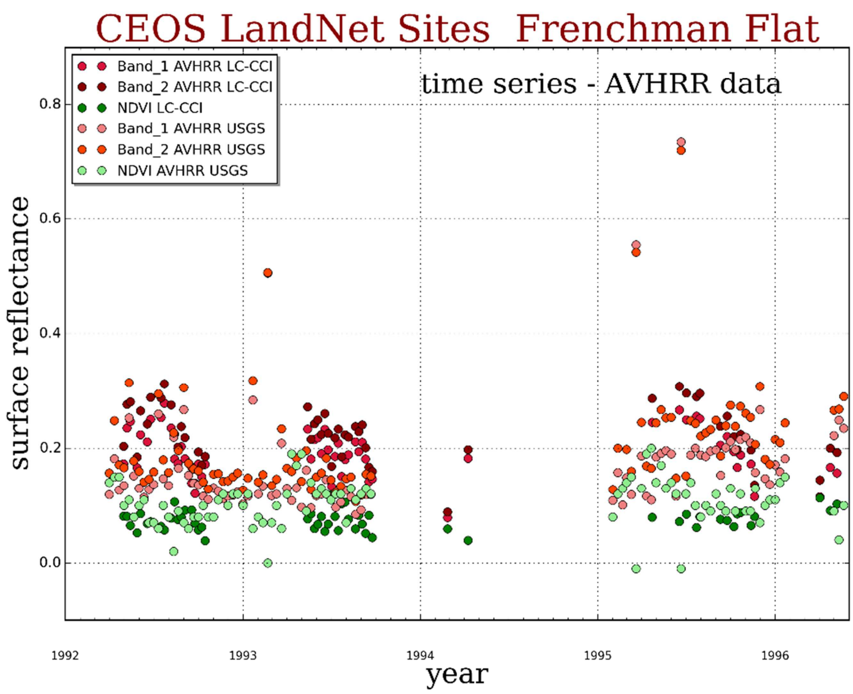

Figure 3-180: SR time series from AVHRR data - 1992-1997 - CEOS-LANDNET SITES – Frenchman Flat – LC-CCI & Global Land 1km dataset

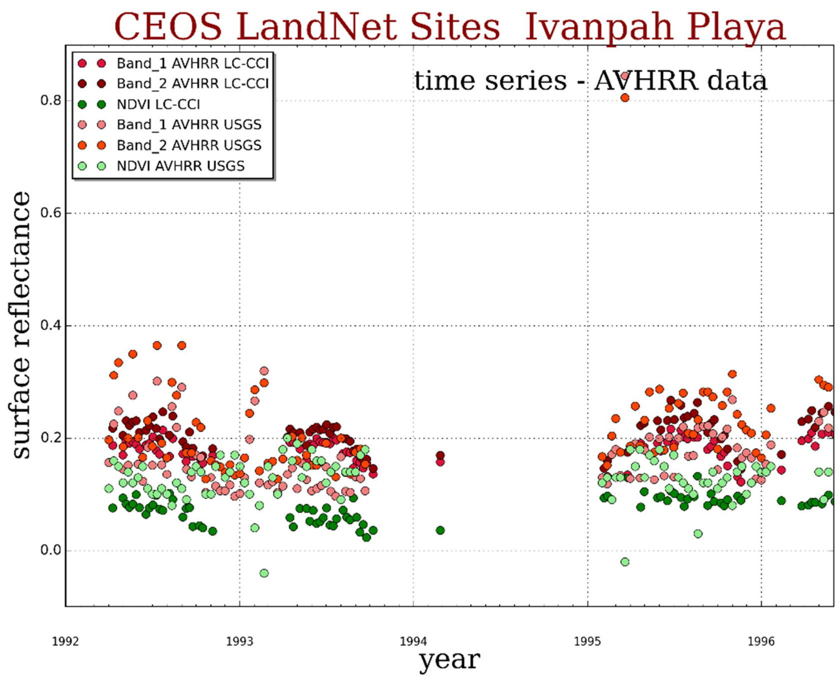

Figure 3-181: SR time series from AVHRR data - 1992-1997 - CEOS-LANDNET SITES – Ivanpah Playa – LC-CCI & Global Land 1km dataset

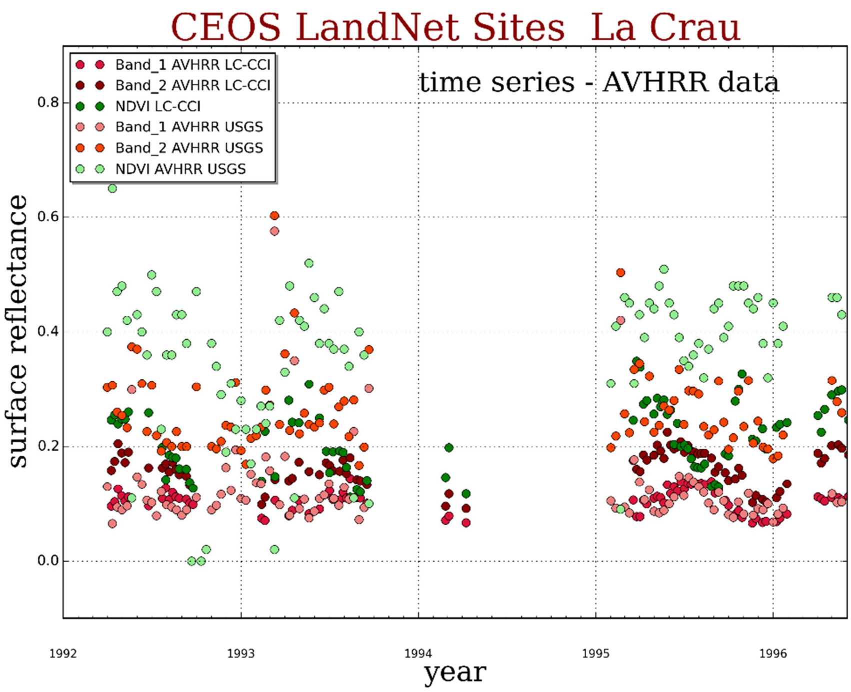

Figure 3-182: SR time series from AVHRR data - 1992-1997 - CEOS-LANDNET SITES –La Crau – LC-CCI & Global Land 1km dataset

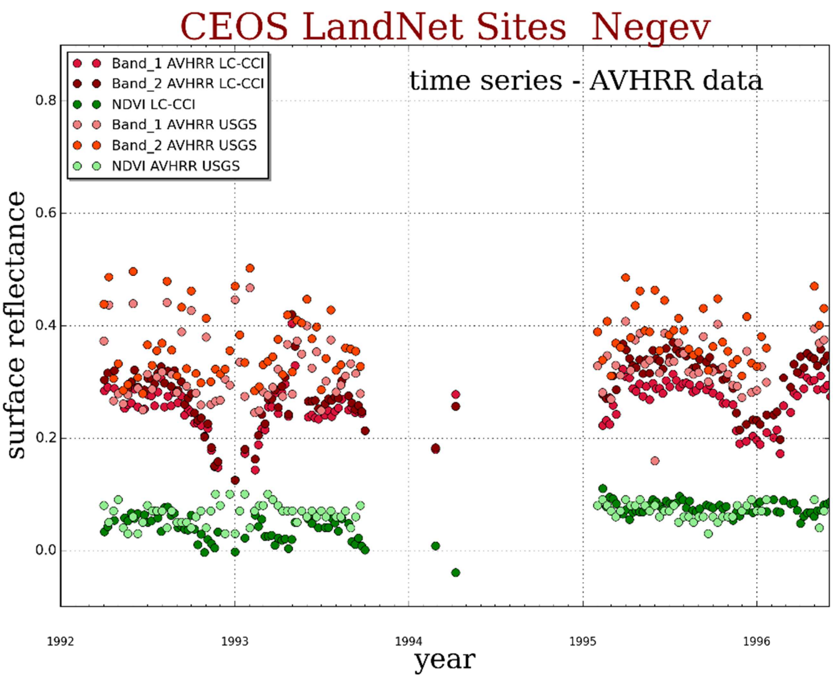

Figure 3-183: SR time series from AVHRR data - 1992-1997 - CEOS-LANDNET SITES – Negev – LC-CCI & Global Land 1km dataset

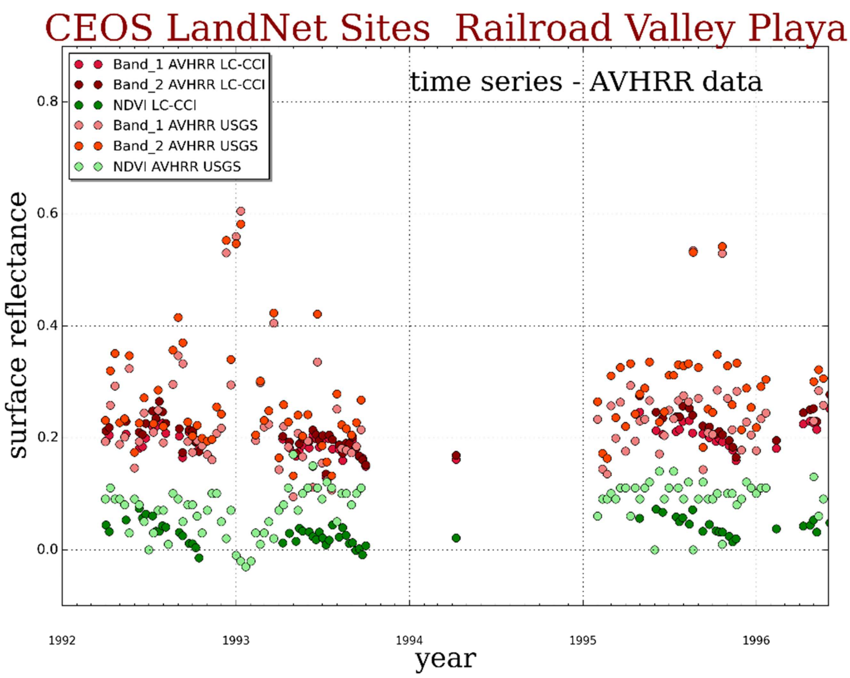

Figure 3-184: *SR time series from AVHRR data - 1992-1997 - CEOS-LANDNET SITES – Railroad Valley Playa – LC-CCI & Global Land 1km dataset*

3.6.5 Long-term NDVI time series over the CEOS sites from MERIS FR, PROBA V and AVHRR

Additionally, for the intercomparison of the global 7-day MERIS FR, PROBA-V and AVHRR SR composites the long-term time series of the NDVI have been calculated over the CEOS LANDNET sites (without Dome C and Tuz Golu).

The following figures (Figure 3-185 - Figure 3-190) show the time series of the NDVI for the 6 CEOS LANDNET sites. The characteristic of the NDVI time series from MERIS FR and PROBA-V looks very similar and only differ slightly from the absolute values. The NDVI values calculated from the AVHRR data indicate a greater variability except over La Crau and differ strongly in terms of the absolute values in comparison to the NDVI values calculated from MERIS FR and PROBA-V data. These differences can be caused by the different sensor configurations, different spatial resolution of the sensors considered here and by the uncertainty of the determination of atmospheric conditions used in the atmospheric correction.

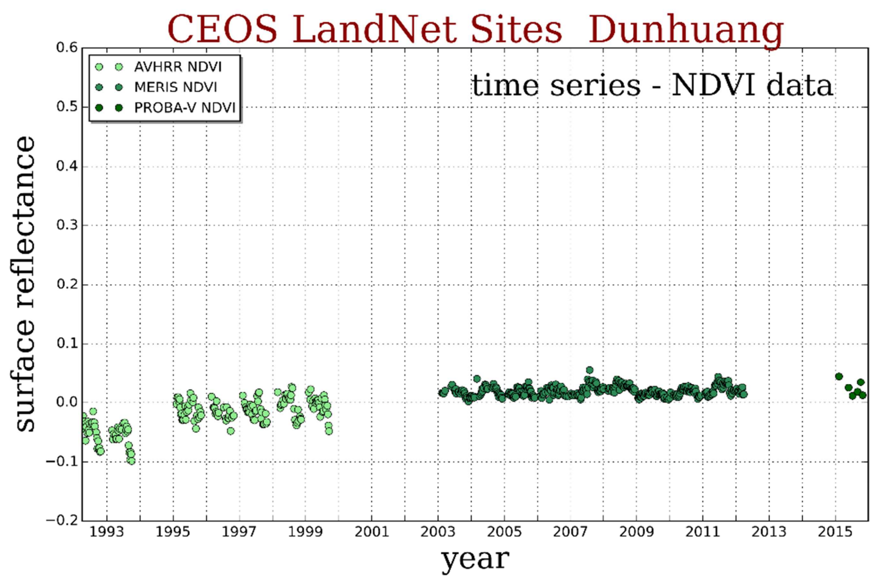

Figure 3-185: NDVI time series - CEOS-LANDNET SITES – Dunhuang – MERIS FR 2003-2012; PROBA-V 2014-2016 and AVHRR 1992-1999

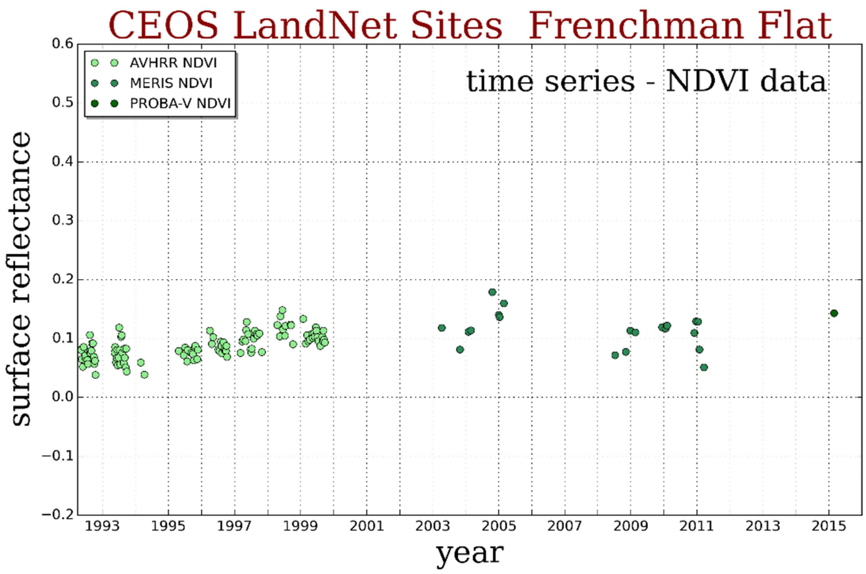

Figure 3-186: NDVI time series - CEOS-LANDNET SITES – Frenchman Flat – MERIS FR 2003-2012; PROBA-V 2014-2016 and AVHRR 1992-1999

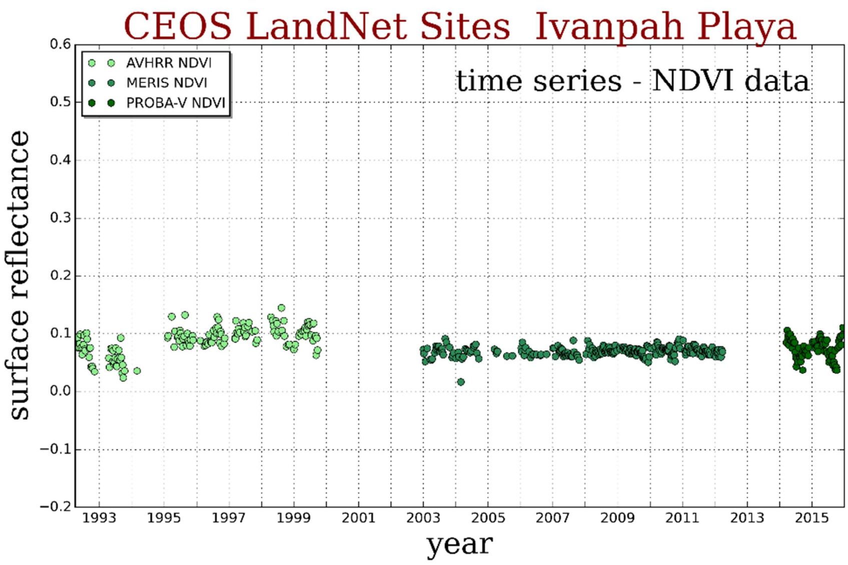

Figure 3-187: NDVI time series - CEOS-LANDNET SITES – Ivanpah Playa – MERIS FR 2003-2012; PROBA-V 2014-2016 and AVHRR 1992-1999

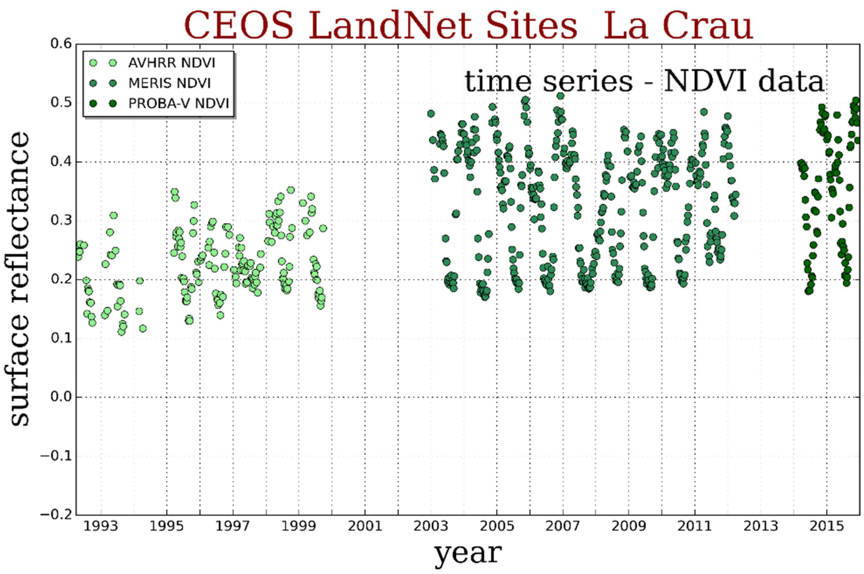

Figure 3-188: NDVI time series - CEOS-LANDNET SITES –La Crau – MERIS FR 2003-2012; PROBA-V 2014-2016 and AVHRR 1992-1999

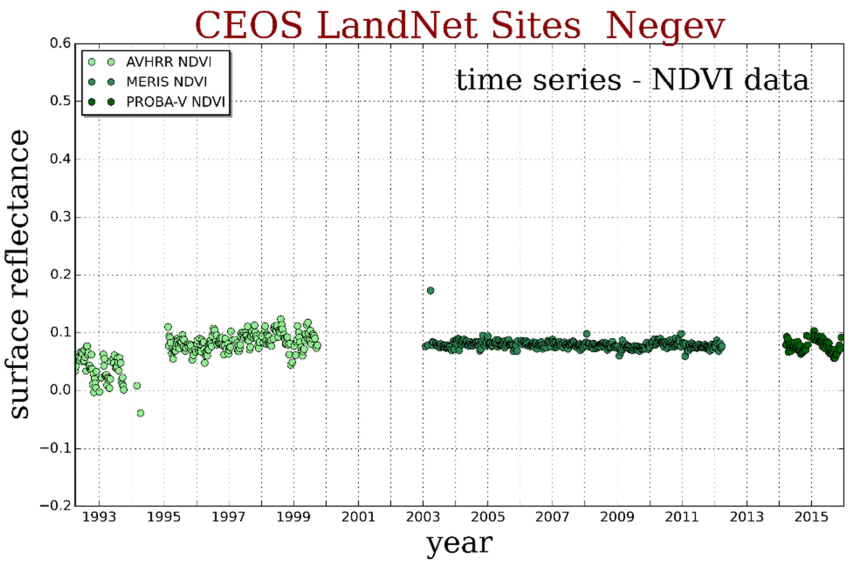

Figure 3-189: NDVI time series - CEOS-LANDNET SITES – Negev – MERIS FR 2003-2012; PROBA-V 2014-2016 and AVHRR 1992-1999

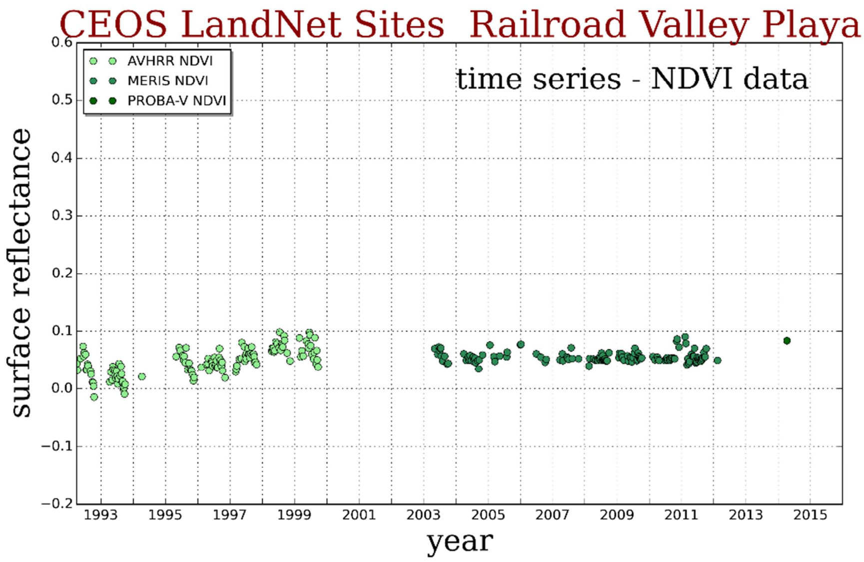

Figure 3-190: *NDVI time series- CEOS-LANDNET SITES – Railroad Valley Playa - MERIS FR 2003-2012; PROBA-V 2014-2016 and AVHRR 1992-1999*

3.7 Visual quality assessment of LC-CCI global SR-7day composites

The MERIS FR and RR, PROBA-V and AVHRR 7-day composites have been also systematically assessed by visual inspection after mosaicing.

3.7.1 MERIS FR and RR

The overall quality of the SR composite from FR and RR data is very good and highlights the impact of the pre-processing improvements since GlobCover for instance. A set of issues has been identified and concern limited areas of the composites. The following list summarizes these issues.

- **Issue 1: missing lakes and island**
- **Issue 2: NoData (NaN value) in the desert over bright areas**
- **Issue 3: cloud/ snow ice discrimination**
- **Issue 4: undetected semi-transparent clouds and clouds**

Figure 3-191: Example for Issue 4: Undetected semi-transparent clouds - ESACCI-LC-L3-SR-MERIS-300m-P7D-h35v15-20090604-v2.0.nc

3.7.2 PROBA-V

The overall quality of the SR composite from PROBA-V data is very good but a set of issues has been identified and concern limited areas of the composites (see also section 3.6.3). The following list summarizes these issues.

- **Issue 1: NoData (NaN value) in the desert over bright areas**
- **Issue 2: cloud/ snow ice discrimination**
- **Issue 3: undetected semi-transparent clouds and clouds**

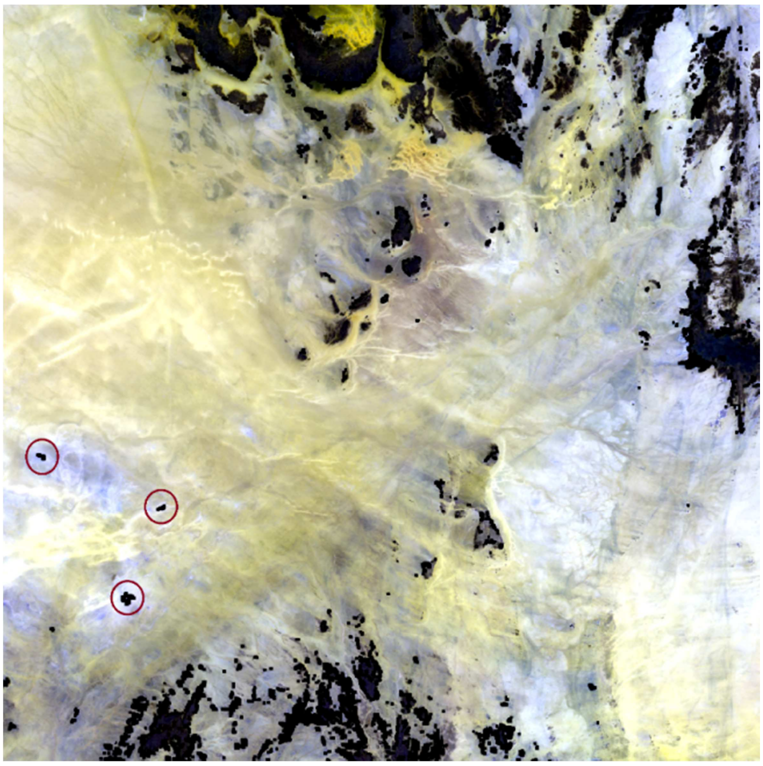

Figure 3-192: Example for Issue 1: NoData (NaN value) in the desert over bright areas-ESACCI-LC-L3-SR-VEGETATION-300m-P7D-h36v13-20140528-v2.0.nc

3.7.3 AVHRR

The overall quality of the SR composite from AVHRR data is very good and but again a set of issues has been identified and concern limited areas of the composites (see also section 3.6.4). The following list summarizes these issues.

- **Issue 1: NoData (NaN value) in the desert over bright areas**
- **Issue 2: Cloud/ snow ice discrimination**
- **Issue 3: Undetected semi-transparent clouds**

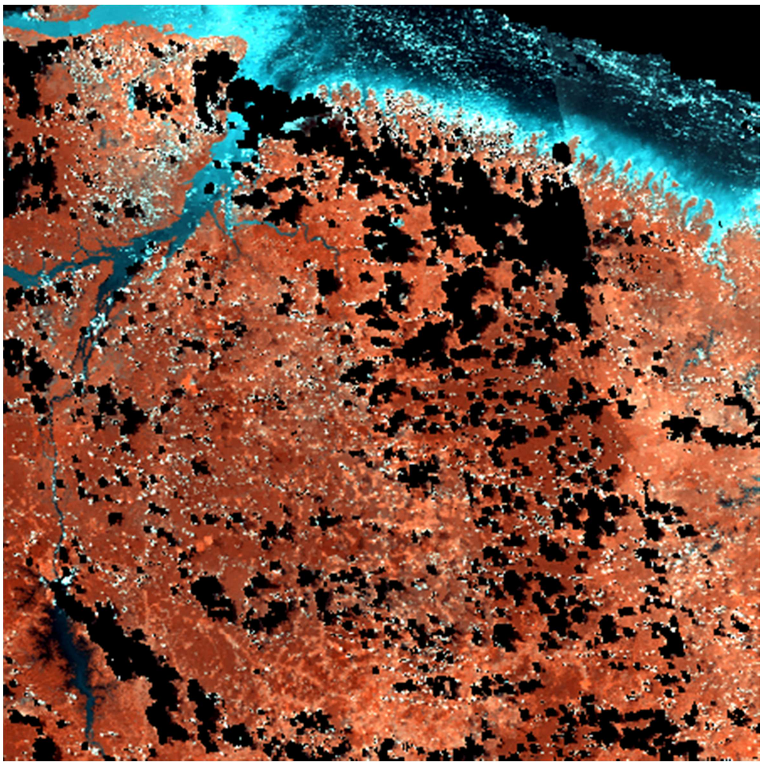

Figure 3-193: Example for Issue 4: undetected semi-transparent clouds and clouds - ESACCI-LC-L3-SR-AVHRR-1000m-P7D-h26v18-19930521-v2.2.nc

3.8 Concluding remarks

The overall quality of the LC-CCI global SR-7day composite time series of the correspondent epochs was found quite well according to the current validation results.

The number of pixels which contribute to the analysis of the time series is very variable whereas this can be caused by the data availability or by the cloud coverage or by the commission and omission errors of the pixel identification.

Visual quality assessment of LC-CCI global SR-7day composites: The overall quality of the SR composite from FR and RR and PROBA-V data is very good and highlights the impact of the pre-processing improvements since GlobCover for instance in case of MERIS FR and RR. The quality of SR composite from AVHRR data is sufficient. A set of issues has been identified and concern limited areas of the composites.

Temporal variance at the pixel level for the various spectral reflectance values: The impact of undetected clouds, data availability and the commission and omission errors of the pixel identification is visible in the time series and influences the statistical parameter estimate. The standard deviation values reach an order of magnitude:

- from 1.6 through 55 % (mean 22%) for MERIS data
- from 2.0 through 86 % (mean 18%) for PROBA-V data
- from 6.3 through 67 % (mean 26%) for AVHRR data

Local variance for the various spectral reflectance values within a LC class and across LC classes: The results of ANOVA for the all analysed combinations of LC-CCI classes show that the differences between class means and their variation among and between classes are statistical significance. The ANOVA of individual bands can also result in rejection of the null hypothesis, e.g. MERIS FR band 9 for the ANOVA for cropland and grassland (see Table 3-18).

Analysis of the intra- and inter-annual reflectance dynamic: The spectra inside the class over the years are very similar but the standard deviation shows a great dispersion from the average, the very high standard deviation over the LC-CCCI class 'bare areas' reflects the natural variability of soils. The analysis of the multi-annual temporal profiles of the mean and the range highlights similar intra-annual "structures" from year to year inside the class and no significant inter-annual changes.

Validation against in-situ data: The comparison of the mean spectra retrieved from time series of the CEOS LANDNET site Dunhuang, La Crau, Negev and Railroad Valley Playa and the in-situ spectrum shows that the characteristic of the spectra is similar, but the absolute values may differ.

Intercomparison with other products:

- The 7-day MERIS FR SR composite products processed in phase I and phase II data have been compared in their radiometric attributes at SR (surface reflectance) level and the scatterplots indicate in all cases a linear correlation.

- The characteristic of the time series of the 7 day SR composites from the LC-CCI project and the CultureMeris project for the 6 CEOS LANDNET sites is similar, but the absolute values may differ.
- The intercomparison of the PROBA-V 7-day SR composite and the PROBA-V S10 TOC products points out, that the characteristic of both time series is similar, but the absolute values may differ.
- The intercomparison of the AVHRR 7-day SR composite and the Global Land 1km AVHRR products indicates again, that the characteristic of both time series is similar, but the absolute values may differ.
- The characteristic of the NDVI time series from MERIS FR and PROBA-V looks very similar and only differ slightly from the absolute values. The NDVI values calculated from the AVHRR data indicate a greater variability except over La Crau and differ strongly in terms of the absolute values in comparison to the NDVI values calculated from MERIS FR and PROBA-V data.

4 CCI GLOBAL LAND COVER MAP V2

4.1 Product description

The CCI-LC project delivers consistent global LC maps at 300 m spatial resolution on an annual basis from 1992 to 2015. The Coordinate Reference System used for the global land cover database is a geographic coordinate system (GCS) based on the World Geodetic System 84 (WGS84) reference ellipsoid.

Figure 4-1 presents the LC map from the year 2015 at global scale and Figure 4-2 shows the classification obtained throughout the years over a region of Argentina.

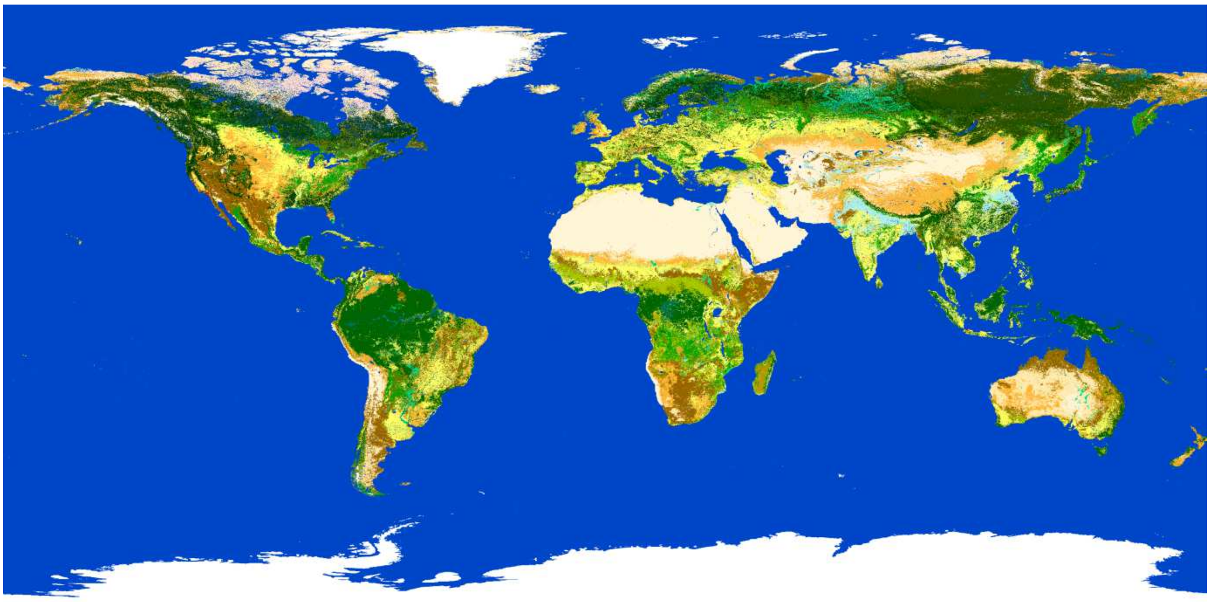

Figure 4-1: The most recent map from the LC map series from the year 2015, at 300 m spatial resolution.

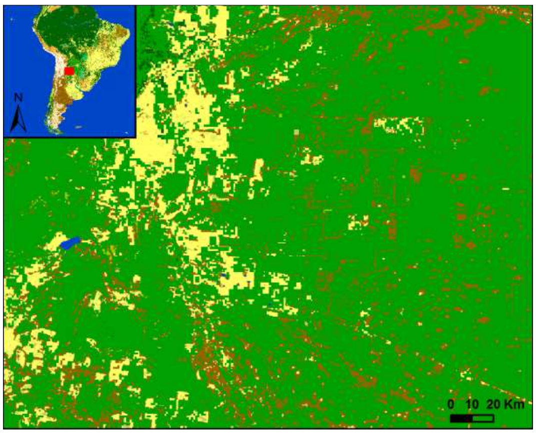

Year 1992

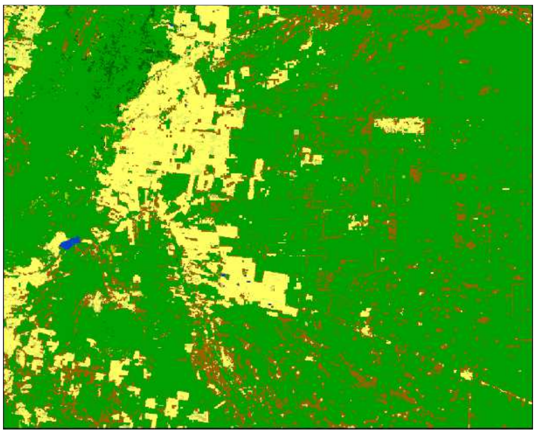

Year 2000

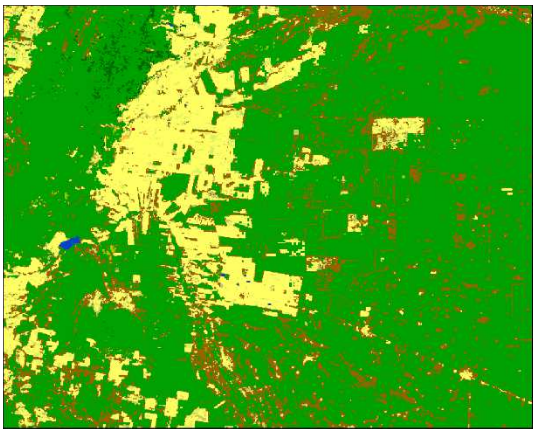

Year 2004

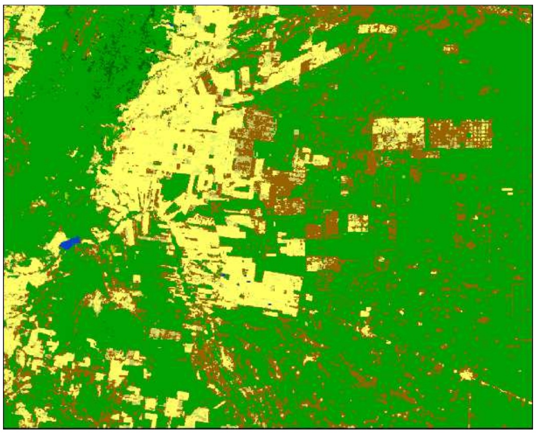

Year 2007

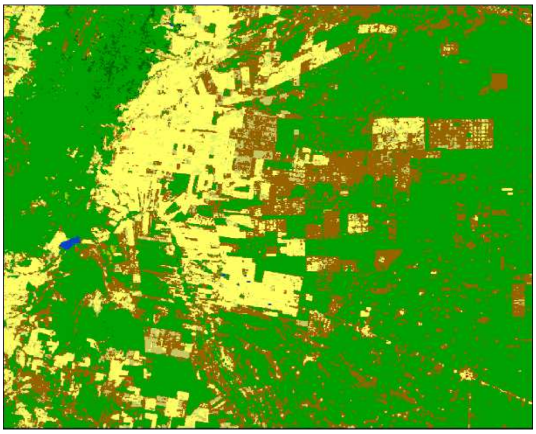

Year 2011

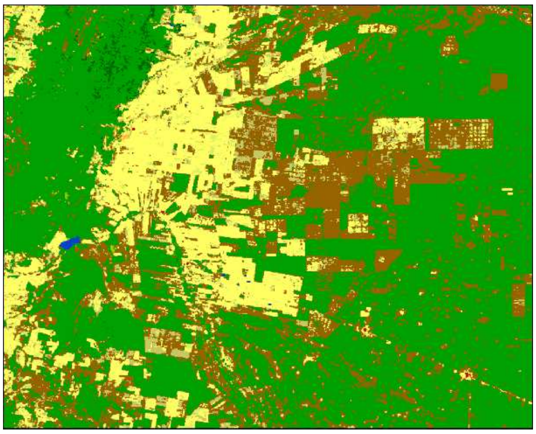

Year 2015

Figure 4-2: Illustration of a sequence of the CCI global annual land cover maps for years 1992, 2000, 2004, 2007, 2011 and 2015 for an area of the Salta Province in Argentina.

The following sections describe the legend of the CCI-LC maps and give an overview of the processing chain.

4.1.1 Legend

The typology was defined using the Land Cover Classification System (LCCS) developed by the United Nations (UN) Food and Agriculture Organization (FAO), with the view to be as much as possible compatible with the GLC2000, GlobCover 2005 and 2009 products. In addition, the UN-LCCS was found quite compatible with the Plant Functional Types (PFTs) used in climate models [Ph2_URDv1.0, 2014].

The UN-LCCS defines LC classes using a set of classifiers. The system was designed as a hierarchical classification, which allows adjusting the thematic detail of the legend to the amount of information available to describe each LC class, whilst following a standardized classification approach.

As the CCI-LC maps are designed to be globally consistent, their legend is determined by the level of information that is available and that makes sense at the scale of the entire world. The "level 1" legend – also called "global" legend – presented in Table 4-1 meets this requirement. This legend counts 22 classes and each class is associated with a ten values code (i.e. class codes of 10, 20, 30, etc.). The CCI-LC maps are also described by a more detailed legend, called "level 2" or "regional". This level 2 legend makes use of more accurate and regional information – where available – to define more LCCS classifiers and so to reach a higher level of detail in the legend. The regional classes are associated with non-ten values (i.e. class codes such as 11, 12, etc.). They are not present all over the world since they were not properly discriminated at the global scale.

Table 4-1: Level 1 (or global) legend of the CCI-LC maps, based on the UN-LCCS.

VALUE	LABEL	COLOR
0	No Data	
10	Cropland, rainfed	
20	Cropland, irrigated or post-flooding	
30	Mosaic cropland (>50%) / natural vegetation (tree, shrub, herbaceous cover) (<50%)	
40	Mosaic natural vegetation (tree, shrub, herbaceous cover) (>50%) / cropland (<50%)	
50	Tree cover, broadleaved, evergreen, closed to open (>15%)	
60	Tree cover, broadleaved, deciduous, closed to open (>15%)	
70	Tree cover, needleleaved, evergreen, closed to open (>15%)	
80	Tree cover, needleleaved, deciduous, closed to open (>15%)	
90	Tree cover, mixed leaf type (broadleaved and needleleaved)	
100	Mosaic tree and shrub (>50%) / herbaceous cover (<50%)	
110	Mosaic herbaceous cover (>50%) / tree and shrub (<50%)	
120	Shrubland	
130	Grassland	
140	Lichens and mosses	
150	Sparse vegetation (tree, shrub, herbaceous cover) (<15%)	

160	Tree cover, flooded, fresh or brakish water	
170	Tree cover, flooded, saline water	
180	Shrub or herbaceous cover, flooded, fresh/saline/brakish water	
190	Urban areas	
200	Bare areas	
210	Water bodies	
220	Permanent snow and ice	

Among these LC classes, four were largely identified thanks to external dataset: the "tree cover, flooded, saline water" (class value 170) class which is based on the global mangrove atlas (http://geodata.grid.unep.ch/results.php), the "urban areas" (class value 190) which relies both on the Global Human Settlement Layer [Pesaresi et al., 2016] and on the Global Urban Footprint [DLR, 2016], the "water bodies" (class value 210) which have been inherited from the CCI global map of open water bodies and the "permanent snow and ice" (class value 220) which comes from the Randolph Glaciers Inventory (http://www.glims.org/RGI/), to which the CCI-Glaciers project is one of the main contributors.

4.1.2 Processing chain

A key aspect of the CCI-LC maps consists in their consistency over time. As a result, the set of annual maps are not produced independently but they are derived from a unique baseline LC map which is generated thanks to the entire MERIS FR and RR archive from 2003 to 2012. Independently from this baseline, LC changes are detected at 1 km based on the AVHRR time series between 1992 to 1999, SPOT-VGT time series between 1999 and 2013 and PROBA-V data for years 2013, 2014 and 2015. When MERIS FR or PROBA-V time series are available, changes detected at 1 km are re-mapped at 300 m. The last step consists in back- and up-dating the 10-year baseline LC map to produce the 24 annual LC maps from 1992 to 2015. The logical model underlying this processing chain is illustrated in Figure 2-3.

4.2 Visual quality assessment

The following figures present the annual LC products, with a focus on the year 2015 which is the most recent one of the map series. This presentation is done, through snapshots and visual comparison with reference datasets and with the previous version of the CCI-LC map for the 2010 epoch (v1.6.1), in various regions of the world. These comparisons show the accomplished progress.

The high level of thematic detail present in the CCI-LC maps is illustrated in Figure 4-3 and Figure 4-4.

In general, good agreement between the CCI-LC map 2015 and other existing reference maps is observed, even if these reference datasets are of higher spatial resolution. This is the case with the SERVIR datasets (https://www.nasa.gov/mission_pages/servir/africa.html), as illustrated over Zambia in Figure 4-3. Good agreement is also observed with lower spatial resolution datasets, as illustrated in Figure 4-4 in Angola.

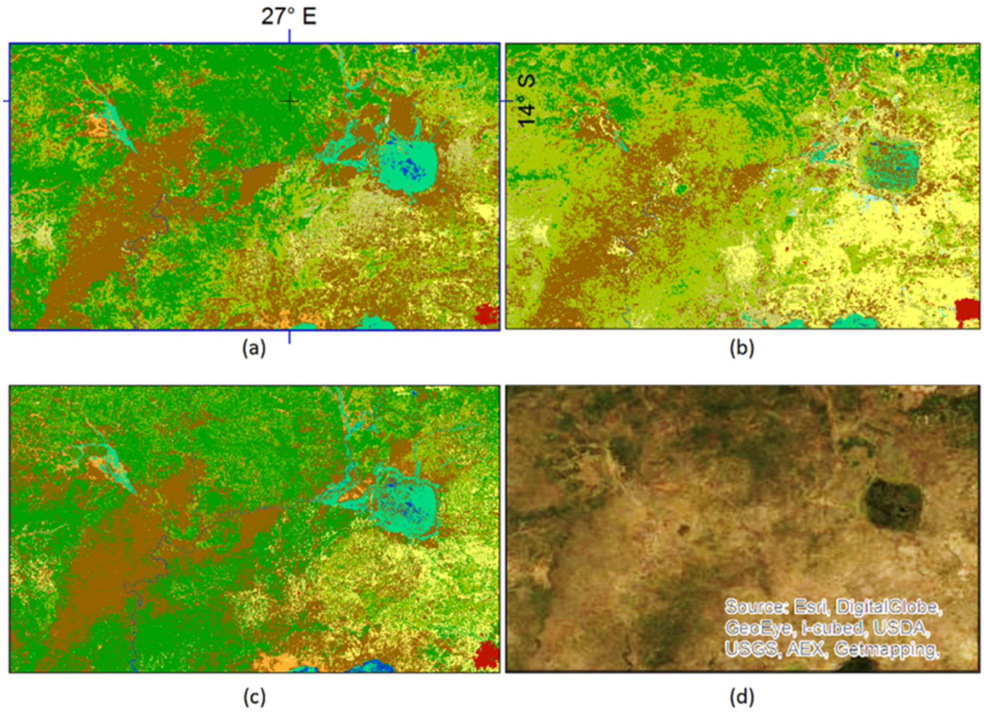

Figure 4-3: Comparison, over Zambia, between the 2015 LC map (a), the CCI-LC v1.6.1 from the 2010 epoch (b), the SERVIR land cover of Zambia (c) and the ESRI high resolution base map layer (d).

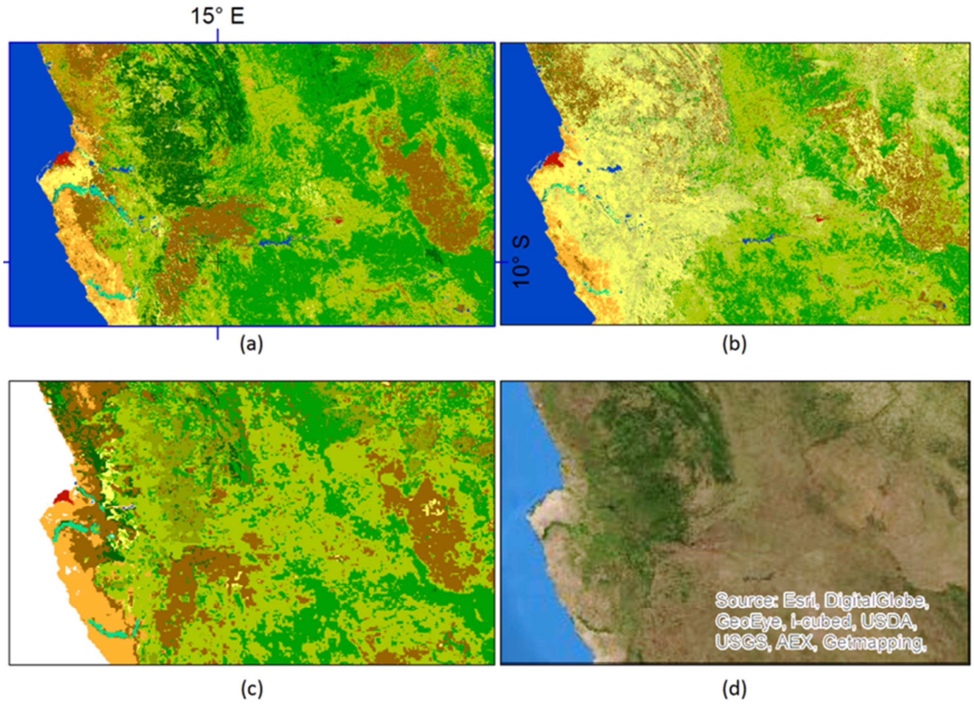

Figure 4-4: Comparison, over Angola, between the 2015 LC map (a), the CCI-LC v1.6.1 from the 2010 epoch (b), the regional GLC2000 for Africa [Bartholome and Belward, 2005] (c) and the ESRI high resolution base map layer (d).

Improvements in cropland and forest mapping with respect to the previous v1.6.1 version are illustrated in Figure 4-5 to Figure 4-8.

Figure 4-5 illustrates the better discrimination between crops (class 10 in yellow) and natural vegetation (green classes), with a clear decrease of the crop area in Democratic Republic of Congo. Figure 4-6 shows the improvement reached in the distinction between crop and grassland, through an example in South America. As for the forest mapping, the better identification and delineation of patches is shown in Figure 4-7and Figure 4-8.

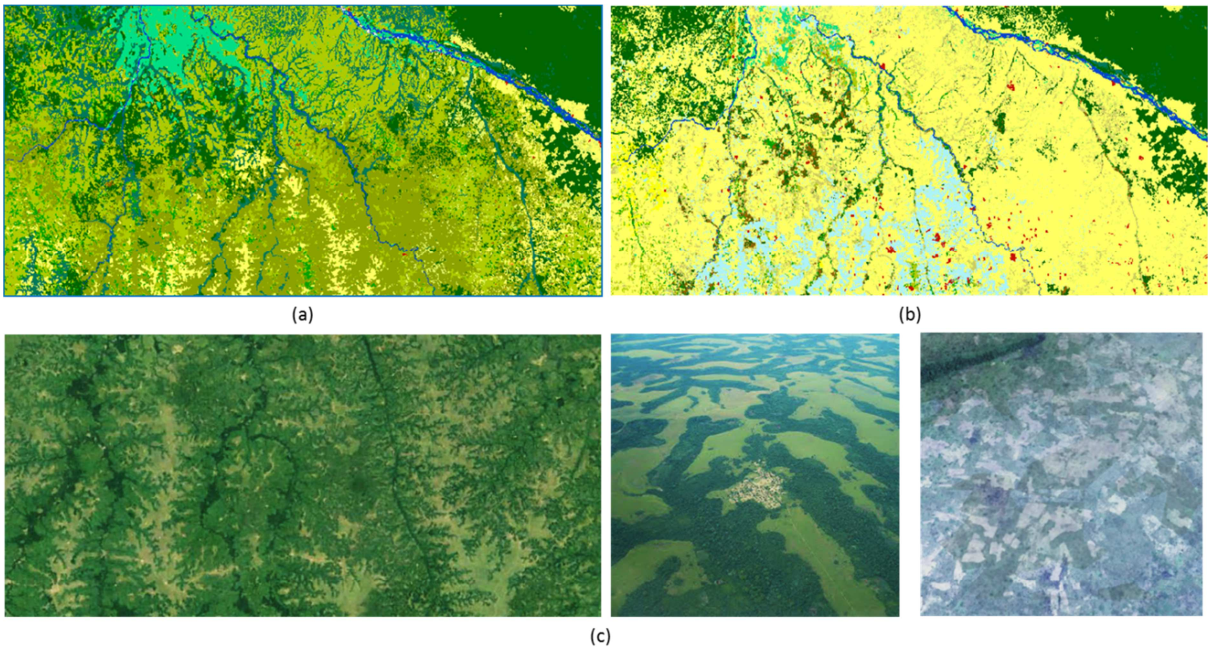

Figure 4-5: Cropland mapping in Democratic Republic of Congo. Comparison between the 2015 LC map (a), the CCI-LC v1.6.1 from the 2010 epoch (b) and ESRI high resolution base map layer (c).

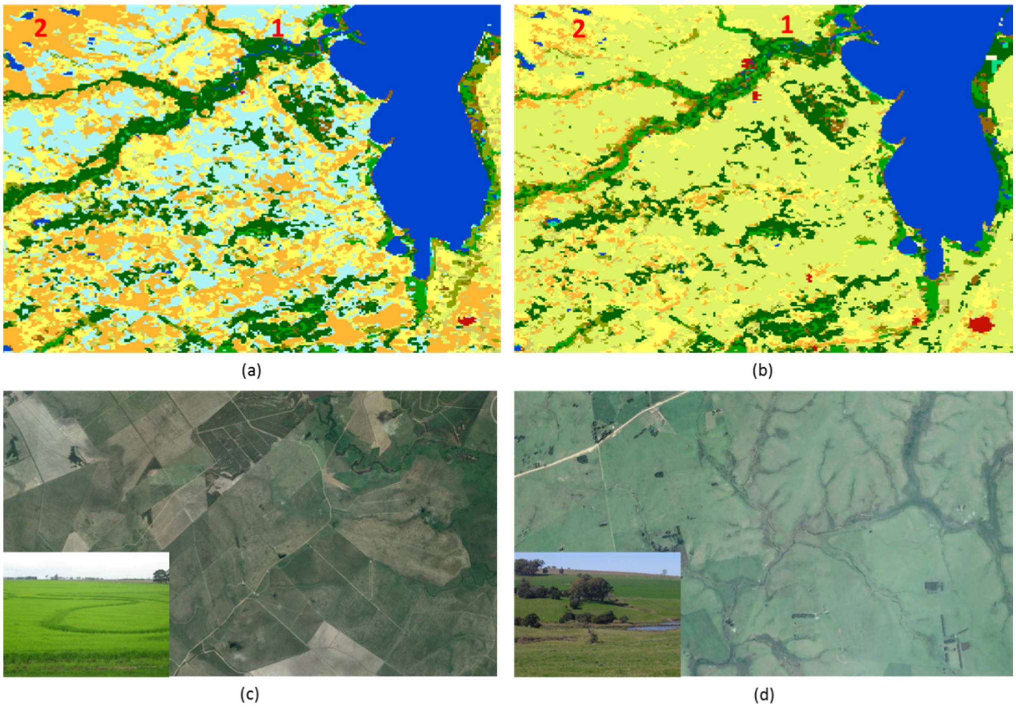

Figure 4-6: Cropland mapping in Uruguay (southeastern boundary). Comparison between the 2015 LC map (a), the CCI-LC v1.6.1 from the 2010 epoch (b) and ESRI high resolution base map layer (c-d) Zooms in (c) and (d) illustrate the areas (1) and (2), respectively shown in the images (a) and (b)

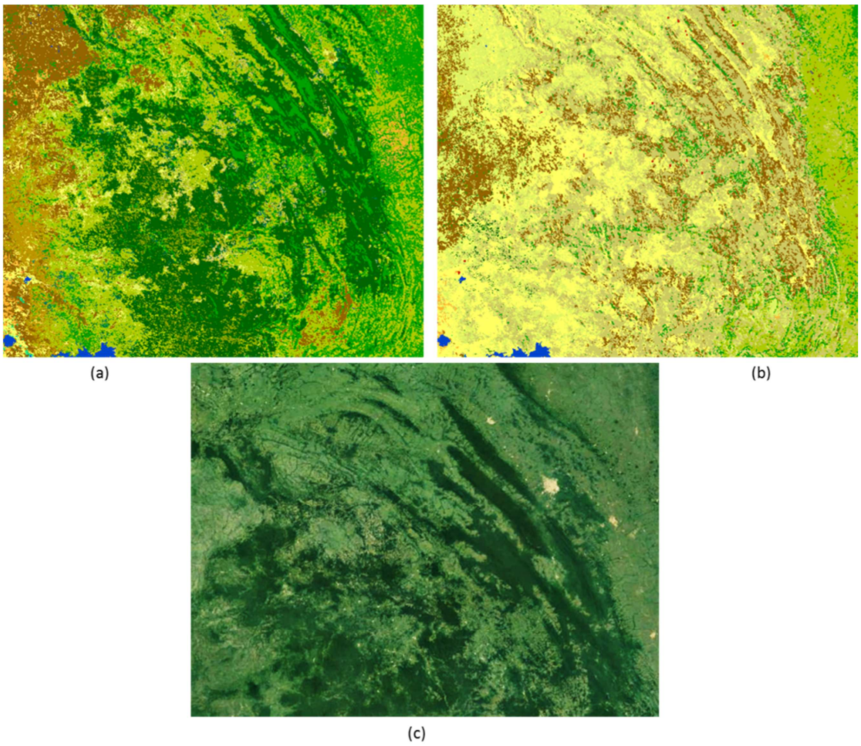

Figure 4-7: Forest mapping in North of Angola (Uige). Comparison between the 2015 LC map (a), the CCI-LC v1.6.1 from the 2010 epoch (b) and ESRI high resolution base map layer (c).

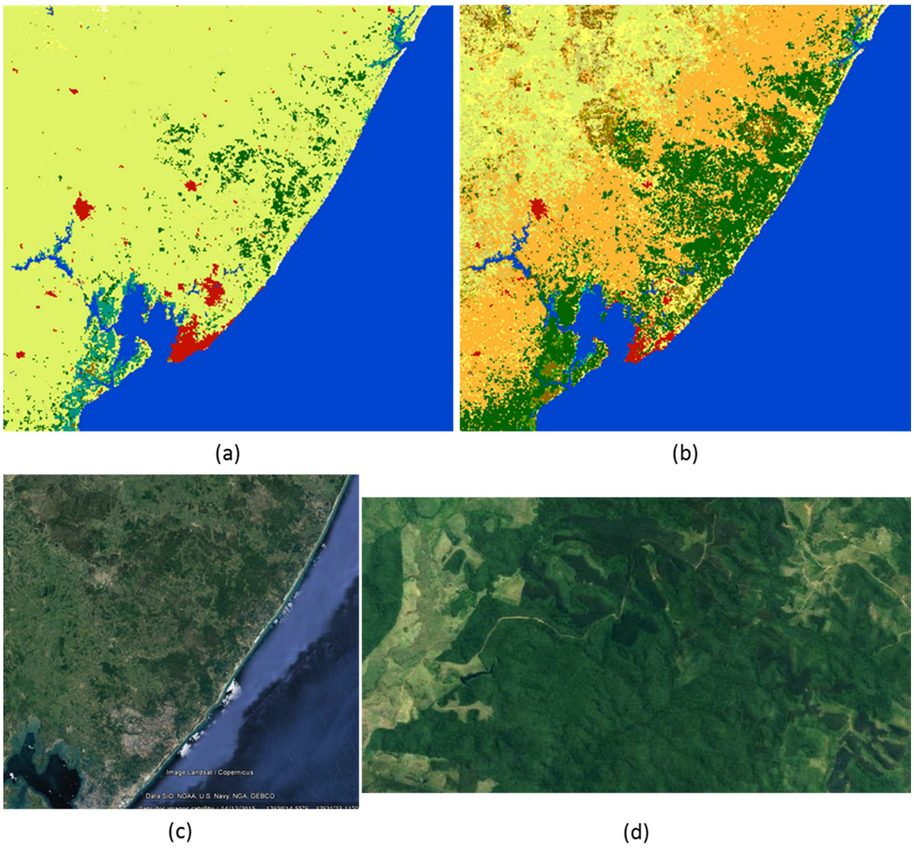

Figure 4-8: Forest mapping in Brazil (Salvador de Bahia). Comparison between the 2015 LC map (a), the CCI-LC v1.6.1 from the 2010 epoch (b) and ESRI high resolution base map layer (c-d).

Progress has also been made in the mapping of Northern regions, which were mostly labelled as "bare areas" in the previous 1.6.1 version, while vegetation was clearly present. Vegetation is now also visible in the map, through a better gradient of shrubland, grassland, sparse vegetation and bare classes, as illustrated in Figure 4-9 and Figure 4-10.

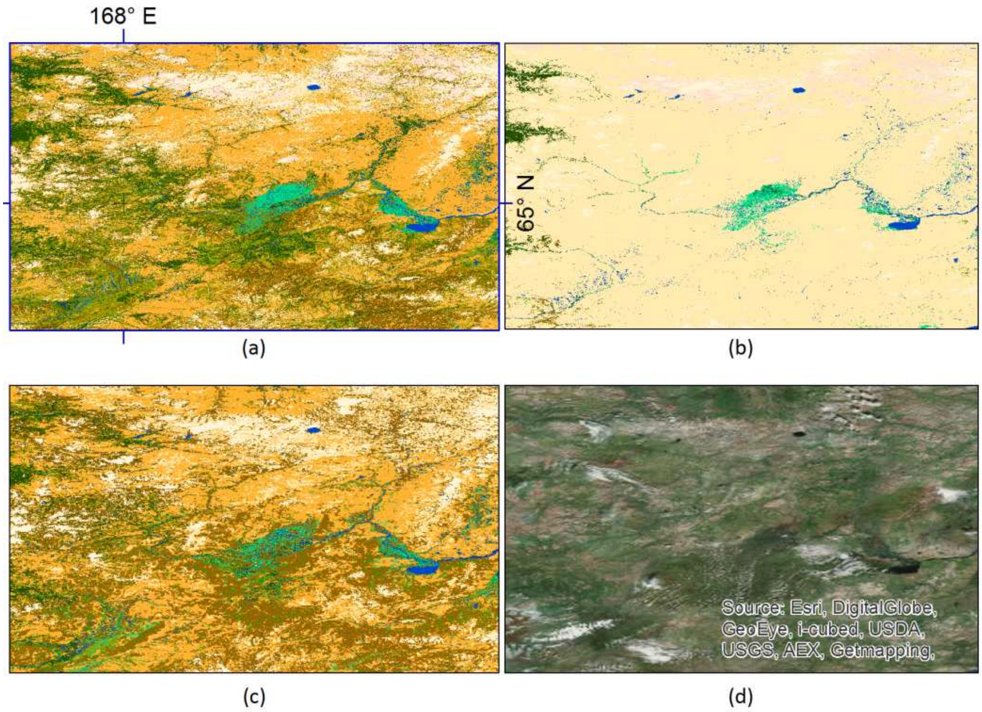

Figure 4-9: Comparison, over Russia, between the 2015 LC map (a), the CCI LC v1.6.1 from the 2010 epoch (b), the Northern Eurasia Land Cover database [Sulla-Menashe et al., 2011] (c) and the ESRI high resolution base map layer (d).

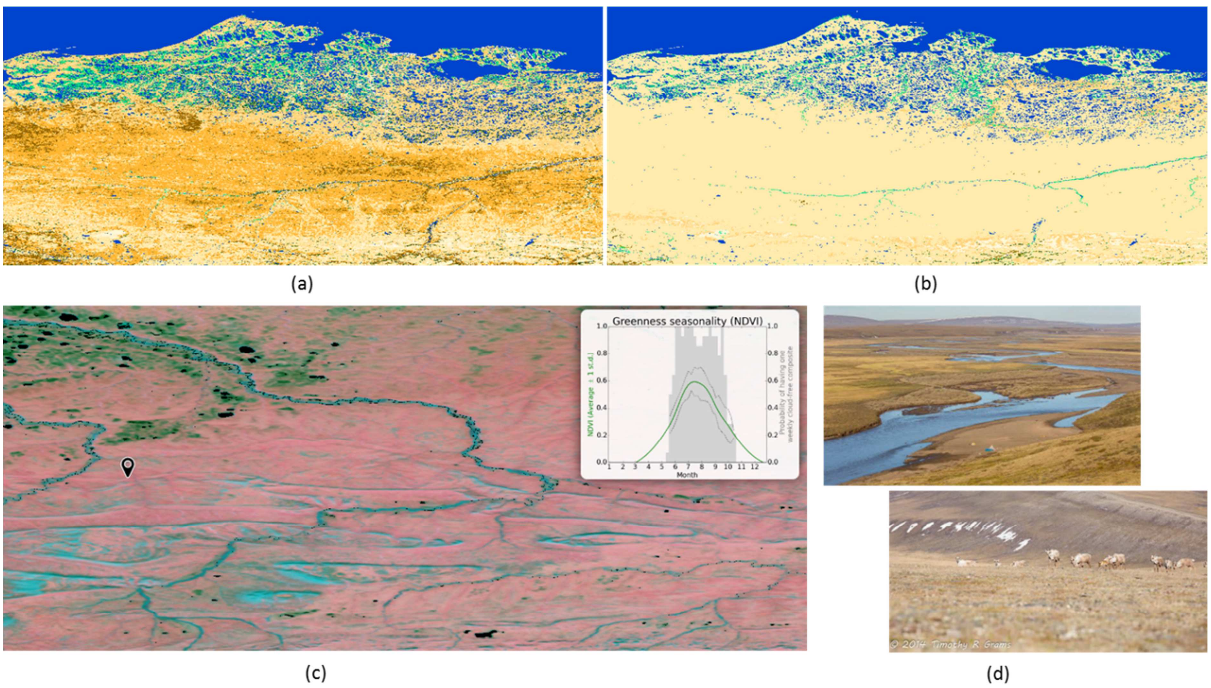

Figure 4-10: Comparison, over Canada, between the 2015 LC map (a), the CCI LC v1.6.1 from the 2010 epoch (b), the MERIS annual composite over the full archive 2004-2012, with an indicative NDVI profile of the area (c) and the ESRI high resolution base map layer (d).

Finally, Figure 4-11 to Figure 4-13 give examples of the wetland and urban mapping. On Figure 4-12, it can be noted that urban areas are better identified, with a higher density of the “red” class. On Figure 4-13, it is shown that the urban delineation has also been improved, with more realistic limits of the cities.

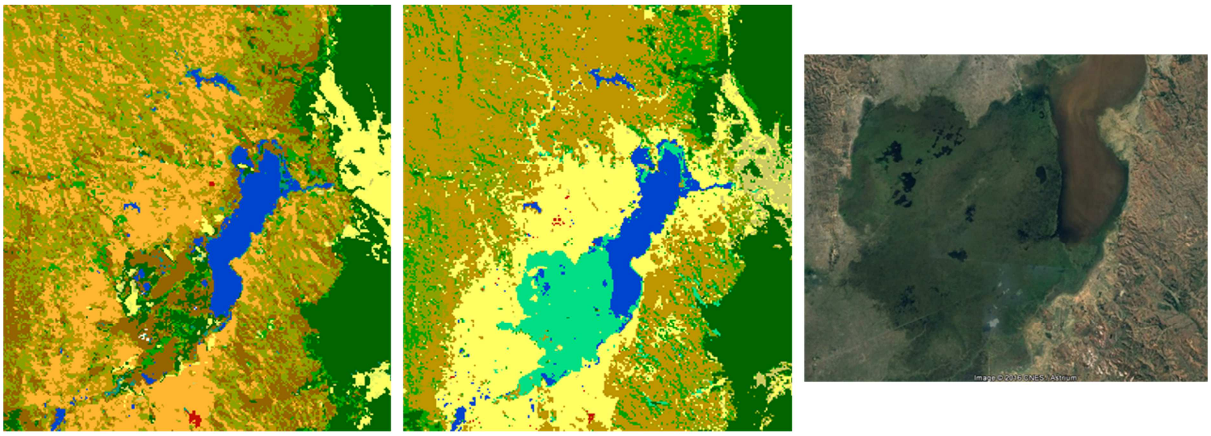

(a) (b) (c)

Figure 4-11: Wetland mapping in South Africa. Comparison between the 2015 LC map (b), the CCI-LC v1.6.1 from the 2010 epoch (a) and ESRI high resolution base map layer (c-d).

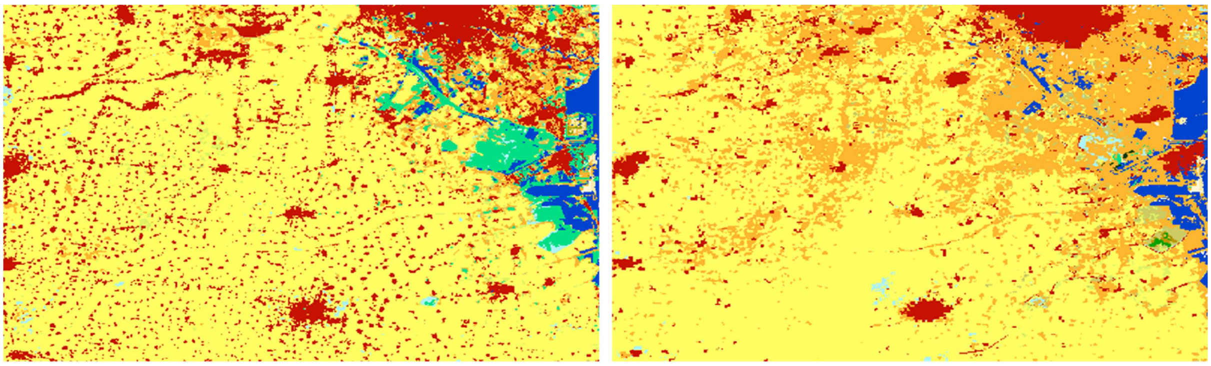

(a) (b)

Figure 4-12: Urban mapping in China, North East of Tianjin. Comparison between the 2015 LC map (a) and the CCI-LC v1.6.1 from the 2010 epoch (b).

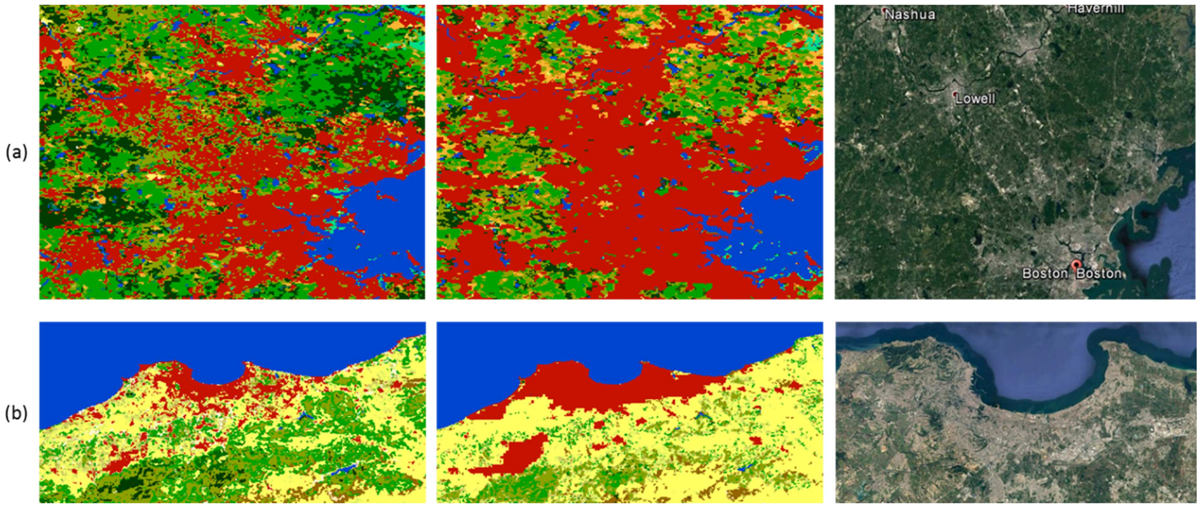

Figure 4-13: Mapping of the cities of Boston, USA (a) and Alger, Algeria (b), with the 2015 LC map (left), the CCI-LC v1.6.1 from the 2010 epoch (centre) and ESRI high resolution base map layer (right).

Figure 4-14 and Figure 4-15 illustrate the land cover dynamics of major LC changes captured in the annual CCI-LC maps from 1992 to 2015 over an area in Brazil and over the Aral Sea, respectively.

In Brazil, the evolution of the deforestation patterns is consistent with what is observed in the Landsat imagery from the Timelapse Google Earth Engine. The slight underestimation of croplands in 1992 is explained by the use of the 1-km AVHRR in the 1990s. The drying up of the Aral Sea is in agreement with recent published research [Pekel et al., 2016].

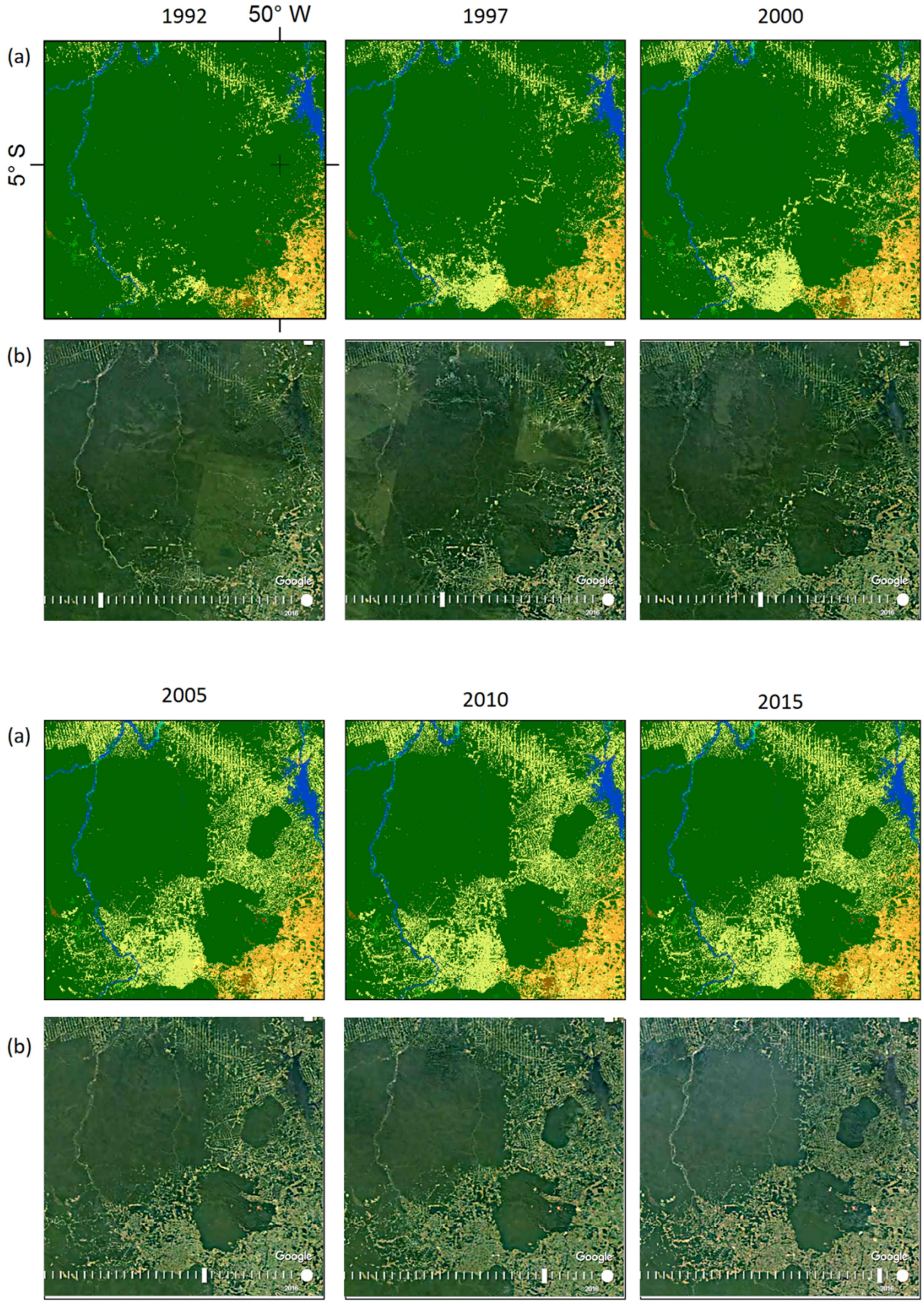

Figure 4-14: Comparison of deforestation patterns in Brazil between annual LC maps for years 1992, 1997, 2000, 2005, 2010 and 2015 (a) and the corresponding Landsat imagery from Timelapse Google Earth Engine (b).

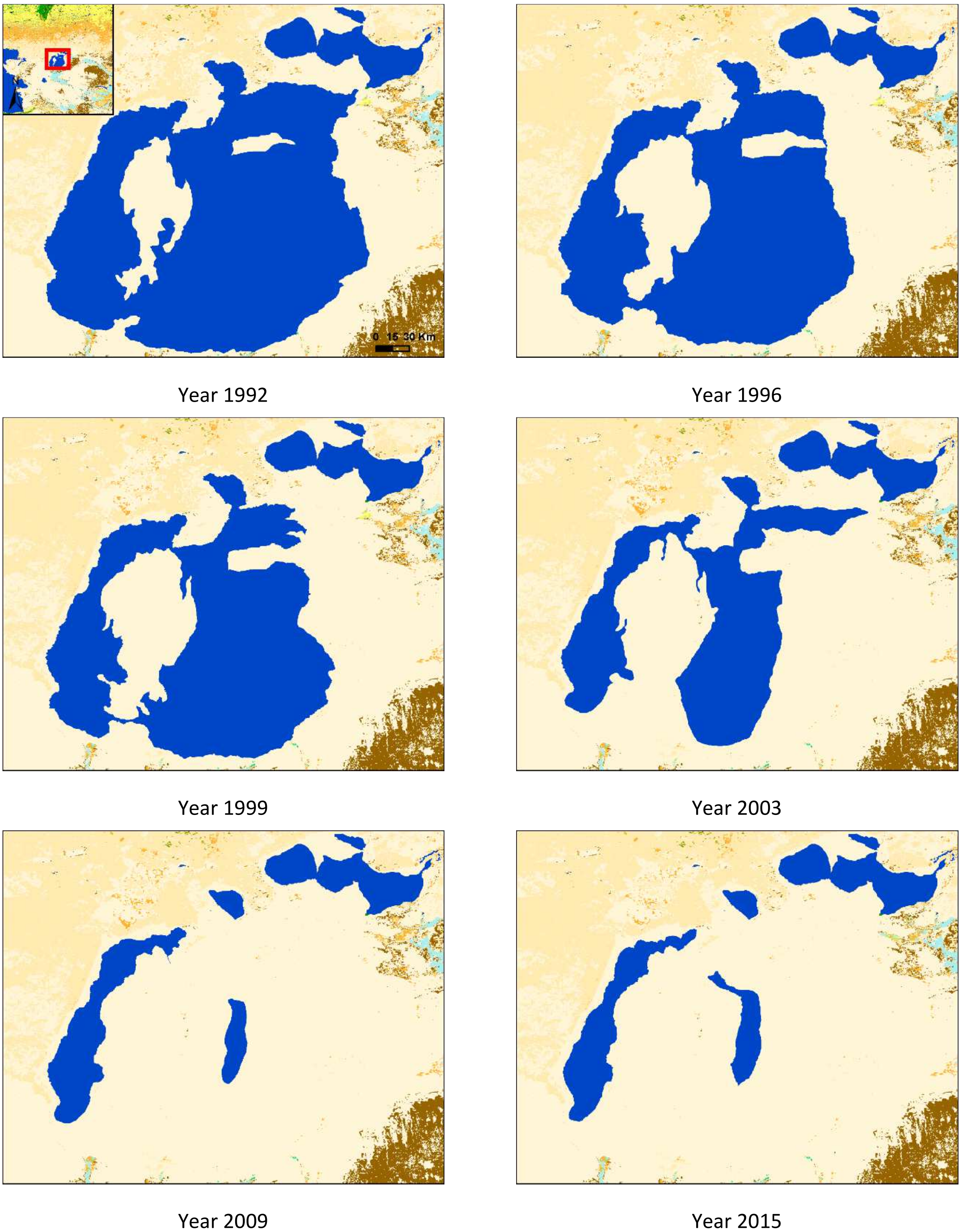

Figure 4-15: Dynamics of the Aral Sea illustrated by the CCI global annual land cover maps for years 1992, 1996, 1999, 2003, 2009 and 2015.

4.3 Accuracy assessment

A critical step in the acceptance of the CCI-LC maps by the user communities is providing confidence in their quality through validation against independent data such as ground-based reference measurements or alternate estimates from other projects and sensors.

The main objective of the validation is to allow a potential user to determine the "map's fitness for use" for his / her application. There are several definitions of validation available from various agencies, and it was agreed that the Committee on Earth Observing Satellites Working Group on Calibration and Validation (CEOS-WGCV) definition would be adopted within the CCI program, which defines validation as:

> *"The process of assessing, by independent means, the quality of the data products derived from the system outputs".*

The validation process independence has been ensured using validation datasets that were not used during the production of the LC maps.

The statistical accuracy assessment relies on several steps, as illustrated in Figure 4-16.

The three first steps have been achieved several times during the GlobCover and the CCI LC project, in order to build what is called the CCI / GlobCover validation database. The last step consists in exploiting the database to assess the maps accuracy. It shall be noted that the validation, along with the building of validation databases, is a continuous process since the understanding of the database is a continuous effort, since successive versions of the maps are generated and since maps are updated to reflect the current years.

Figure 4-16: Different components of the independent statistical validation component

This validation is presented here below. For the sake of comparison, it has been performed mainly using the GlobCover 2009 validation database, in order to validate the most recent 2015 LC map. Quantitative figures obtained with the CCI LC validation database are also provided but it shall be emphasized that comparisons with previous figures are to be avoided, especially because the concepts underlying the building of this database are totally new and its exploitation therefore also needs new methods.

4.3.1 Validation Database

The building of the CCI validation database is described in the following section. A complete description of the GlobCover validation database can be found in [Bontemps et al., 2010].

4.3.1.1 *Collection of reference data sources*

The collection of "ground truth" is considered as the best option to support the validation of remote sensing products in general and of the CCI-LC maps in particular. Normally, this is performed by carrying out field surveys. For global land cover products such as the CCI-LC maps, this approach would be too costly due to the amount of man power and logistic effort needed to organize field visits to remote areas with difficult access. However surrogate to "ground truth" can be obtained from existing "reference data sources" to be subsequently interpreted by experts. Existing reference data sources were collected; they were made of several types of datasets:

- High and very high spatial resolution imagery: Google Earth/Virtual Earth imagery + 1 Landsat TM or ETM+ image over each epoch obtained from the Global Land Survey (GLS) dataset from 2000, 2005 and 2010;
- Multi-temporal Normalized Difference Vegetation Index (NDVI) profiles derived from SPOT-VGT time series: aggregated NDVI profiles built from 10 years of SPOT-VGT daily top of canopy SR syntheses (S1 products) + yearly NDVI profiles for the years 2000/2005/2010.
- Google Earth facilities.

4.3.1.2 *Sampling design*

The sampling scheme was designed with the following requirements:

- to be statistically valid for accuracy assessment of the CCI-LC products;
- to be reusable for future global products of similar type;
- to be designed before (i.e. independently) the CCI-LC product;
- to use the most recent picture of global land cover distribution (as best proxy of the actual land-cover distribution);
- to address the issue of rare classes with a strong impact on the climate system (urban areas, wetlands, etc).

The sampling used in the CCI-LC project relied on the systematic sampling of the TREES dataset combined with a two-stage stratified clustered sampling, since it is generally recognized as the most efficient sampling strategy [Strahler et al., 2006]. This stratified random sampling allowed selecting the ***Primary Sampling Units*** (PSUs).

To generate an accuracy measurement with a precision of 0.03, it was determined that around 900 sample plots would be needed for validating the global CCI-LC product [Ph1_PVPv1.3, 2011].

However, in order to be consistent with the previous exercises, 2600 PSUs were selected (Figure 4-17).

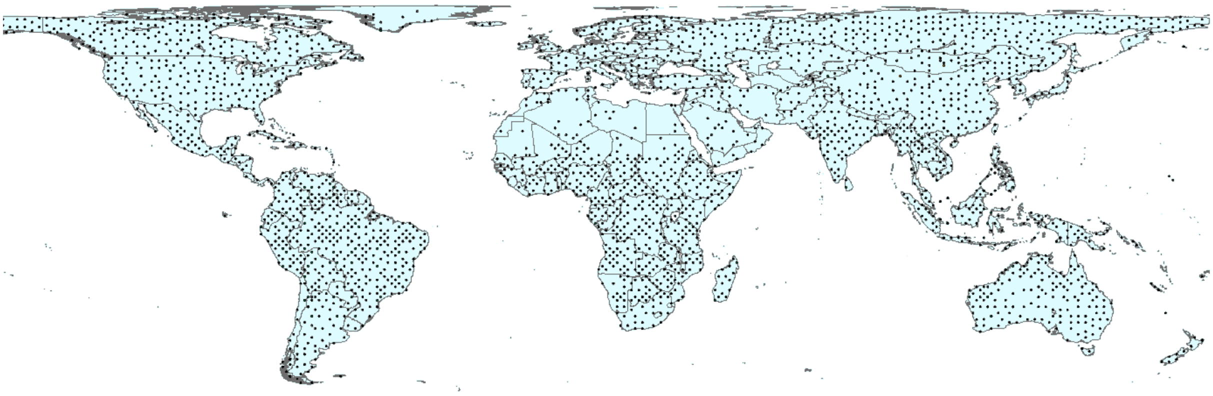

Figure 4-17: Selected sample frame displaying the 2600 PSUs

A 20-km × 20-km box was defined around each PSU and Secondary Sampling Units (SSUs), which correspond to the actual "sample plots", were then selected by systematically distributing them within these boxes. 5 SSUs were located at the center of each 20-km × 20-km box and at a distance of 4-km × 4-km from the center of each box (Figure 4-18).

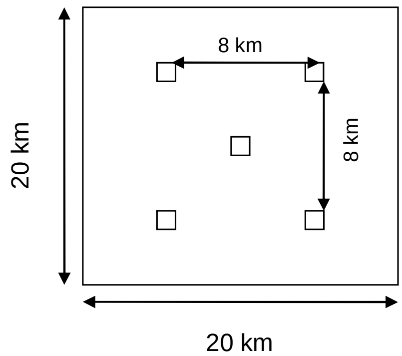

Figure 4-18: Selection of SSUs within a PSU

This nested sampling approach (i.e. the multiplication of the number of sample sites compared with the option of using only one single sample plot per box) provides a larger number of sample sites and therefore leads to lower standard error of accuracy estimates.

The elementary unit in the CCI-LC product is a 300m spatial resolution pixel. However, the same unit placed over higher spatial resolution imagery may represent something quite different. It is thus necessary to distinguish the Minimum Mapping Unit (MMU), which is a cartographic term, and the observational unit, which will correspond to the size of the sample plot. The CCI-LC products' MMU is the 300m spatial resolution pixel (i.e. 9 hectares). Due to the fact that single pixels will often cover several land cover types, the observational unit is larger than the MMU and thus gives more weight to the neighborhood of the pixel. The main reason for assigning more weight to the neighborhood of the pixel is that it is not realistic for an expert to interpret land cover class of single MERIS-size pixels. The expert needs sufficient information (pixels in this case) to decide which land cover type is the dominant one. It was decided to define the observation unit as a window of 3 × 3 pixels at 300-m × 300-m spatial resolution (i.e. 81 hectares).

4.3.1.3 *Independent interpretation*

The reference data sources are then intended to be interpreted over each sample (SSU) through an international network of experts in a standardized manner.

Selecting appropriate experts is a key element of the validation process. The selection / involvement of experts were based on the following criteria:

- Recognized expertise on land cover over large areas;
- Familiarity with interpretation of remote sensing imagery;
- Commitment to perform the interpretation;
- Complementarities with the other experts.

The experts' network involved in this project is presented in Table 4-2.

Table 4-2: Name and affiliation of the international land cover experts involved in the CCI-LC project

REGION	EXPERTS	INSTITUTION
Africa	TREBOSSEN Hervé	Independent international consultant
	NONGUIERMA André	Centre Agrhymet – Niger / Economic Commission of Africa
Europe	COLDITZ René	Comision Nacional para el Conocimiento y Uso de la Biodiversidad (CONABIO) – Mexico
	SANNIER Christophe CONRAD Roland	Systèmes d'Information à Référence Spatiale (SIRS) – France
Russia	BARTALEV Slava	Institute for Environment and Sustainability – Joint Research Centre
	KRANKINA Olga	Oregon State University
Asia	HEINIMANN Andreas	National Centre of Competence in Research North-South Centre for Development and Environment (CDE)
	KUANG Wenhui	Institute of Geographical Sciences and Natural Resources Research – Chinese Academy of Sciences
	MIETTINEN Juka	Institute for Environment and Sustainability – Joint Research Centre
	RASI Ratislav	Institute for Environment and Sustainability – Joint Research Centre
	STIBIG Hans-Jürgen	Institute for Environment and Sustainability – Joint Research Centre
	TSENDBAZAR Nandika	Wageningen University – Netherlands
North and	COLDITZ René	Comision Nacional para el Conocimiento y Uso de la Biodiversidad (CONABIO) – Mexico

Central America	GIRI Chandra	United States Geological Servey – EROS Data Center
	LATIFOVIC Rasim	Canada Centre for Remote Sensing – Ottawa – Canada
South America	DI BELLA Carlos	Instituto Nacional de Tecnología Agropecuaria – Argentina
	GOND Valéry	CIRAD-Guyane – Université Laval
	SHIMABUKUO Yosio	INPE
Australia	CACETTA Peter	Commonwealth Scientific and Industrial Research Organisation – Australia

Experience from previous projects (notably the GLC2000 and GlobCover projects) has shown that the most efficient way to obtain commitment – and hence, the required information from these experts – is to invite the experts to visit the premises of one of the CCI-LC team members in Europe. This approach overcomes misunderstanding in the needs of the CCI-LC project, in particular the ambiguity in the interpretation of findings.

A total of 4 workshops of one week was organised at UCL premises in Louvain-la-Neuve (Belgium) and 1 workshop was held at JRC premises. All necessary datasets and infrastructure (hardware / software) was put at the disposal of the experts in order to comply with the requirements of the project.

Three experts (already involved in previous GLC2000 and/or GlobCover 2005-2009 experiences) performed the interpretation in remote, working at their own premises with an on-line support from UCL for any question.

The experts were asked to interpret each SSU over the three epochs through a sequential procedure. First, they were invited to interpret the 2010 epoch, based on very high spatial resolution data available from Google Satellite/Virtual Earth. The interpretation was helped through the application of an a priori segmentation and a land cover class had to be assigned to each object. Second, the change in LC between epochs was determined at the SSU scale, using the 3 Landsat TM or ETM+ images obtained from the 2000, 2005 and 2010 GLS datasets. For each diagnostic (2010 interpretation and LC change between epochs), the experts had to provide their level of confidence.

A new validation tool was developed for hosting this interpretation process, based on the experience gained during the previous validation exercises of the GLC2000 and GlobCover projects. The validation tool provides an online interface available to the expert on reception of the URL. Figure 4-19 presents this interface, highlighting different functionalities.

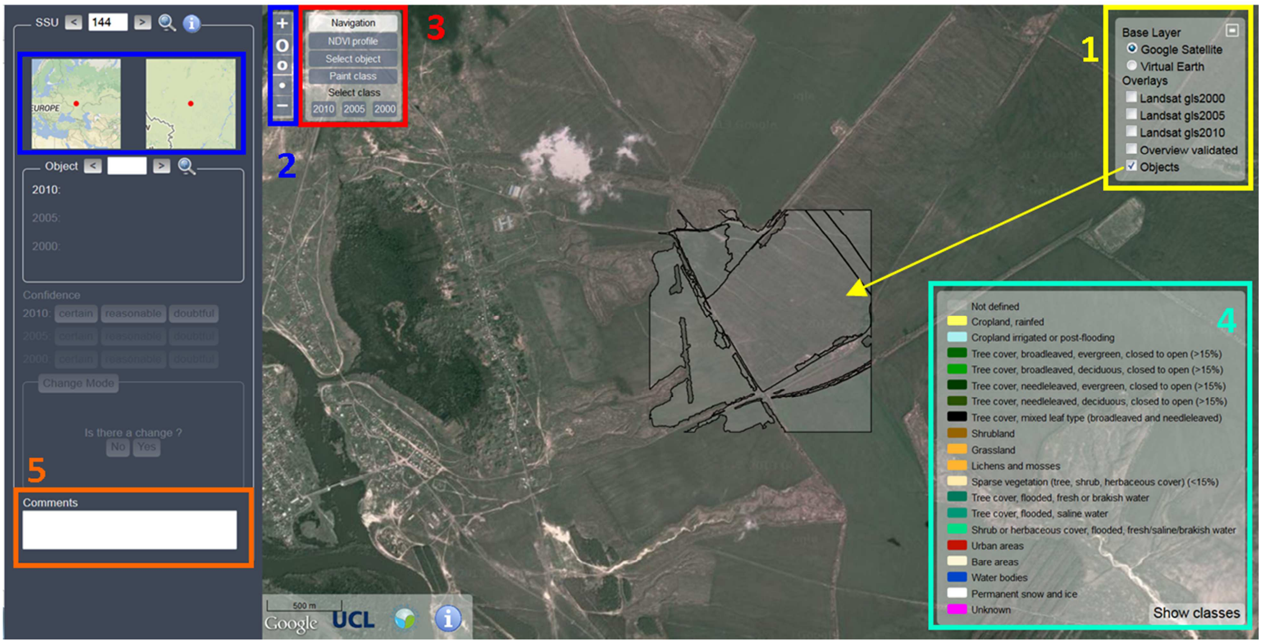

Figure 4-19: Main page of the validation tool, with the following functionalities: 1) Layer box to display different layouts; 2) Zooming functionalities; 3) Tools box to activate navigation, display NDVI profile, select objects or assign a LC class; 4) Legend description; 5) Comments box to include free text that should help understanding the labelling choices

Figure 4-20 and Figure 4-21 illustrate the interfaces developed for the two main steps of the interpretation process: the 2010 epoch interpretation based on very high spatial resolution data available from Google Satellite/Virtual Earth and the LC change evaluation using the 3 Landsat TM or ETM+ images obtained from the GLS datasets.

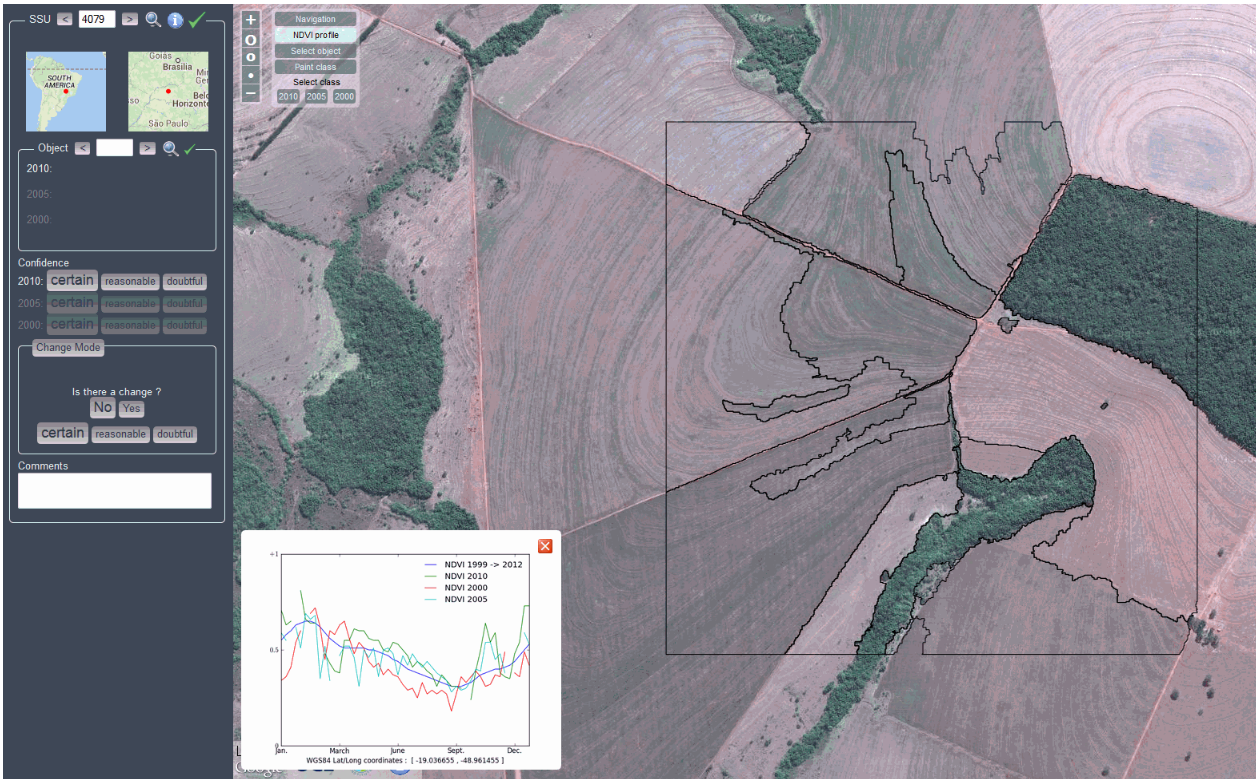

Figure 4-20: Example of segmented SSU over Brazil to be interpreted for the 2010 epoch

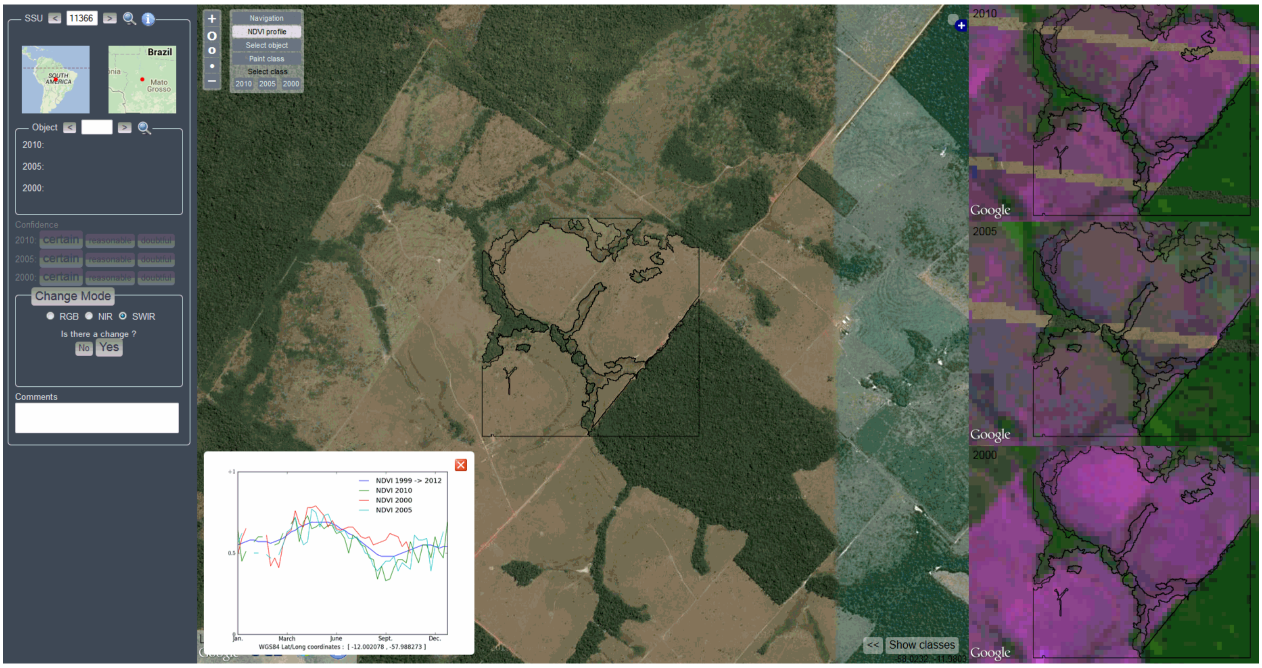

Figure 4-21: Example of segmented SSU over Brazil to be interpreted for the 2000-2005-2010 epochs (the right panel providing the 3 Landsat images associated with the 3 epochs)

4.3.2 Validation dataset

4.3.2.1 *GlobCover 2009 validation dataset*

The GlobCover 2009 validation sample was based on the GlobCover 2005 sampling and adjusted in order to (i) ensure a better representation of each continent and of each land cover class and (ii) ensure minimum 30 point per class. According to these criteria, the final sampling (Figure 4-22) counted 4164 points, of which 2036 belonged to the 2005 sampling and 2128 were new.

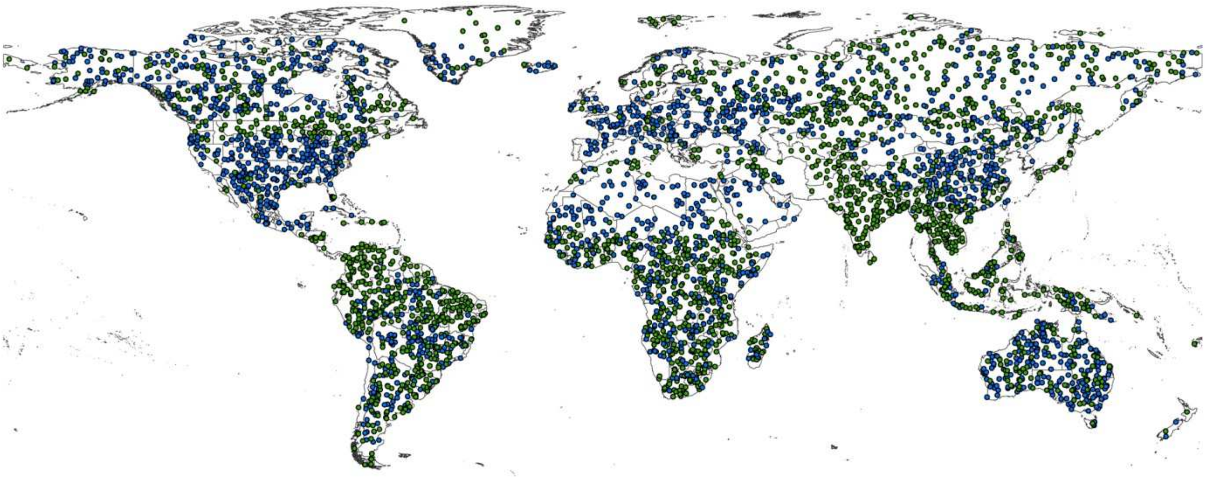

Figure 4-22: Distribution of the points sample used for the validation of the GlobCover 2009 land cover map. Blue points are the ones derived from the 2005 database and green points are the new ones.

The set of classifiers and attributes that were selected by the experts in order to characterise the land cover of a particular site was transformed to the CCI-LC legend. The same translation rules than the ones defined for the GlobCover products [GlobCover - PVR, 2008] were followed, with some adaptations to account for the small differences existing between the GlobCover and CCI-LC legends. Like for the GlobCover validation exercise, the translation was rather straightforward in most of the cases. Yet, there were some sources of confusion that prevented from an easy translation between the experts classifiers and the CCI-LC land cover class.

A first source of confusion comes from the way the forests have been interpreted by the experts. The classifiers proposed to the experts to characterize the forests are presented in Table 4-3.

Table 4-3: Set of classifiers available to characterize the validation points corresponding to a forest

Dichotomous category	Life form of the main strata	Leaf type	Leaf phenology	Cover
A12 - Natural & semi-natural terrestrial vegetation	A3 - Trees	D1 - Broadleaved	E1 - Evergreen	A11 - Open (70-60 - 20-10%)
		D2 - Needleleaved	E2 - Deciduous	A12 - Open (70-60 - 40%)
			E4 - Semi-deciduous	A13 - Open (40-20 - 10%)
				A14 - Sparse (20-10 - 1%)

				A20 - Closed to open (100 - 15%)
				A21 - Closed to open (100 - 40%)

The experts often did not provide the information (typically the leaf type and the leaf phenology) that allowed us to assign the points to a specific forest type. In order to avoid removing many "forest points" from the validation datasets, they were assigned to the class of "mixed forest". In the contingency matrix, the "mixed forest" class will be considered in possible agreement with all "pure" forest classes from the CCI-LC product (classes 50 to 90). This generalization was also applied in the GlobCover validation procedure [GlobCover - PVR, 2008].

A second source of confusion is related to the need to discriminate between "Irrigated or post-flooding" and "Rainfed" agriculture in the Cultivated and Managed land category. Indeed, depending on the date of the high spatial resolution images which are available for the validation, this distinction can prove to be very difficult. As a result, possible agreement between the two corresponding land cover classes (10 - Rainfed cropland & 20 - Irrigated and post-flooding cropland) was decided [GlobCover - PVR, 2008].

A third source of confusion comes from the fact that the experts could characterize each validation point with up to 3 land cover classes. In these cases, it was often difficult to interpret unambiguously all the information provided by the experts. These points were assigned to up to 2 "pure classes" (corresponding to the 2 first classes mentioned by the expert) and when possible, up to 2 "mosaic classes". The comparison between the CCI-LC map and the validation dataset accounted for all these possibilities.

In parallel of the interpretation of the mosaic classes in the validation dataset, the interpretation of the mixed classes of the CCI-LC products constitutes a third source of confusion. Indeed, these mixed classes cover a wide range of land cover types:

- classes 30 & 40: mixed classes of agriculture and natural vegetation;
- classes 100 & 110: mixed classes of natural vegetation.

In the assessment of these units with the validation dataset, an agreement between the product and the validation dataset is accepted when the validation dataset gives a class that falls within the range of land cover types included in the mosaic class and complies with the dominance criteria given in the class definition. This is the procedure that was applied for the GlobCover validation [GlobCover - PVR, 2008].

Finally, in some cases, the information provided by the experts was limited and not specific enough to convert the classifiers into land cover classes. Especially in the case of the Natural and Semi-natural terrestrial vegetation, it was essential to have a minimum number of classifiers. But, if the expert just specified "Trees", "Woody vegetation" or "Shrubs", the practical use of the point was almost absent. In the same vein, in the case of the Cultivated and Managed Lands, it was not possible to derive a land cover class if the expert did not specify the irrigation practice ("Rainfed", "Irrigated" or "Post-flooding"). As a result, the classifiers could not be interpreted to any land cover class at all.

Considering these sources of confusions, new possibilities of agreement between the product and the validation dataset (which are different from the diagonal cells) were foreseen. They are summarized in Table 4-4.

Table 4-4: Cells of the contingency matrix that are not diagonal cells but that show agreement between the two datasets, and that are thus taken into account in the overall accuracy calculation

PRODUCT CLASS	IN AGREEMENT WITH	VALIDATION CLASS
10 - Rainfed croplands	↔	20 - Post-flooding or irrigated croplands
20 - Post-flooding or irrigated croplands	↔	10 - Rainfed croplands
30 - Mosaic cropland (>50%) / natural vegetation (tree, shrub, herbaceous cover) (<50%)	↔	10 - Rainfed croplands 20 - Post-flooding or irrigated croplands 30 - Mosaic cropland (>50%) / natural vegetation (tree, shrub, herbaceous cover) (<50%)
40 - Mosaic natural vegetation (tree, shrub, herbaceous cover) (>50%) / cropland (<50%)	↔	40 - Mosaic natural vegetation (tree, shrub, herbaceous cover) (>50%) / cropland (<50%) evergreen and/or semi-deciduous forest (>5m) 50 - Tree cover, broadleaved, evergreen, closed to open (>15%) 60 - Tree cover, broadleaved, deciduous, closed to open (>15%) 70 - Tree cover, needleleaved, evergreen, closed to open (>15%) 80 - Tree cover, needleleaved, deciduous, closed to open (>15%) 90 - Tree cover, mixed leaf type (broadleaved and needleleaved) 120 - Shrubland 130 - Grassland
100 - Mosaic tree and shrub (>50%) / herbaceous cover (<50%)	↔	50 - Tree cover, broadleaved, evergreen, closed to open (>15%) 60 - Tree cover, broadleaved, deciduous, closed to open (>15%) 70 - Tree cover, needleleaved, evergreen, closed to open (>15%) 80 - Tree cover, needleleaved, deciduous, closed to open (>15%) 90 - Tree cover, mixed leaf type (broadleaved and needleleaved) 120 - Shrublan
110 - Mosaic herbaceous cover (>50%) / tree and shrub (<50%)	↔	130 - Grassland
50 - Tree cover, broadleaved, evergreen, closed to open (>15%)	↔	90 - Tree cover, mixed leaf type (broadleaved and needleleaved)

60 - Tree cover, broadleaved, deciduous, closed to open (>15%) 70 - Tree cover, needleleaved, evergreen, closed to open (>15%) 80 - Tree cover, needleleaved, deciduous, closed to open (>15%) 90 - Tree cover, mixed leaf type (broadleaved and needleleaved)		

In the matrix representation, diagonal cells will be coloured in green while cells which don't belong to this diagonal while marking an agreement between the two datasets (see Table 4-4) will be coloured in yellow.

4.3.2.2 *CCI LC validation dataset*

At the end of the selection of the SSUs, the sample was made of 13.000 units. However, due to time constraints related to the interpretation of each date, not all SSUs were interpreted. At a minimum, the SSU corresponding to the centre was selected and possibly, one or two other SSUs of the PSU were also proposed to the experts. In average, 2.4 SSU were interpreted by PSU.

In total, 1450 PSUs were proposed to the experts and 1352 were interpreted, which corresponds to 90%. In terms of SSUs, 2746 SSUs were interpreted by the experts out of the 3433 which were proposed to them (i.e. 80%). Figure 4-23 illustrates this figure. It also shows that there is no point over South America. 158 SSU, belonging to 86 PSU were interpreted in this region and are part of the database but at the time of writing this report, we face an issue reading these interpretations. It will be solved in the near future.

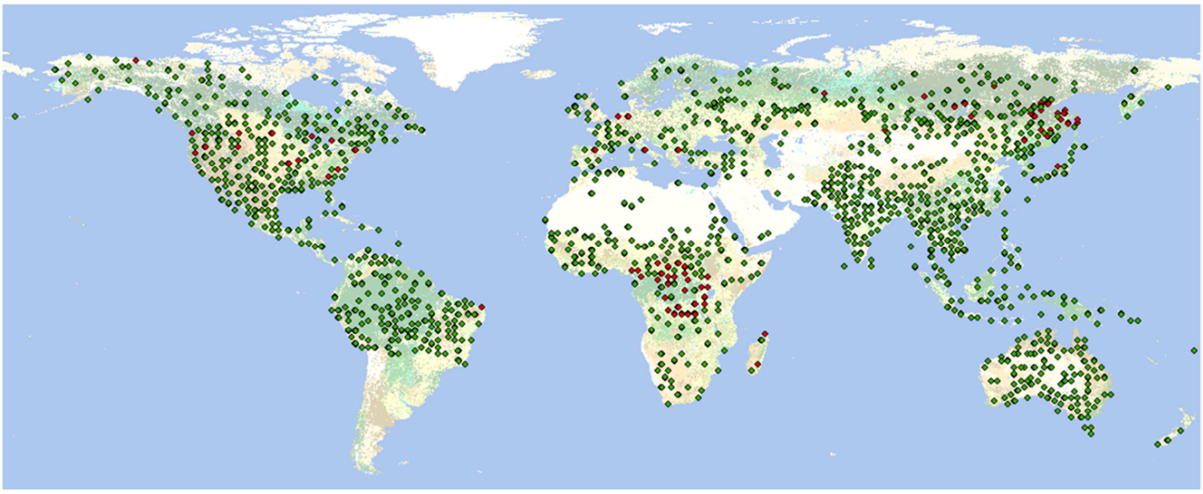

Figure 4-23: Spatial distribution of the samples included in the CCI-LC validation database, where points in red represent PSUs interpreted by the experts while those in red are the ones that were proposed but not interpreted due to time constraints

For each SSUs, the database contains the following information (Table 4-5). Information in bold correspond to information given by the expert during the interpretation process.

Table 4-5: Information included in the validation database for each SSU

FIELD NAME	DETAILS
FOR EACH SSU	
SSU ID	Unique identifier
PSU ID	Identifier of the associated PSU
Lat / Long	Coordinates of the 3*3 MERIS pixels corresponding to the observational unit to interpret
Level of certainty	**Level of certainty (certain, reasonable, doubtful) associated with the interpretation of the expert for the 3 epochs (2000, 2005, 2010)**
Land cover change	**Presence / absence of LC change between epochs within the SSU**
Comments	**Comments given by the expert to explain / detail its interpretation**
FOR EACH OBJECT IN THE SSU, FOR THE 2000, 2005 AND 2010 EPOCHS	
Objet IC	Unique identifier
SSU ID	Identifier of the associated SSU
PSU ID	Identifier of the associated PSU
Object geometry	Area and perimeter
Land cover class	**Class ID of the CCI-LC legend (Table 4-1) associated to each object, for each epoch**

When looking at the level of certainty indicated by the experts, 65% of SSUs have been interpreted as certain, 31% as reasonable and 4% as doubtful. The SSUs associated with a doubtful interpretation were removed from the database.

Figure 4-24 shows how certain, reasonable and doubtful samples are spatially distributed. This illustration allows pointing areas that are more difficult to interpret. But it also shows that this exercise asked to the expert to evaluate their certainty is highly subjective and that each of them had a personal interpretation of what is a certain, reasonable and doubtful diagnostic.

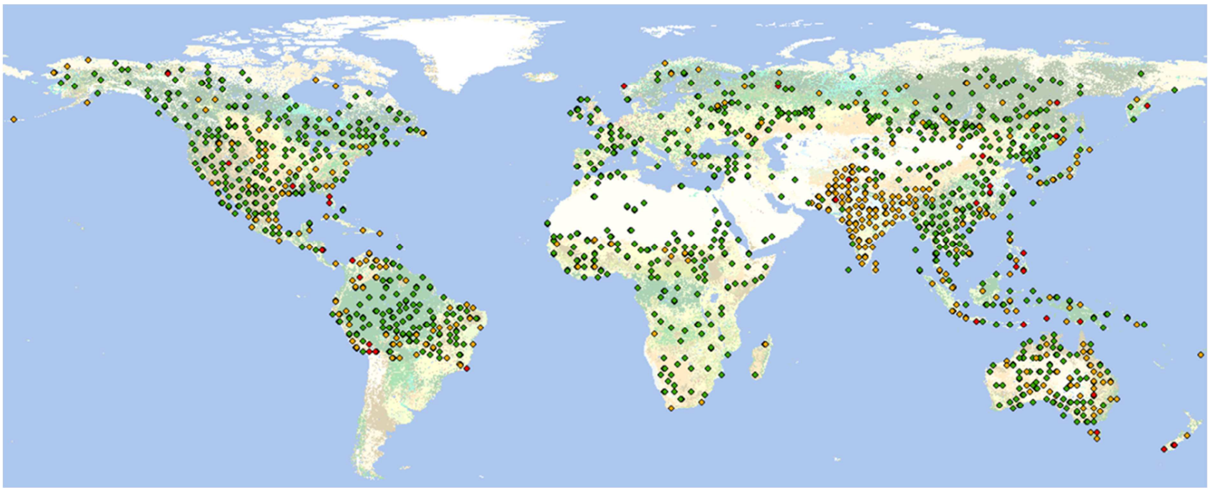

Figure 4-24: Samples included in the CCI-LC validation database associated with the level of certainty of their interpretation (green = certain, orange = reasonable, red = doubtful)

As for the land cover change, 8% of the SSUs were concerned by at least one change between the three epochs (Figure 4-25). These land cover changes are mainly located in Central and South America, Europe and Amazon, then in China, Central and South Asia (Figure 4-26).

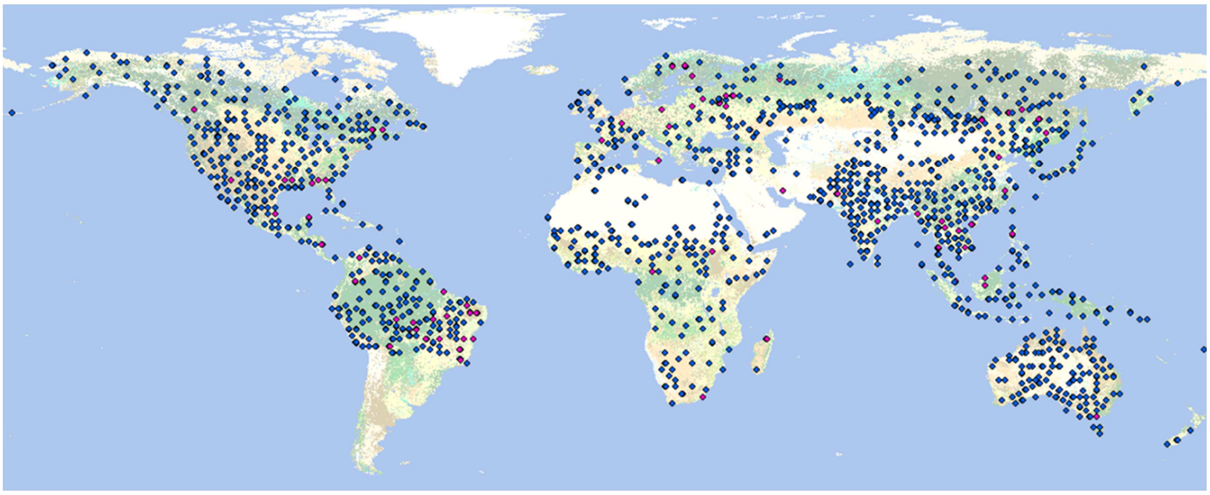

Figure 4-25: Presence of land cover change within the samples included in the CCI-LC validation database (blue = no change, pink = change)

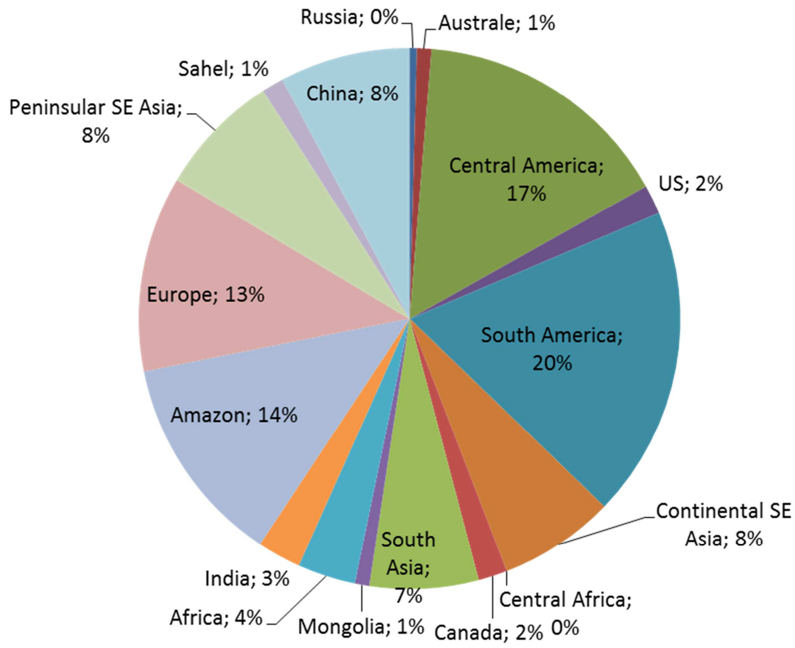

Figure 4-26: Spatial distribution of land cover changes identified in the CCI-LC validation database (8% of the SSUs)

With regard of the homogeneity of the SSUs, it was evaluated by looking at the number of polygons by SSUs (Figure 4-27) and at the number of LC classes by SSUs (Figure 4-28). Figure 4-27 shows that 80% of the SSUs are covered by less than 35 polygons, which is a reasonable amount for the interpretation. Conversely, it might be suspected that SSUs covered by more than 50 objects (less than 5%) will be interpreted with more difficulty or precision.

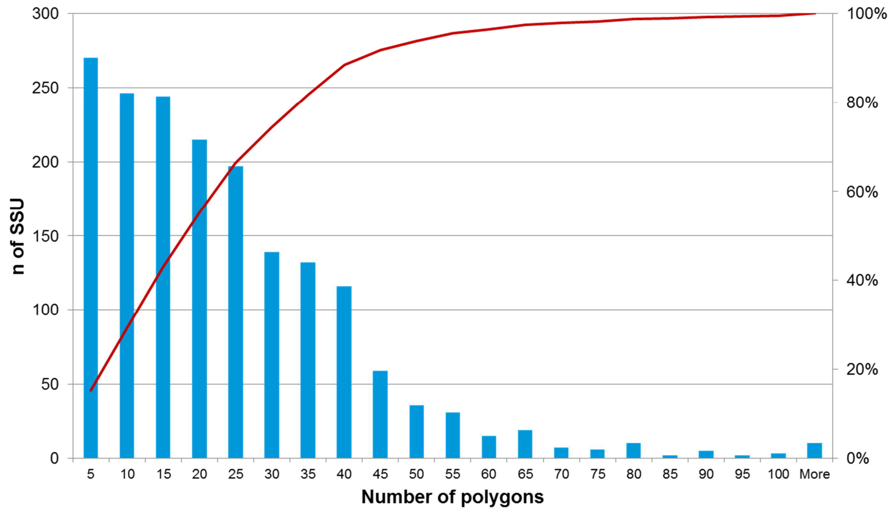

Figure 4-27: Distribution of the number of objects by SSUs

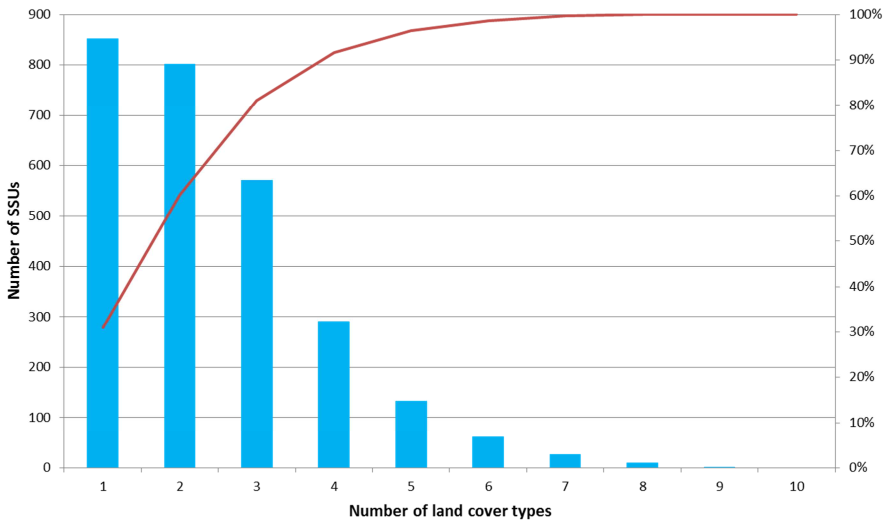

Figure 4-28: Distribution of the number of land cover classes by SSUs

In average, the SSUs were covered by 2.3 land cover classes, with a minimum of 1 and a maximum of 9 land cover classes. 31% of the SSUs are fully homogeneous, i.e. covered by a single land cover class. Then, 29%, 21% and 11% of the SSUs are respectively covered by 2, 3 and 4 different land cover classes. Looking at cumulative figures, it means that 60% of the SSUs are covered by 2 or less land cover types, 81% are covered by 3 or less land cover types and 92% are covered by 4 or less land cover types.

4.3.3 Results

For the sake of comparison with previous global LC mapping exercises, the accuracy of the CCI-LC map (year 2015) has been assessed using the GlobCover 2009 validation dataset. As explained in section 4.3.2.1, not all the points of the GlobCover 2009 validation database could be used.

Contingency matrices were built and overall accuracies were not only calculated based on the diagonal cells of the matrix but also accounted for other cells which mark agreement between the product and the validation dataset. Table 4-6 presents a first contingency matrix calculated by comparing the CCI-LC map from 2015 with the points interpreted as “certain” by the experts and “homogeneous” (i.e. made of a single LC class). This matrix indicates that the accuracy level is of 75.4%.

Table 4-6: Adjusted contingency matrix that considers the CCI-LC 2015 map and the "certain" and "homogeneous" points of the GlobCover 2009 validation dataset. Green cells mark diagonal cells while yellow cells represent other samples that also mark a clear agreement between the product and the reference.

		REFERENCE: GLOBCOVER 2009 VALIDATION DATASET																							
	0	**10**	**20**	**30**	**40**	**50**	**60**	**70**	**80**	**90**	**100**	**110**	**120**	**130**	**140**	**150**	**160**	**170**	**180**	**190**	**200**	**210**	**220**	**SUM**	**User Acc. (%)**
PRODUCT: CCI-LC 2015 MAP	**10**	245	27	0	0	4	0	0	0	1	0	0	6	7	0	0	0	0	2	5	0	0	0	297	**92**
	20	5	5	0	0	0	0	0	0	0	0	0	0	1	0	0	0	0	0	0	1	0	0	12	**83**
	30	18	2	0	0	2	1	0	0	1	0	0	2	1	0	0	0	0	0	1	0	0	0	28	**71**
	40	12	0	0	0	3	1	0	0	0	0	0	2	3	0	2	0	0	0	0	0	0	0	23	**39**
	50	4	2	0	0	224	2	1	0	8	0	0	0	0	0	0	0	0	0	0	0	0	0	241	**96**
	60	5	0	0	0	18	44	1	4	31	0	0	16	3	0	1	0	0	2	0	0	1	0	126	**60**
	70	1	0	0	0	2	2	35	2	28	0	0	8	5	1	1	0	0	5	0	2	2	1	95	**66**
	80	0	0	0	0	0	0	0	12	2	0	0	2	1	0	0	0	0	0	0	0	0	0	17	**82**
	90	0	0	0	0	1	6	2	0	4	0	0	0	0	0	0	0	0	0	0	0	0	0	13	**31**
	100	5	0	0	0	3	1	0	0	1	0	0	3	6	1	1	0	0	0	1	1	0	0	23	**35**
	110	1	0	0	0	1	0	0	0	0	0	0	1	2	0	2	0	0	2	0	0	0	0	9	**22**
	120	15	2	0	0	4	4	1	0	1	0	0	92	10	0	10	0	0	1	1	7	0	1	149	**62**
	130	25	1	0	0	0	0	1	1	1	0	0	13	48	0	8	0	0	0	2	2	1	1	104	**46**
	140	0	0	0	0	0	0	0	0	0	0	0	0	2	3	0	0	0	1	0	2	0	1	9	**33**
	150	3	0	0	0	0	0	0	0	0	0	0	7	4	1	9	0	0	0	1	17	0	0	42	**21**
	160	0	0	0	0	4	1	0	0	0	0	0	0	1	1	0	5	1	1	0	0	0	0	14	**36**
	170	0	0	0	0	1	0	0	0	0	0	0	0	0	0	0	1	5	0	0	0	0	0	7	**71**
	180	0	0	0	0	0	0	0	0	0	0	0	1	3	1	0	0	0	3	0	0	1	0	9	**33**
	190	1	2	0	0	0	0	0	0	0	0	0	0	0	0	0	0	0	0	18	0	0	0	21	**86**
	200	0	1	0	0	0	0	0	0	1	0	0	1	2	1	4	0	0	0	1	135	1	6	153	**88**
	210	0	1	0	0	0	0	0	0	0	0	0	0	0	1	0	0	0	1	0	0	78	0	81	**96**
	220	0	0	0	0	0	0	0	0	0	0	0	0	0	0	0	0	0	0	0	1	0	25	26	**96**
	SUM	340	43	0	0	267	62	41	19	79	0	0	154	99	10	38	6	6	18	30	168	84	35	1499	
	Prod. Acc (%)	**79**	**79**	**N/A**	**N/A**	**86**	**74**	**85**	**63**	**94**	**N/A**	**N/A**	**63**	**54**	**30**	**24**	**83**	**83**	**17**	**60**	**80**	**93**	**71**		**75.38**

The same kind of analysis has been made using the “homogeneous” samples of the CCI LC validation database. In this database, each sample is associated to a certain number of objects, which have been labelled by the experts. The “homogeneity” of the samples is therefore more complicated to define than in the case of the GlobCover validation database. Two options were identified to define the samples “homogeneity”:

- the dominant class is identified based on given thresholds on the area. Thresholds of 100%, 90%, 80%, 70%, 60% and 50% were tested;
- the dominant class is identified as the majority classes, independently from the area it covers.

The LC maps from the years 2000, 2005, 2010 and 2015 were validated, 2010 and 2015 being validated with the same 2010 epoch of the validation database. Confusion matrices were generated for the various scenarios (years and homogeneity definition) and overall accuracy values were calculated. The results are summarized in Figure 4-29. As an example, Table 4-7 provides the contingency matrix for the year 2015 validation using the samples covered at 100% by the same LC class.

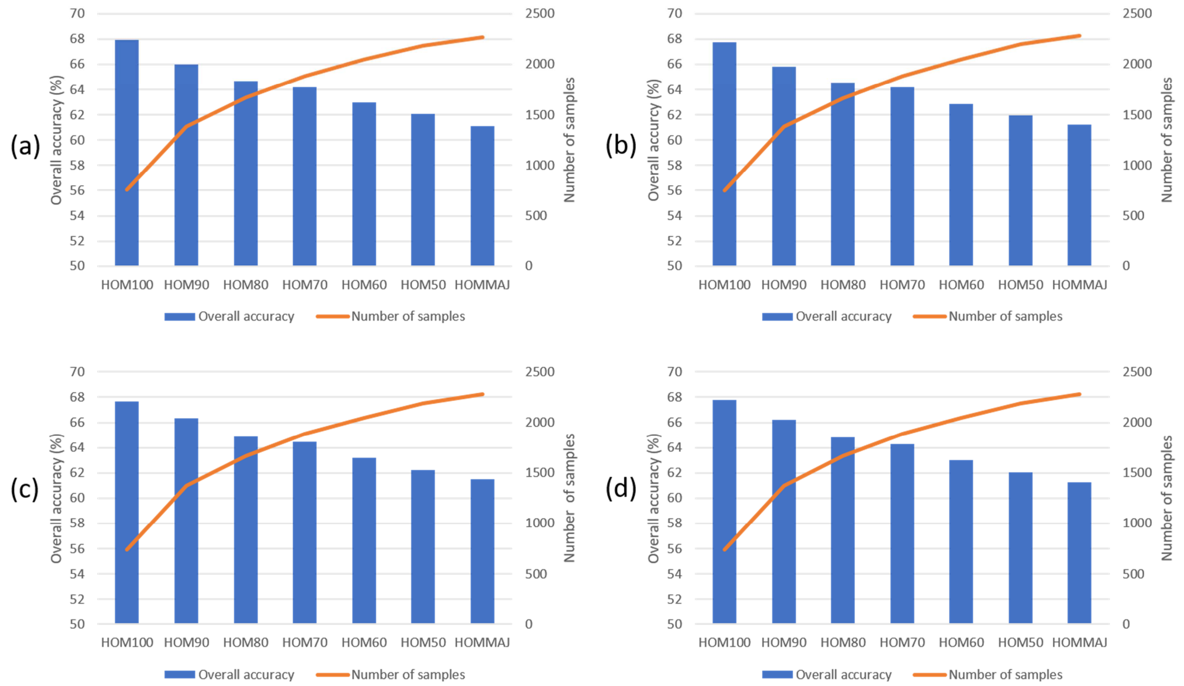

Figure 4-29: Evolution of the overall accuracy values for the LC maps 2000 (a), 2005 (b), 2010 (c) and 2015 (d) depending on the definition of the “homogeneity” of the samples of the CCI LC validation database (HOM100 to HOM50 meaning the homogeneity defined based on a threshold of the area covered by the dominant LC class, this threshold varying from 100 to 50%; HOMMAJ meaning that the majority LC class is considered as the only LC class associated with the sample)

It can be noted on Figure 4-29 that there are very few differences between the 4 maps. This was expected since the sampling was not at all designed to validate the LC changes. At global scale, LC change represents a few percent of the total area and is thus not well rendered in classical validation approaches. Change validation would require working with an alternative sampling design focusing on hot-spot change areas and on LC classes known to drive major LC changes.

Table 4-7: Adjusted contingency matrix that considers the CCI-LC 2015 map and the samples covered at 100% with a same LC class from the CCI LC database. Green cells mark diagonal cells while yellow cells represent other samples that also mark a clear agreement between the product and the reference.

	REFERENCE: CCI LC VALIDATION DATASET																							
	0	**10**	**20**	**30**	**40**	**50**	**60**	**70**	**80**	**90**	**100**	**110**	**120**	**130**	**140**	**150**	**160**	**170**	**180**	**190**	**200**	**210**	**220**	**SUM**	**User Acc. (%)**
PRODUCT: CCI-LC 2015 MAP	**10**	38	11	0	0	0	0	0	0	0	0	0	5	1	0	0	0	0	1	0	1	0	0	57	**86**
	20	2	12	0	0	0	0	0	0	0	0	0	0	1	0	0	0	0	0	0	0	0	0	15	**93**
	30	5	0	0	0	0	0	0	0	0	0	0	1	1	0	0	0	0	0	0	0	0	0	7	**71**
	40	3	0	0	0	0	1	0	0	0	0	0	2	2	0	0	0	0	0	0	0	0	0	8	**63**
	50	3	0	0	0	163	6	1	0	0	0	0	4	0	0	0	1	0	0	0	0	0	0	178	**92**
	60	0	0	0	0	7	26	0	3	5	0	0	10	1	0	0	0	0	0	0	0	0	0	52	**60**
	70	0	0	0	0	4	3	16	0	1	0	0	0	0	0	0	0	0	1	0	0	0	0	25	**68**
	80	0	0	0	0	0	0	3	13	0	0	0	2	2	0	0	0	0	0	0	0	0	0	20	**65**
	90	0	0	0	0	0	2	0	0	2	0	0	0	0	0	0	0	0	0	0	0	0	0	4	**50**
	100	2	0	0	0	0	4	2	0	0	0	0	3	4	0	3	1	0	0	0	0	0	0	19	**47**
	110	0	0	0	0	0	0	0	0	0	0	0	1	0	0	0	0	0	0	0	0	0	0	1	**0**
	120	3	0	0	0	9	7	1	0	0	0	0	51	17	1	8	0	0	1	0	2	0	0	100	**51**
	130	1	0	0	0	0	0	0	0	0	0	0	14	25	0	9	0	0	0	0	18	0	0	67	**37**
	140	0	0	0	0	0	0	0	0	0	0	0	0	0	0	0	0	0	0	0	0	0	0	0	**N/A**
	150	5	0	0	0	0	0	0	0	0	0	0	12	23	1	22	0	0	0	0	6	0	0	69	**32**
	160	0	0	0	0	3	0	0	0	0	0	0	0	0	0	0	1	0	0	0	0	0	0	4	**25**
	170	0	0	0	0	0	0	0	0	0	0	0	0	0	0	0	0	1	0	0	0	0	0	1	**100**
	180	0	0	0	0	0	0	0	0	0	0	0	1	0	0	1	1	0	2	0	0	0	0	5	**40**
	190	0	0	0	0	0	0	0	0	0	0	0	0	0	0	0	0	0	0	0	0	0	0	0	**N/A**
	200	2	0	0	0	0	0	0	0	0	0	0	1	1	0	10	0	0	1	0	52	0	0	67	**78**
	210	0	1	0	0	0	0	0	0	0	0	0	0	0	0	0	0	0	0	0	0	41	0	42	**98**
	220	0	0	0	0	0	0	0	0	0	0	0	0	0	0	0	0	0	0	0	1	0	0	1	**0**
	SUM	64	24	0	0	186	49	23	16	8	0	0	107	78	2	53	4	1	6	0	80	41	0	742	
	Prod. Acc (%)	**70**	**96**	**N/A**	**N/A**	**88**	**63**	**78**	**81**	**100**	**N/A**	**N/A**	**52**	**35**	**0**	**42**	**25**	**100**	**33**	**N/A**	**65**	**100**	**N/A**		**67,79**

Coming back to the GlobCover validation database, a second contingency matrix is derived using all the "certain" points, whether they are "homogeneous" or "heterogeneous" (i.e. made of several or mosaic LC classes), which is presented in Table 4-8. This second matrix indicates that the accuracy level is found to be 71.45%.

According to the CEOS recommendations, overall accuracy values weighted by the area proportions of the land cover classes are also calculated. The surfaces of the various land cover classes were determined based on the CCI-LC 2015 product itself, projected in an equal area projection. Using the 1499 "certain" and "homogeneous" points, the weighted-area overall accuracy figure of the 2015 CCI-LC map is of 71.1%, while with the 2329 "certain" points (without homogeneity constraint), it is of 71.7%. In the first case, accounting for the LC classes area decreases a little bit the overall accuracy while in the second case, it does not modify it the value significantly. These figures are higher than the ones of GlobCover 2009 product.

Table 4-8: Adjusted contingency matrix that considers the CCI-LC 2015 map and the "certain" ("homogeneous" and "heterogeneous") points of the GlobCover 2009 validation dataset. Green cells mark diagonal cells while yellow cells represent other samples that also mark a clear agreement between the product and the reference.

	REFERENCE: GLOBCOVER 2009 VALIDATION DATASET																								
	0	**10**	**20**	**30**	**40**	**50**	**60**	**70**	**80**	**90**	**100**	**110**	**120**	**130**	**140**	**150**	**160**	**170**	**180**	**190**	**200**	**210**	**220**	**SUM**	**User Acc. (%)**
PRODUCT: CCI-LC 2015 MAP	**10**	342	50	0	0	7	0	0	0	6	0	0	9	13	0	1	0	0	3	7	4	0	0	442	**89**
	20	9	16	0	0	0	0	0	0	0	0	0	0	1	0	0	0	0	0	1	1	0	0	28	**89**
	30	22	2	21	0	3	2	1	0	4	0	0	5	1	0	0	0	0	0	1	0	0	0	62	**73**
	40	15	0	0	13	3	2	0	0	0	0	0	2	4	0	2	0	0	0	0	0	0	0	41	**59**
	50	9	2	0	0	257	2	1	0	15	0	0	1	1	0	0	0	0	0	0	0	0	0	288	**94**
	60	13	1	0	0	21	74	2	5	43	0	0	26	8	0	1	0	0	3	0	1	2	0	200	**59**
	70	3	0	0	0	3	3	63	3	57	0	0	13	14	7	2	0	0	7	0	7	3	2	187	**64**
	80	0	0	0	0	0	2	0	37	3	0	0	2	1	3	1	0	0	0	0	2	0	0	51	**78**
	90	0	0	0	0	1	9	11	1	12	0	0	0	0	0	0	0	0	0	0	0	0	0	34	**35**
	100	20	0	0	0	3	2	3	0	2	5	0	6	8	3	2	0	0	0	2	2	0	0	58	**36**
	110	1	0	0	0	1	0	0	0	0	0	2	1	2	0	2	0	0	2	0	0	0	0	11	**36**
	120	20	2	0	0	4	5	2	0	5	0	0	118	24	3	11	0	0	1	1	12	1	2	211	**56**
	130	33	3	0	0	0	0	1	1	4	0	0	19	99	2	12	0	0	0	4	23	1	2	204	**49**
	140	0	0	0	0	0	0	1	0	0	0	0	0	4	10	0	0	0	5	0	4	0	2	26	**38**
	150	3	0	0	0	0	0	0	1	0	0	0	10	9	6	33	0	0	0	2	28	0	2	94	**35**
	160	1	0	0	0	8	1	0	0	0	0	0	0	1	2	0	6	1	3	0	0	0	0	23	**26**
	170	0	0	0	0	1	0	0	0	0	0	0	0	0	0	0	1	6	0	0	0	0	0	8	**75**
	180	0	0	0	0	0	0	0	0	0	0	0	1	3	1	0	0	0	8	0	0	2	0	15	**53**
	190	1	2	0	0	0	0	0	0	0	0	0	0	0	0	0	0	0	0	22	0	0	0	25	**88**
	200	1	1	0	0	0	0	0	0	1	0	0	1	2	1	4	0	0	0	2	160	2	6	181	**88**
	210	0	2	0	0	0	0	0	0	1	0	0	1	0	1	1	0	0	1	1	0	102	1	111	**92**
	220	0	0	0	0	0	0	0	0	0	0	0	0	0	0	0	0	0	0	0	1	0	28	29	**97**
	SUM	493	81	21	13	312	102	85	48	153	5	2	215	195	39	72	7	7	33	43	245	113	45	2329	
	Prod. Acc (%)	**76**	**84**	**100**	**100**	**84**	**76**	**78**	**77**	**86**	**100**	**100**	**59**	**54**	**26**	**46**	**86**	**86**	**24**	**51**	**65**	**90**	**62**		**71.45**

4.4 Concluding remarks

- ***Classification accuracy interpreted in the light of producers and users accuracy values***

Attention should also be paid to the producer and user accuracy values, which give more information about the accuracy of the different thematic classes and which can also explain the effects observed when weighting the overall accuracy values by the land cover class areas.

The highest user accuracy values[5] are found for the classes of rainfed cropland (class value 10; 89-92%), irrigated cropland (class value 20; 89-83%), broadleaved evergreen forest (class value 50; 94-96%), urban areas (class value 190; 88-86%), bare areas (class value 200; 88-88%), water bodies (class value 210; 92-96%) and permanent snow and ice (class value 220; 97-96%). This is generally not surprising as these classes are homogeneous, unambiguous and recognisable. What is more unexpected - and therefore a highly positive result - is the high accuracy associated with the cropland classes. These classes are of paramount importance for food security but which are unfortunately often poorly captured in global land cover products due to their dynamic nature and the large variety of agro-systems.

Conversely, mosaic classes of natural vegetation (class values 100, 110) are associated with the lowest user accuracy values, as well as the three classes of lichens and mosses (class value 140), sparse vegetation (class value 150) and flooded forest with fresh water (class value 160). The class of mixed broadleaved and needleleaved forest (class value 90) has also a low user accuracy value, but all errors relate to confusion between this class and other forest classes, which very much limits the impact of this low value.

- ***Classification accuracy related to the number of observations in the MERIS archive***

It has to be clear that the quality of the map varies according to the region of interest. Looking at the number of valid observations available over a region (information which is provided in the quality flag 3) can give a first indication about the input data quality and the expected classification reliability. Areas affected by a lower MERIS FR coverage are the western part of the Amazon basin, Chili and the southern part of Argentina, the western part of Congo basin as well as the gulf of Guinea, the eastern part of Russia, the eastern coast of China and Indonesia.

- ***Classification accuracy in the light of the contingency matrix***

The overall accuracy figures presented in the previous section must be balanced by the fact that the LC maps quality varies according to the thematic class. In particular, land cover classes such as rainfed and irrigated croplands, broadleaved evergreen forest, urban areas, bare areas, water bodies and permanent snow are found quite accurately mapped. On the other hand, classes such as lichens

[5] The figures given into brackets correspond to the ones given in Table 4-8 first (certain points, homogeneous and heterogeneous) and in Table 4-6 second (certain points, homogeneous only)

and mosses, sparse vegetation and flooded forest with fresh water can be affected by errors. The mosaic classes of natural vegetation have also lower user accuracy values, such as the class of mixed broadleaved and needleleaved forest. Yet, in this latter case, most of the errors occur between this class and other forest classes, which very much limits the thematic impact of this lower accuracy value.

- ***Not possible to validate the changes properly***

The sampling design underlying the building of both GlobCover and CCI LC validation database is not relevant for validate LC changes. Indeed, at global scale, LC change represents a few percent of the total area and is thus not well rendered in classical validation approaches. Change validation would require working with an alternative sampling design focusing on hot-spot change areas and on LC classes known to drive major LC changes.

Independently of what can be validated, it is nevertheless known that the set of annual LC maps don't capture all changes that have occurred between the 22 LC classes defined in Table 4-1. This limitation is inherent to the methodology developed to detect the change in a consistent way over years [Ph2_ATBDv2_1.0, 2017]. The different shortcomings related to the change detection method are reminded here below:

  - *Not all possible changes between the 22 LC classes are captured in the dataset*

The 22 LCCS land cover classes are indeed grouped into the 6 IPCC land categories, with the consideration of the subcategories shrubland, sparse vegetation, bare area and water (forming the "Other" IPCC main land category). Consequently, any change occurring between LCCS classes being part of the same IPCC land category is not captured by the CCI-LC dataset. More precisely, the CCI-LC dataset does not provide information on:

- the conversions between rainfed (class values 10, 11 and 12) and irrigated agriculture (class value 20). As a result, the agriculture intensification through the irrigation will not be detected as a change;
- the conversion between forest classes (e.g. conversion of broadleaved to mixed forests, flooded forest dewatering or salinization of a forest flooded with fresh water);
- the conversion between sparse vegetation (class value 150) and lichens and mosses (class value 140);
- the conversion between a "pure"[6] class and a mosaic class (e.g. forest degradation characterized by the evolution of a pure forest (class values 50 to 90) to a mosaic of natural vegetation (class values 100 and 110); cropland intensification characterized by the conversion of a mosaic of cropland and natural vegetation (class values 30 and 40) to a rainfed or irrigated cropland (class values 10 to 20); forest regeneration characterized a mosaic of natural vegetation (class values 100 and 110) to a pure forest (class values 50 to 90).

[6] "pure" is here expressed as opposed to "mosaic" or "mixed" class, which have the values 30, 40, 100 and 110

- the conversion between “level 2” or “regional” classes (see section 4.1.1), whatever the IPCC land category. This corresponds to any dynamics specific to herbaceous vs woody cropland (class values 11 and 12), to the density of the forests (depicted in the level 2 of the forest classes 61, 62, 71, 72, 81 and 82), to the phenology of the shrubland (class values 121 and 122), to the type of the sparse vegetation (class values 151, 152, 153) or the type of bare area (class values 201 and 202).
    - *Change delineated at 300 m based on hot spots of change detected at 1 km*

All annual CCI-LC maps are delivered at 300 m spatial resolution but it is to be reminded that the change detection is performed at 1 km spatial resolution, based on the AVHRR, SPOT-VGT and PROBA-V missions. It means that only land cover changes visible at 1 km are detected. These hot spots of change and their surroundings (up to 5 km) are then further delineated at 300 m starting 2004 onwards thanks to the availability of the 300 m MERIS and PROBA-V time series at this period.

As a result, several cases of change omissions are observed in the annual LC maps. First, changes of low intensity and/or surface below 1 km² are not detected. Second, changes are not delineated at 300 m if it does not occur in the surroundings of a hot spot of change detected at 1 km. In other words, if the change occurs at a distance greater than 5 km away from the 1 km change hot spot. Finally, changes will not be delineated at 300 m if they occur before year 2004 as no MERIS and PROBA-V time series exist at 300 m before 2003.

- *Changes along the coastlines and of permanent snow and ice class not included in the CCI-LC products*

Changes along the coastlines are not captured with a change detection algorithm based on 1-km observations. Yet, an exception is made for changes related to the Saudi Arabia manmade islands.

In addition, the permanent snow and ice (class value 220) remains constant over time and relies solely on the Randolph Glaciers Inventory.

- *Changes occurring in the 2014 - 2015 period*

Changes occurring in the 2014 - 2015 period are limited to forests changes. This is a consequence of the methodology that needs to have confirmation of the land cover change during at least 2 years. During this period, this confirmation cannot be ensured and so, only the forest changes – which are the easiest to detect – are included in the maps.

- *Change during the AVHRR 1992 - 1999 period*

The performance of the change detection is highly dependent on the input data quality and availability. The general lower quality of AVHRR surface reflectances and georeferencing implies a less reliable change detection. In addition, the lack of AVHRR data in year 1994 reduces the change detection reliability for this particular year.

5 APPENDIX

Table 5-1 presents the other selected reference points used for validation.[7]

Table 5-1: Selected reference points

NAME	LONGITUDE	LATITUDE	COMMENTS
Africa			
Mikumi National Park	37.64	-6.64	http://en.wikipedia.org/wiki/Mikumi_National_Park vegetation of this area consists of savannah dotted with acacia, baobab, tamarinds, and some rare palm
New Valley - Sahara	27.18	24.49	http://en.wikipedia.org/wiki/New_Valley_Governorate http://en.wikipedia.org/wiki/Libyan_Desert Sand plains, dunes, ridges and some depressions (basins)
Timbuktu - Sahara	-3.75	21.04	http://en.wikipedia.org/wiki/Timbuktu http://en.wikipedia.org/wiki/Sahara_Desert_(ecoregion) sand dunes (erg), to stone plateaus (hamadas), gravel plains (reg), dry valleys (wadis), and salt flats
Tumba Lediima Kongo	17.10	-1.61	-
Asia			
Boreal Forest - Wladiwostok	132.01	43.20	-
Tundra - Tajmyr	87.98	74.35	http://en.wikipedia.org/wiki/Tundra dwarf shrubs, sedges and grasses, mosses, and lichens
Australia			
Coen - tropical	143.29	-13.95	http://en.wikipedia.org/wiki/Coen,_Queensland
Great Sandy Dessert	125.43	-21.01	http://en.wikipedia.org/wiki/Great_Sandy_Desert large ergs
Great Basalt Wall National Park	145.35	-20.04	http://en.wikipedia.org/wiki/Great_Basalt_Wall_National_Park basalt flows

[7] Note: Further examination and verification regarding the uncertainty is needed.

NAME	LONGITUDE	LATITUDE	COMMENTS
Mackenzie Country New Zealand	170.33	-44.05	http://en.wikipedia.org/wiki/Mackenzie_Basin grassland, wilding conifers, farmland
Europe			
Kalevalsky Bor National Park	29.94	65.00	http://www.gov.karelia.ru/News/2006/12/1206_01_e.html natural forestland
National Park Horto Bagy	21.11	47.54	http://www.hnp.hu/index_en.php grassland
National Park Peneda Geres	-8.16	41.72	http://en.wikipedia.org/wiki/Peneda-Ger%C3%AAs_National_Park oak forest, shrubbery, marshes and riparian vegatation
North America			
Great Bear Rainforest	-127.30	51.97	http://en.wikipedia.org/wiki/Great_Bear_Rainforest Coastal rainforest
Sheyenne National Grassland	-97.32	46.44	http://en.wikipedia.org/wiki/Sheyenne_National_Grassland tallgrass prairie
White Mountain National Forest	-71.67	43.82	http://en.wikipedia.org/wiki/White_Mountain_National_Forest forest
South America			
Amazon	-53.44	0.48	http://en.wikipedia.org/wiki/Amazon_Basin Amazon rainforest
Atacama Dessert	-70.13	-23.64	http://en.wikipedia.org/wiki/Atacama_Desert salt lakes, sand, and felsic lava flows
Gran Sabana	-61.70	5.35	http://en.wikipedia.org/wiki/Gran_Sabana rivers, waterfalls and gorges, deep and vast valleys, impenetrable jungles and savannahs
Yungas Coroico	-67.20	-16.19	http://en.wikipedia.org/wiki/Cloud_forest fog forest

The following figures (Figure 5-1 through Figure 5-140) show SR time series of MERIS FR and RR, PROBA-V and AVHRR data for the correspondent epochs and the other reference points as well as the mean spectra, except AVHRR

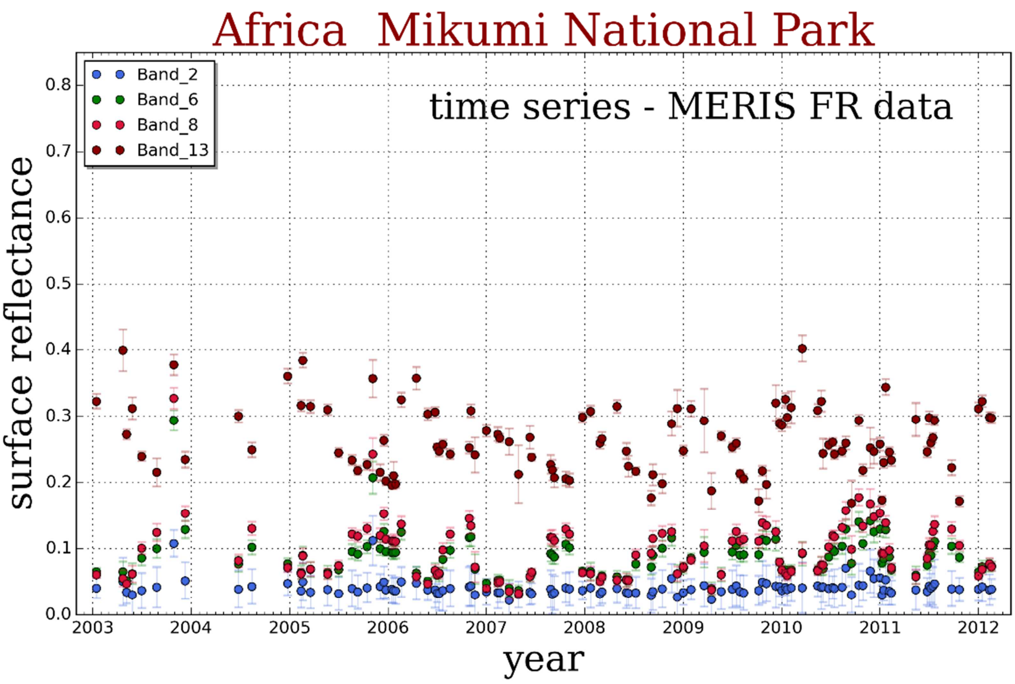

Figure 5-1: SR time series from MERIS FR data - 2003-2012 - Africa - Mikumi National Park

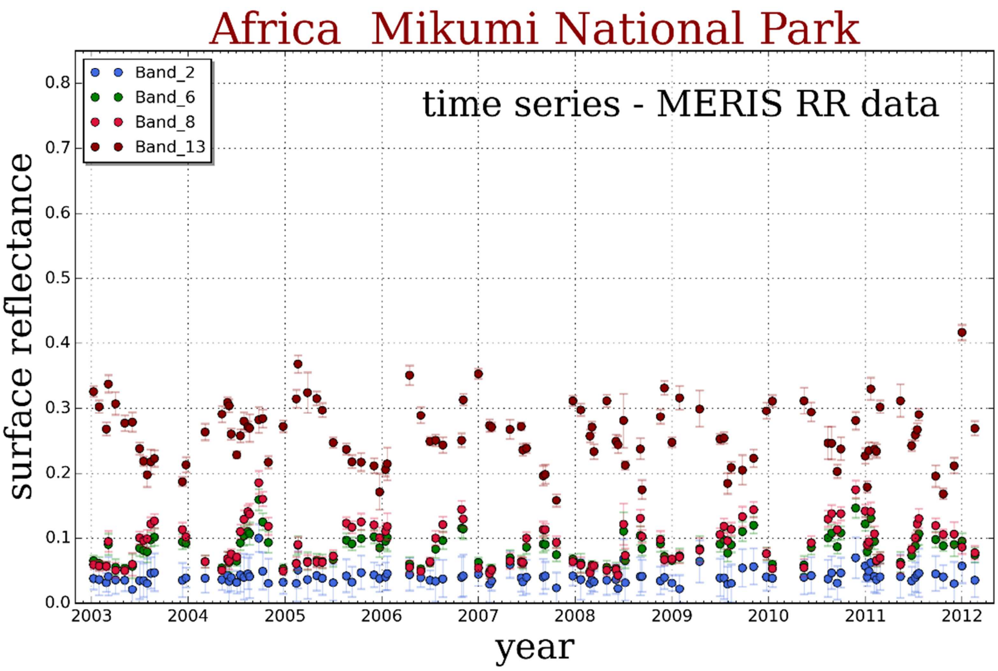

Figure 5-2: SR time series from MERIS RR data - 2003-2012 - Africa - Mikumi National Park

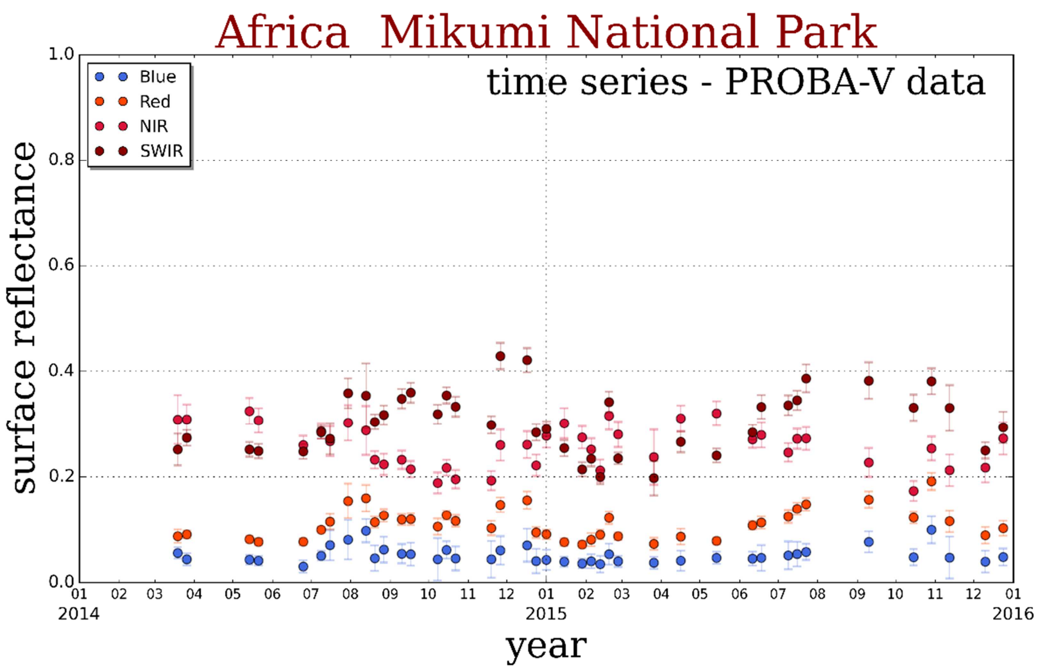

Figure 5-3: SR time series from PROBA-V data - 2014-2016 - Africa - Mikumi National Park

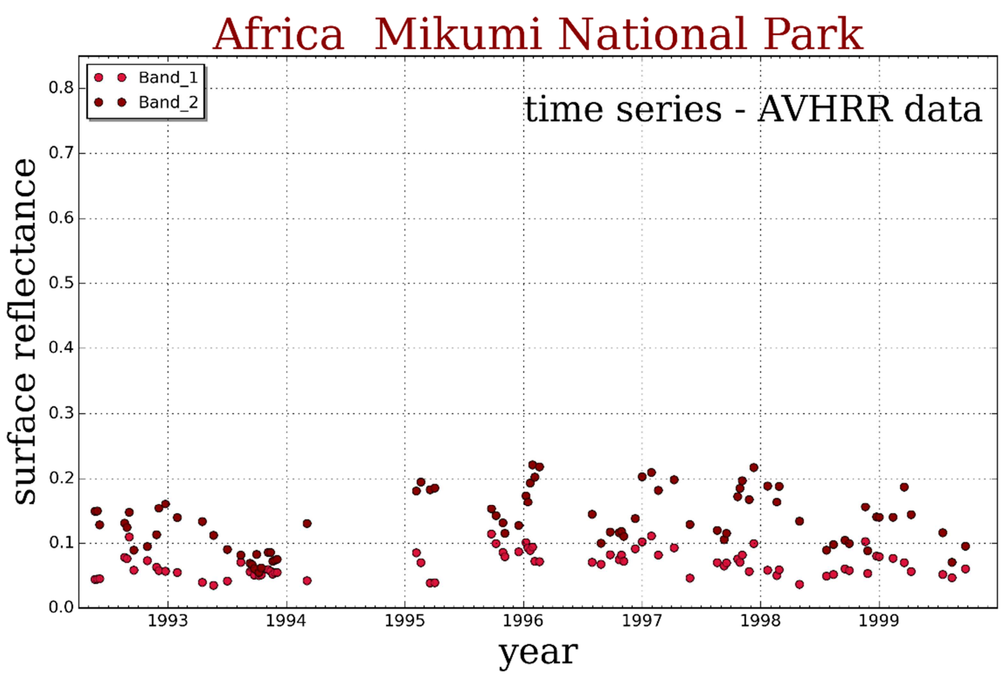

Figure 5-4: SR time series from AVHRR data - 1992-1999 - Africa - Mikumi National Park

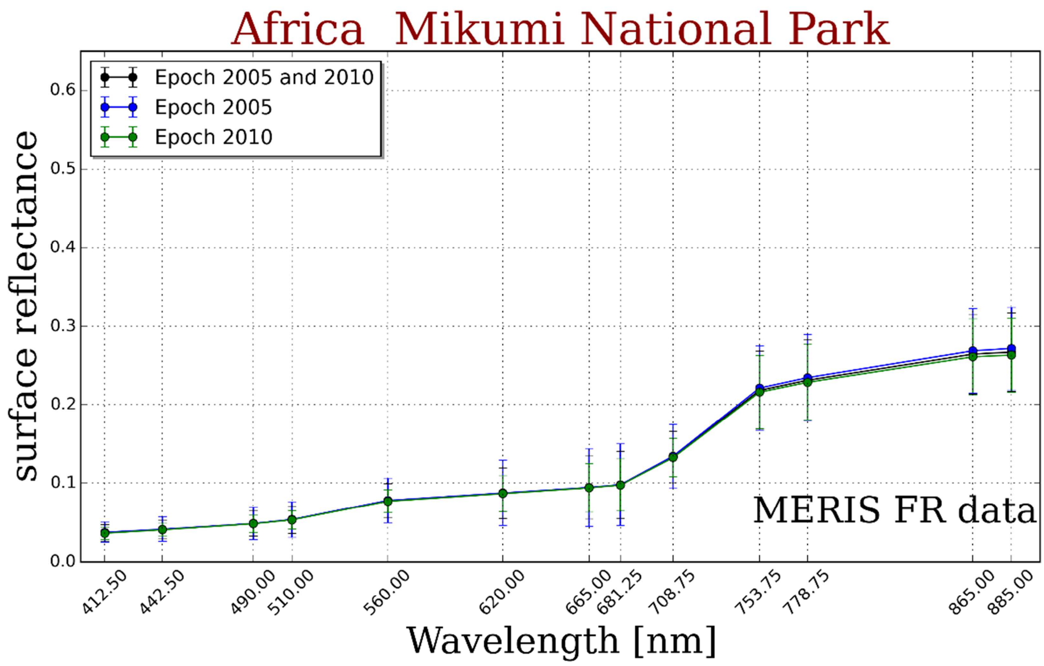

Figure 5-5: Spectra - Africa - Mikumi National Park - MERIS FR data

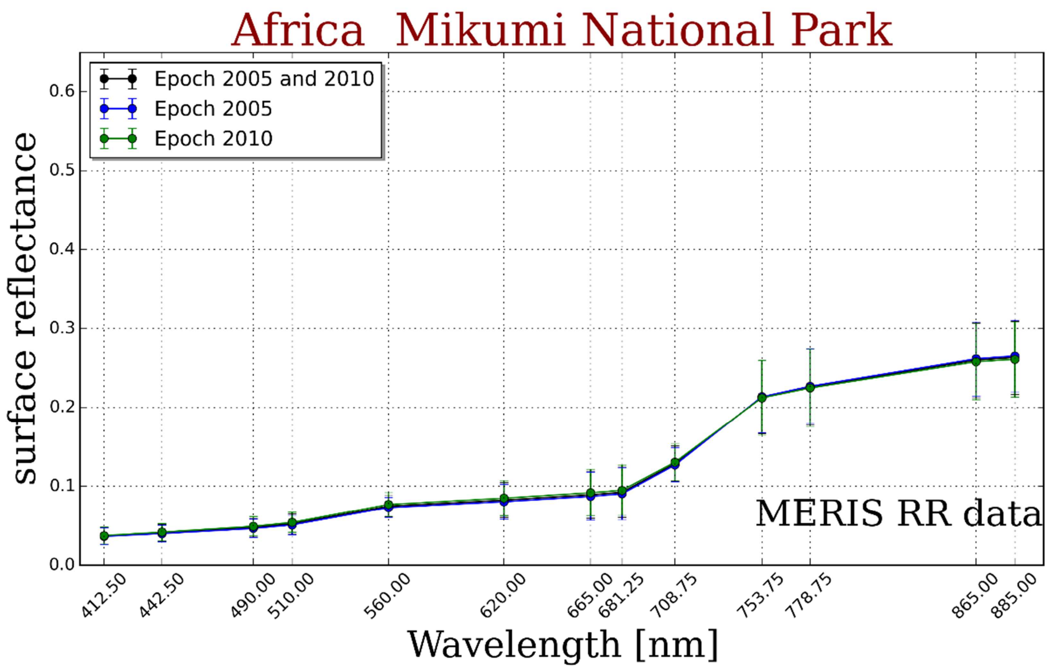

Figure 5-6: Spectra - Africa - Mikumi National Park - MERIS RR data

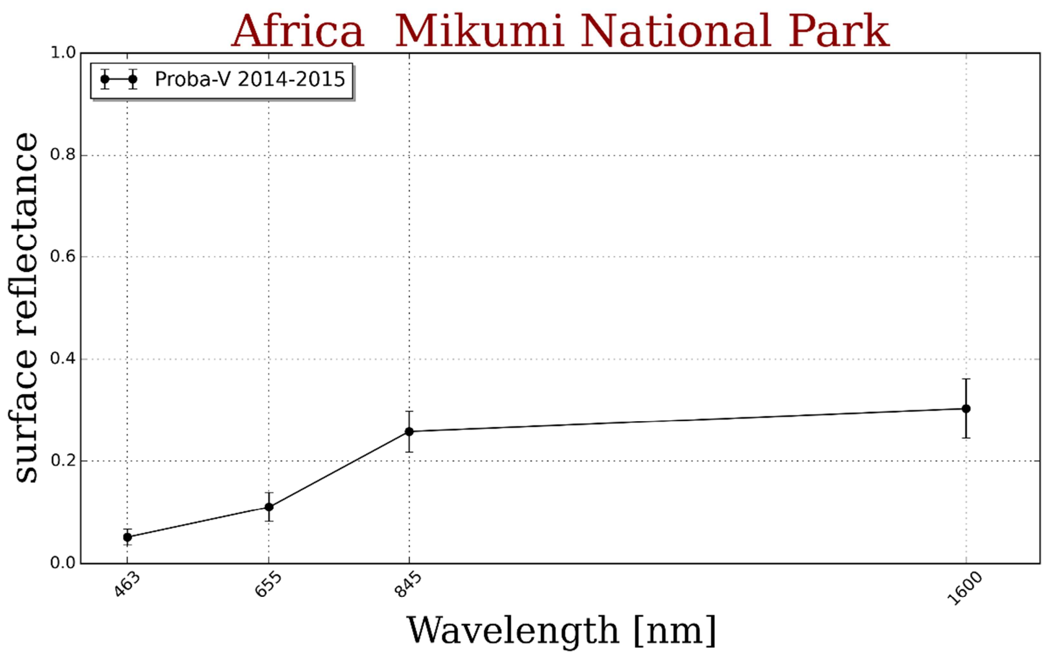

Figure 5-7: Spectra - Africa - Mikumi National Park – PROBA-V data

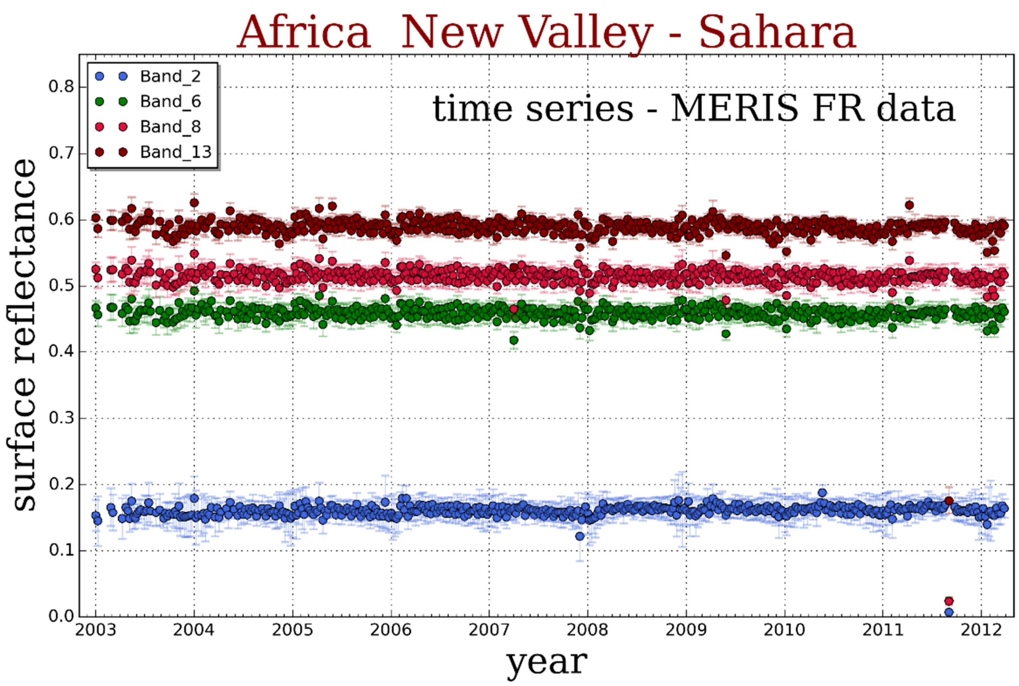

Figure 5-8: SR time series from MERIS FR data - 2003-2012 - Africa - New Valley Sahara

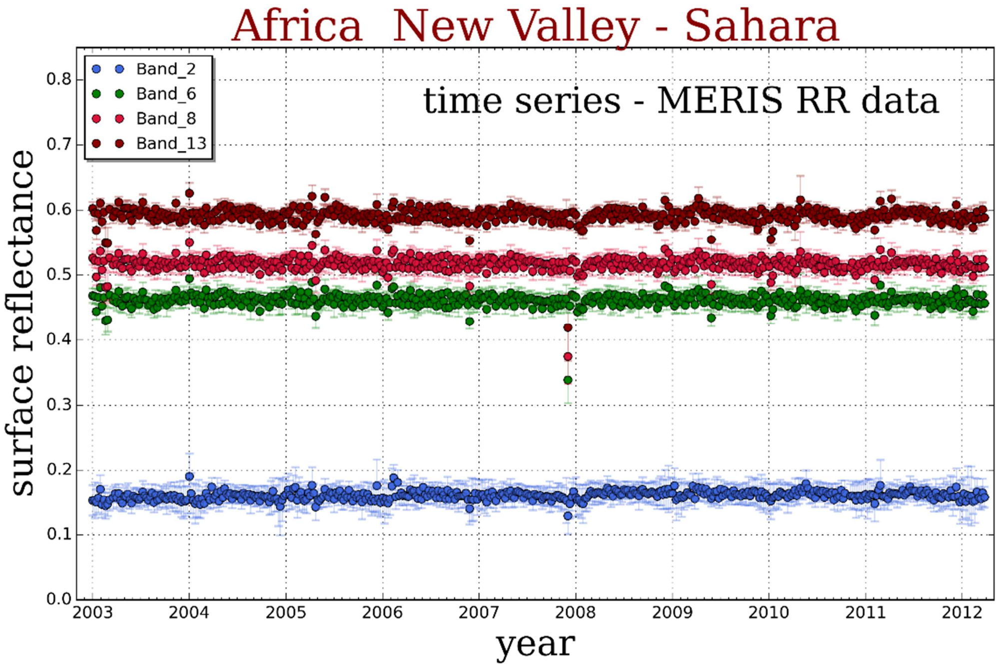

Figure 5-9: SR time series from MERIS RR data - 2003-2012 - Africa - New Valley Sahara

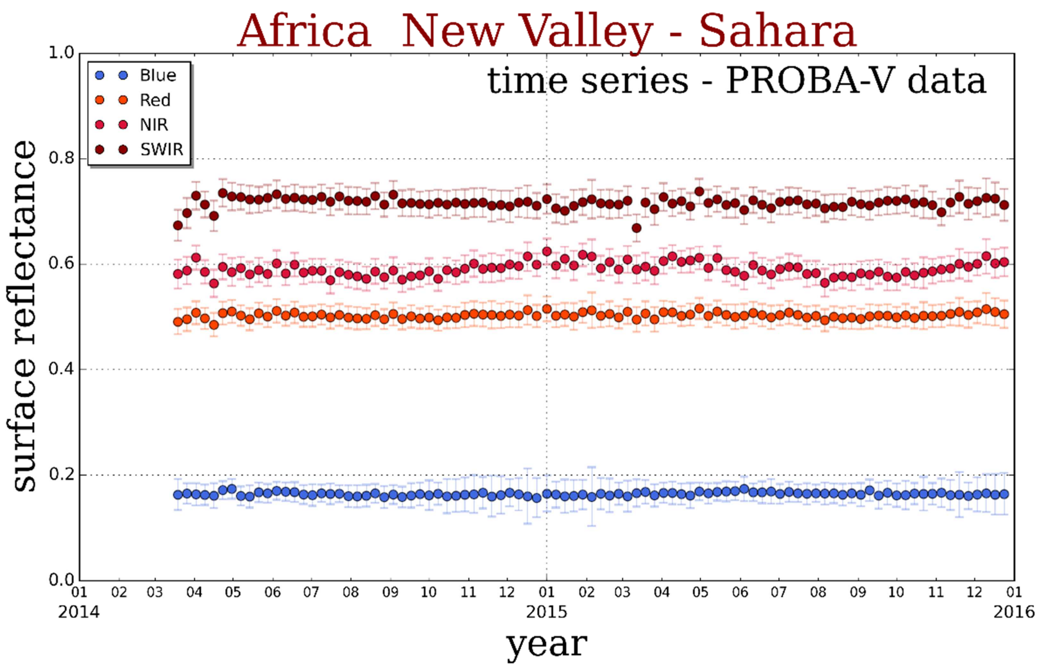

Figure 5-10: SR time series from PROBA-V data - 2014-2016 - Africa - New Valley Sahara

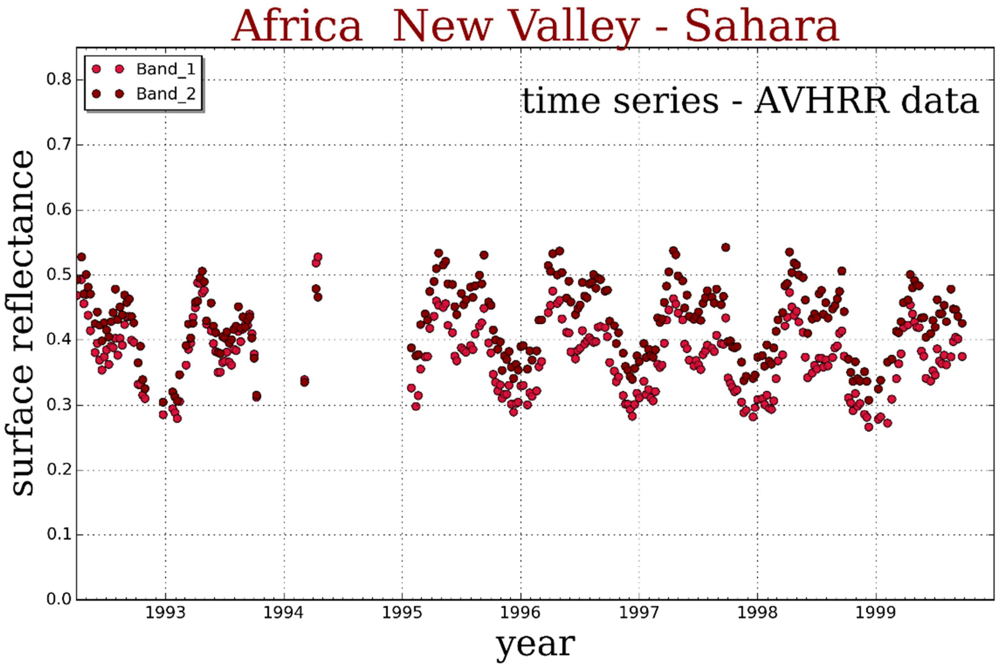

Figure 5-11: SR time series from AVHRR data - 1992-1999 - Africa - New Valley Sahara

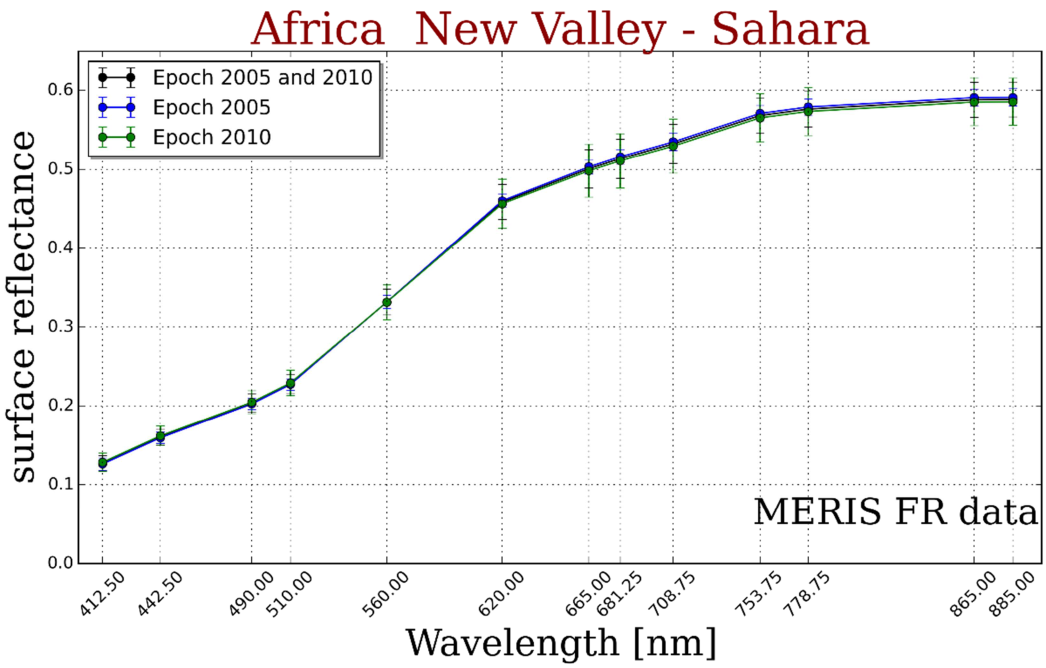

Figure 5-12: Spectra - Africa - New Valley Sahara - MERIS FR data

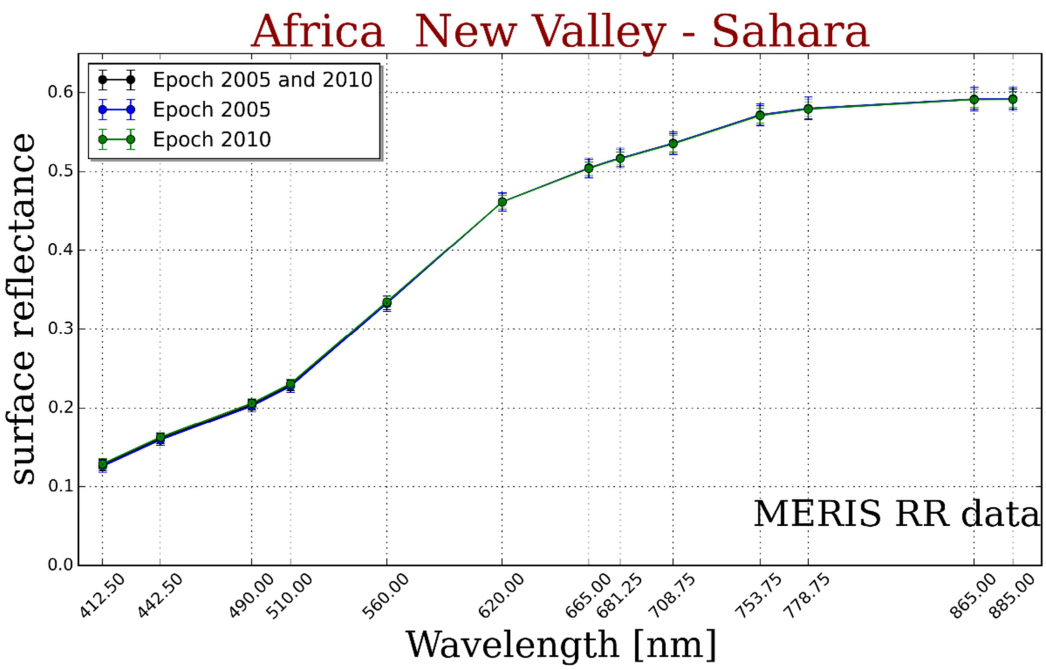

Figure 5-13: Spectra - Africa - New Valley Sahara - MERIS RR data

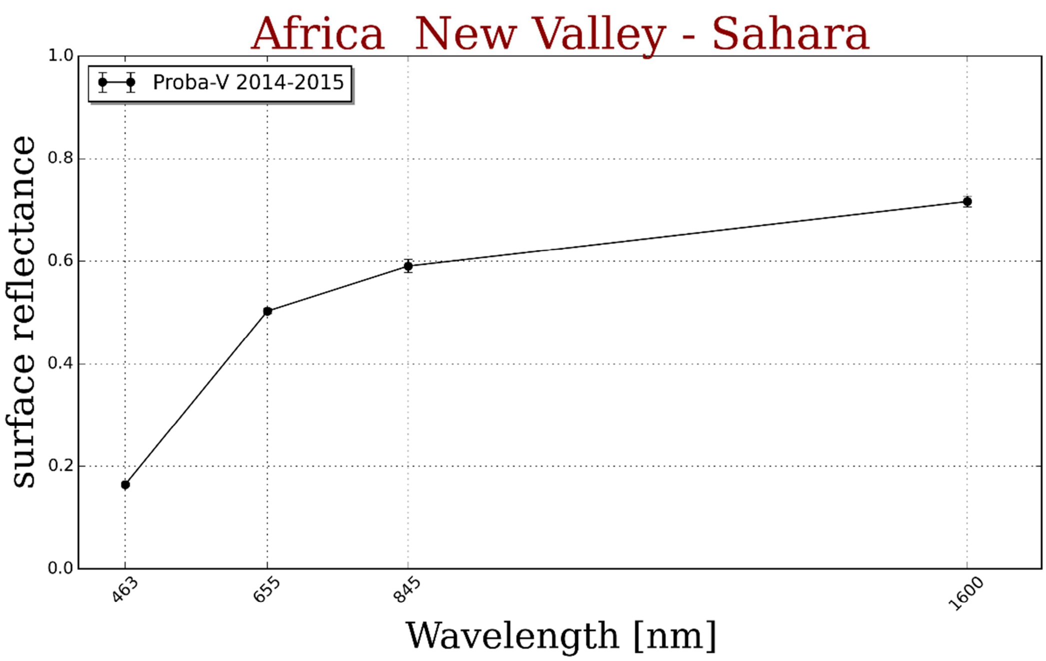

Figure 5-14: Spectra - Africa - New Valley Sahara – PROBA-V data

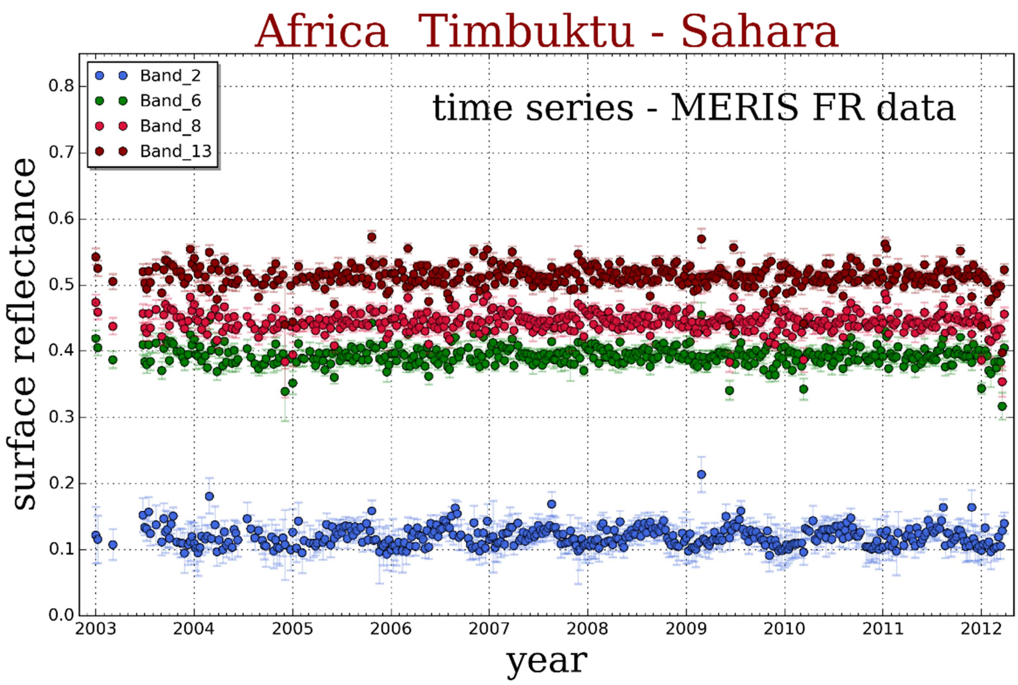

Figure 5-15: SR time series from MERIS FR data - 2003-2012 - Africa - Timbuktu Sahara

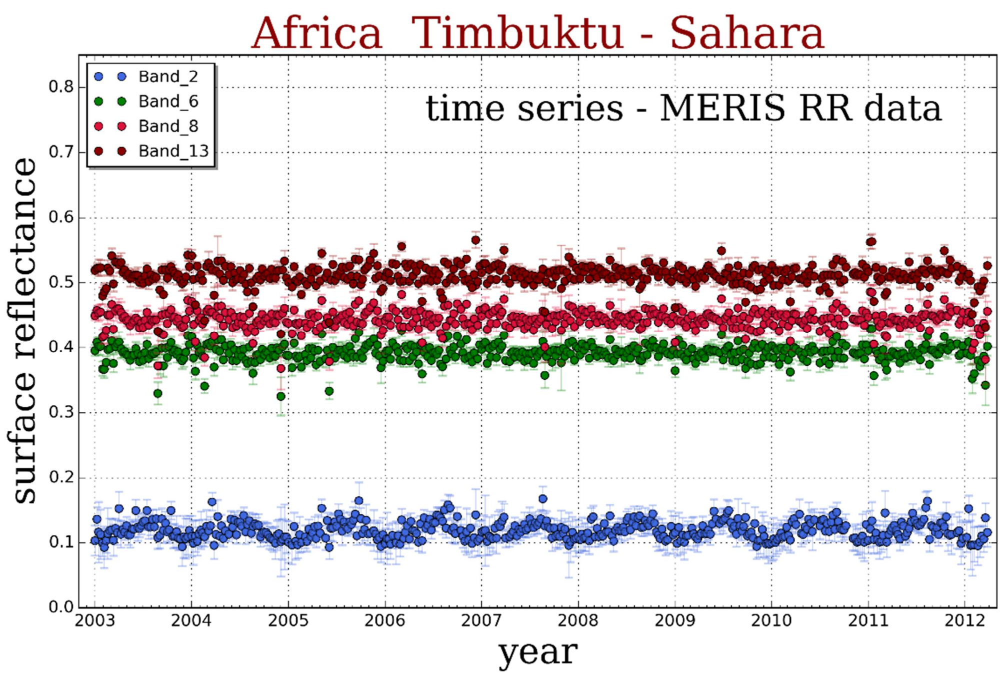

Figure 5-16: SR time series from MERIS RR data - 2003-2012 - Africa - Timbuktu Sahara

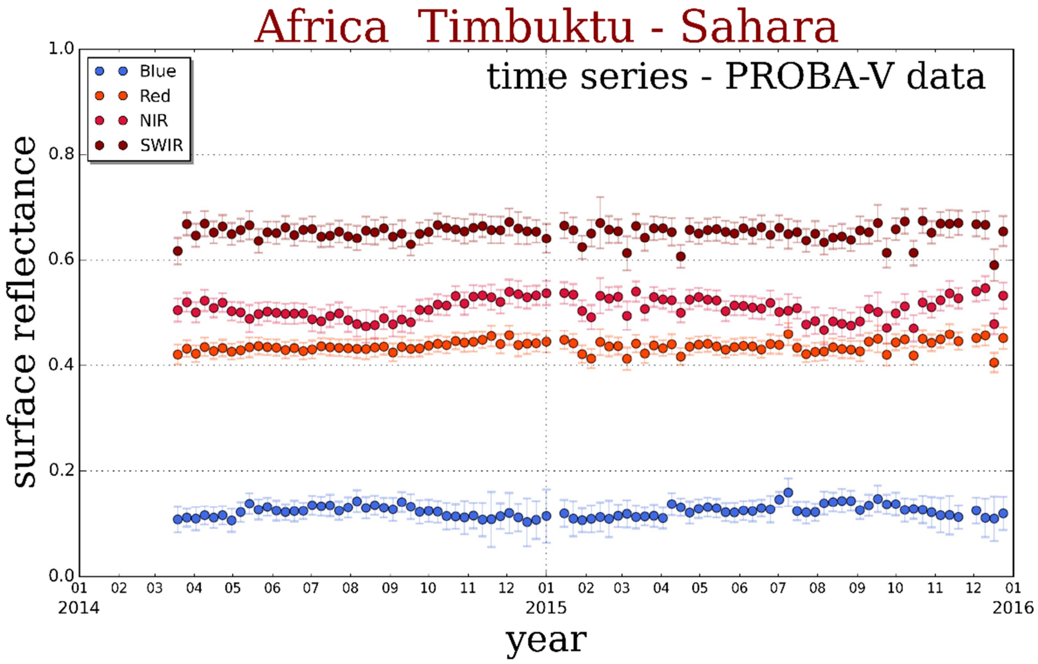

Figure 5-17: SR time series from PROBA-V data - 2014-2016 - Africa - Timbuktu Sahara

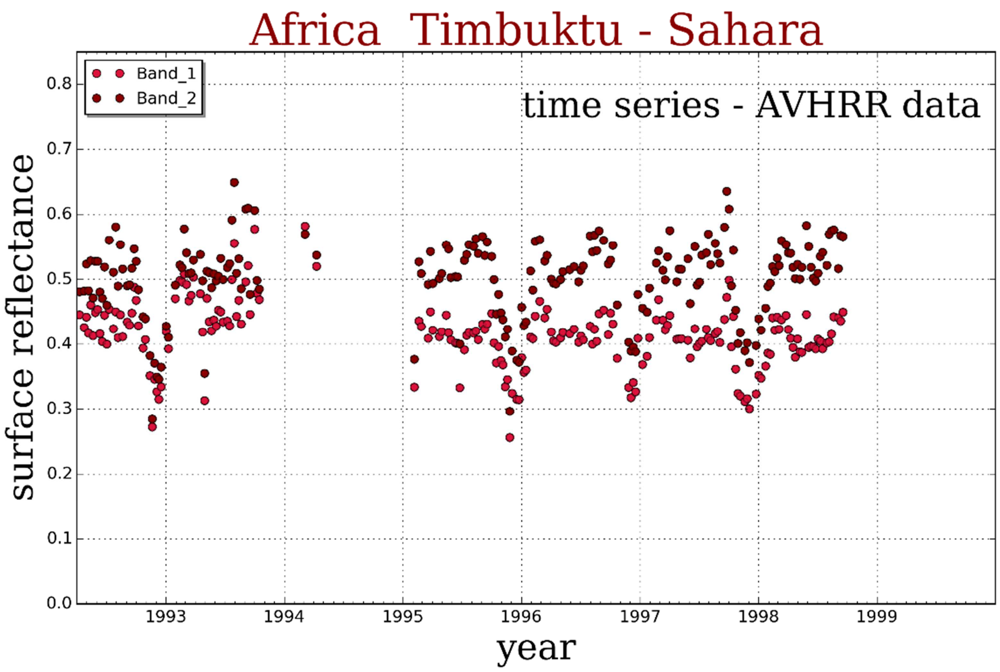

Figure 5-18: SR time series from AVHRR data - 1992-1999 - Africa - Timbuktu Sahara

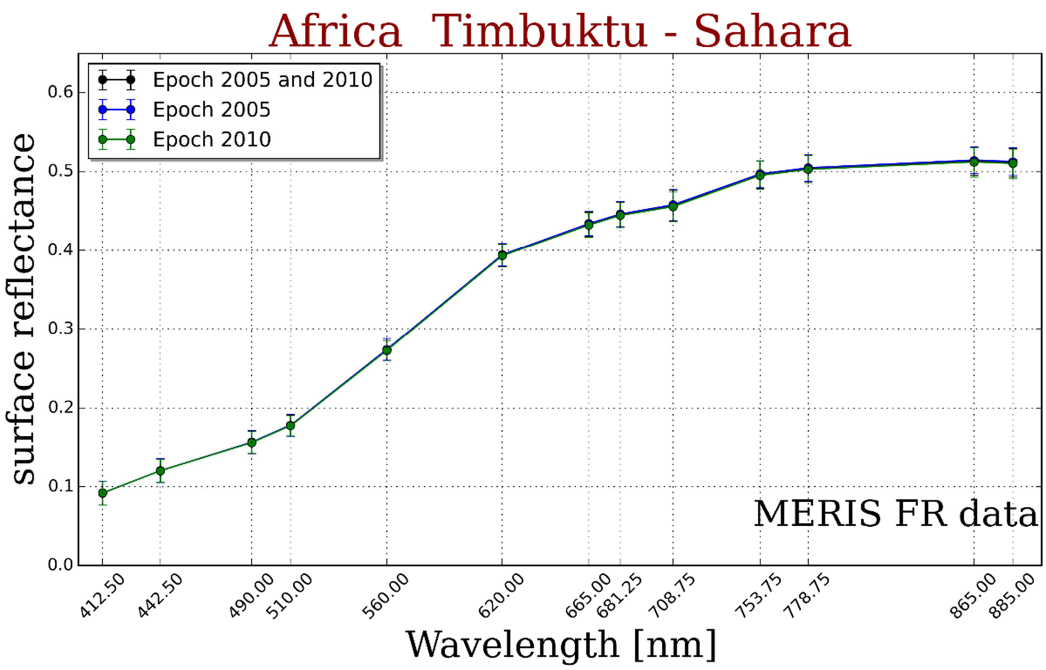

Figure 5-19: Spectra - Africa - Timbuktu Sahara - MERIS FR data

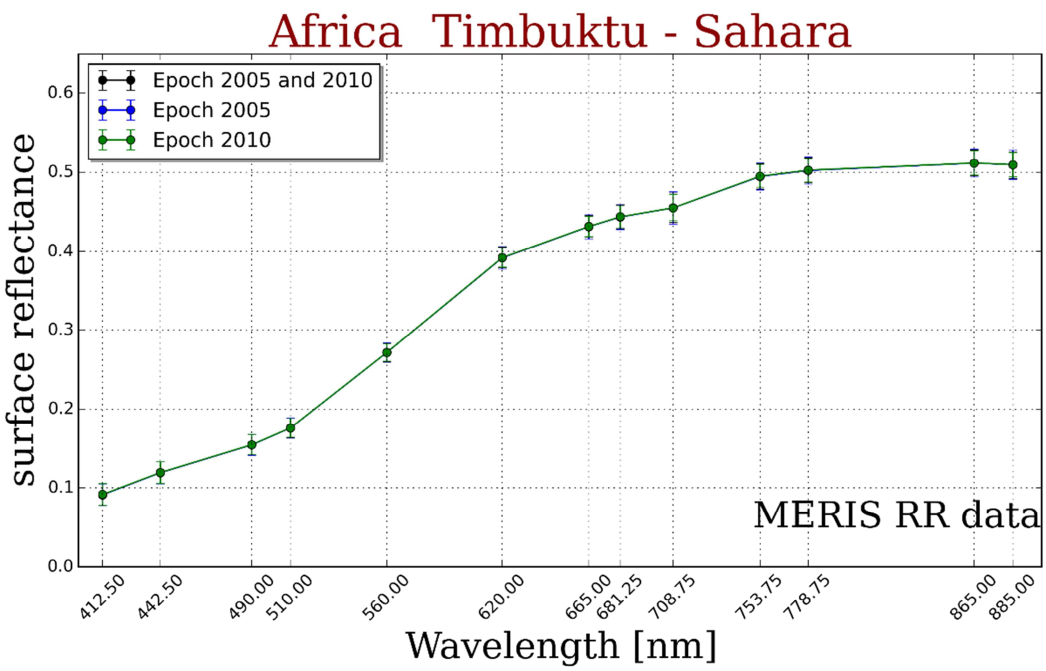

Figure 5-20: Spectra - Africa - Timbuktu Sahara - MERIS RR data

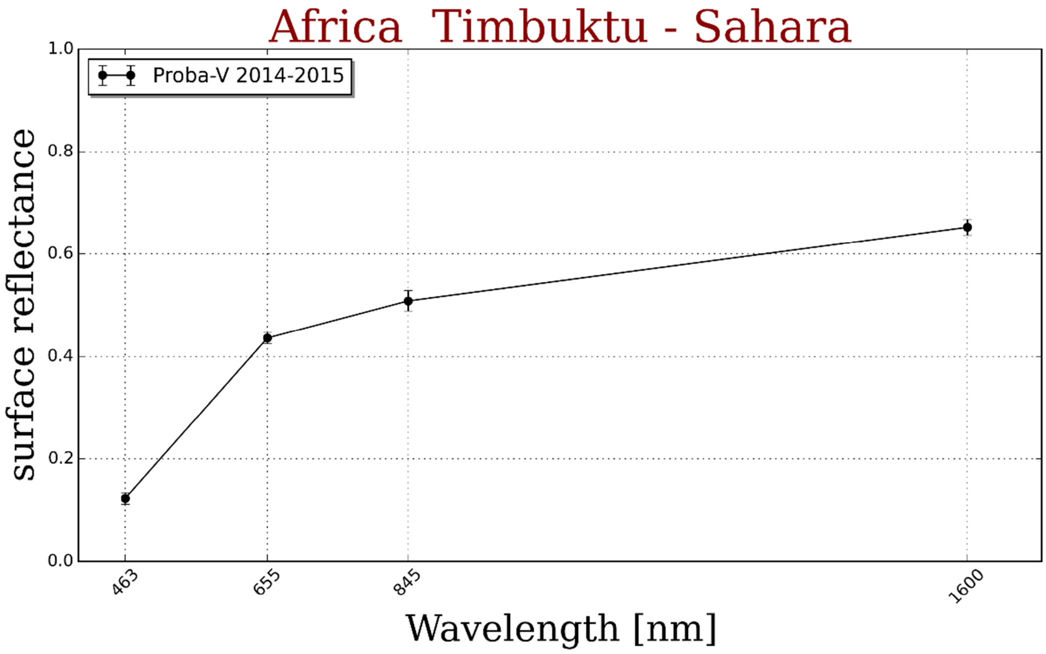

Figure 5-21: Spectra - Africa - Timbuktu Sahara – PROBA-V data

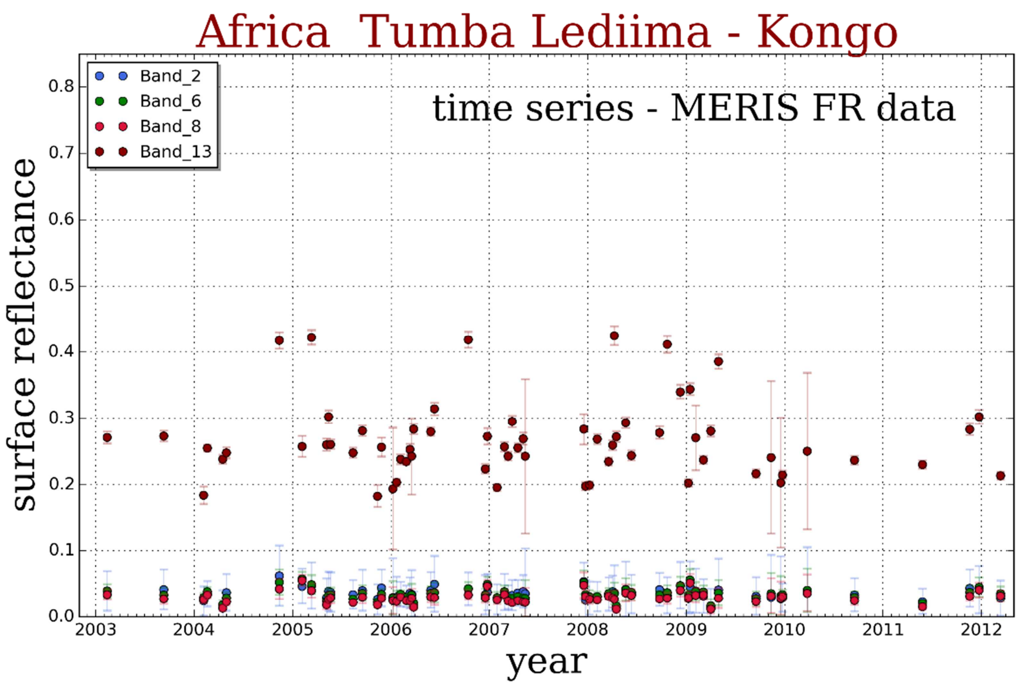

Figure 5-22: SR time series from MERIS FR data - 2003-2012 - Africa - Tumba Lediima Kongo

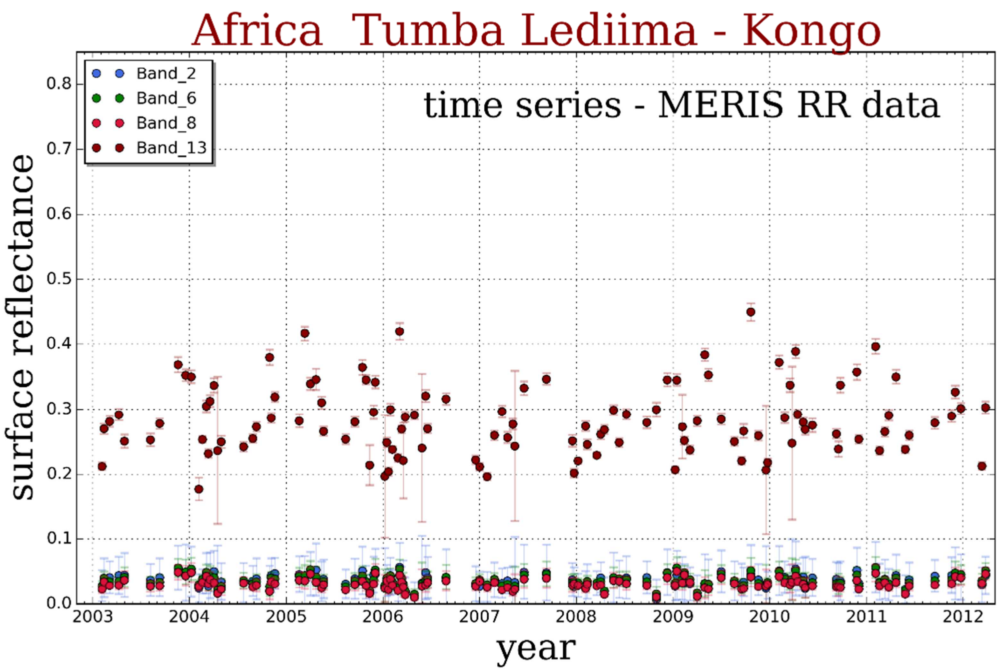

Figure 5-23: SR time series from MERIS RR data - 2003-2012 - Africa - Tumba Lediima Kongo

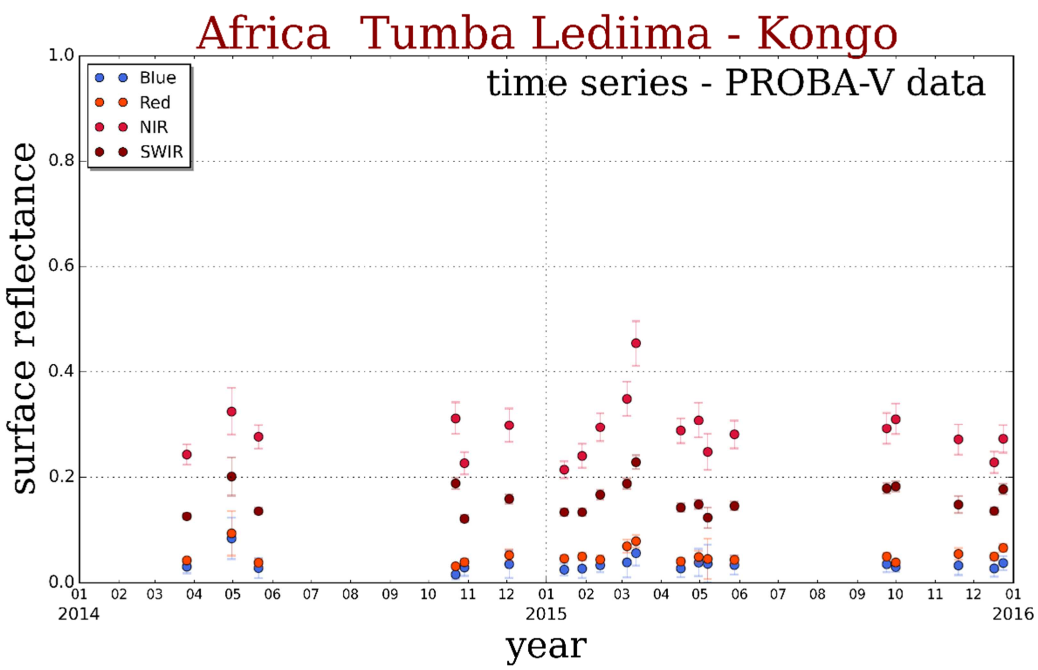

Figure 5-24: SR time series from PROBA-V data - 2014-2016 - Africa - Tumba Lediima Kongo

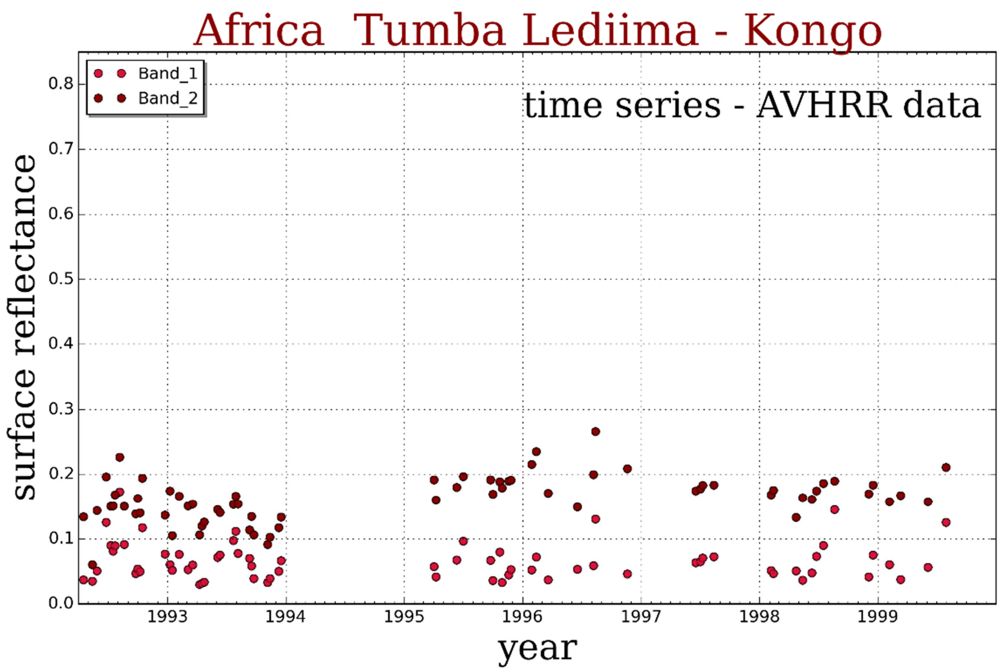

Figure 5-25: SR time series from AVHRR data - 1992-1999 - Africa - Tumba Lediima Kongo

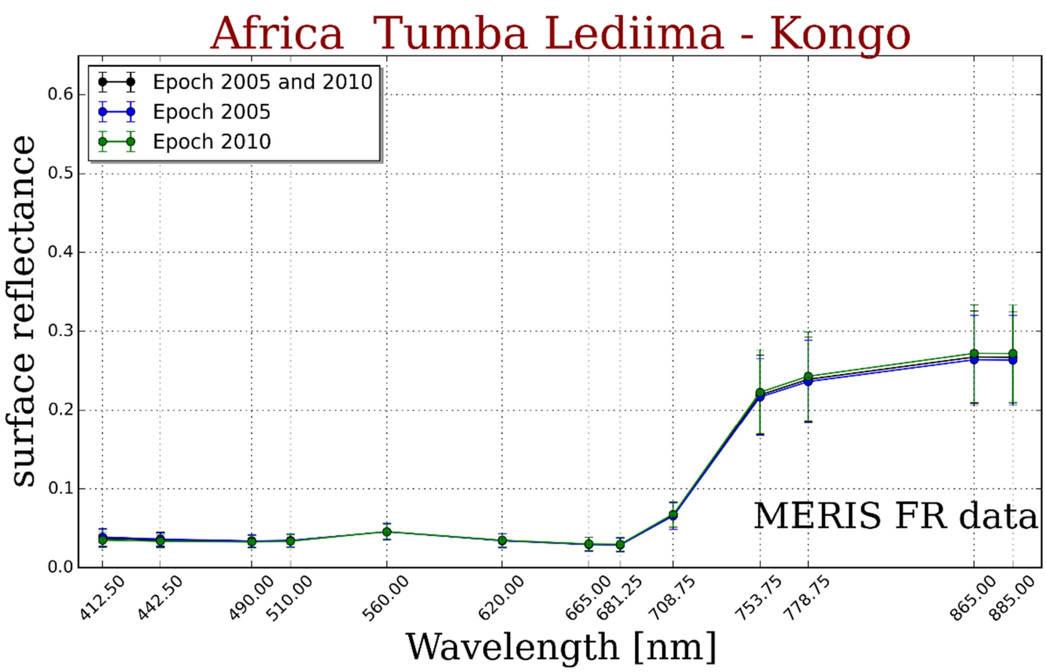

Figure 5-26: Spectra - Africa - Tumba Lediima Kongo - MERIS FR data

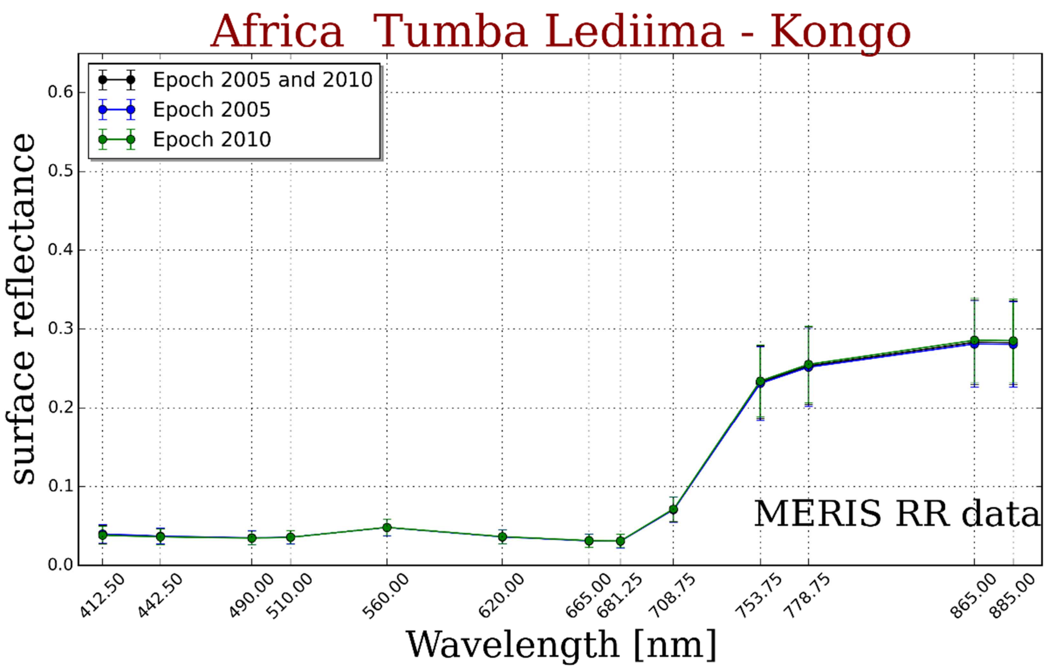

Figure 5-27: Spectra - Africa - Tumba Lediima Kongo - MERIS RR data

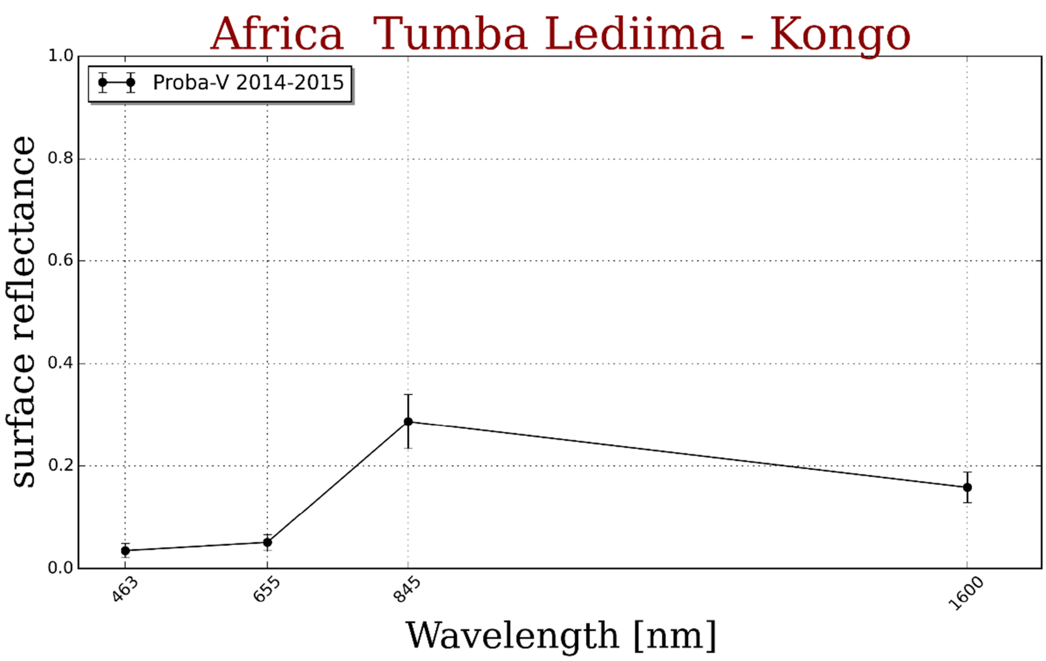

Figure 5-28: Spectra - Africa - Tumba Lediima Kongo – PROBA-V data

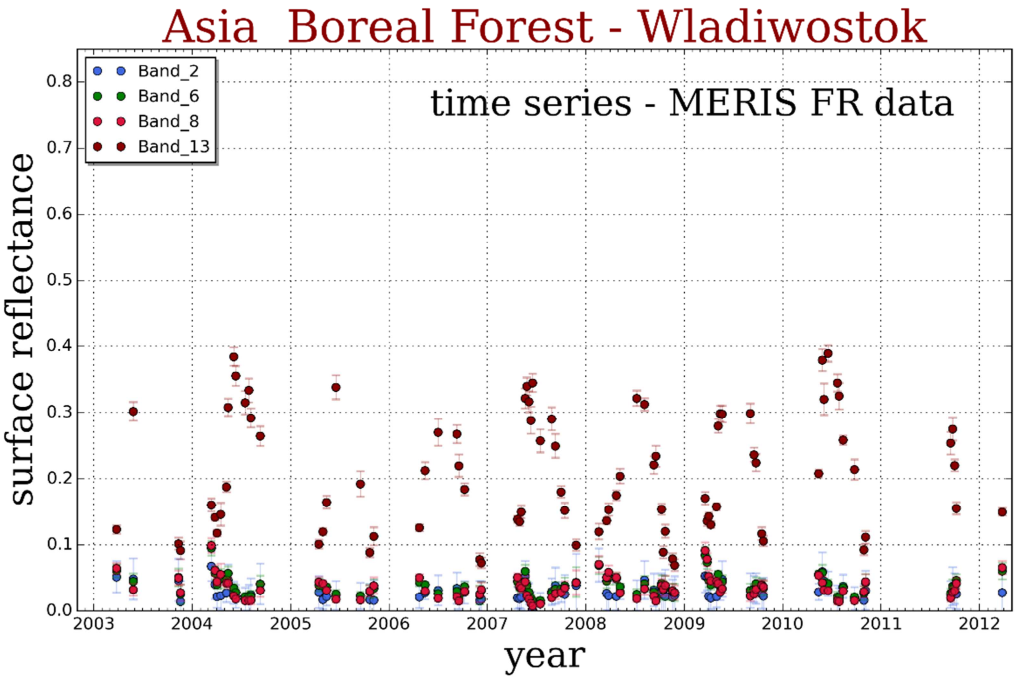

Figure 5-29: SR time series from MERIS FR data - 2003-2012 - Asia - Boreal Forest Wladiwostok

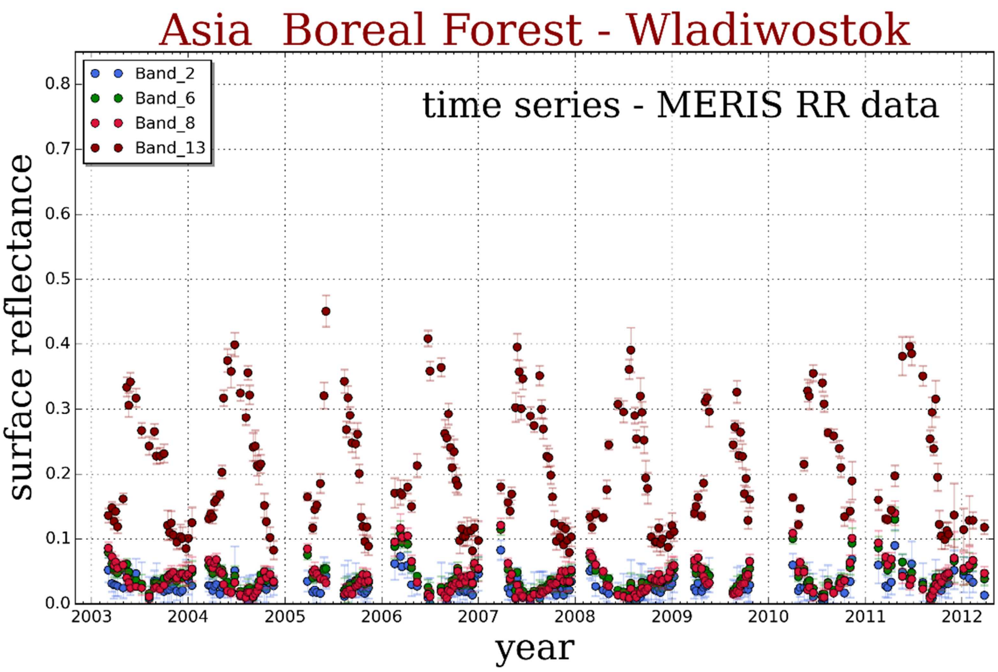

Figure 5-30: SR time series from MERIS RR data - 2003-2012 - Asia - Boreal Forest Wladiwostok

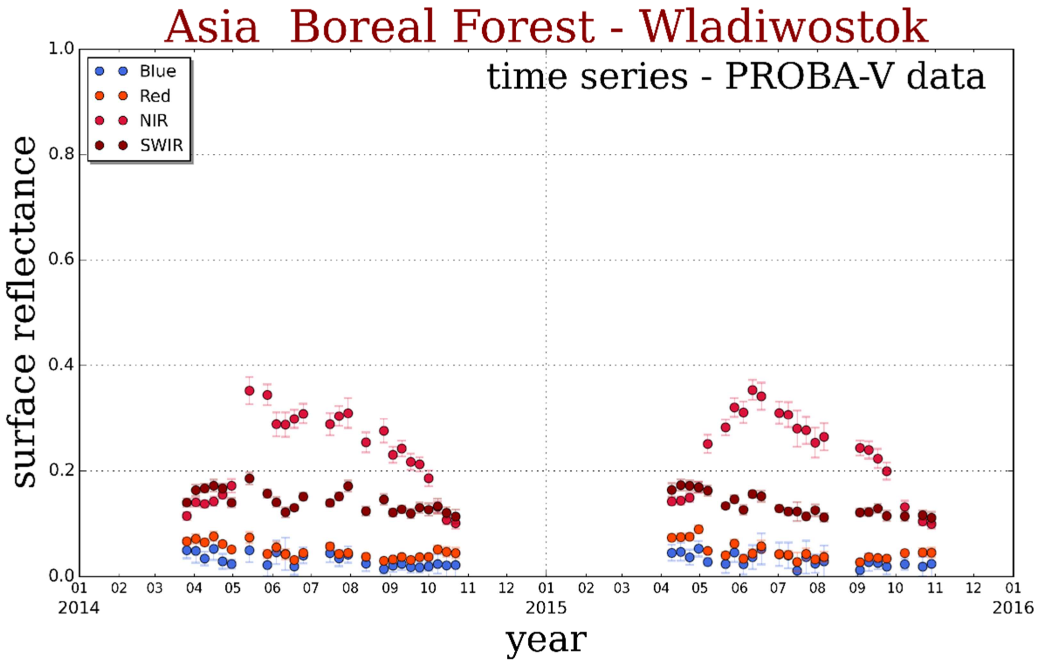

Figure 5-31: SR time series from PROBA-V data - 2014-2016 - Asia - Boreal Forest Wladiwostok

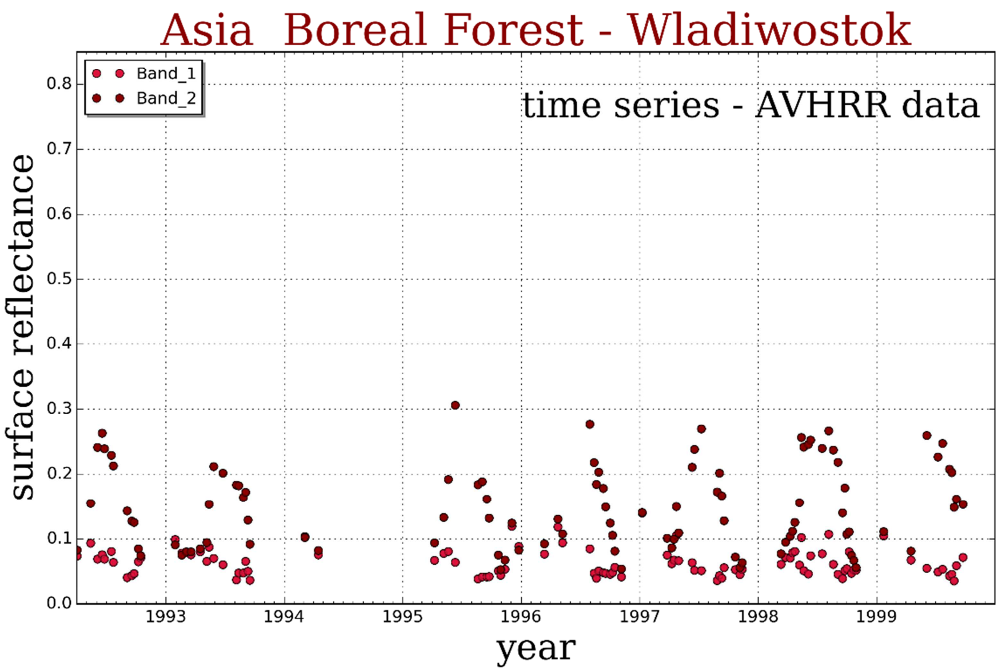

Figure 5-32: SR time series from AVHRR data - 1992-1999 - Asia - Boreal Forest Wladiwostok

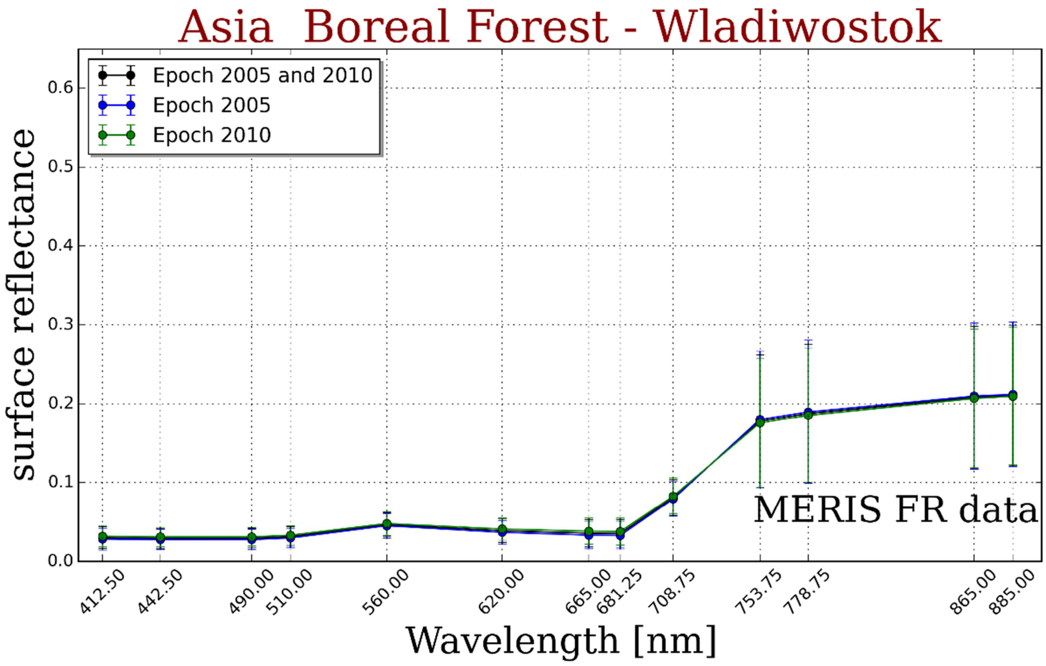

Figure 5-33: Spectra - Asia - Boreal Forest Wladiwostok - MERIS FR data

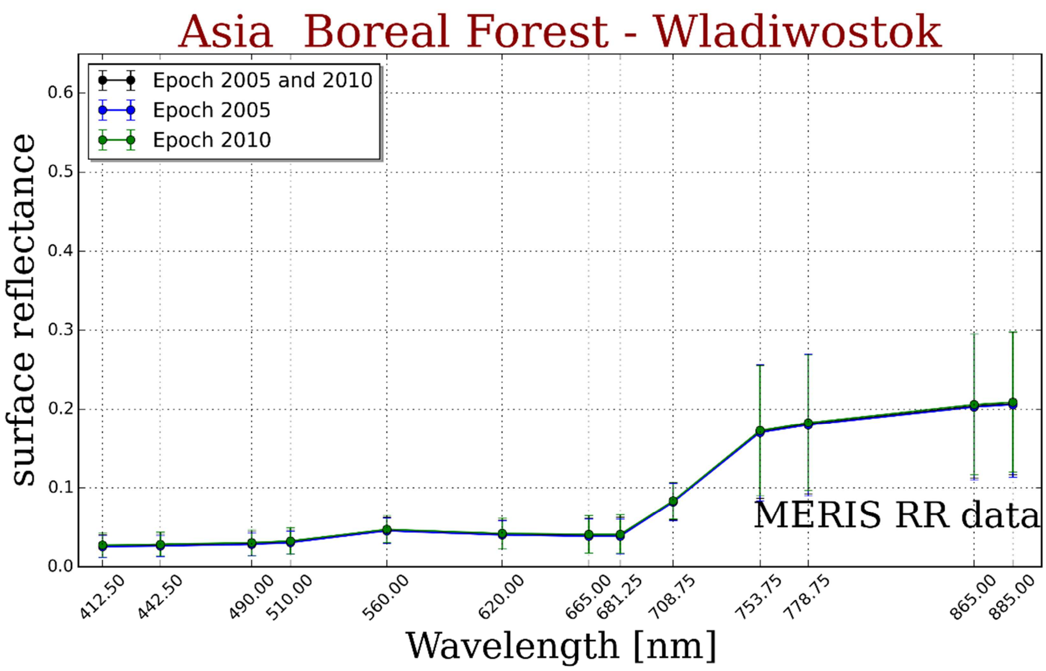

Figure 5-34: Spectra - Asia - Boreal Forest Wladiwostok - MERIS RR data

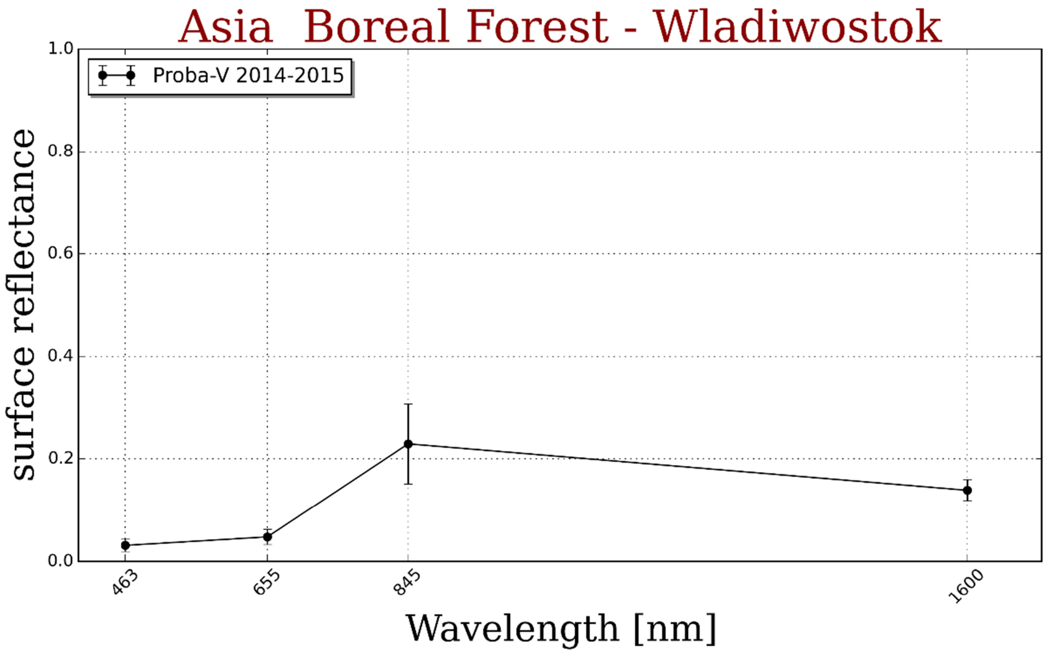

Figure 5-35: Spectra - Asia - Boreal Forest Wladiwostok – PROBA-V data

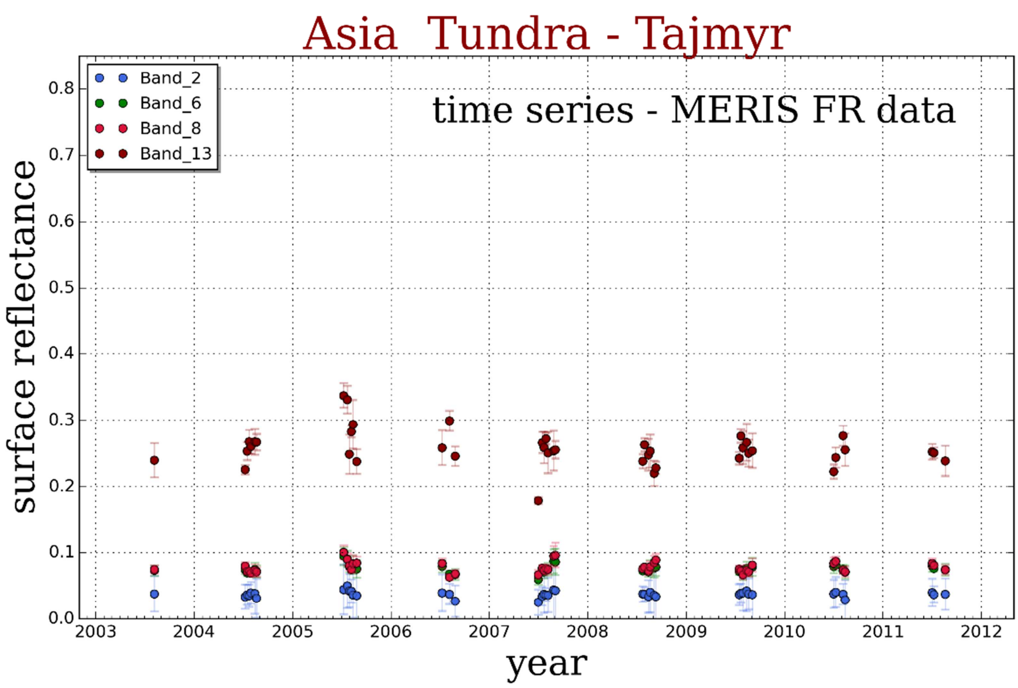

Figure 5-36: SR time series from MERIS FR data - 2003-2012 - Asia - Tundra Tajmyr

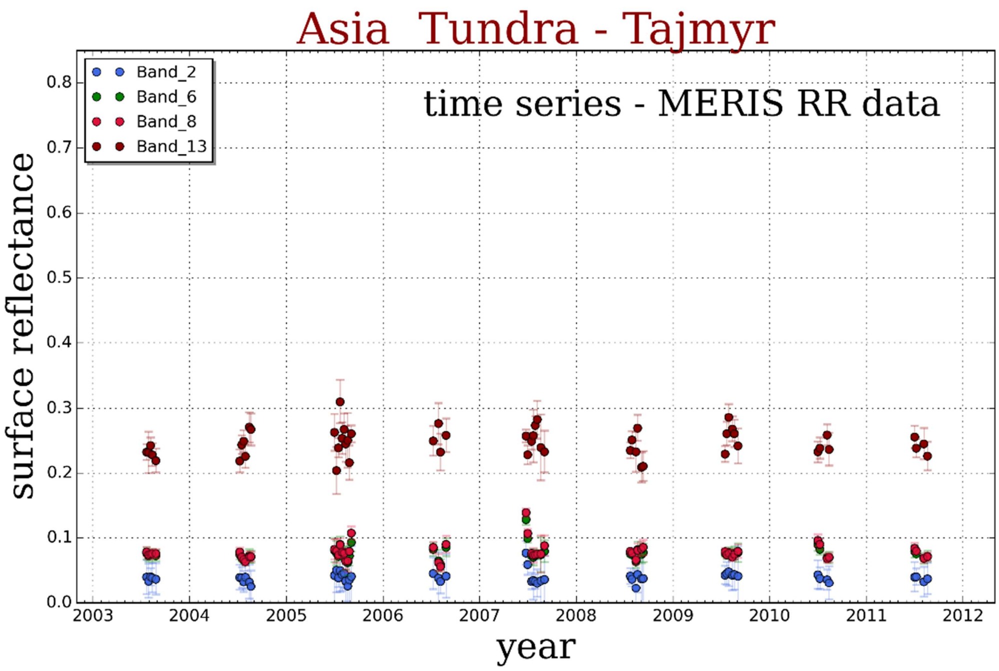

Figure 5-37: SR time series from MERIS RR data - 2003-2012 - Asia - Tundra Tajmyr

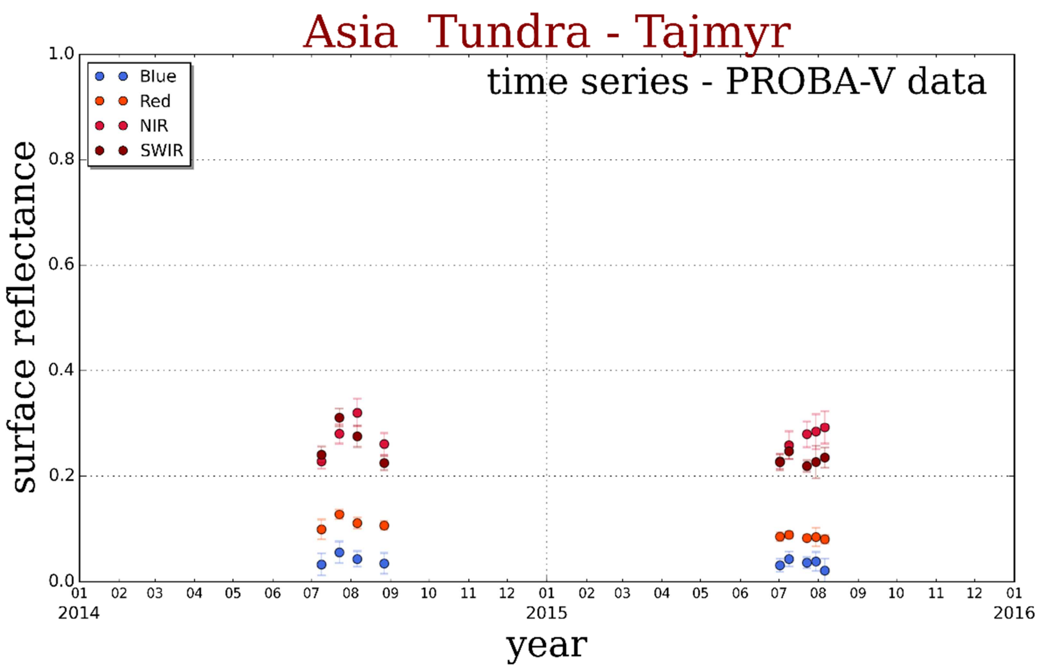

Figure 5-38: SR time series from PROBA-V data - 2014-2016 - Asia - Tundra Tajmyr

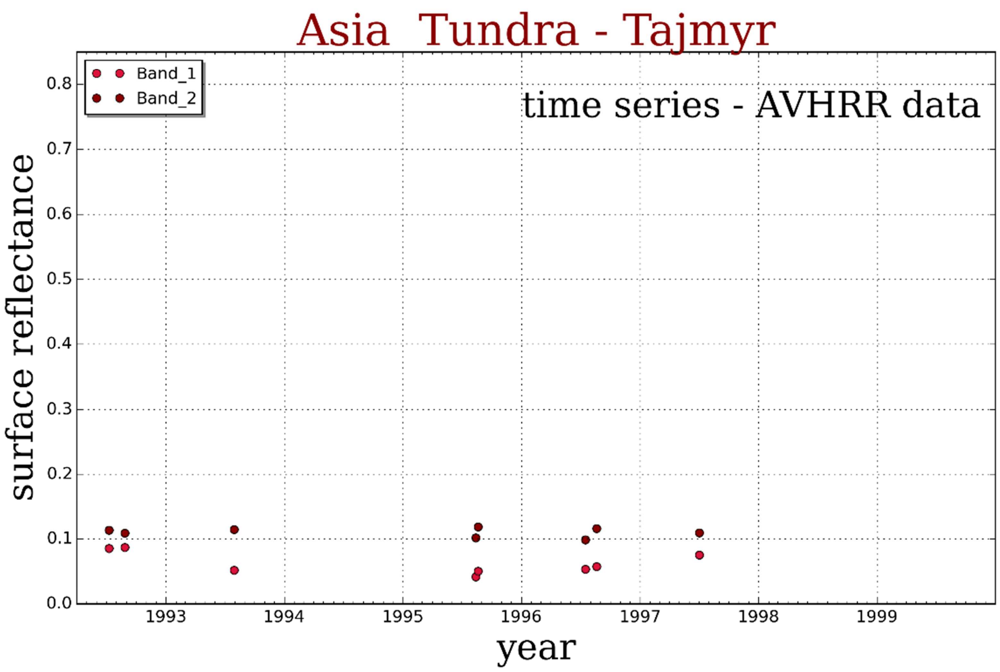

Figure 5-39: SR time series from AVHRR data - 1992-1999 - Asia - Tundra Tajmyr

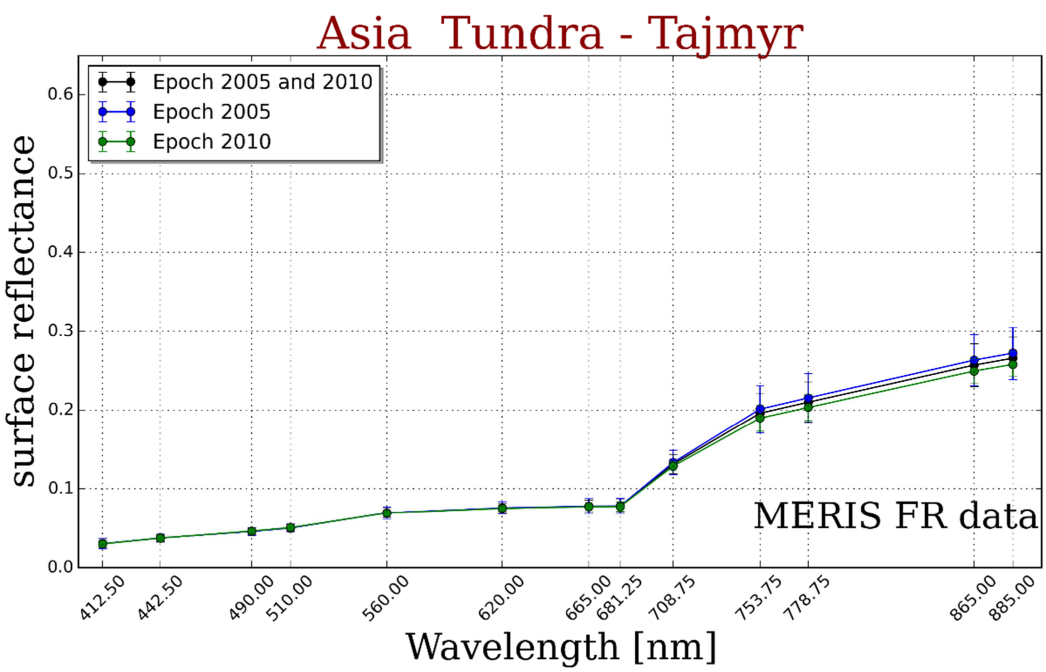

Figure 5-40: Spectra - Asia - Tundra Tajmyr - MERIS FR data

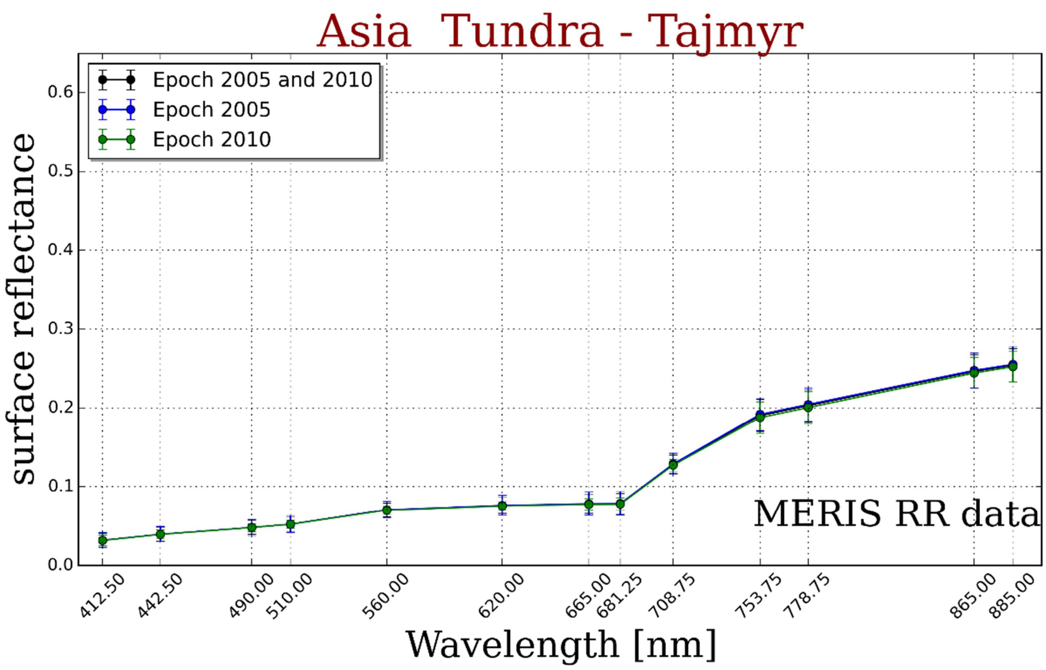

Figure 5-41: Spectra - Asia - Tundra Tajmyr - MERIS RR data

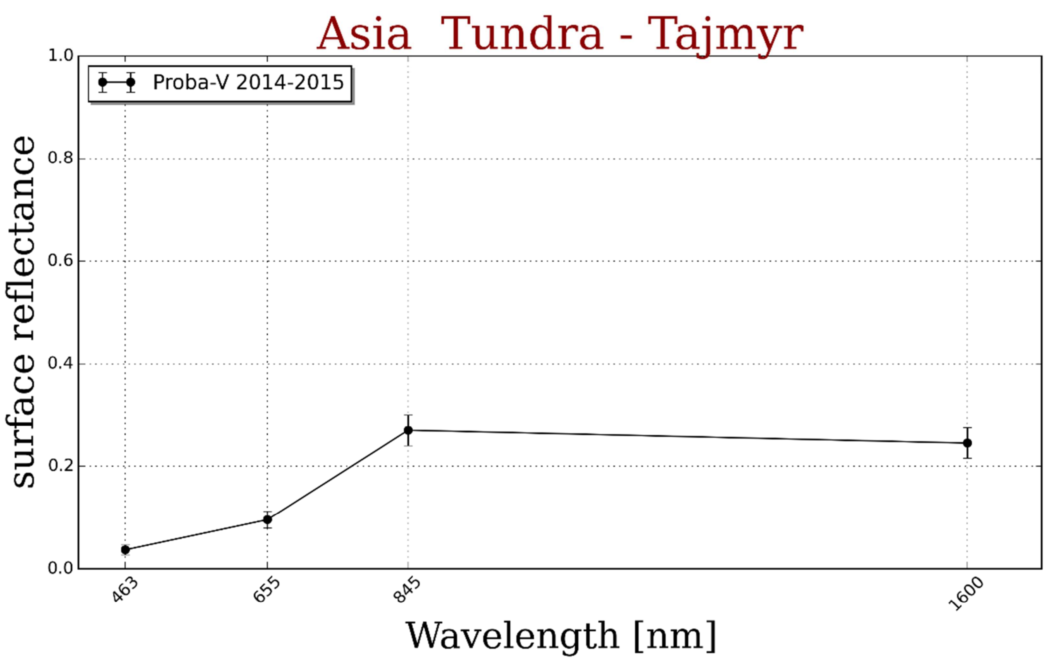

Figure 5-42: Spectra - Asia - Tundra Tajmyr – PROBA-V data

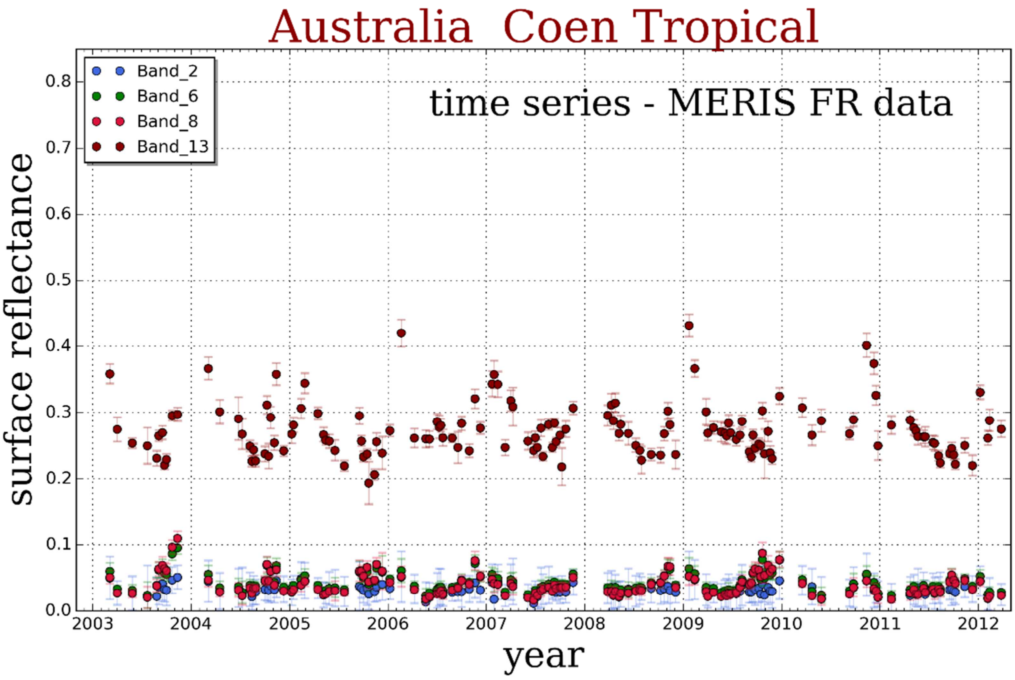

Figure 5-43: SR time series from MERIS FR data - 2003-2012 – Australia and Oceania - Coen Tropical

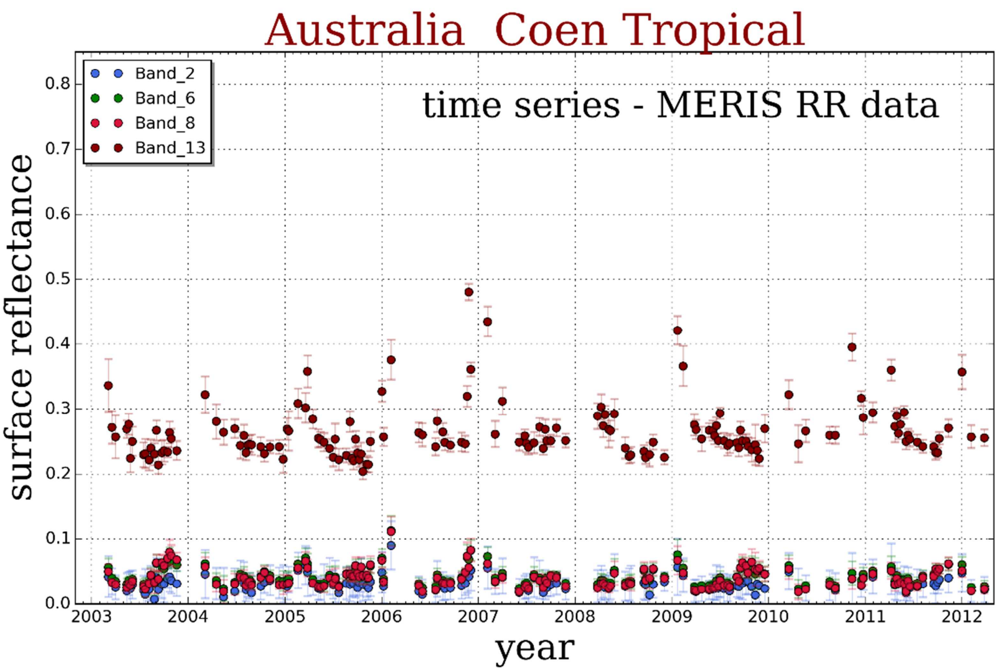

Figure 5-44: SR time series from MERIS RR data - 2003-2012 – Australia and Oceania - Coen Tropical

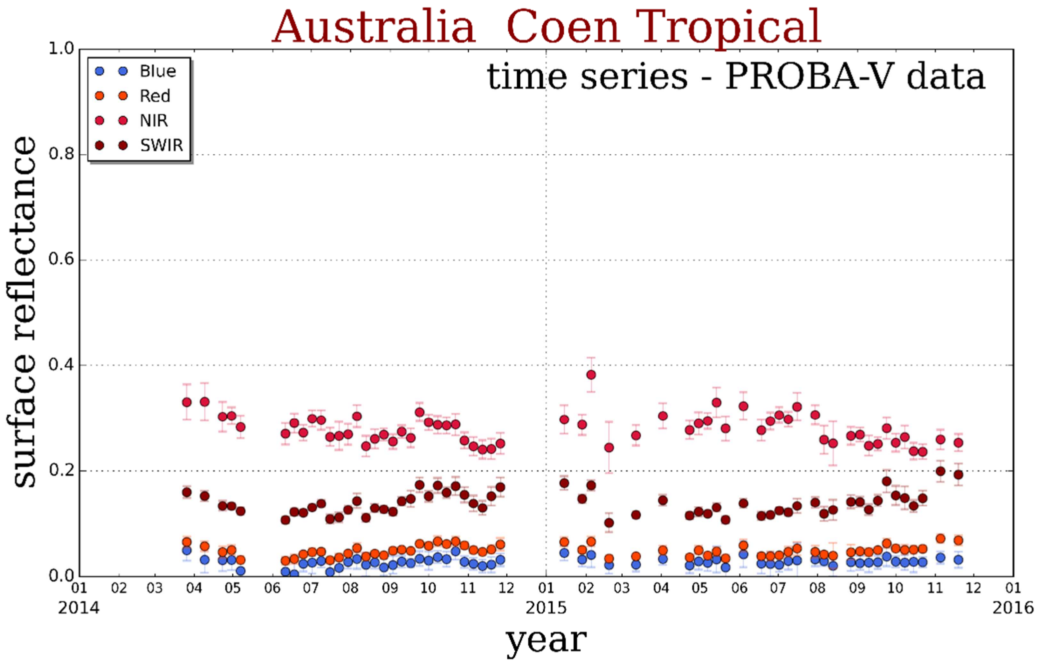

Figure 5-45: SR time series from PROBA-V data - 2014-2016 – Australia and Oceania - Coen Tropical

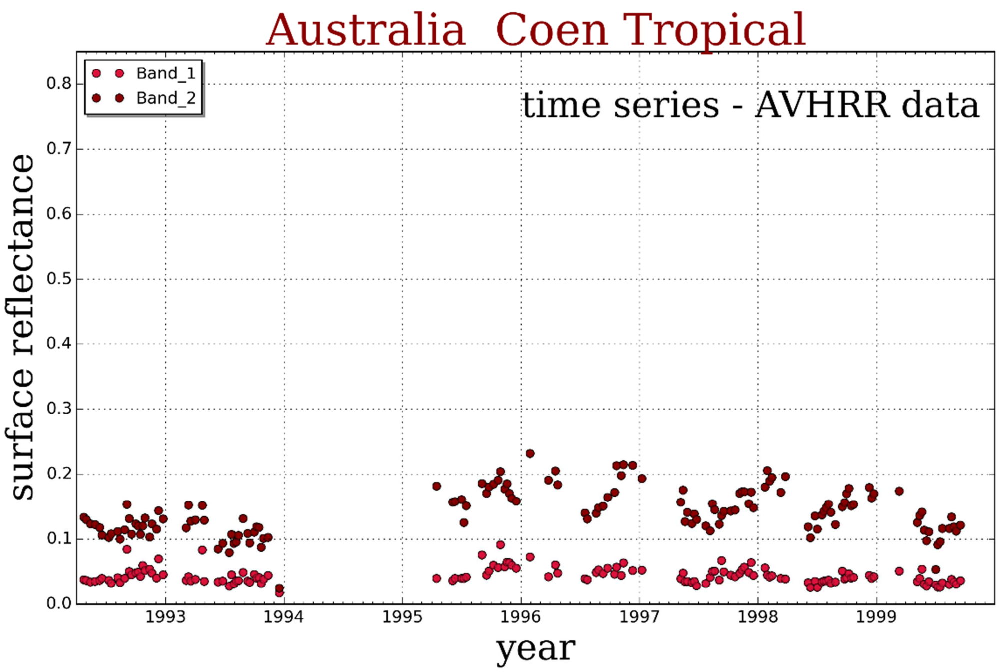

Figure 5-46: SR time series from AVHRR data - 1992-1999 – Australia and Oceania - Coen Tropical

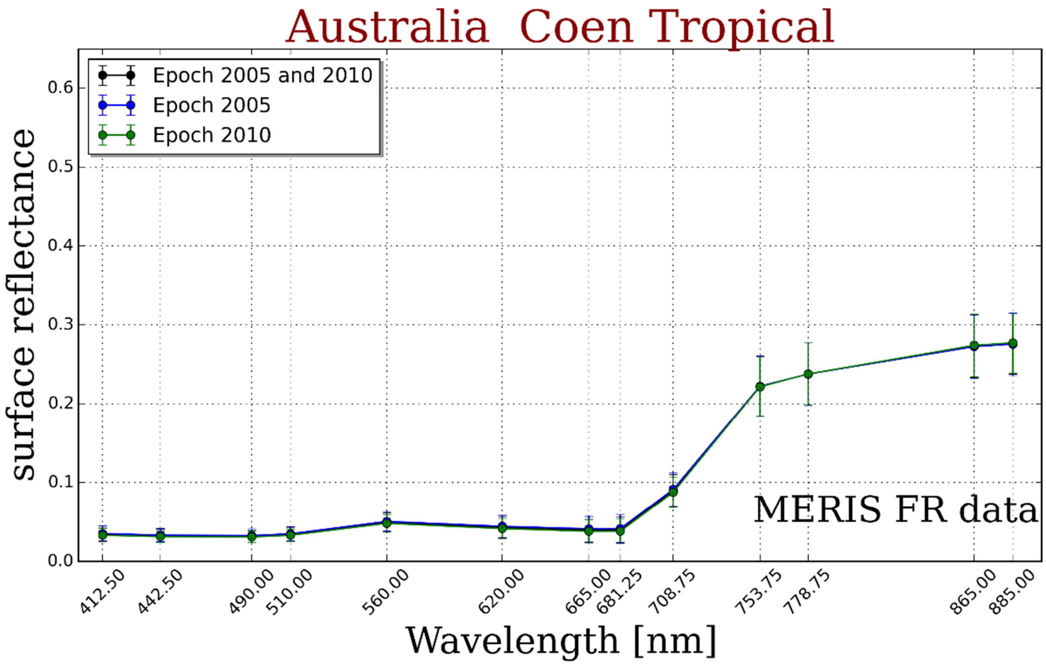

Figure 5-47: Spectra – Australia and Oceania - Coen Tropical - MERIS FR data

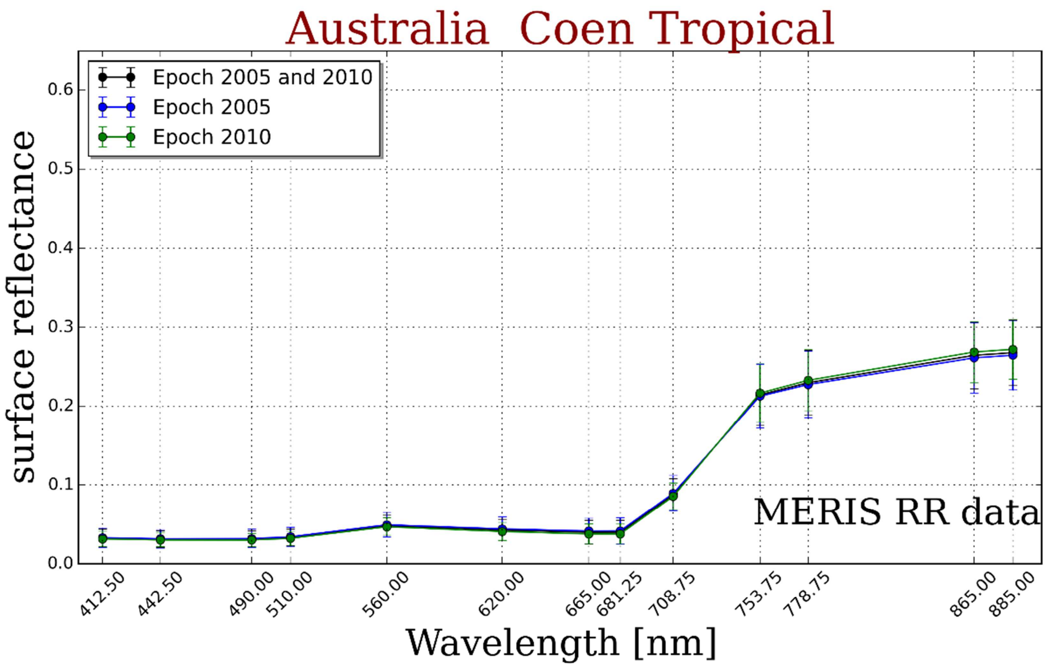

Figure 5-48: Spectra – Australia and Oceania - Coen Tropical - MERIS RR data

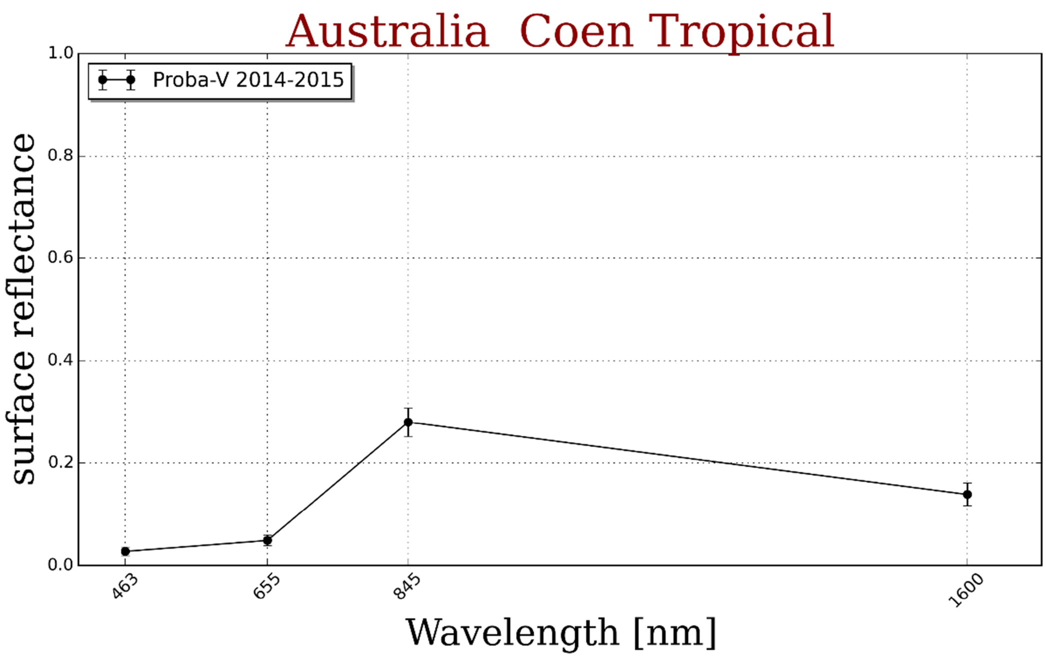

Figure 5-49: Spectra – Australia and Oceania - Coen Tropical – PROBA-V data

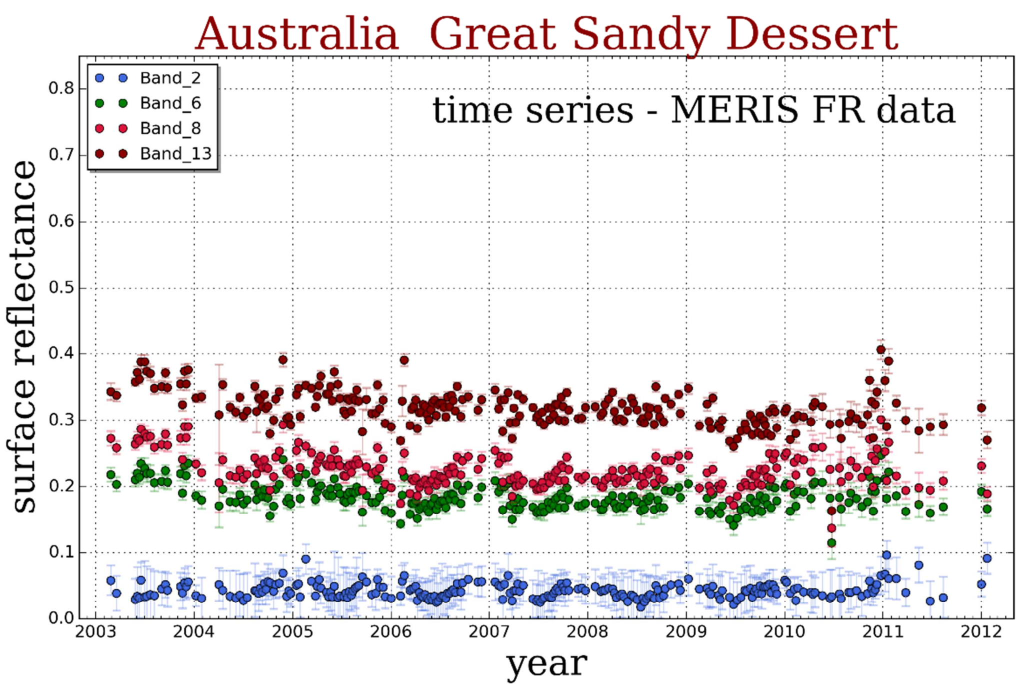

Figure 5-50: SR time series from MERIS FR data - 2003-2012 – Australia and Oceania - Great Sandy Dessert

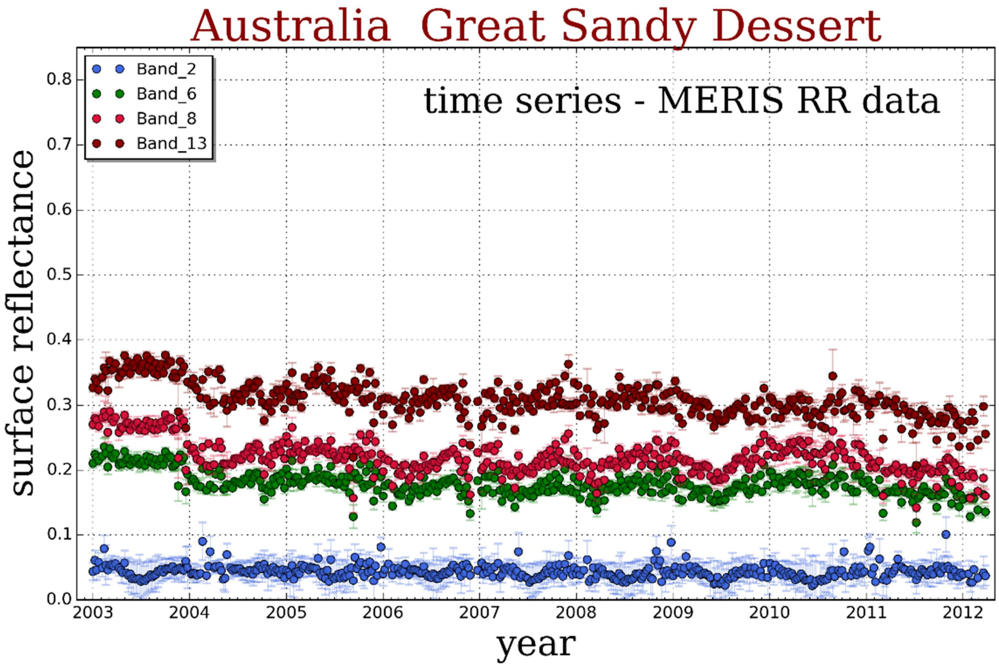

Figure 5-51: SR time series from MERIS RR data - 2003-2012 – Australia and Oceania - Great Sandy Dessert

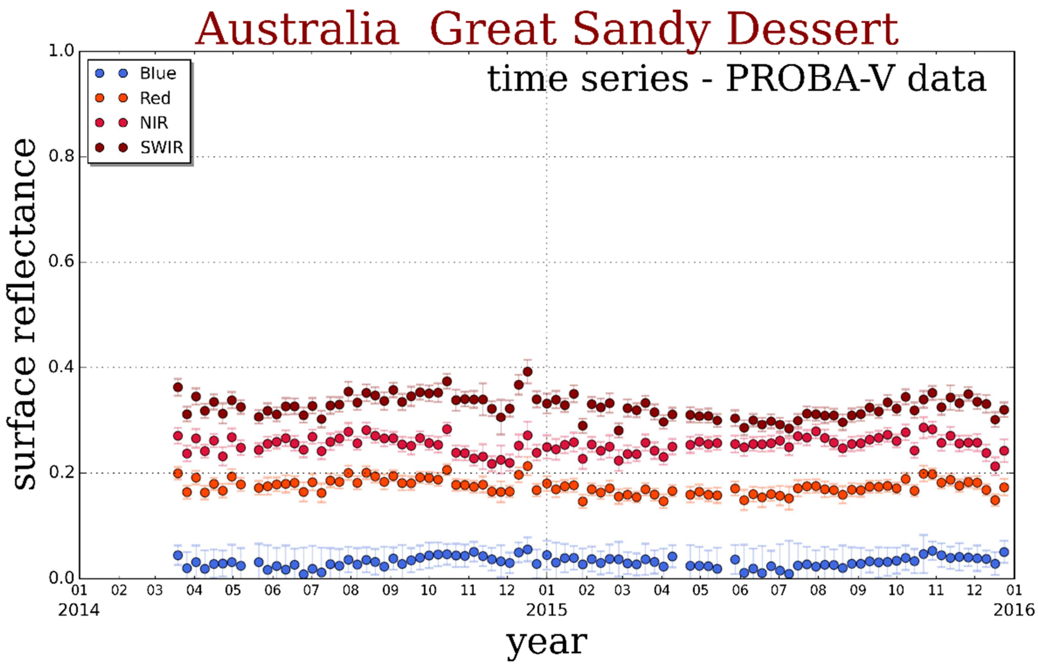

Figure 5-52: SR time series from PROBA-V data - 2014-2016 – Australia and Oceania - Great Sandy Dessert

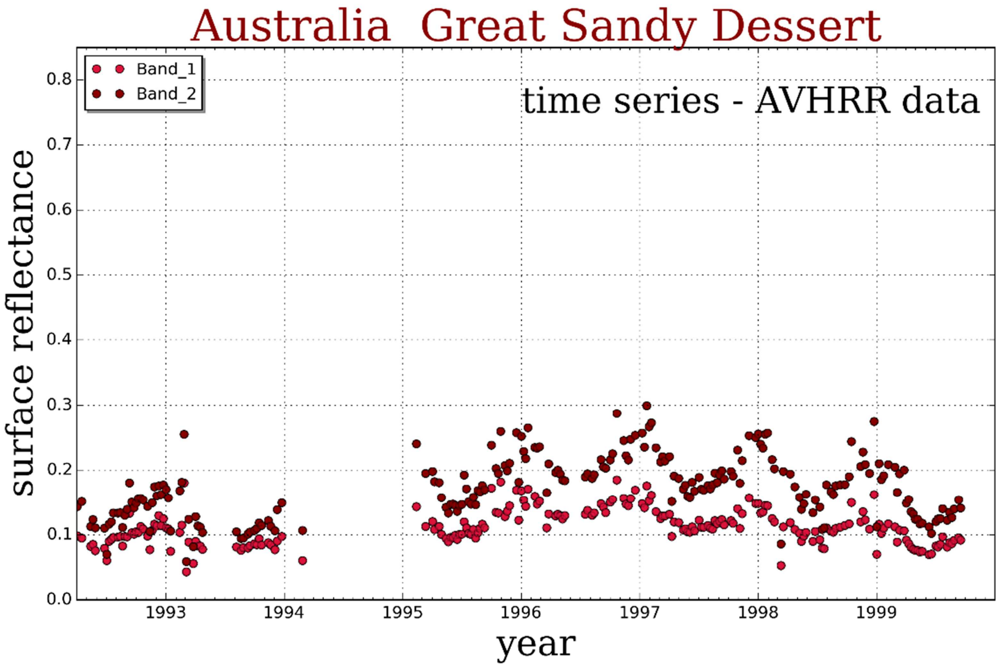

Figure 5-53: SR time series from AVHRR data - 1992-1999 – Australia and Oceania - Great Sandy Dessert

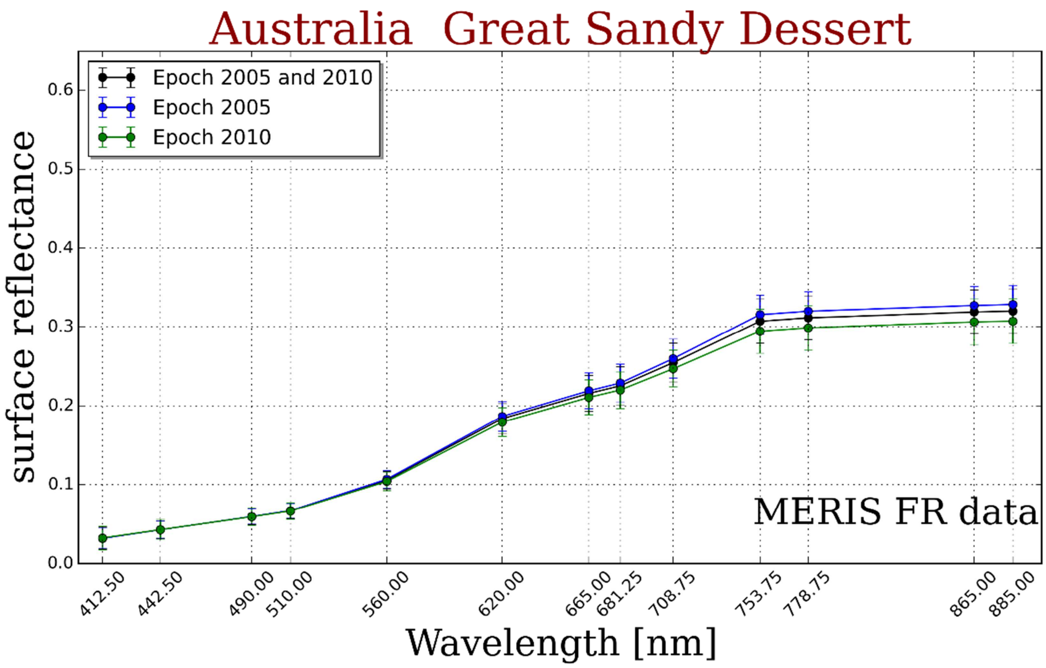

Figure 5-54: Spectra – Australia and Oceania - Great Sandy Dessert - MERIS FR data

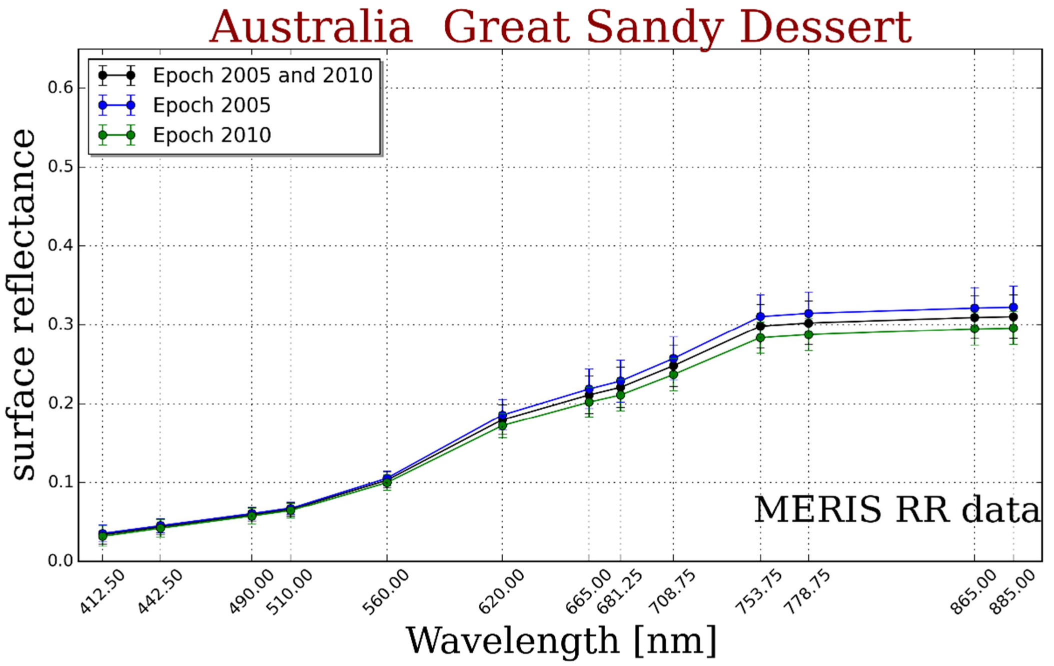

Figure 5-55: Spectra – Australia and Oceania - Great Sandy Dessert - MERIS RR data

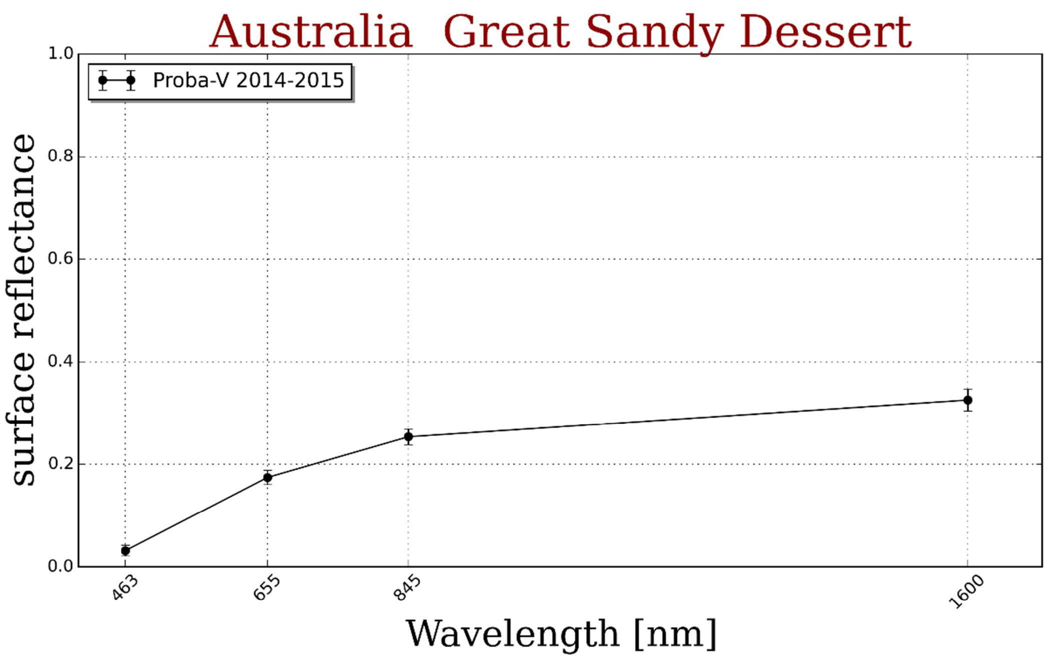

Figure 5-56: Spectra – Australia and Oceania - Great Sandy Dessert – PROBA-V data

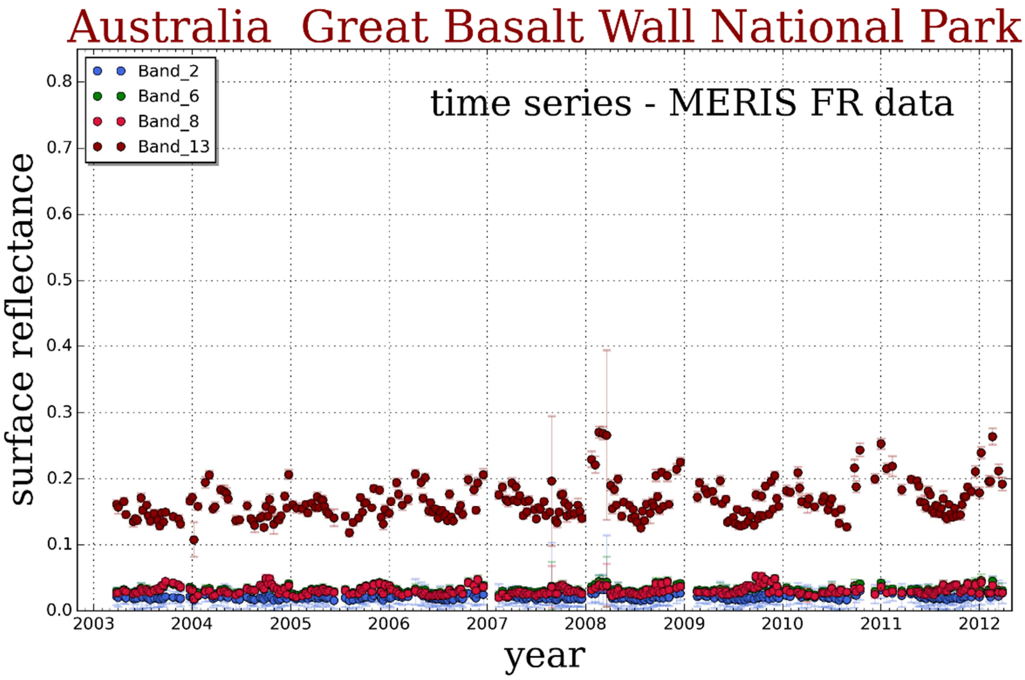

Figure 5-57: SR time series from MERIS FR data - 2003-2012 – Australia and Oceania - Great Basalt Wall National Park

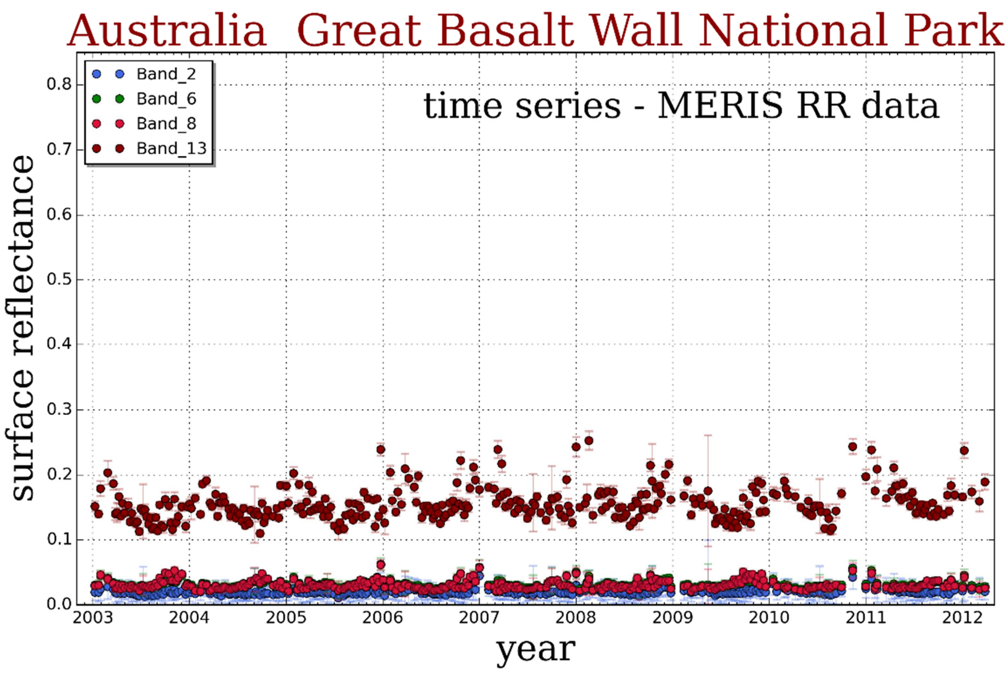

Figure 5-58: SR time series from MERIS RR data - 2003-2012 – Australia and Oceania - Great Basalt Wall National Park

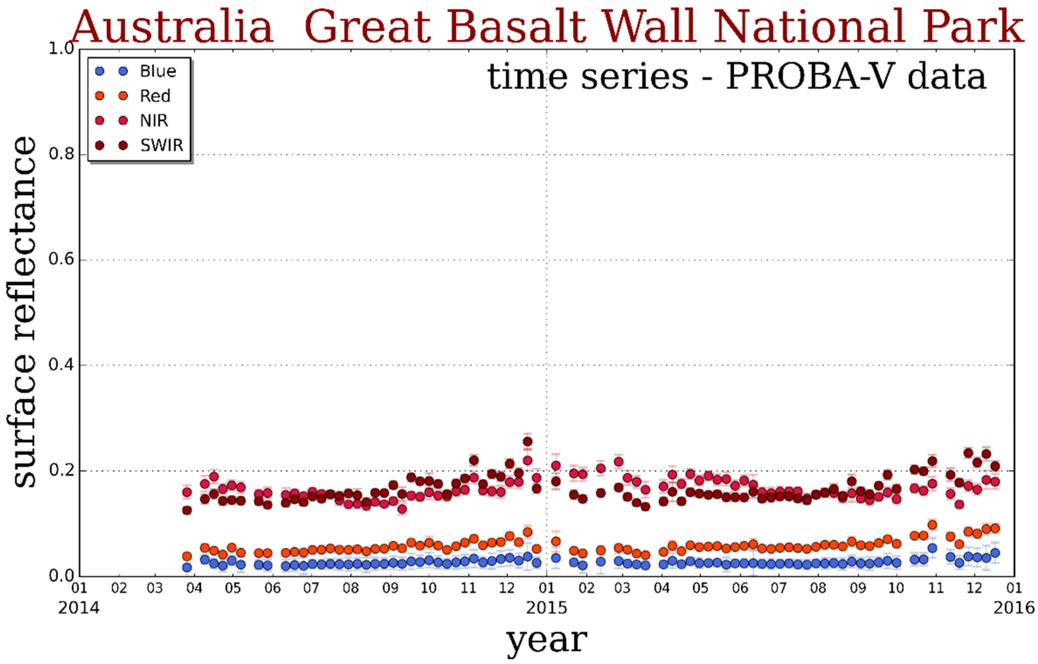

Figure 5-59: SR time series from PROBA-V data - 2014-2016 – Australia and Oceania - Great Basalt Wall National Park

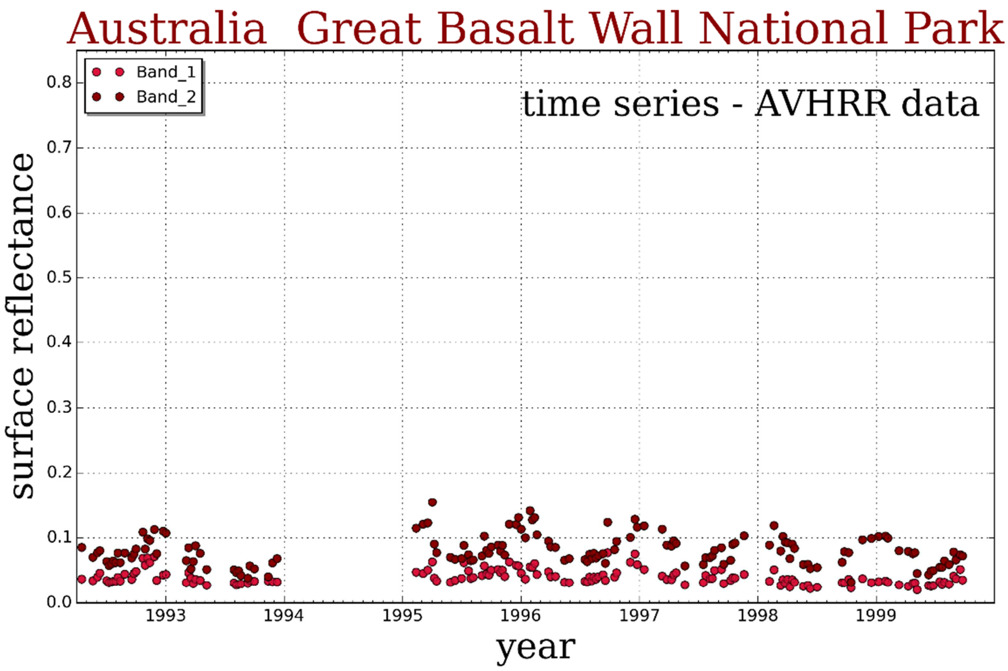

Figure 5-60: SR time series from AVHRR data - 1992-1999 – Australia and Oceania - Great Basalt Wall National Park

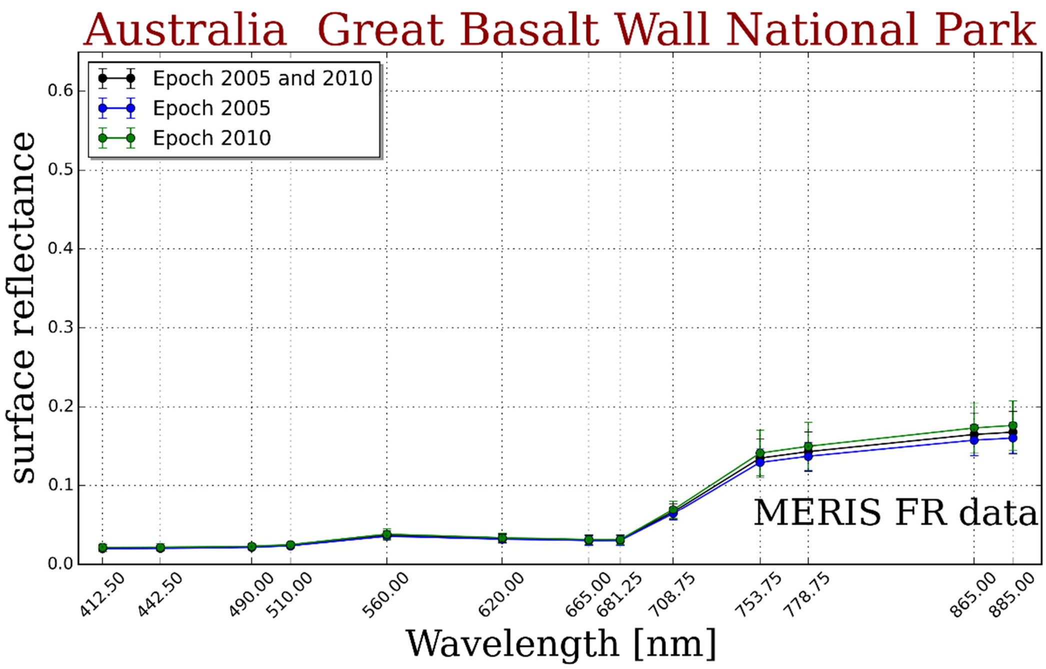

Figure 5-61: Spectra – Australia and Oceania - Great Basalt Wall National Park - MERIS FR data

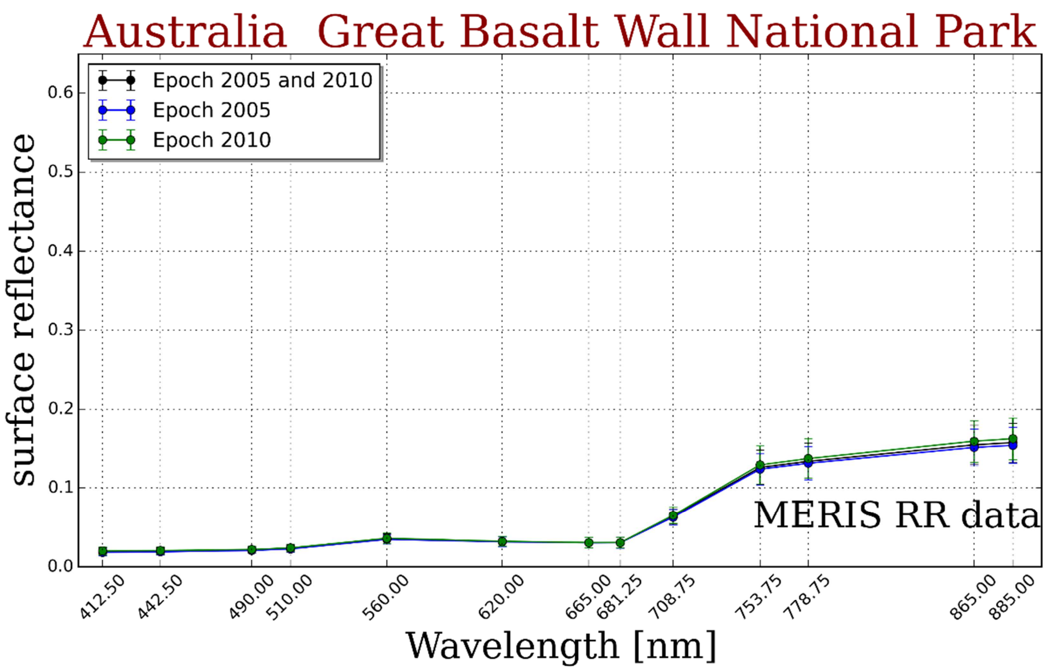

Figure 5-62: Spectra – Australia and Oceania - Great Basalt Wall National Park - MERIS RR data

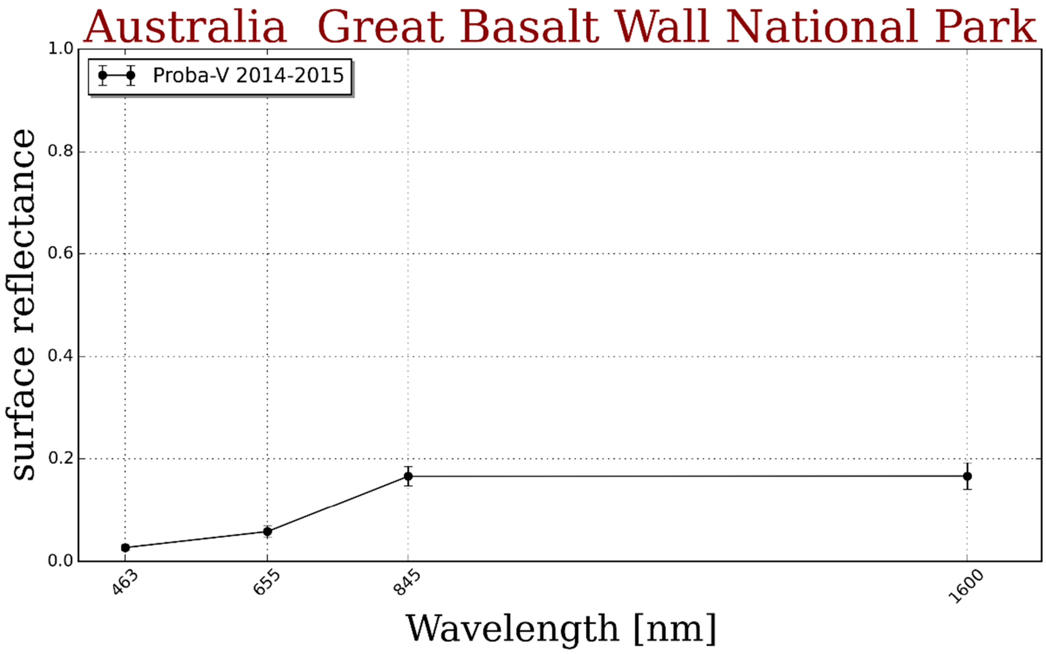

Figure 5-63: Spectra – Australia and Oceania - Great Basalt Wall National Park – PROBA-V data

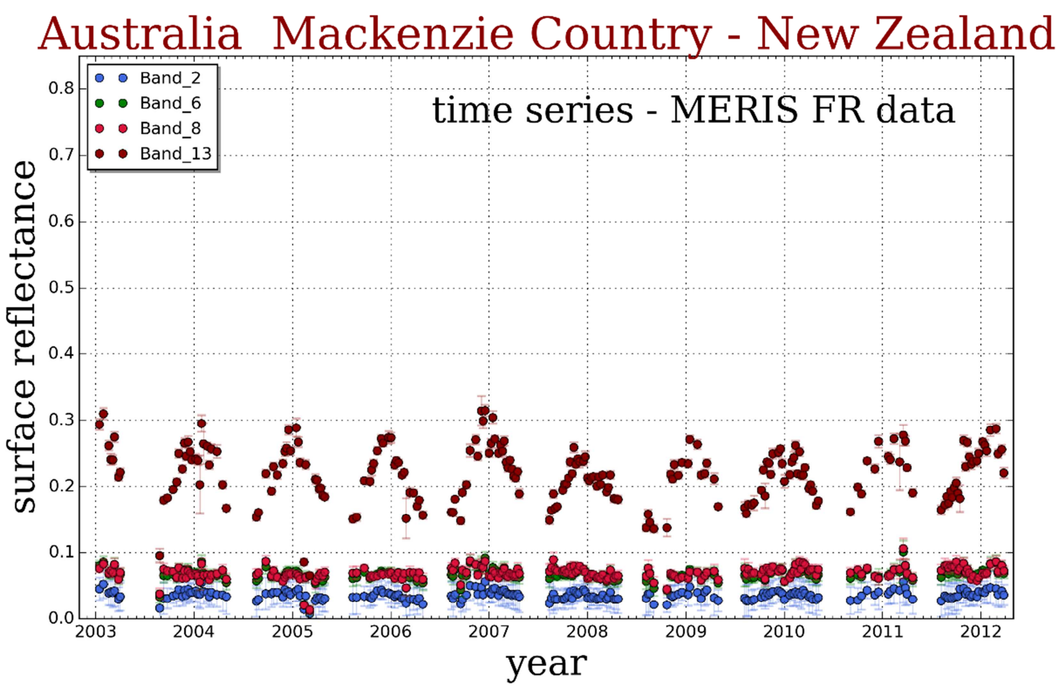

Figure 5-64: SR time series from MERIS FR data - 2003-2012 – Australia and Oceania - Mackenzie Country New Zealand

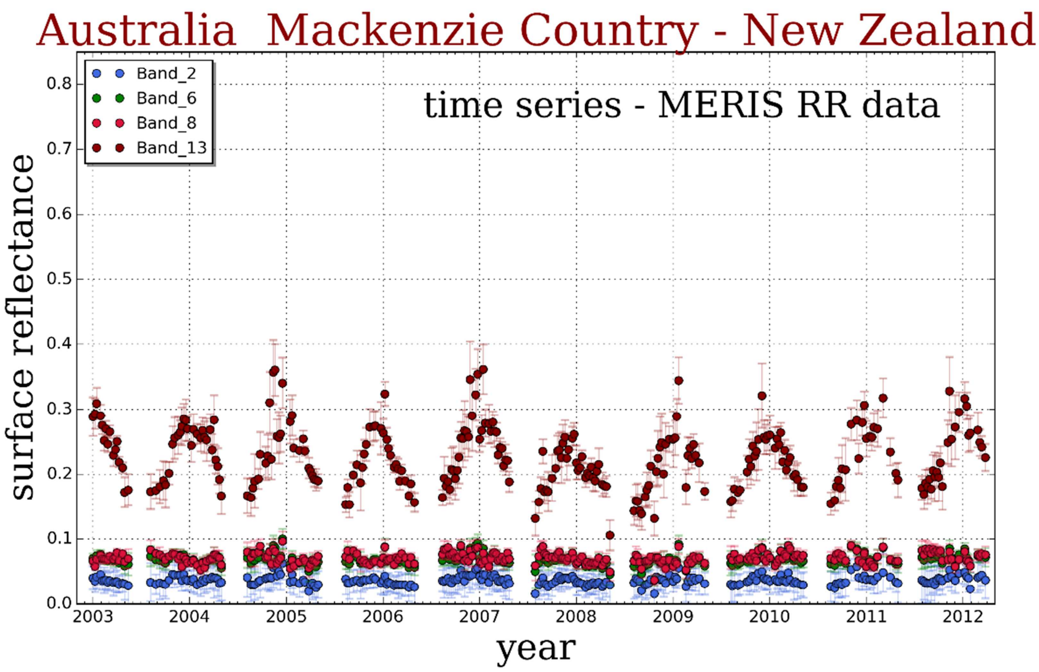

Figure 5-65: SR time series from MERIS RR data - 2003-2012 – Australia and Oceania - Mackenzie Country New Zealand

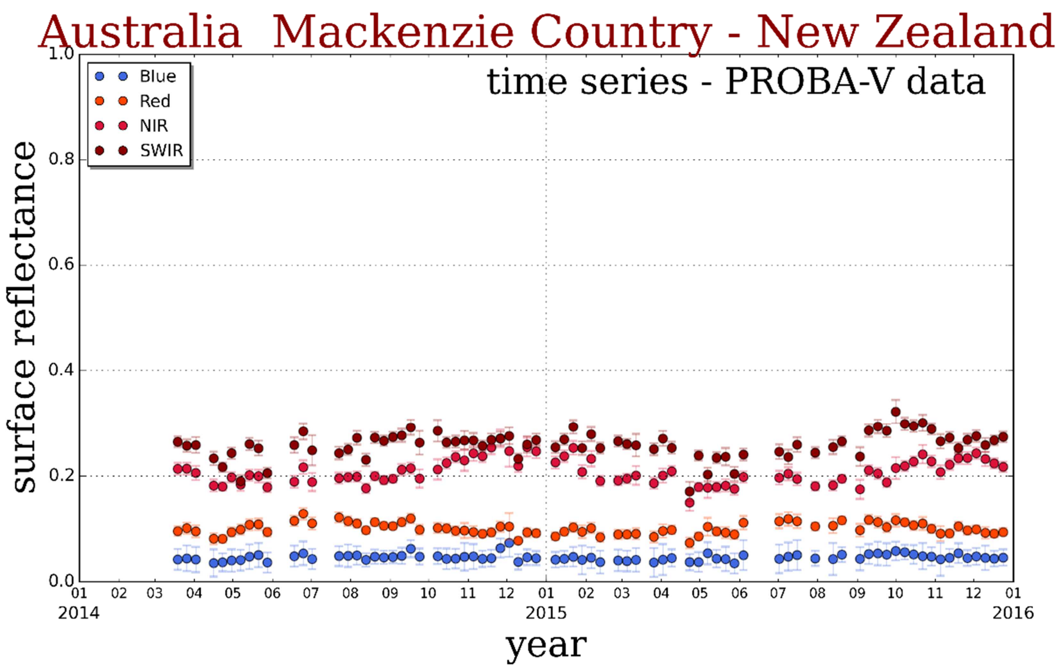

Figure 5-66: SR time series from PROBA-V data - 2014-2016 – Australia and Oceania - Mackenzie Country New Zealand

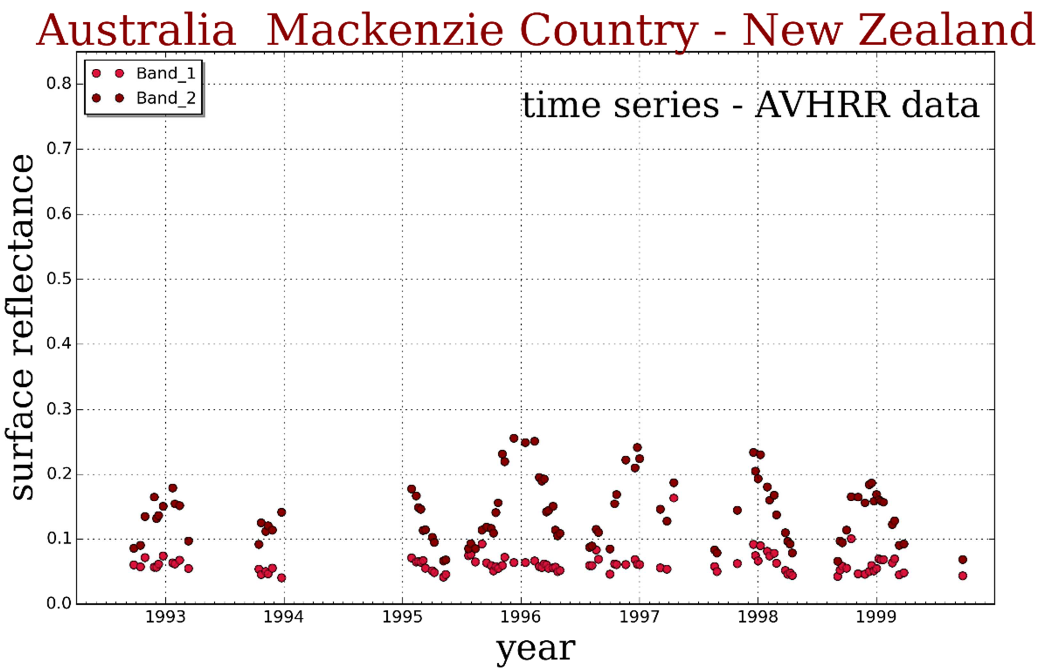

Figure 5-67: SR time series from AVHRR data - 1992-1999 – Australia and Oceania - Mackenzie Country New Zealand

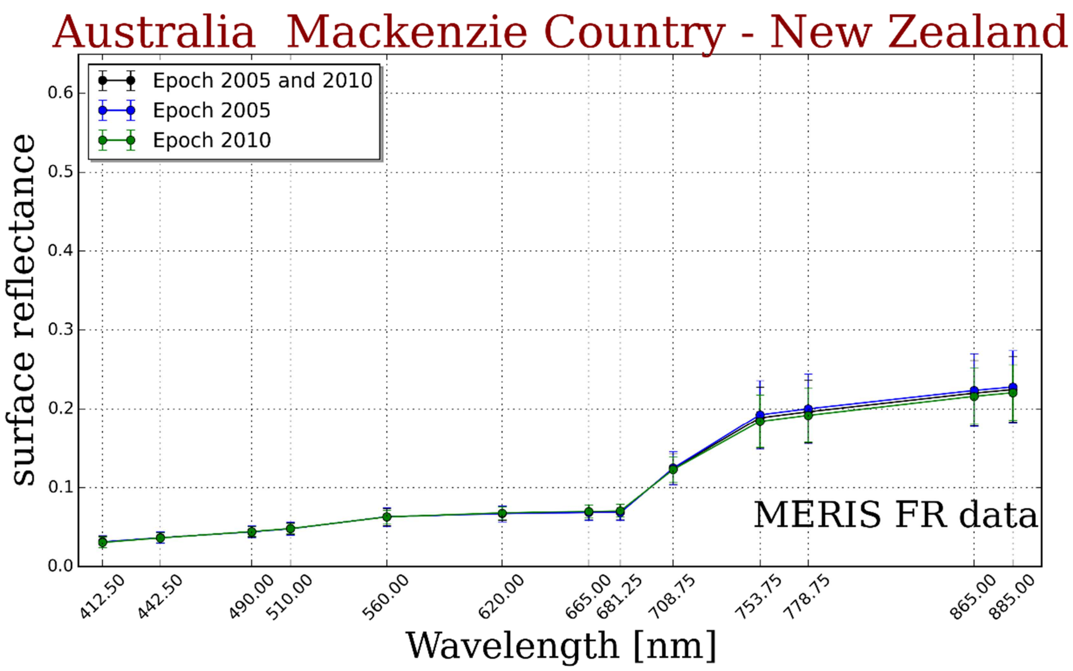

Figure 5-68: Spectra – Australia and Oceania - Mackenzie Country New Zealand - MERIS FR data

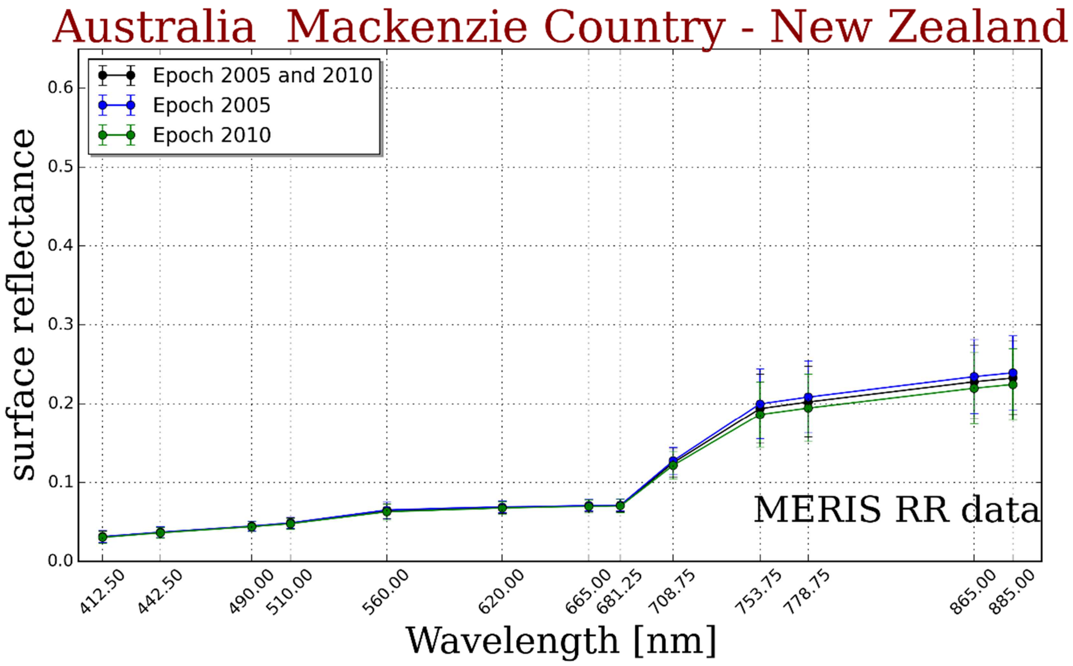

Figure 5-69: Spectra – Australia and Oceania - Mackenzie Country New Zealand - MERIS RR data

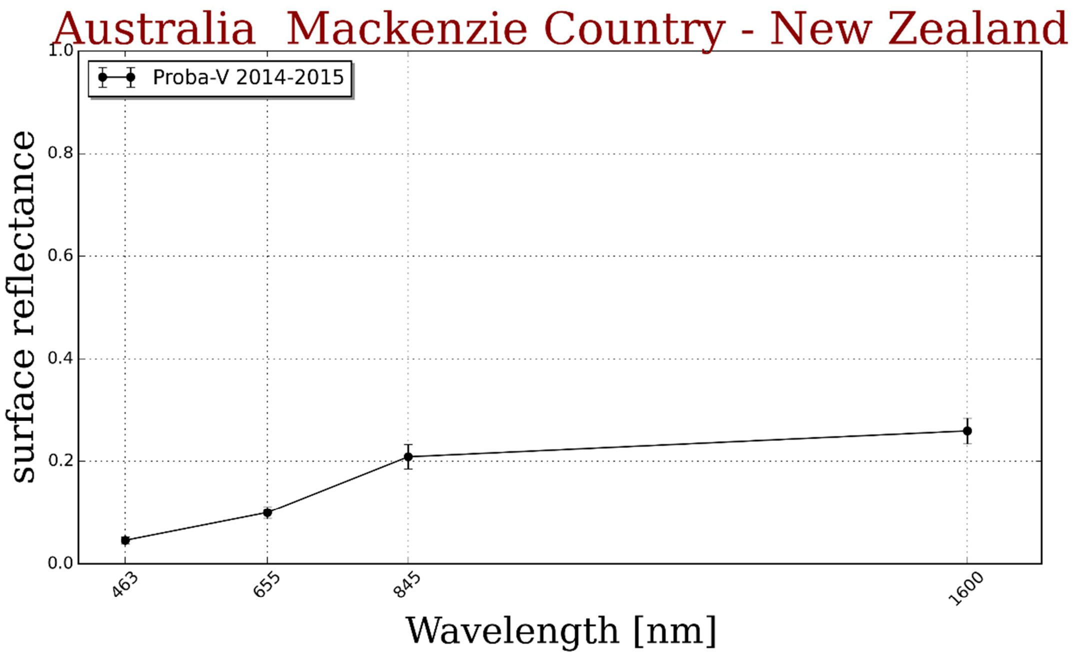

Figure 5-70: Spectra – Australia and Oceania - Mackenzie Country New Zealand – PROBA-V data

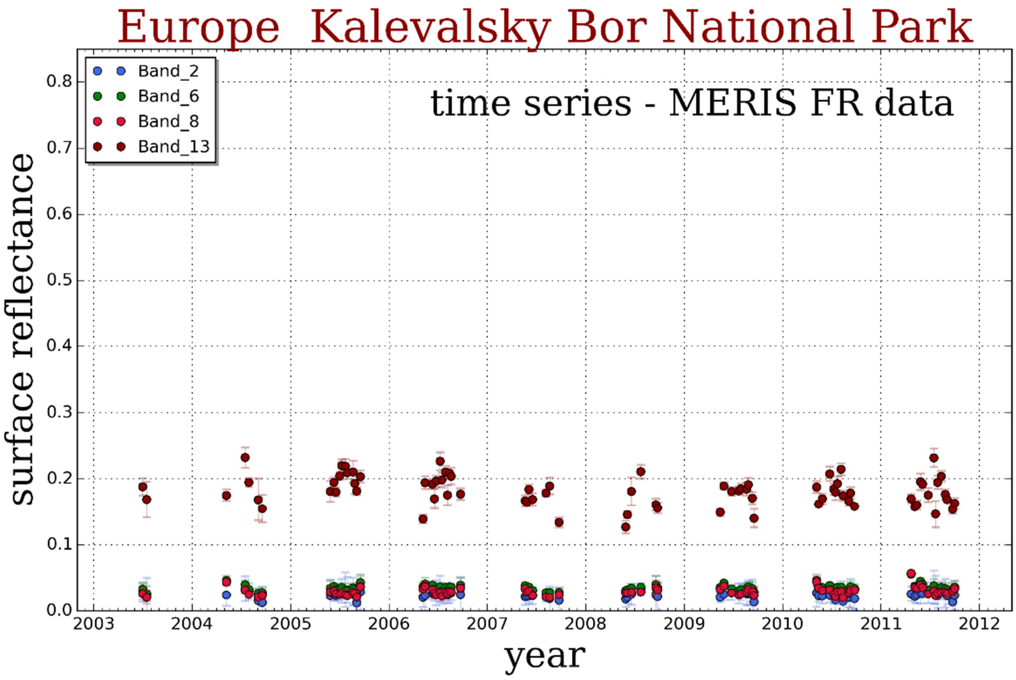

Figure 5-71: SR time series from MERIS FR data - 2003-2012 - Europa - Kalevalsky Bor National Park

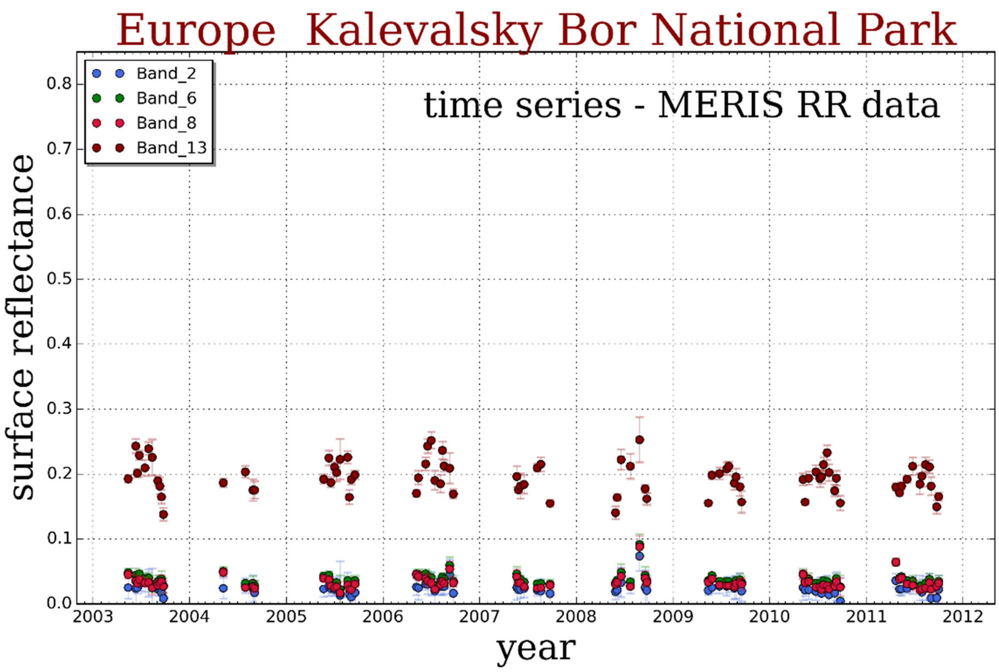

Figure 5-72: SR time series from MERIS RR data - 2003-2012 - Europa - Kalevalsky Bor National Park

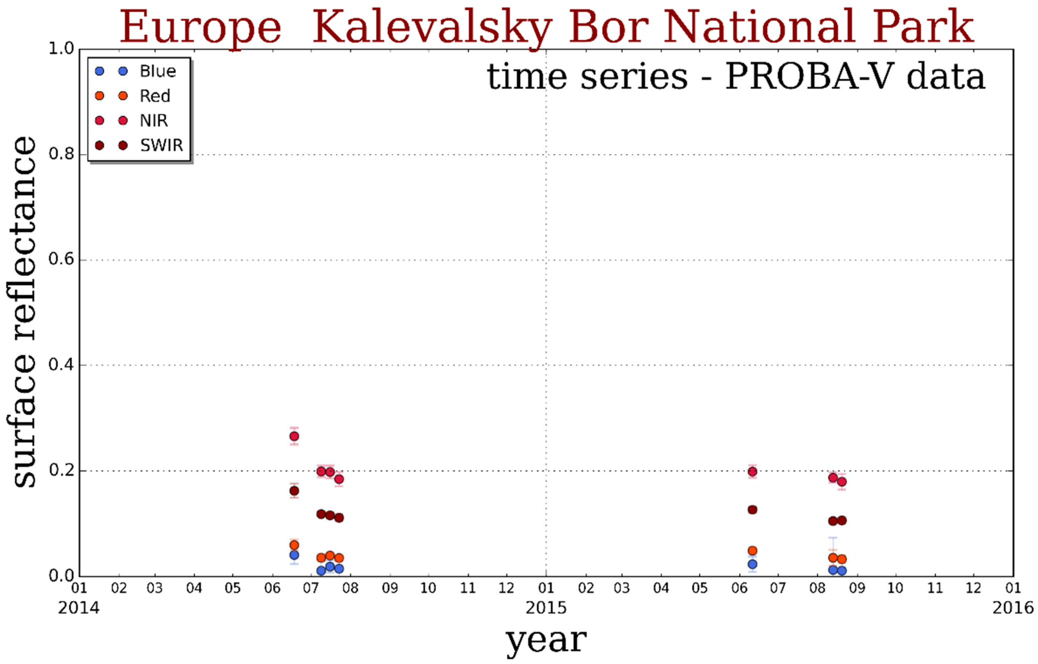

Figure 5-73: SR time series from PROBA-V data - 2014-2016 - Europa - Kalevalsky Bor National Park

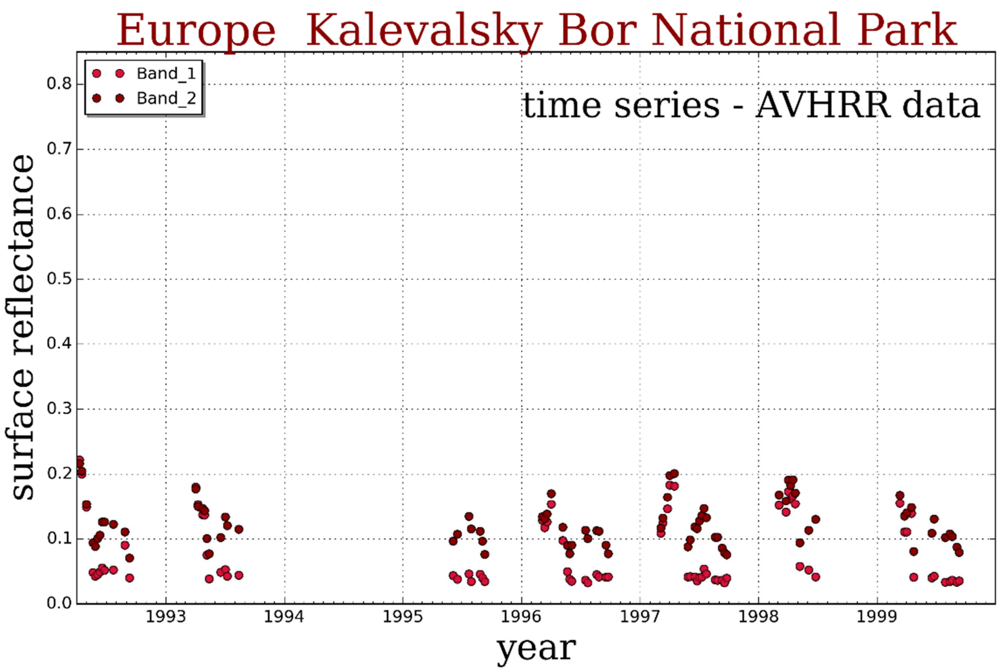

Figure 5-74: SR time series from AVHRR data - 1992-1999 - Europa - Kalevalsky Bor National Park

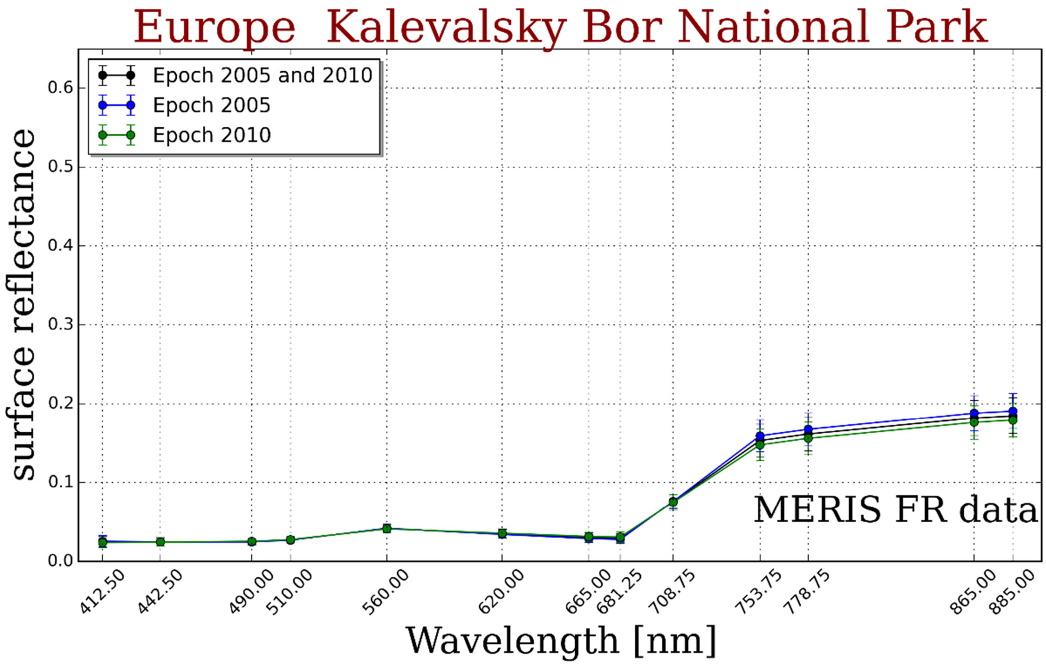

Figure 5-75: Spectra - Europa - Kalevalsky Bor National Park - MERIS FR data

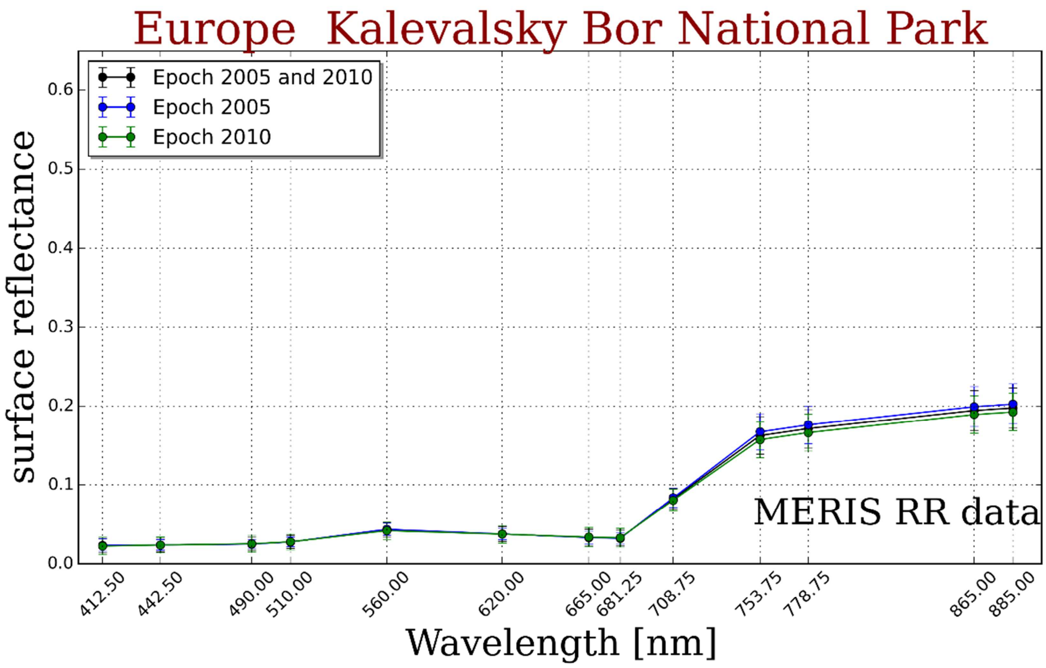

Figure 5-76: Spectra - Europa - Kalevalsky Bor National Park - MERIS RR data

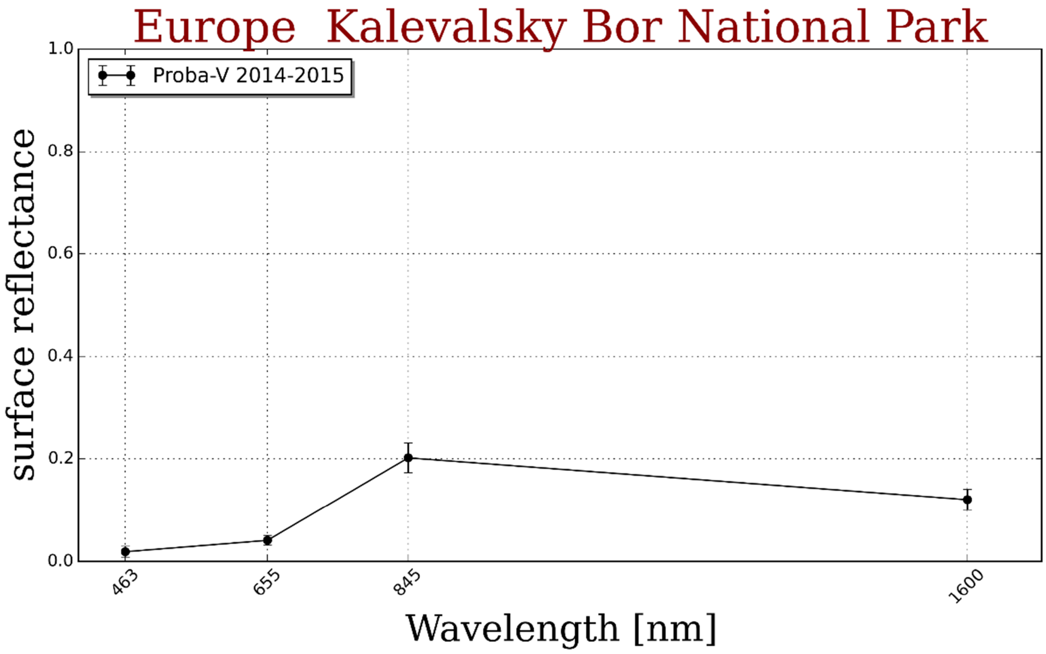

Figure 5-77: Spectra - Europa - Kalevalsky Bor National Park – PROBA-V data

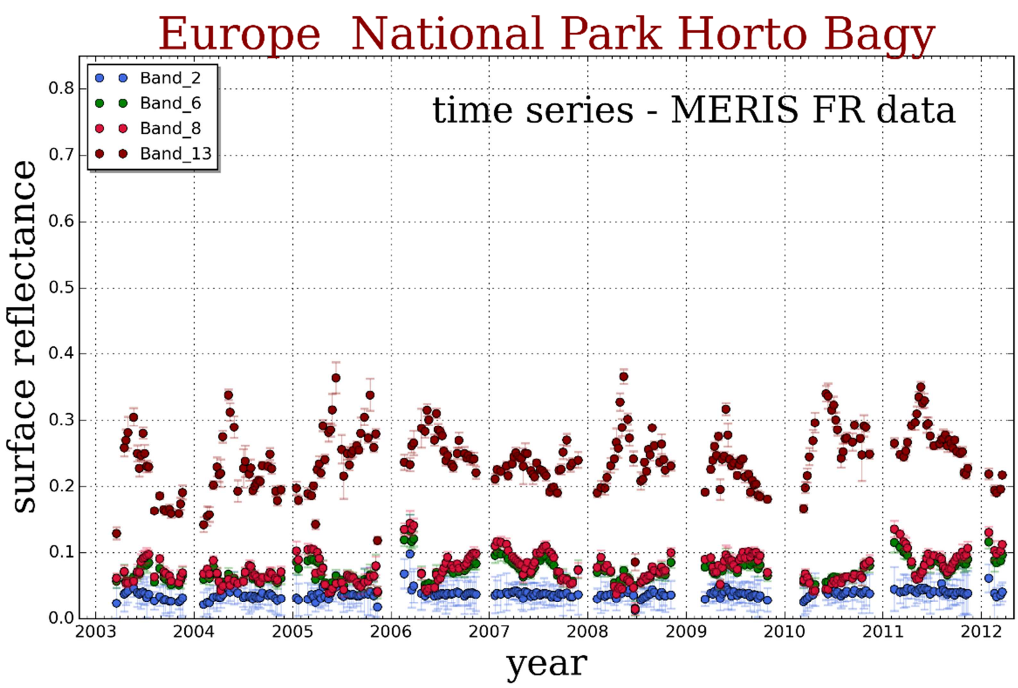

Figure 5-78: SR time series from MERIS FR data - 2003-2012 - Europa - National Park Horto Bagy

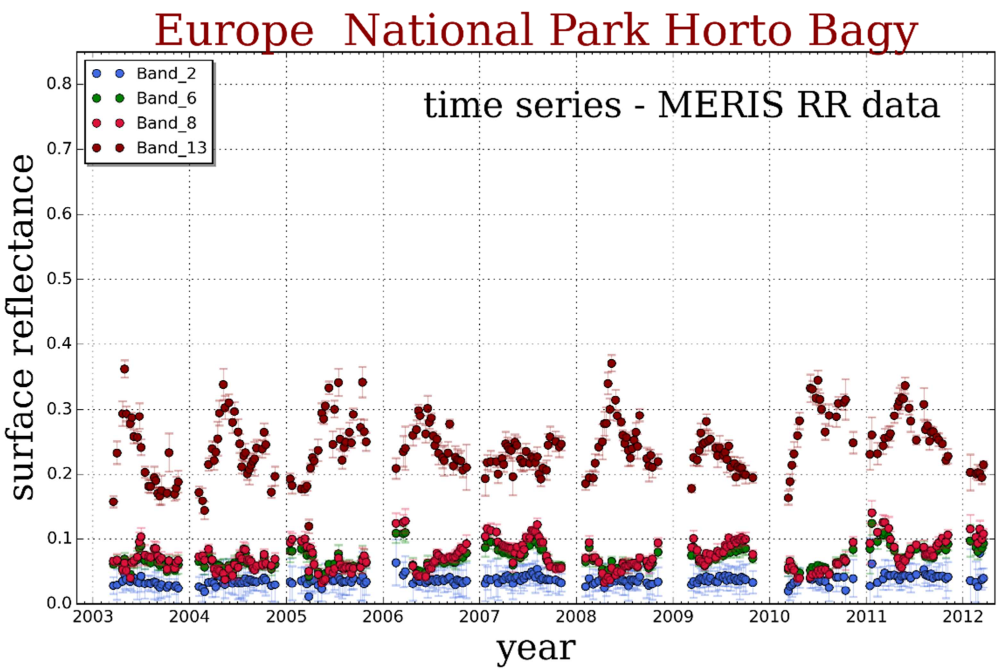

Figure 5-79: SR time series from MERIS RR data - 2003-2012 - Europa - National Park Horto Bagy

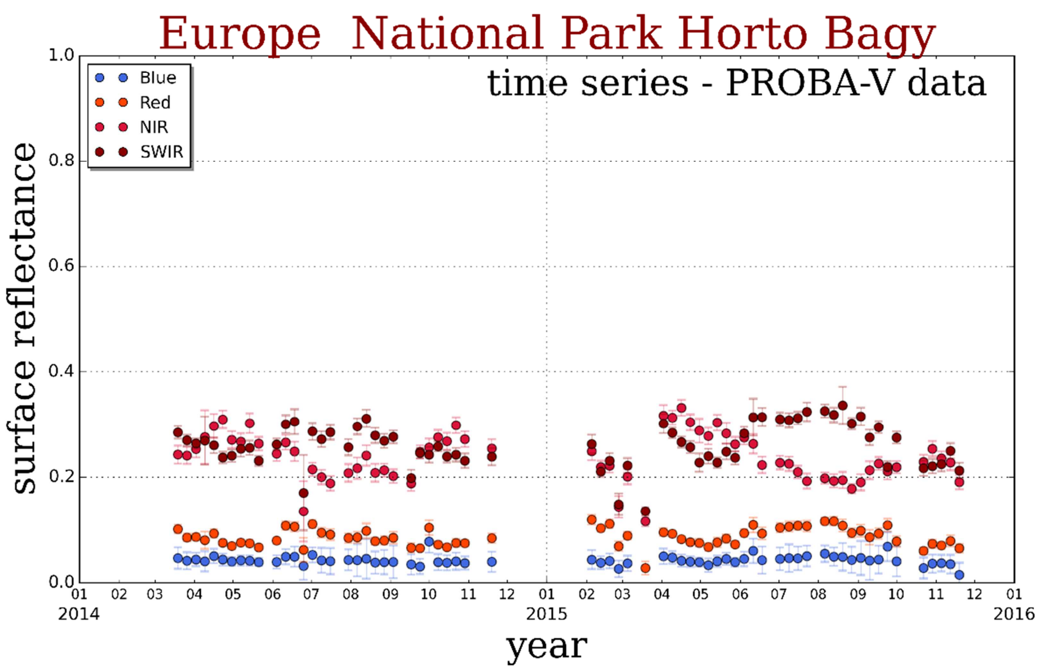

Figure 5-80: SR time series from PROBA-V data - 2014-2016 - Europa - National Park Horto Bagy

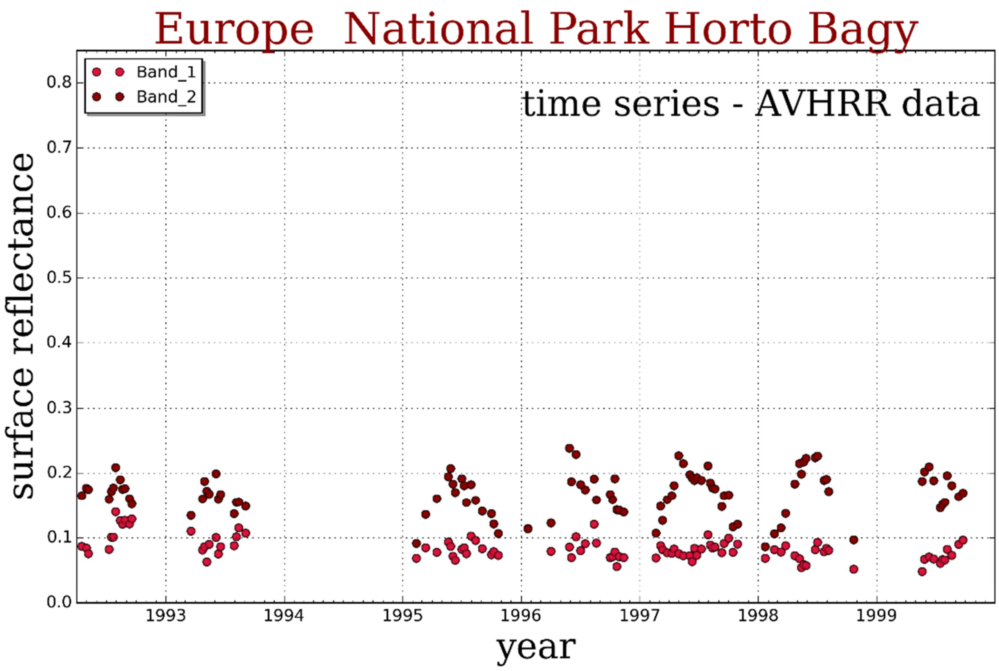

Figure 5-81: SR time series from AVHRR data - 1992-1999 - Europa - National Park Horto Bagy

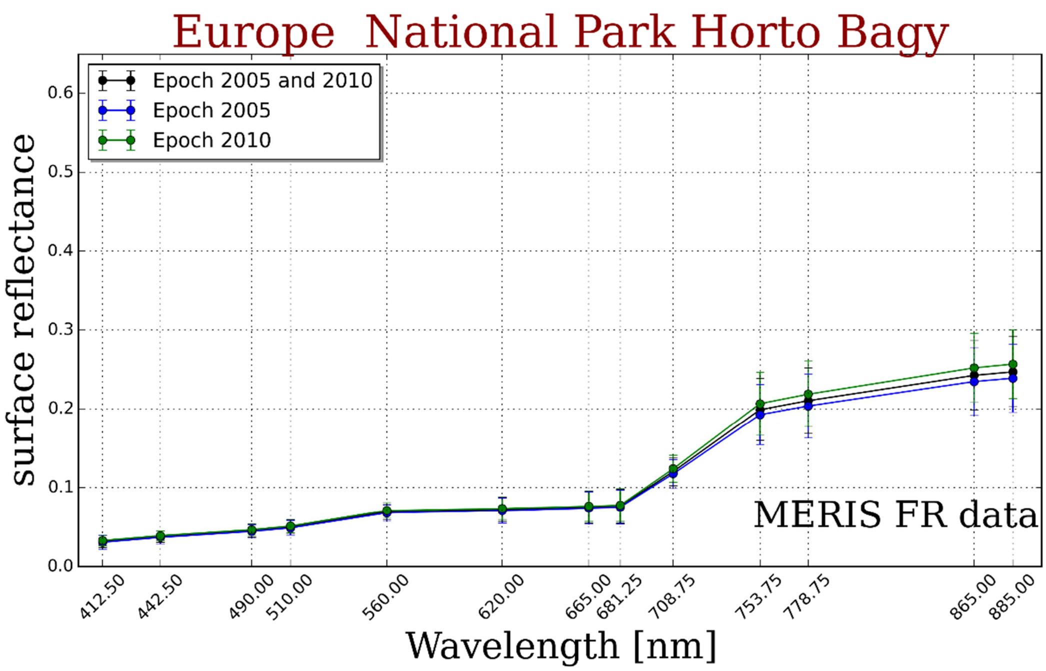

Figure 5-82: Spectra - Europa - National Park Horto Bagy - MERIS FR data

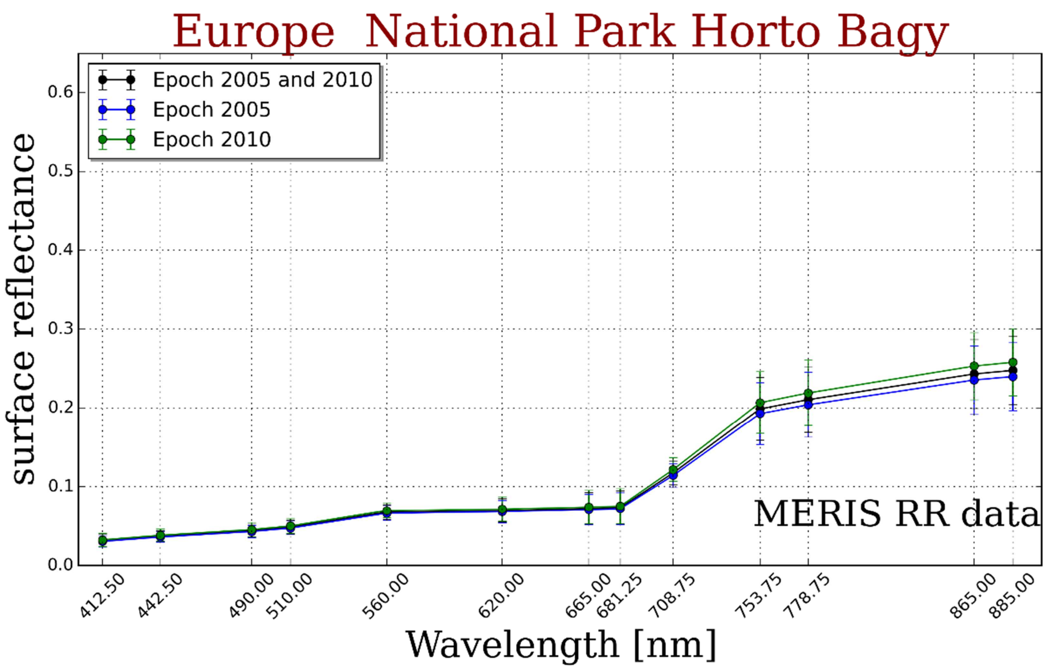

Figure 5-83: Spectra - Europa - National Park Horto Bagy - MERIS RR data

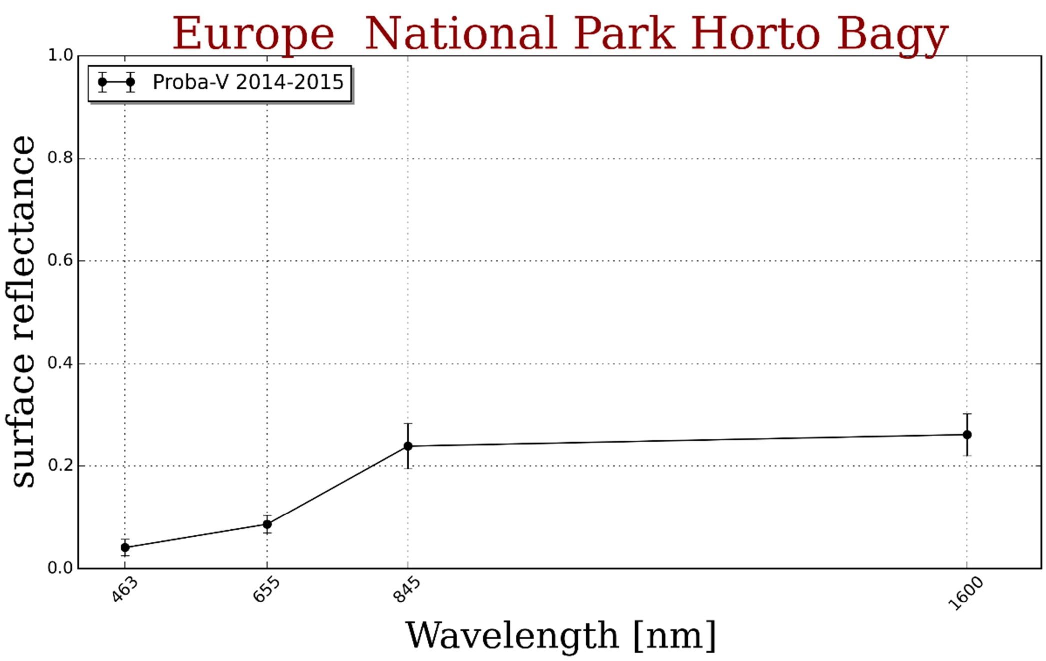

Figure 5-84: Spectra - Europa - National Park Horto Bagy – PROBA-V data

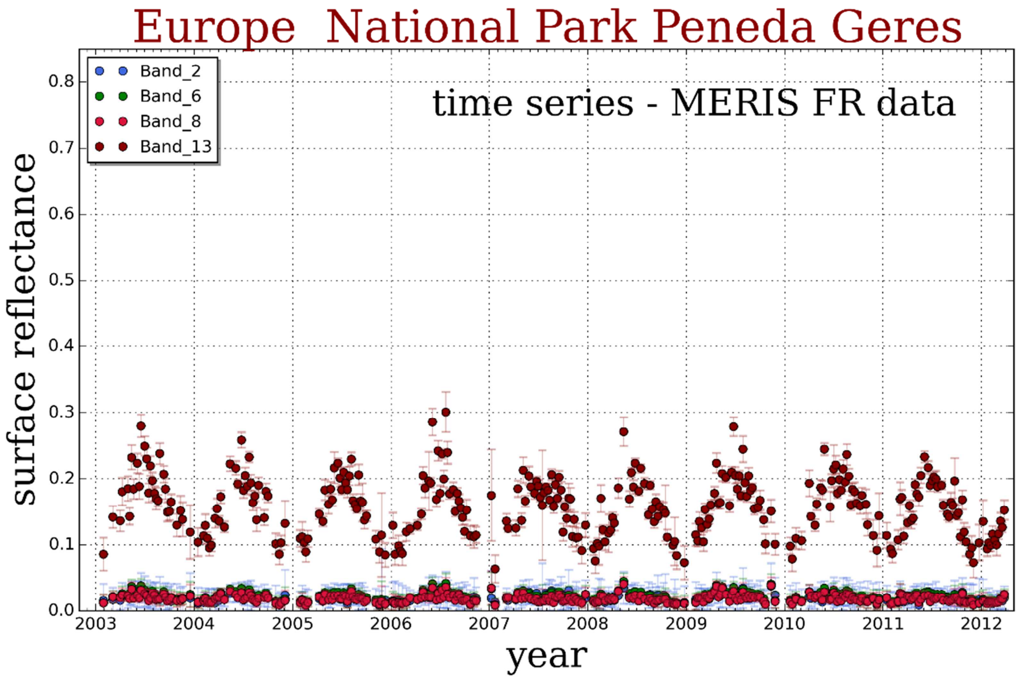

Figure 5-85: SR time series from MERIS FR data - 2003-2012 - Europa - National Park Peneda Geres

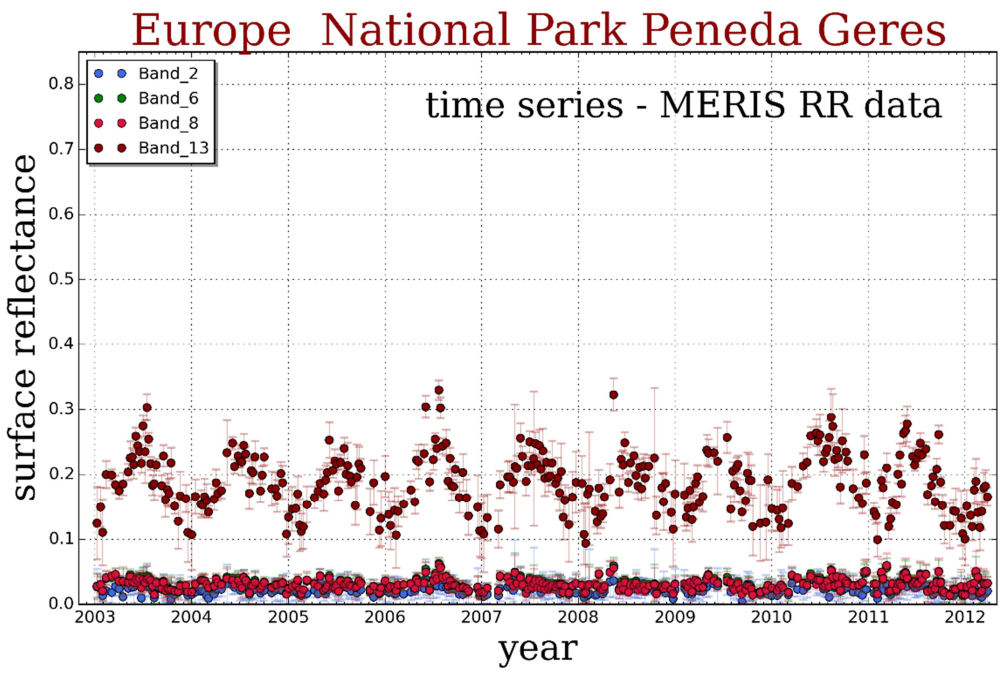

Figure 5-86: SR time series from MERIS RR data - 2003-2012 - Europa - National Park Peneda Geres

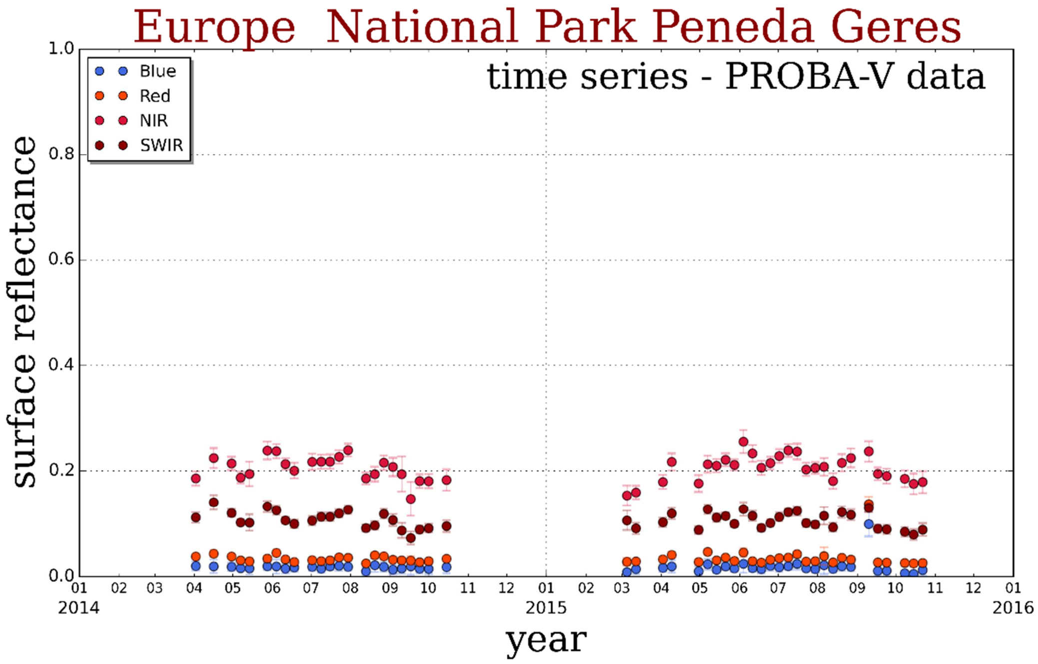

Figure 5-87: SR time series from PROBA-V data - 2014-2016 - Europa - National Park Peneda Geres

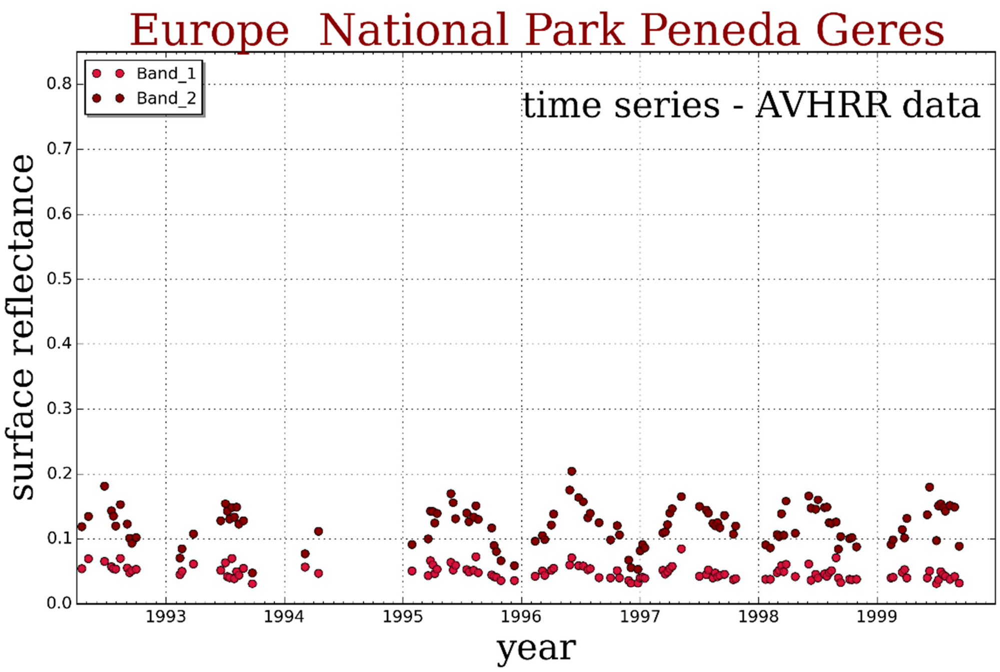

Figure 5-88: SR time series from AVHRR data - 1992-1999 - Europa - National Park Peneda Geres

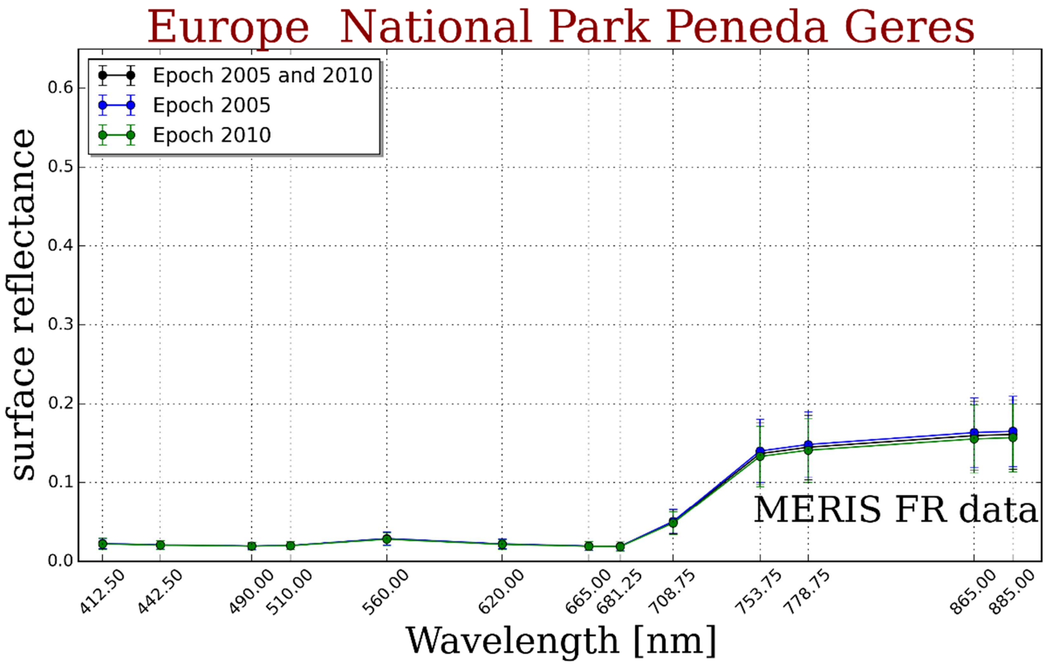

Figure 5-89: Spectra - Europa - National Park Peneda Geres - MERIS FR data

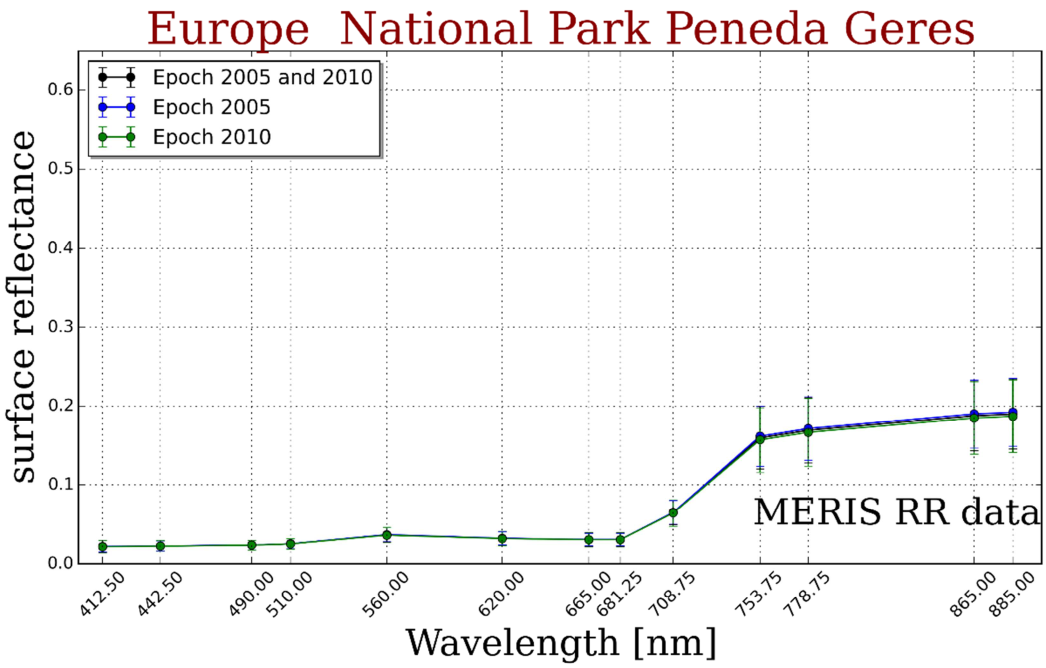

Figure 5-90: Spectra - Europa - National Park Peneda Geres - MERIS FR data

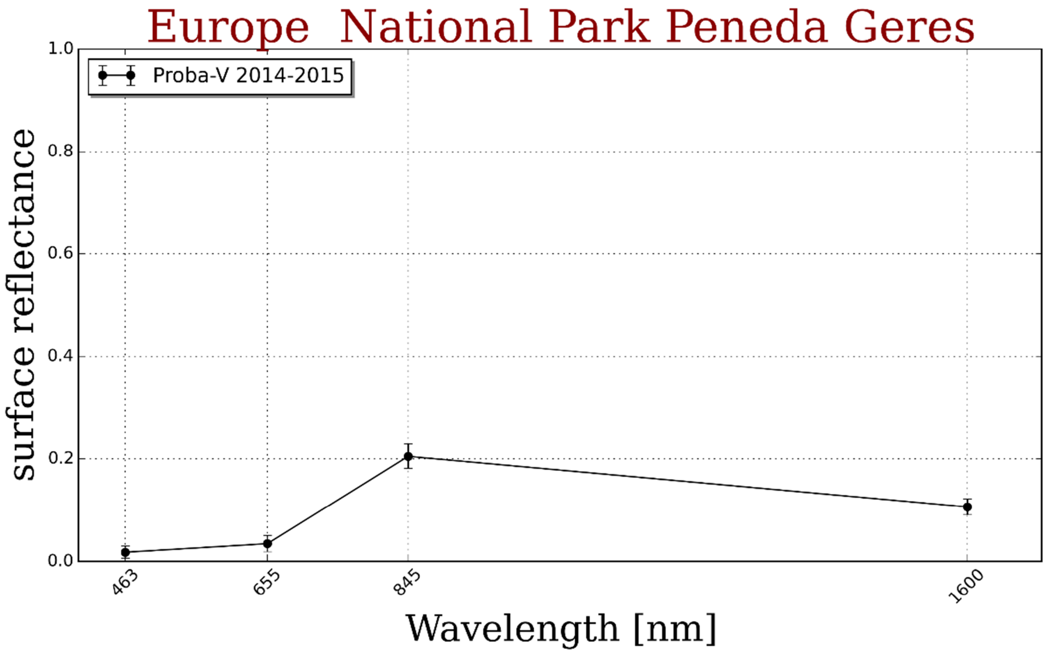

Figure 5-91: Spectra - Europa - National Park Peneda Geres – PROBA-V data

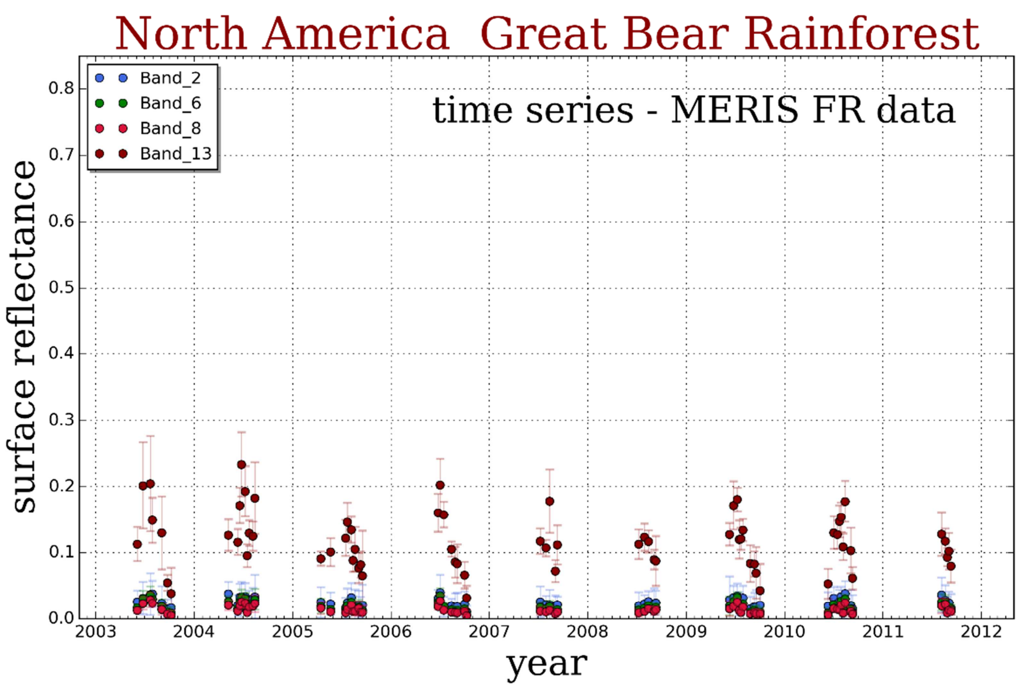

Figure 5-92: SR time series from MERIS FR data - 2003-2012 – North America - Great Bear Rainforest

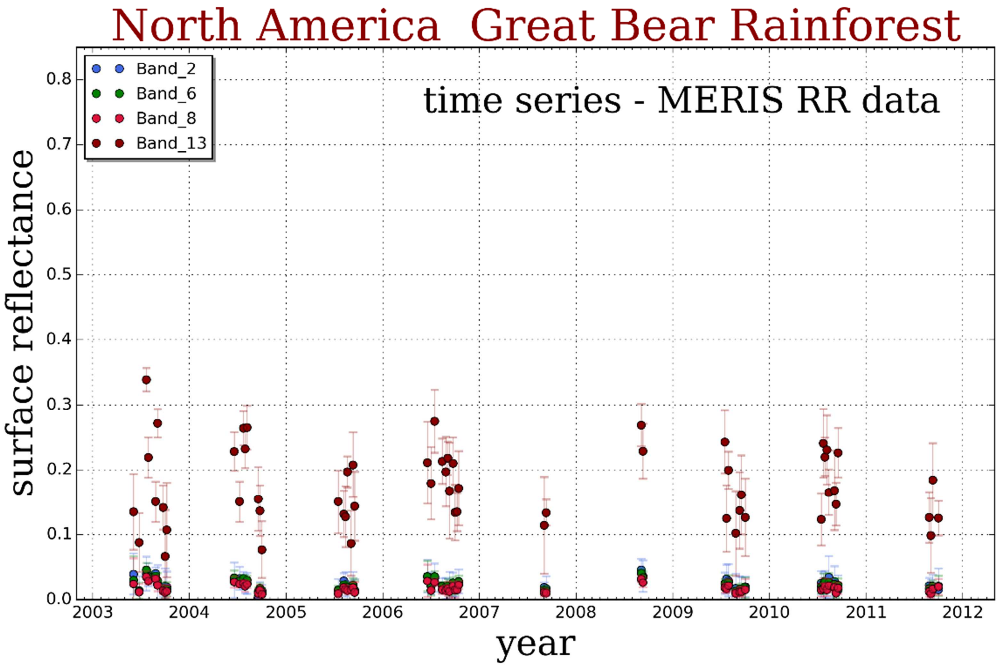

Figure 5-93: SR time series from MERIS RR data - 2003-2012 – North America - Great Bear Rainforest

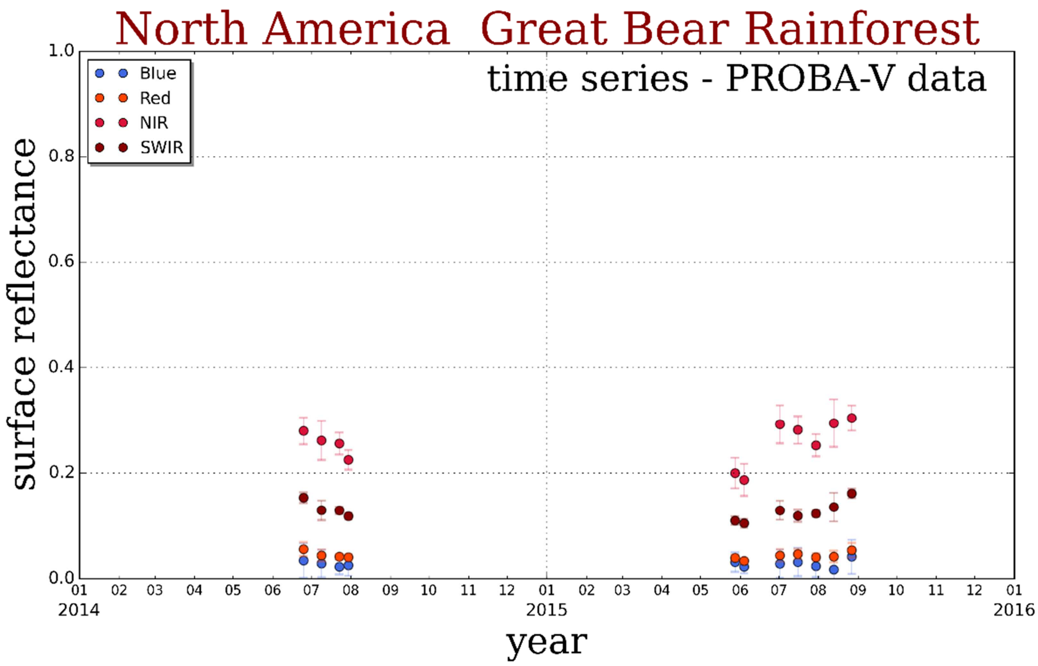

Figure 5-94: SR time series from PROBA-V data - 2014-2016 – North America - Great Bear Rainforest

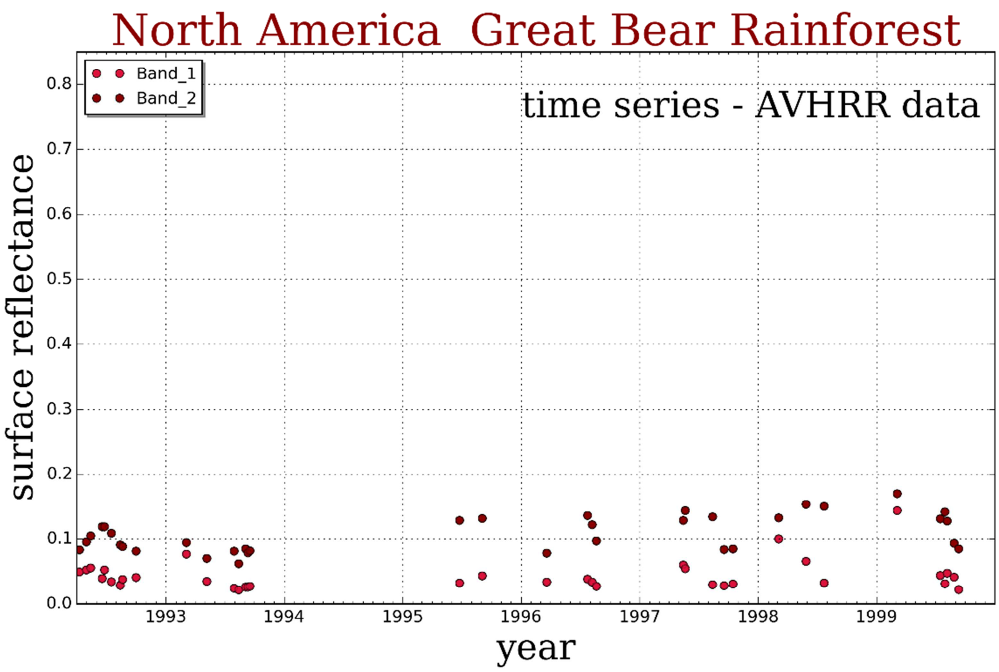

Figure 5-95: SR time series from AVHRR data - 1992-1999 – North America - Great Bear Rainforest

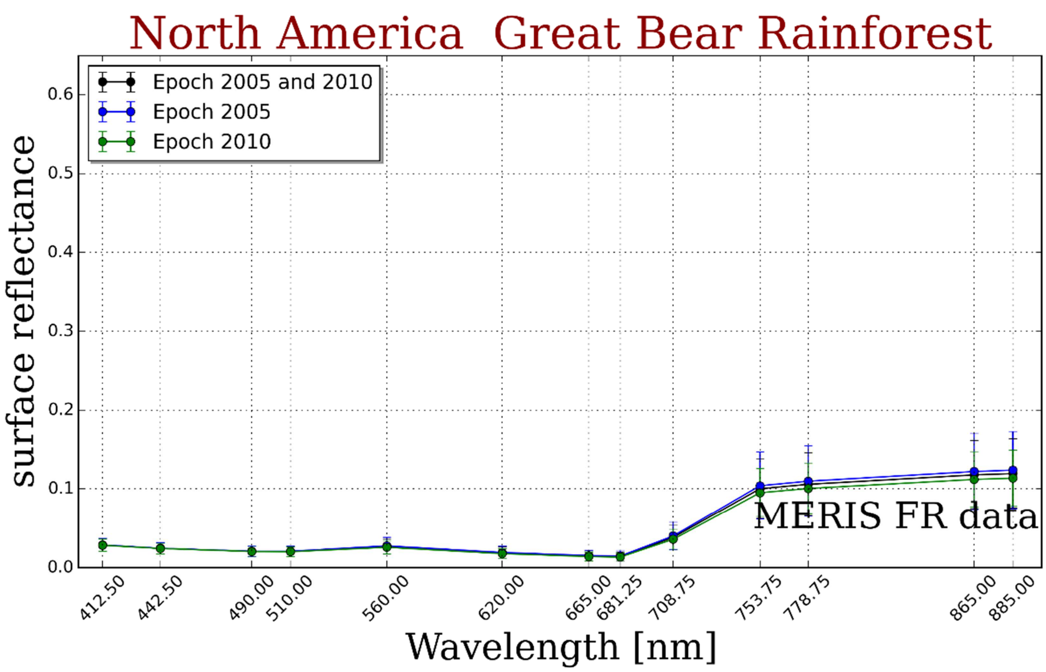

Figure 5-96: Spectra – North America - Great Bear Rainforest - MERIS FR data

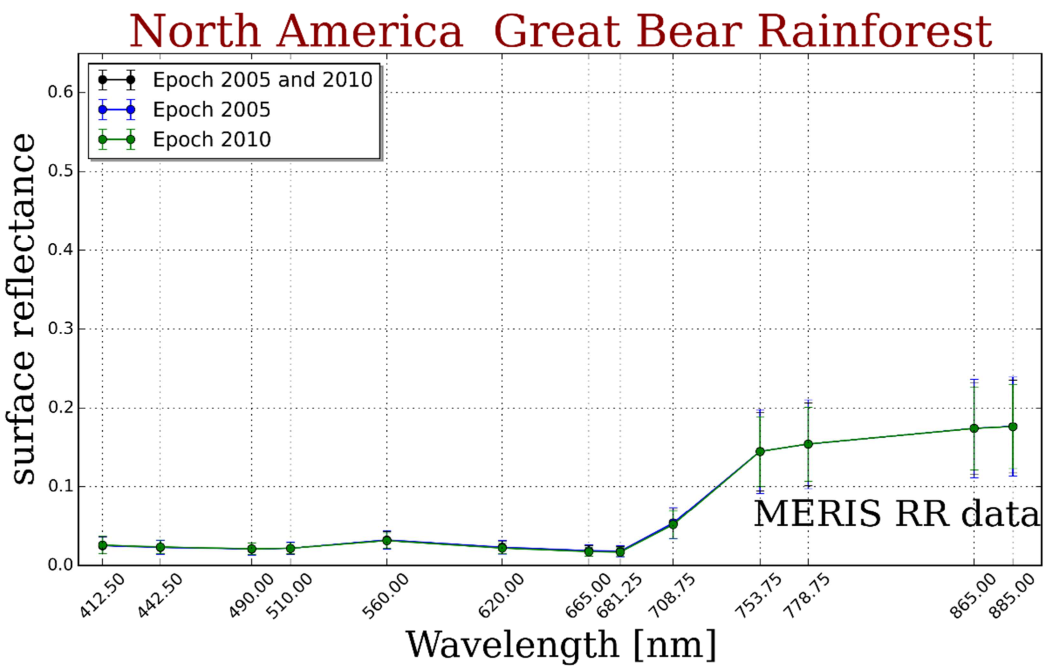

Figure 5-97: Spectra – North America - Great Bear Rainforest - MERIS RR data

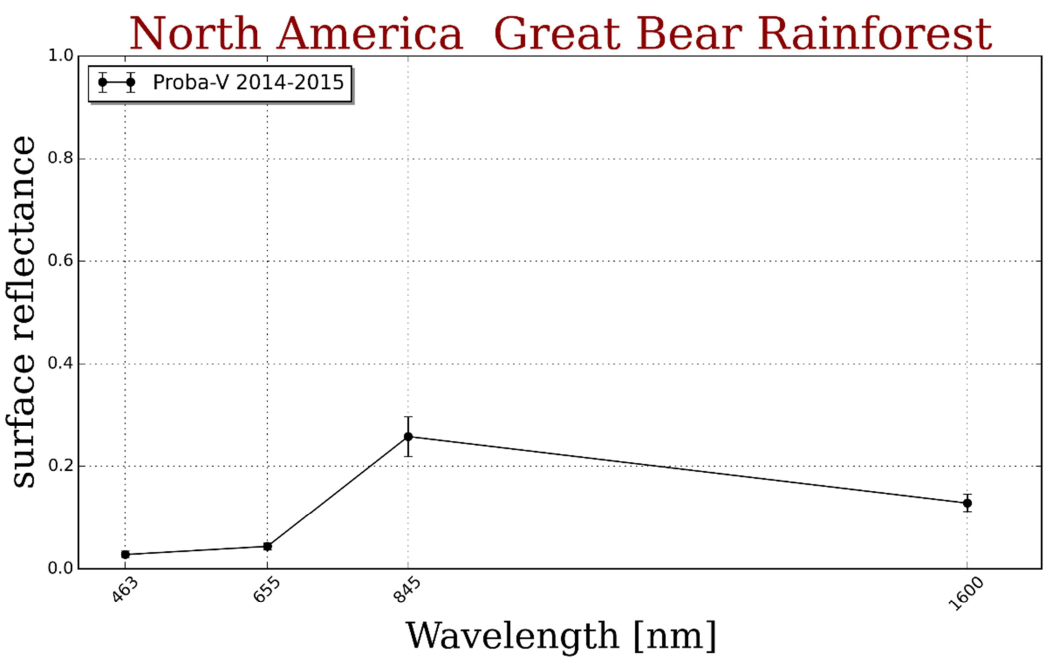

Figure 5-98: Spectra – North America - Great Bear Rainforest – PROBA-V data

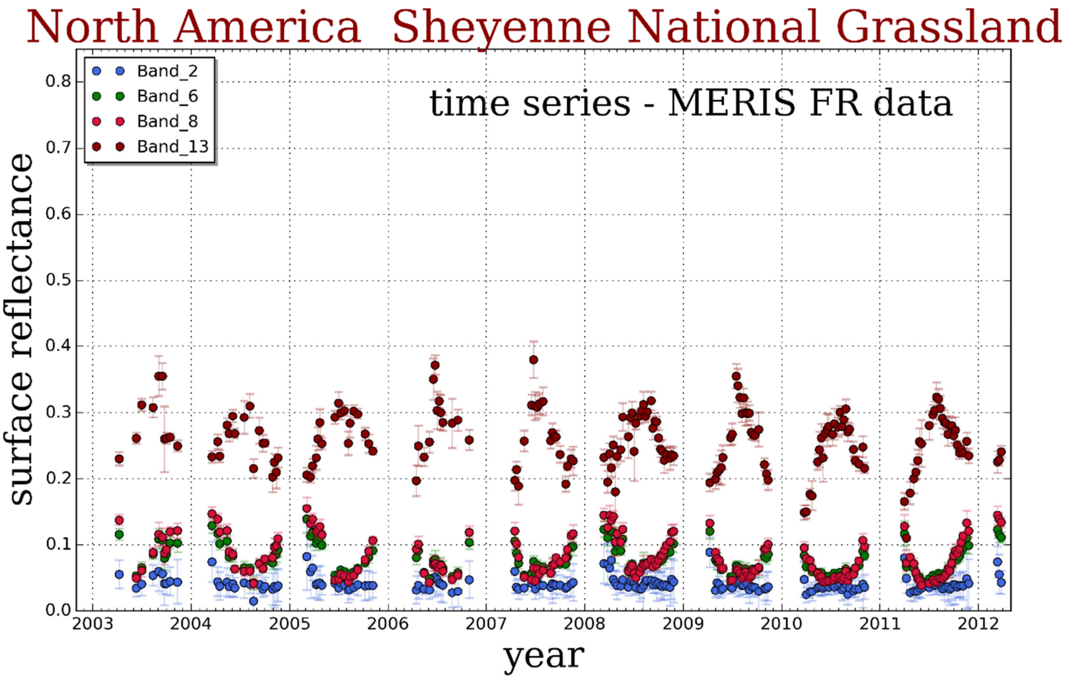

Figure 5-99: SR time series from MERIS FR data - 2003-2012 – North America - Sheyenne National Grassland

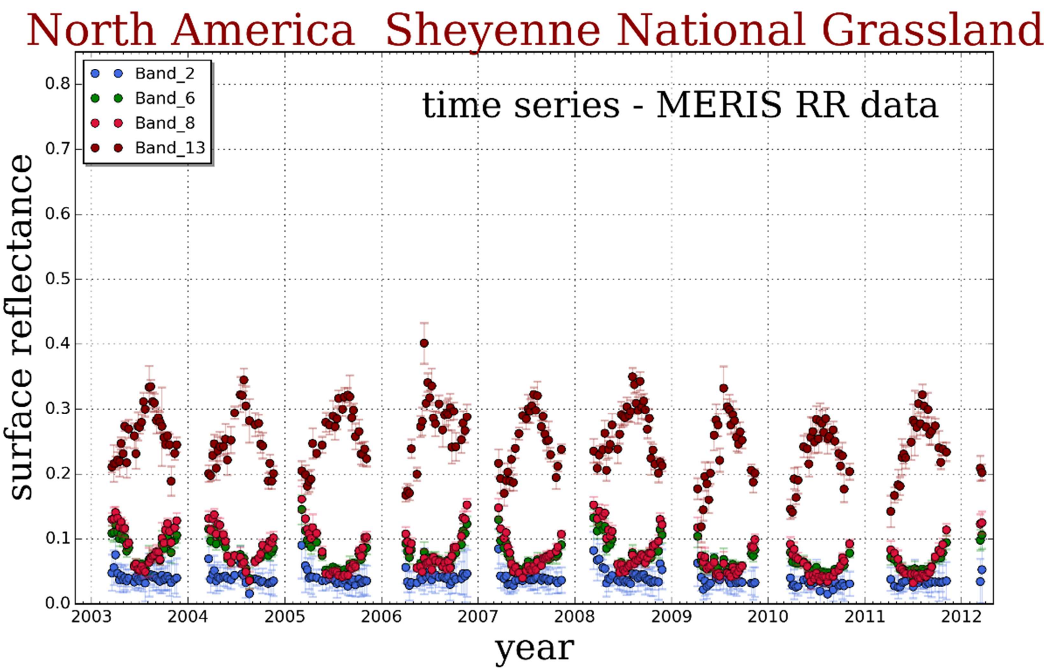

Figure 5-100: SR time series from MERIS RR data - 2003-2012 – North America - Sheyenne National Grassland

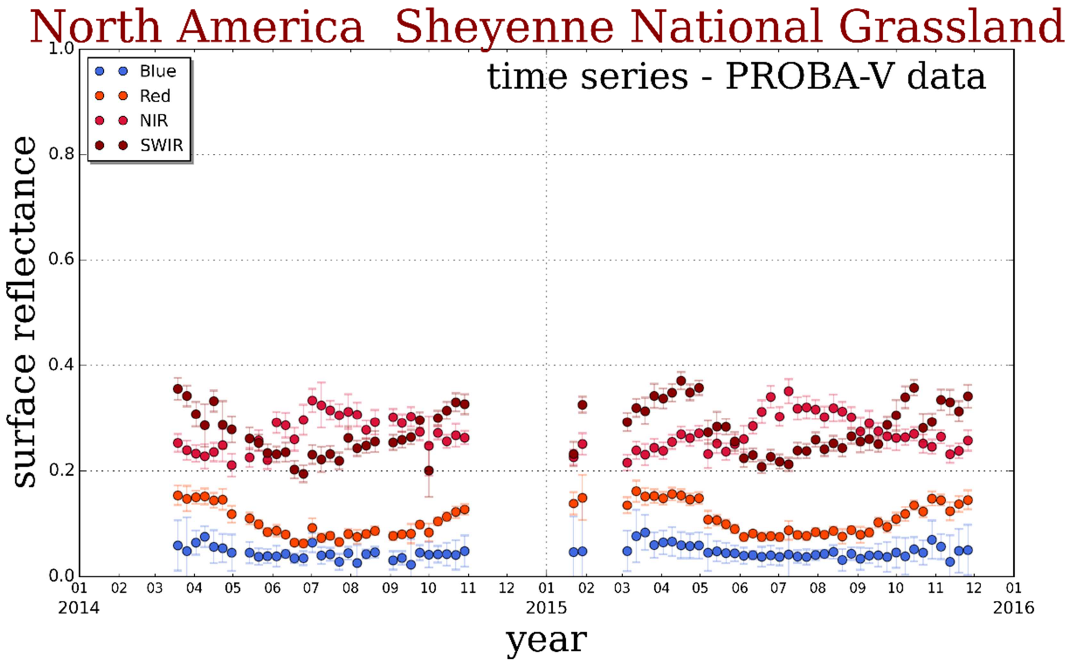

Figure 5-101: SR time series from PROBA-V data - 2014-2016 – North America - Sheyenne National Grassland

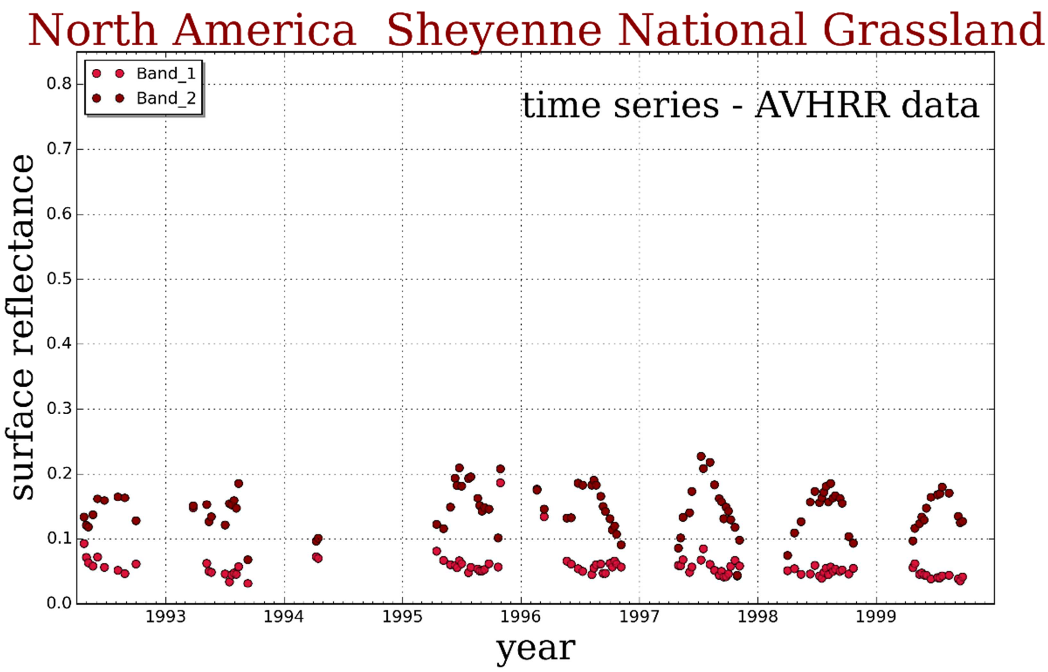

Figure 5-102: SR time series from AVHRR data - 1992-1999 – North America - Sheyenne National Grassland

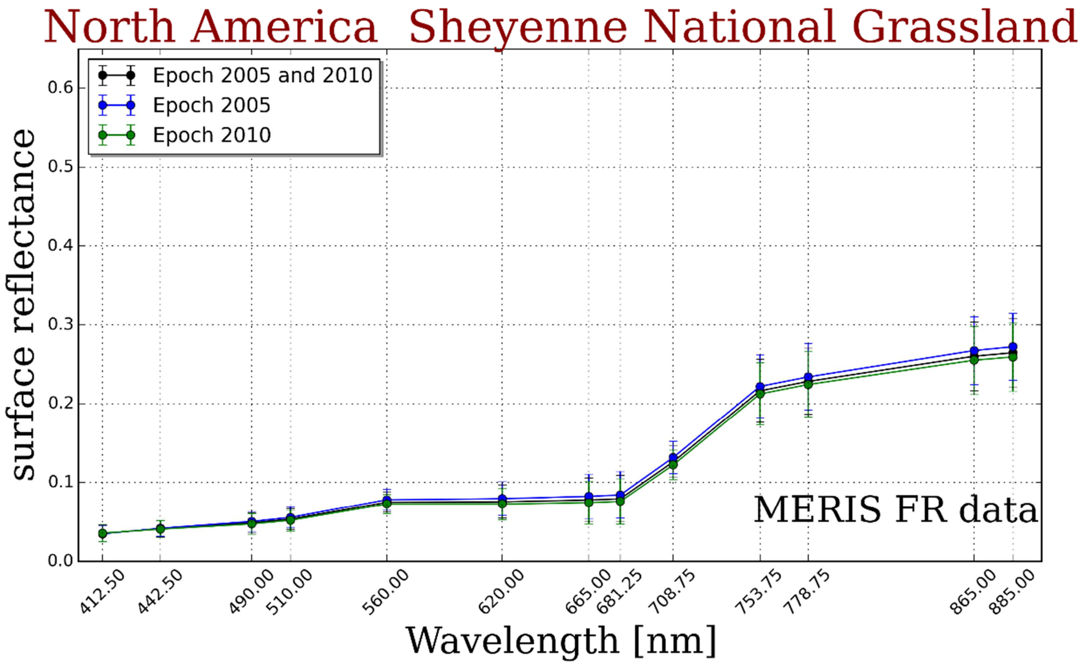

Figure 5-103: Spectra – North America - Sheyenne National Grassland - MERIS FR data

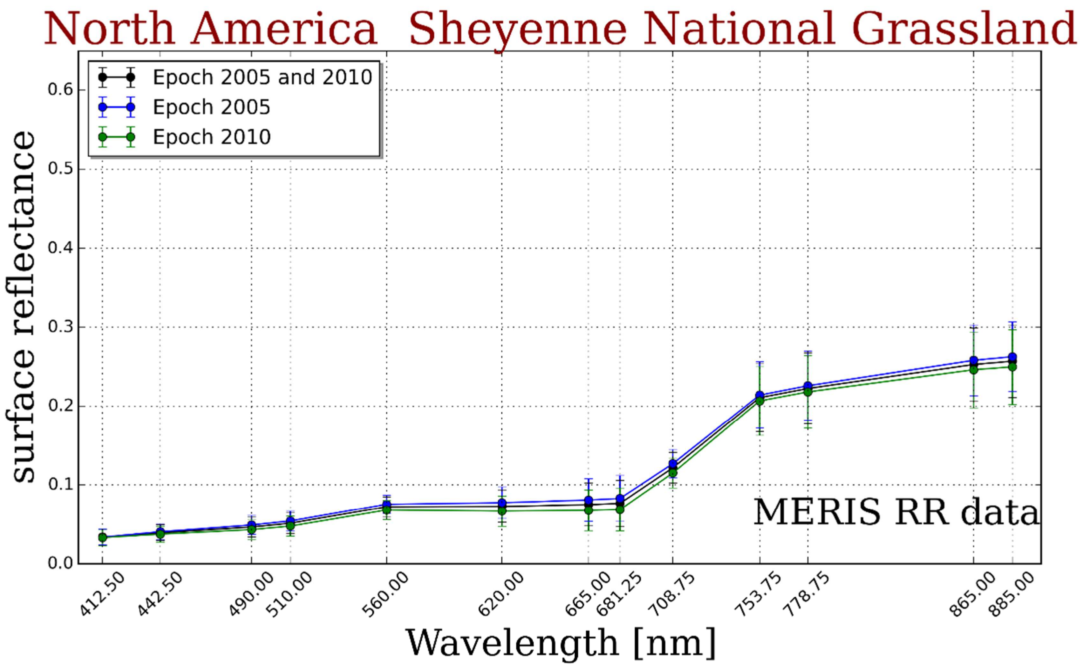

Figure 5-104: Spectra – North America - Sheyenne National Grassland - MERIS RR data

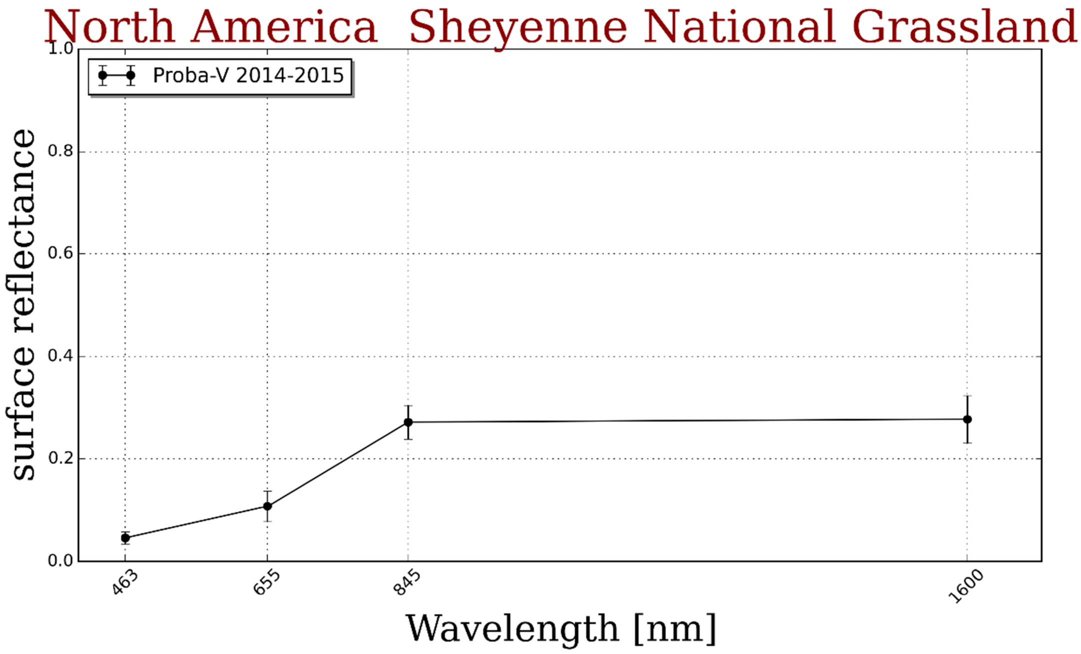

Figure 5-105: Spectra – North America - Sheyenne National Grassland – PROBA-V data

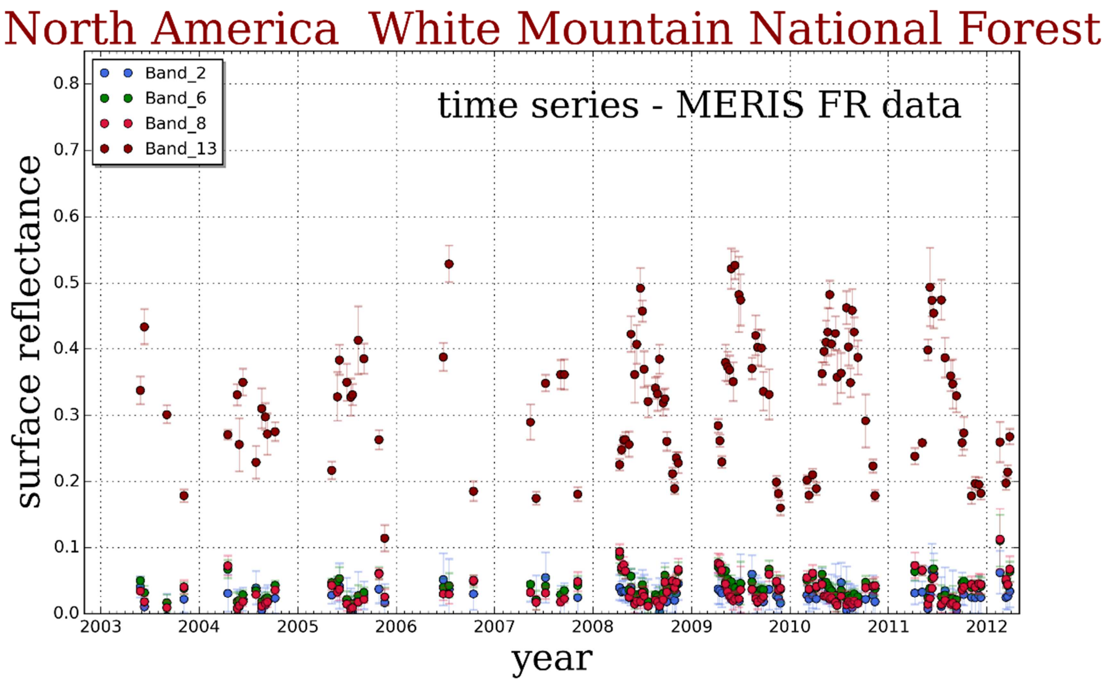

Figure 5-106: SR time series from MERIS FR data - 2003-2012 – North America - White Mountain National Forest

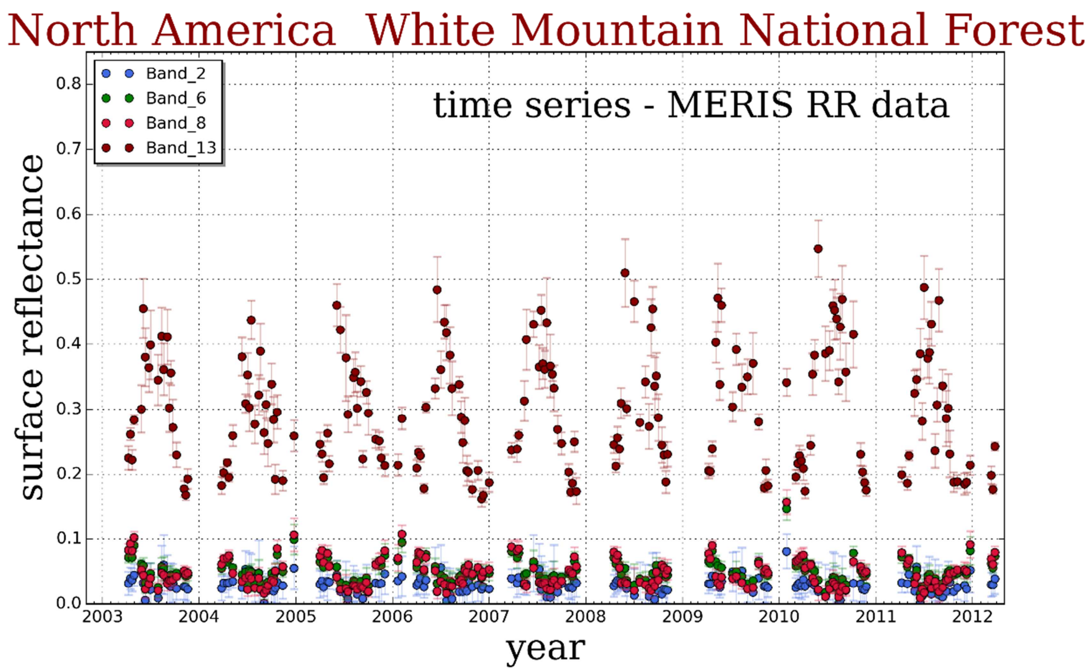

Figure 5-107: SR time series from MERIS RR data - 2003-2012 – North America - White Mountain National Forest

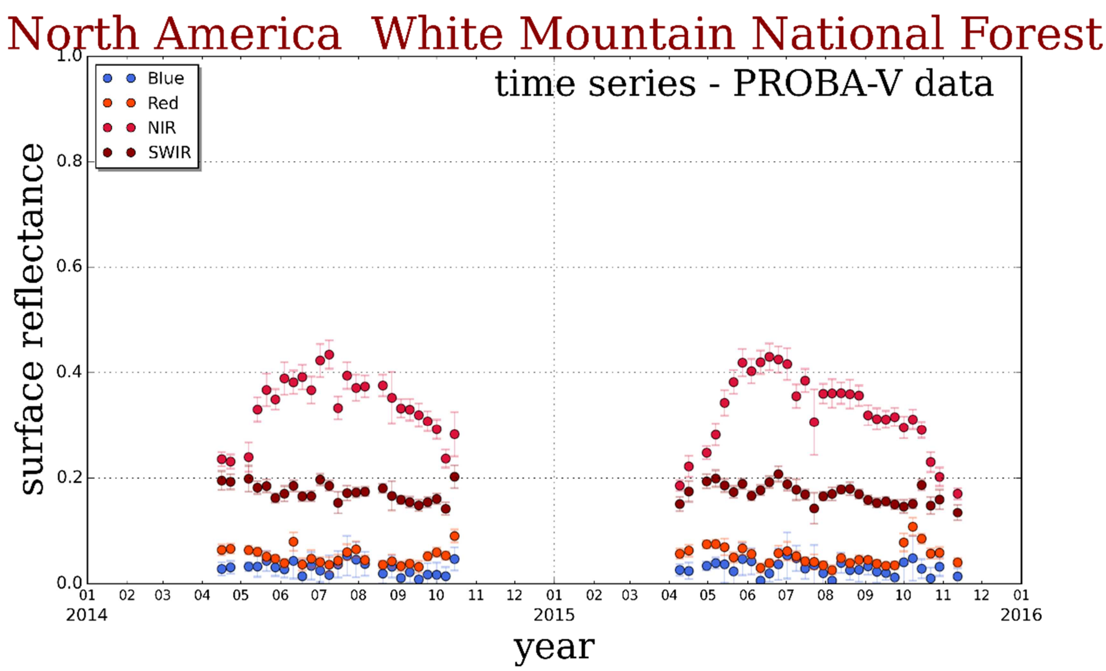

Figure 5-108: SR time series from PROBA-V data - 2014-2016 – North America - White Mountain National Forest

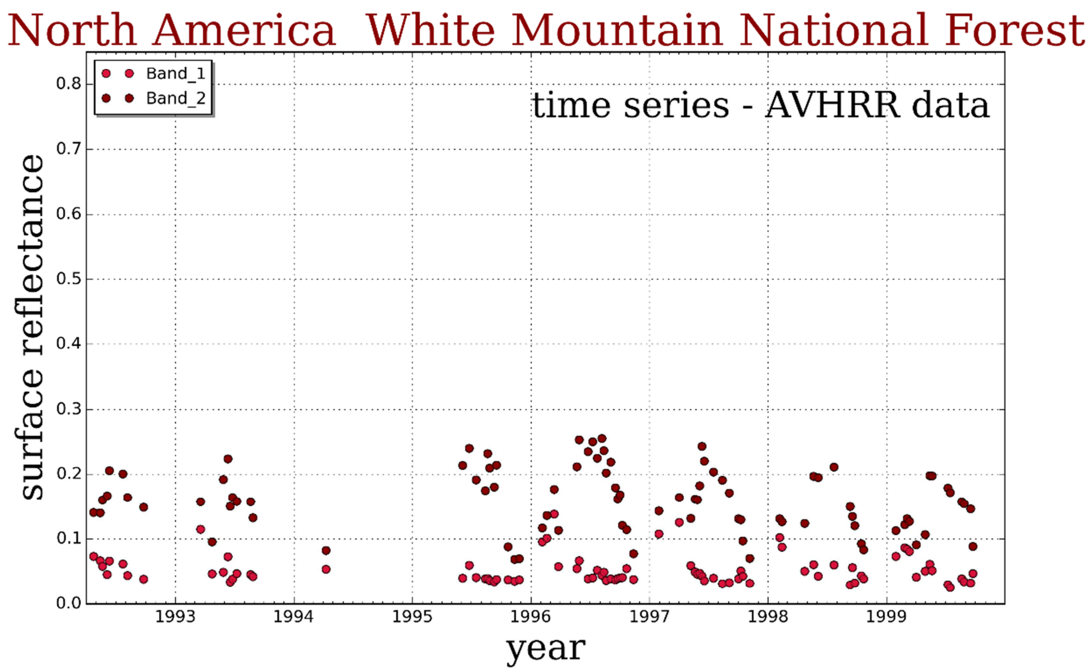

Figure 5-109: SR time series from AVHRR data - 1992-1999 – North America - White Mountain National Forest

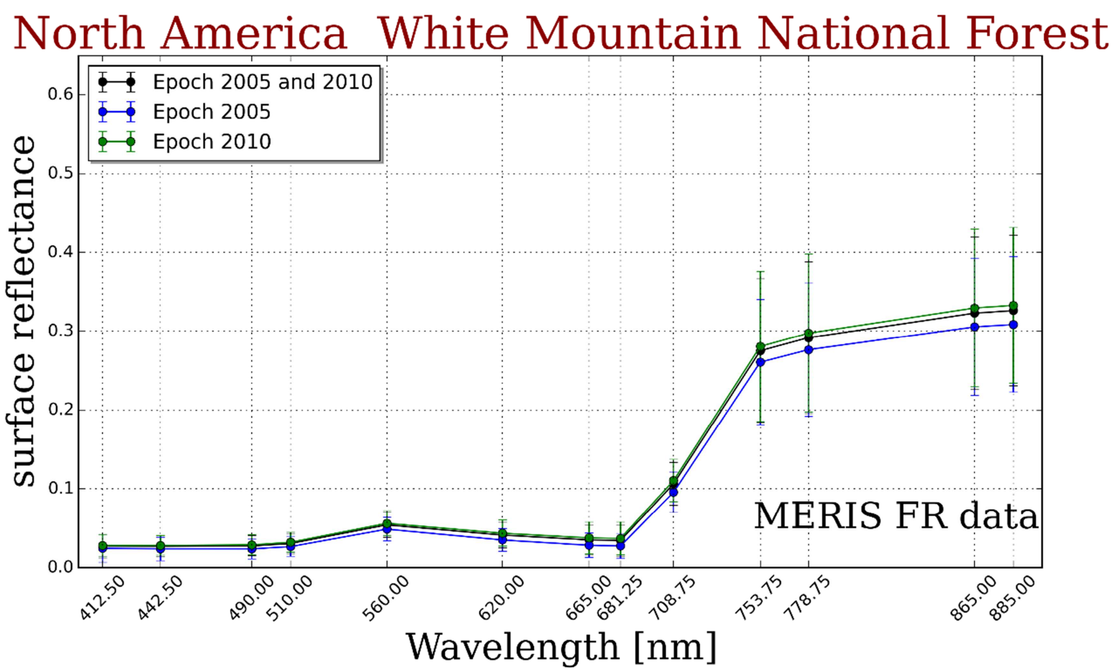

Figure 5-110: Spectra – North America - White Mountain National Forest - MERIS FR data

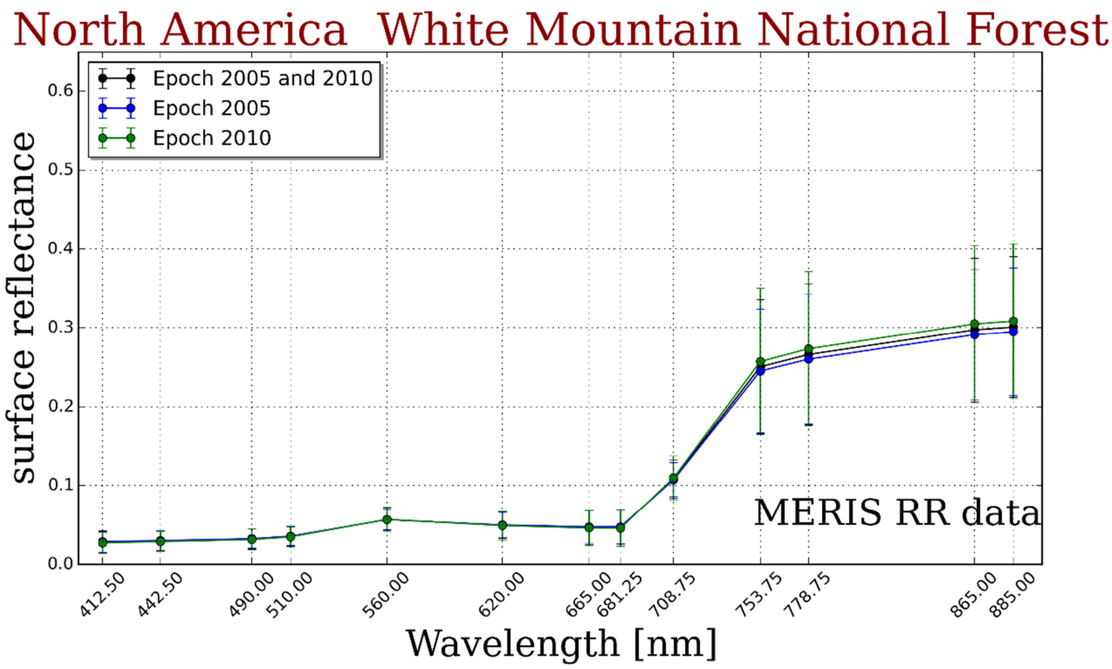

Figure 5-111: Spectra – North America - White Mountain National Forest - MERIS RR data

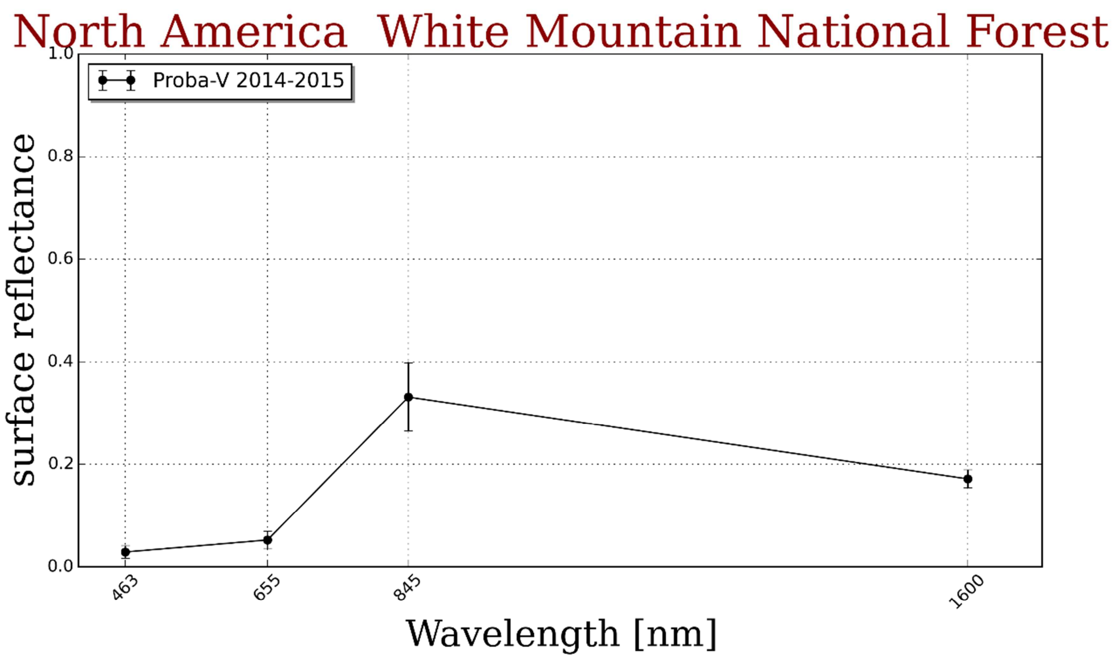

Figure 5-112: Spectra – North America - White Mountain National Forest – PROBA-V data

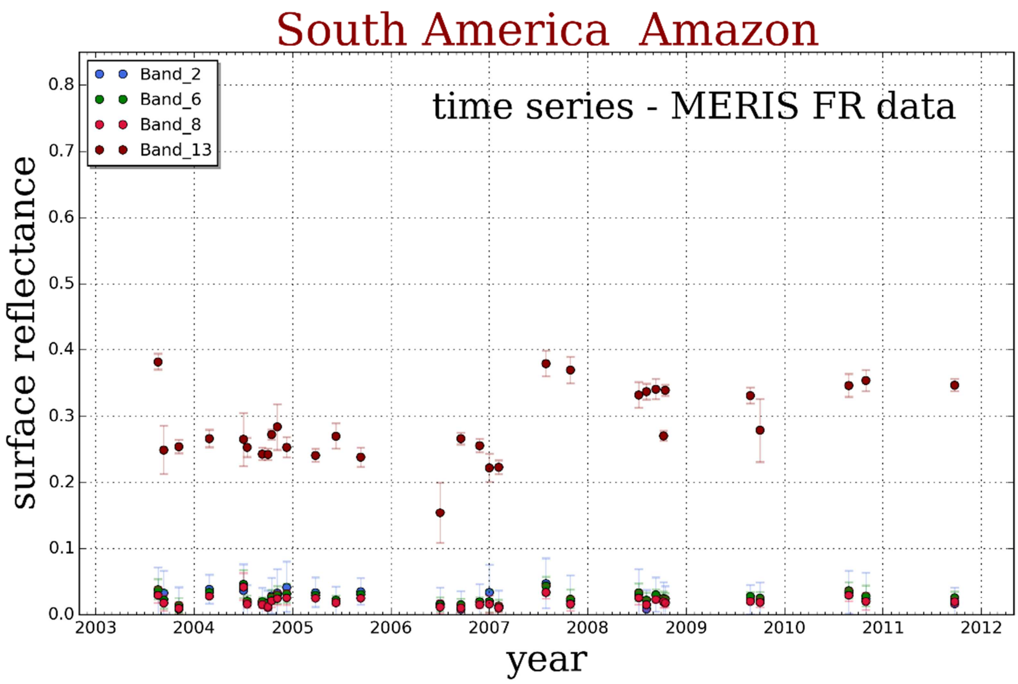

Figure 5-113: SR time series from MERIS FR data - 2003-2012 – South America – Amazon

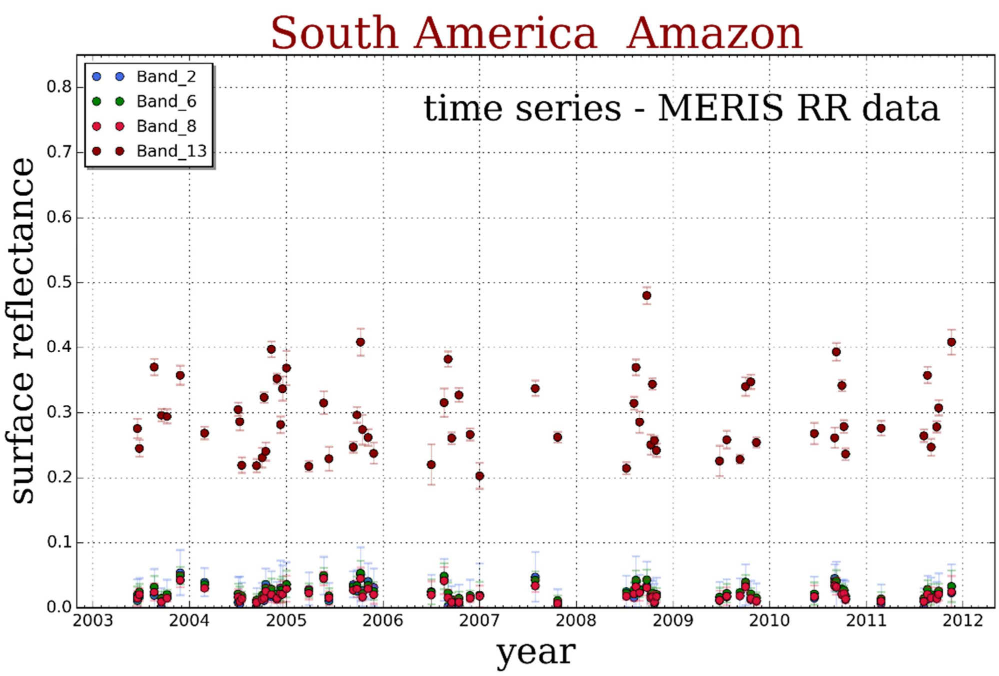

Figure 5-114: SR time series from MERIS RR data - 2003-2012 – South America – Amazon

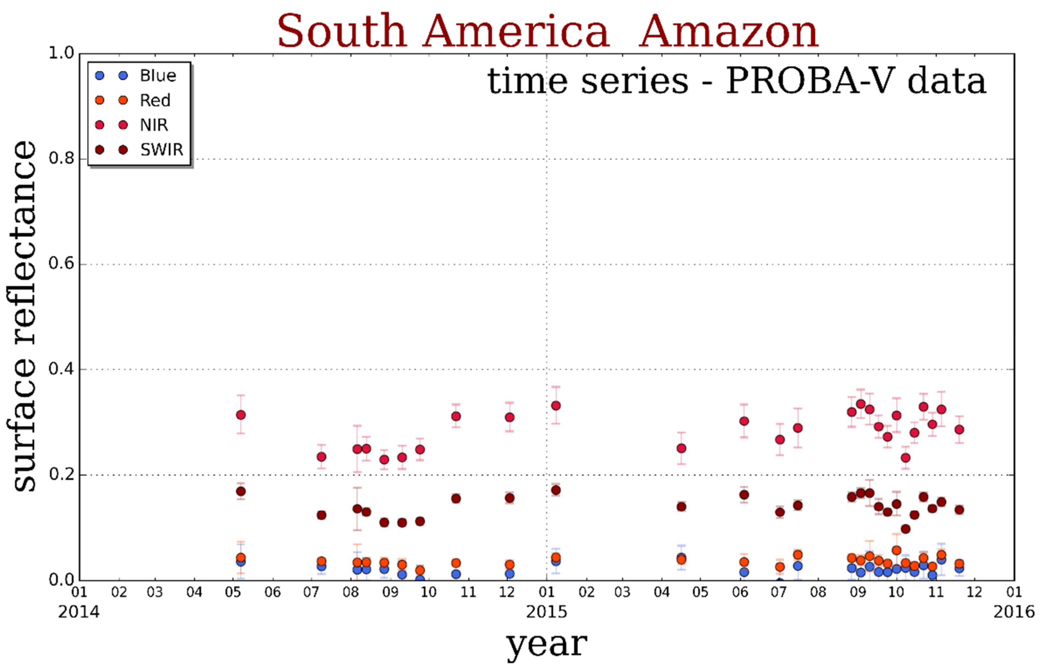

Figure 5-115: SR time series from PROBA-V data - 2014-2016 – South America – Amazon

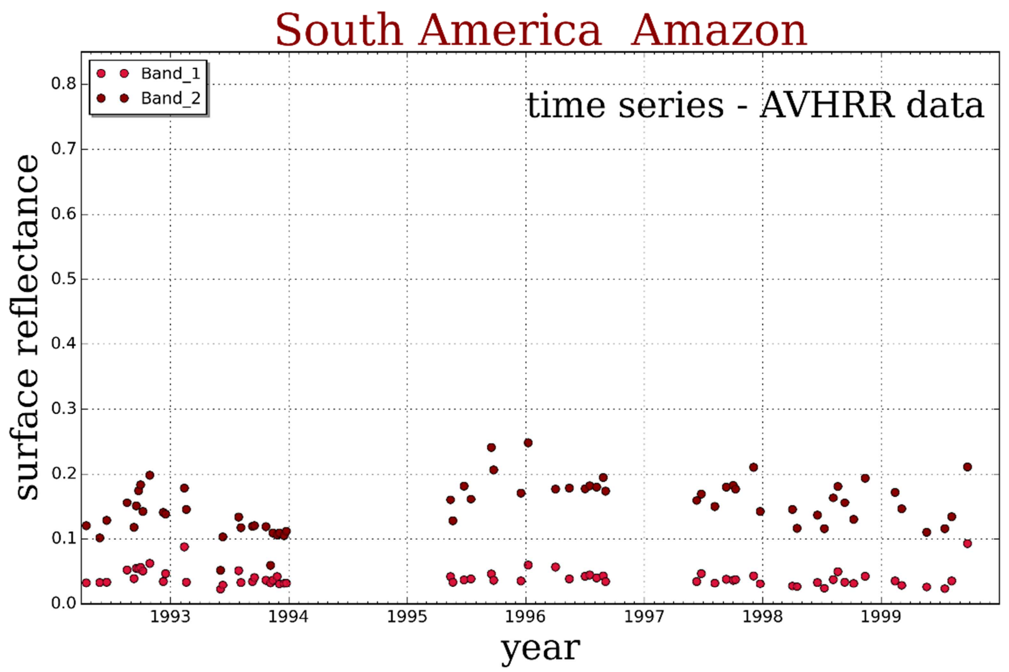

Figure 5-116: SR time series from AVHRR data - 1992-1999 – South America – Amazon

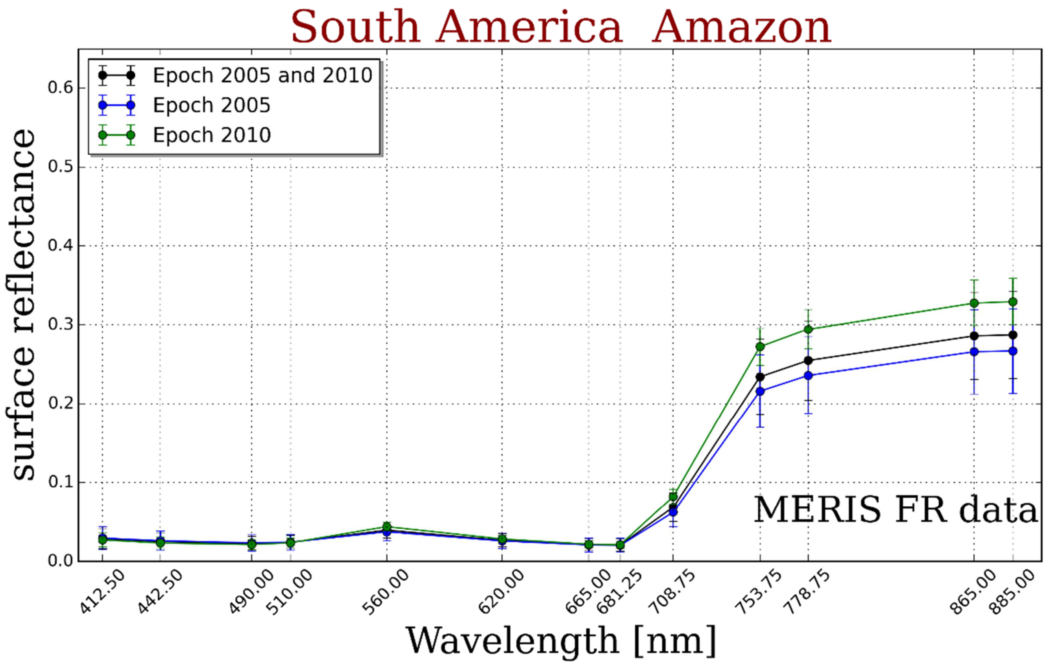

Figure 5-117: Spectra – South America – Amazon - MERIS FR data

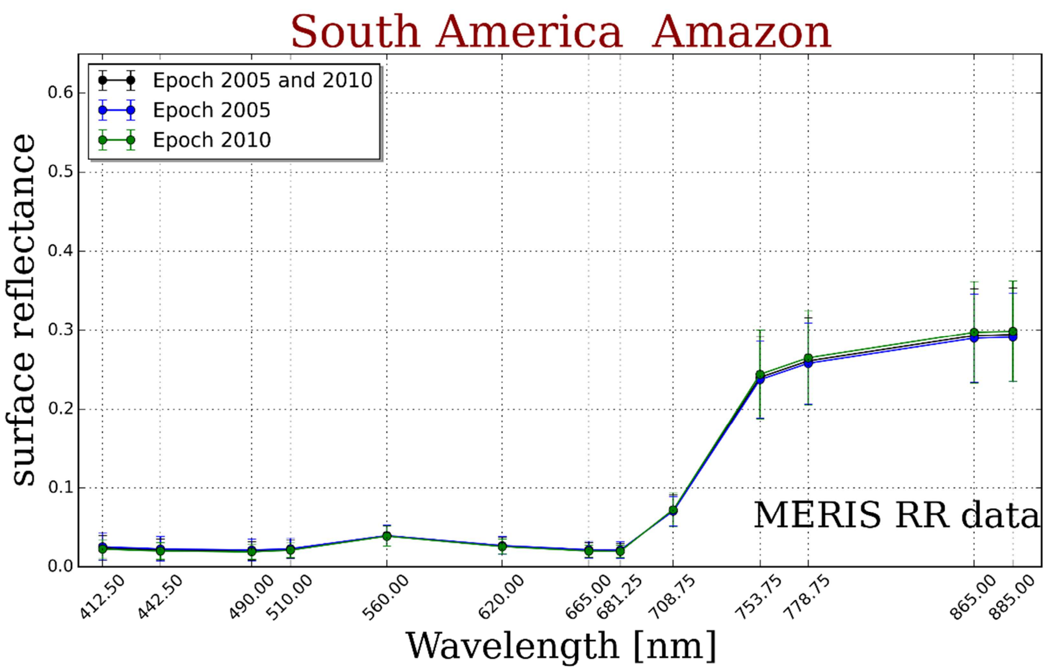

Figure 5-118: Spectra – South America – Amazon - MERIS RR data

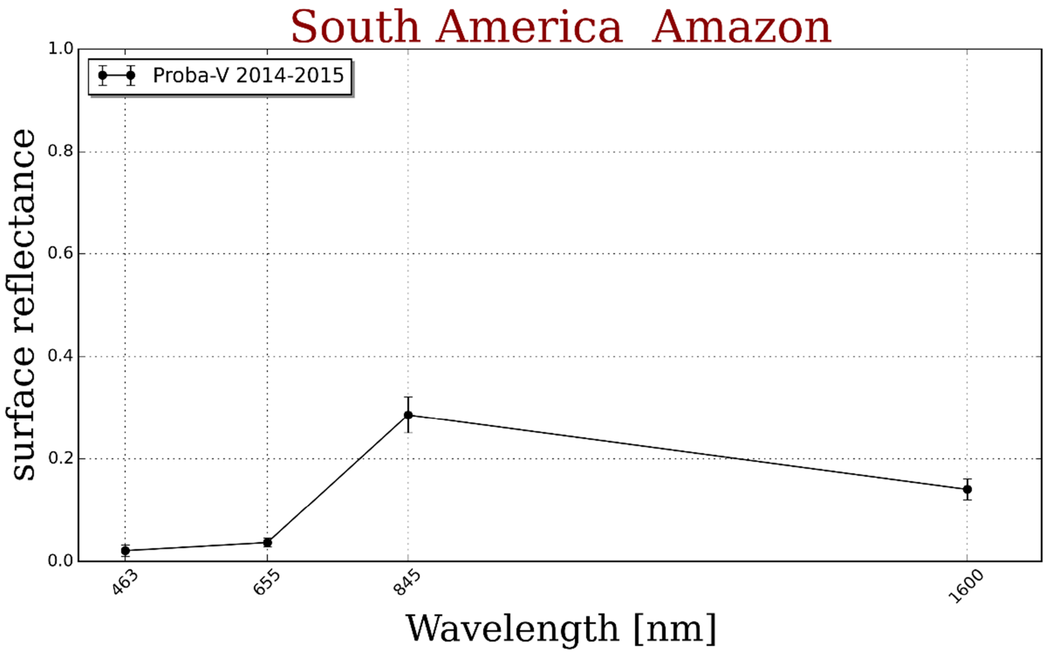

Figure 5-119: Spectra – South America – Amazon – PROBA-V data

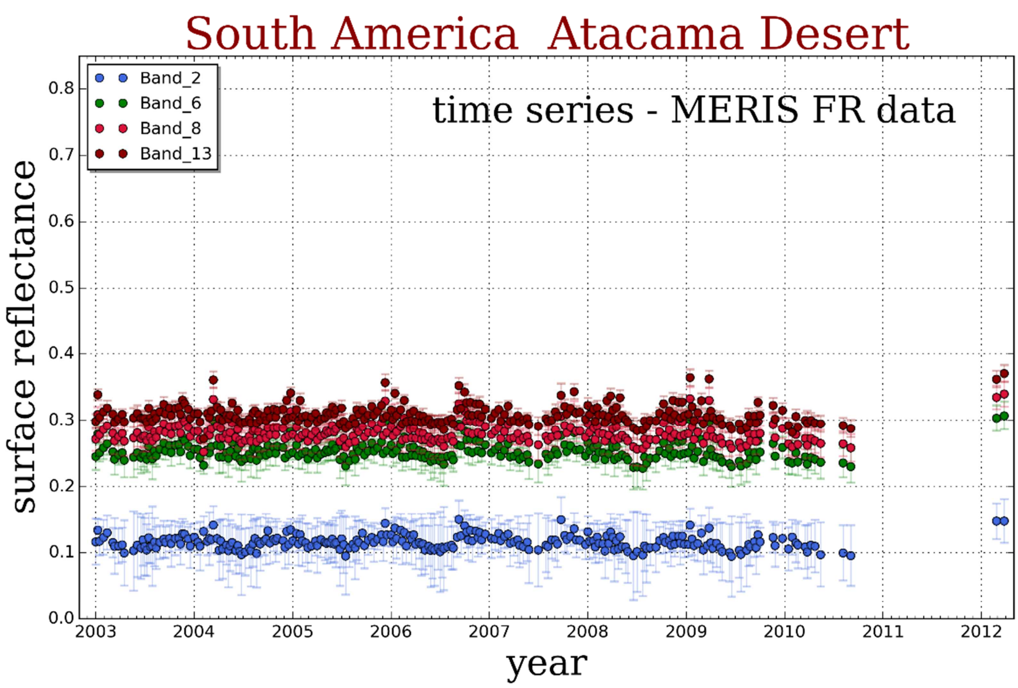

Figure 5-120: SR time series from MERIS FR data - 2003-2012 – South America – Atacama Desert

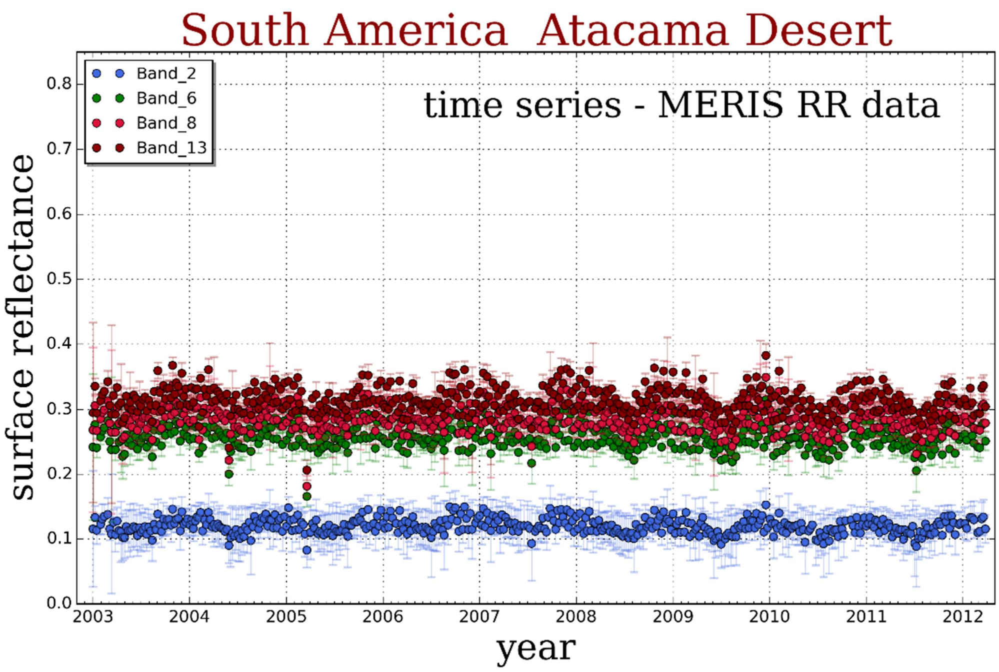

Figure 5-121: SR time series from MERIS RR data - 2003-2012 – South America – Atacama Desert

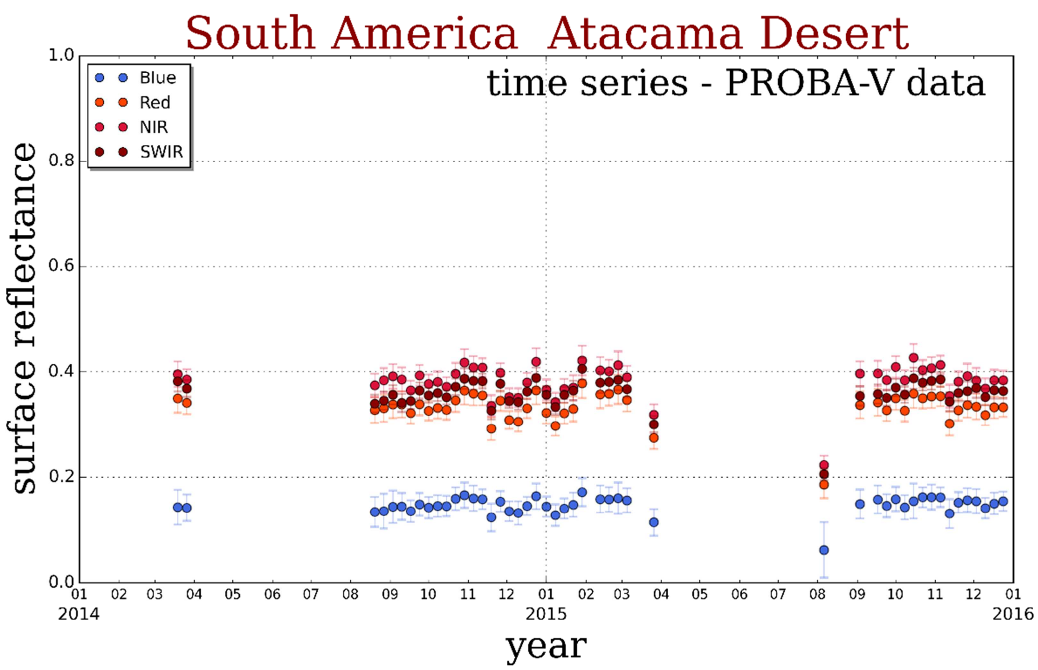

Figure 5-122: SR time series from PROBA-V data - 2014-2016 – South America – Atacama Desert

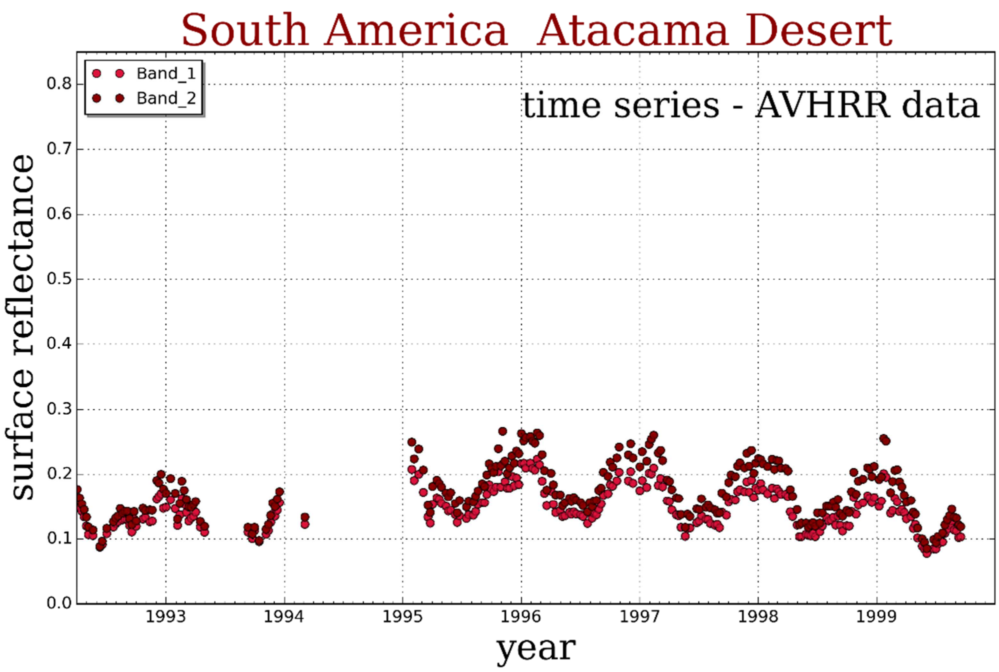

Figure 5-123: SR time series from AVHRR data - 1992-1999 – South America – Atacama Desert

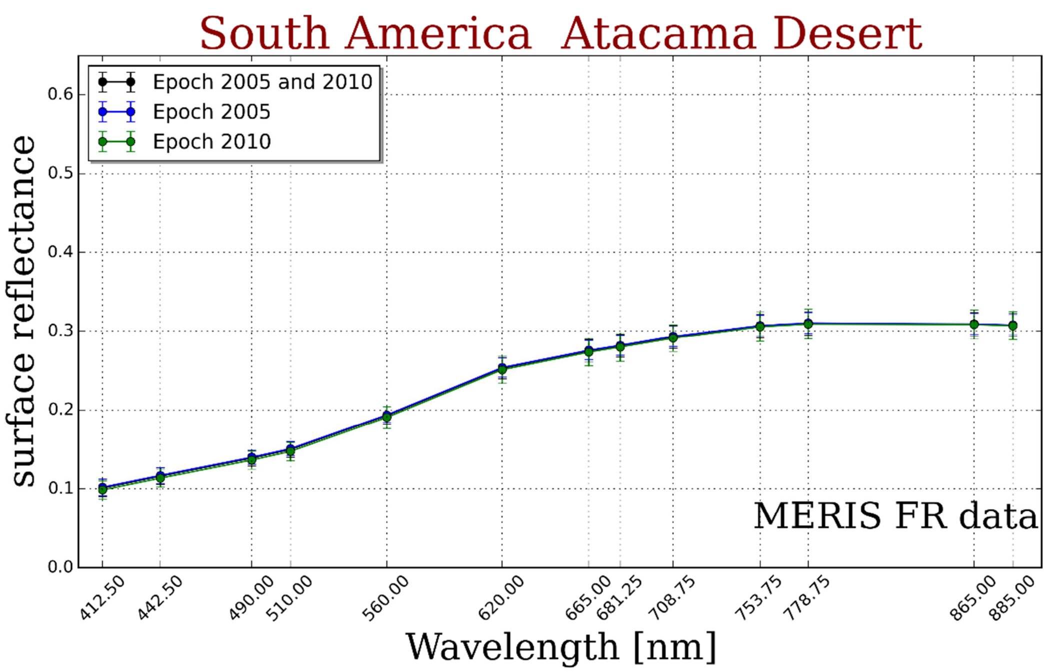

Figure 5-124: Spectra – South America – Atacama Desert - MERIS FR data

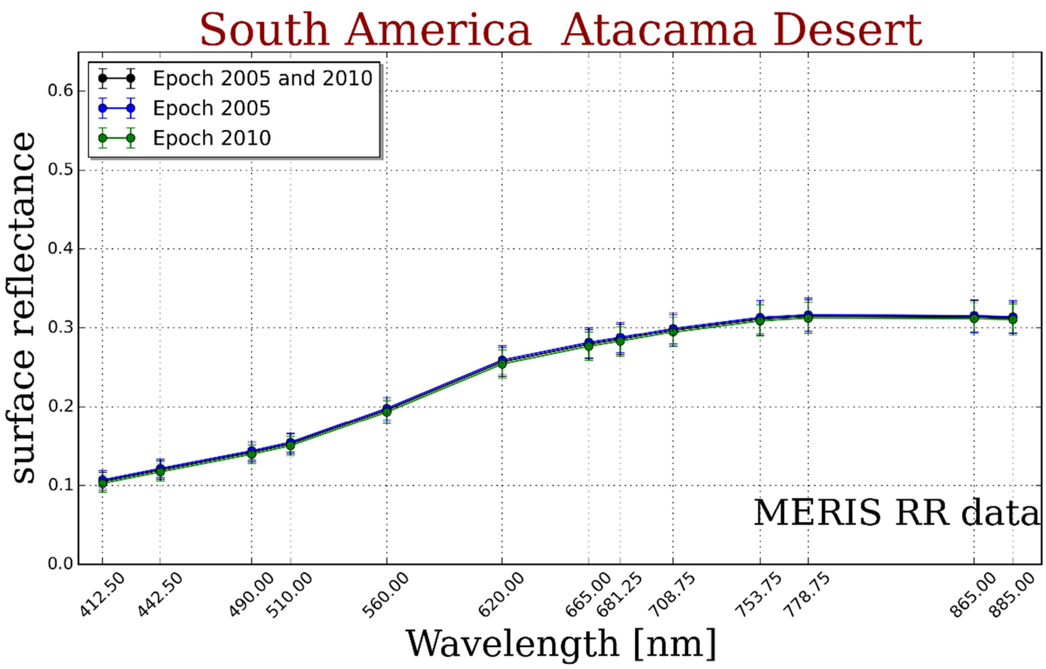

Figure 5-125: Spectra – South America – Atacama Desert - MERIS RR data

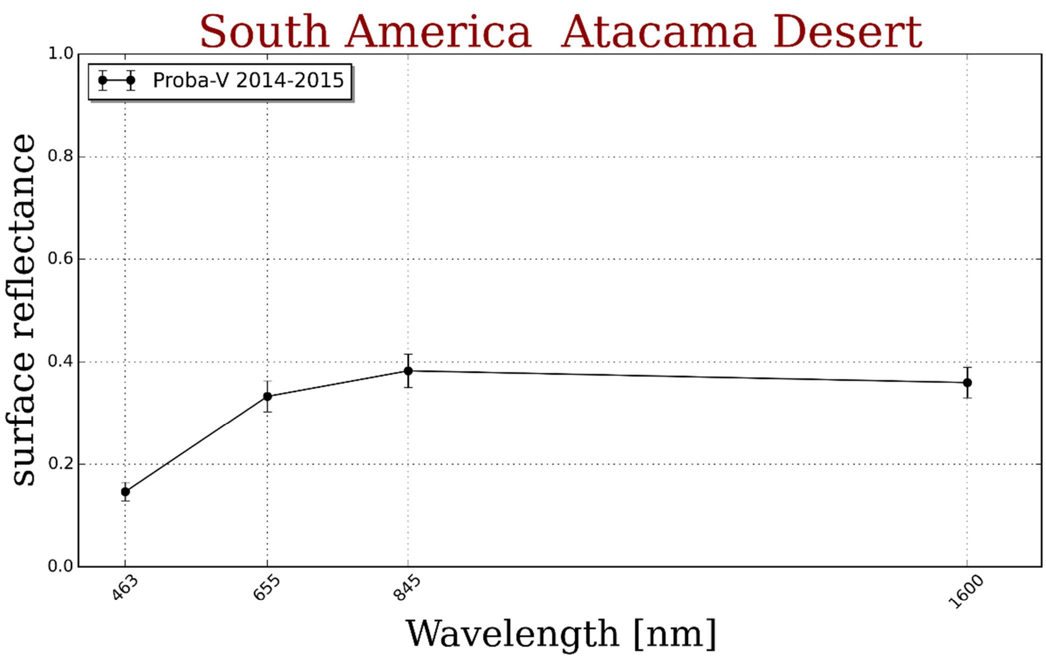

Figure 5-126: Spectra – South America – Atacama Desert – PROBA-V data

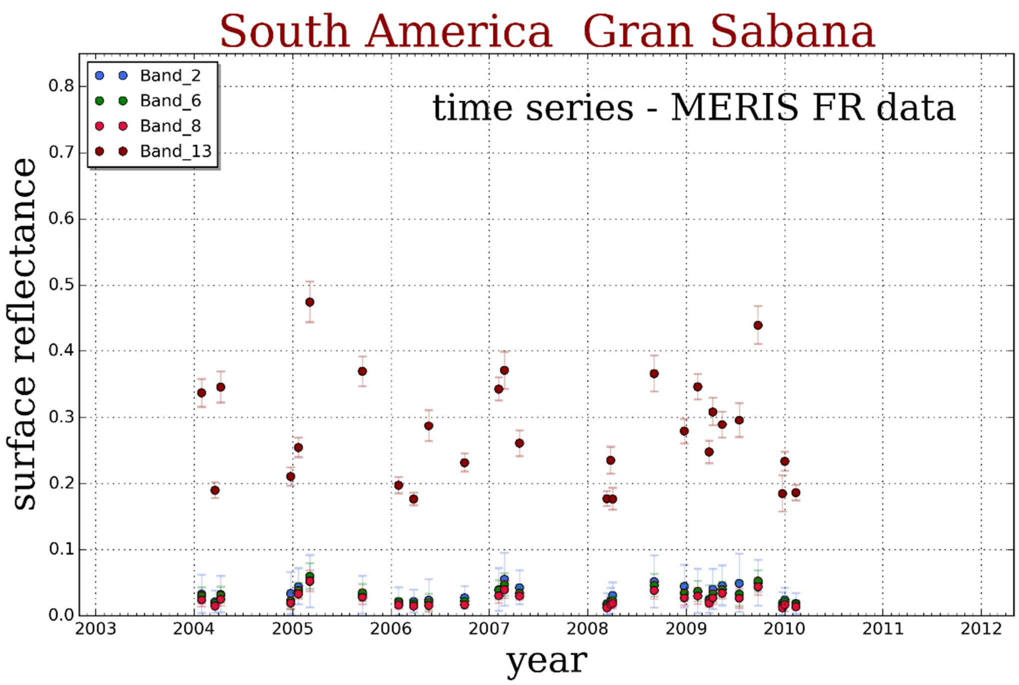

Figure 5-127: SR time series from MERIS FR data - 2003-2012 – South America – Gran Sabana

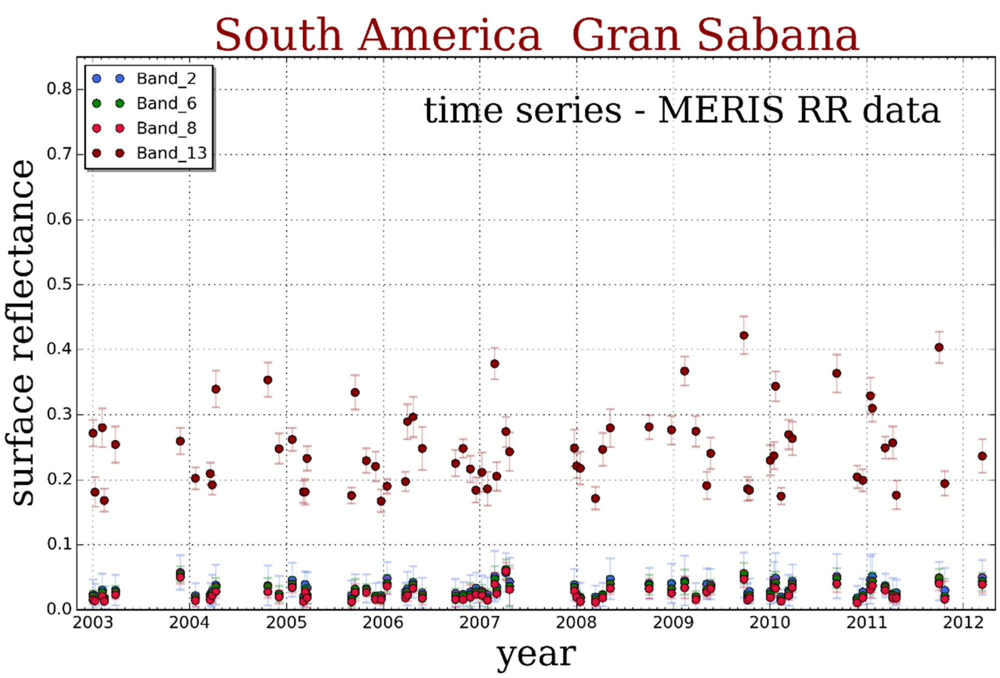

Figure 5-128: SR time series from MERIS RR data - 2003-2012 – South America – Gran Sabana

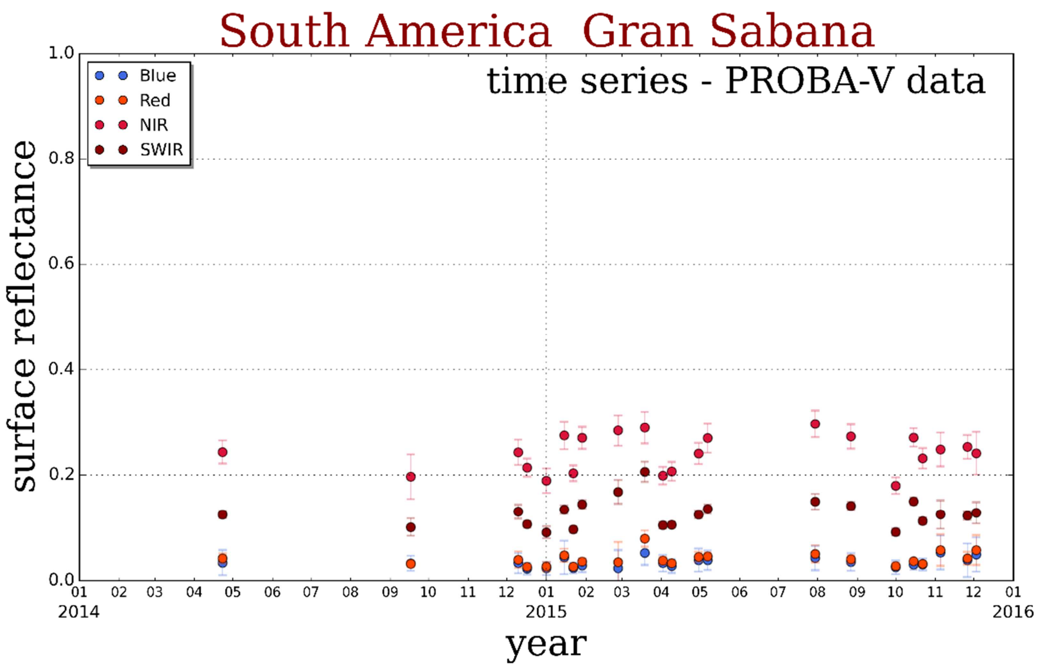

Figure 5-129: SR time series from PROBA-V data - 2014-2016 – South America – Gran Sabana

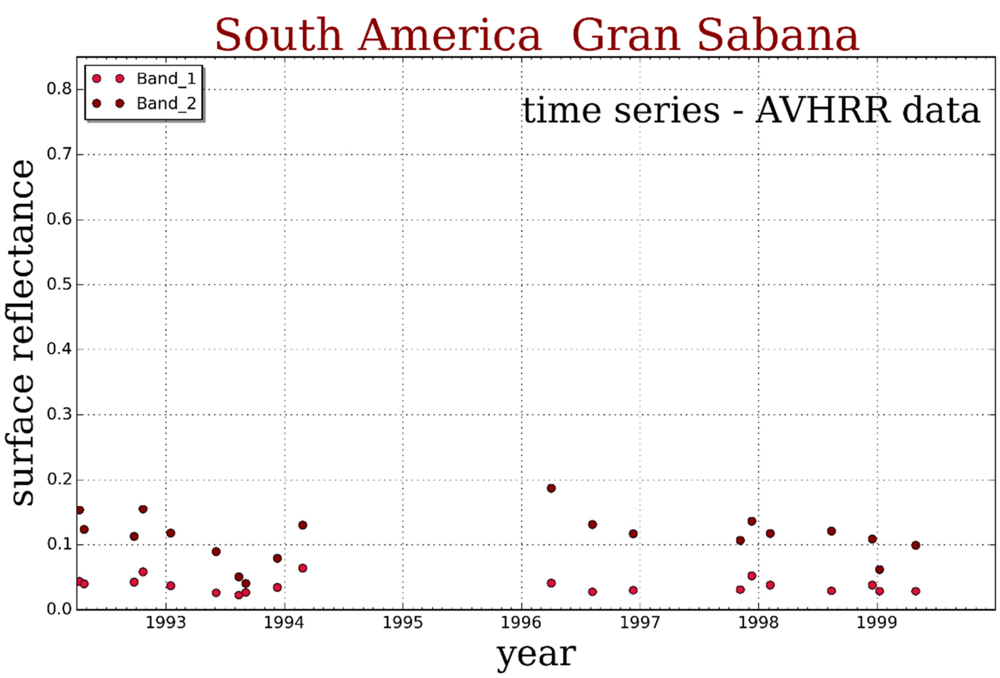

Figure 5-130: SR time series from AVHRR data - 1992-1999 – South America – Gran Sabana

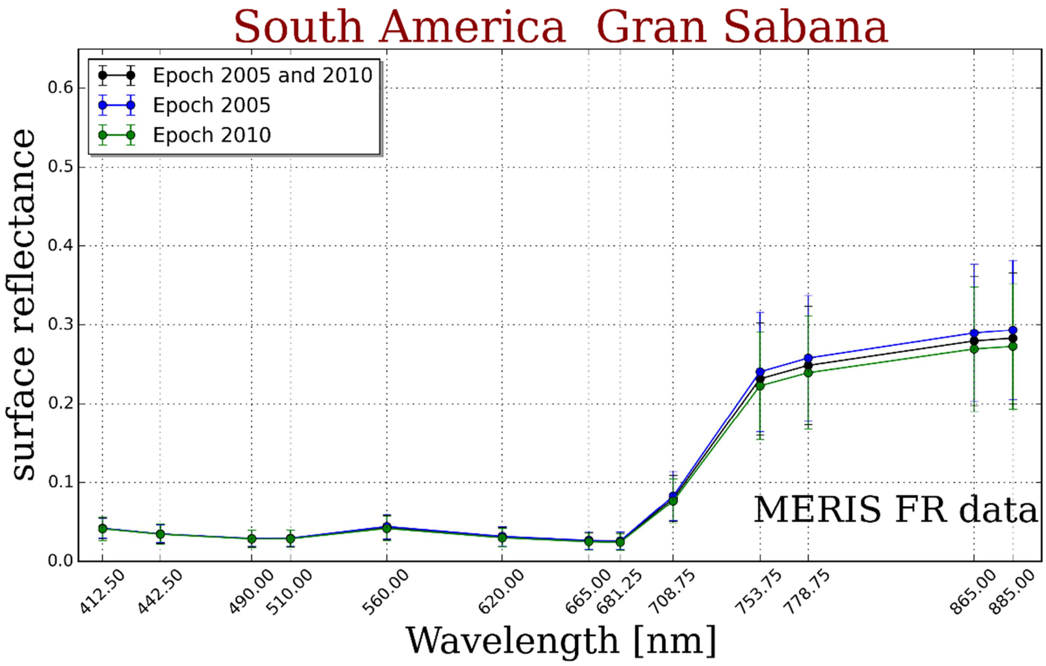

Figure 5-131: Spectra – South America – Gran Sabana - MERIS FR data

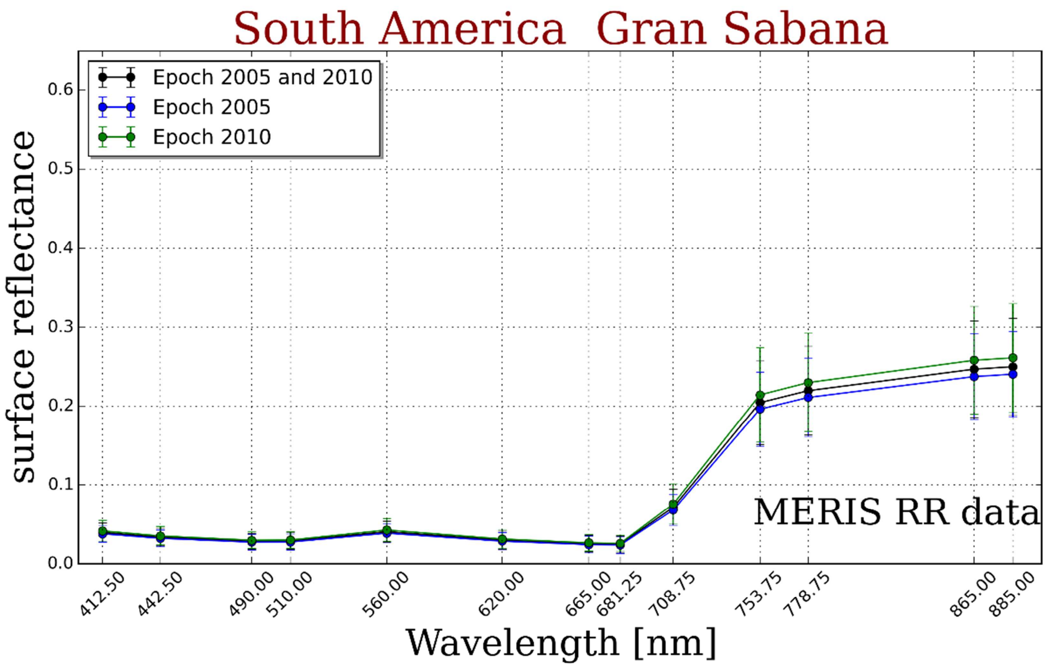

Figure 5-132: Spectra – South America – Gran Sabana - MERIS RR data

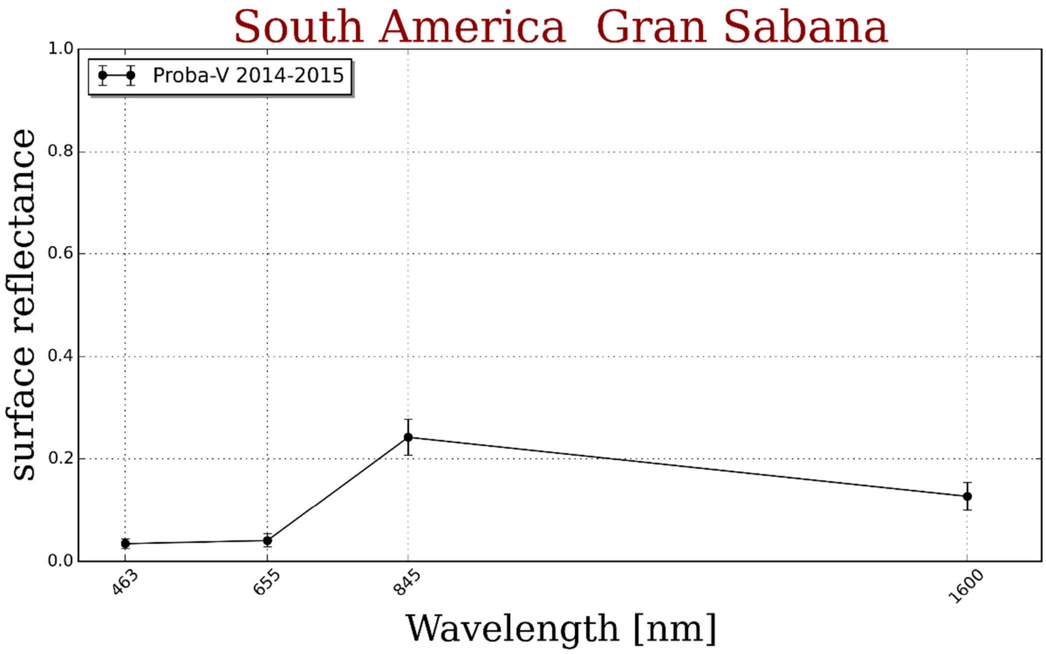

Figure 5-133: Spectra – South America – Gran Sabana – PROBA-V data

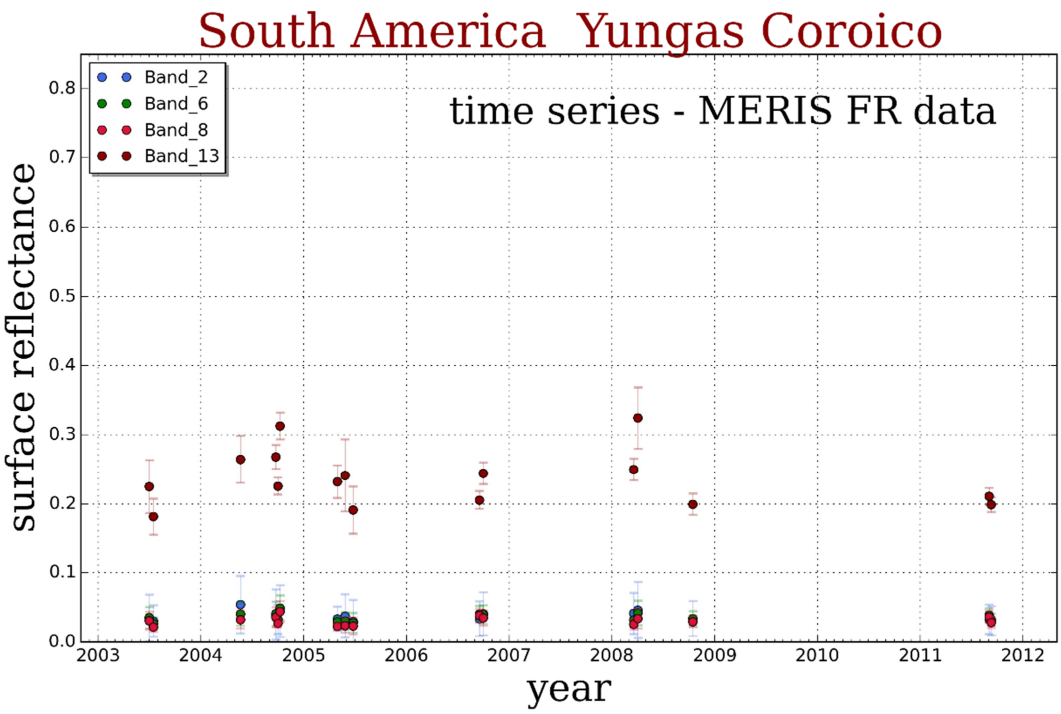

Figure 5-134: SR time series from MERIS FR data - 2003-2012 – South America – Yungas Coroico

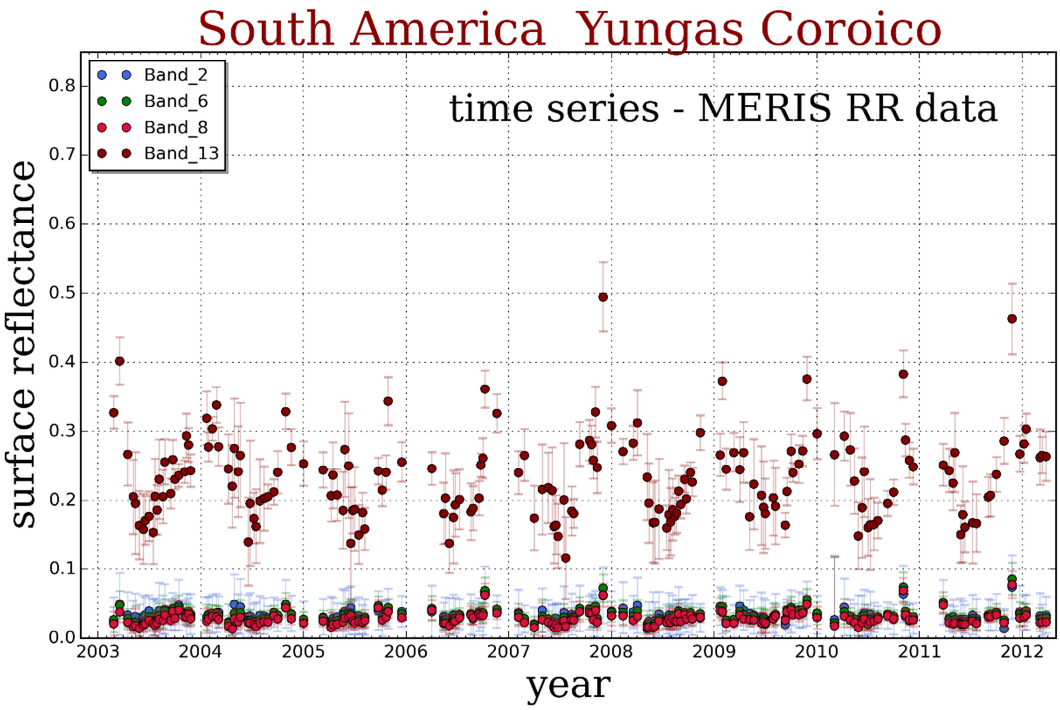

Figure 5-135: SR time series from MERIS RR data - 2003-2012 – South America – Yungas Coroico

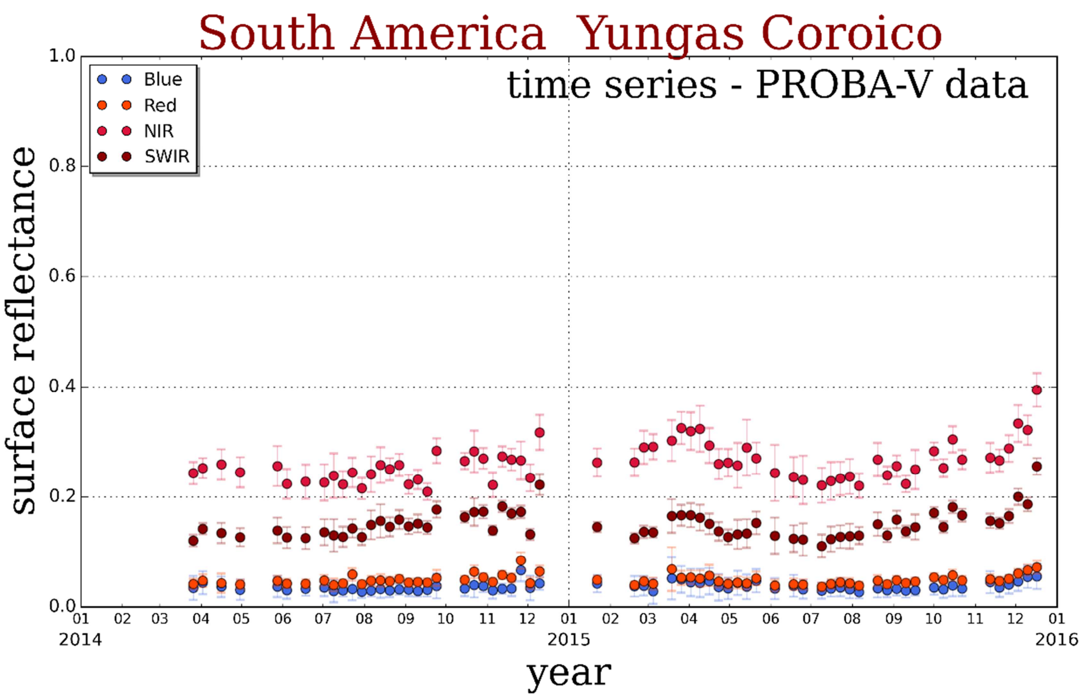

Figure 5-136: SR time series from PROBA-V data - 2014-2016 – South America – Yungas Coroico

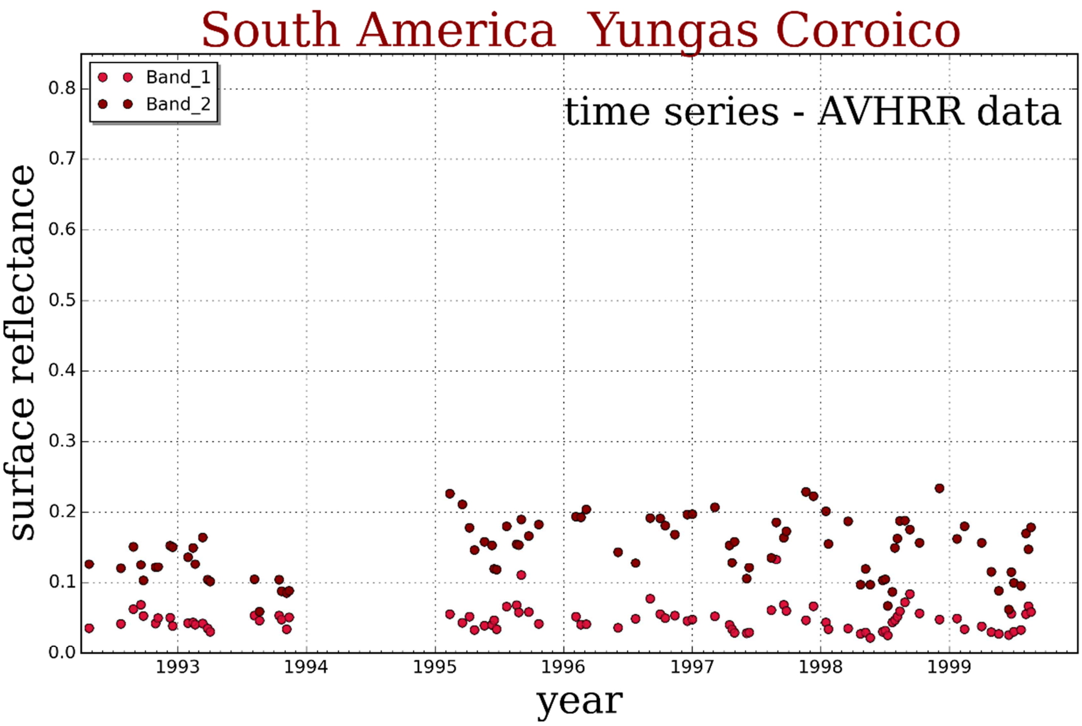

Figure 5-137: SR time series from AVHRR data - 1992-1999 – South America – Yungas Coroico

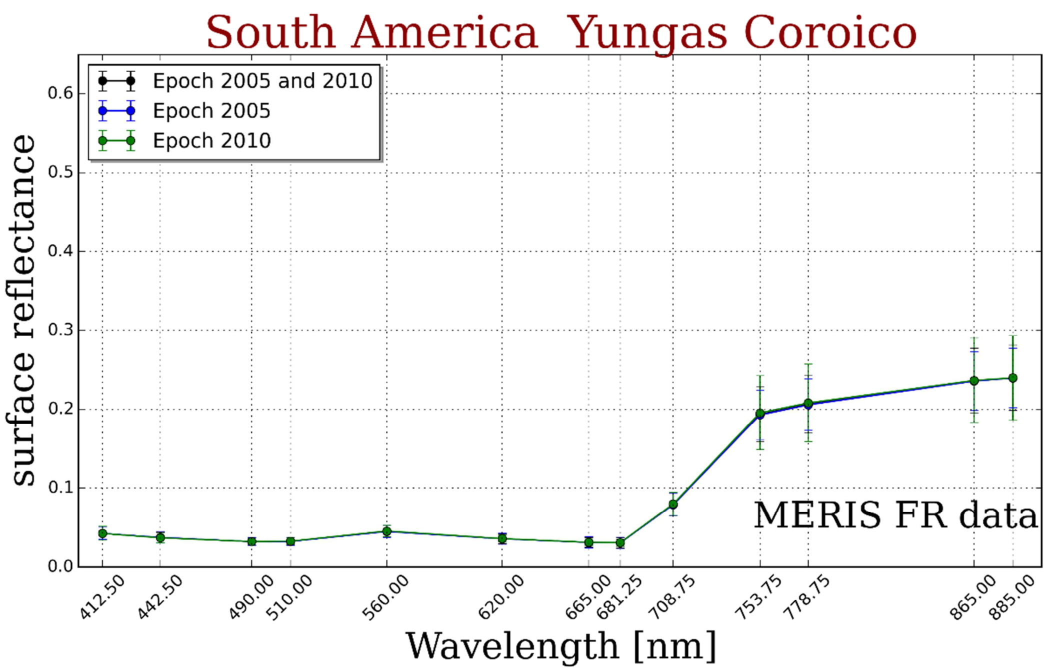

Figure 5-138: Spectra – South America – Yungas Coroico - MERIS FR data

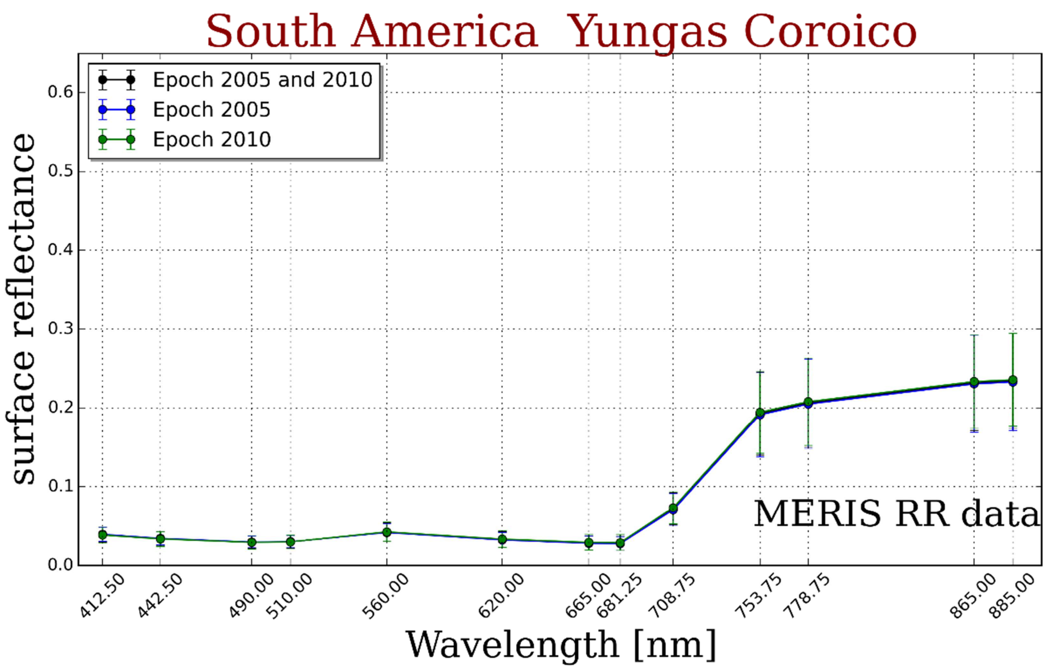

Figure 5-139: Spectra – South America – Yungas Coroico - MERIS RR data

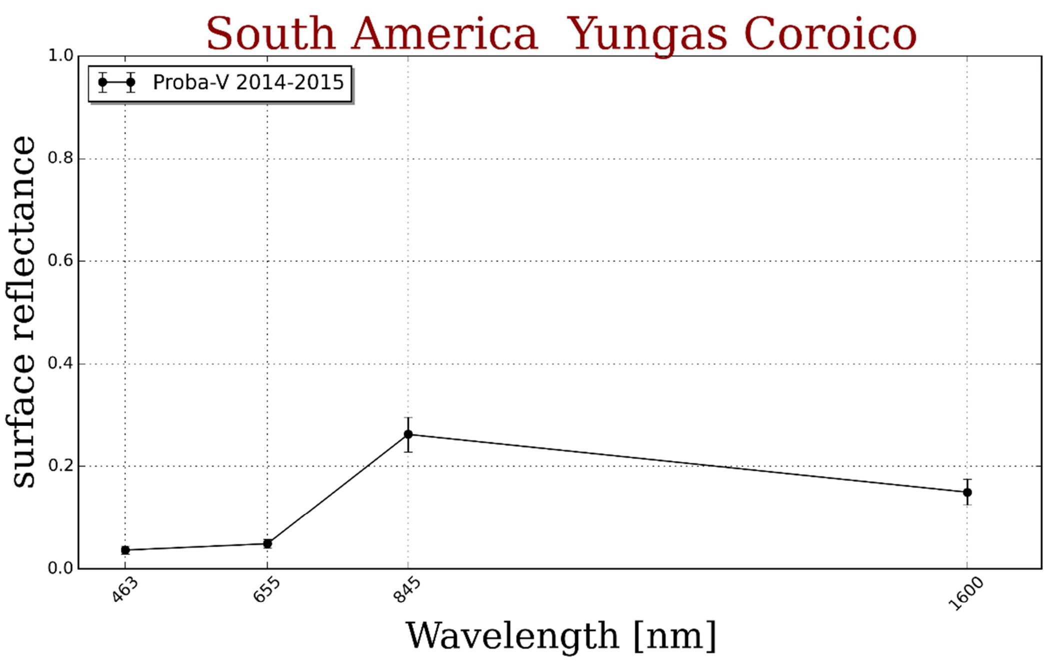

Figure 5-140: Spectra – South America – Yungas Coroico – PROBA-V data

Table 5-2: Temporal mean and variance (σ^2) at the pixel level for the various spectral reflectance values - selected reference points - MERIS FR time series and band1 to band7

	OBS. COUNTS CLEAR LAND		MERIS FR SR BAND 1	MERIS FR SR BAND 2	MERIS FR SR BAND 3	MERIS FR SR BAND 4	MERIS FR SR BAND 5	MERIS FR SR BAND 6	MERIS FR SR BAND 7
Yungas Coroico	67	mean	0.0424	0.0372	0.0321	0.0324	0.0451	0.0357	0.0312
		sigma	0.0076	0.0067	0.0047	0.0047	0.0073	0.0061	0.0061
Gran Sabana	230	mean	0.0415	0.0346	0.0287	0.0290	0.0429	0.0308	0.0257
		sigma	0.0135	0.0117	0.0103	0.0106	0.0153	0.0119	0.0108
Atacama Desert	269	mean	0.1011	0.1161	0.1391	0.1499	0.1930	0.2531	0.2751
		sigma	0.0110	0.0104	0.0100	0.0101	0.0113	0.0136	0.0141
Amazon	273	mean	0.0288	0.0252	0.0228	0.0240	0.0395	0.0267	0.0212
		sigma	0.0125	0.0106	0.0091	0.0085	0.0103	0.0083	0.0077
White Mountain National Forest	309	mean	0.0271	0.0270	0.0275	0.0306	0.0541	0.0412	0.0351
		sigma	0.0150	0.0134	0.0128	0.0127	0.0159	0.0163	0.0193
Sheyenne National Grassland	419	mean	0.0354	0.0412	0.0487	0.0536	0.0750	0.0756	0.0780
		sigma	0.0106	0.0104	0.0130	0.0134	0.0126	0.0209	0.0278
Great Bear Rainforest	395	mean	0.0286	0.0244	0.0206	0.0205	0.0268	0.0186	0.0148
		sigma	0.0079	0.0070	0.0064	0.0066	0.0097	0.0073	0.0062
National Park Peneda Geres	461	mean	0.0224	0.0207	0.0194	0.0200	0.0285	0.0219	0.0193
		sigma	0.0066	0.0054	0.0046	0.0049	0.0081	0.0062	0.0056
National Park Horto Bagy	470	mean	0.0318	0.0379	0.0455	0.0499	0.0694	0.0722	0.0752
		sigma	0.0081	0.0072	0.0083	0.0089	0.0103	0.0154	0.0202

	OBS. COUNTS CLEAR LAND		MERIS FR SR BAND 1	MERIS FR SR BAND 2	MERIS FR SR BAND 3	MERIS FR SR BAND 4	MERIS FR SR BAND 5	MERIS FR SR BAND 6	MERIS FR SR BAND 7
Kalevalsky Bor National Park	292	mean	0.0246	0.0246	0.0251	0.0272	0.0415	0.0349	0.0303
		sigma	0.0068	0.0050	0.0036	0.0037	0.0050	0.0052	0.0060
Mackenzie Country - New Zealand	353	mean	0.0309	0.0363	0.0440	0.0478	0.0628	0.0673	0.0691
		sigma	0.0072	0.0068	0.0068	0.0074	0.0109	0.0093	0.0094
Great Basalt Wall National Park	422	mean	0.0206	0.0209	0.0222	0.0242	0.0368	0.0327	0.0308
		sigma	0.0043	0.0034	0.0030	0.0034	0.0058	0.0054	0.0060
Great Sandy Dessert	297	mean	0.0321	0.0428	0.0595	0.0668	0.1058	0.1838	0.2158
		sigma	0.0136	0.0115	0.0100	0.0098	0.0113	0.0189	0.0229
Coen Tropical	392	mean	0.0342	0.0324	0.0319	0.0340	0.0494	0.0430	0.0397
		sigma	0.0091	0.0080	0.0080	0.0085	0.0119	0.0136	0.0157
Tundra - Tajmyr	227	mean	0.0302	0.0375	0.0461	0.0504	0.0694	0.0756	0.0779
		sigma	0.0054	0.0045	0.0041	0.0044	0.0059	0.0063	0.0078
Boreal Forest - Wladiwostok	256	mean	0.0300	0.0292	0.0293	0.0313	0.0464	0.0388	0.0357
		sigma	0.0138	0.0126	0.0123	0.0122	0.0151	0.0145	0.0169
Tumba Lediima - Kongo	337	mean	0.0370	0.0350	0.0332	0.0340	0.0455	0.0343	0.0295
		sigma	0.0107	0.0088	0.0080	0.0080	0.0101	0.0087	0.0086
Timbuktu - Sahara	435	mean	0.0921	0.1203	0.1561	0.1775	0.2733	0.3936	0.4331
		sigma	0.0149	0.0149	0.0143	0.0137	0.0131	0.0145	0.0155
New Valley - Sahara	456	mean	0.1273	0.1606	0.2036	0.2280	0.3317	0.4584	0.5008

	OBS. COUNTS CLEAR LAND		MERIS FR SR BAND 1	MERIS FR SR BAND 2	MERIS FR SR BAND 3	MERIS FR SR BAND 4	MERIS FR SR BAND 5	MERIS FR SR BAND 6	MERIS FR SR BAND 7
		sigma	0.0097	0.0099	0.0112	0.0122	0.0164	0.0222	0.0243
Mikumi National Park	415	mean	0.0367	0.0409	0.0484	0.0534	0.0774	0.0871	0.0944
		sigma	0.0103	0.0120	0.0159	0.0174	0.0217	0.0326	0.0402

Table 5-3: Temporal mean and variance (σ^2) at the pixel level for the various spectral reflectance values - selected reference points - MERIS FR time series and band8 to band14

	OBS. COUNTS CLEAR LAND		MERIS FR SR BAND 8	MERIS FR SR BAND 9	MERIS FR SR BAND 10	MERIS FR SR BAND 12	MERIS FR SR BAND 13	MERIS FR SR BAND 14
Yungas Coroico	67	mean	0.0306	0.0793	0.1937	0.2065	0.2360	0.2397
		sigma	0.0064	0.0139	0.0351	0.0369	0.0411	0.0413
Gran Sabana	230	mean	0.0251	0.0798	0.2316	0.2485	0.2794	0.2830
		sigma	0.0106	0.0292	0.0714	0.0750	0.0821	0.0829
Atacama Desert	269	mean	0.2815	0.2929	0.3068	0.3102	0.3091	0.3078
		sigma	0.0144	0.0143	0.0151	0.0152	0.0148	0.0145
Amazon	273	mean	0.0206	0.0686	0.2341	0.2547	0.2858	0.2870
		sigma	0.0075	0.0181	0.0477	0.0504	0.0550	0.0553
White Mountain National Forest	309	mean	0.0344	0.1064	0.2752	0.2919	0.3231	0.3263
		sigma	0.0200	0.0273	0.0913	0.0961	0.0969	0.0956
Sheyenne National Grassland	419	mean	0.0795	0.1263	0.2163	0.2283	0.2601	0.2645
		sigma	0.0295	0.0198	0.0399	0.0417	0.0437	0.0433
Great Bear Rainforest	395	mean	0.0141	0.0384	0.1002	0.1058	0.1177	0.1194

	OBS. COUNTS CLEAR LAND		MERIS FR SR BAND 8	MERIS FR SR BAND 9	MERIS FR SR BAND 10	MERIS FR SR BAND 12	MERIS FR SR BAND 13	MERIS FR SR BAND 14
		sigma	0.0060	0.0158	0.0380	0.0399	0.0433	0.0436
National Park Peneda Geres	461	mean	0.0190	0.0496	0.1366	0.1446	0.1593	0.1609
		sigma	0.0055	0.0148	0.0392	0.0411	0.0441	0.0441
National Park Horto Bagy	470	mean	0.0766	0.1205	0.1990	0.2104	0.2424	0.2469
		sigma	0.0213	0.0179	0.0393	0.0413	0.0442	0.0442
Kalevalsky Bor National Park	292	mean	0.0294	0.0756	0.1531	0.1614	0.1818	0.1846
		sigma	0.0060	0.0092	0.0206	0.0214	0.0226	0.0226
Mackenzie Country - New Zealand	353	mean	0.0695	0.1241	0.1887	0.1964	0.2200	0.2245
		sigma	0.0095	0.0188	0.0391	0.0401	0.0413	0.0412
Great Basalt Wall National Park	422	mean	0.0308	0.0667	0.1347	0.1429	0.1645	0.1675
		sigma	0.0062	0.0100	0.0239	0.0251	0.0271	0.0269
Great Sandy Dessert	297	mean	0.2255	0.2549	0.3074	0.3117	0.3191	0.3203
		sigma	0.0242	0.0248	0.0279	0.0280	0.0279	0.0280
Coen Tropical	392	mean	0.0398	0.0897	0.2219	0.2377	0.2730	0.2762
		sigma	0.0166	0.0206	0.0376	0.0392	0.0400	0.0389
Tundra - Tajmyr	227	mean	0.0781	0.1314	0.1961	0.2100	0.2570	0.2657
		sigma	0.0082	0.0122	0.0253	0.0259	0.0271	0.0274
Boreal Forest - Wladiwostok	256	mean	0.0353	0.0810	0.1779	0.1875	0.2084	0.2108
		sigma	0.0173	0.0225	0.0836	0.0874	0.0900	0.0891

	OBS. COUNTS CLEAR LAND		MERIS FR SR BAND 8	MERIS FR SR BAND 9	MERIS FR SR BAND 10	MERIS FR SR BAND 12	MERIS FR SR BAND 13	MERIS FR SR BAND 14
Tumba Lediima - Kongo	337	mean	0.0290	0.0664	0.2192	0.2390	0.2672	0.2668
		sigma	0.0086	0.0166	0.0502	0.0536	0.0587	0.0585
Timbuktu - Sahara	435	mean	0.4452	0.4567	0.4958	0.5035	0.5131	0.5112
		sigma	0.0158	0.0193	0.0171	0.0174	0.0180	0.0184
New Valley - Sahara	456	mean	0.5135	0.5324	0.5683	0.5764	0.5883	0.5885
		sigma	0.0249	0.0249	0.0225	0.0224	0.0221	0.0221
Mikumi National Park	415	mean	0.0978	0.1334	0.2184	0.2313	0.2645	0.2671
		sigma	0.0426	0.0323	0.0498	0.0512	0.0510	0.0499

Table 5-4: Temporal mean and variance at the pixel level for the various spectral reflectance values - selected reference points - MERIS RR time series and band1 to band7

	OBS. COUNTS CLEAR LAND		MERIS RR SR BAND 1	MERIS RR SR BAND 2	MERIS RR SR BAND 3	MERIS RR SR BAND 4	MERIS RR SR BAND 5	MERIS RR SR BAND 6	MERIS RR SR BAND 7
Yungas Coroico	473	mean	0.0390	0.0340	0.0294	0.0299	0.0421	0.0328	0.0286
		sigma	0.0095	0.0085	0.0078	0.0081	0.0117	0.0099	0.0092
Gran Sabana	473	mean	0.0396	0.0336	0.0285	0.0287	0.0406	0.0299	0.0253
		sigma	0.0120	0.0110	0.0103	0.0104	0.0132	0.0112	0.0105
Atacama Desert	475	mean	0.1052	0.1198	0.1421	0.1528	0.1959	0.2568	0.2791
		sigma	0.0118	0.0116	0.0120	0.0124	0.0146	0.0179	0.0190
Amazon	473	mean	0.0240	0.0215	0.0202	0.0221	0.0391	0.0263	0.0209
		sigma	0.0152	0.0135	0.0117	0.0112	0.0127	0.0103	0.0096

	OBS. COUNTS CLEAR LAND		MERIS RR SR BAND 1	MERIS RR SR BAND 2	MERIS RR SR BAND 3	MERIS RR SR BAND 4	MERIS RR SR BAND 5	MERIS RR SR BAND 6	MERIS RR SR BAND 7
White Mountain National Forest	478	mean	0.0281	0.0295	0.0320	0.0353	0.0568	0.0495	0.0469
		sigma	0.0135	0.0124	0.0127	0.0126	0.0143	0.0170	0.0215
Sheyenne National Grassland	474	mean	0.0335	0.0392	0.0466	0.0514	0.0723	0.0728	0.0751
		sigma	0.0100	0.0099	0.0125	0.0130	0.0123	0.0204	0.0274
Great Bear Rainforest	398	mean	0.0254	0.0231	0.0210	0.0218	0.0320	0.0227	0.0183
		sigma	0.0105	0.0088	0.0075	0.0076	0.0109	0.0081	0.0068
National Park Peneda Geres	478	mean	0.0218	0.0225	0.0236	0.0253	0.0366	0.0322	0.0306
		sigma	0.0076	0.0065	0.0060	0.0063	0.0093	0.0085	0.0086
National Park Horto Bagy	471	mean	0.0313	0.0370	0.0440	0.0484	0.0677	0.0697	0.0723
		sigma	0.0078	0.0069	0.0083	0.0087	0.0093	0.0150	0.0202
Kalevalsky Bor National Park	302	mean	0.0230	0.0238	0.0252	0.0277	0.0429	0.0377	0.0335
		sigma	0.0094	0.0085	0.0082	0.0082	0.0093	0.0093	0.0100
Mackenzie Country - New Zealand	391	mean	0.0309	0.0366	0.0443	0.0482	0.0639	0.0684	0.0705
		sigma	0.0076	0.0068	0.0063	0.0068	0.0105	0.0080	0.0081
Great Basalt Wall National Park	477	mean	0.0191	0.0196	0.0212	0.0232	0.0353	0.0319	0.0305
		sigma	0.0046	0.0039	0.0038	0.0041	0.0062	0.0061	0.0067
Great Sandy Dessert	478	mean	0.0337	0.0437	0.0591	0.0660	0.1031	0.1797	0.2113
		sigma	0.0119	0.0103	0.0090	0.0088	0.0099	0.0191	0.0238

	OBS. COUNTS CLEAR LAND		MERIS RR SR BAND 1	MERIS RR SR BAND 2	MERIS RR SR BAND 3	MERIS RR SR BAND 4	MERIS RR SR BAND 5	MERIS RR SR BAND 6	MERIS RR SR BAND 7
Coen Tropical	474	mean	0.0324	0.0311	0.0312	0.0334	0.0483	0.0428	0.0399
		sigma	0.0114	0.0105	0.0104	0.0108	0.0138	0.0137	0.0147
Tundra - Tajmyr	243	mean	0.0318	0.0394	0.0481	0.0522	0.0705	0.0761	0.0782
		sigma	0.0085	0.0083	0.0088	0.0089	0.0089	0.0104	0.0124
Boreal Forest - Wladiwostok	475	mean	0.0261	0.0272	0.0293	0.0315	0.0462	0.0410	0.0397
		sigma	0.0142	0.0141	0.0151	0.0152	0.0164	0.0186	0.0224
Tumba Lediima - Kongo	477	mean	0.0390	0.0366	0.0347	0.0356	0.0480	0.0362	0.0312
		sigma	0.0116	0.0098	0.0087	0.0086	0.0104	0.0089	0.0085
Timbuktu - Sahara	479	mean	0.0916	0.1194	0.1547	0.1760	0.2717	0.3920	0.4315
		sigma	0.0137	0.0138	0.0131	0.0125	0.0118	0.0133	0.0143
New Valley - Sahara	478	mean	0.1273	0.1608	0.2042	0.2288	0.3335	0.4615	0.5041
		sigma	0.0074	0.0067	0.0068	0.0071	0.0086	0.0100	0.0107
Mikumi National Park	474	mean	0.0369	0.0408	0.0477	0.0524	0.0748	0.0826	0.0894
		sigma	0.0106	0.0105	0.0121	0.0125	0.0139	0.0220	0.0300

Table 5-5: Temporal mean and variance (σ^2) at the pixel level for the various spectral reflectance values - selected reference points - MERIS RR time series and band8 to band14

	OBS. COUNTS CLEAR LAND		MERIS RR SR BAND 8	MERIS RR SR BAND 9	MERIS RR SR BAND 10	MERIS RR SR BAND 12	MERIS RR SR BAND 13	MERIS RR SR BAND 14
Yungas Coroico	473	mean	0.0283	0.0719	0.1929	0.2063	0.2318	0.2342
		sigma	0.0093	0.0207	0.0528	0.0558	0.0605	0.0605

	OBS. COUNTS CLEAR LAND		MERIS RR SR BAND 8	MERIS RR SR BAND 9	MERIS RR SR BAND 10	MERIS RR SR BAND 12	MERIS RR SR BAND 13	MERIS RR SR BAND 14
Gran Sabana	473	mean	0.0247	0.0717	0.2045	0.2196	0.2469	0.2499
		sigma	0.0105	0.0228	0.0535	0.0562	0.0613	0.0617
Atacama Desert	475	mean	0.2856	0.2973	0.3115	0.3149	0.3140	0.3127
		sigma	0.0193	0.0197	0.0206	0.0207	0.0204	0.0201
Amazon	473	mean	0.0205	0.0713	0.2402	0.2610	0.2932	0.2945
		sigma	0.0094	0.0198	0.0517	0.0547	0.0592	0.0591
White Mountain National Forest	478	mean	0.0469	0.1084	0.2506	0.2662	0.2975	0.3011
		sigma	0.0224	0.0246	0.0852	0.0899	0.0905	0.0891
Sheyenne National Grassland	474	mean	0.0767	0.1218	0.2107	0.2224	0.2528	0.2569
		sigma	0.0291	0.0192	0.0428	0.0449	0.0466	0.0462
Great Bear Rainforest	398	mean	0.0177	0.0531	0.1446	0.1540	0.1738	0.1763
		sigma	0.0066	0.0188	0.0498	0.0527	0.0584	0.0588
National Park Peneda Geres	478	mean	0.0306	0.0648	0.1596	0.1693	0.1878	0.1899
		sigma	0.0087	0.0158	0.0396	0.0418	0.0445	0.0444
National Park Horto Bagy	471	mean	0.0736	0.1176	0.1988	0.2105	0.2431	0.2476
		sigma	0.0213	0.0153	0.0397	0.0418	0.0437	0.0435
Kalevalsky Bor National Park	302	mean	0.0326	0.0823	0.1625	0.1715	0.1945	0.1978
		sigma	0.0099	0.0130	0.0235	0.0242	0.0252	0.0252
Mackenzie Country - New	391	mean	0.0709	0.1251	0.1938	0.2023	0.2278	0.2326

	OBS. COUNTS CLEAR LAND		MERIS RR SR BAND 8	MERIS RR SR BAND 9	MERIS RR SR BAND 10	MERIS RR SR BAND 12	MERIS RR SR BAND 13	MERIS RR SR BAND 14
Zealand								
		sigma	0.0083	0.0176	0.0435	0.0448	0.0465	0.0465
Great Basalt Wall National Park	477	mean	0.0306	0.0639	0.1260	0.1337	0.1545	0.1574
		sigma	0.0069	0.0104	0.0218	0.0228	0.0248	0.0247
Great Sandy Dessert	478	mean	0.2209	0.2482	0.2984	0.3025	0.3094	0.3105
		sigma	0.0253	0.0264	0.0276	0.0276	0.0271	0.0275
Coen Tropical	474	mean	0.0400	0.0879	0.2144	0.2297	0.2643	0.2676
		sigma	0.0152	0.0203	0.0390	0.0407	0.0423	0.0416
Tundra - Tajmyr	243	mean	0.0784	0.1283	0.1903	0.2030	0.2463	0.2540
		sigma	0.0129	0.0117	0.0204	0.0206	0.0210	0.0212
Boreal Forest - Wladiwostok	475	mean	0.0397	0.0828	0.1712	0.1810	0.2041	0.2071
		sigma	0.0231	0.0236	0.0844	0.0883	0.0913	0.0907
Tumba Lediima - Kongo	477	mean	0.0308	0.0709	0.2324	0.2532	0.2830	0.2826
		sigma	0.0084	0.0161	0.0458	0.0490	0.0536	0.0534
Timbuktu - Sahara	479	mean	0.4436	0.4550	0.4946	0.5023	0.5114	0.5094
		sigma	0.0146	0.0188	0.0160	0.0163	0.0168	0.0174
New Valley - Sahara	478	mean	0.5169	0.5359	0.5716	0.5797	0.5917	0.5919
		sigma	0.0109	0.0125	0.0120	0.0122	0.0127	0.0128
Mikumi National Park	474	mean	0.0926	0.1287	0.2129	0.2258	0.2600	0.2632

	OBS. COUNTS CLEAR LAND		MERIS RR SR BAND 8	MERIS RR SR BAND 9	MERIS RR SR BAND 10	MERIS RR SR BAND 12	MERIS RR SR BAND 13	MERIS RR SR BAND 14
		sigma	0.0325	0.0224	0.0462	0.0478	0.0475	0.0465

Table 5-6: Temporal mean and variance (σ^2) at the pixel level for the various spectral reflectance values - selected reference points - PROBA-V time series and band1 to band4

	OBS. COUNTS CLEAR LAND		PROBA-V SR BAND 1	PROBA-V SR BAND 2	PROBA-V SR BAND 3	PROBA-V SR BAND 4
Yungas Coroico	66	mean	0.0365	0.0488	0.2619	0.1497
		sigma	0.0077	0.0089	0.0344	0.0250
Gran Sabana	22	mean	0.0344	0.0406	0.2419	0.1272
		sigma	0.0093	0.0127	0.0351	0.0270
Atacama Desert	48	mean	0.1466	0.3327	0.3824	0.3595
		sigma	0.0172	0.0298	0.0327	0.0296
Amazon	26	mean	0.0210	0.0367	0.2858	0.1407
		sigma	0.0110	0.0083	0.0354	0.0205
White Mountain National Forest	55	mean	0.0289	0.0523	0.3313	0.1715
		sigma	0.0124	0.0167	0.0664	0.0176
Sheyenne National Grassland	72	mean	0.0457	0.1073	0.2713	0.2772
		sigma	0.0118	0.0305	0.0332	0.0466
Great Bear Rainforest	11	mean	0.0278	0.0437	0.2578	0.1284
		sigma	0.0067	0.0063	0.0391	0.0171
National Park Peneda Geres	51	mean	0.0179	0.0345	0.2050	0.1063

	OBS. COUNTS CLEAR LAND		PROBA-V SR BAND 1	PROBA-V SR BAND 2	PROBA-V SR BAND 3	PROBA-V SR BAND 4
		sigma	0.0123	0.0157	0.0239	0.0154
National Park Horto Bagy	67	mean	0.0408	0.0864	0.2386	0.2611
		sigma	0.0161	0.0172	0.0445	0.0411
Kalevalsky Bor National Park	7	mean	0.0188	0.0410	0.2019	0.1206
		sigma	0.0106	0.0098	0.0291	0.0200
Mackenzie Country - New Zealand	77	mean	0.0458	0.1000	0.2087	0.2590
		sigma	0.0066	0.0111	0.0237	0.0254
Great Basalt Wall National Park	81	mean	0.0269	0.0580	0.1662	0.1666
		sigma	0.0058	0.0119	0.0191	0.0258
Great Sandy Dessert	90	mean	0.0314	0.1744	0.2536	0.3255
		sigma	0.0103	0.0141	0.0154	0.0213
Coen Tropical	61	mean	0.0274	0.0487	0.2798	0.1387
		sigma	0.0086	0.0104	0.0283	0.0222
Tundra - Tajmyr	9	mean	0.0370	0.0958	0.2701	0.2451
		sigma	0.0095	0.0161	0.0301	0.0300
Boreal Forest - Wladiwostok	48	mean	0.0312	0.0477	0.2292	0.1389
		sigma	0.0121	0.0152	0.0783	0.0211
Tumba Lediima - Kongo	20	mean	0.0349	0.0509	0.2868	0.1584
		sigma	0.0139	0.0151	0.0532	0.0296
Timbuktu - Sahara	91	mean	0.1231	0.4358	0.5084	0.6522

	OBS. COUNTS CLEAR LAND		PROBA-V SR BAND 1	PROBA-V SR BAND 2	PROBA-V SR BAND 3	PROBA-V SR BAND 4
		sigma	0.0113	0.0105	0.0201	0.0153
New Valley - Sahara	93	mean	0.1644	0.5030	0.5905	0.7162
		sigma	0.0034	0.0054	0.0126	0.0104
Mikumi National Park	41	mean	0.0516	0.1107	0.2579	0.3033
		sigma	0.0155	0.0287	0.0403	0.0580

Table 5-7: Temporal mean and variance (σ^2) at the pixel level for the various spectral reflectance values - selected reference points - AVHRR time series and band1 to band2

	OBS. COUNTS CLEAR LAND		AVHRR SR BAND 1	AVHRR SR BAND 2
Yungas Coroico	87	mean	0.0480	0.1477
		sigma	0.0173	0.0412
Gran Sabana	20	mean	0.0373	0.1120
		sigma	0.0111	0.0354
Atacama Desert	246	mean	0.1468	0.1730
		sigma	0.0313	0.0420
Amazon	65	mean	0.0404	0.1508
		sigma	0.0127	0.0381
White Mountain National Forest	88	mean	0.0526	0.1604
		sigma	0.0224	0.0480
Sheyenne National Grassland	104	mean	0.0585	0.1468
		sigma	0.0235	0.0338

	OBS. COUNTS CLEAR LAND		AVHRR SR BAND 1	AVHRR SR BAND 2
Great Bear Rainforest	36	mean	0.0437	0.1083
		sigma	0.0237	0.0274
National Park Peneda Geres	119	mean	0.0489	0.1222
		sigma	0.0101	0.0294
National Park Horto Bagy	103	mean	0.0840	0.1685
		sigma	0.0175	0.0321
Kalevalsky Bor National Park	82	mean	0.0783	0.1231
		sigma	0.0528	0.0344
Mackenzie Country - New Zealand	98	mean	0.0617	0.1412
		sigma	0.0155	0.0475
Great Basalt Wall National Park	147	mean	0.0399	0.0808
		sigma	0.0113	0.0229
Great Sandy Dessert	219	mean	0.1118	0.1722
		sigma	0.0267	0.0470
Coen Tropical	143	mean	0.0439	0.1408
		sigma	0.0121	0.0345
Tundra - Tajmyr	8	mean	0.0630	0.1100
		sigma	0.0171	0.0069
Boreal Forest - Wladiwostok	102	mean	0.0642	0.1498
		sigma	0.0208	0.0645
Tumba Lediima - Kongo	69	mean	0.0661	0.1623

	OBS. COUNTS CLEAR LAND		AVHRR SR BAND 1	AVHRR SR BAND 2
		sigma	0.0289	0.0349
Timbuktu - Sahara	206	mean	0.4148	0.5017
		sigma	0.0501	0.0608
New Valley - Sahara	264	mean	0.3744	0.4303
		sigma	0.0534	0.0543
Mikumi National Park	81	mean	0.0679	0.1346
		sigma	0.0192	0.0436